Prediction of Mobility Profile with Minimum Real Time Measurements using Artificial Intelligence

BY

MUBARAK AOUDAH AL-DHUFAIRI

A Thesis Presented to the

DEANSHIP OF GRADUATE STUDIES

KING FAHD UNIVERSITY OF PETROLEUM & MINERALS

DHAHRAN, SAUDI ARABIA

In Partial Fulfillment of the
Requirements for the Degree of

MASTER OF SCIENCE

In

PETROLEUM ENGINEERING

MAY 2011

KING FAHD UNIVERSITY OF PRTROLEUM AND MINERALS
DHAHRAN 31261, SAUDI ARABIA
DEANSHIP OF GRADUATE STUDIES

This thesis, written by **MUBARAK AOUDAH AL-DHUFAIRI** under the direction of this thesis advisor and approval by this thesis committee, has been presented to and accepted by the Dean of Graduate Studies, in partial fulfillment of the requirements for the degree of **MASTER OF SCIENCE IN PETROLEUM ENGINEERING.**

Thesis Committee

a. a. almajed
Dr. Abdulaziz A. Al-Majed (Thesis Advisor)

Dr. Abdulazeez Abdulraheem (Member)

Hossain
Dr. M. Enamul Hossain (Member)

Dr. Abdulaziz A. Al-Majed
(Department Chairman)

Dr. Salam A. Zummo
(Dean of Graduate Studies)

22/5/11
Date

DEDICATION

My loving parents & my wife

ACKNOWLEDGEMENTS

In the name of Allah, The Most Gracious and The Most Merciful, all praises and adoration are due to Allah, the lord of incomparable Majesty, and peace be upon the last messenger, Mohammad, his family and companions, for giving me the help and guidance that enabled me to work successfully.

I would like to appreciate my family members for their prayers, encouragement and support that permitted me to indulge in my passion for the long task to completing this work.

My profound gratitude goes to my thesis advisor, Dr. Abdulaziz Al-Majed, and my thesis committee members, Dr. Abdulaziz Abdulraheem and Dr. Enamul Al-Hossain for the advice and assistance accorded me during the course of this work. Their advice and constructive criticism have made this thesis an unqualified success. Many thanks go to the Chairman and other faculty members and staff of the Petroleum Engineering department.

TABLE OF CONTENTS

LIST OF TABLES

LIST OF FIGURES

THESIS ABSTRACT

NAME: MUBARAK AOUDAH AL-DHUFAIRI

TITLE: PREDICTION OF MOBILITY PROFILE WITH MINIMUM REAL TIME MEASUREMENTS USING ARTIFICIAL INTELLIGENCE

MAJOR: PETROLEUM ENGINEERING

DATE OF DEGREE: September, 2011

In the oil business, information equals cost-effective productivity. The more that is known about reservoir conditions, the better the reservoir can be produced. Acquiring knowledge and information to add value to oilfield operations has always been the area of active research programs. In the fields with multiple viscosity values, the ability to measure the mobility is one of the main keys to plan the field development and production strategies for optimum reservoir management aspects.

This thesis work will present a novel idea, trying to develop a prediction model that can reduce the investment of acquiring mobility data measurements utilizing Artificial Intelligent (AI) tools. A mobility profile is generated (using Formation Testing Tools) which involves significant costs for mobilizing the equipments to the rig site and then acquiring the data for a large number of sampling points. The mobility profile thus generated can help in efficient geo-steering for better placement of the horizontal section.

This thesis deals with the prediction of the mobility profile using three AI tools (Artificial neural network (ANN), Functional network (FunNet) and Support vector machine (SVM)) while employing only minimum number of real time mobility sampling data points. The three AI tool showed excellent performance but the ANN performed the best among the three tools.

خلاصــة الرســالــة

أسم الطالب : مبارك عودة الظفيري

عنوان البحث : التنبؤ بقيم اللزوجة باستخدام الحد الأدنى من البيانات القادمة مباشرة من أداة الحفر بواسطة أدوات الذكاء الاصطناعي

مجال التخصص : هندسة النفط

تاريخ الدرجة العلمية : فبراير 2011

إن للمعلومات في قطاع النفط دور كبير في تحقيق الإنتاجية الفعالة و تقليل التكلفة. كلما زادت معرفتنا أكثر عن حال المكمن، كلما تمكنا من إدارته و إنتاجه بشكل أفضل.إن برامج الأبحاث النشطة تركز على إكتساب المعارف والمعلومات لإضافة قيمة إلى عمليات النفط. إن القدرة على قياس سرعه حركة الزيت داخل المكمن تعد أحد أهم المفاتيح لتخطيط استراتيجيات تطوير وإنتاج الحقل بأفضل أساليب الإدارة الممكنة خصوصاً في الحقول متعددة قيم اللزوجة.

إن أطروحة البحث هذه تقدم فكرة جديدة، وذلك بمحاولة تطوير نموذج للتنبؤ، يمكن أن يقلل من الاستثمارات المرصودة للحصول على قياسات قيم اللزوجة وذلك باستخدام أدوات الذكاء الاصطناعية.

يمكن فهم هذا من حقيقة أن قيم اللزوجة تستخلص باستخدام أدوات اختبار المكمن وهي التي تنطوي على تكاليف كبيرة ابتداء بنقل المعدات إلى موقع الحفر وثم الحصول على بيانات قيم اللزوجة وهي التي تتطلب أخذ قرابة 100عينه لتمكين المهندسين من قيادة الجزء الأفقي من البئر النفطي للمكان الأفضل في المكمن.

هذه الأطروحة تقدم دراسة التنبؤ لقيم اللزوجة با ستخدام ثلاث أدوات ذكاء اصطناعية (الشبكة العصبية الاصطناعية, الشبكات الوظيفية وأجهزة المتجهات الاعتمادية) و باستخدام الحد الأدنى فقط من البيانات القادمة مباشرة من أداة الحفر. إن الأدوات الذكية الاصطناعية الثلاث أظهرت أداء ممتاز ولكن أداء الشبكة العصبية الاصطناعية كان الأفضل بين أداوت المحاكاة الثلاث.

CHAPTER 1

INTRODUCTION

1.1 Introduction of the Thesis

Traditionally, due to technological restrictions and economic considerations, wells were drilled mainly vertical to the oil bearing formation. However, thanks to recent advances in oil-well drilling technology and a decrease in drilling cost, horizontal wells are now being drilled routinely to drain oil reservoirs. The biggest challenge in horizontal well drilling is placement of the horizontal sections.

The best placement technique for oil producers in fields where bottom water aquifer and gas cap exists is to target the middle of the layer as illustrated in Figure 1. This can be achieved by geo-steering, Geologically Navigation Process, and making use of Measurement While Drilling (MWD) tools which provide basic reservoir characteristics like porosity, gamma ray and water saturation.

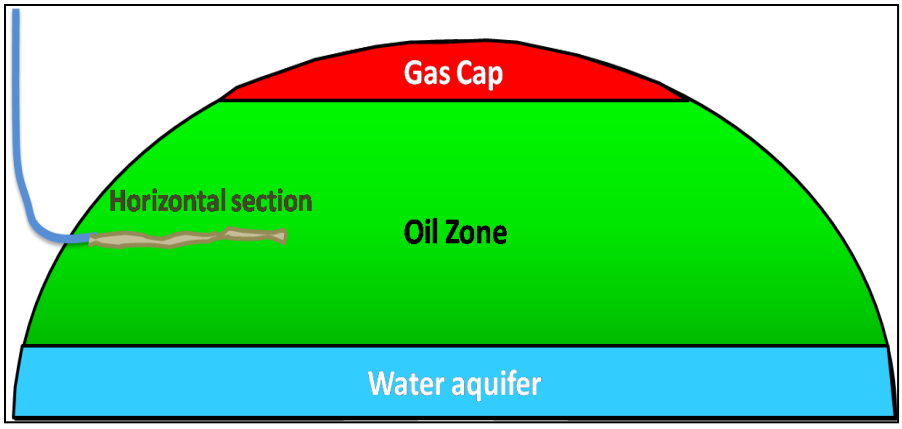

Figure 1: Reservoir with bottom water aquifer and gas cap

This method will help in delaying the gas and water encroachment by reducing the pressure depression in the well's neighborhood due to the smaller flow rate per unit length. It will also maximize the field's oil recovery.

The task gets extremely complex for a horizontal water injection well in a field underlay by irregular thickness tarmat zone isolating the aquifer support from oil zone as shown in Figure 2.

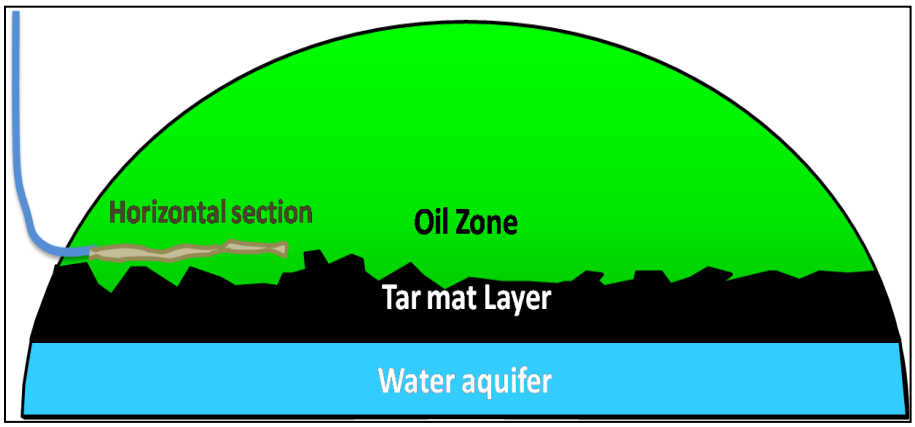

Figure 2: Reservoir with bottom water aquifer and Tarmat layer

In such case, placement of horizontal sections is a real challenge as the MWD tool will fail in identifying the stand-off the tarmat layer. The MWD tool alone can't provide mobility values to

properly geo-steer the horizontal well, therefore, the formation testing tool should be added to the MWD tool to provide mobility profiles and enhance the placement effectiveness.

The power of mobility profiling in geo-steering is explained through the mobility definition. The mobility is defined as the ratio of the permeability to the flow of the liquid to the dynamic viscosity of that liquid. On other words, it is the measure of the liquid ability to flow in the porous media which generally giving in the following expression:

$$M = \left(\frac{k}{\mu}\right)\left(md/cp\right)$$

Knowing the mobility profile distribution per unit length across the horizontal section of a well is fairly important for the engineers to, especially with the existence of tarmat or high viscosity variation, accurately generate field development/production plans. The mobility profile can be obtained using the formation testing tools which will help in

- Identification of in situ reservoir fluids
- Evaluation of near wellbore reservoir properties with a single probe
- Determination of well productivity
- Collection of representative reservoir fluid samples
- Identification and characterization of faults and boundaries (i.e. Tarmat)

Utilizing mobility measurement in geo-steering is very expensive, risky and time consuming process; this thesis work will investigate the possibility of employing artificial intelligence to predict the mobility profile using the minimum number of sampling data points.

1.2.1 Literature Review in General

1.2.1.1 Artificial Intelligence

The science of artificial intelligence or what is synonymously known as soft computing shows better performance over the conventional solutions. Sage[1] defined the aim of artificial intelligence as the development of paradigms or algorithms that require machines to perform tasks that apparently require cognition when performed by humans.

This definition is widely broadened to include preceptrons, language, and problems solving as well as conscious, unconscious processes[2]. Many techniques are classified under the name of artificial intelligence such as genetic algorithms, expert systems, and fuzzy logic because of their ability, one at least, to make certain reasoning, representation, problem solving, and generalization. Artificial neural network is also considered one of the important components of artificial intelligence system.

1.2.1.2 Artificial Neural Networks (ANN)

Generally, ANN is a machine that is designed to model the way in which the brain performs a particular task or function of interest. The system of ANN has received different definitions[3]. A widely accepted term is that adopted by Alexander and Morton[4]: “A neural

network is a massively parallel distributed processor that has a natural propensity for storing experiential knowledge and making it available for use".

ANN resembles the brain in two aspects; knowledge is acquired by the network through a learning process, and the interneuron connection strengths known as synaptic weights are used to store the knowledge[5]. In other way, neural networks are simply a way of mapping a set of input variables to a set of output variables through a typical learning process. So, it has certain features in common with biological nervous system. The relationship between the two systems and the brain system mechanism is further explained in the next subsection. Figure 3 shows a typical topology of neural network.

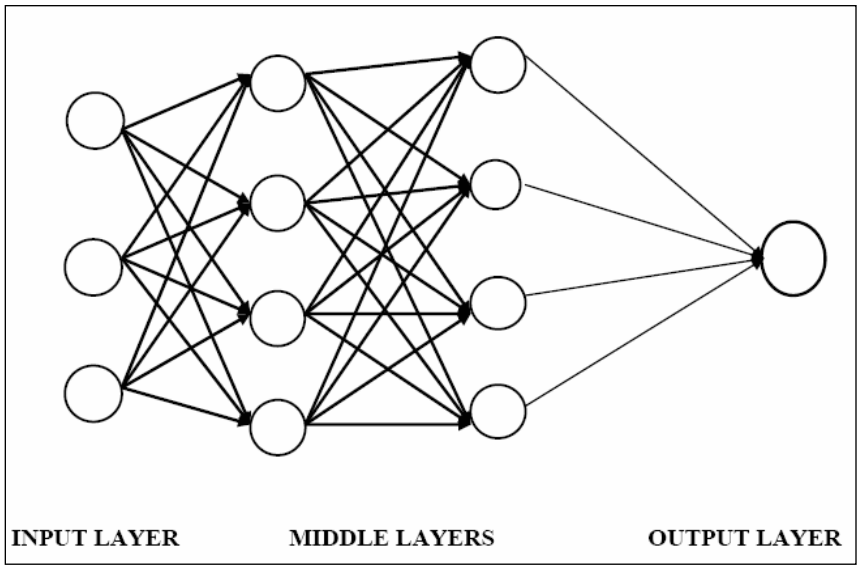

Figure 3: Fully Connected Network with Two Hidden Layers and Output Layer

1.2.1.3 Functional network (FunNet)

Functional networks (FunNet) were recently introduced as a generalization of the standard neural networks, which deal with general functional models instead of sigmoidal-like

ones. The neuron functions are learned instead of weights as in the standard neural networks. Further, the FunNet doesn't require inputs and outputs to be normalized similar to the neural networks providing different computational method. This makes the FunNet one of the powerful data modeling tools as it demonstrated strong ability to capture and represent complex input and output relationships[6].

FunNet is not black boxes and the network is able to reproduce some physical or engineering properties to the corresponding network. Thus, the initial functional network can arise directly from the problem under consideration. However, the constraints imposed by functional equations allow derive a simplified functional network structure, which normally transforms the complex initial neural functions in another much simpler functions[7]. Figure 4 shows a typical topology of functional networks.

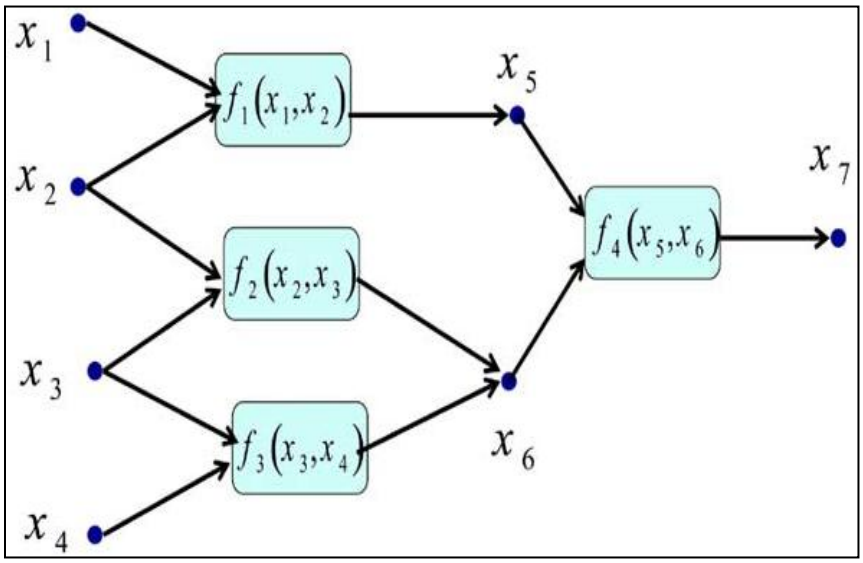

Figure 4: Typical FunNet structure

1.2.1.4 Support vector machine (SVM)

A Support Vector Machine (SVM) performs classification by constructing an N-dimensional hyperplane that optimally separates the data into two categories using a sigmoid kernel function is equivalent to a two-layer, perceptron neural network[8].

SVM is a classifier derived from statistical learning theory by Vapnik and Chervonenkis which was first introduced in the conference of computational learning theory (COLT 1992), July 27-29, 1992, Pittsburgh, PA, USA. The SVM became famous when, using pixel maps as input; it gave higher accuracy when compared to NNs with hand-designed features in a pattern recognition task such as[9]

- Handwriting recognition
- Face Detection recognition
- Text region detection

Support Vector Machines (SVMs) are a set of related supervised learning methods used for classification and regression which make SVMs part of Generalized Linear Classifiers family[10]. They can also be considered as a special case of Tikhonov Regularization. SVMs map input vectors to a higher dimensional space where a maximal separating hyperplane is constructed[11]. This is described in Figure 5 below

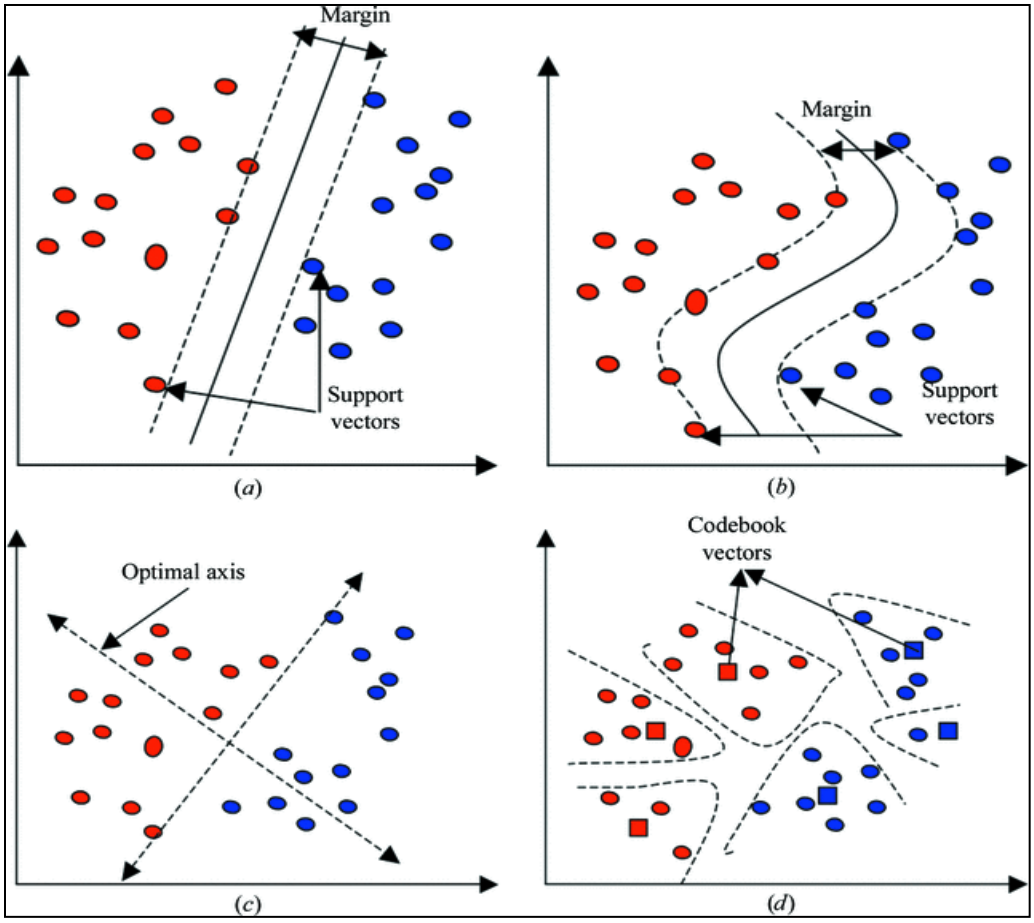

Figure 5: SVM mapping techniques

The SVM is a tool that maps the input vectors into a very high-dimensional feature space. The task of finding the maximum-margin separator becomes computationally intractable. Luckily all the mathematics is linear, but the vectors have a huge number of components which can be addressed through taking the scalar product of two vectors which is very expensive way[12]. To go over this issue and keep things tractable, the use "the kernel trick" is suggested, the trick that MatLab community uses for Linearization is to use a function that redefines distances between points. As shown below in the example[13]

$$K(x,z) = e^{-\|x-z\|^2/2\sigma}$$

SVM performance is strongly related to the Kernel methods selection, the use of the large margin classifiers and the re production of kernel Hilbert space.

1.2.2 Literature Review in General

1.2.2.1 The Use of Artificial Neural Networks in Petroleum Industry

The acceptance of Artificial Intelligence (AI) techniques in the E&P industry has been slow compared to other mainstream industries and can be tracked back just almost ten years. Throughout that time the employment of AI techniques significantly increased in data mining, learning and knowledge management which lead to the development of complex decision support tools. These tools enabled short and long term optimizations with uncertainty assessments and risk mitigation.

Artificial Neural Networks have been used to solve many problems in petroleum industry that is extended but not limited to reservoir characterization and simulation, optimum stimulation treatment design, virtual measurements, and production optimization. The following are the most active areas on the petroleum industry that tried to employ Artificial Neural Networks

<u>Geology and Geophysics</u>

- Reserve estimation[14]
- Mineral identification from well logs[15]
- Location of subsurface targets in geophysical data[16]
- Identification of lithofacies pattern features[17]
- Seismic phase identification[18]

- Seismic pattern recognition[19]
- Seismic data compression[20]
- Sedimentology - sequence stratigraphy[21]

Reservoir simulation characterization

- History matching[22]
- Formation and relative permeability and porosity prediction[23]
- Electric & magnetic resonance logs[24]
- Reservoir Stochastic modeling[25]
- Reconstruction of Irreducible water saturation distribution for water flooding projects[26]
- Lithofacies identification[27]
- Productivity estimation[28]
- Reservoir zonal identification[29]
- Predicting minimum miscibility pressure in hydrocarbon gas injection[30]
- EOR project risk analysis[31]

Drilling & Completion

- MWD data analysis[32]
- Drill bit diagnosis[33]
- Selection and monitoring of drilling bits and drilling mud[34]

Stimulation Treatments Design:

- Hydraulic fracturing analysis[35]
- Post-fracture deliverability prediction[35]
- Optimal candidate selection[35]
- Water shut off candidate selection[36]

Virtual Measurement in the Oil Field:

- Prediction of PVT properties[37]
- Prediction of bottomhole pressure[38]
- Prediction of hold-up[38]
- Prediction of flow regime[38]
- Well testing analysis[39]
- Temperature profile prediction[39]
- Flow regimes in horizontal wells prediction[38]
- Multiphase flow metering prediction[27]
- Prediction of critical gas flow rate[27]

Field Operations Optimization:

- Resource allocation, pressure and production prediction[39]
- Surface hydraulic simulation for production optimization[35]
- Well placement and location water flooding optimization[24]
- Tracking the state and diagnosing down hole permanent sensors in intelligent well completions[39]
- Pump operation diagnosis[40]
- Well test model selection & interpretation[38]
- Gas-lift optimization[40]
- EOR project risk analysis[23]
- Fluid flow in pipes[27]

Neural networks development has faced a renaissance in the last decade, with a large number of application areas which can be clearly seen from increasing number of publications and studies in the recent literature. The application of ANN in the industry is growing rapidly in all directions especially in geology and geophysics, formation evaluation and reservoir engineering. Yet going hybrid in employing different AI tools together (fuzzy logic, expert systems, genetic algorithms, etc.) will be the way foreword to increase problems handling efficiency.

1.3 Statement of the Problem and Objectives

1.3.1 Statement of the Problem

Some of oil fields are characterized with presence of tarmat layer underlying the oil zone preventing adequate aquifer support reaching the oil producing wells. To address the need for pressure support, water injection wells are usually planed to be drilled and placed accurately above the tarmat zone in order to achieve the desired reservoir pressure throughout the field life with minimum loss of reserves and minimum oil to be left behind the flood front. In such case, geo-steering the horizontal wells using the proper tool is the key of successful peripheral water flooding scheme. This is achieved by combining the formation tester tool measuring mobility along with the basic logging while drilling (LWD) package measuring the Permeability transforms, Porosity, Water saturation and Gamma ray.

Geo-steering with the formation tester tool Figure 6 is an extremely expensive process. The drilling rig consumes great times (30 minutes per sample) during which the tool collect's fluid sample. In reality, to generate a reasonable mobility profile for effective geo-steering an average of 60 to 80 sampling points need to be collected.

The samples measures for viscosity in centipoises (cp) coupled with accurate pressure measurements in (psi) to calculate the permeability measured in millidarcy (md) which is then transformed in to mobility (cp/md). Figure 7 is showing a typical mobility profile log[41].

Figure 6: Formation tester tool

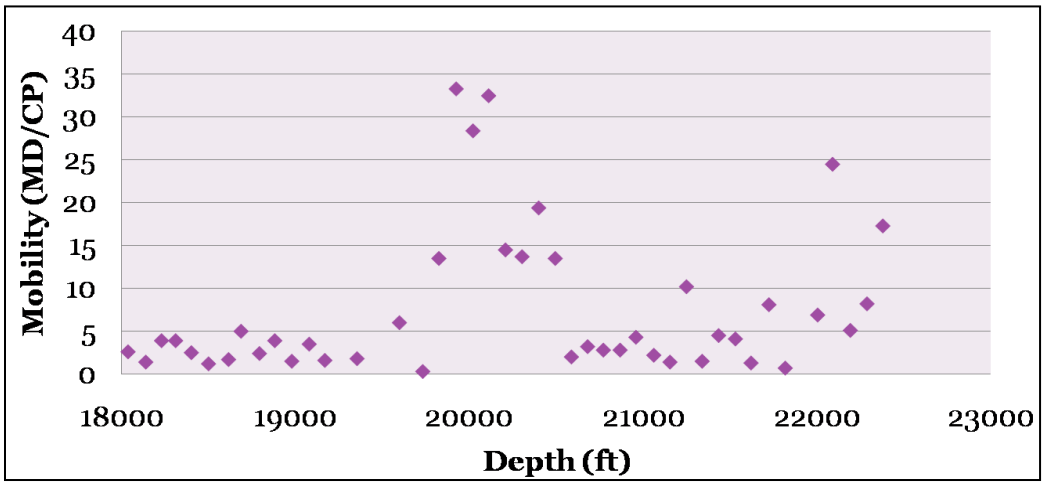

Figure 7: Typical mobility profile log

1.3.2 Objective

In complex reservoirs with irregular thickness tarmat layer, the typical horizontal geo-steering package (MWD) alone fails to provide accurate horizontal section placement. To overcome this challenge, formation tester tool was deployed to accurately map the mobility profile along the horizontal section. Introducing the formation tester tool increased the placement efficiency and increases the drilling process complexity and cost as will. This thesis work will examine the possibility of utilizing artificial intelligence to predict the mobility profile using the limited number of sampling data points and generating the rest using AI tools. This will have significant improvement to the drilling time and huge reduction of the well cost.

The AI model will develop a relation between the input parameters and mobility to optimize the sampling requirements and provide better guidance to investment.

1.3.3 Motivation

The biggest stimulus of this work is to develop a prediction model that can reduce the investment of acquiring mobility data measurements utilizing Artificial Intelligent (AI) tools to minimize the operation expenses and increase drilling process efficiency.

This can be understood from the fact that mobility profile is generated (using Formation Testing Tools) which involves significant costs for mobilizing the equipments to the rig site and then acquiring the data for almost 100 sampling points. The mobility profile thus generated can help in efficient geo-steering for better placement of the horizontal section.

The objective of this study is to predict the mobility profile using AI tools while employing only minimum number of sampling data points. To achieve this objective three different AI tools will be used

- Artificial neural network (ANN)
- Functional network (FunNet)
- Support vector machine (SVM)

1.4 Methodology or Solution Procedure

To investigate this novel idea that will lead to cost optimization and simplifying operation, the following is the planned course of action

- Collection of mobility data from two different fields (5 wells each)
- Data preparation and pre- processing for building the data base
- Building the Matlab codes for the following AI tools
    - Artificial neural network (ANN) using several backpropagation functions
    - Functional network (FunNet) involving different selection methods
    - Support vector machine (SVM) using various kernels
- Analyzing the output data to explore the potential application

CHAPTER 2

MOBILITY PROFILING

2.1 Mobility Measurement Background

In the oil and gas industry, the mobility of a specific fluid is defined as the ratio of the relative permeability to the viscosity of that fluid. It's derived from the Darcy's law which states that the velocity of a homogeneous fluid in a porous medium is proportional to the pressure gradient, and inversely proportional to the fluid viscosity, or:

$$V = \frac{k}{\mu}\frac{dp}{ds} \ldots (1)$$

"v" is the apparent velocity in centimeters per second and it is equal to (q/A), where "q" is the volumetric flow rate in cubic centimeters per second and "A" is the apparent or total cross-sectional area of the rock in square centimeters. The fluid viscosity, μ, is expressed in centipoises units, and the pressure gradient, dp/ds, is in atmospheres per centimeter, taken in the same direction as v and q. The proportionality constant, k, is the permeability of the rock expressed in darcy units.

Based on the definition of mobility,

$M=k/\mu \ldots$. (2)

Substitute (2) into equation (1), then equation (1) can be rewritten as below:

$$\mathbf{v} = -\mathbf{M}\frac{\mathbf{dp}}{\mathbf{ds}} \quad \ldots(3)$$

The velocity and the pressure gradient are related by the mobility.

Where two fluids are flowing simultaneously, it is the ratio of the mobility of both fluids which determines their individual flow rates. The mobility ratio is an important factor affecting the displacement efficiency of displaced fluid by displacing fluid. In oil and gas industry, the displaced fluid always refers to oil and the displacing fluid might refer to water in a waterflooding project or gas in a chemical flooding project.

The mathematical model of two-phase immiscible displacement reveals that the approximate fractional flow of the wetting phase is given by

$$\mathbf{F_w} = \frac{\mathbf{1}}{\left(\mathbf{1} + \frac{\mathbf{1}}{\mathbf{M}}\right)} \quad \ldots..(4)$$

Where, the mobility ratio is defined as a ratio of the mobility of wetting phase to that of the non-wetting phase, i.e.,

$$\mathbf{M} = \frac{\frac{\mathbf{K_{wr}}}{\mu_w}}{\frac{\mathbf{K_{nwr}}}{\mu_{nw}}} = \frac{\mathbf{K_{wr}} \times \mu_{nw}}{\mathbf{K_{wr}} \times \mu_w} = \frac{\mathbf{M_w}}{\mathbf{M_{nw}}} \quad \ldots(5)$$

Where, the subscription,

M_w is the wetting phase Mobility

M_{nw} is the non-wetting phase Mobility

In order to maximize the displacement efficiency of the non-wetting phase, we need to minimize the fractional flow of the wetting phase (F_w) at each point in the porous medium. Much can be

deduced about the immiscible displacement from the fractional flow equation, (5). Examination of this equation leads to the following qualitative deductions about immiscible displacements in porous media:

> The displacement efficiency can be increased by reducing the mobility ratio or by reducing the mobility of the wetting phase assuming the mobility of the non-wetting phase in the system remains unchanged to some extent. This can be accomplished in practice by increasing the viscosity of the wetting phase (the injected fluid) by use of a polymer. This is the basis for polymer flooding as an improved oil recovery technique.

The fractional flow equation indicates that the displacement efficiency can be improved by injecting the wetting phase at a high enough rate to minimize capillary smearing of the displacement front. This is generally true for a favorable mobility ratio displacement. If the mobility ratio is unfavorable, an increase in rate can result in viscous instability which reduces the displacement efficiency. The fractional flow equation suggests that the effect of gravity will be eliminated if the porous medium is horizontal. This is misleading because, in practice, if there is a density contrast between the fluids, the injection rate is sufficiently low and the core has a vertical dimension (which it does), gravity segregation will occur even in a horizontal medium. In this case, the one dimensional displacement model is inadequate to describe the displacement. A multidimensional model is needed to correctly describe the gravity-dominated displacement. The only fail proof way to eliminate the effect of gravity is to eliminate the density contrast between the fluids or perform the displacement in outer space[42].

Many global EOR and IOR projects have been successfully done based on the principle that the displacement efficiency can be increased by reducing the mobility ratio or by reducing the mobility of the wetting phase. Moreover, mobility ratio has also been successfully employed in the interpretation of well logging such as nuclear magnetic resonance logging, specifically in the estimate of viscosity of heavy oils.

Heavy oil reservoirs may contain several grades of oil. A complex reservoir might be composed of stacked porous beds separated by impermeable layers. Each bed can contain oil with properties different from the oils in adjacent beds. Moreover, viscosity can vary vertically within a single bed. Given vertical and lateral variations in viscosity, description of fluid properties from samples collected in reservoirs is impractical because the process requires an impossibly large number of samples for representative coverage. In addition, obtaining representative heavy oil fluid samples is extremely difficult due to the viscosity of the fluid and relative permeability. Operationally, fluid sampling can be very difficult in the high-angle or extended reach wells that would have to be drilled to understand lateral variations. Borehole logging tools are the most accurate and cost-effective means of determining properties of fluids found in subsurface geological formations, and therefore offer a practical solution to this complex problem.

Nuclear magnetic resonance (NMR) is the most widely used log in the estimation of viscosity, as the bulk relaxation properties of a hydrocarbon depend on its viscosity. Several techniques, most of which are based on transforms that relate logarithmic-mean relaxation times to viscosity, have been developed to estimate viscosity from NMR logs. Although the introduction of 2-D NMR

methods has increased the robustness of these methods, they tend to work better in light oils where the overlap of oil and water relaxation spectra in the free-fluid window is minimal.

Heavy oils introduce a series of challenges into the applicability of NMR-Only viscosity estimation methods. As the oil gets more viscous, the oil and water spectra overlap in both bound and free-fluid regimes, minimizing the effectiveness of the methods developed for light oils. An additional complication arises from the portion of the oil spectrum that contains decay times too short to be detected by the logging tools. Although the porosity associated with it, called the missing-porosity, can be quantified with the use of other logs, there is no easy solution for the proper reconstruction of the actual relaxation spectrum.

These limitations have forced the researchers to consider the use of volumetric information in the estimation of heavy oil viscosity. Earlier work has focused on the use of the missing-porosity, and its various related attributes. The fraction of the missing-porosity in the oil signal dominates the response in very high viscosities, and this sensitivity makes such methods more suitable for applications where viscosity exceeds 1000 cp.

Recent work has aimed to bridge the gap that exists at intermediate viscosities, where the overlap of oil and water spectra in the bound-fluid window can be substantial, particularly in carbonates. Akkurt et al (2008) have introduced qualitative estimators to characterize viscosity trends in carbonate heavy oil reservoirs. At the same time, Burcam et al (2008) have introduced a log-based method that uses a new correlation to estimate dead-oil viscosity of heavy oil[43].

The new methodology introduced here for viscosity estimation is a natural continuation of the work done earlier as it expands on concepts of the two tar indicators discussed in Akkur et al (2008). The spectral boundaries used to compute the indicators offer a natural and intuitive breakdown of the hydrocarbon relaxation spectrum into three regions, leading to the definition of a three-component fluid model for heavy oil.

Conceptually, each component represents a range of molecule sizes, characterized by a specific range of relaxation times and a specific molecular weight. SARA (Saturates, Aromatics, Resins and Asphaltenes) analysis, which is used to classify heavy oils based on the solubility of four different molecular weight fractions, serves as a good analogue to relate to the compositional model introduced here.

Viscosity information is encoded in the characteristic molecular weight and relaxation time of a component (or constituent). Viscosity of a constituent is directly proportional to its molecular weight and inversely proportional to its relaxation time. The relative volume fractions of the constituents determine the overall macroscopic viscosity and the governing relationship is empirical. The associated workflow is straightforward: first the volume fractions of the constituents are estimated, and then using the empirical transform, viscosity is calculated.

2.2 Definition

Mobility can be defined as the quality or state of being mobile when looking to the English meaning of the word[44]. This definition is close to the accepted definition among the petroleum engineering society

- The mobility is defined as the ratio of the permeability to the flow of the liquid to the dynamic viscosity of that liquid

$$\mathbf{M} = \frac{\mathbf{k}}{\mu}\left(\frac{\mathbf{md}}{\mathbf{cp}}\right)$$

- In different mathematical words Mobility, $\mathbf{M} = \frac{\mathbf{k}}{\mu}\left(\frac{\mathbf{md}}{\mathbf{cp}}\right)$, is defined as permeability of a porous material to a given phase divided by the viscosity of that phase

In oil and gas industry, mobility is always transformed to mobility ratio. The mobility ratio is defined as mobility of the displacing phase divided by the mobility of the displaced phase.

- Oil Mobility Ratio= (ko/μo)
- Water Mobility Ratio= (kw/μw)

2.3 Mobility Measurement Tool

In combination with LWD tools the mobility is being measured real time using the formation testing tool which can provide accurate pressure measurements, permeability, permeability anisotropy, and downhole fluid analysis as described in Figure 8. This information is obtained to develop a drawdown and buildup tests where the pressure transient analysis are conducted at the same point used to create the flow disturbance in the reservoir[45].

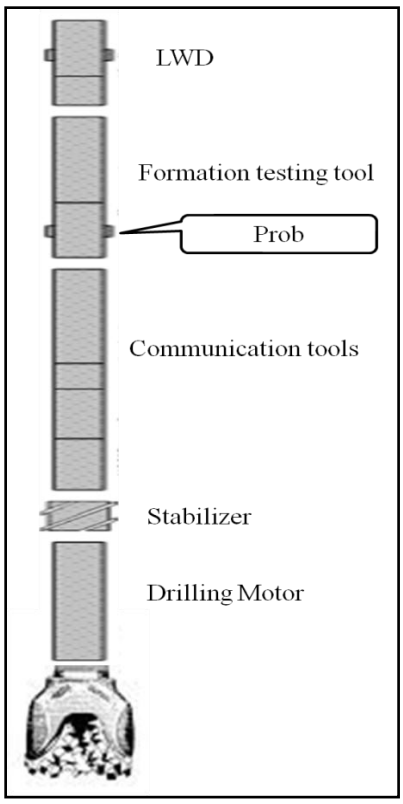

Figure 8: Bottom Hole assembly

In a single trip, the formation tester tool can collect a large number of representative formation fluid samples which required inserting a probe against the reservoir allowing a small amount of fluid to flow into a closed volume chamber within the tool body. Obtaining the fluid samples to create pressure drop requires accurate pressure and temperature recording which is achieved by accuracy and resolution gauge as seen in Figure 9. The precise flow control during testing ensures efficient and accurate permeability determination and representative sample collection.

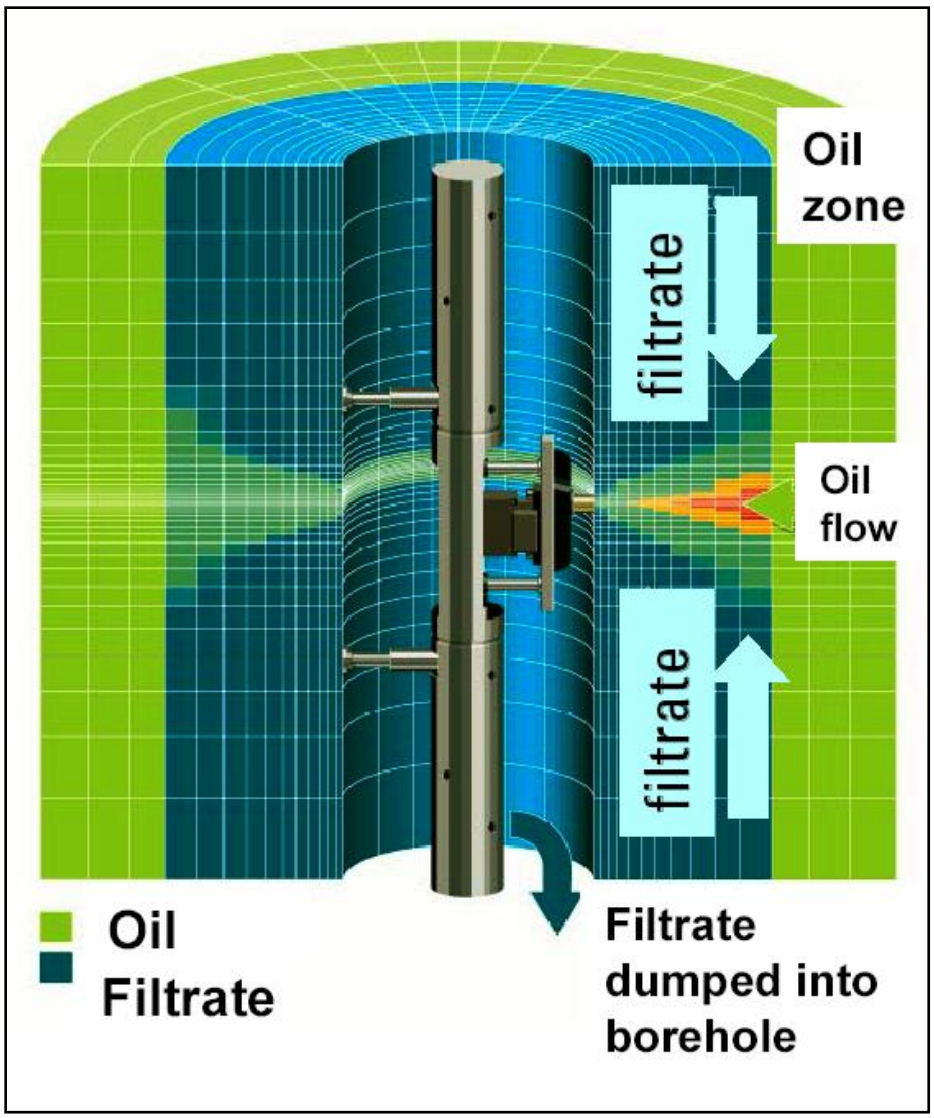

Figure 9: Clean up During Pumpout

Because pressure, volume, and temperature (PVT) analysis needs single phase samples, pumping and sampling pressure must be maintained above the pressure at which gases, liquids, or solids separate. With the Formation Testing tool, the sampling pressure and pretest flow rate and volume can be fully controlled from the surface in real time. When the transition is made from pumping out to sample capture, there is no disturbance to the pressure or flow rate, thus avoiding probe flowline plugging or losing the packer seal. In addition, full surface control of the downhole probe allows the selection of an optimal flow schedule during a pressure transient test.

To complete the package, sophisticated real time interpretation programs generate accurate pressure gradient, permeability, and fluid sampling answers. In addition, the software is able to provide real-time plotting of pressure, resistivity, and optical properties versus time to generate derivatives and to perform interpretation at the wellsite as can be understood from Figure 10. This capability is essential for real-time quality control and ongoing optimization of the job.

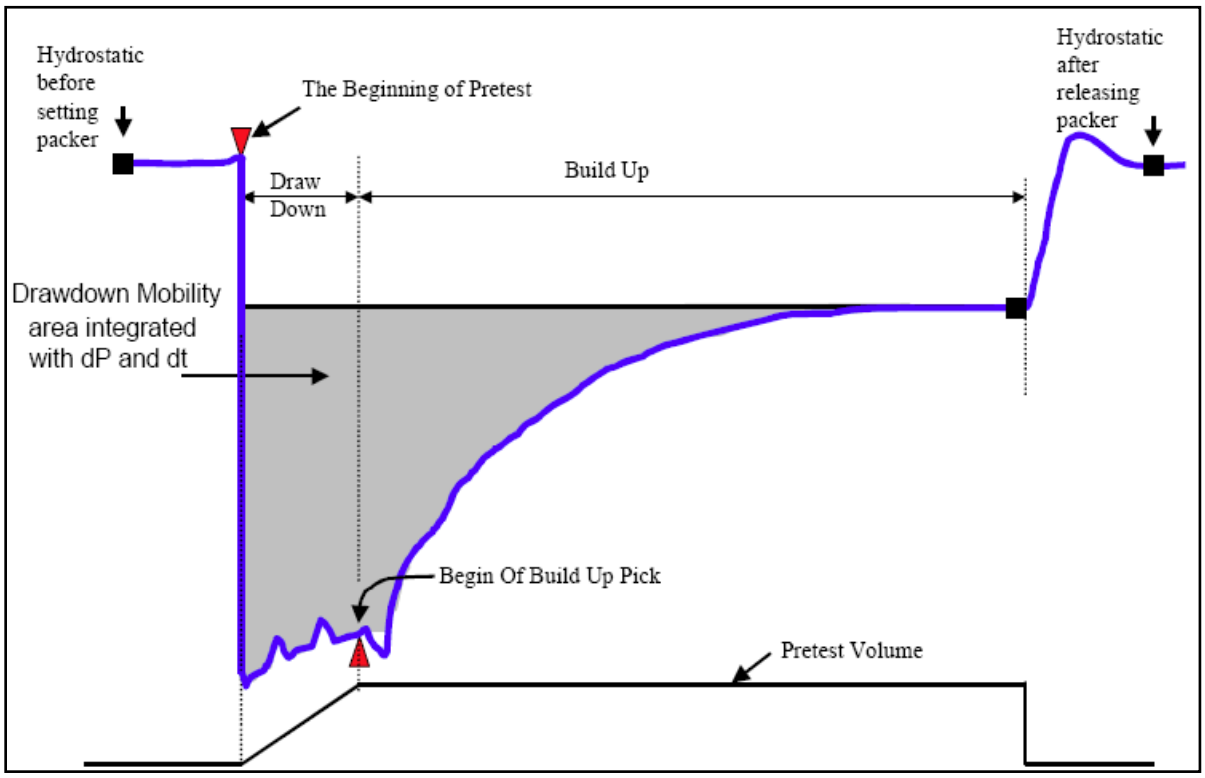

Figure 10: Drawdown Mobility Processing

2.4 Mobility from Drawdown Analysis

When the probe is set in the wellbore, a short pretest measures formation pressure. The pretest takes approximately 20 cm3 of fluid from the formation, through the probe, and into the pretest chamber. Each pretest acquires both drawdown and buildup pressure data. This generates

a localized flow in the formation with an essentially spherical pattern. The drawdown pressure depends on the mobility (permeability normalized for fluid viscosity) of the flowing fluid, which is usually mud filtrate from the invaded zone. At the end of the drawdown period, the pretest chamber is full, and the buildup period starts. The pressure disturbance continues to advance in a pattern similar to the drawdown period because of fluid flowing from the undisturbed part of the formation toward the low-pressure area near the probe.

The pressure measured at the probe rises until it reaches the formation pressure. The time required for this buildup is essentially a function of the formation fluid mobility and the producing time.

During the drawdown, most of the fluid movement takes place in a small volume immediately surrounding the probe. Using the solution to the spherical flow equation for a slightly compressible fluid in a homogeneous medium with correct boundary conditions, the drawdown mobility (M) can be expressed as follows:

$$M = \frac{K_d}{\mu} = \frac{C_{pf} \times V}{\Sigma(\Delta P \times \Delta t)} \ldots . (6)$$

Where:

Kd = drawdown permeability

μ = viscosity

Cpf = proportionality factor [(md/cp) psi/ (cm3/s)]

The drawdown proportionality factor depends on the packer-probe configuration and should specified by the manufacturer

V = pretest volume (cm3)

Dp = pressure drop during flow and following buildup period (psi)

The term $\sum(\Delta P \times \Delta t)$ is computed from the beginning of the pretest to the beginning of the retract cycle for all positive pressure changes (i.e., for all pressures less than the final buildup pressure) like shown in Figure 11.

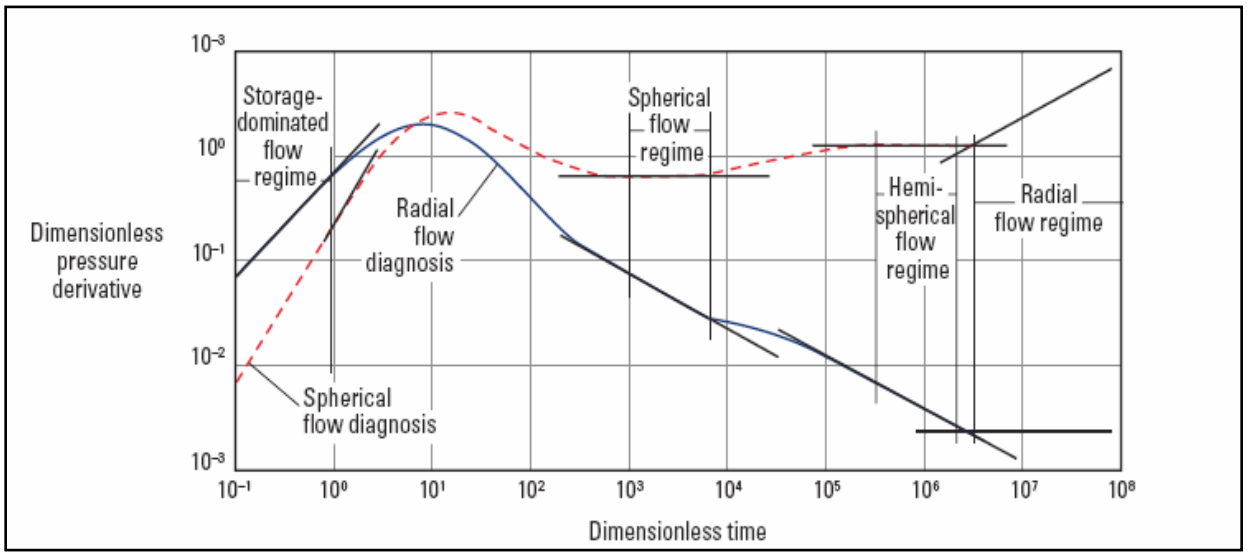

Figure 11: Theoretical log-log plot of the pressure derivative for a sink probe buildup

2.4 Mobility Analysis Limitations

The mobility analysis using this method has some limitations[46].

- High-permeability formations:

  In very high-permeability formations, the pressure gauge resolution is too small to accurately measure the drawdown pressures.

- Low-permeability formations:

  At very low permeability, the long time that it may take to reach the final pressure affects mobility results.

- Depth of investigation and borehole damage:

Virtually all the pressure disturbance during a pretest drawdown occurs near the probe (approximately 50% of the pressure drop occurs within 0.393 in. [1.0 cm]. Therefore, the permeability the tool sees during a drawdown may differ significantly from the actual formation permeability. The effects of drilling and invasion may damage the formation or change its permeability.

- These changes in reservoir characteristics (skin factor):

  Generally, soft formations have a negative skin factor and a reduced permeability value. Hard formations have a positive skin factor and an enhanced permeability value.

- Formation and invading fluid type:

  The relative (effective or measured) mobility changes with increased water saturation. If the invading fluid is water based mud, it can significantly reduce the relative permeability.

CHAPTER 3

DATA PREPARATION AND MODEL DEVELOPMENT

In this chapter, first, data preparation and handling is discussed in terms of data collection, pre-processing and post-processing. Then, a detailed discussion of the developed artificial intelligence models, including model features, selected topology, and model optimization are presented.

3.1 Data Preparation

3.1.1 Data Handling

Data handling is the most important step before feeding to the networks since it determines the success of any model. Artificial intelligence models training can be made efficient if a certain pre-processing steps are performed on the networks inputs and targets. Another post-processing step is needed to transform the output of the trained network to its original format. This step involves transforming the data into a suitable form to the network inputs like arranging input data to fall within the same number of digest as possible which can be achieved by many mathematical ways[47]. The most popular normalization scheme is applying the natural logs to reduce the number of digest in certain input value. Also, normalizing the mean and standard deviation of the training set is considered one of the powerful network inputs and targets scaling techniques[48].

3.1.2 Data Collection

The data utilized in this thesis work was extracted together from MWD logs and Formation testing data gathered from ten wells making two sets of data representing two different fields from Middle East.

Real emphasis was drawn on selecting the most relevant parameters involved in estimation of mobility based on the correlation coefficient analysis of the selected Predictor Variables relation to the output which is the mobility.

Predictor Variables		Full Meaning
1	PERM	Transformed Permeability
2	PHIE	Porosity Log
3	SWE	Water Saturation Log
4	GR	Gamma Ray Log

Table 1: Predictor Variables

The database composes of two sets of well logs, every five wells are coming from one field and every well has a total of 12,000 data points distributed evenly among the four input parameters listed in Table 1. Furthermore, the wells from 1 to 5 are representing field-A where the wells from 6 to 10 are representing field-B with an objective of diversity to assure network functionality and to test the network ability to predict different ranges of data. In order to understand the data diversity, tables from 2 to 11 have been generated to display a descriptive statistical analysis for the ten wells used in database development.

This database was used when designing the MATLAB codes and MATLAB toolboxes: ANN, SVM and FunNet to implement these methods and validate accuracy.

Well # 1	PERM	PHIE	SWE	GR
Std	252.805	0.031	0.030	3.248
Min	15.623	0.130	0.044	11.010
Max	988.703	0.263	0.152	21.236
Mean	204.145	0.204	0.078	15.058
Median	83.100	0.205	0.069	14.166
Mode	53.000	0.200	0.044	12.400
Var	63910.162	0.001	0.001	10.550

Table 2: Descriptive statistics of Well 1

Well # 2	PERM	PHIE	SWE	GR
Std	209.570	0.052	0.051	4.310
Min	1.524	0.103	0.101	19.177
Max	642.180	0.255	0.297	35.951
Mean	318.505	0.210	0.169	26.675
Median	412.801	0.237	0.166	26.171
Mode	2.990	0.247	0.103	22.510
Var	43919.706	0.003	0.003	18.577

Table 3: Descriptive statistics of Well 2

Well # 3	PERM	PHIE	SWE	GR
Std	51.241	0.008	0.023	2.364
Min	86.988	0.177	0.155	10.136
Max	300.443	0.209	0.232	17.450
Mean	176.969	0.195	0.195	14.406
Median	166.905	0.195	0.196	14.171
Mode	146.700	0.189	0.217	17.440
Var	2625.675	0.000	0.001	5.588

Table 4: Descriptive statistics of Well 3

Well # 4	PERM	PHIE	SWE	GR
Std	145.020	0.016	0.038	2.457
Min	78.534	0.164	0.111	10.860
Max	568.910	0.216	0.229	19.405
Mean	220.922	0.191	0.168	13.602
Median	159.487	0.194	0.160	12.756
Mode	162.360	0.169	0.228	12.880
Var	21030.658	0.000	0.001	6.038

Table 5: Descriptive statistics of Well 4

Well # 5	PERM	PHIE	SWE	GR
Std	52.392	0.005	0.014	1.566
Min	186.184	0.248	0.223	17.064
Max	412.031	0.269	0.274	22.199
Mean	263.999	0.257	0.251	19.166
Median	251.963	0.256	0.251	19.048
Mode	215.030	0.254	0.267	17.060
Var	2744.953	0.000	0.000	2.452

Table 6: Descriptive statistics of Well 5

Well # 6	PERM	PHIE	SWE	GR
Std	542.588	0.032	0.027	1.853
Min	20.627	0.149	0.045	12.079
Max	1909.082	0.257	0.140	18.723
Mean	591.634	0.213	0.082	15.812
Median	383.237	0.215	0.073	16.476
Mode	70.230	0.246	0.045	16.940
Var	294401.651	0.001	0.001	3.434

Table 7: Descriptive statistics of Well 6

Well # 7	PERM	PHIE	SWE	GR
Std	37.691	0.014	0.029	4.059
Min	90.128	0.210	0.267	12.013
Max	278.646	0.279	0.413	28.259
Mean	212.048	0.260	0.352	21.355
Median	216.556	0.264	0.350	20.613
Mode	216.160	0.263	0.343	25.940
Var	1420.621	0.000	0.001	16.473

Table 8: Descriptive statistics of Well 7

Well # 8	PERM	PHIE	SWE	GR
Std	219.830	0.036	0.091	4.238
Min	12.295	0.174	0.094	8.037
Max	655.786	0.281	0.441	23.364
Mean	360.909	0.249	0.261	17.695
Median	422.891	0.268	0.270	19.630
Mode	12.290	0.280	1.910	19.630
Var	48325.299	0.001	0.008	17.962

Table 9: Descriptive statistics of Well 8

Well # 9	PERM	PHIE	SWE	GR
Std	119.727	0.022	0.036	3.581
Min	22.888	0.190	0.204	12.982
Max	435.058	0.273	0.351	25.534
Mean	270.409	0.251	0.262	19.079
Median	316.563	0.260	0.265	17.813
Mode	359.260	0.265	0.282	17.610
Var	14334.459	0.000	0.001	12.821

Table 10: Descriptive statistics of Well 9

Well # 10	PERM	PHIE	SWE	GR
Std	491.586	0.020	0.033	1.933
Min	28.496	0.169	0.088	6.487
Max	2026.038	0.264	0.259	14.214
Mean	917.397	0.237	0.116	9.452
Median	895.965	0.242	0.104	9.206
Mode	332.180	0.239	0.102	7.310
Var	241656.453	0.000	0.001	3.735

Table 11: Descriptive statistics of Well 10

Tables from 12 to 21 describe the Correlation coefficient of the input data which measures the strength and the direction of a linear relationship between the variables[49].

In definition, the correlation coefficient is a measure of how well trends in the predicted values follow trends in past actual values[50]. It is a measure of how well the predicted values from a forecast model "fit" with the real-life data.

The correlation coefficient is a number between 0 and 1. If there is no relationship between the predicted values and the actual values the correlation coefficient is zero or very low, i.e., the predicted values are no better than random numbers[51]. As the strength of the relationship between the predicted values and actual values increases so does the correlation coefficient[52].

	PERM	**PHIE**	**SWE**	**GR**
PERM	1.0000	0.7857	0.0988	0.2402
PHIE	0.7857	1.0000	0.2691	0.5835
SWE	0.0988	0.2691	1.0000	0.0427
GR	0.2402	0.5835	0.0427	1.0000

Table 12: Correlation coefficients for Well 1

	PERM	**PHIE**	**SWE**	**GR**
PERM	1.0000	0.8348	0.0556	0.6391
PHIE	0.8348	1.0000	0.1066	0.7437
SWE	0.0556	0.1066	1.0000	0.4395
GR	0.6391	0.7437	0.4395	1.0000

Table 13: Correlation coefficients for Well 2

	PERM	PHIE	SWE	GR
PERM	1.0000	0.7604	0.0230	0.1224
PHIE	0.7604	1.0000	0.1151	0.1377
SWE	0.0230	0.1151	1.0000	0.0616
GR	0.1224	0.1377	0.0616	1.0000

Table 14: Correlation coefficients for Well 3

	PERM	PHIE	SWE	GR
PERM	1.0000	0.7724	0.1140	0.1324
PHIE	0.7724	1.0000	0.4236	0.4098
SWE	0.1140	0.4236	1.0000	0.5341
GR	0.1324	0.4098	0.5341	1.0000

Table 15: Correlation coefficients for Well 4

	PERM	PHIE	SWE	GR
PERM	1.0000	0.9892	0.4928	0.6787
PHIE	0.9892	1.0000	0.4914	0.7020
SWE	0.4928	0.4914	1.0000	0.0602
GR	0.6787	0.7020	0.0602	1.0000

Table 16: Correlation coefficients for Well 5

	PERM	PHIE	SWE	GR
PERM	1.0000	0.8757	0.0878	0.6098
PHIE	0.8757	1.0000	0.0945	0.4588
SWE	0.0878	0.0945	1.0000	0.6407
GR	0.6098	0.4588	0.6407	1.0000

Table 17: Correlation coefficients for Well 6

	PERM	PHIE	SWE	GR
PERM	1.0000	0.9904	0.4645	0.6406
PHIE	0.9904	1.0000	0.4550	0.6654
SWE	0.4645	0.4550	1.0000	0.5235
GR	0.6406	0.6654	0.5235	1.0000

Table 18: Correlation coefficients for Well 7

	PERM	PHIE	SWE	GR
PERM	1.0000	0.8338	0.1828	0.3562
PHIE	0.8338	1.0000	0.1254	0.2550
SWE	0.1828	0.1254	1.0000	0.7809
GR	0.3562	0.2550	0.7809	1.0000

Table 19: Correlation coefficients for Well 8

	PERM	PHIE	SWE	GR
PERM	1.0000	0.9660	0.0843	0.2279
PHIE	0.9660	1.0000	0.1551	0.1146
SWE	0.0843	0.1551	1.0000	0.6153
GR	0.2279	0.1146	0.6153	1.0000

Table 20: Correlation coefficients for Well 9

	PERM	PHIE	SWE	GR
PERM	1.0000	0.8968	0.1107	0.2772
PHIE	0.8968	1.0000	0.3782	0.3994
SWE	0.1107	0.3782	1.0000	0.0213
GR	0.2772	0.3994	0.0213	1.0000

Table 21: Correlation coefficients for Well 10

The Correlation coefficient exercise reflected strong relationship between all the input parameters.

3.2 Model Development

3.2.1 ANN

Back propagation is based on the well known steepest descent method and thus proceeds to minimize an error function by searching along the direction of the negative gradient The back propagation training algorithm has proven to be a robust method for supervised training of multi-layered neural networks[52]. A major drawback however is that the last weight has to be stored and the storage requirements can become substantial with increasing network size. Further, the

backpropagation may encounter slow rate of convergence which increases the computational requirement and might lead to unsatisfactory performance[53]. The artificial intelligence community got around these drawbacks by introducing different training functions. During the model development several training functions were examined to find the best training function that delivers the most accurate prediction without running through the major drawbacks[54]. The ANN model was developed using eight different training functions as they are described below:

Trainlm: The default backpropagation training algorithm is Levenberg-Marquardt (trainlm)[55]. This is the fastest method in the toolbox, but it can use large amounts of memory[56]. The Levenberg-Marquardt algorithm was designed to approach second-order training speed without having to compute the Hessian matrix. This method divides the data into training data, validation data, and test data sets using the following split 60%, 20% and 20% respectively[57].

In general, on function approximation problems, the Levenberg-Marquardt algorithm will have the fastest convergence. This advantage is especially noticeable if very accurate training is required[58]. In many cases, trainlm is able to obtain lower mean square errors than any of the other algorithms tested. However, as the number of weights in the network increases, the advantage of trainlm decreases. In addition, trainlm performance is relatively poor on pattern recognition problems[59].

Traingd: It is batch steepest descent training function. In batch mode the weights and biases of the network are updated only after the entire training set has been applied to the network[60]. The gradients calculated at each training example are added together to

determine the change in the weights and biases which makes this method often too slow for practical problems.

Traingdx: Traingdx is a Variable Learning Rate function with standard steepest descent, the learning rate is held constant throughout training. The performance of the algorithm is very sensitive to the proper setting of the learning rate. If the learning rate is set too high, the algorithm can oscillate and become unstable. If the learning rate is too small, the algorithm takes too long to converge. The performance can be increased by including some adaptive learning rate attempts to keep the learning step size as large as possible while keeping learning stable[61].

Traincgf: Traincgf is a Fletcher-Reeves Update which is a Conjugate Gradient Algorithm based on numerical optimization techniques for neural network training. The conjugate gradient algorithms are usually much faster than variable learning rate backpropagation which makes it good for networks with a large number of weights[62].

Trainoss: Trainoss is defined as One Step Secant function built on Quasi-Newton Algorithm. This method is an attempt to bridge the gap between the Conjugate Gradient algorithms and the Secant algorithms it terms of storage and computation requirements[63].

Trainrp: Resilient backpropagation function is the fastest algorithm on pattern recognition problems which makes it excellent in handling very large network. However, it does not perform well on function approximation problems[64].

Traincgb: The Traincgb is a Powell-Beale Restarts with Conjugate Gradient Algorithm that searches direction which periodically reset the function to the negative of the gradient[65].

Trainbfg: BFGS quasi-Newton backpropagation. It is an alternative to the conjugate gradient methods for fast optimization. The trainbfg function is similar to that of trainlm but it does not require much of storage memory[66]. The weakness of this function is that the computation requirement does increase geometrically with the size of the network since the Newton's algorithm requires computing the equivalent of a matrix inverse for each iteration[67].

Neural network training can be made more efficient when performing certain preprocessing steps on inputs and targets. Network-input processing functions transform inputs into a better form for the network use which should be applied to the network output to transform targets into a better form for network training, and then reverse transformed outputs back to the original target data form[68]. During the model development two different pre-processing and Post-processing functions where used as described below:

Mapstd: It is a Preprocessing technique using the Mean and Standard Deviation. Neural network training can be made more efficient if you perform certain preprocessing steps on the network inputs and targets. It is often useful to scale the inputs and targets to normalize the mean and standard deviation of the training set so that they always fall within a specified range[69].

Processpca: Principal Component Analysis is a preprocessing technique that is used when the input vector and the components the vectors are not of the same size but highly correlated. Therefore, the Processpca performs the following orthogonalizes the components of the input vectors, orders the resulting orthogonal components and eliminates those components that contribute the least to the variation in the data set[70].

The ANN training models also considered investigation of different number on neurons and different multiplier layers. Therefore, the final model was constructed using ten different cases listed in Table 12, where they were built with different training functions, different number of neurons and different preprocessing and postprocessing techniques.

Case	Backpropagation Function Type
1	trainlm (One Layer, 20 Neurons)
2	trainlm (Two Layer, 15,20 Neurons)
3	traingd (Two Layer, 15,20 Neurons)
4	traingdx (Two Layer, 15,20 Neurons)
5	traincgf (Two Layer, 15,20 Neurons)
6	trainoss (Two Layer, 15,20 Neurons)
7	trainrp (Two Layer, 15,20 Neurons)
8	traincgb (Two Layer, 15,20 Neurons, mapstd)
9	trainbfg (Two Layer, 15,20 Neurons, mapstd, processpca)
10	trainlm (Two Layer, 15,20 Neurons, mapstd, processpca)

Table 22: Constructed ANN models

3.2.2 Functional Networks (FunNet)

Functional networks as a new modeling scheme has been used in solving both prediction and classification problems. It is a general framework useful for solving a wide range of problems[71].

Functional network is a generalization of the standard neural network but it differs from the neural network since it is a problem driven and it deals with general functional models instead of sigmoid-like networks. In functional networks there are no weights associated with the links connecting neurons, and it uses unknown neuron functions, that are learned from given families of linearly independent functions during the training process[72].

Therefore, Functional networks has a great feature as it allow the neurons to be of multi-argument and different from any learnable function, instead of fixed functions. Also, it allows easier neuron outputs convergence forcing the outputs to be concurrent. This leads to functional equations or systems of functional equations, which require some compatibility conditions on the neuron functions[73]. Functional networks have the possibility of dealing with functional constraints that are determined by the functional properties of the network model[74].

The best functional networks model is chosen based on the minimum description length and some other quality measurements, such as, the correlation coefficients and the root-meansquared errors[75]. The selection is achieved using one of the well known selection schemes, such as,

	Method	
1	FNESM	Functional Network Elimination Selection Method using liner and Non-Linear of the 1st order regression.
2	FNFSM	Functional Network Forward Selection Method using liner and Non-Linear of the 1st order regression.
3	FNBEM	Functional Network Backward Elimination Method using liner and Non-Linear of the 1st order regression.
4	FNFBM	Functional Network Forward Backward Selection Method using liner and Non-Linear of the 1st order regression.
5	FNBFM	Functional Network Backward Forward Selection Method using liner and Non-Linear of the 1st order regression.

Table 23: Constructed FunNet models

3.2.3 SVM

Support vector machines (SVMs) are a set of related supervised learning methods that analyze data and recognize patterns, used for classification and regression analysis. The SVMs are powerful, state-of-the-art algorithms with strong theoretical foundations based on the Vapnik-Chervonenkis theory[76].

SVM models have similar functional form to neural networks and radial basis functions, both popular data mining techniques. However, neither of these algorithms has the well-founded theoretical approach to regularization that forms the basis of SVM[77]. The quality of generalization and ease of training of SVM is far beyond the capacities of these more traditional methods[78].

SVM can model complex, real-world problems such as text and image classification, hand-writing recognition, and bioinformatics and biosequence analysis[79].

SVM performs well on data sets that have many attributes, even if there are very few cases on which to train the model. There is no upper limit on the number of attributes; the only constraints are those imposed by hardware. Traditional neural nets do not perform well under these circumstances[80].

The SVMs are kernel-based algorithm and the kernels are functions that transform the input data to a high-dimensional space where the problem is solved. Kernel functions can be linear or nonlinear[81]. In different words, kernel functions operate in the feature space without ever computing the coordinates of the data in that space, but rather by simply computing the inner products between the images of all pairs of data in the feature space. This operation is often computationally cheaper than the explicit computation of the coordinates[82]. Kernel functions have been introduced for sequence data, graphs, text, images, as well as vectors.

Since the kernel function selection of a support vector machine has great influence on its performance four different kernel functions where investigated on this thesis.

1. **Gaussian kernel:** In general, Gaussian is a characteristic symmetric "bell curve"[83]. The Gaussian kernel transforms each case in the training data to a point in an *n*-dimensional space, where *n* is the number of cases. The algorithm attempts to separate the points into subsets with homogeneous target values[84]. The Gaussian kernel uses nonlinear separators, but within the kernel space it constructs a linear equation[85].
2. **Polynomial kernel:** This kernel is a classifier which nonlinearly (explicitly) maps[86] an input vector to a vector in a high-dimensional feature space and linearly discriminates it there, it has a similar learning curve to a linear dichotomy that has an average generalization error proportional to the dimension of the input space and inversely proportional to the number of given examples in the asymptotic limit[87].
3. **Polyhomogeneous kernel:** The polyhomogeneous kernel is a nonlinear classification function[88]. It is an advancement of polynomial kernels where polyhomogeneous function are displaying better performance on data mapping approximation and strength on solving nonlinear elliptic systems[89].

4. **JCB kernel:** is a kernel function developed by Christopher J. C. B., as a combination of some of common kernel functions. It is a nonlinear mapping of a data to reach into symmetry[90].

CHAPTER 4

RESULTS AND DISCUSSION

4.1 Statistical Error Analysis

The error analysis is utilized to check the accuracy of the models. Several statistical parameters were used in the presented work and they are the Regression Value (R), Average Absolute Percent Relative Error (AAPE), Root Mean Square Error (RMSE) and the Correlation Coefficient (CC) and they will be discussed next.

4.1.1 Definition of Regression Value

The term "regression" was coined in the nineteenth century and the regression value indicates the match between the actual verses the predict values. This value ranges from 1 to 0, with 1 corresponding to a perfect match between the actual and predict values. Further, as the deviation increases, the regression value decreases, with a lower limit of 0 indicating poor relation.

4.1.1.1 Calculating the Regression Value

Linear regression or "least squares" method works by minimizing the sum of the square of the vertical distances of the points from the regression line[91]. Where, the regression line is a plot of the expected value of the dependent variable for all values of the independent variable.

The regression line is actually a running series of means of the predicted value (Y) for each actual value (X) and is calculated from the following equation[92]:

$$y = a + bx$$

Where

$$a = \frac{\Sigma y - b\Sigma x}{n}$$

$$b = \frac{n\Sigma(xy) - \Sigma x \Sigma y}{n\ \Sigma x^2 - (\Sigma[x])^2}$$

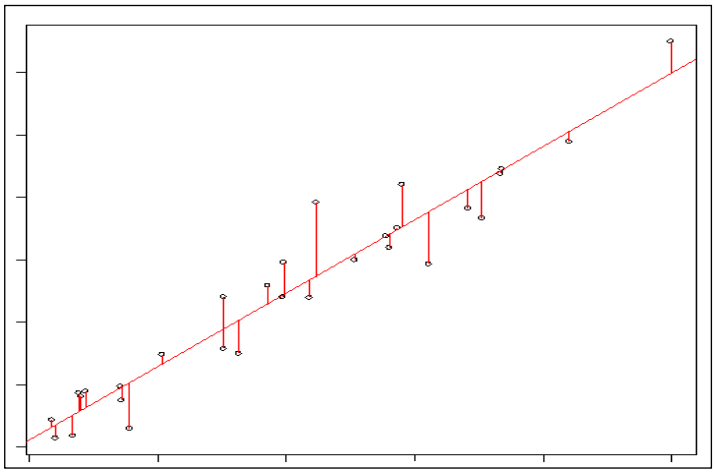

Figure 12: Regression line plot[93]

4.1.2 Average Absolute Percent Relative Error (AAPE):

It measures the relative absolute deviation from the experimental values, defined by:

$$E_a = \frac{1}{n}\sum_{i=1}^{n}|E_i|$$

4.1.3 Root Mean Square Error (RMSE):

Measures the data dispersion around zero deviation, defined by:

$$RMSE = \left[\frac{1}{n}\sum_{i=1}^{n} E_i^2\right]^{0.5}$$

4.1.4 The Correlation Coefficient (R):

It represents the degree of success in reducing the standard deviation by regression analysis, defined by:

$$R = \sqrt{1 - \frac{\sum_{i=1}^{n}[act - pred]}{\sum_{i=1}^{n} act - \overline{\Delta(act - pred)}}}$$

'R' values range between 0 and 1. The closer value to 1 represents perfect correlation whereas 0 indicates no correlation at all among the independent variables.

4.2 Graphical Error Analysis

Graphical tools aid in visualizing the performance and accuracy of a correlation or a model. For the presented work, one graphical analysis technique was utilized which was the crossplot.

4.2.1 Crossplots

In this graphical based technique, all predicted mobility values are plotted against the measured values and thus a crossplot is formed. A 45° straight line between the predicted mobility versus actual mobilitydata points is drawn on the crossplot, which denotes a perfect

correlation line. The tighter the cluster about the unity slope line, the better the agreement between the experimental and the predicted results.

4.3 Results for the Prediction of Mobility

The following sections of the thesis will describe the results of each model individually

4.3.1 ANN Model Prediction Results

The neural network prediction was oscillating between perfect to very poor depending on the training function when looking to the following

- Slope of the linear regression (M)
- The Y intercept of the linear regression (B)
- The regression value (R)

ANN Used Function for Well # 1	M	B	R
Trainlm with single layer	1	0.02	1
Trainlm with two layers	1	0	1
Traingd with two layers	0.12	215	0.07
Traingdx with two layers	0.8	9.63	0.92
Traincgf with two layers	0.99	1.67	0.98
Trainoss with two layers	0.86	7.08	0.94
Trainrp with two layers	0.98	0.46	1
Traincgb with two layers & mapstd	0.97	1.29	0.99
Trainbfg with two layers & mapstd, processpca	0.86	8.92	0.91
Trainlm with two layers & mapstd, processpca	1	0	1

Table 24: ANN Model Prediction Results for well 1

ANN Used Function for Well # 2	M	B	R
Trainlm with single layer	1	0	1
Trainlm with two layers	1	0	1
Traingd with two layers	2.07	68.05	0.78
Traingdx with two layers	0.81	7.8	0.8
Traincgf with two layers	0.99	0.56	1
Trainoss with two layers	0.96	1.37	0.99
Trainrp with two layers	1	0.04	1
Traincgb with two layers & mapstd	1	0.08	1
Trainbfg with two layers & mapstd, processpca	0.95	2.24	0.98
Trainlm with two layers & mapstd, processpca	1	0	1

Table 25: ANN Model Prediction Results for well 2

ANN Used Function for Well # 3	M	B	R
Trainlm with single layer	1	0	1
Trainlm with two layers	1	0	1
Traingd with two layers	0.34	14.76	0.34
Traingdx with two layers	0.83	2.05	0.92
Traincgf with two layers	0.98	0.25	0.98
Trainoss with two layers	0.96	0.35	0.98
Trainrp with two layers	0.99	0.08	1
Traincgb with two layers & mapstd	1	0	1
Trainbfg with two layers & mapstd, processpca	0.93	0.76	0.97
Trainlm with two layers & mapstd, processpca	1	0	1

Table 26: ANN Model Prediction Results for well 3

ANN Used Function for Well # 4	M	B	R
Trainlm with single layer	1	0	1
Trainlm with two layers	1	0	1
Traingd with two layers	1.05	29.29	0.5
Traingdx with two layers	0.82	2.52	0.91
Traincgf with two layers	1	0.07	1
Trainoss with two layers	0.8	2.41	0.9
Trainrp with two layers	1	0	1
Traincgb with two layers & mapstd	1	0	1
Trainbfg with two layers & mapstd, processpca	1	0	1
Trainlm with two layers & mapstd, processpca	1	0	1

Table 27: ANN Model Prediction Results for well 4

ANN Used Function for Well # 5	M	B	R
Trainlm with single layer	1	0.05	1
Trainlm with two layers	1	0	1
Traingd with two layers	0.23	94.21	0.12
Traingdx with two layers	0.47	13.09	0.72
Traincgf with two layers	0.9	2.63	0.95
Trainoss with two layers	0.86	4.11	0.94
Trainrp with two layers	0.95	1.32	0.98
Traincgb with two layers & mapstd	0.97	0.82	0.98
Trainbfg with two layers & mapstd, processpca	0.7	8.63	0.85
Trainlm with two layers & mapstd, processpca	1	0	1

Table 28: ANN Model Prediction Results for well 5

ANN Used Function for Well # 6	M	B	R
Trainlm with single layer	1	0.01	1
Trainlm with two layers	1	0	1
Traingd with two layers	0.24	119.3	0.13
Traingdx with two layers	0.94	2.76	0.97
Traincgf with two layers	0.99	0.5	0.99
Trainoss with two layers	0.98	0.8	0.99
Trainrp with two layers	0.99	0.23	1
Traincgb with two layers & mapstd	0.99	0.47	1
Trainbfg with two layers & mapstd, processpca	0.94	2.22	0.97
Trainlm with two layers & mapstd, processpca	1	0	1

Table 29: ANN Model Prediction Results for well 6

ANN Used Function for Well # 7	M	B	R
Trainlm with single layer	1	0	1
Trainlm with two layers	1	0	1
Traingd with two layers	0.05	34.2	0.04
Traingdx with two layers	0.73	2.74	0.88
Traincgf with two layers	0.97	0.27	0.98
Trainoss with two layers	0.96	0.28	0.99
Trainrp with two layers	0.99	0.08	1
Traincgb with two layers & mapstd	0.99	0.04	1
Trainbfg with two layers & mapstd, processpca	0.89	1	0.96
Trainlm with two layers & mapstd, processpca	1	0	1

Table 30: ANN Model Prediction Results for well 7

ANN Used Function for Well # 8	M	B	R
Trainlm with single layer	1	0.02	1
Trainlm with two layers	1	0.02	1
Traingd with two layers	0.92	168.02	0.53
Traingdx with two layers	0.46	17.43	0.63
Traincgf with two layers	0.97	0.48	0.99
Trainoss with two layers	0.96	1.09	0.98
Trainrp with two layers	0.99	0.18	1
Traincgb with two layers & mapstd	0.98	0.32	0.99
Trainbfg with two layers & mapstd, processpca	0.9	3.08	0.95
Trainlm with two layers & mapstd, processpca	1	0	1

Table 31: ANN Model Prediction Results for well 8

ANN Used Function for Well # 9	M	B	R
Trainlm with single layer	1	0.02	1
Trainlm with two layers	1	0	1
Traingd with two layers	0.29	475.18	0.1
Traingdx with two layers	0.68	18.34	0.81
Traincgf with two layers	0.99	0.21	1
Trainoss with two layers	1	0.18	1
Trainrp with two layers	1	0.2	1
Traincgb with two layers & mapstd	0.96	1.99	0.98
Trainbfg with two layers & mapstd, processpca	0.81	8.36	0.92
Trainlm with two layers & mapstd, processpca	1	0	1

Table 32: ANN Model Prediction Results for well 9

ANN Used Function for Well # 10	M	B	R
Trainlm with single layer	1	0.01	1
Trainlm with two layers	1	0	1
Traingd with two layers	1.3	165.44	0.39
Traingdx with two layers	0.71	33.57	0.81
Traincgf with two layers	0.99	1.32	1
Trainoss with two layers	1	0.3	1
Trainrp with two layers	1	0.15	1
Traincgb with two layers & mapstd	1	0.16	1
Trainbfg with two layers & mapstd, processpca	0.97	1.79	0.99
Trainlm with two layers & mapstd, processpca	1	0	1

Table 33: ANN Model Prediction Results for well 10

The other evaluation method adopted during this thesis is the graphical plots of the actual and predicted outputs in addition to their corresponding error crossplots. An example is presented below that reflects the perfect network model in terms of performance.

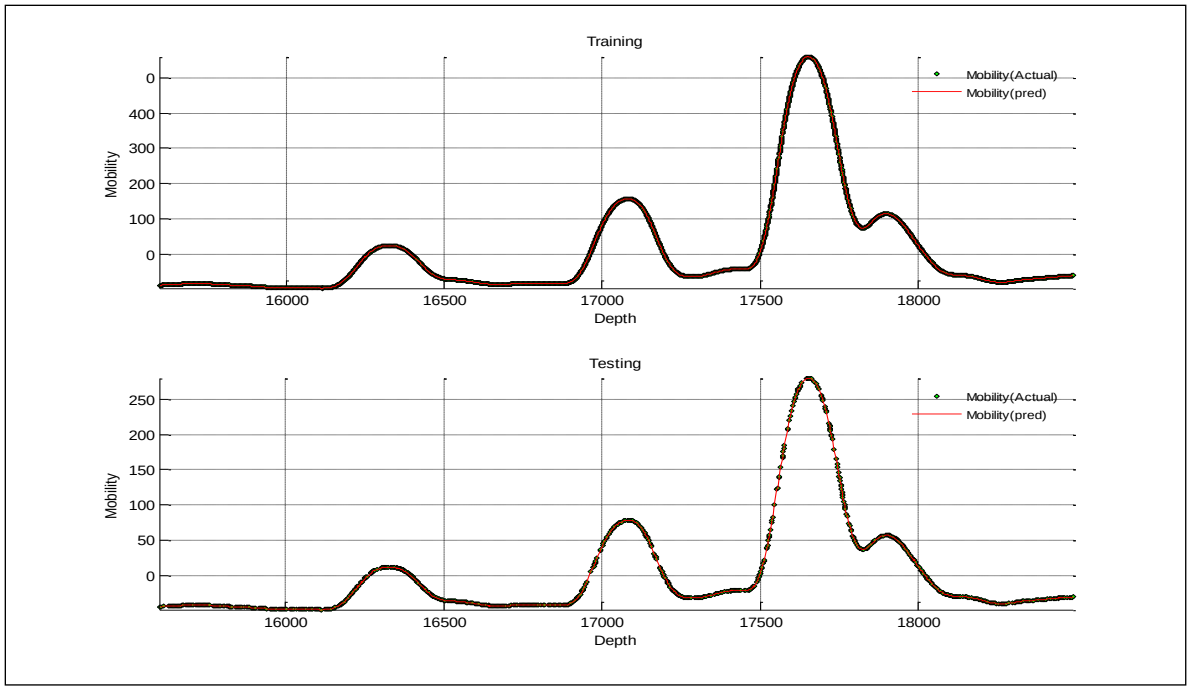

Figure 13: Example of Trainlm with two layers & mapstd, processpca for Well#1

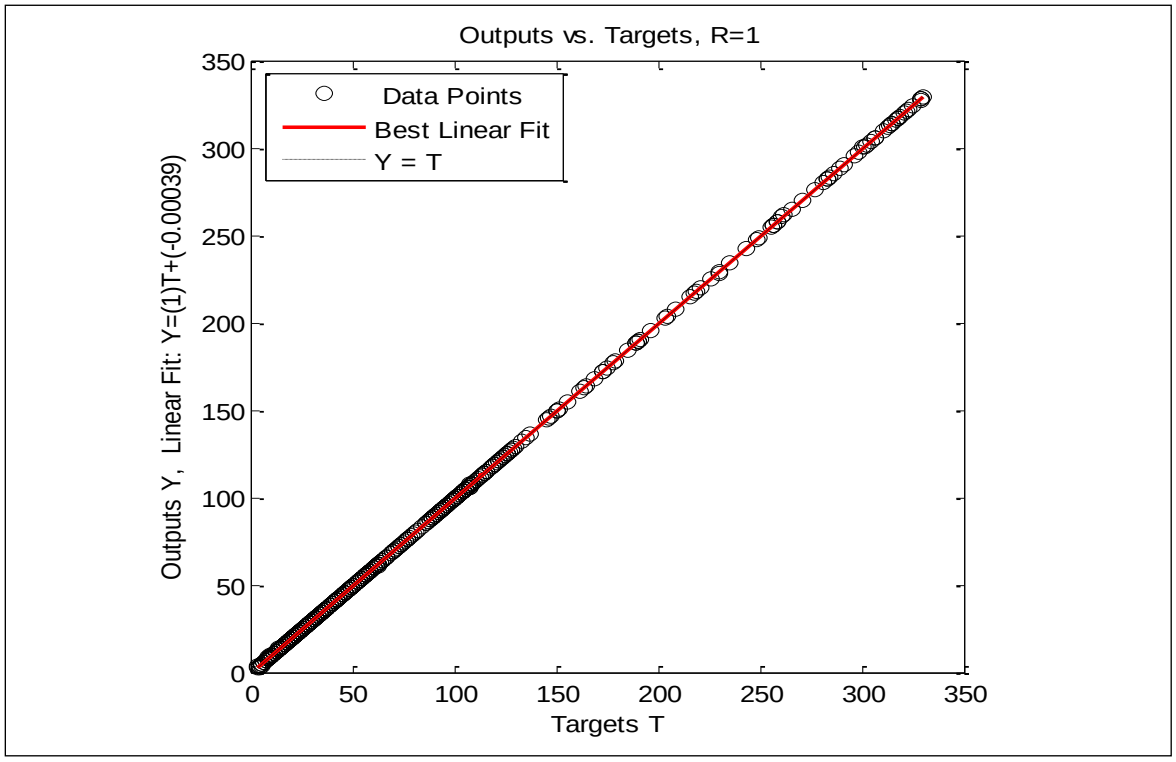

Figure 14: Example of the Trainlm with two layers & mapstd, processpca for Well#1 crossplot

Note: The remaining ANN graphical plots of the actual and predicted outputs in addition to their corresponding error crossplots are presented in appendix-A.

4.3.2 FunNet Model Prediction Results

The function network prediction was ranging from average to poor depending on the range of data. The following tables summarize the resulst using **AAPE,** RMSE and **CC.**

Well-1		**CC**	**RMSE**	**AAPE**
FNESM	Linear	0.96	8.37	61.51
	Non-Linear	1.00	2.46	19.05
FNFSM	Linear	0.96	8.37	61.51
	Non-Linear	1	2.50	17.43
FNBEM	Linear	0.96	8.37	60.87
	Non-Linear	1.00	2.46	19.05
FNFBM	Linear	0.95	9.79	67.18
	Non-Linear	1.00	2.73	20.82
FNBFM	Linear	0.96	8.37	60.87
	Non-Linear	1.00	2.46	19.05

Table 34: FunNet Model Prediction Results for well 1

Well-2		CC	RMSE	AAPE
FNESM	Linear	0.86	12.57	106.54
	Non-Linear	0.89	11.27	90.97
FNFSM	Linear	0.86	12.57	106.48
	Non-Linear	0.88	11.79	100.05
FNBEM	Linear	0.86	12.57	106.54
	Non-Linear	0.89	11.26	91.01
FNFBM	Linear	0.63	19.02	146.82
	Non-Linear	0.86	12.57	105.63
FNBFM	Linear	0.86	12.57	106.54
	Non-Linear	0.89	11.26	91.01

Table 35: FunNet Model Prediction Results for well 2

Well-3		CC	RMSE	AAPE
FNESM	Linear	0.79	9.36	70.44
	Non-Linear	0.86	7.69	87.17
FNFSM	Linear	0.79	9.36	70.44
	Non-Linear	0.80	9.11	84.32
FNBEM	Linear	0.79	9.36	70.44
	Non-Linear	0.86	7.69	87.17
FNFBM	Linear	0.52	12.99	156.04
	Non-Linear	0.79	9.36	70.72
FNBFM	Linear	0.79	9.36	70.44
	Non-Linear	0.86	7.69	87.17

Table 36: FunNet Model Prediction Results for well 3

Well-4		CC	RMSE	AAPE
FNESM	Linear	0.94	2.46	23.50
	Non-Linear	0.98	1.54	13.27
FNFSM	Linear	0.94	2.46	23.50
	Non-Linear	0.98	1.54	12.89
FNBEM	Linear	0.94	2.46	23.50
	Non-Linear	0.98	1.54	13.27
FNFBM	Linear	0.94	2.46	23.50
	Non-Linear	0.97	1.65	13.67
FNBFM	Linear	0.94	2.46	23.50
	Non-Linear	0.98	1.54	13.27

Table 37: FunNet Model Prediction Results for well 4

Well-5		CC	RMSE	AAPE
FNESM	Linear	0.43	19.77	133.77
	Non-Linear	0.68	16.09	96.99
FNFSM	Linear	0.43	19.77	133.77
	Non-Linear	0.47	19.35	128.52
FNBEM	Linear	0.43	19.77	133.77
	Non-Linear	0.68	16.09	96.99
FNFBM	Linear	0.43	19.77	133.77
	Non-Linear	0.39	20.18	175.97
FNBFM	Linear	0.43	19.77	133.77
	Non-Linear	0.68	16.09	96.99

Table 38: FunNet Model Prediction Results for well 5

Well-6		CC	RMSE	AAPE
FNESM	Linear	0.72	17.44	197.74
	Non-Linear	0.91	10.33	82.34
FNFSM	Linear	0.72	17.44	197.74
	Non-Linear	0.86	12.75	139.19
FNBEM	Linear	0.72	17.44	197.74
	Non-Linear	0.91	10.33	82.34
FNFBM	Linear	0.72	17.44	197.74
	Non-Linear	0.84	13.59	129.64
FNBFM	Linear	0.72	17.44	197.74
	Non-Linear	0.91	10.33	82.34

Table 39: FunNet Model Prediction Results for well 6

Well-7		CC	RMSE	AAPE
FNESM	Linear	0.68	9.39	138.30
	Non-Linear	0.95	4.15	73.22
FNFSM	Linear	0.68	9.39	138.30
	Non-Linear	0.95	4.20	72.85
FNBEM	Linear	0.68	9.39	138.30
	Non-Linear	0.95	4.16	73.41
FNFBM	Linear	0.68	9.39	138.30
	Non-Linear	0.93	4.58	87.00
FNBFM	Linear	0.68	9.39	138.30
	Non-Linear	0.95	4.16	73.41

Table 40: FunNet Model Prediction Results for well 7

Well-8		CC	RMSE	AAPE
FNESM	Linear	0.84	31.92	485.65
	Non-Linear	0.99	8.42	176.30
FNFSM	Linear	0.84	31.92	485.65
	Non-Linear	0.99	8.42	176.30
FNBEM	Linear	0.84	31.92	485.65
	Non-Linear	0.99	8.42	176.30
FNFBM	Linear	0.83	32.34	372.05
	Non-Linear	0.98	10.73	105.55
FNBFM	Linear	0.84	31.92	485.65
	Non-Linear	0.99	8.42	176.30

Table 41: FunNet Model Prediction Results for well 8

Well-9		CC	RMSE	AAPE
FNESM	Linear	0.76	42.81	111.89
	Non-Linear	0.90	29.39	72.00
FNFSM	Linear	0.76	42.81	111.89
	Non-Linear	0.89	30.13	73.57
FNBEM	Linear	0.76	42.81	111.89
	Non-Linear	0.90	29.39	72.00
FNFBM	Linear	0.45	59.17	91.13
	Non-Linear	0.81	38.49	110.64
FNBFM	Linear	0.76	42.81	111.89
	Non-Linear	0.90	29.39	72.00

Table 42: FunNet Model Prediction Results for well 9

Well-10		CC	RMSE	AAPE
FNESM	Linear	0.71	93.56	247.93
	Non-Linear	0.90	57.75	164.03
FNFSM	Linear	0.71	93.56	247.93
	Non-Linear	0.89	60.36	204.07
FNBEM	Linear	0.71	93.56	247.93
	Non-Linear	0.90	57.75	163.97
FNFBM	Linear	0.71	93.56	247.93
	Non-Linear	0.87	65.20	172.31
FNBFM	Linear	0.71	93.56	247.93
	Non-Linear	0.90	57.75	163.97

Table 43: FunNet Model Prediction Results for well 10

An example of the FunNet graphical plots of the actual and predicted outputs is presented below that reflects the acceptable nonlinear FNESM network performance.

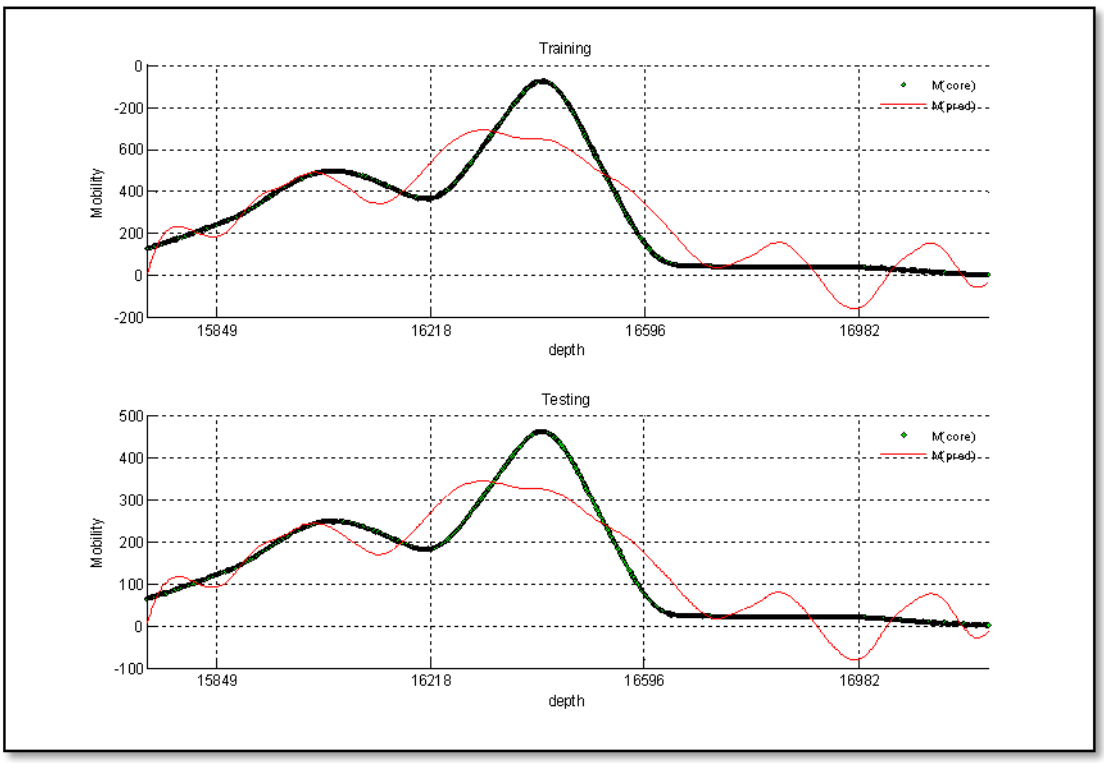

Figure 15: Example of the FunNet graphical plots (Well-10)

Note: All the FunNet graphical plots of the actual and predicted outputs are presented in appendix-B.

4.3.3 SVM Model Prediction Results

The support vector machine prediction was ranging from average to poor depending on the range of data. The following tables summarize the results using AAPE, RMSE and CC.

Well # 1			
KERNEL TYPE	**CC**	**RMSE**	**AAPE**
GAUSSIAN	0.99	2.5	32.08
POLY	0.99	2.06	28.86
POLYHOMOG	0.99	2.96	33.28
JCB	0.96	4.89	51.88

Table 44: SVM Model Prediction Results for well 1

Well # 2			
KERNEL TYPE	**CC**	**RMSE**	**AAPE**
GAUSSIAN	0.89	10.86	61.81
POLY	0.99	3.11	26.19
POLYHOMOG	0.95	7.59	35.91
JCB	0.84	13.19	75.26

Table 45: SVM Model Prediction Results for well 2

Well # 3			
KERNEL TYPE	**CC**	**RMSE**	**AAPE**
GAUSSIAN	0.85	8.07	57.97
POLY	0.97	3.87	39.85
POLYHOMOG	0.89	6.88	55.28
JCB	0.79	9.51	75.14

Table 46: SVM Model Prediction Results for well 3

Well # 4			
KERNEL TYPE	**CC**	**RMSE**	**AAPE**
GAUSSIAN	0.99	1.43	13.27
POLY	0.99	1.03	10.99
POLYHOMOG	0.99	0.95	9.99
JCB	0.96	2.35	18.63

Table 47: SVM Model Prediction Results for well 4

Well # 5			
KERNEL TYPE	**CC**	**RMSE**	**AAPE**
GAUSSIAN	0.56	18.65	103.99
POLY	0.82	12.53	46.98
POLYHOMOG	0.74	14.87	62.91
JCB	0.41	20.39	121.2

Table 48: SVM Model Prediction Results for well 5

Well # 6			
KERNEL TYPE	**CC**	**RMSE**	**AAPE**
GAUSSIAN	0.89	12.29	99.85
POLY	0.98	5.51	44.66
POLYHOMOG	0.96	7.69	62.06
JCB	0.72	19.22	173.74

Table 49: SVM Model Prediction Results for well 6

Well # 7			
KERNEL TYPE	**CC**	**RMSE**	**AAPE**
GAUSSIAN	0.74	10.08	69.95
POLY	0.99	2.09	46.04
POLYHOMOG	0.97	3.27	54.88
JCB	0.66	10.9	90.26

Table 50: SVM Model Prediction Results for well 7

Well # 8			
KERNEL TYPE	**CC**	**RMSE**	**AAPE**
GAUSSIAN	0.93	21.25	143.7
POLY	0.99	5.96	133.45
POLYHOMOG	0.99	7.54	176.66
JCB	0.82	33.78	256.73

Table 51: SVM Model Prediction Results for well 8

Well # 9			
KERNEL TYPE	**CC**	**RMSE**	**AAPE**
GAUSSIAN	0.88	38.46	62.16
POLY	0.99	10.83	45.29
POLYHOMOG	0.98	17.17	75.24
JCB	0.9	39.81	116.86

Table 52: SVM Model Prediction Results for well 9

Well # 10			
KERNEL TYPE	**CC**	**RMSE**	**AAPE**
GAUSSIAN	0.87	70.47	58.26
POLY	0.99	10.88	26.77
POLYHOMOG	0.97	30.27	34.11
JCB	0.64	106.78	82.06

Table 53: SVM Model Prediction Results for well 10

An example of the SVM graphical plots of the actual and predicted outputs is presented below that reflects the acceptable Gaussian network model performance.

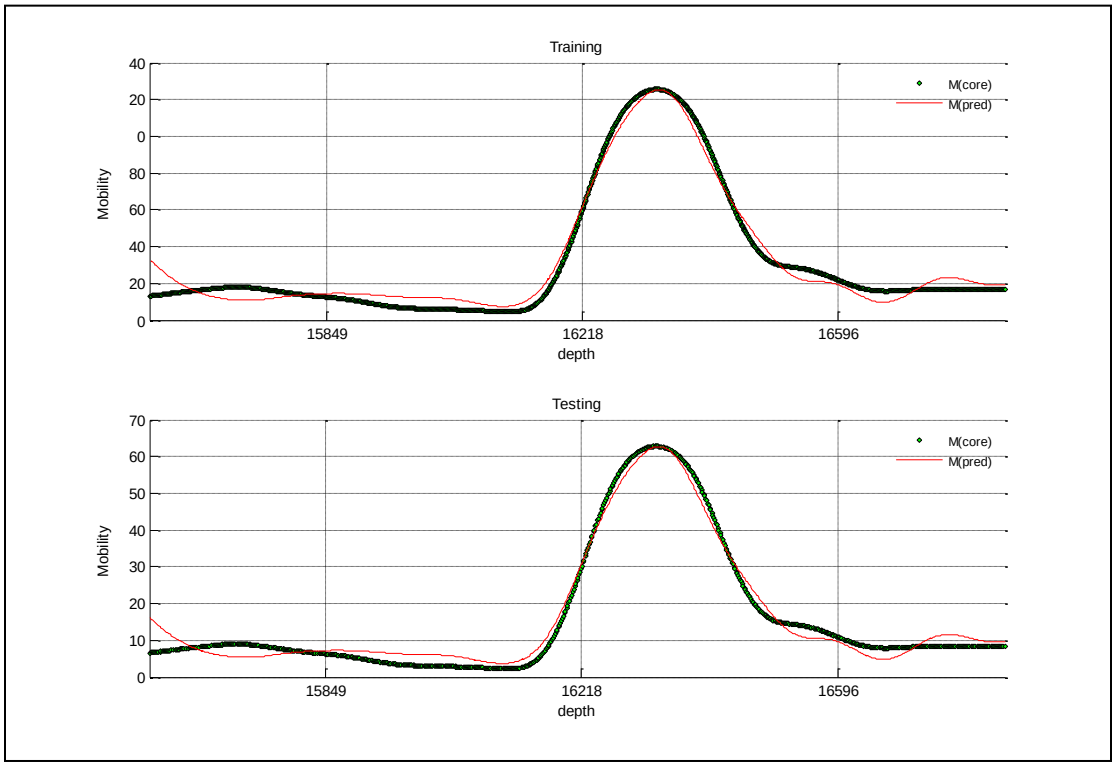

Figure 16: Example of SVM Gaussian kernel graphical plots (Well-1)

Note: All the SVM graphical plots of the actual and predicted outputs are presented in appendix-C.

4.4 Results Analysis

4.4.1 ANN Results Analysis

Trainlm function of the neural network tool box in Matlab environment performed the best when compared to the other functions used during this thesis work as noticed on Figure 17. Zooming more, the Trainlm function with single layer performance was reasonable but when performing visual examination to predicted output plot verses the actual mobility values some discrepancy. The performance was enhanced when the same function was used but with two hidden layers. Yet more perfect matching between prediction verses actual by adding the mapstd and processpca functions to the model of Trainlm and the two layers.

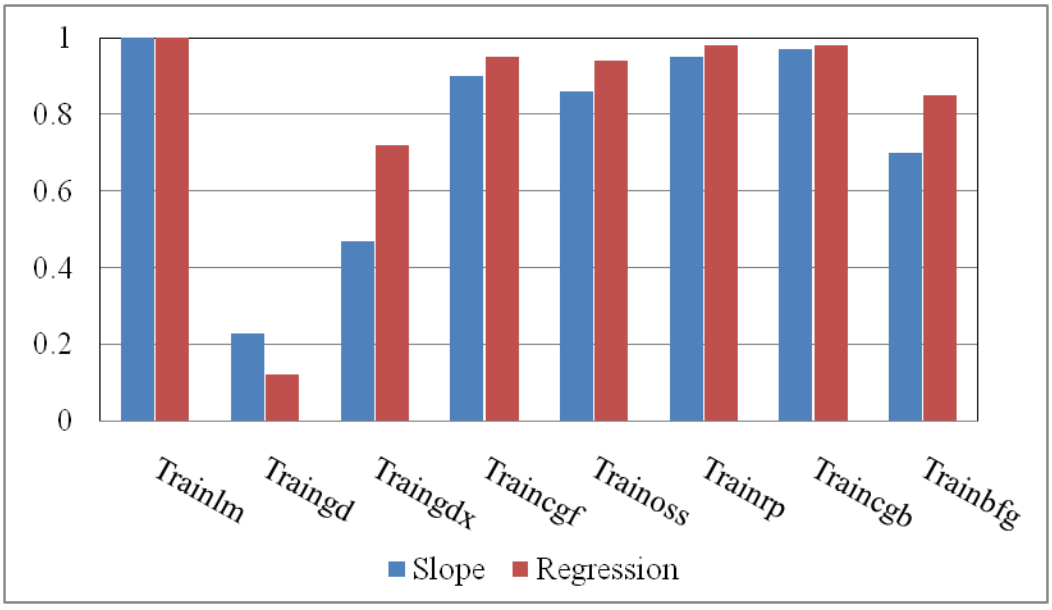

Figure 17: Comparison between ANN functions

4.4.2 FunNet Results Analysis

Functional Network Elimination Selection Method using Non-Linear of the 1st order regression performed the best among the 10 different schemes utilized for this thesis work as observed in Figure 18. Generally, the FunNet performance was not satisfactory when compared to ANN performance.

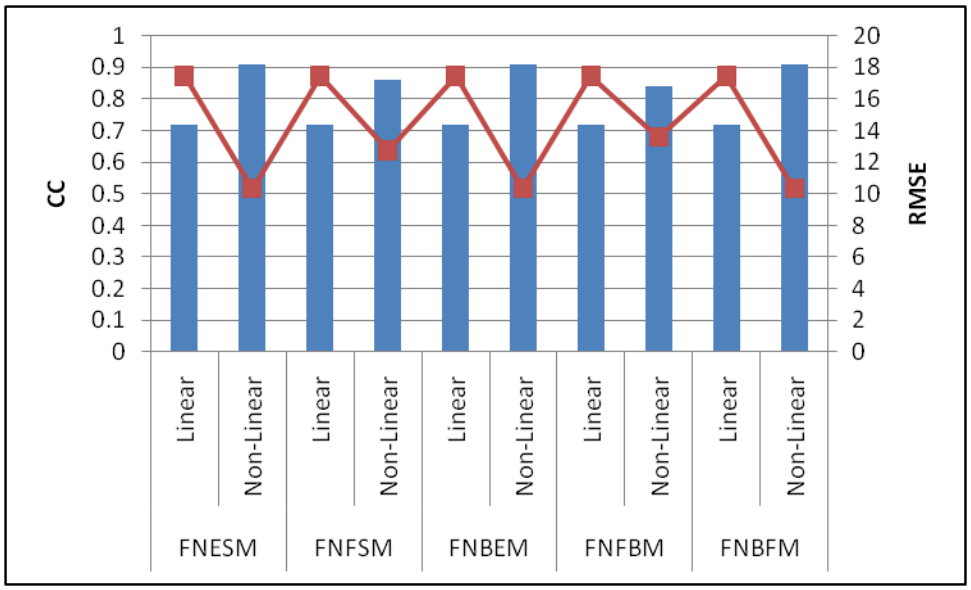

Figure 18: Comparison between FunNet functions

4.4.3 SVM Results Analysis

The polynomial kernel of the SVM tool box performed the best among the four different kernels used in this thesis work as observed on Figure 19. Also, the SVM performance was not satisfactory when compared to ANN performance but generally speaking the polynomial kernel performance was much better and faster in execution time when compared to the FunNet.

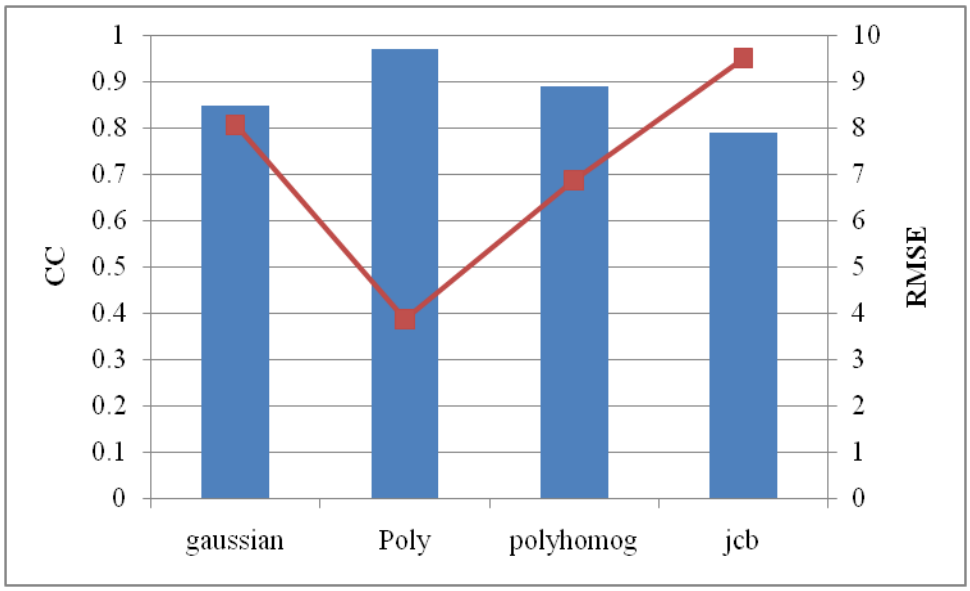

Figure 19: Comparison between SVM kernels

4.5 Values Added to Geosteering with Mobility

Since the ANN tool proved to be the best prediction function within artificial intelligence, it was applied in one well to minimize the sampling requirements while keeping efficient geosteering.

4.5.1 Definition

Geosteering is defined as the direct control of a well path or lateral positioning based on the geological information gathered while drilling. Logging while drilling (LWD) and monitoring while drilling (MWD) tools are responsible to gather downhole geological logging measurements that are of crucial nature to adjust well path and/or update existing geological models. With the advancement of this technology, the Geosteering has become proactive rather than being passive to aid detecting boundaries, sweet spots and other parameters in advance before the bit drills in unfavorable or less desirable zones to avoid the backtrack and ensure smooth borehole and maximum reservoir contact.

4.5.2 Objective

The basic need of Geosteering is simply represented in the direct aid of well placement in real-time fashion rather than using the existing geological modeling with 2D & 3D models of underground substructure. The benefits attained from this approach are clear, but the requirements of the data acquisition tools deployed vary from field to field. Moreover, other factors sometime dictate the need of special tools to compliment or facilitate the interpretations of the conventional logging equipment deployed with the drilling bottom hole assembly (BHA).

4.5.3 Basic Requirements for Efficient Geosteering

The main reason behind bringing this technology to existence is to place the so known well path into the unknown pay zone location and/or in the perfect strata layer that will lead into optimum sweep and recovery.

The conventional logging tools are used mainly to collect geological and petro physical data essential to update the geological and simulation models and to assist in adjusting placement plans based on real-time data collected. The conventional equipment being commonly used today is the triple compo LWD that provides lithology (GR) resistivity and density (Neutron), MWD tools that provide azimuthal positions and well trajectory and a simple gamma ray / rate of penetration (GR/ROP) logs.

For reservoirs with reliable geological models resulted from extensive in-fill programs and with high resolution seismic surveys that reveal the existence of fractures, faults and provide strata dipping, conventional equipment such as triple compo can be used for the purpose of cross checking and data gathering. The requirements might be reduced even further to suggest a very basic logging measurement tools in a classic sandstone reservoir with low heterogeneity factor. However, this is not the case when targeting zones with certain features like:

- Thin bedded pay zones.
- Hydrocarbon bearing zones with different mobility.
- Naturally fractured reservoirs with lack of geological data and low resolution seismic surveys.

For thin bedded pay zones, the pro-active measures are considered to increase reservoir net pay and to place the well away from boundaries to maximize recovery and delay unfavorable fluids production. The conventional resistivity tools have limited capabilities, and the interpretation might require additional information collected while drilling with a lead time to interpretate the petrophysical properties of the fluid. Moreover, anisotropy or mud invasion (based on mud type) has an impact on the data accuracy. Common tool utilized nowadays are the deep azimuthal resistivity tools that has a long radius of investigation capable of detecting boundaries such as formation rocks or even fluids few feet in advance. It also uses the shallow resistivity tools to correct for fluid resistivity since the first is being used to measure the average rock formation resistivity. GR sensors placed at the bit is another requirements needed to assess in the lithology of formation being drilled in real-time rather than waiting for the next few joints to be drilled. Also along with identifying boundaries, the tool can detect maximum hydrocarbon saturation (which is a function of resistivity) and a water wet zones not apparent by the gamma log.

In zones where the hydrocarbon fluid properties varies based on depth, placing the water injection lateral as an example not less vital than targeting thin beds. The concept behind water injection is primarily to maintain pressure and to create a water front for better sweep efficiency. Identifying the mobility of the hydrocarbon dictates the depth and path of the lateral placement for better injecitvity and recovery.

4.5.4 Application

Interpolation technique was used to infill mobility values between the first few actual measurements of mobility obtained from the formation testing tool to generate the initial mobility profile used for training purposes. Thus making first step toward further optimization of the real time sampling requirements very encouraging and consequently reduce total well cost and increase rig safety.

To demonstrate the idea, three wells were selected to evaluate how many sampling point can be reduced without affecting the horizontal section placement quality. First, the measured mobility and the permeability values were plotted against depth and it was noted that in most of the well sections the two profiles behave similarly. This behavior implies that the ANN trainlm function

will be capable of predicting some of these mobility sampling points and eventually cut down the real time sampling requirements. Second, the first few points were used for the model's training after using the Trainlm function to fill in between the actual mobility measurements with more predicted mobility values using gamm-ray, porosity and water saturation to make up a continues mobility profile. Third, the model was run to predict the next mobility point measured and compares the predicted value against the measured one.

When the first well's mobility and permeability data were plotted together as in Figure 20, it was noticed that mobility points No. 1 and 2 easily can be utilized for training purposes to predicted mobility values of points No. 3 and 4. The Trainlm function was used to construct a complete mobility profile between points No. 1 and 2 and use that profile for training and validation purposes and then utilize that model to predict the other two points. Then, the measured points No. 1 and 2 with the predicted mobility values of points No.3 and 4 were used for training to predict the following mobility points. After multiple iterations, that data shown on Table 54 suggested that 45% of the real time measurements of mobility can be dropped and replaced by the data coming from the ANN trainlm function without affecting the quality of geosteering. Also, this exercise clearly established that when a big change (increase or decrease) of permeability values happens then it is an ideal place to take a couple of mobility sampling points to anchor and strengthen the prediction model.

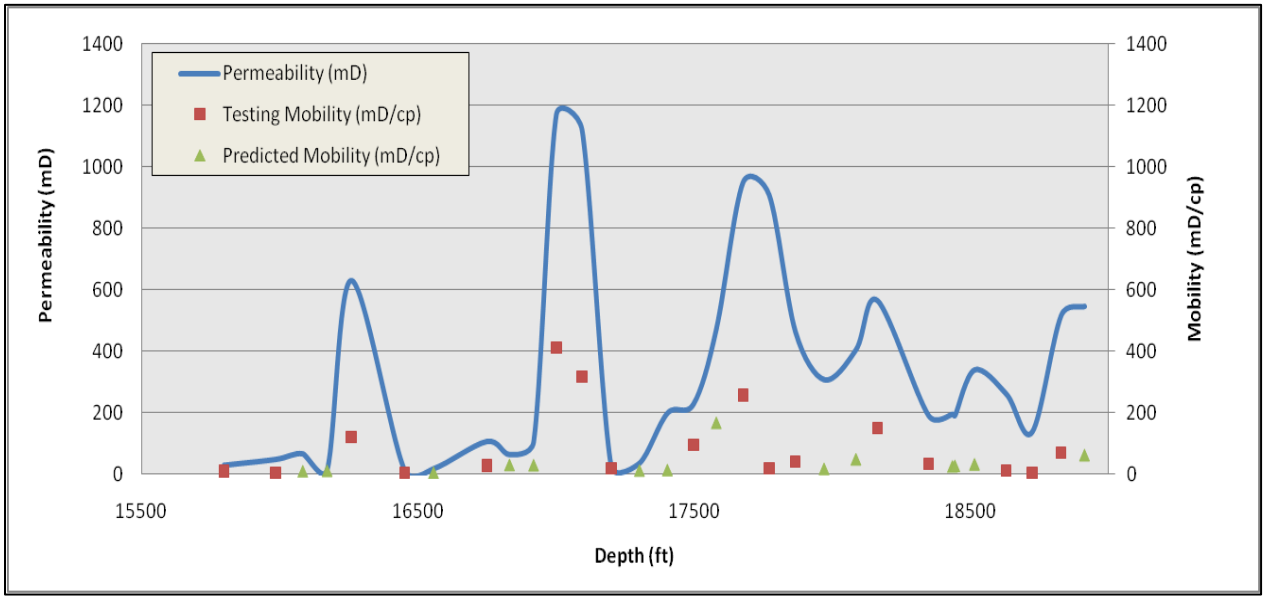

Figure 20: Permeability and Mobility Chart of the First Well

No.	Depth	Permeability (mD)	Mobility			Accuracy (%)
			Measured Mobility (mD/cp)	Mobility Used for Training (mD/cp)	Predicted Mobility (mD/cp)	
1	15800	29.21	9.9	9.9		
2	15986	48.04	4.3	4.3		
3	16085	66.19	9.5		9.5	100
4	16173	14.83	11.2		10.98	98
5	16260	630.96	122	122		
6	16452	14.78	5.3	5.3		
7	16558	17.77	4.7		4.8	98
8	16750	106.46	27.9	27.9		
9	16833	64.03	29.1		29.87	97
10	16920	106.46	29.1		29.12	100
11	17002	1171.66	412	412		
12	17095	1120.99	318	318		
13	17200	27.76	19.3	19.3		
14	17303	36.04	11		11.67	94
15	17404	199.16	13.4		13.33	99
16	17498	228.24	96.2	96.2		
17	17581	473.37	181		167.25	92
18	17677	949.73	258	258		
19	17772	908.66	20	20		
20	17867	463.02	40.3	40.3		
21	17971	307.61	15.8		17.1	92
22	18086	405.51	49		48.33	99
23	18164	564.94	150.3			
24	18348	191.25	34.9			
25	18435	195.52	24		24.84	97
26	18444	191.25	27.1		26.99	99
27	18515	339.78	33.3		31.98	96
28	18630	260.62	12.4			
29	18723	137.28	5			
30	18828	517.13	69.4			
31	18913	546.51	63.1		62.15	98

Table 54: Avoided Sampling Points Comparison of the first well

The second well, showed better capability of the model as shown in Table 55, where the first four real time mobility collected samples were used to train the model after generating the full profile using the Trainlm function helped to avoid the next 7 real time sampling points. Again the mobility and permeability graph shown in Figure 21 was the key to accurately plan the next sampling point location. This technique helped to reduce the real time samples by nearly 50% which equate to 13 hours of rig time and the sampling cost.

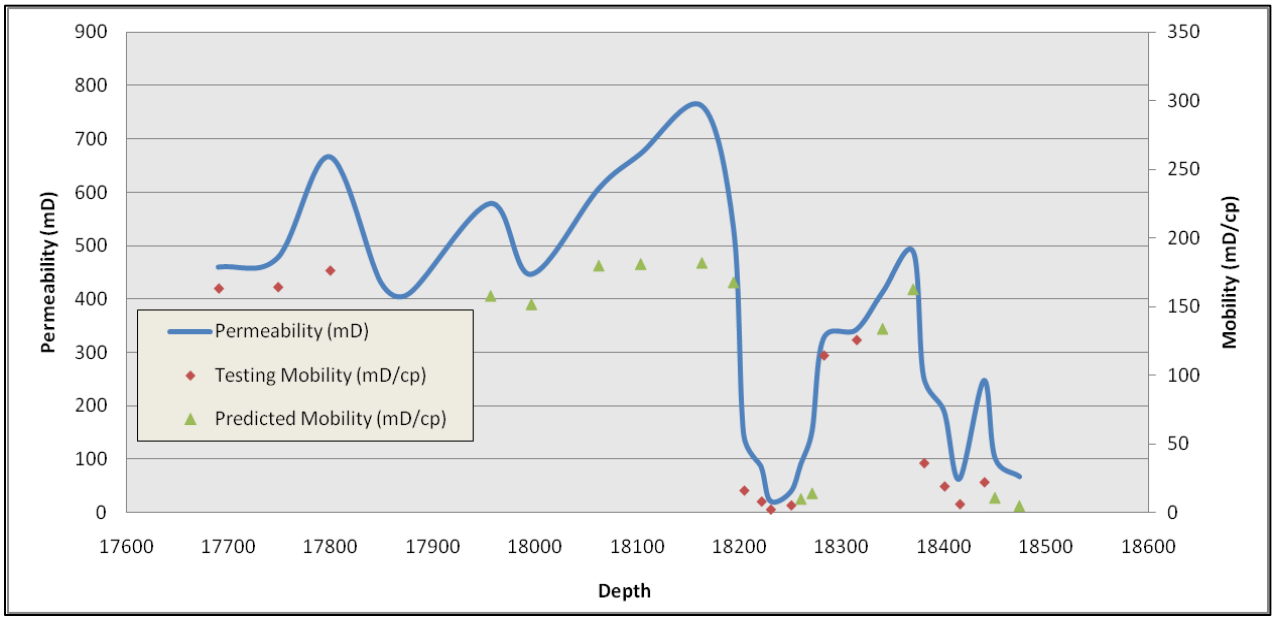

Figure 21: Permeability and Mobility Chart of the Second Well

No.	Depth	Permeability (mD)	Mobility			Accuracy (%)
			Measured Mobility (mD/cp)	Mobility Used for Training (mD/cp)	Predicted Mobility (mD/cp)	
1	17690	460.51	163	163		
2	17748	477.60	164	164		
3	17799	667.01	176.2	176		
4	17849	432.03	143.5	143.4		
5	17877	411.20	140		139	99.3
6	17956	579.44	161.88		157.89	97.5
7	17996	446.90	152		151.81	99.9
8	18062	606.97	179.1		180	99.5
9	18103	672.41	180.73		181.1	99.8
10	18163	762.61	183.33		181.99	99.3
11	18194	533.90	166.42		167.81	99.2
12	18204	146.77	16.3	16.3		
13	18221	87.12	8.3	8.3		
14	18230	22.51	2.5	2.48		
15	18250	39.67	5.4	5.5		
16	18260	91.97	10.89		10	91.8
17	18271	154.06	15.98		14.12	88.4
18	18282	326.23	114.46	114.33		
19	18314	342.95	125.48	125.59		
20	18340	413.65	138.82		133.97	96.5
21	18370	488.98	166		162.72	98.0
22	18380	256.02	26.3	36.2		
23	18400	191.02	19.3	19.3		
24	18415	63.68	6.4	6.4		
25	18439	248.16	22.3	22.3		
26	18450	102.44	13.3		10.89	81.9
27	18474	68.16	4.3		4.9	87.8

Table 55: Avoided Sampling Points Comparison of the second well

Results from the third well demonstrate the same concept, that when drilling horizontally on the same sub-sea depth in presence of different fluid motilities, the change on permeability will most suitable place to take a real time mobility sampling point. This will assure that the well placement is going on the right direction as illustrated in Figure 22. This method in addition to the help of ANN trainlm function model made it very easy to drop nearly 60% of the real sampling requirements to the benefit of the accurate prediction results obtained from the model. Table 56 is showing that 16 real time sampled points can be dropped and replaced by the predicted mobility data from the ANN model with very high accuracy of around 96%.

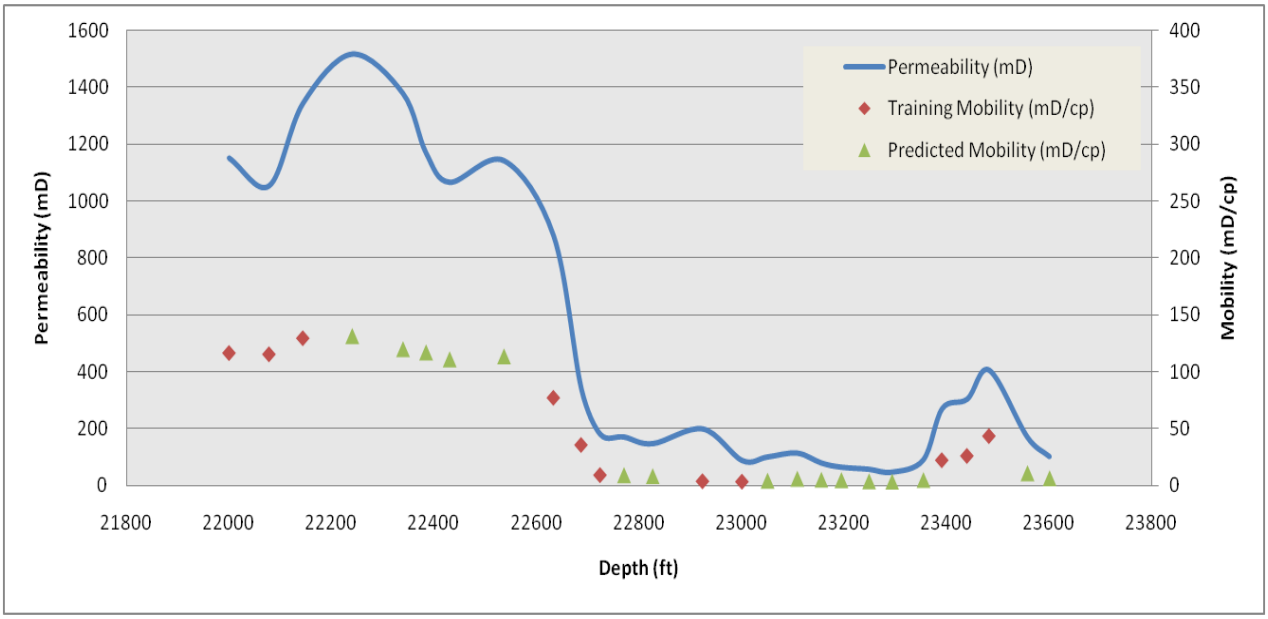

Figure 22: Permeability and Mobility Chart of the Third Well

No.	Depth	Permeability (mD)	Mobility			Accuracy (%)
			Measured Mobility (mD/cp)	Mobility Used for Training (mD/cp)	Predicted Mobility (mD/cp)	
1	22000	1151.119	117.32	116.69		
2	22078	1053.6	116.12	115.63		
3	22144	1343.8	126.66	129.71		
4	22240	1516.8	133.33		131.59	98.7
5	22339	1378.5	120.41		119.93	99.6
6	22384	1169.3	117.63		117.11	99.6
7	22430	1066.1	112.16		110.98	98.9
8	22536	1142.1	118.98		113.56	95.4
9	22633	877.0	78.39	77.41		
10	22687	339.5	35.43	36		
11	22724	179.5	9.61	9.55		
12	22770	170.5	9.01		8.88	98.6
13	22826	146.6	7.71		8.01	96.3
14	22924	198.6	4.08	4.12		
15	23001	87.2	3.71	3.79		
16	23050	99.9	4.01		3.98	99.3
17	23108	113.6	6.75		5.72	84.7
18	23155	79.0	4.9		4.83	98.6
19	23194	64.2	4.4		4.5	97.8
20	23248	56.9	3.1		3.4	91.2
21	23293	46.6	3.06		3.1	98.7
22	23354	89.9	4.7		4.64	98.7
23	23391	270.4	22.62	22.62		
24	23440	304.0	26.33	26.41		
25	23483	404.7	44.04	43.83		
26	23557	169.6	11.32		10.67	94.3
27	23600	101.7	5.96		6.16	96.8

Table 56: Avoided Sampling Points Comparison of the third well

CHAPTER 5

CONCLUSIONS & RECOMMENDATIONS

5.1 Conclusions

Based on the results and discussion presented in this study, the following conclusions can be drawn:

1. The novel idea of optimizing the number of mobility measurements using minimum mobility points using artificial intelligence techniques proved successful.
2. The ANN model with Trainlm function presented the highest accuracy in predicting the mobility.
3. The ANN model with Trainlm function offered a very stable algorithm with very reasonable execution time.
4. This approach proved that the use of artificial intelligence will reduce the risk and cost when acquiring the mobility points in horizontal wells.
5. The new developed model results can only be used within the range of used data.

5.2 Recommendations

The following recommendations are made as a possible extension of the present work

1. The model performance can be tested further using different set of data from different fields with a wider range of variables.
2. The importance of all input variables can be further investigated in a future work to determine the most important parameters that are involved in estimating the mobility; this may result in reducing the number of input variables.
3. The model can be added to the horizontal wells geo-steering software to provide real time prediction of the mobility as a solution to guide the next sampling point and provide better guidance to the investment of the data acquire.

APPENDIX A

ARTIFICIAL NEURAL NETWORKS (ANN) RESULTS SUMMARY

This appendix is showing all the ANN graphical plots of the actual verses the predicted outputs in addition to their corresponding error crossplots of all the ten wells under different cases.

CASES USED

Case No.	Backpropagation Function Type
1	trainlm (One Layer, 20 Neurons)
2	trainlm (Two Layer, 15,20 Neurons)
3	traingd (Two Layer, 15,20 Neurons)
4	traingdx (Two Layer, 15,20 Neurons)
5	traincgf (Two Layer, 15,20 Neurons)
6	trainoss (Two Layer, 15,20 Neurons)
7	trainrp (Two Layer, 15,20 Neurons)
8	traincgb (Two Layer, 15,20 Neurons, mapstd)
9	trainbfg (Two Layer, 15,20 Neurons, mapstd, processpca)
10	trainlm (Two Layer, 15,20 Neurons, mapstd, processpca)

RESULTS

Well No. 1

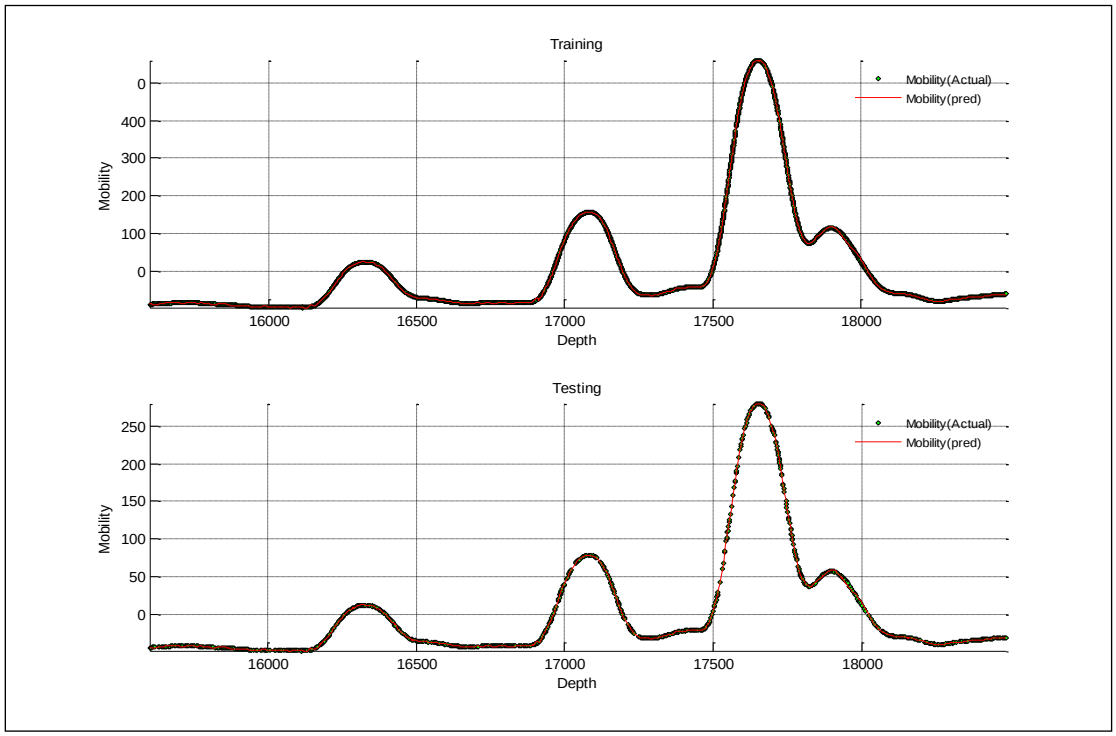

Figure A- 1: Well-1, Case -1

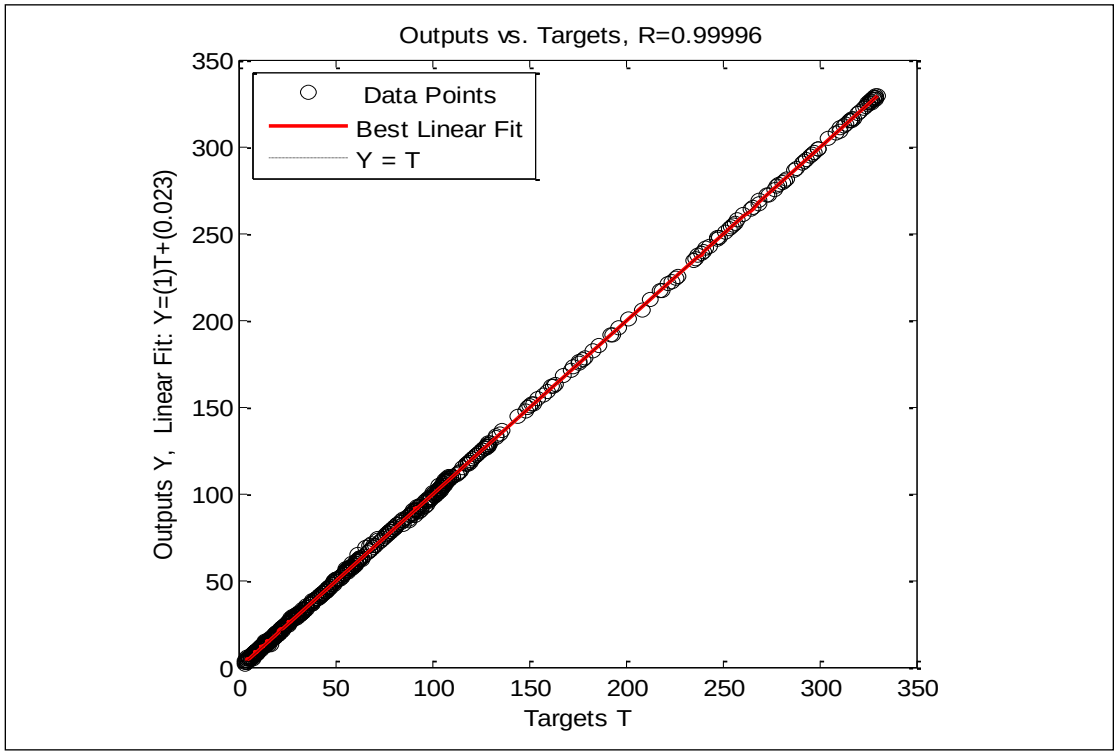

Figure A- 2: Well-1, Case -1, Crossplot

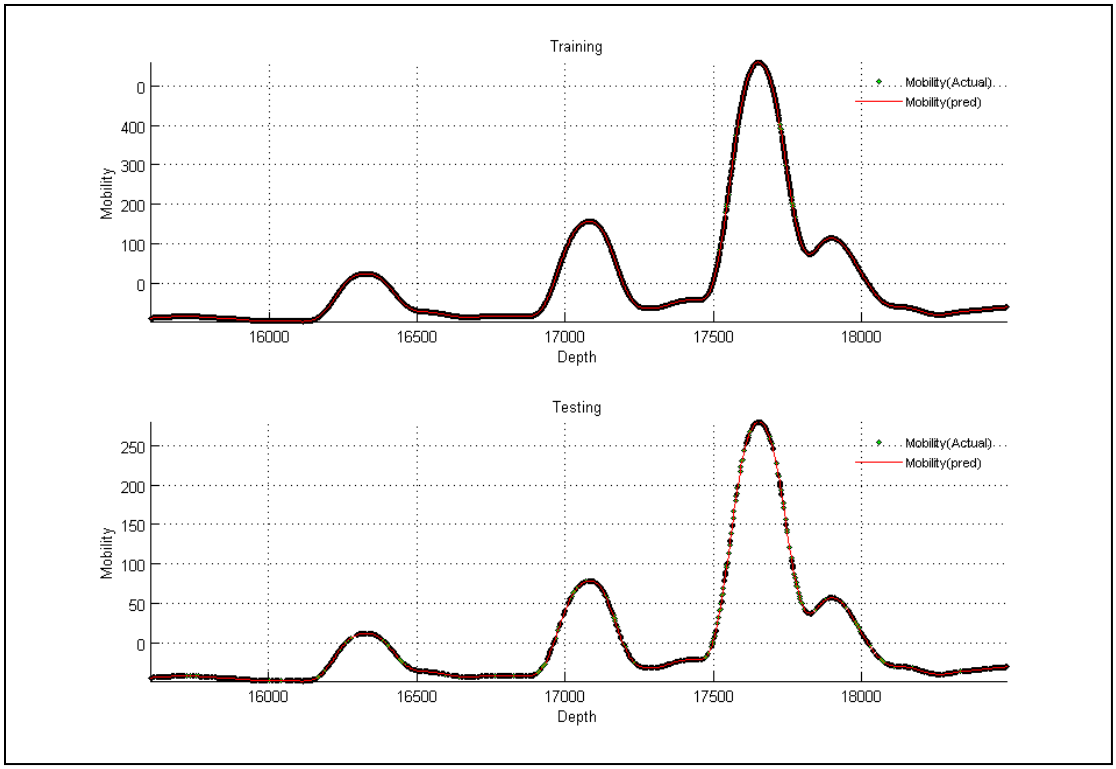

Figure A- 3: Figure A- 2: Well-1, Case -2

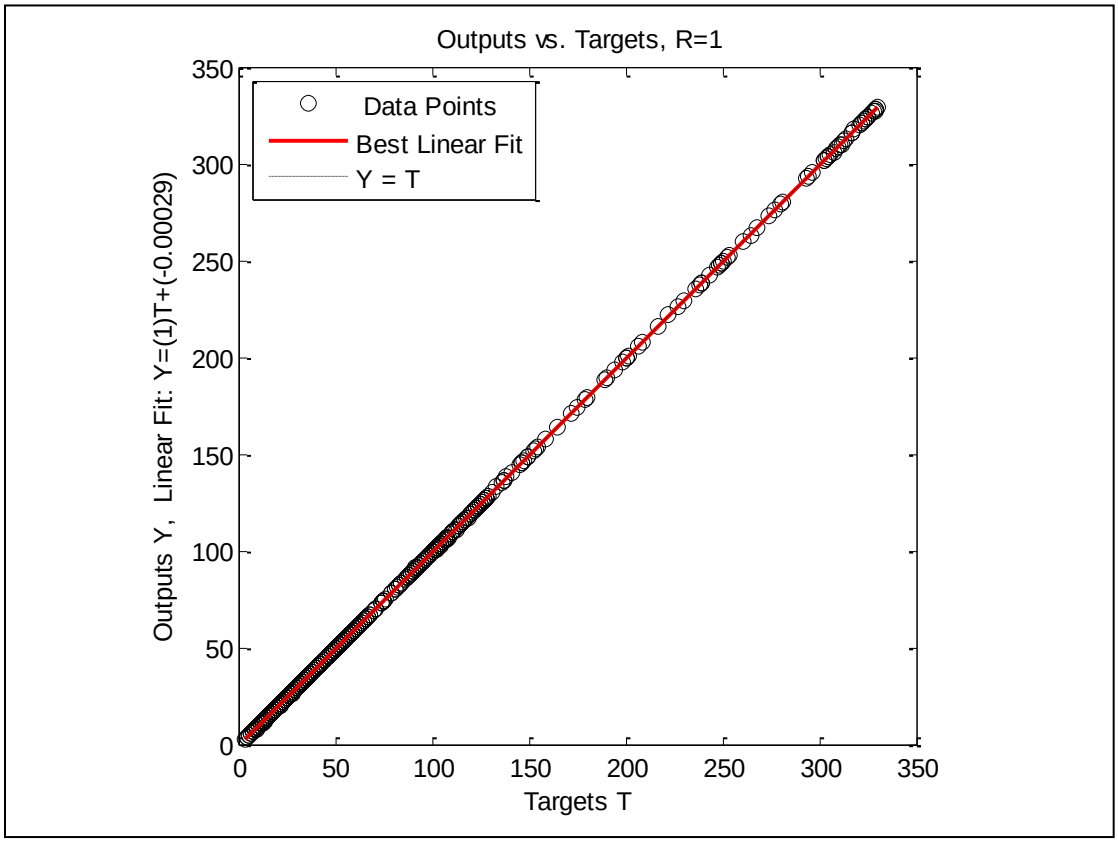

Figure A- 4: Well-1, Case -2, Crossplot

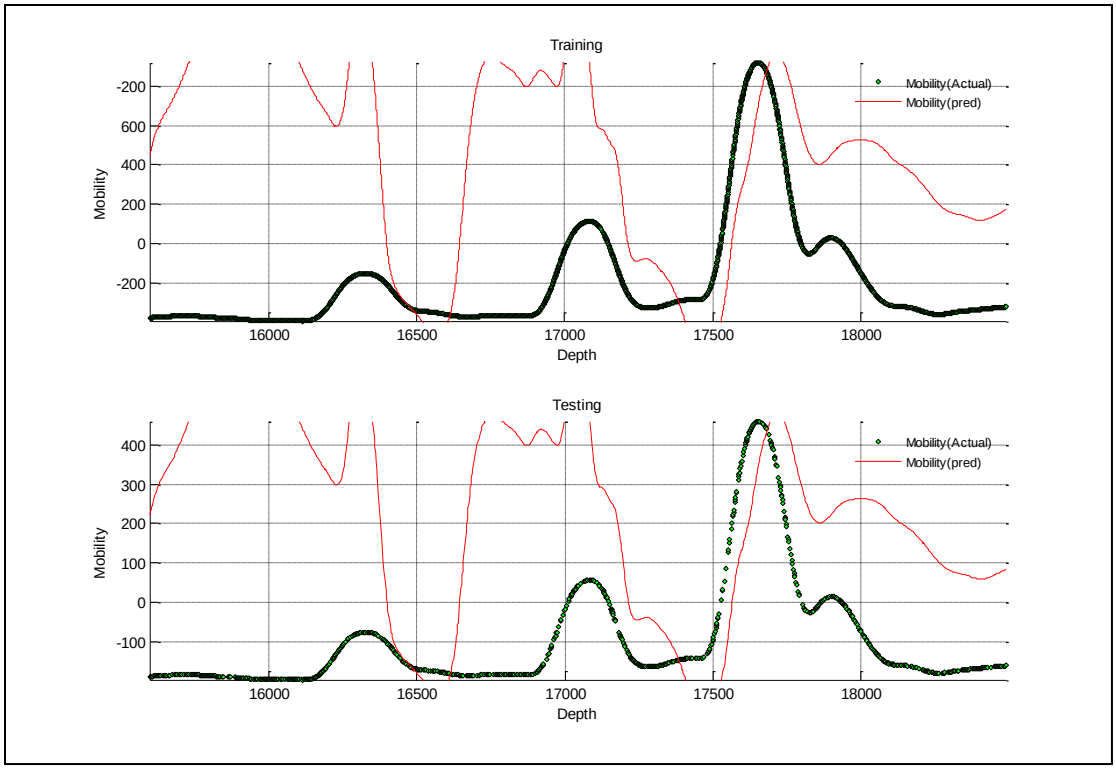

Figure A- 5: Well-1, Case -3

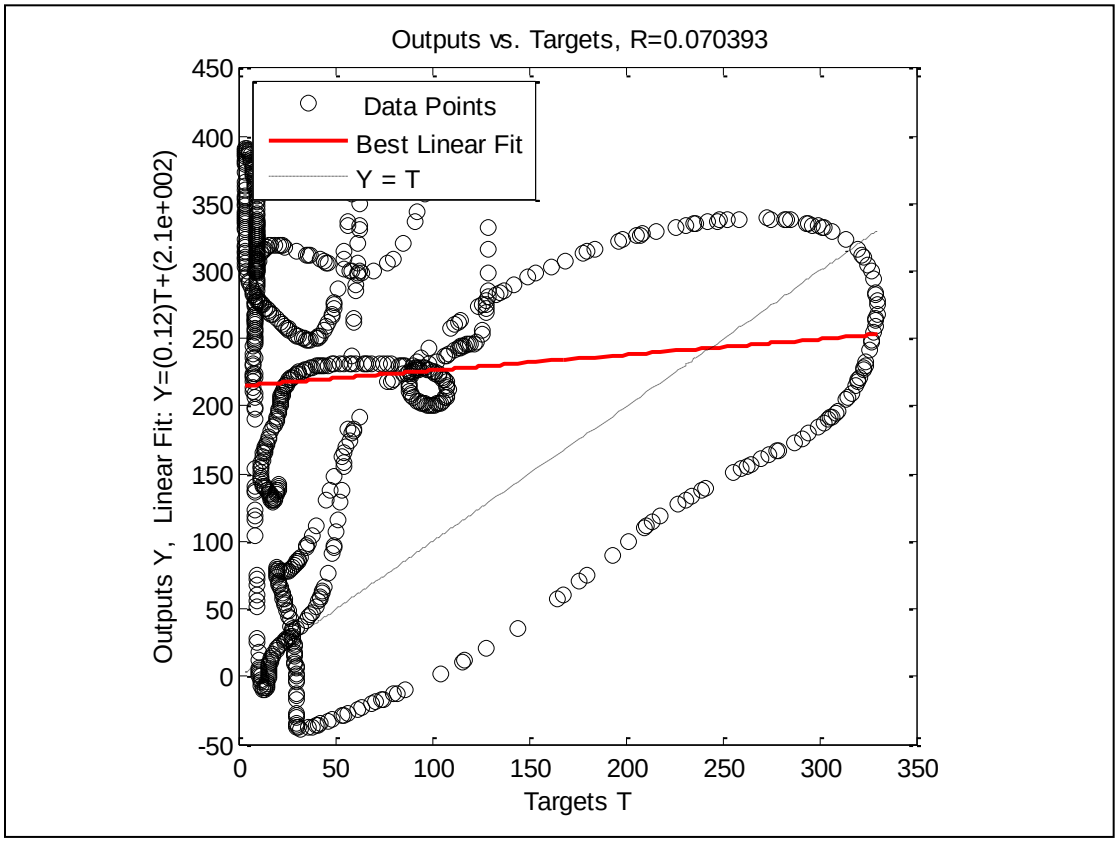

Figure A- 6: Well-1, Case -3, Crossplot

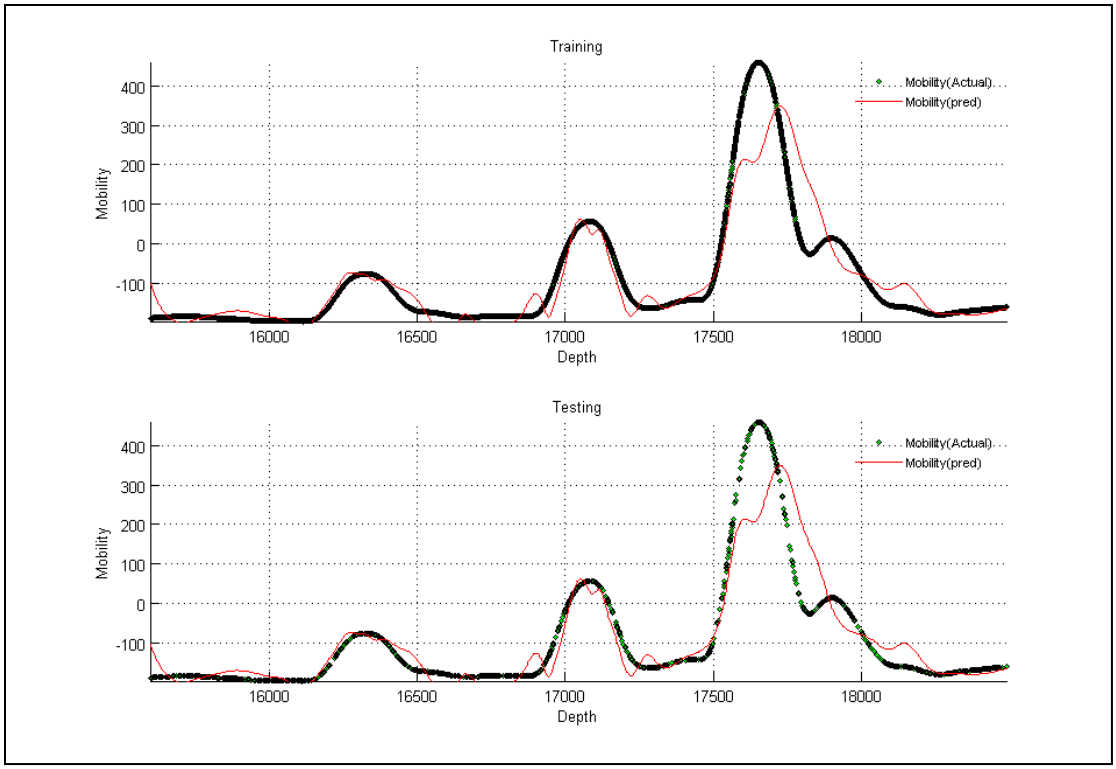

Figure A- 7: Well-1, Case -4

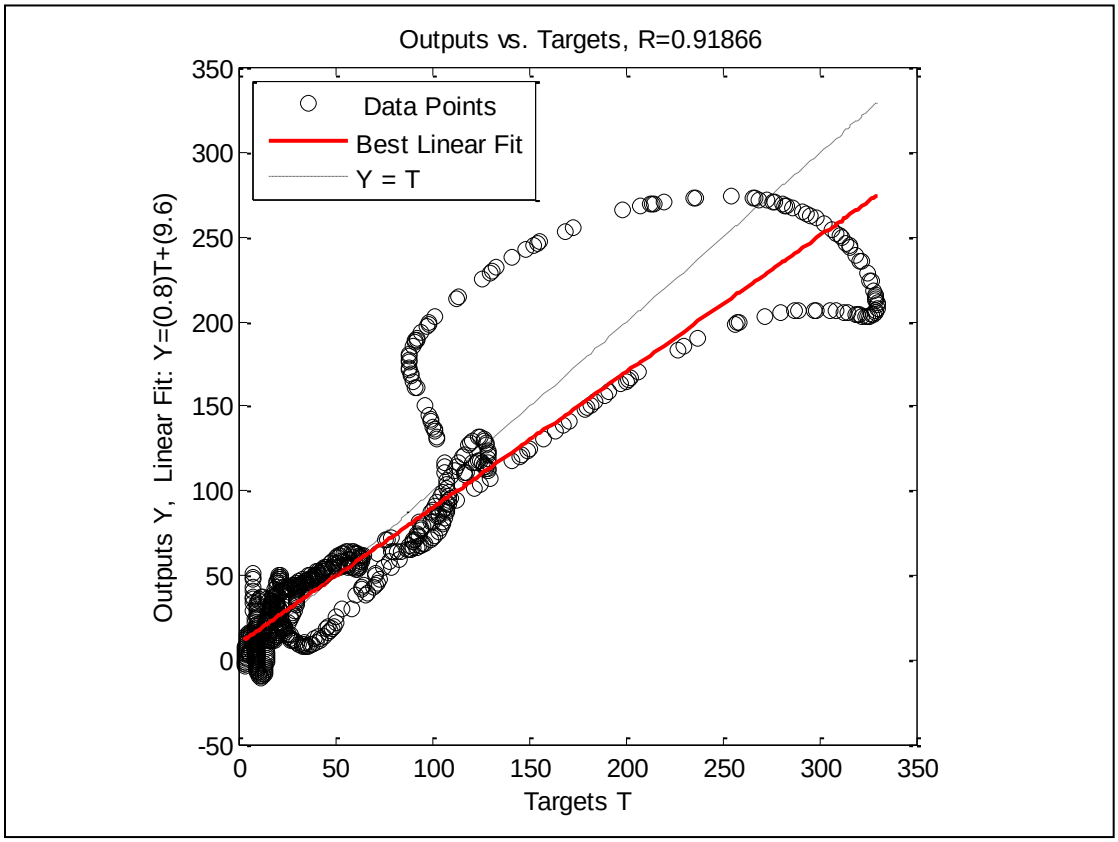

Figure A- 8: Well-1, Case -4, Crossplot

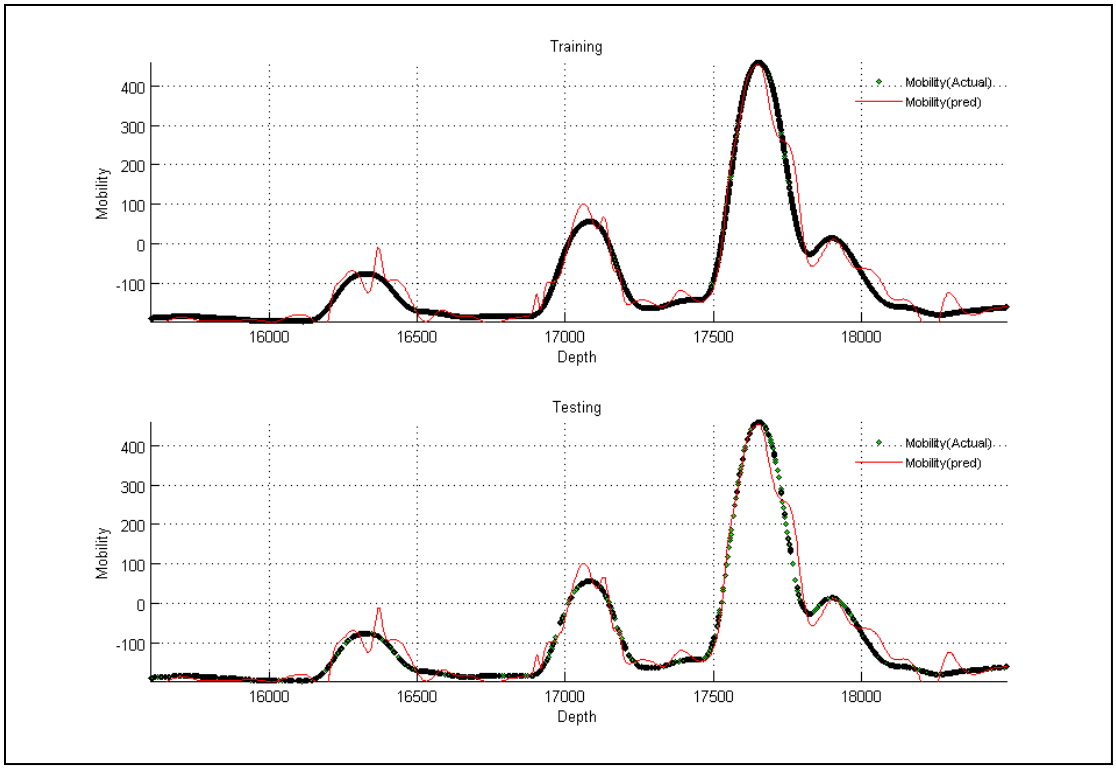

Figure A- 9: Well-1, Case -5

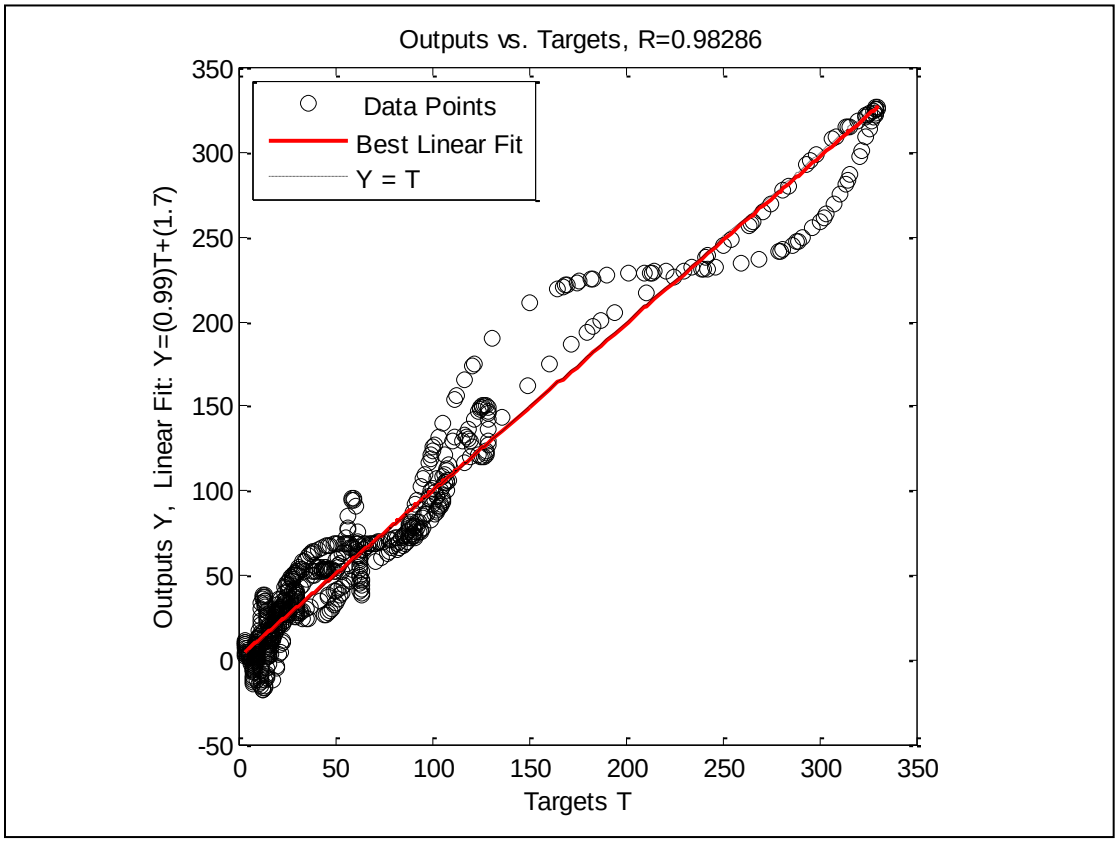

Figure A- 10: Well-1, Case -4, Crossplot

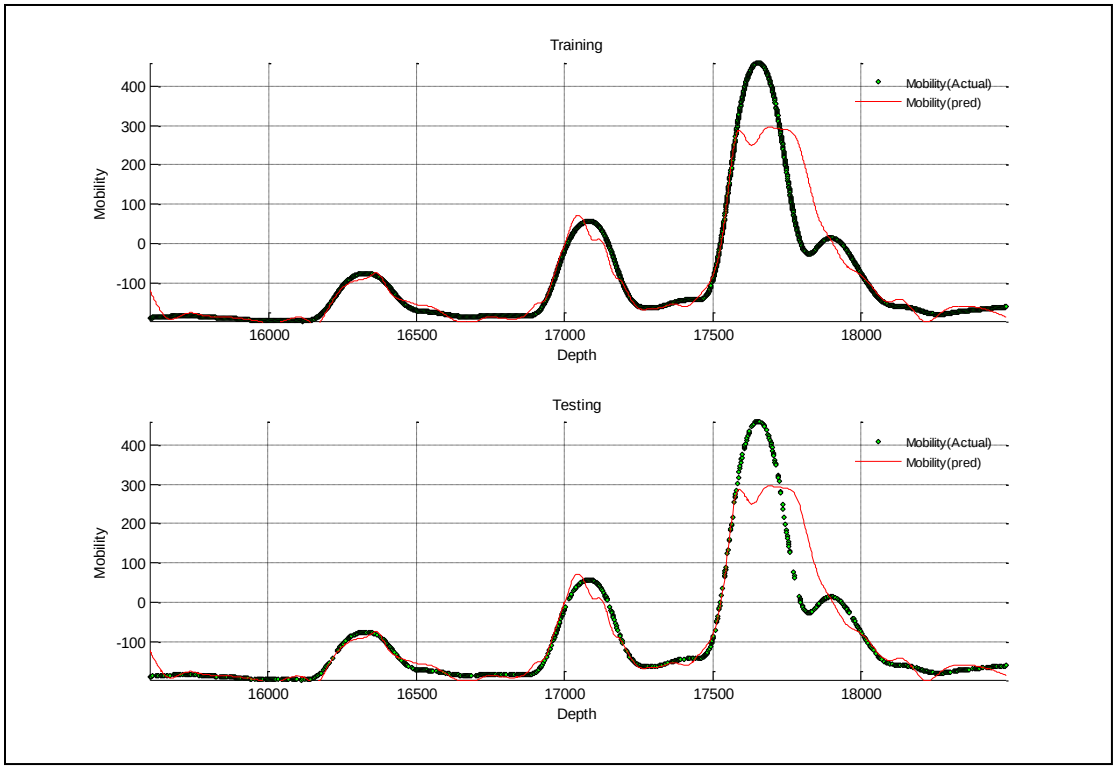

Figure A- 11: Well-1, Case -6

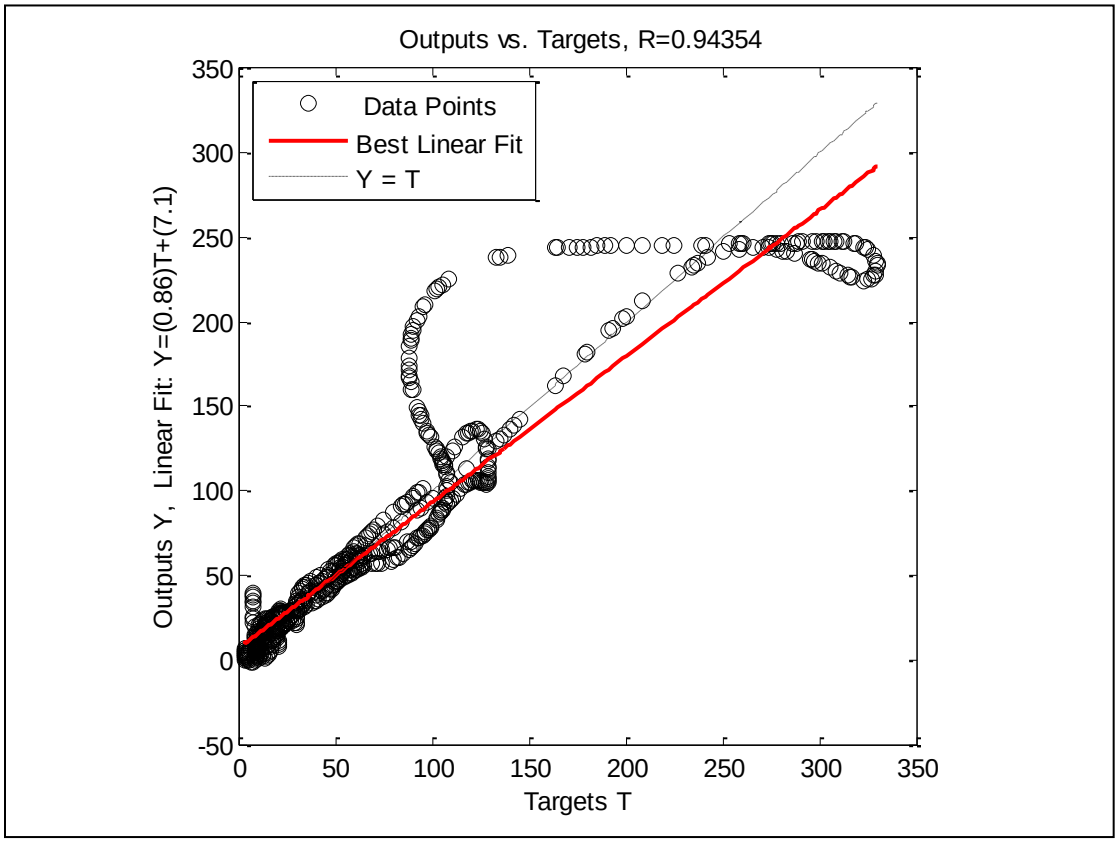

Figure A- 12: Well-1, Case -6, Crossplot

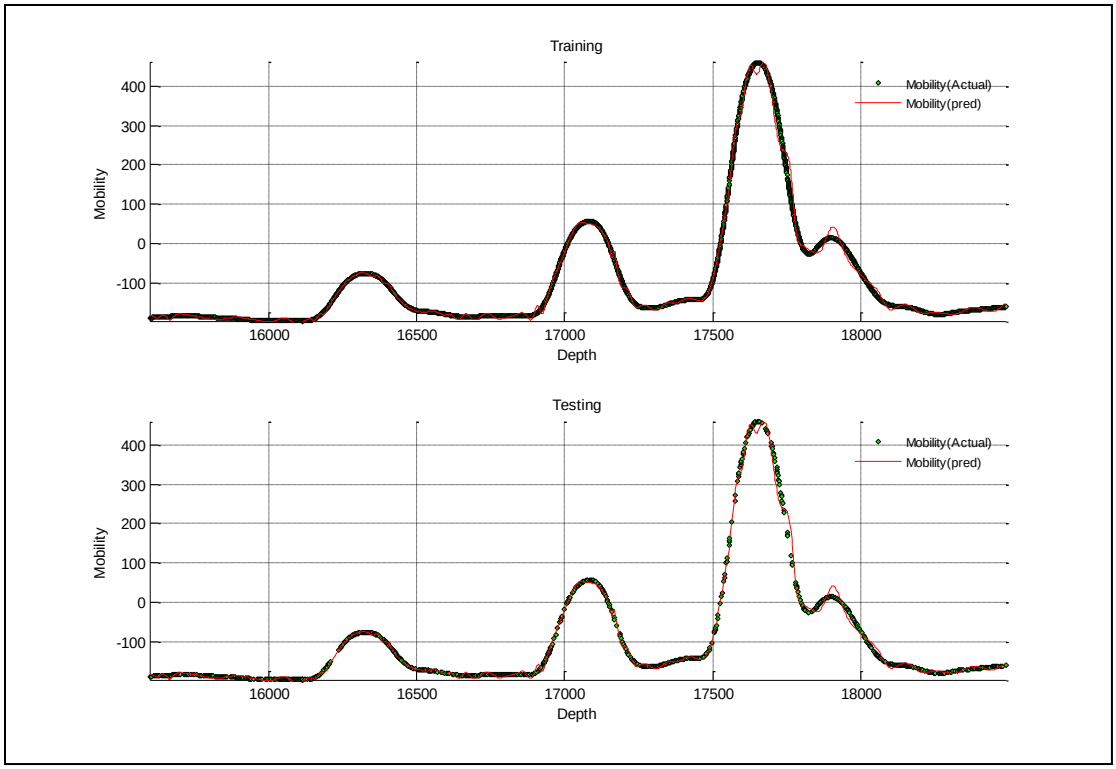

Figure A- 13: Well-1, Case -7

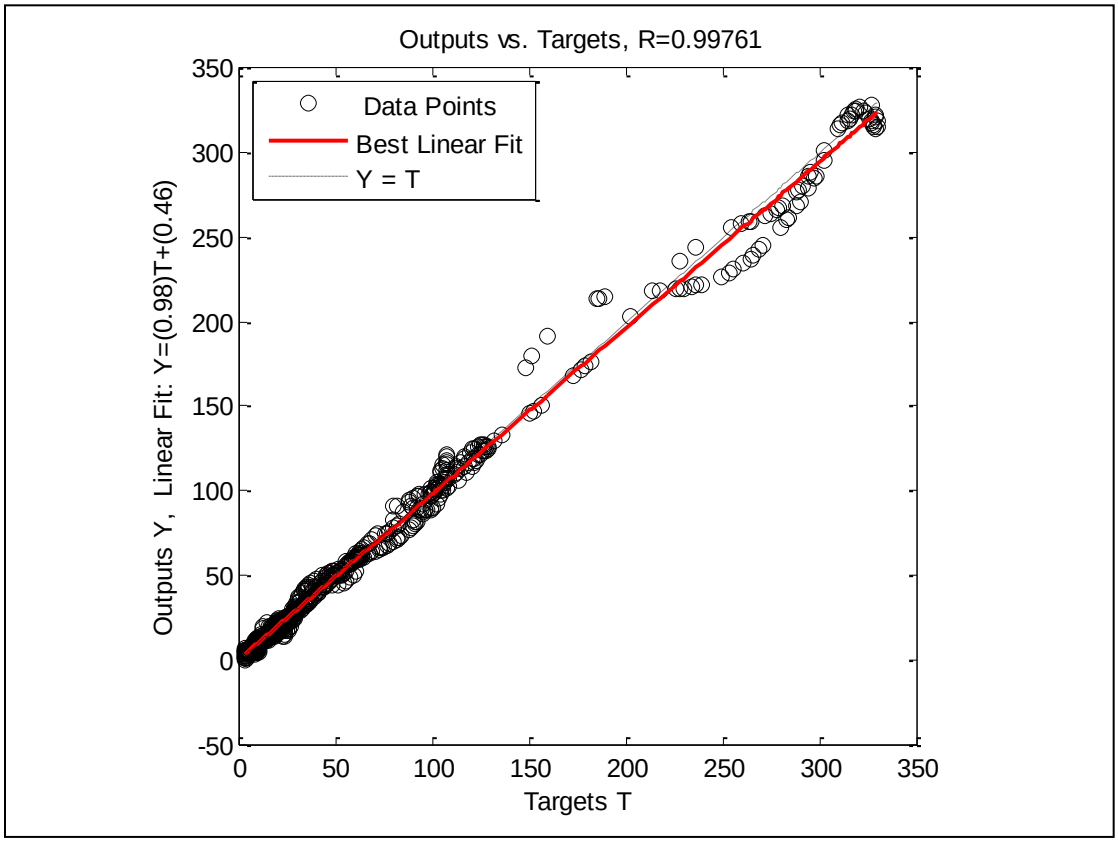

Figure A- 14: Well-1, Case -7, Crossplot

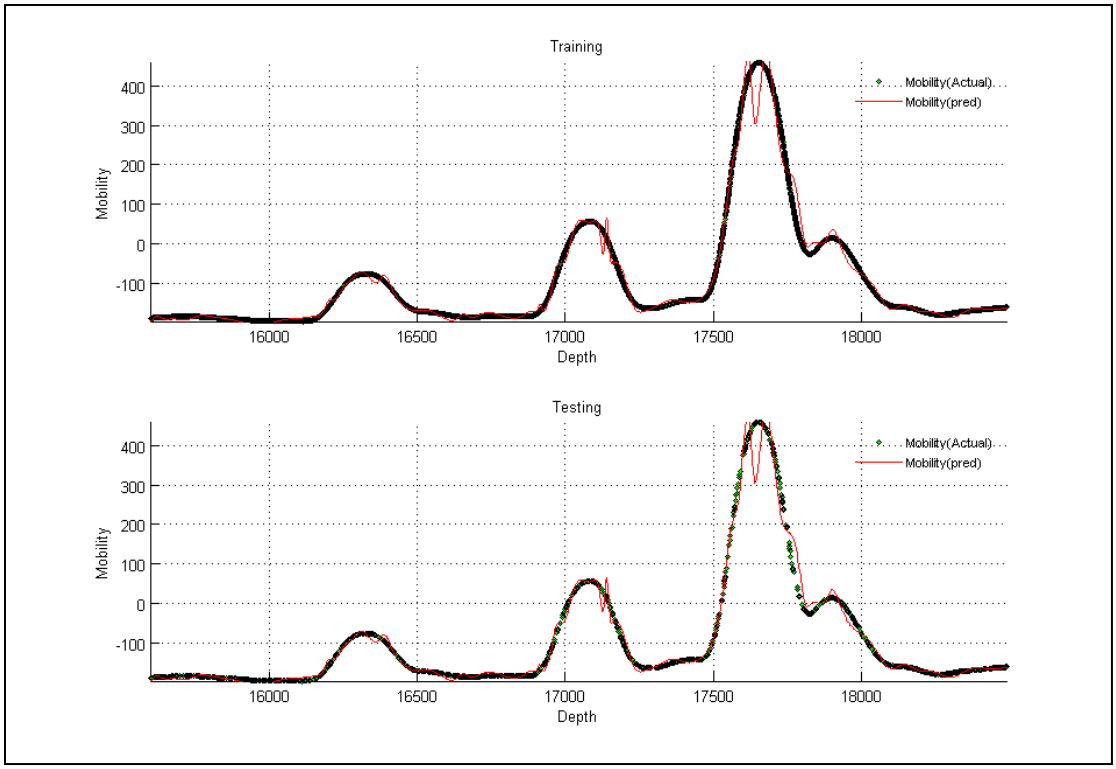

Figure A- 15: Well-1, Case -8

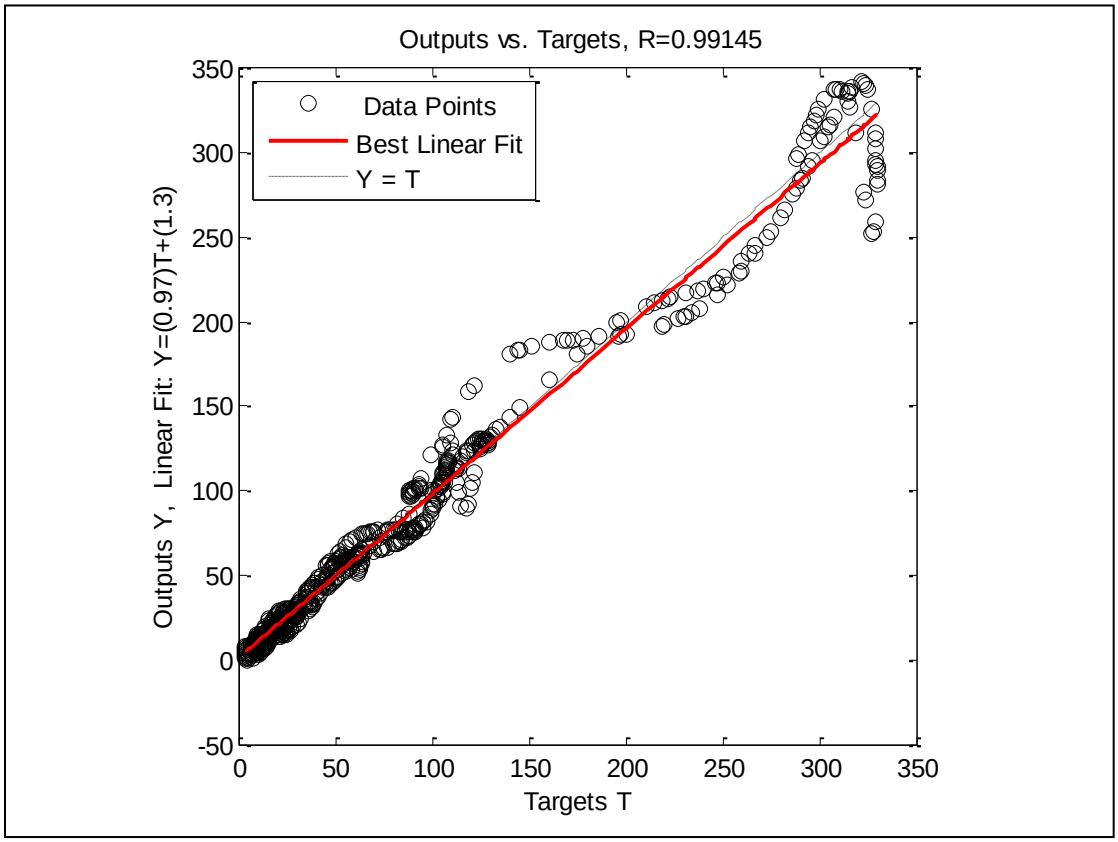

Figure A- 16: Well-1, Case -8, Crossplot

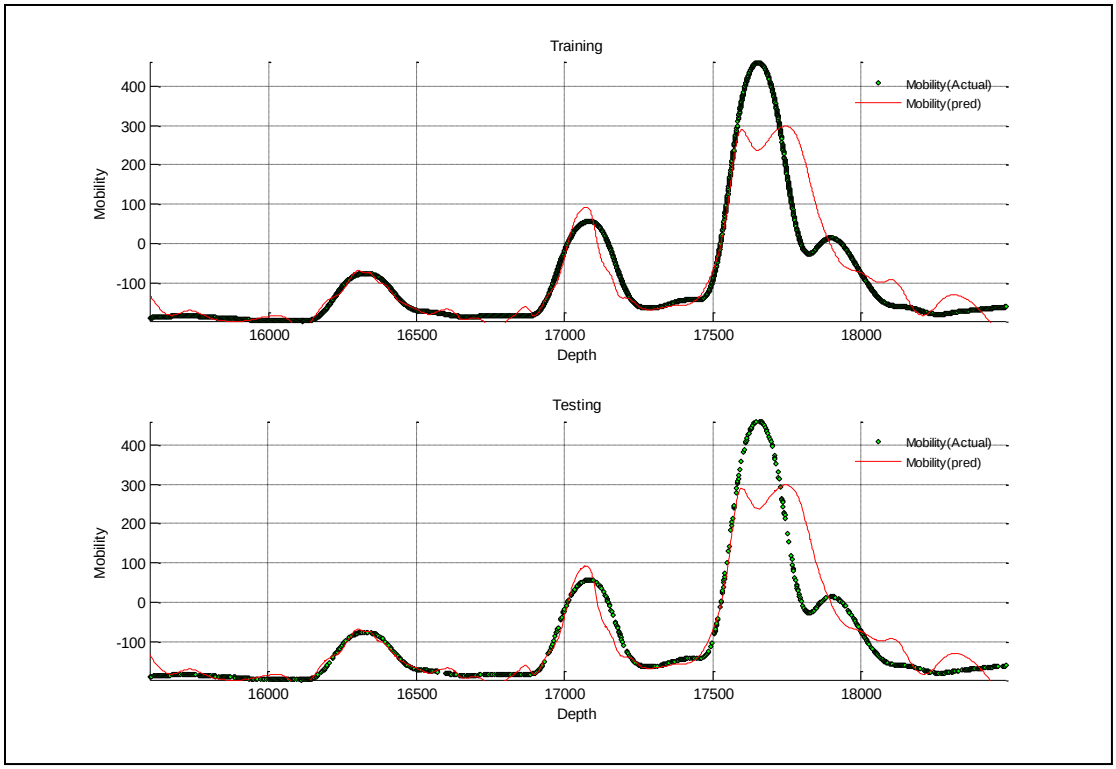

Figure A- 17: Well-1, Case -9

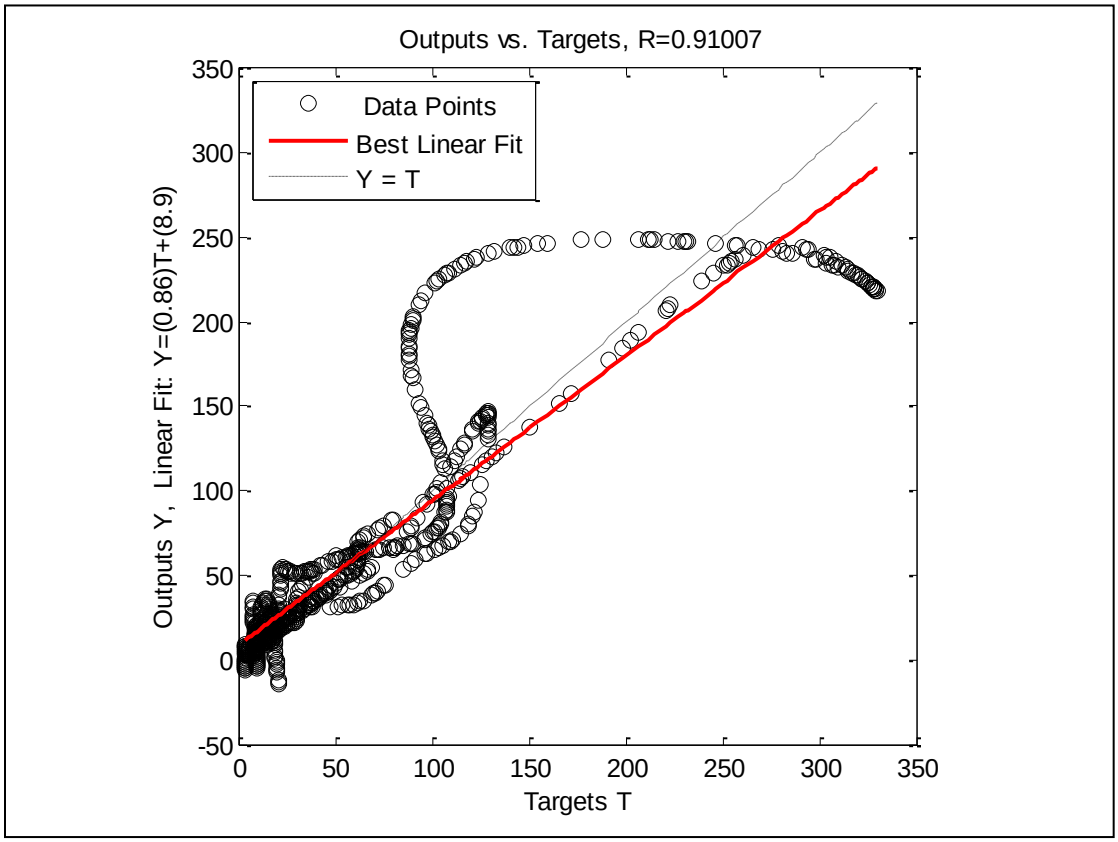

Figure A- 18: Well-1, Case -9, Crossplot

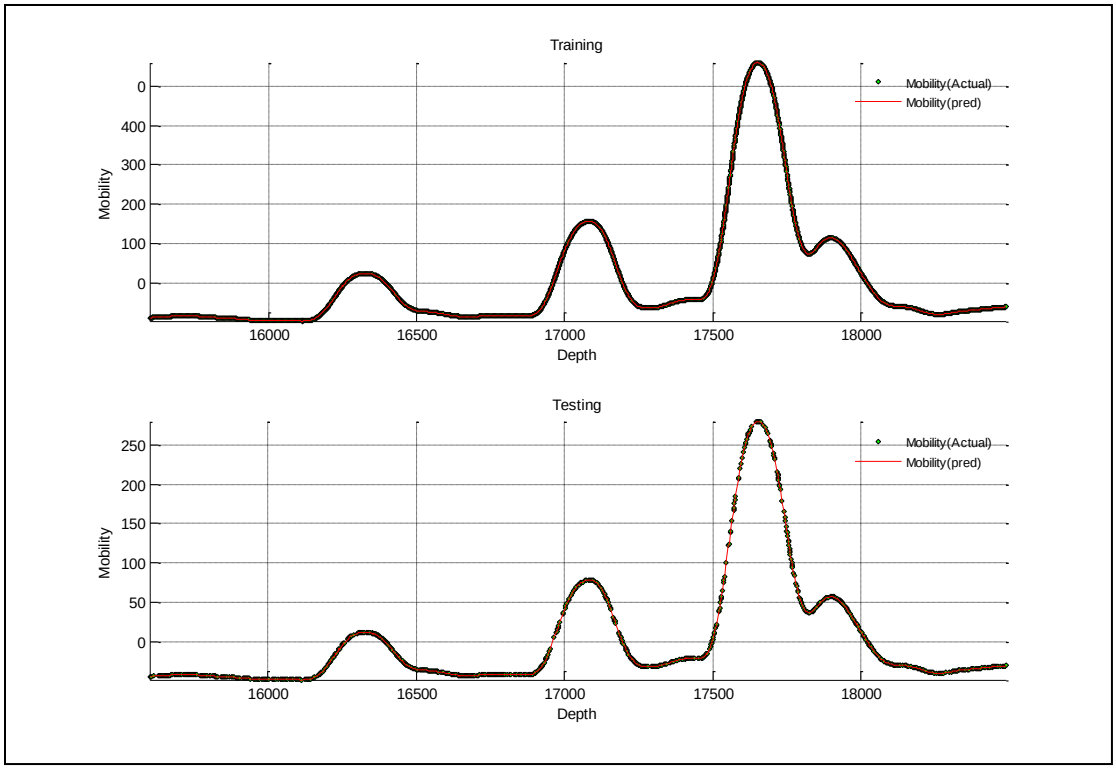

Figure A- 19: Well-1, Case -10

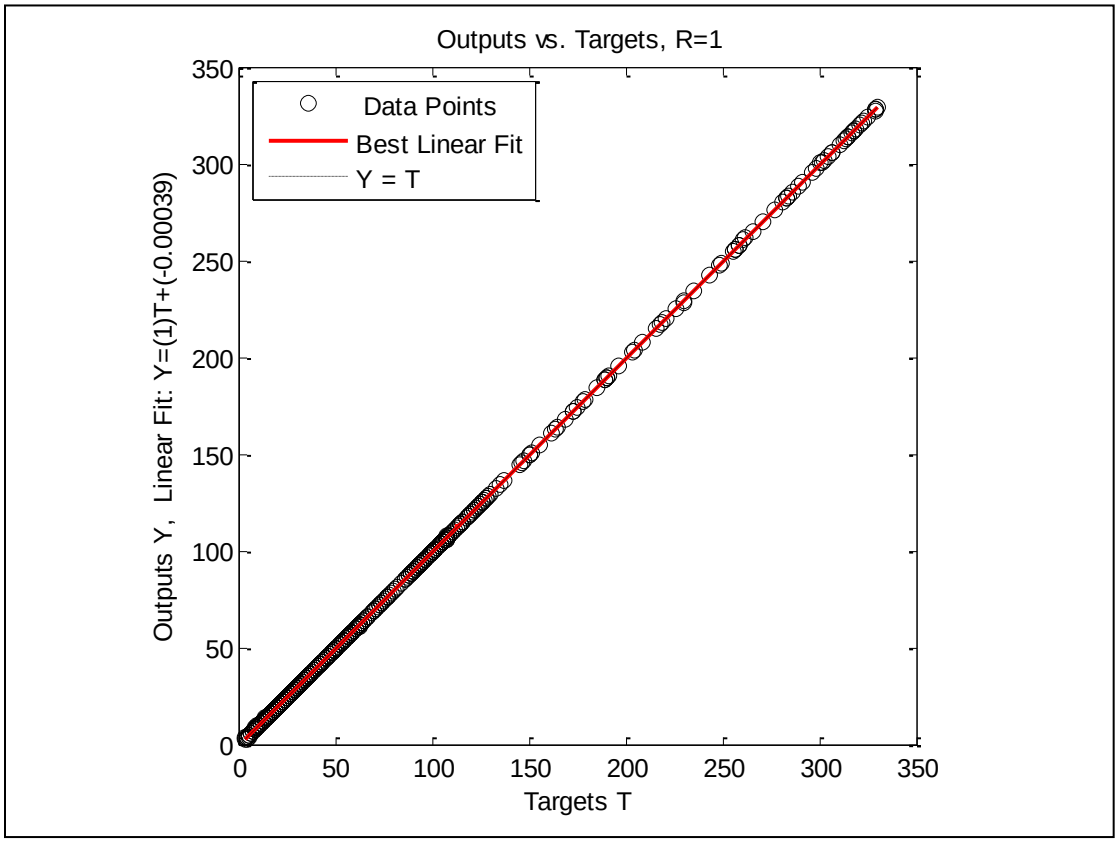

Figure A- 20: Well-1, Case -10, Crossplot

Well No. 2

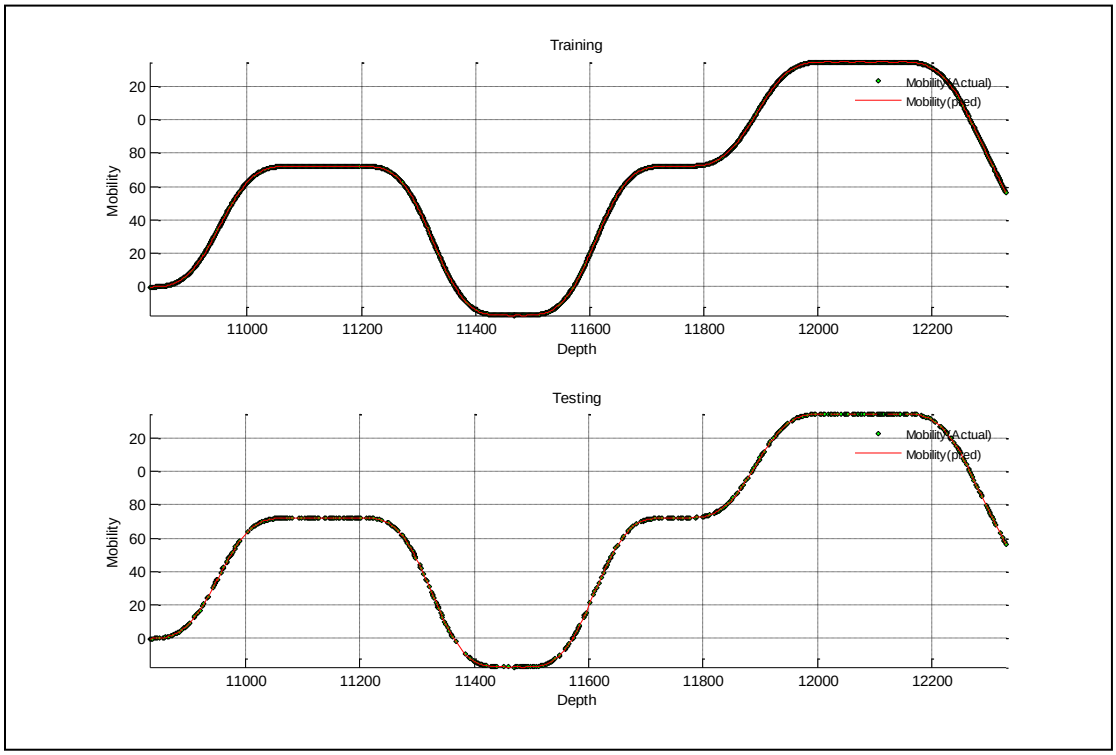

Figure A- 21: Well-2, Case -1

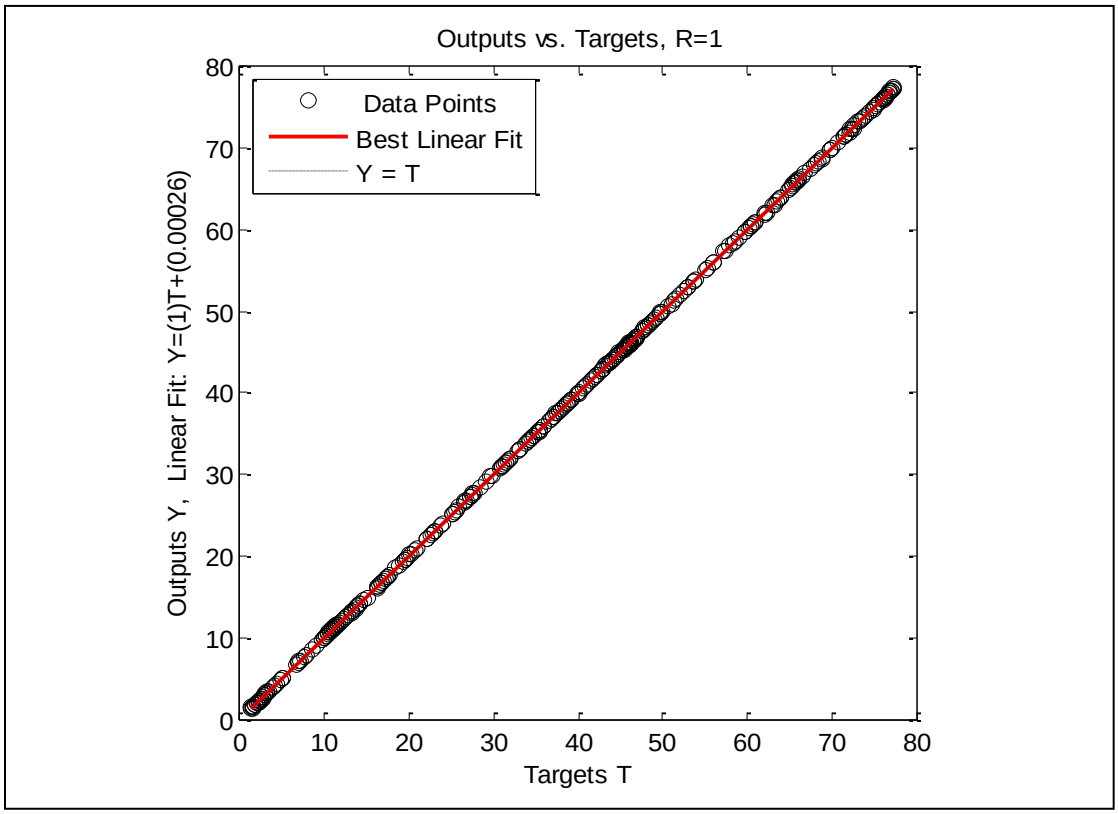

Figure A- 22: Well-2, Case -1, Crossplot

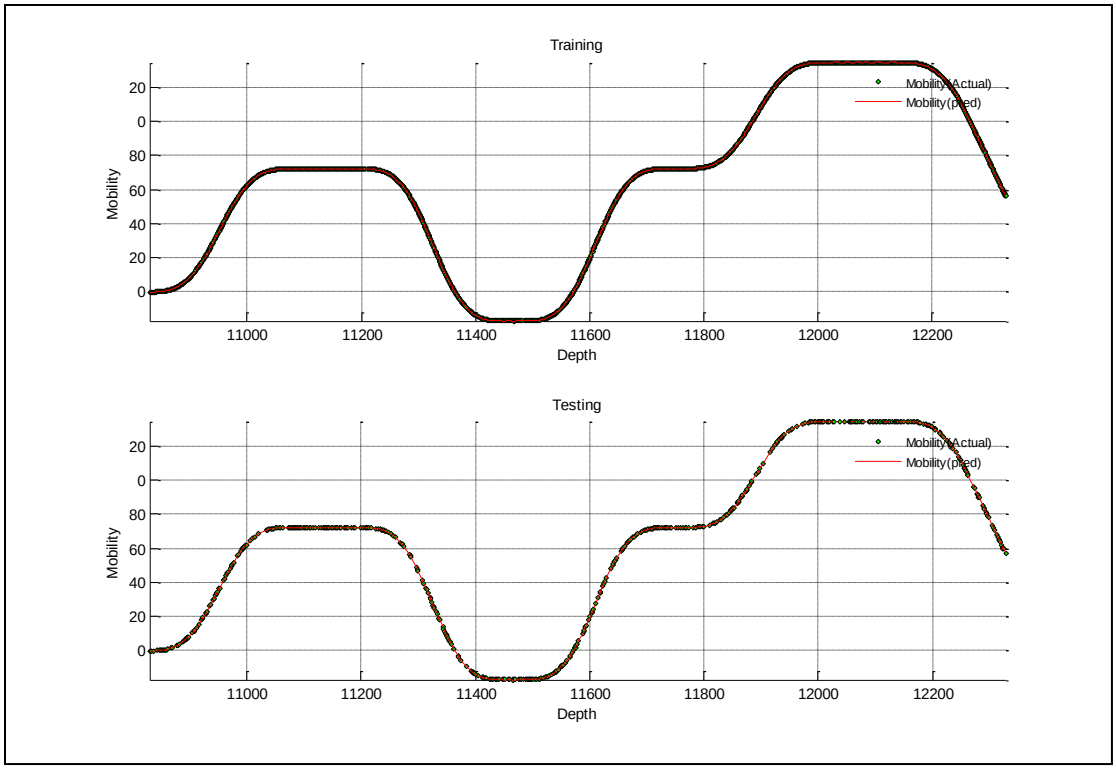

Figure A- 23: Well-2, Case -2

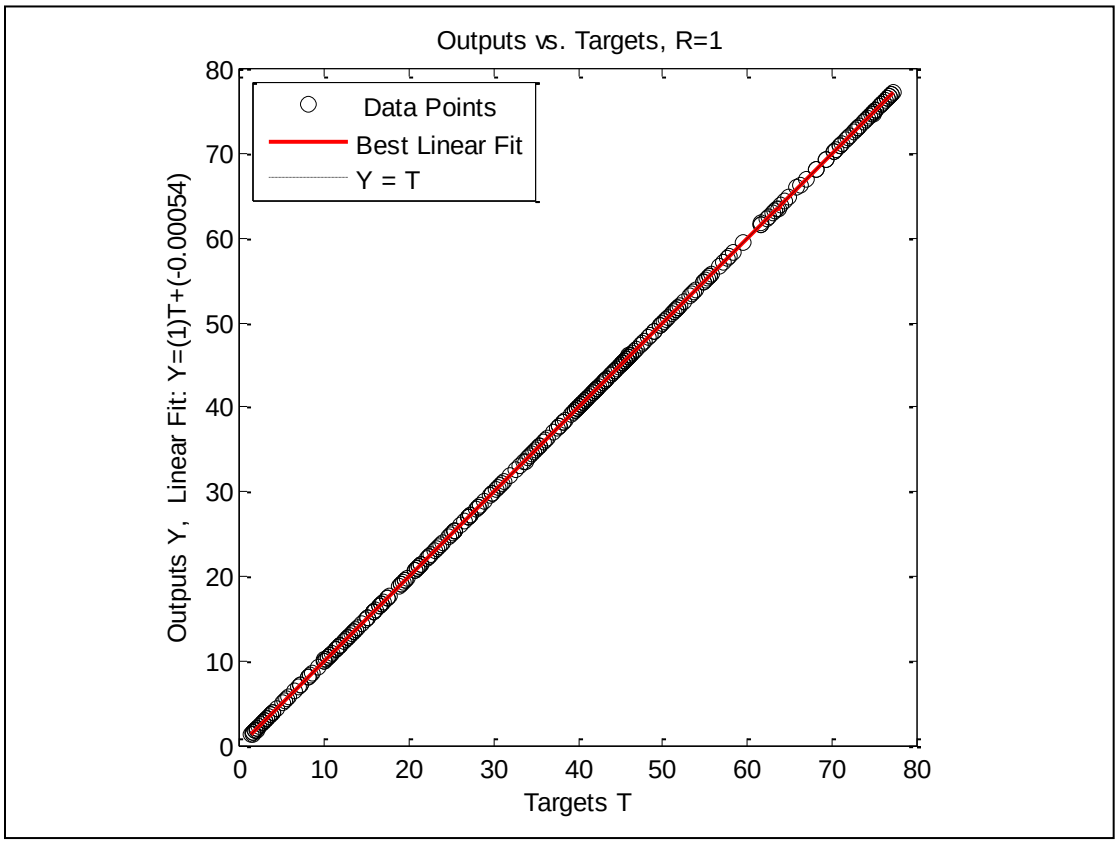

Figure A- 24: Well-2, Case -2, Crossplot

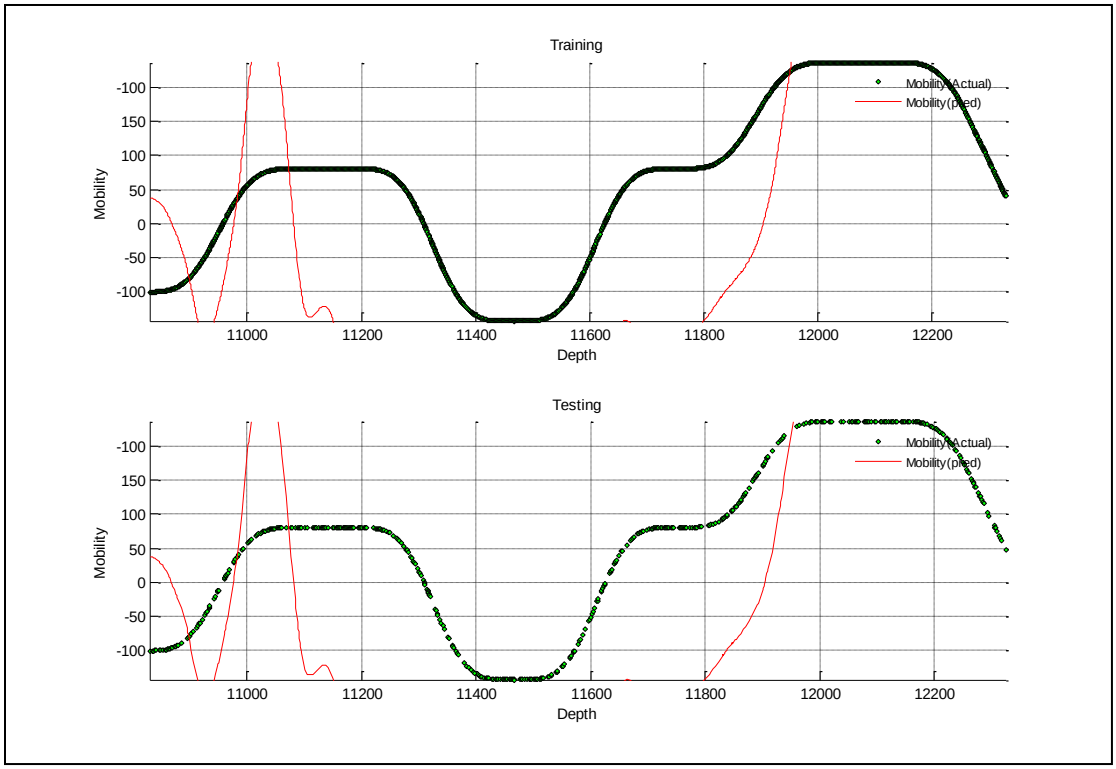

Figure A- 25: Well-2, Case -3

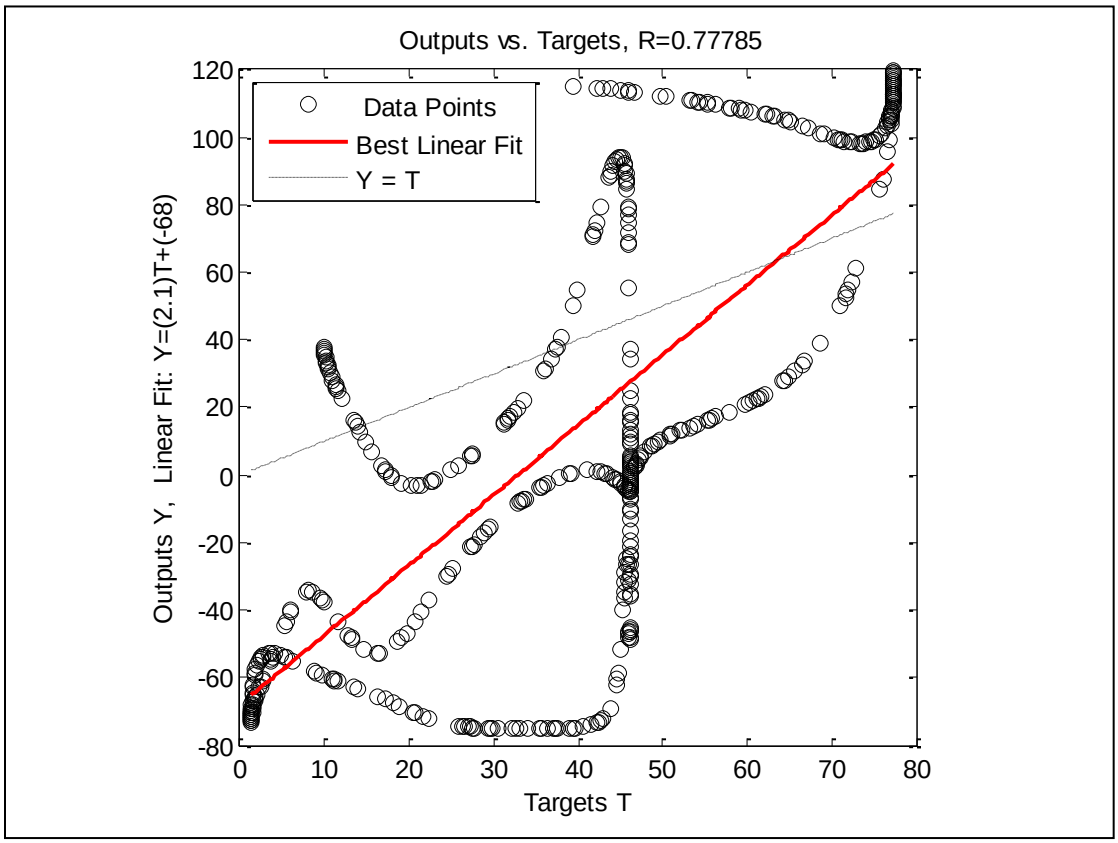

Figure A- 26: Well-2, Case -3, Crossplot

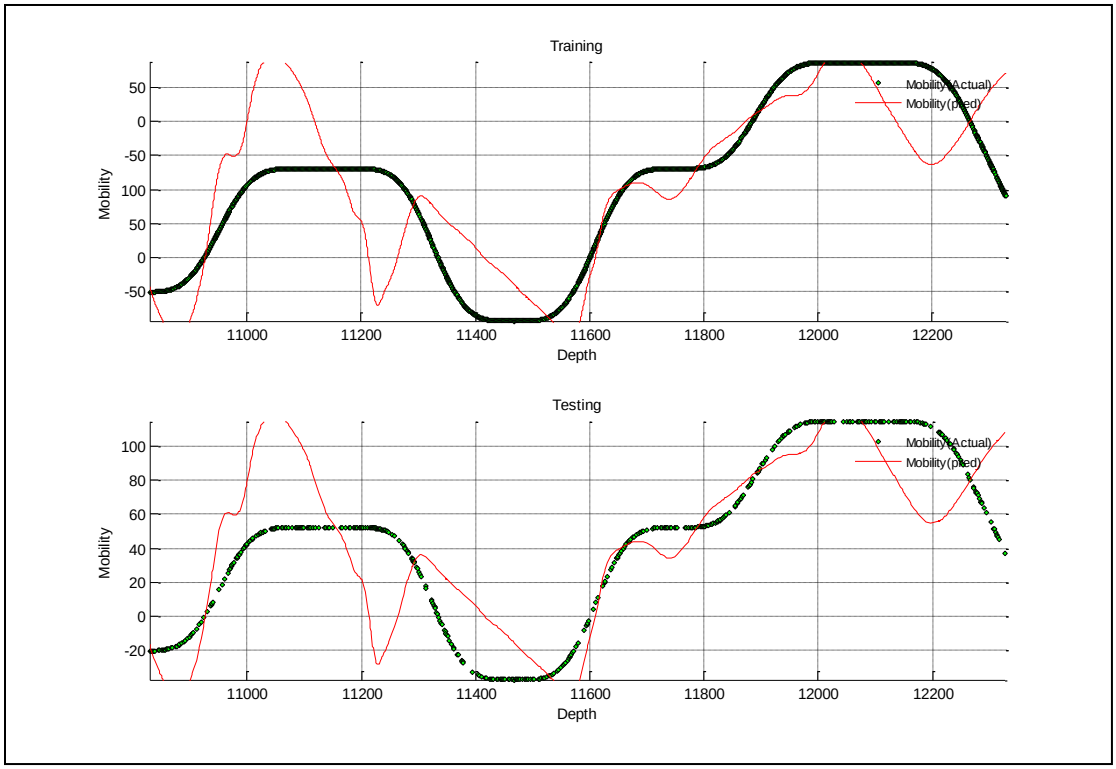

Figure A- 27: Well-2, Case -4

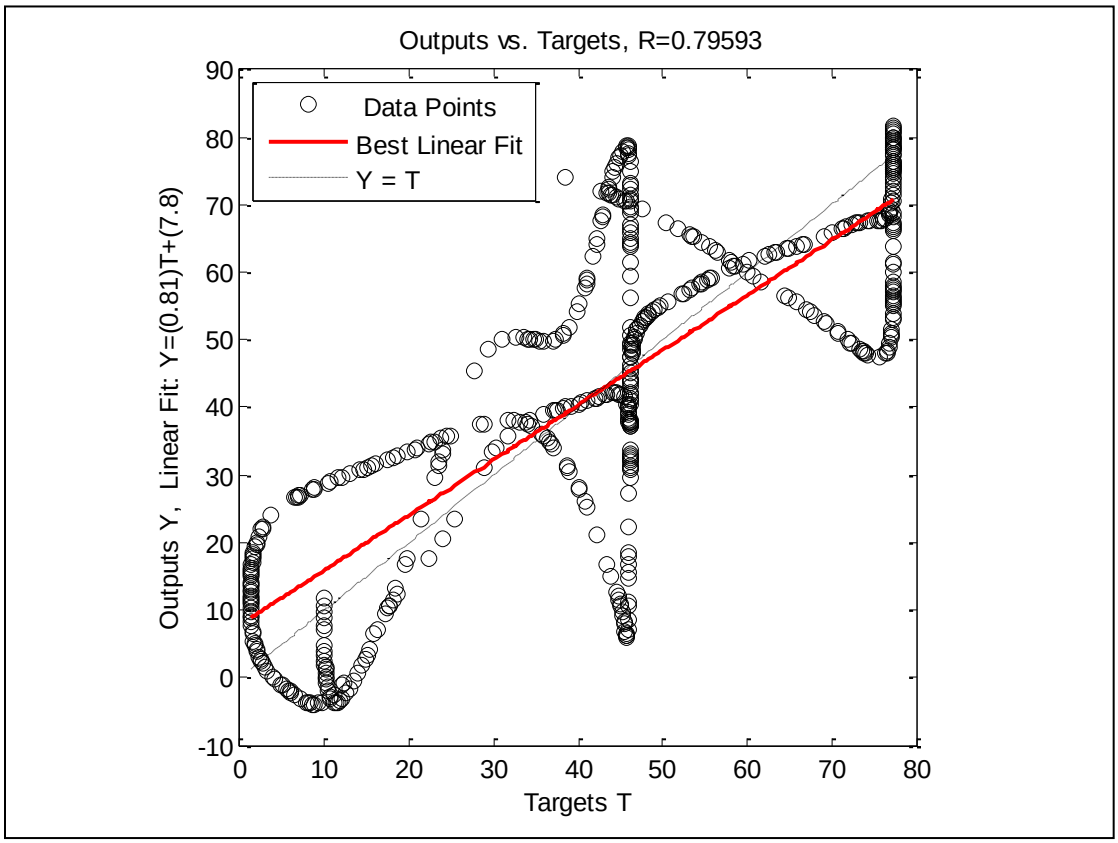

Figure A- 28: Well-2, Case -4, Crossplot

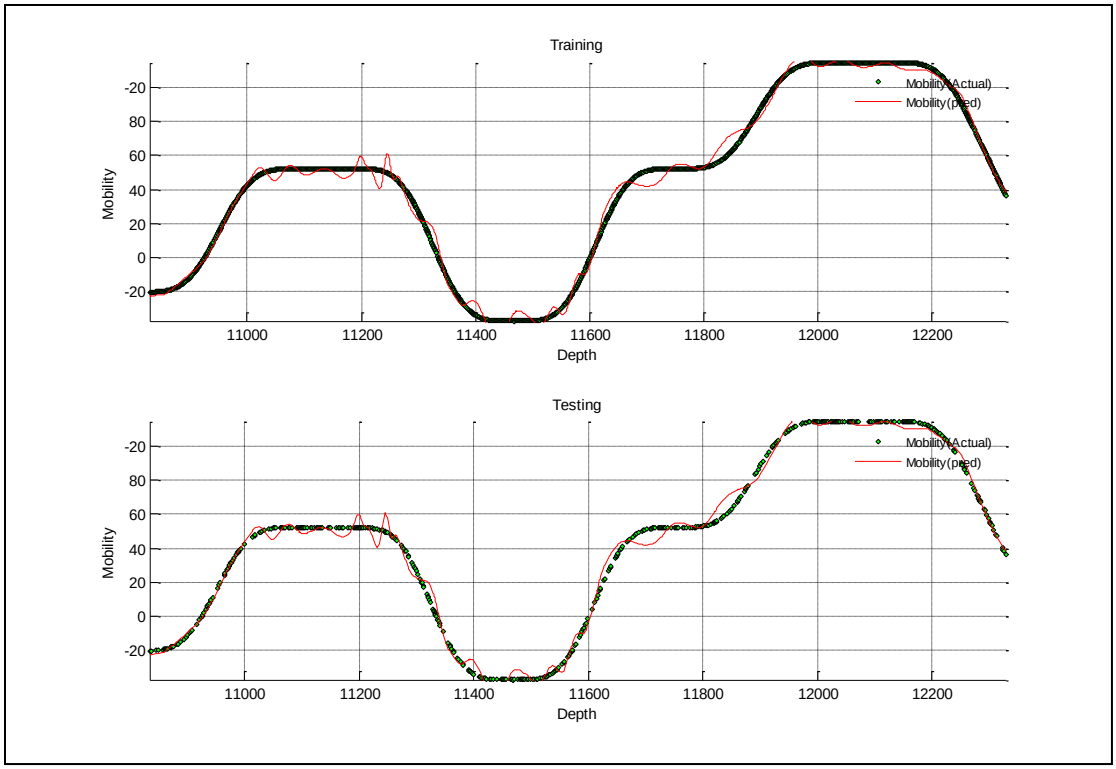

Figure A- 29: Well-2, Case -5

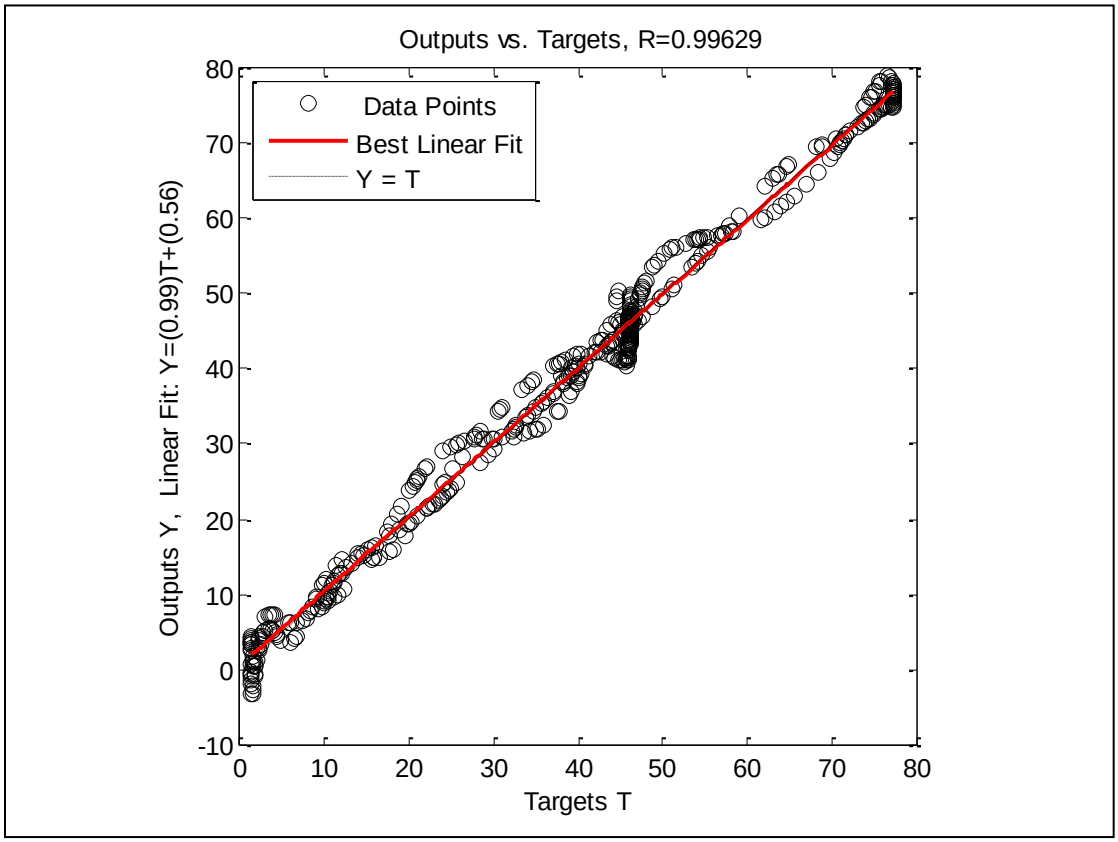

Figure A- 30: Well-2, Case -5, Crossplot

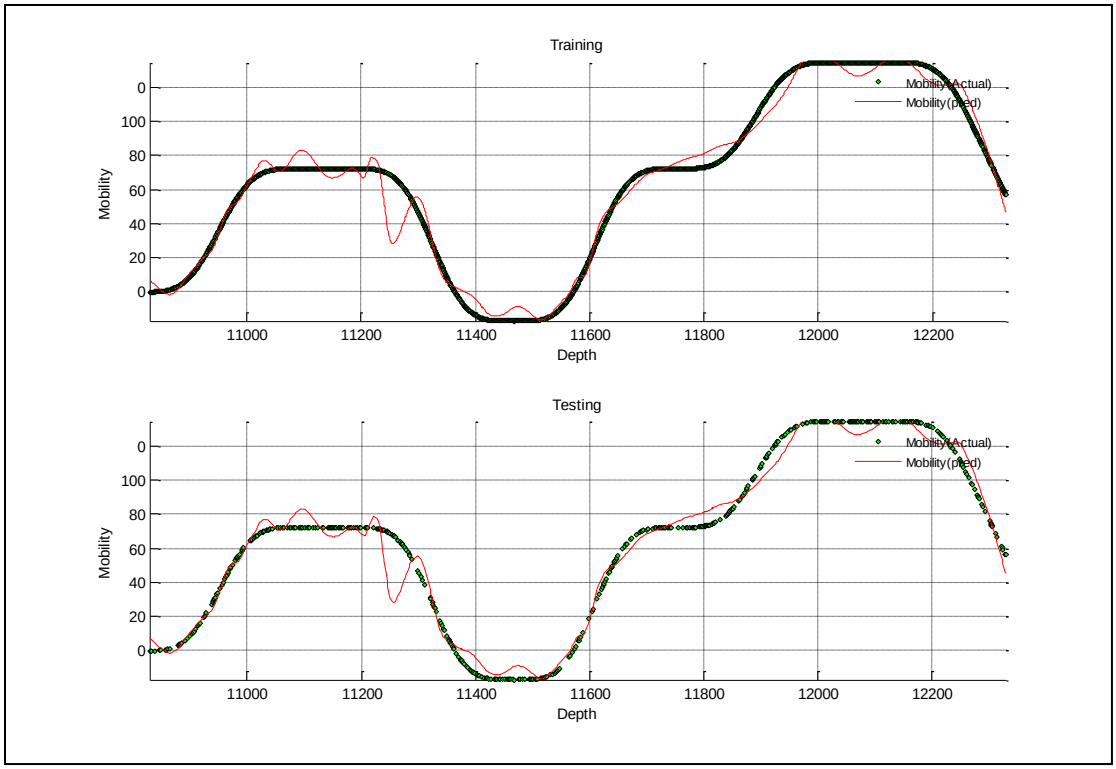

Figure A- 31: Well-2, Case -6

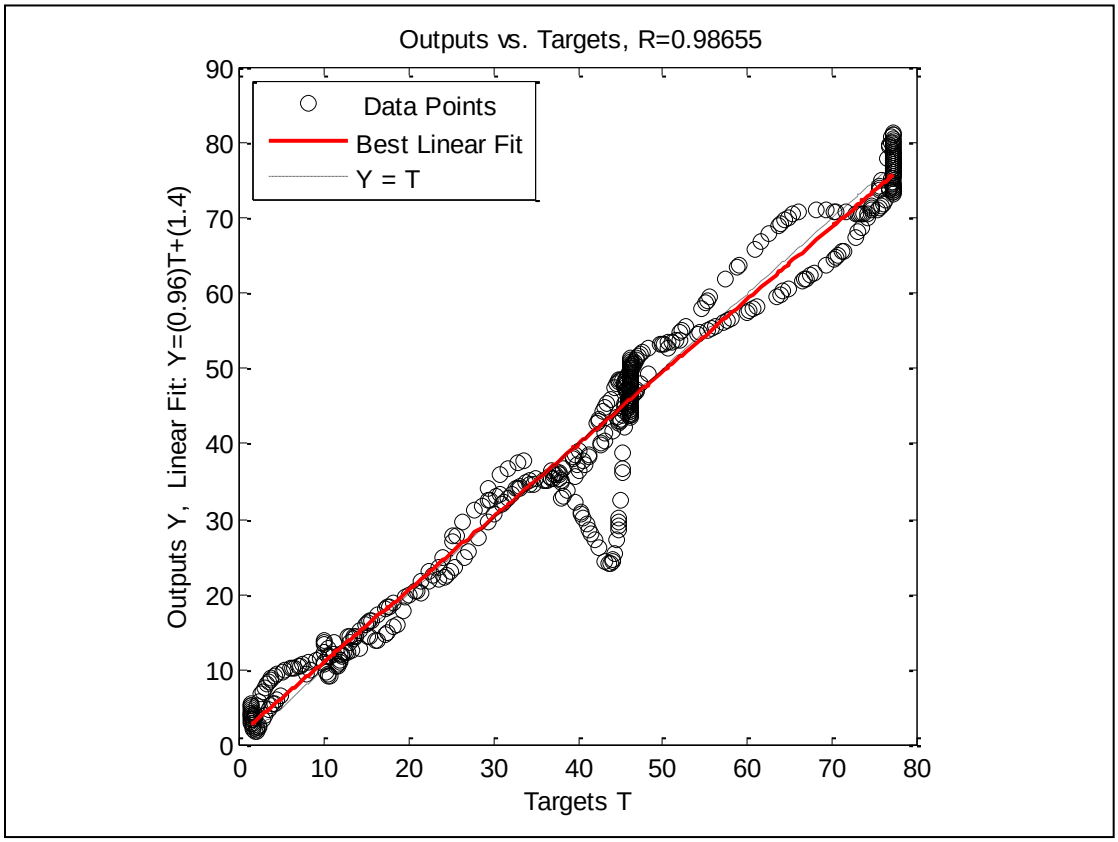

Figure A- 32: Well-2, Case -6, Crossplot

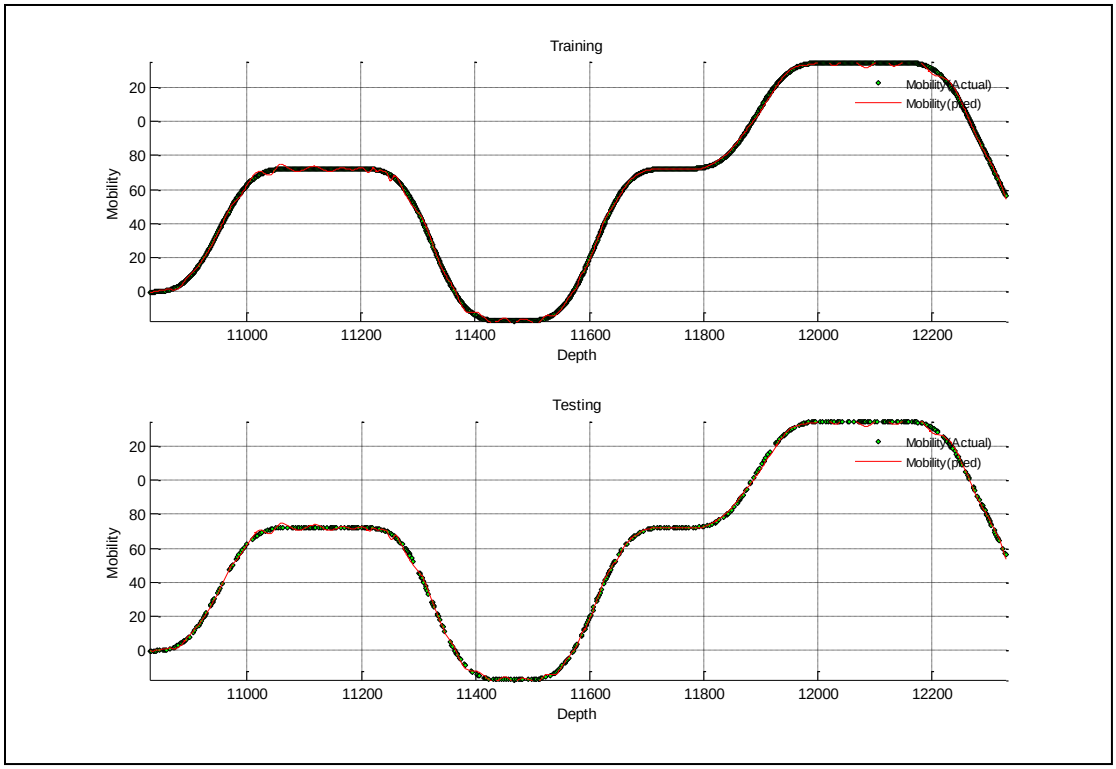

Figure A- 33: Well-2, Case -7

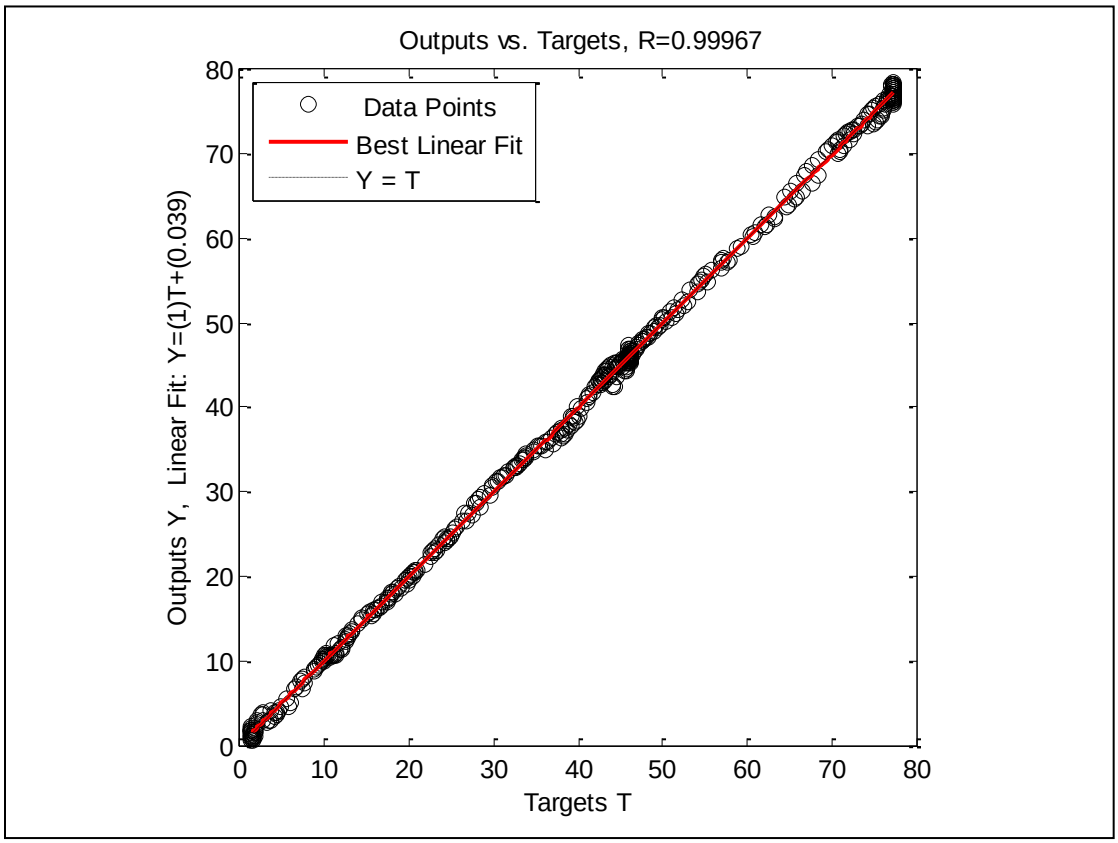

Figure A- 34: Well-2, Case -7, Crossplot

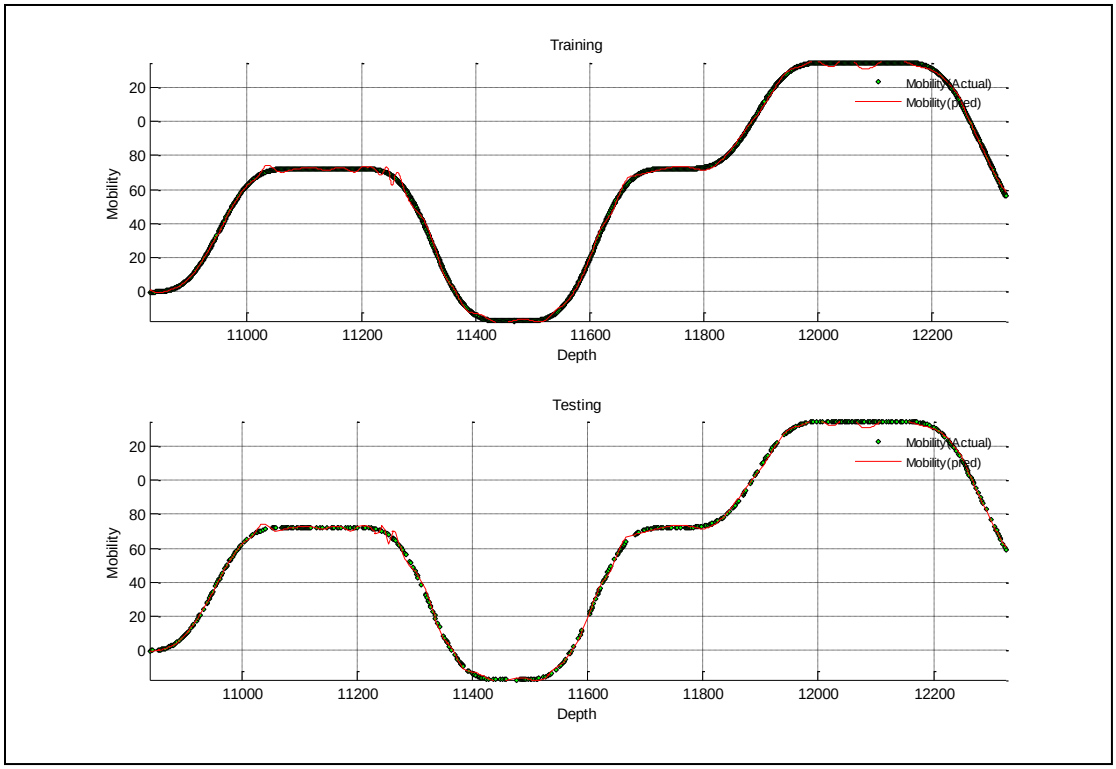

Figure A- 35: Well-2, Case -8

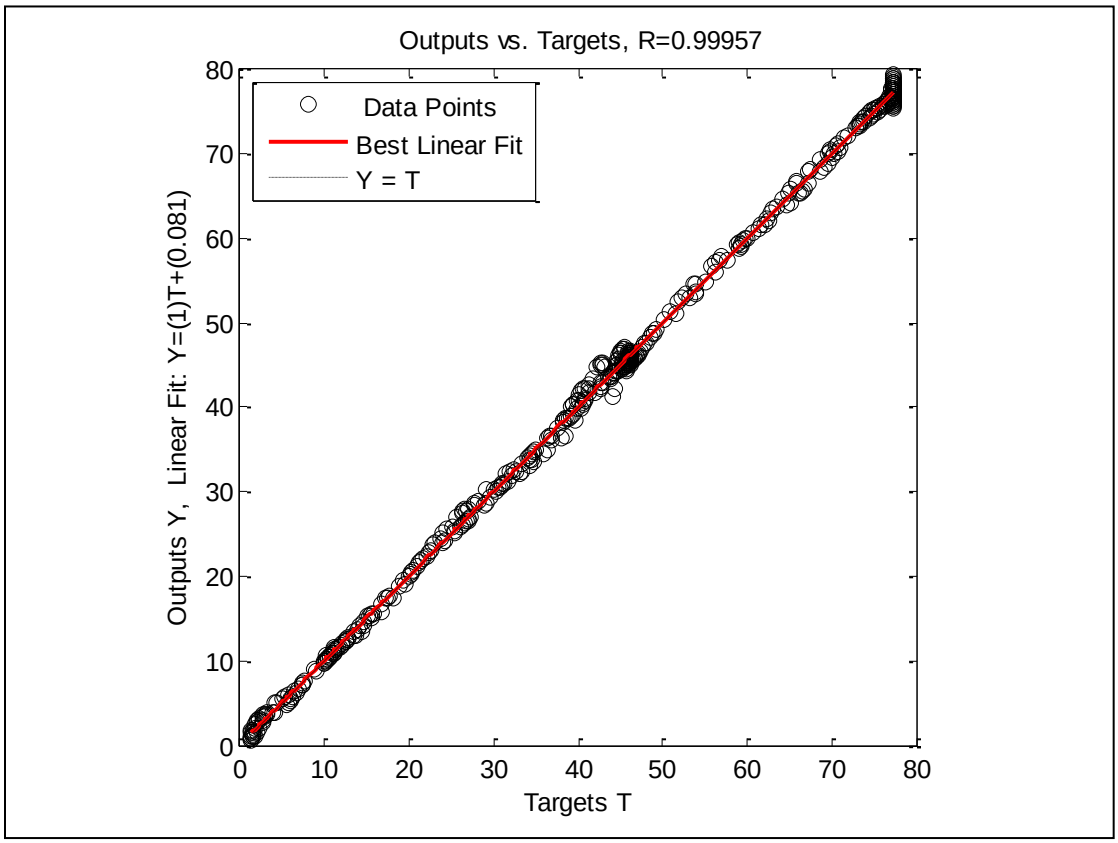

Figure A- 36: Well-2, Case -8, Crossplot

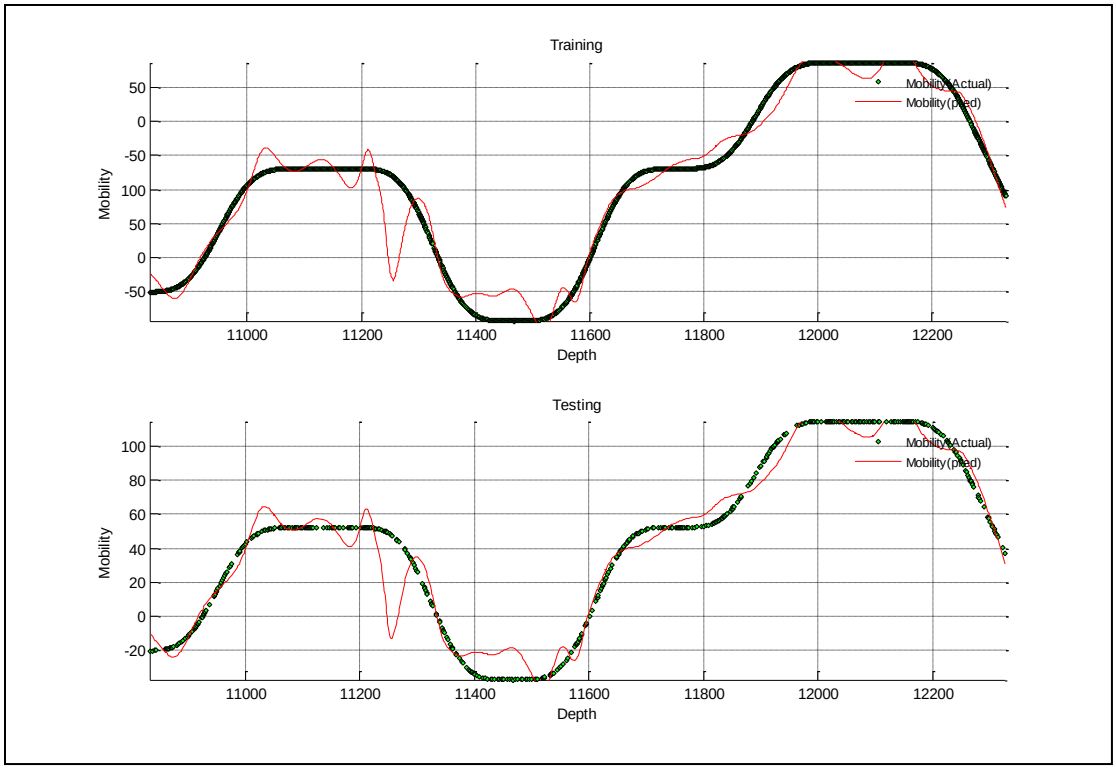

Figure A- 37: Well-2, Case -9

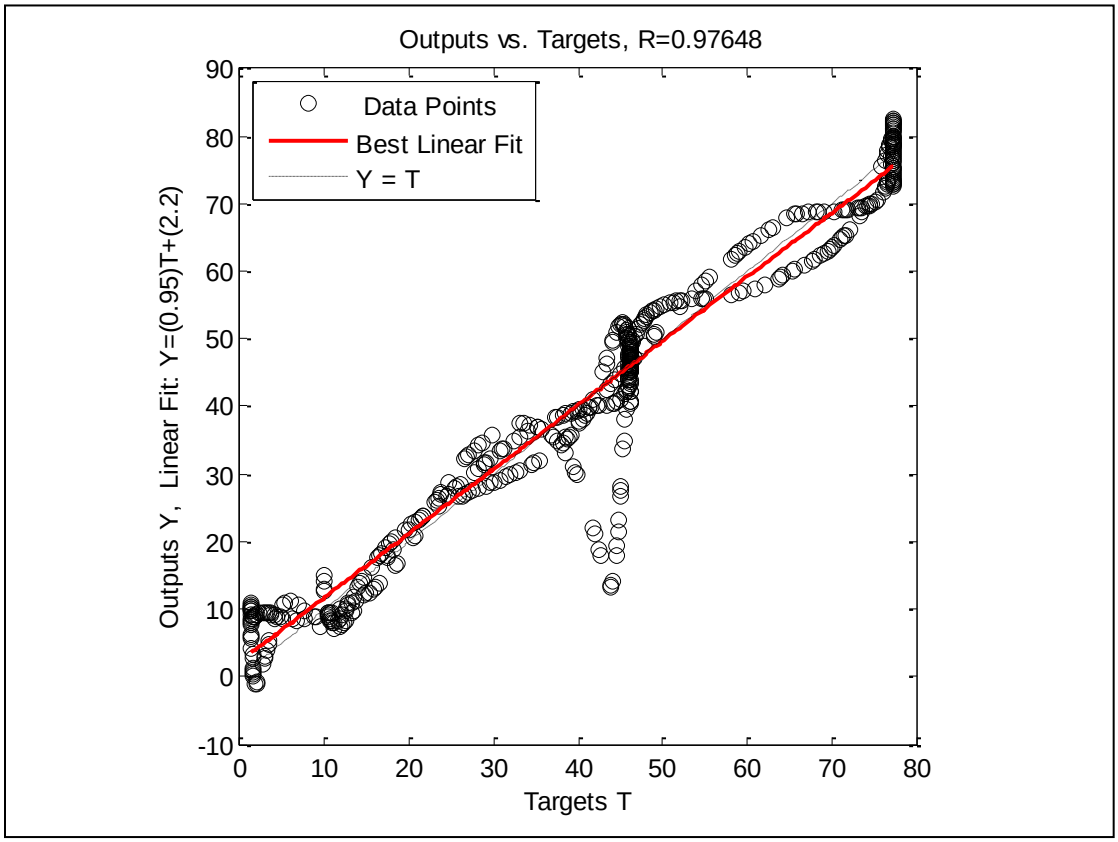

Figure A- 38: Well-2, Case -9, Crossplot

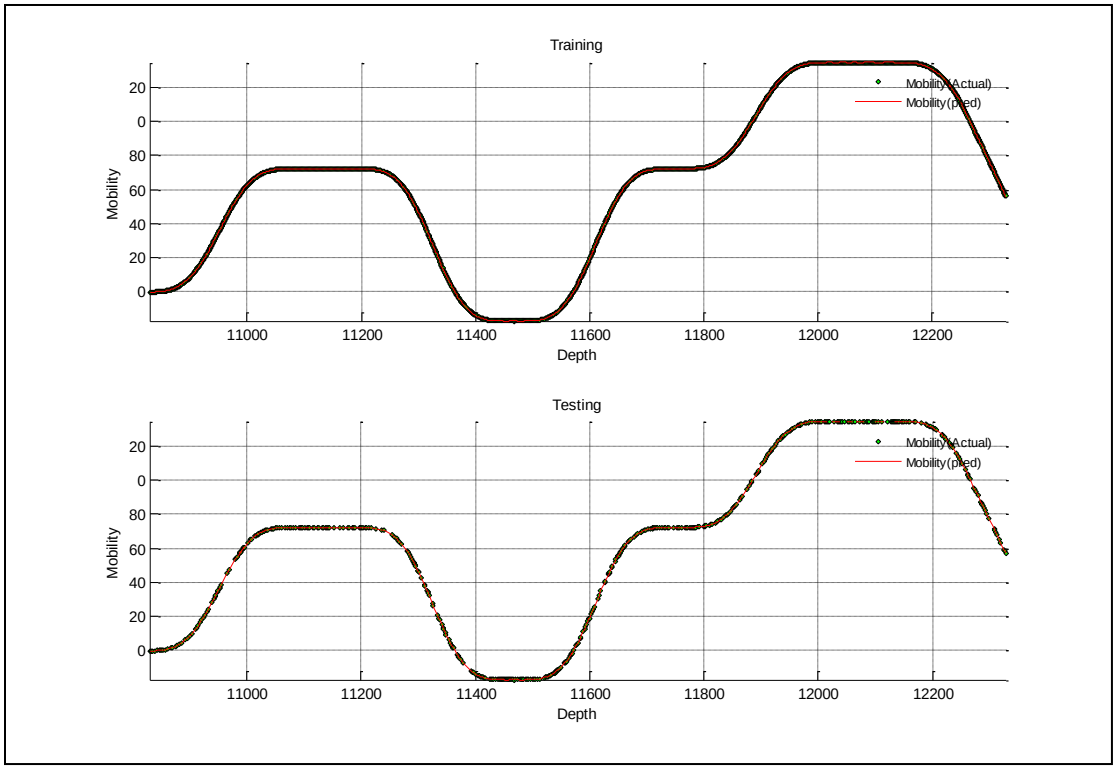

Figure A- 39: Well-2, Case -10

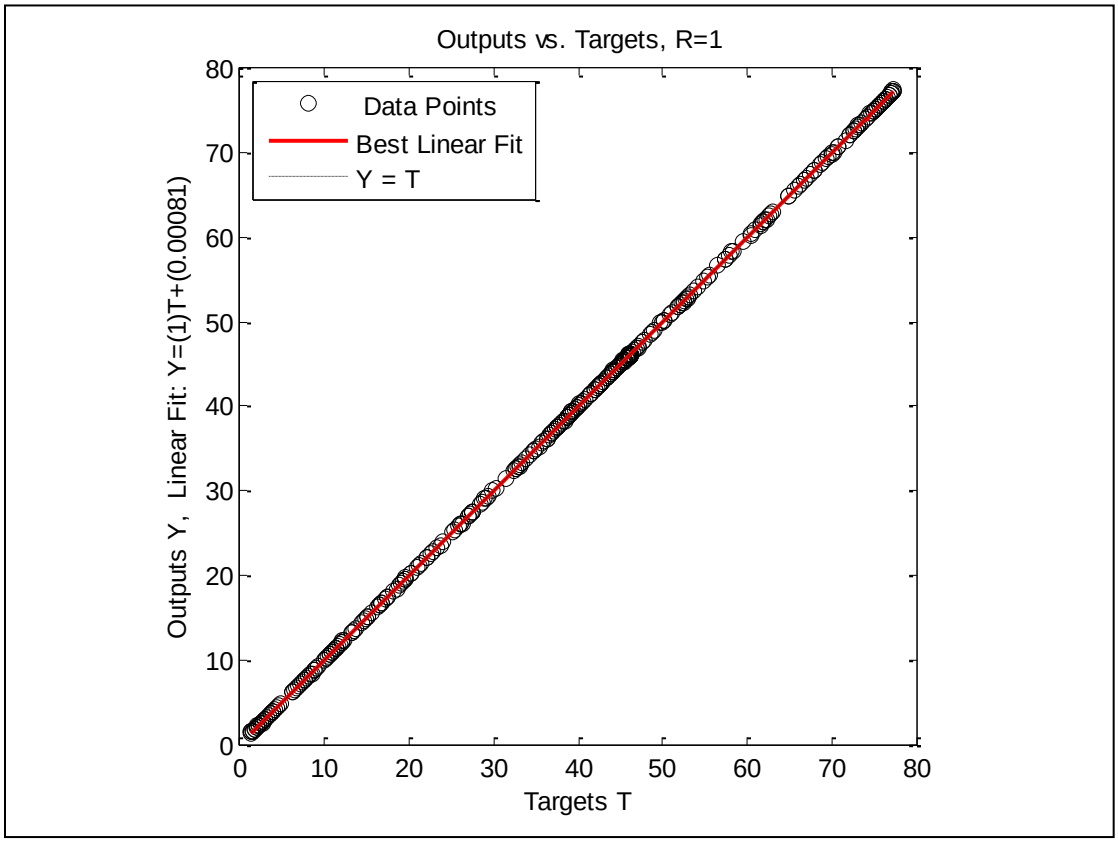

Figure A- 40: Well-2, Case -10, Crossplot

Well No. 3

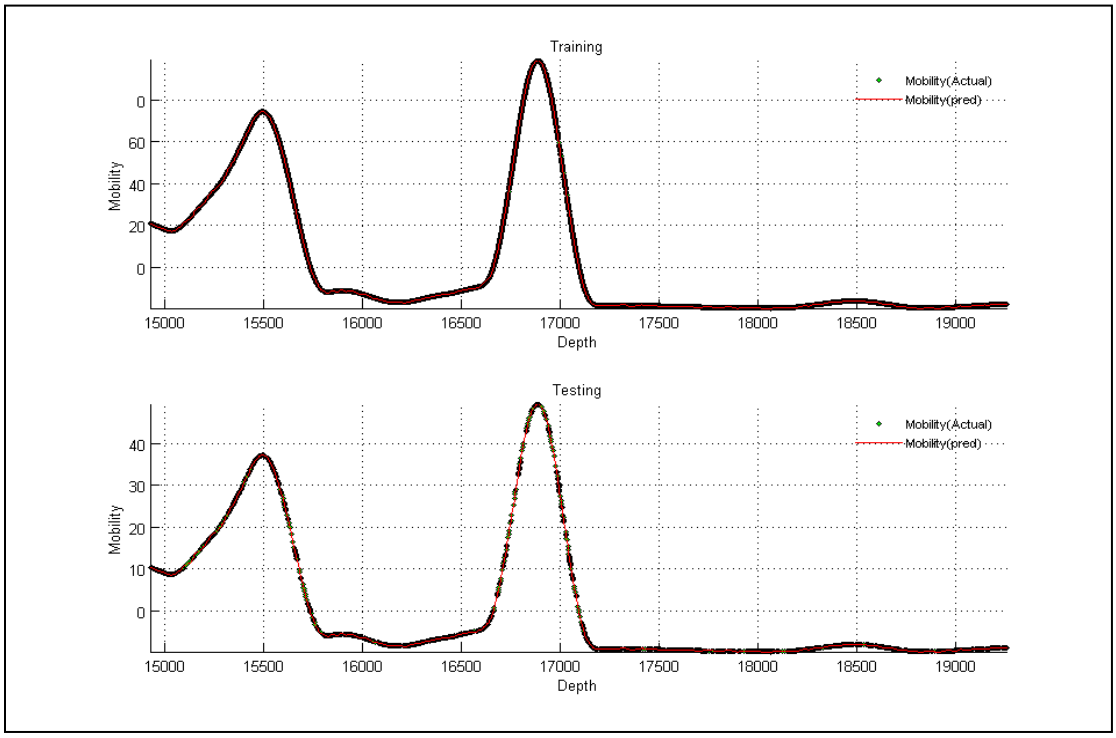

Figure A- 41: Well-3, Case -1

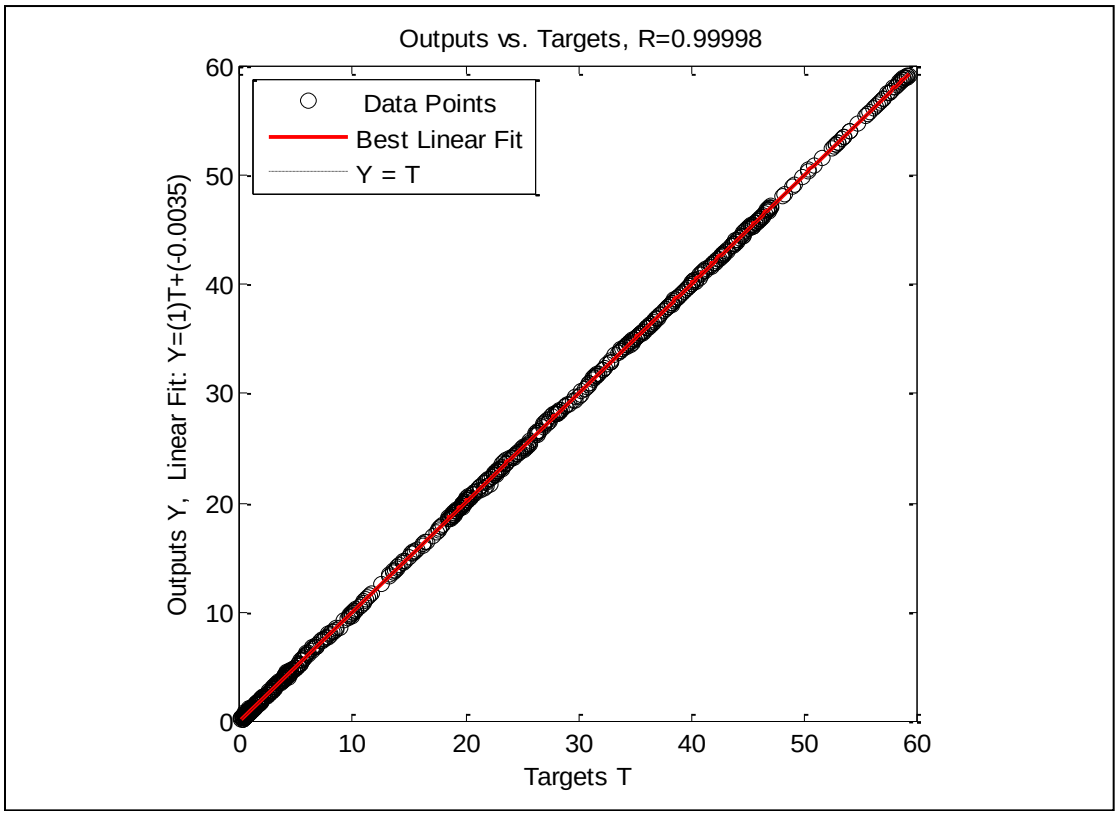

Figure A- 42: Well-3, Case -1, Crossplot

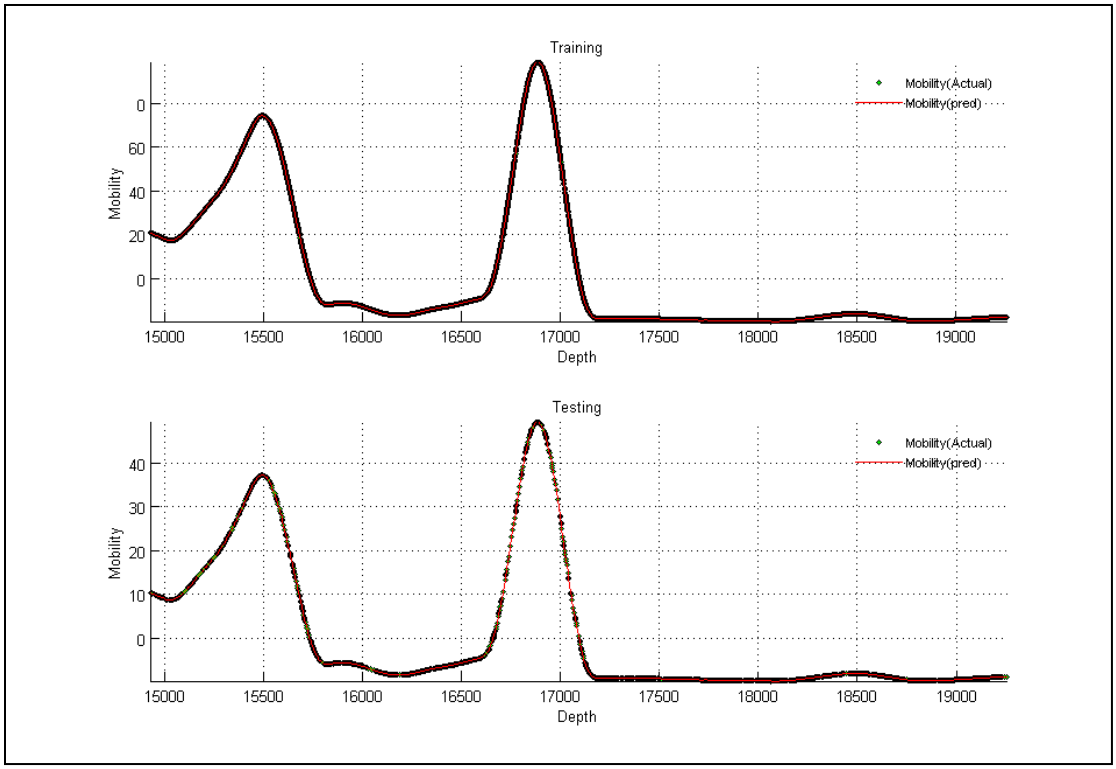

Figure A- 43: Well-3, Case -2

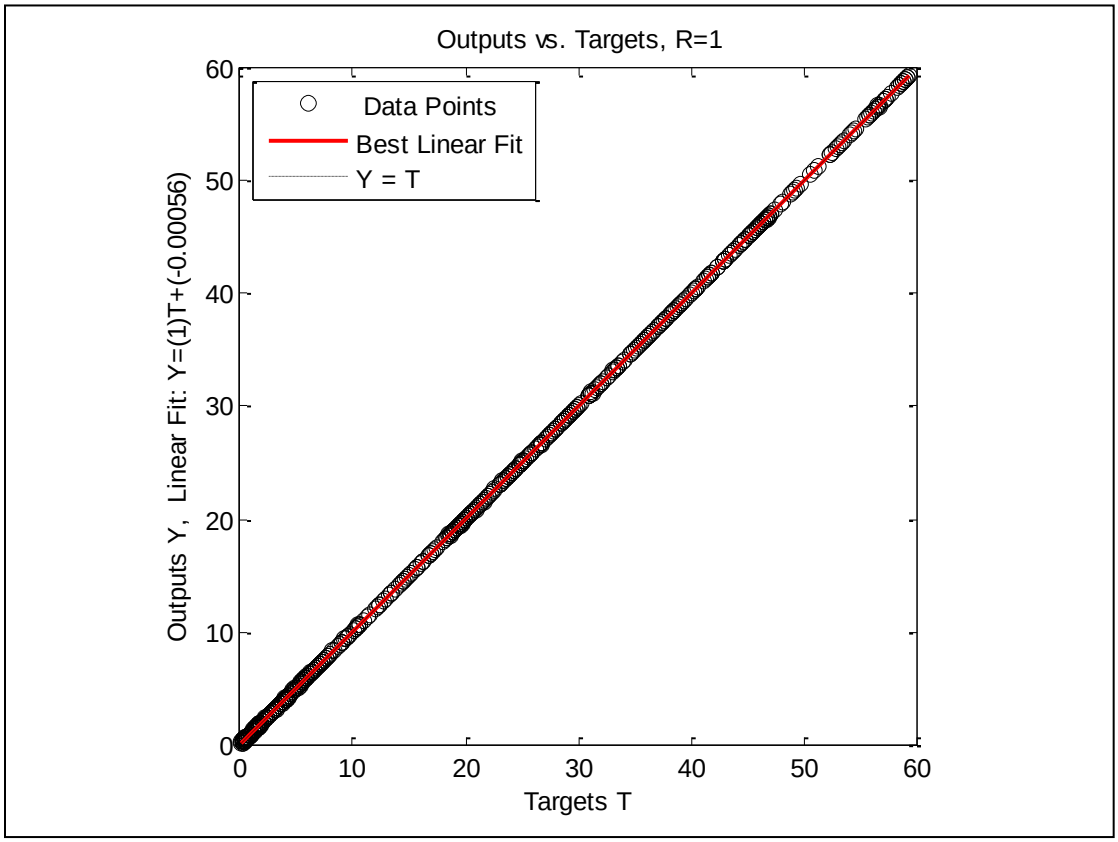

Figure A- 44: Well-3, Case -2, Crossplot

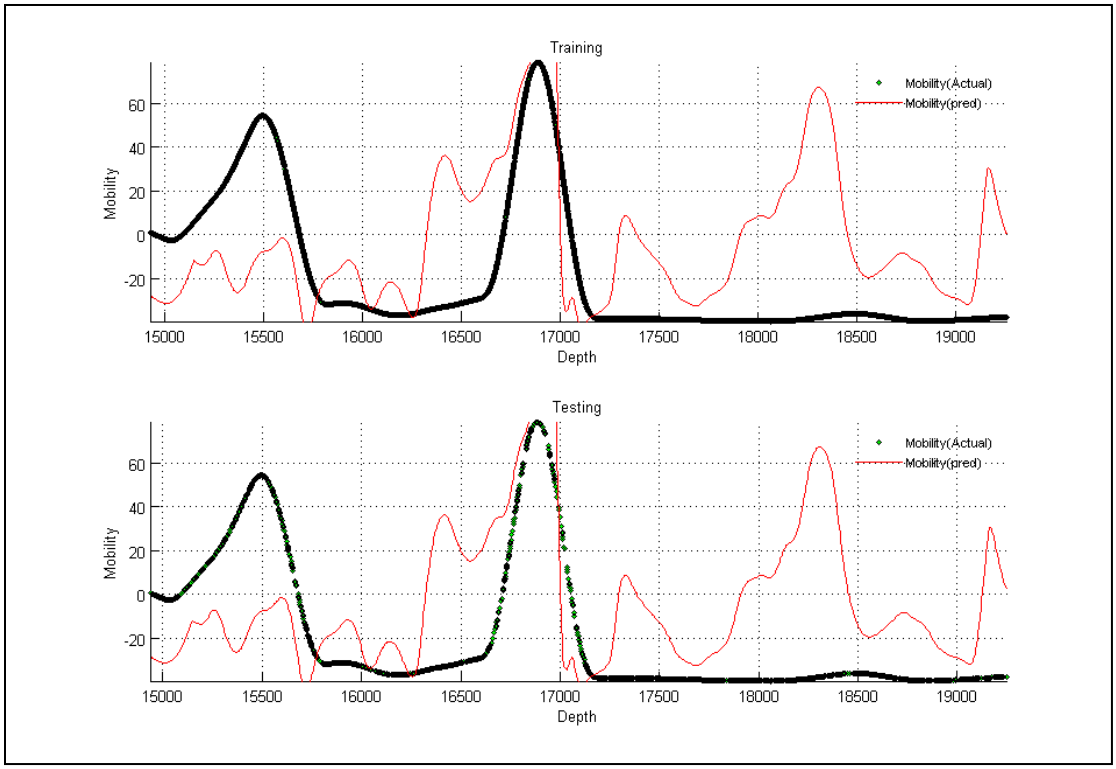

Figure A- 45: Well-3, Case -3

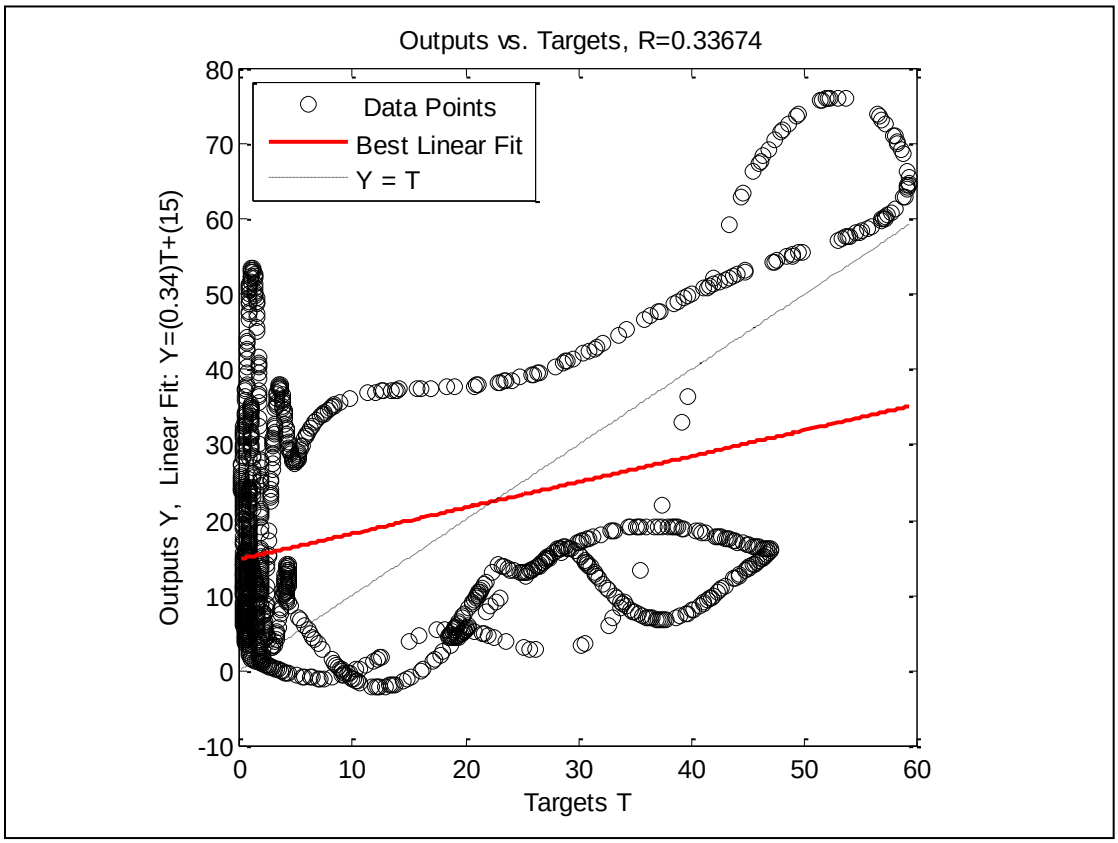

Figure A- 46: Well-3, Case -3, Crossplot

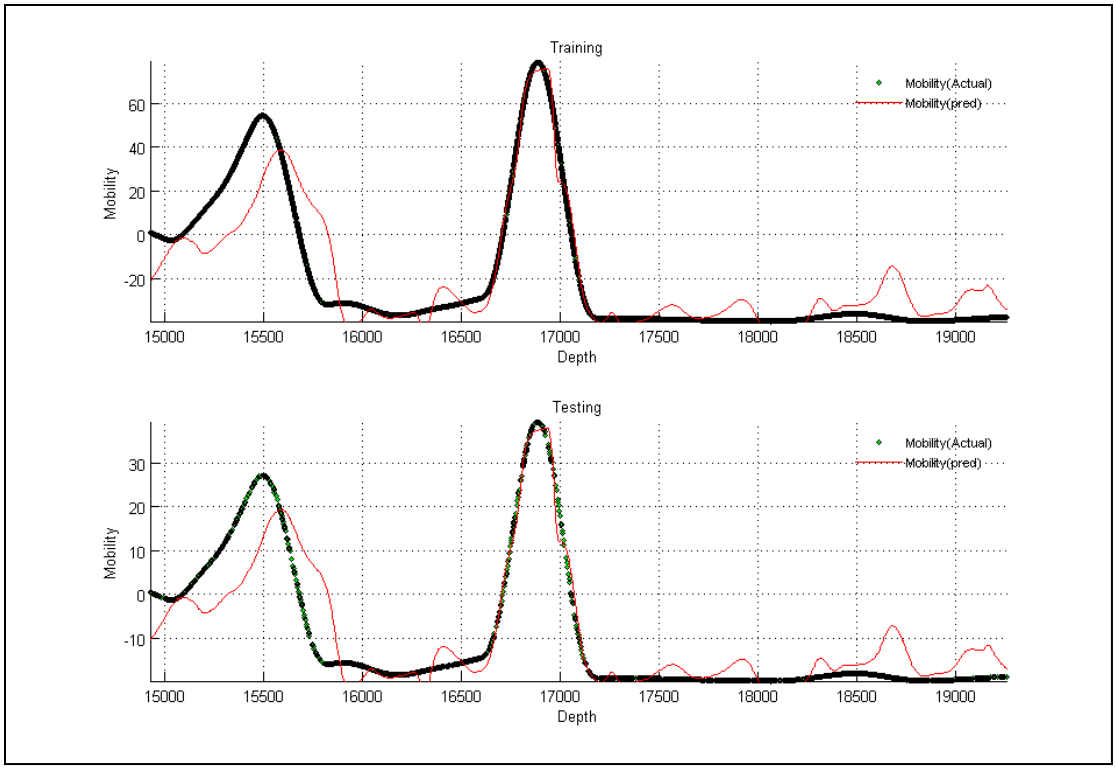

Figure A- 47: Well-3, Case -4

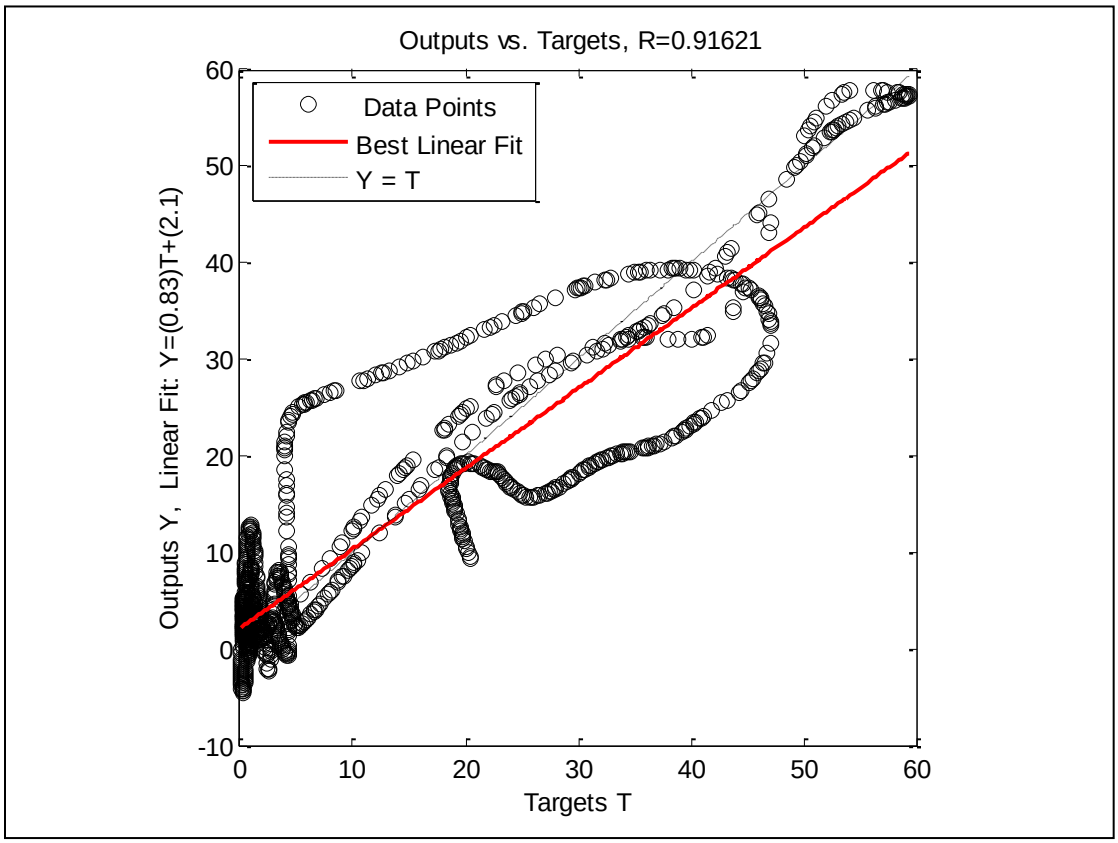

Figure A- 48: Well-3, Case -4, Crossplot

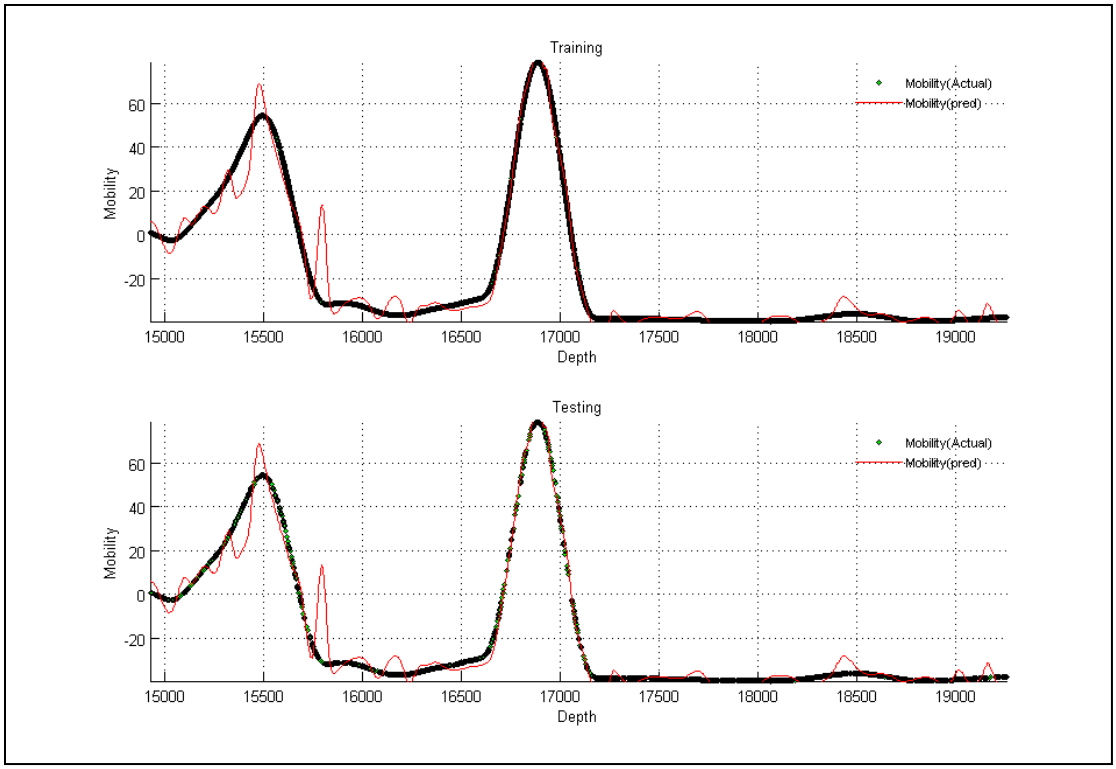

Figure A- 49: Well-3, Case -5

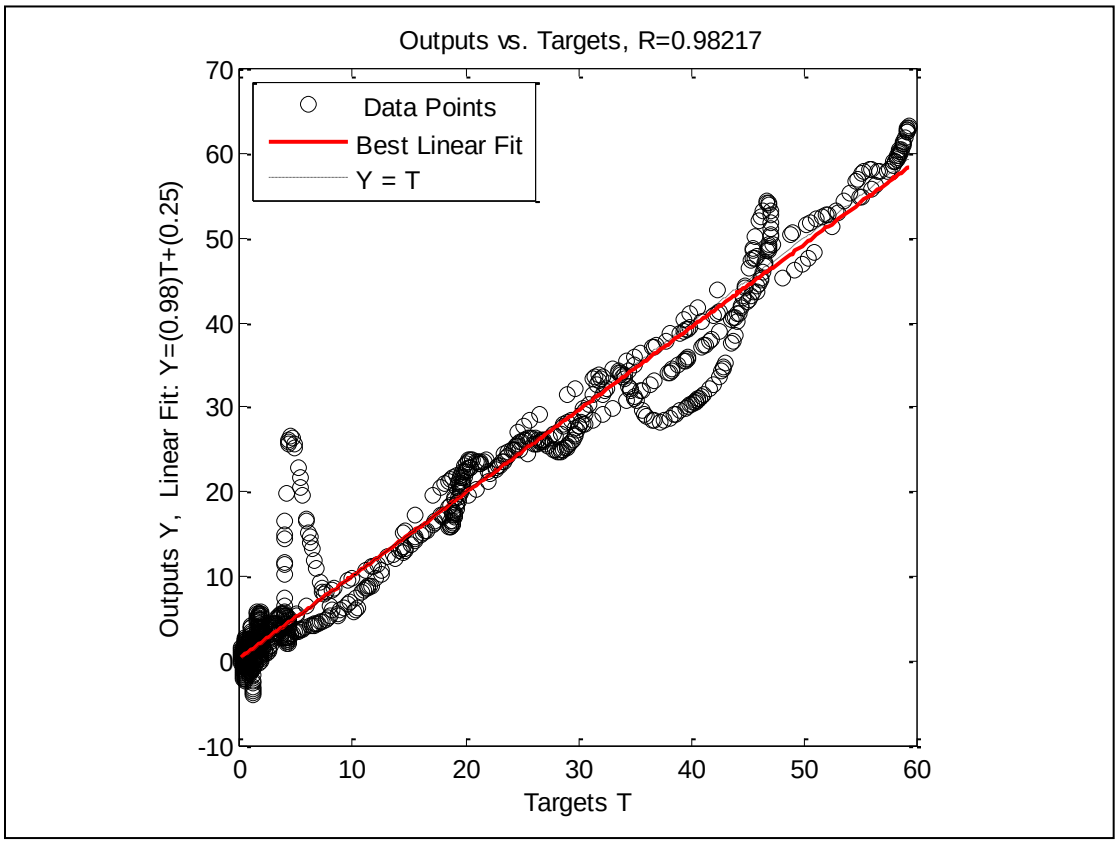

Figure A- 50: Well-3, Case -5, Crossplot

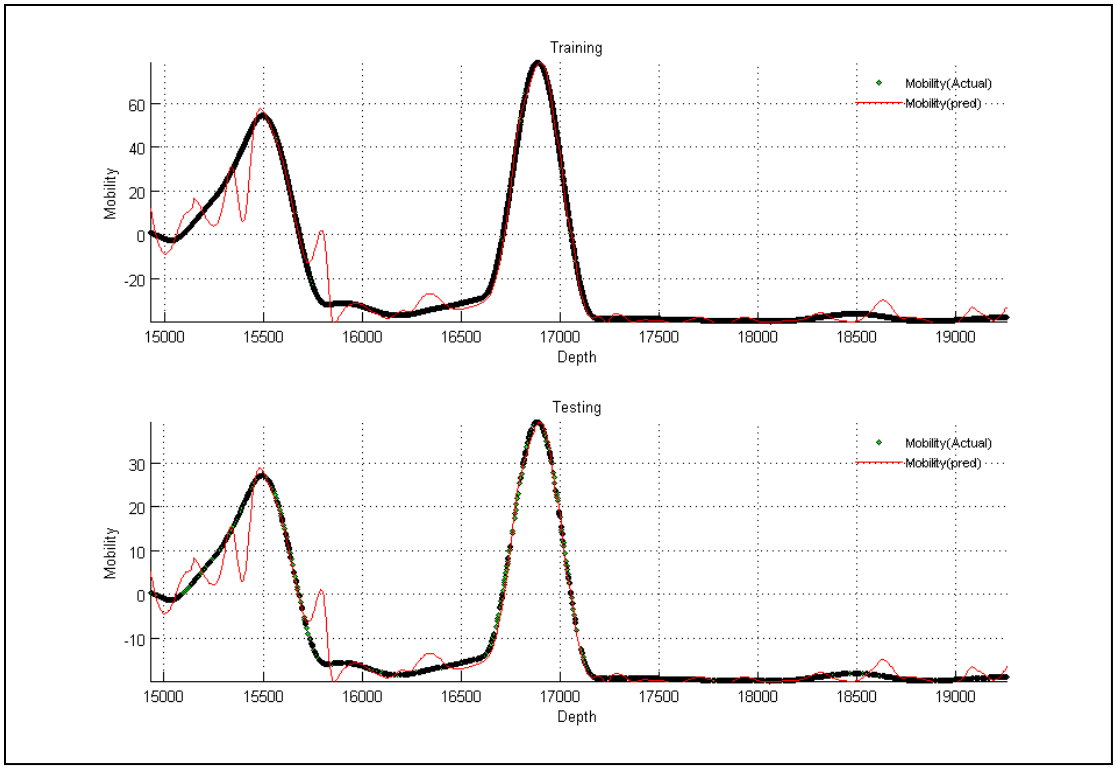

Figure A- 51: Well-3, Case -6

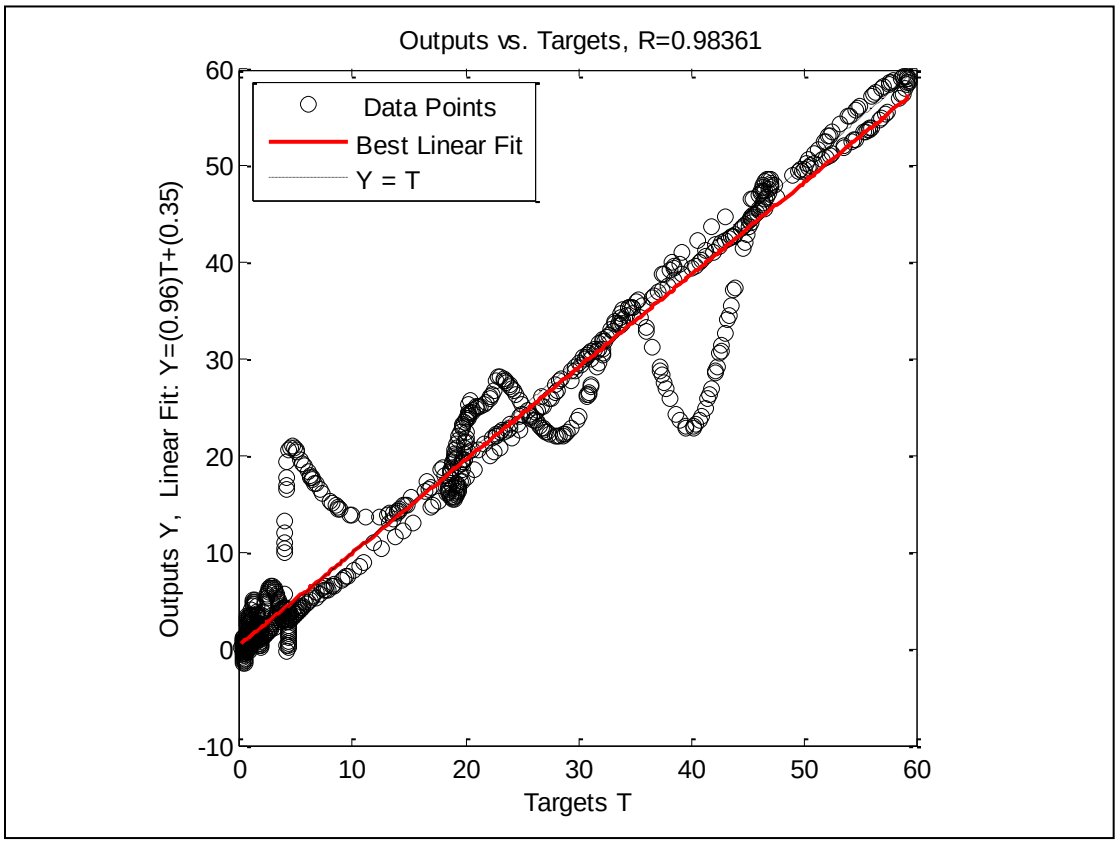

Figure A- 52: Well-3, Case -6, Crossplot

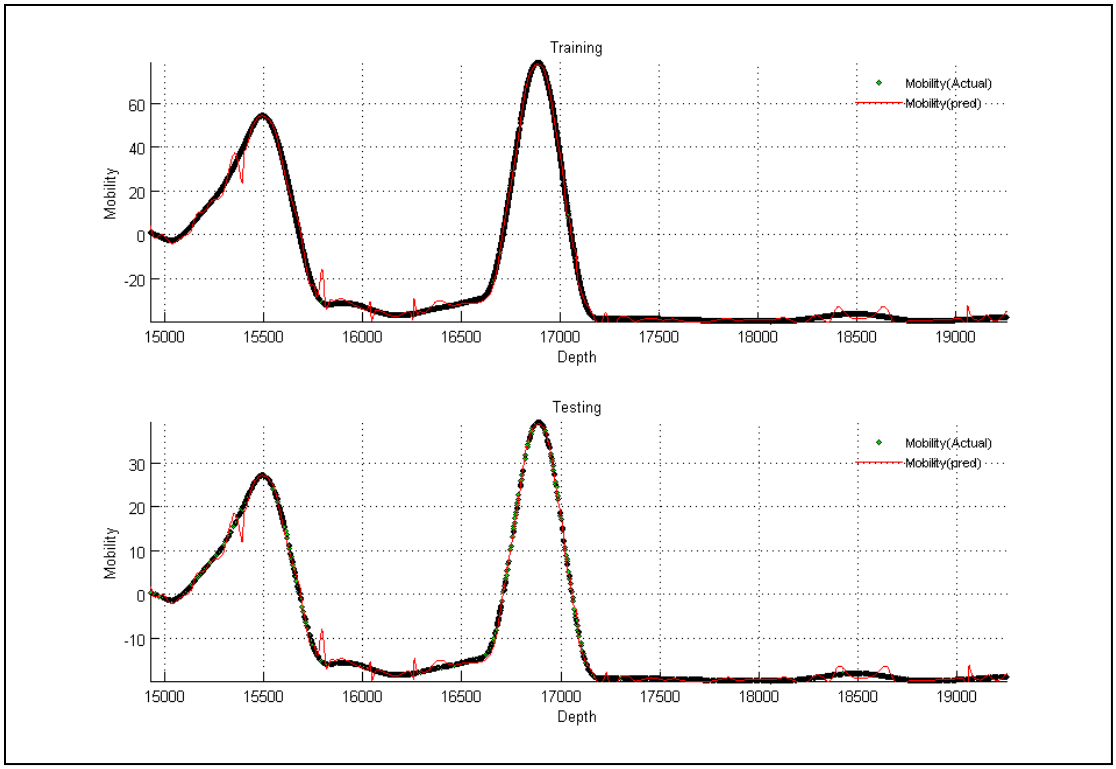

Figure A- 53: Well-3, Case -7

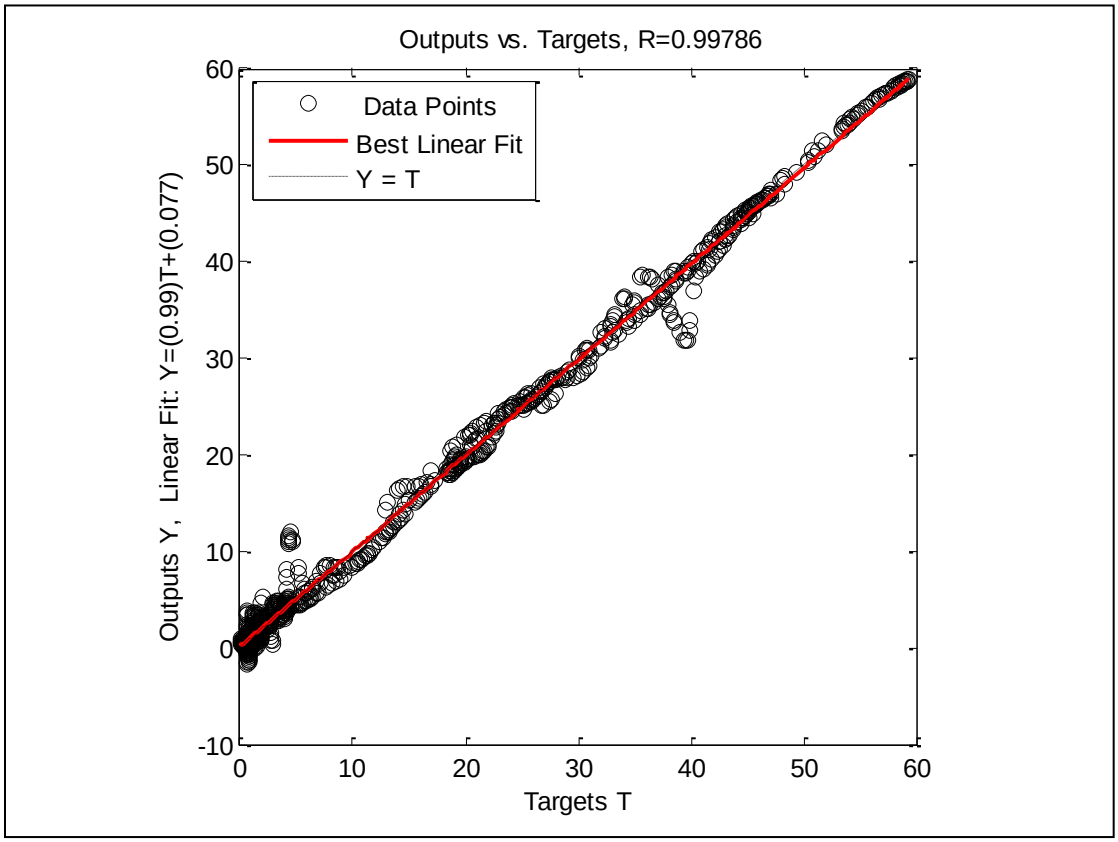

Figure A- 54: Well-3, Case -7, Crossplot

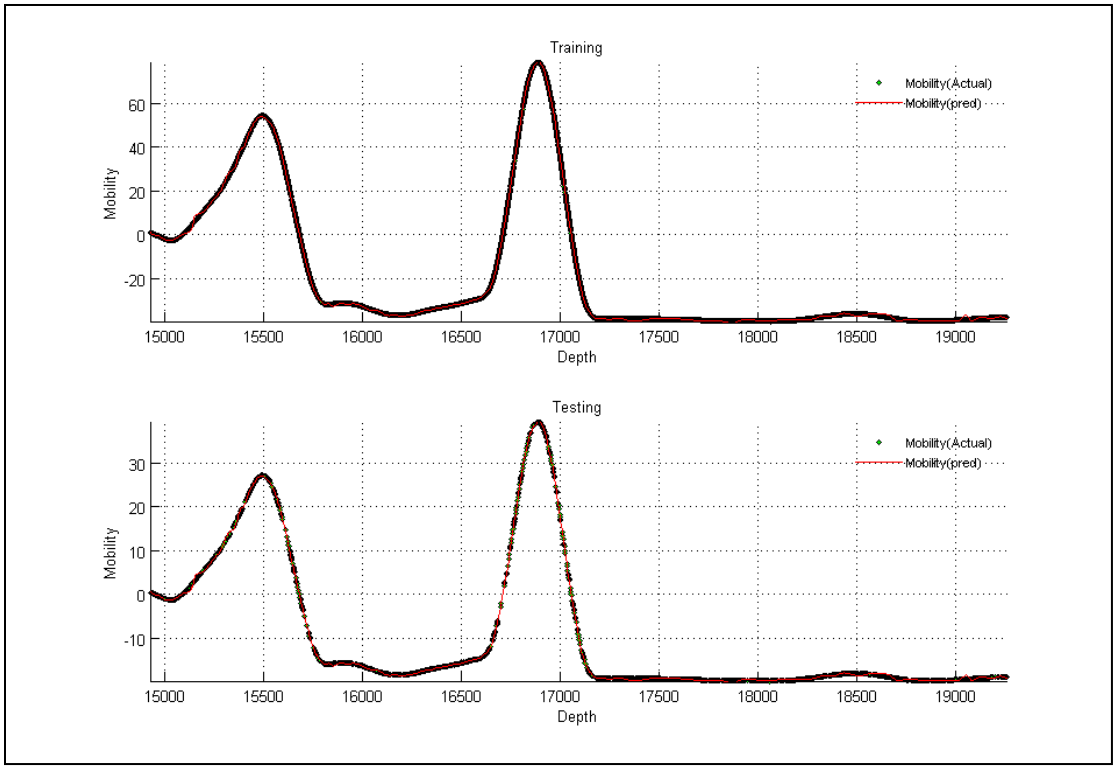

Figure A- 55: Well-3, Case -8

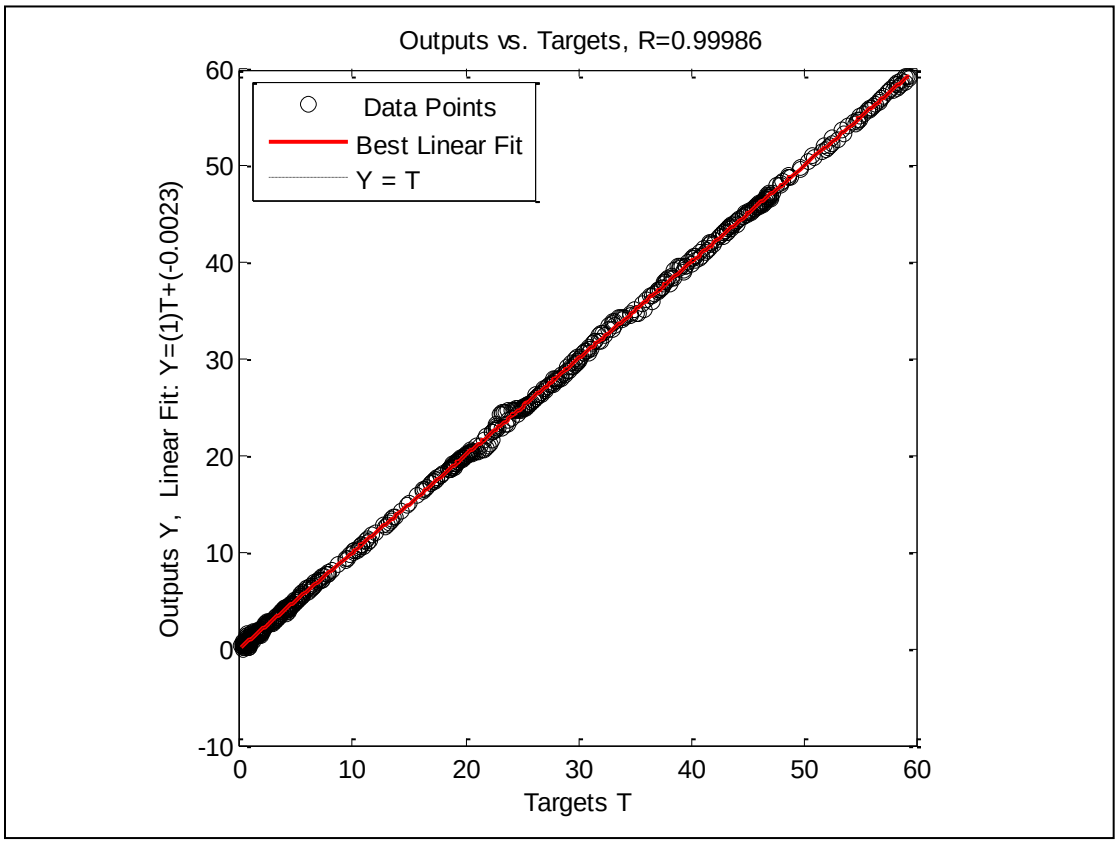

Figure A- 56: Well-3, Case -8, Crossplot

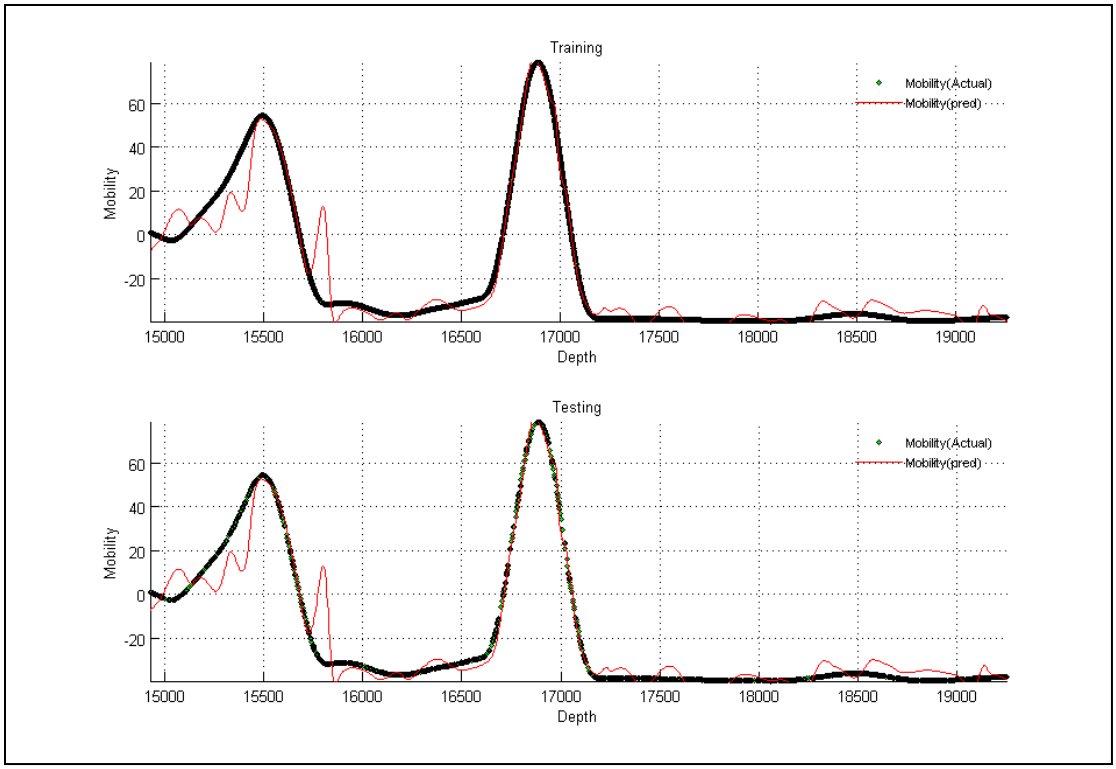

Figure A- 57: Well-3, Case -9

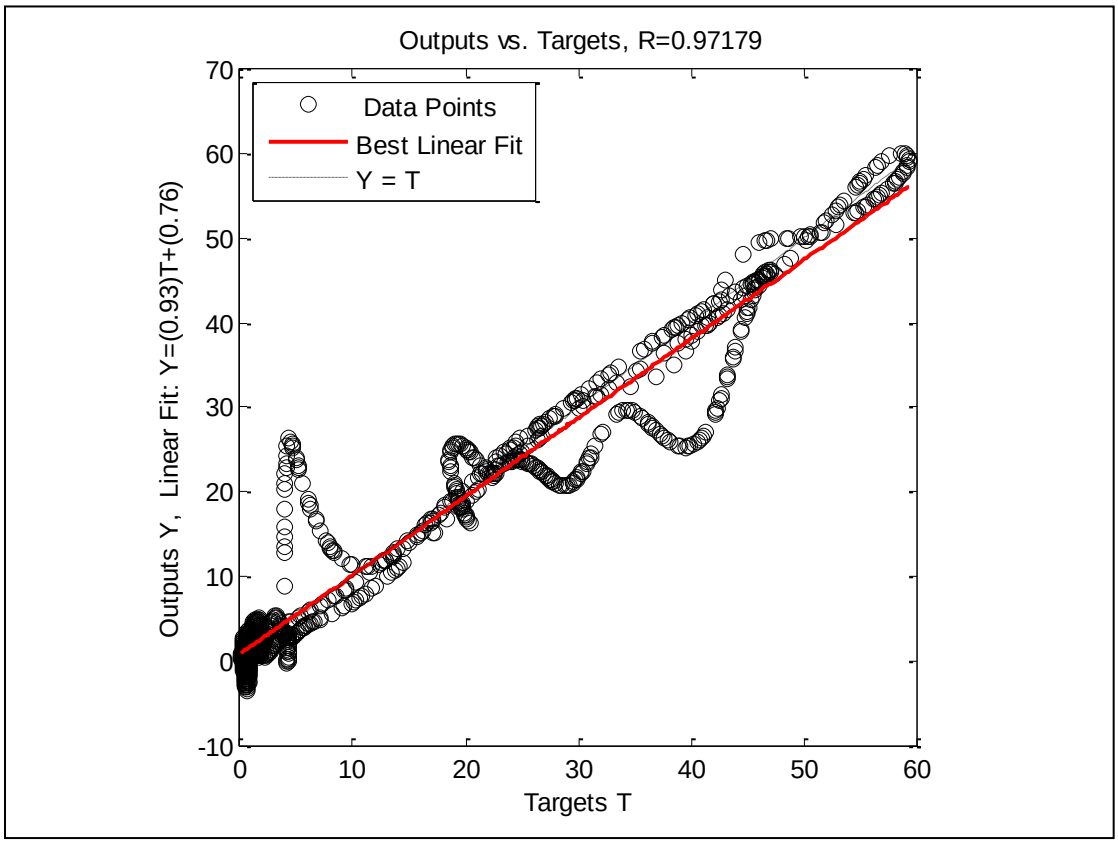

Figure A- 58: Well-3, Case -9, Crossplot

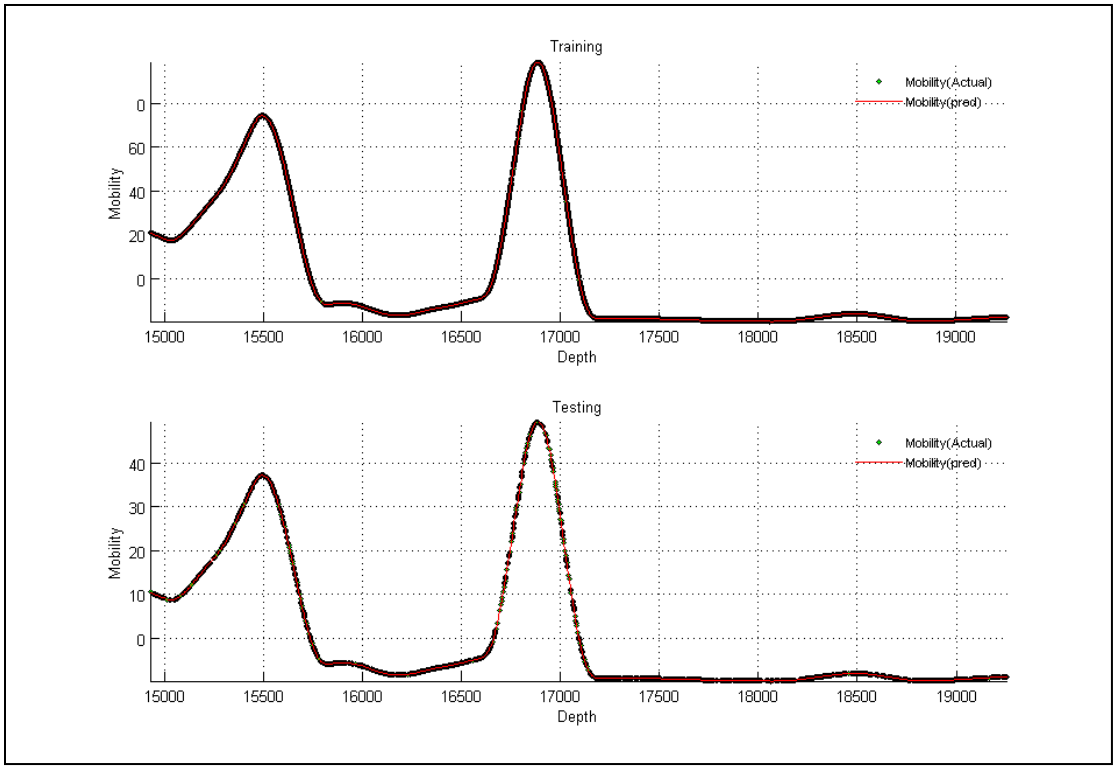

Figure A- 59: Well-3, Case -10

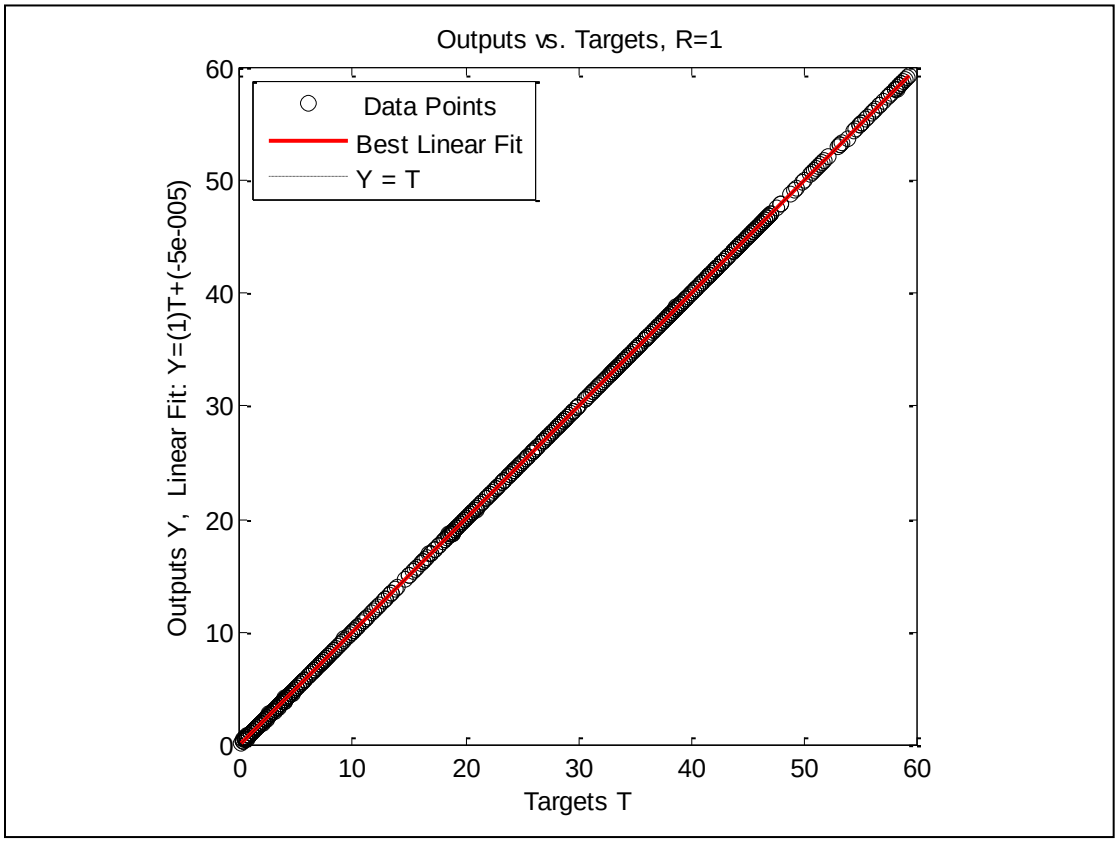

Figure A- 60: Well-3, Case -10, Crossplot

Well No. 4

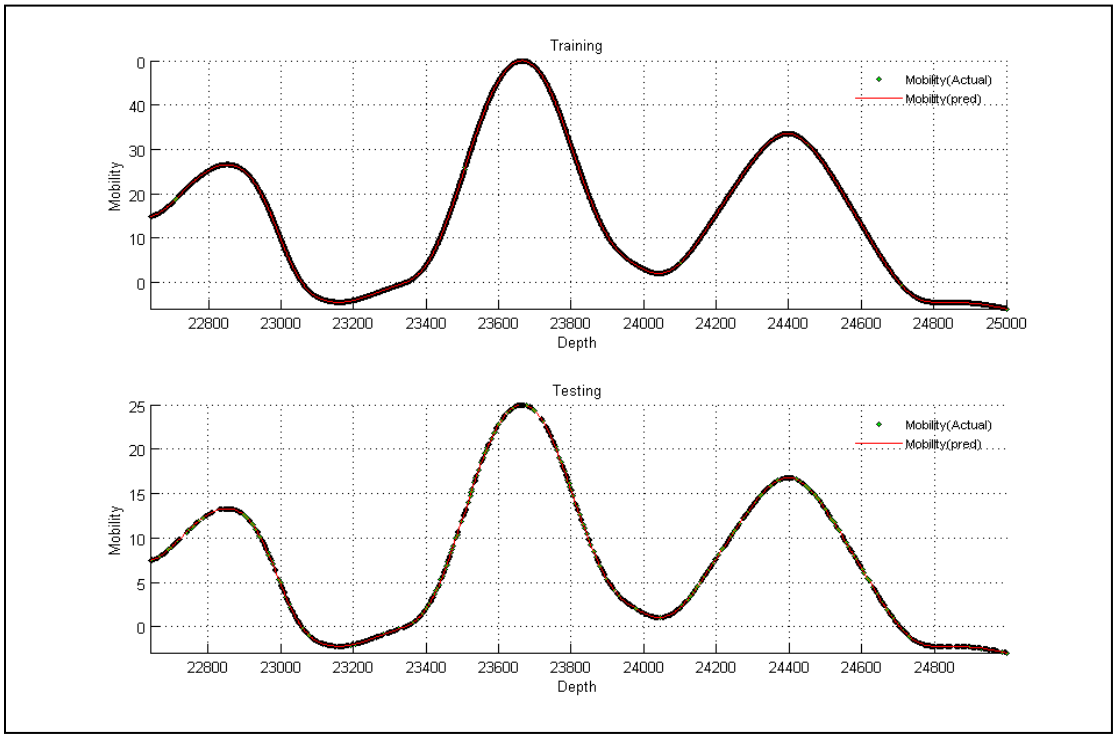

Figure A- 61: Well-4, Case -1

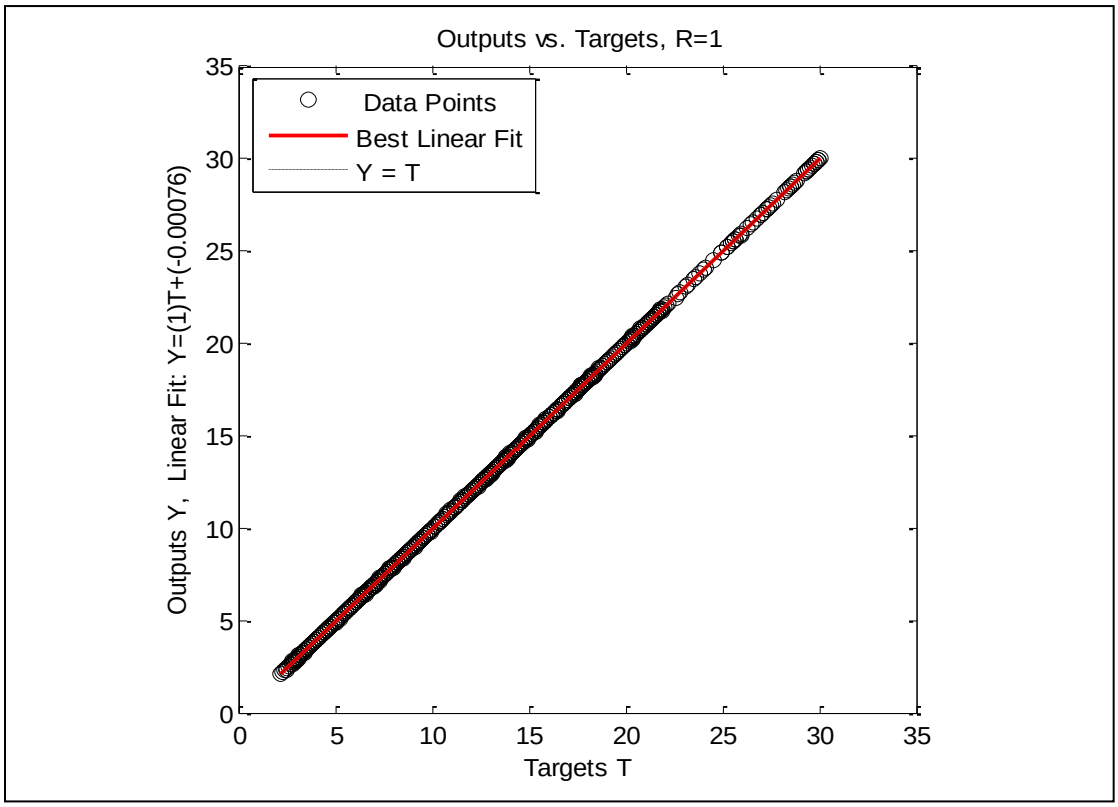

Figure A- 62: Well-4, Case -1, Crossplot

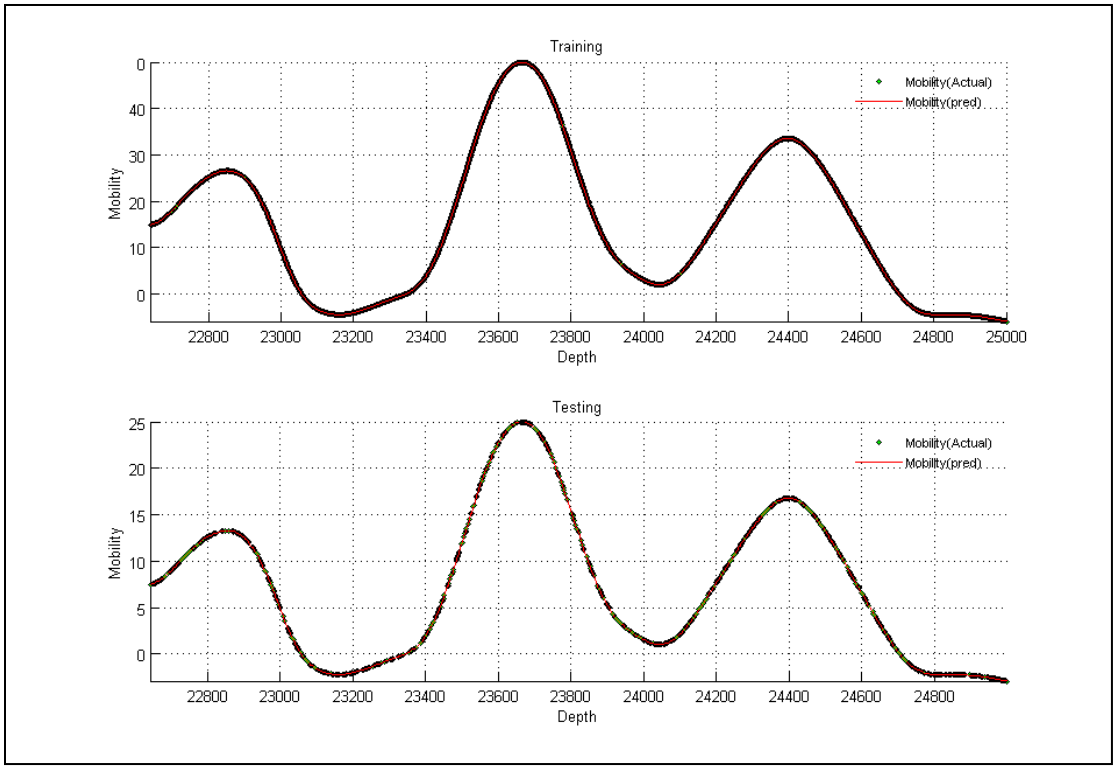

Figure A- 63: Well-4, Case -2

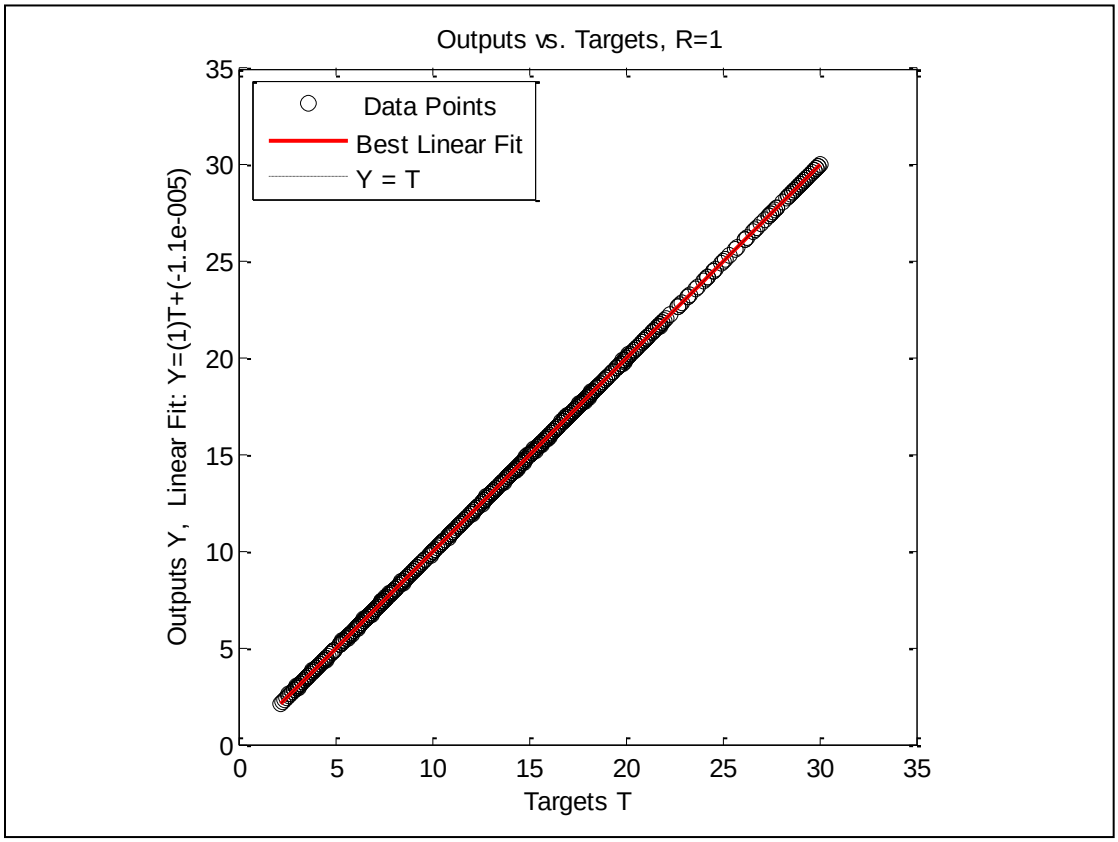

Figure A- 64: Well-4, Case -2, Crossplot

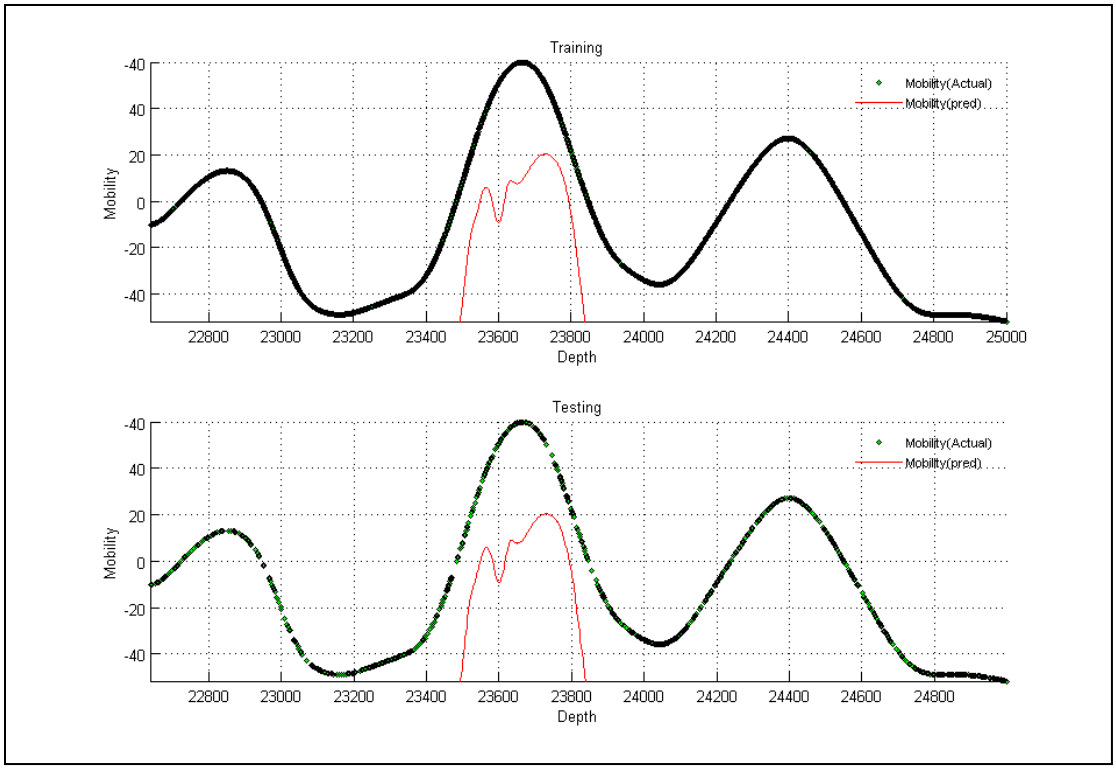

Figure A- 65: Well-4, Case -3

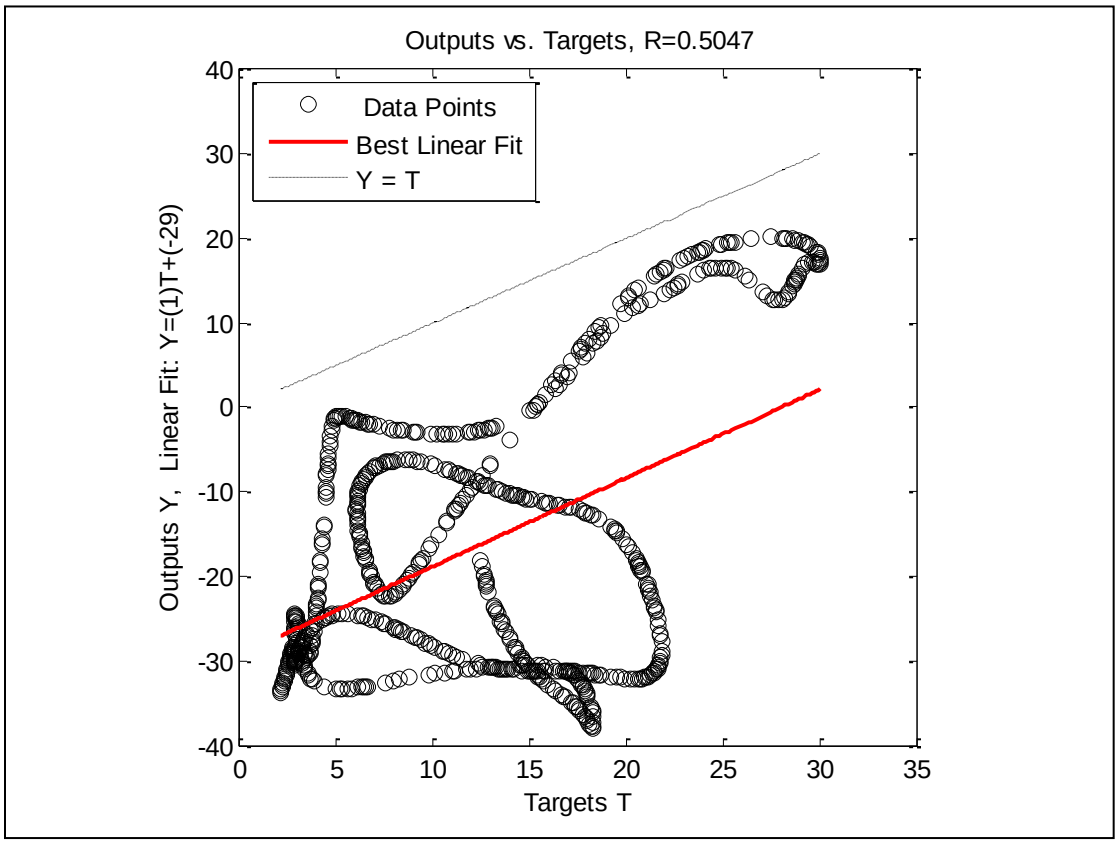

Figure A- 66: Well-4, Case -3, Crossplot

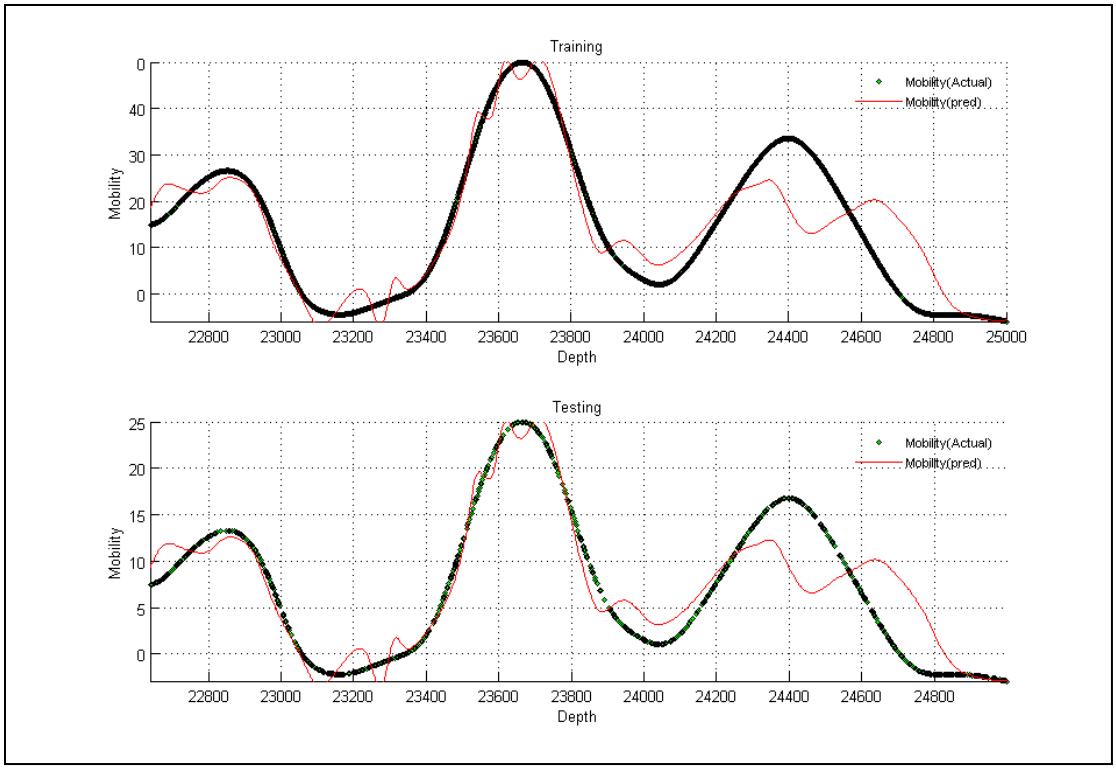

Figure A- 67: Well-4, Case -4

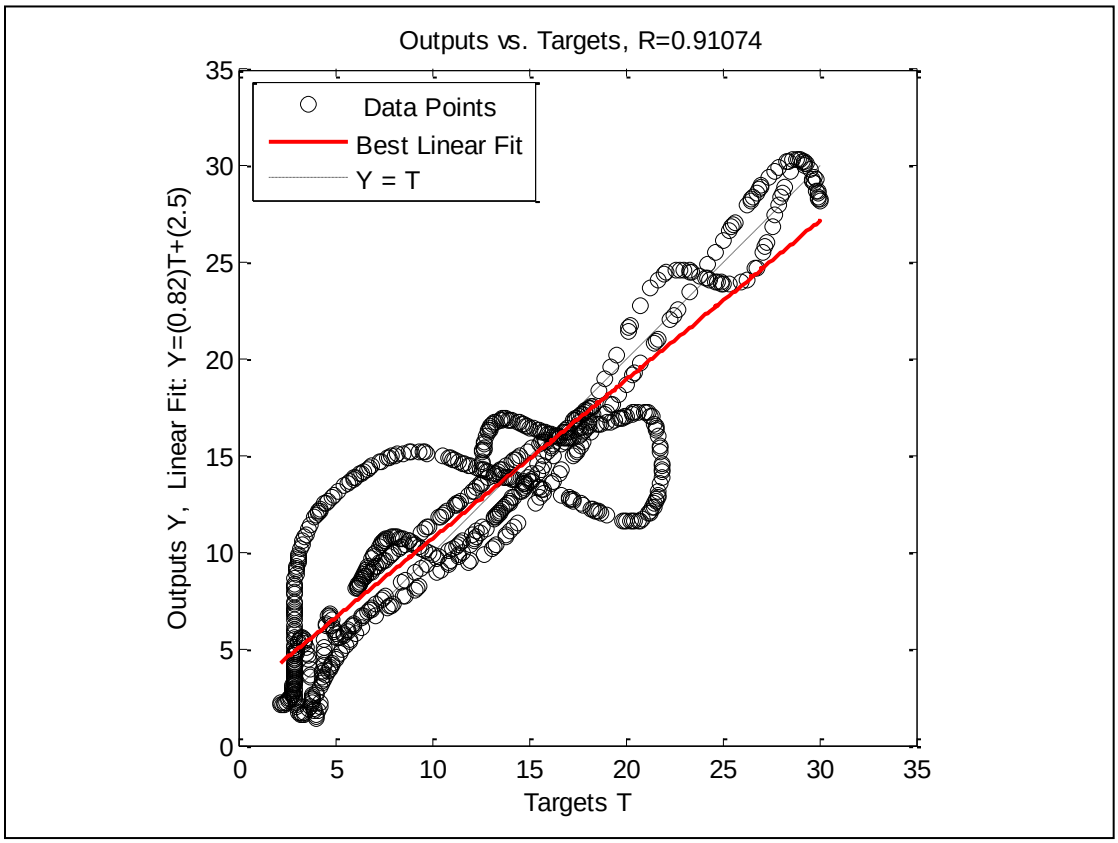

Figure A- 68: Well-4, Case -4, Crossplot

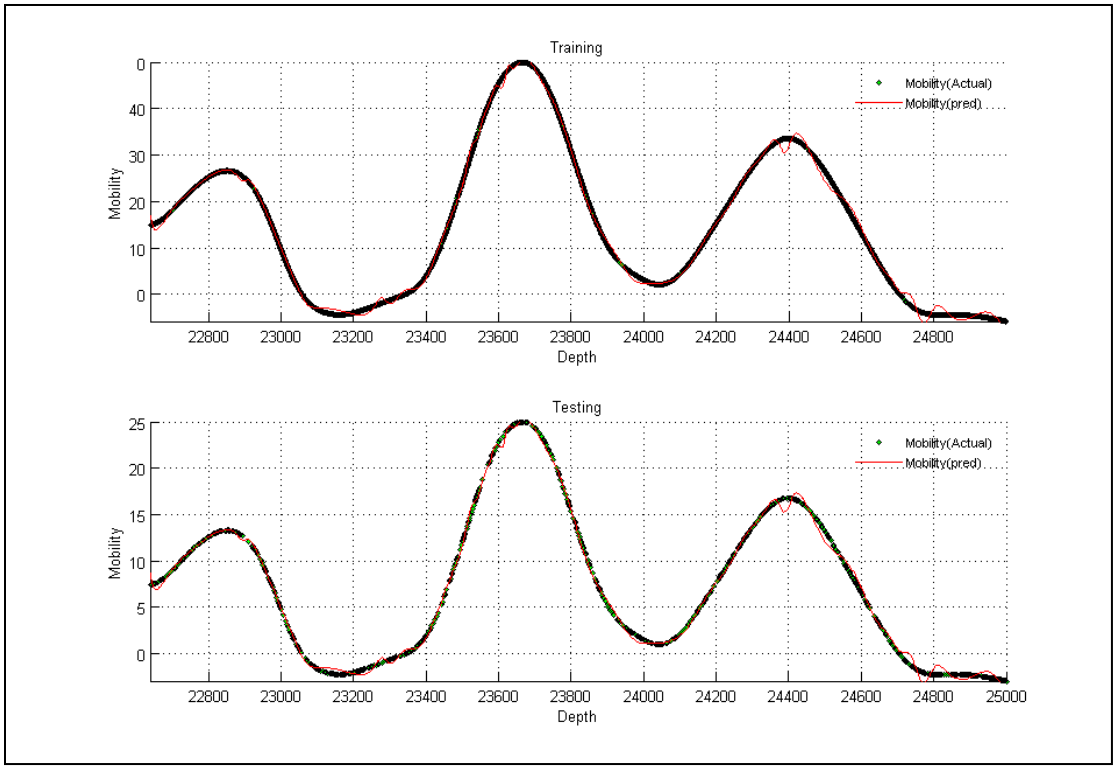

Figure A- 69: Well-4, Case -5

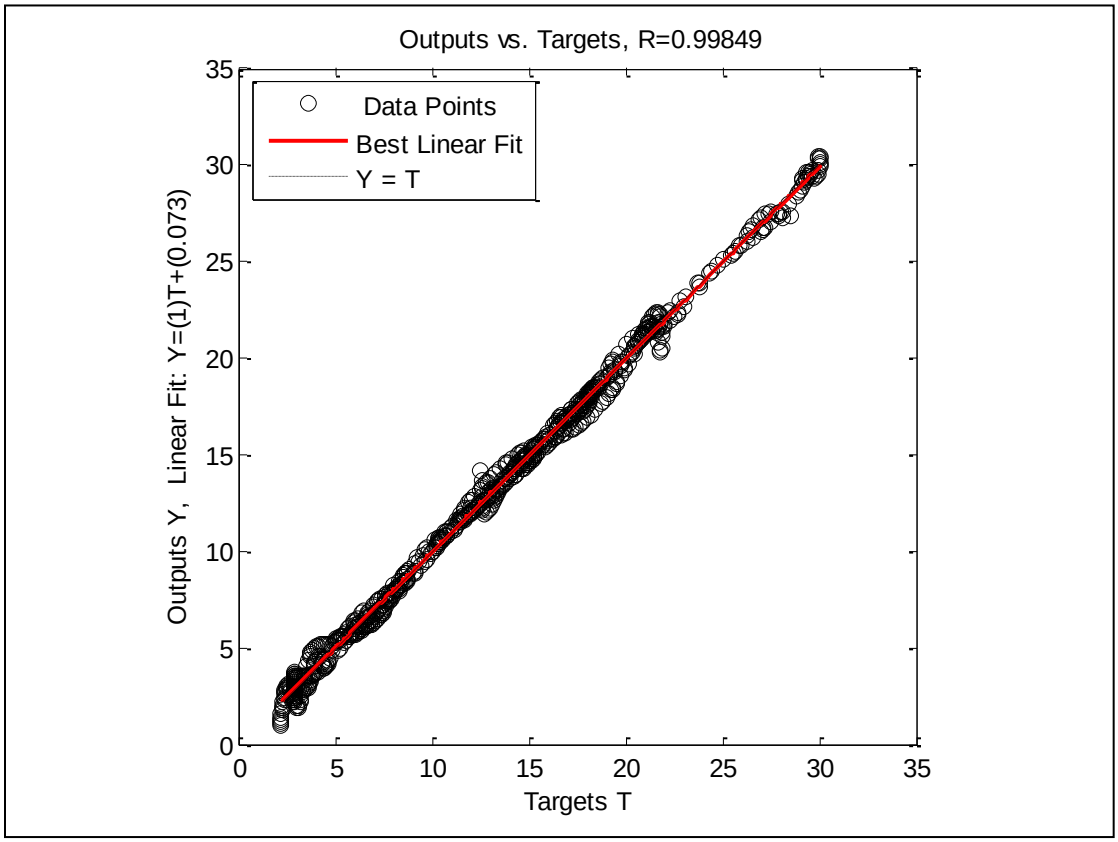

Figure A- 70: Well-4, Case -5, Crossplot

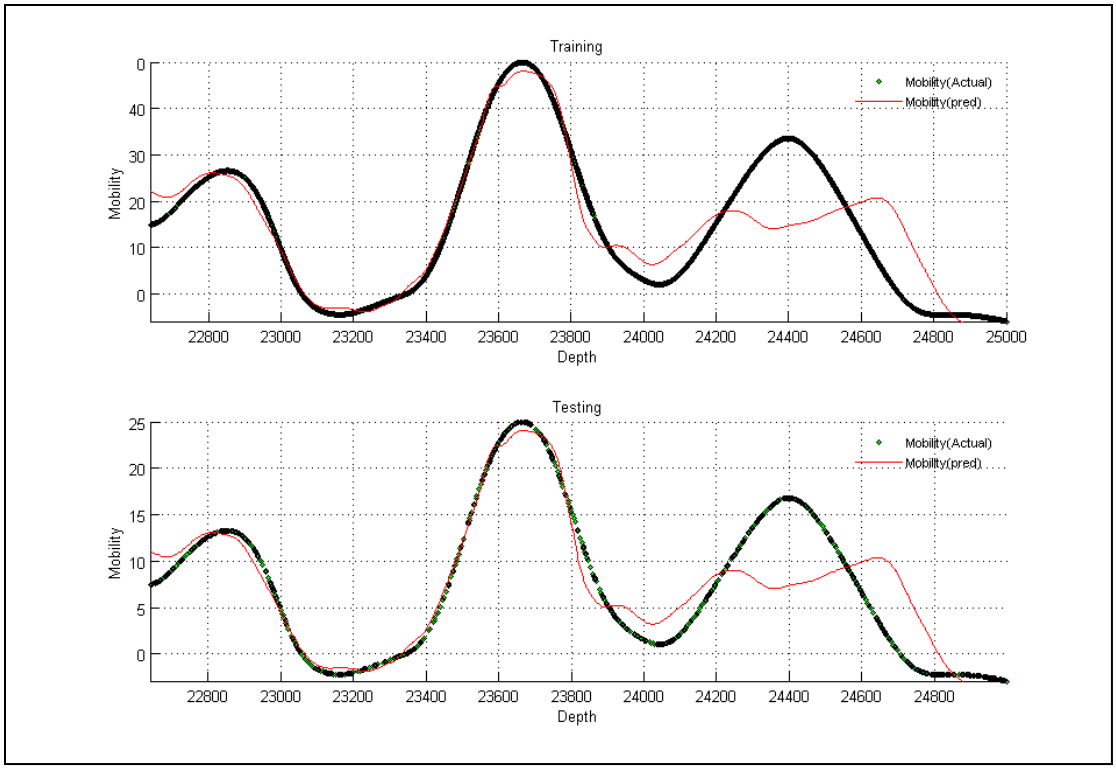

Figure A- 71: Well-4, Case -6

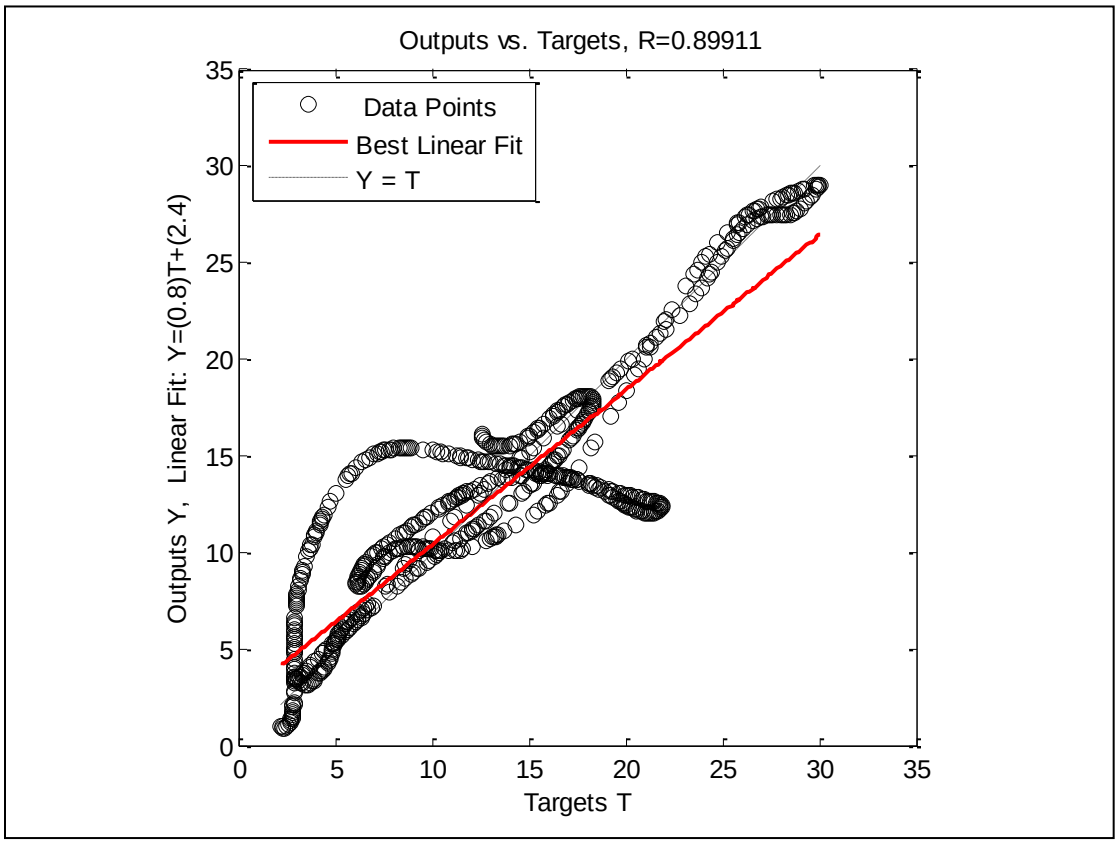

Figure A- 72: Well-4, Case -6, Crossplot

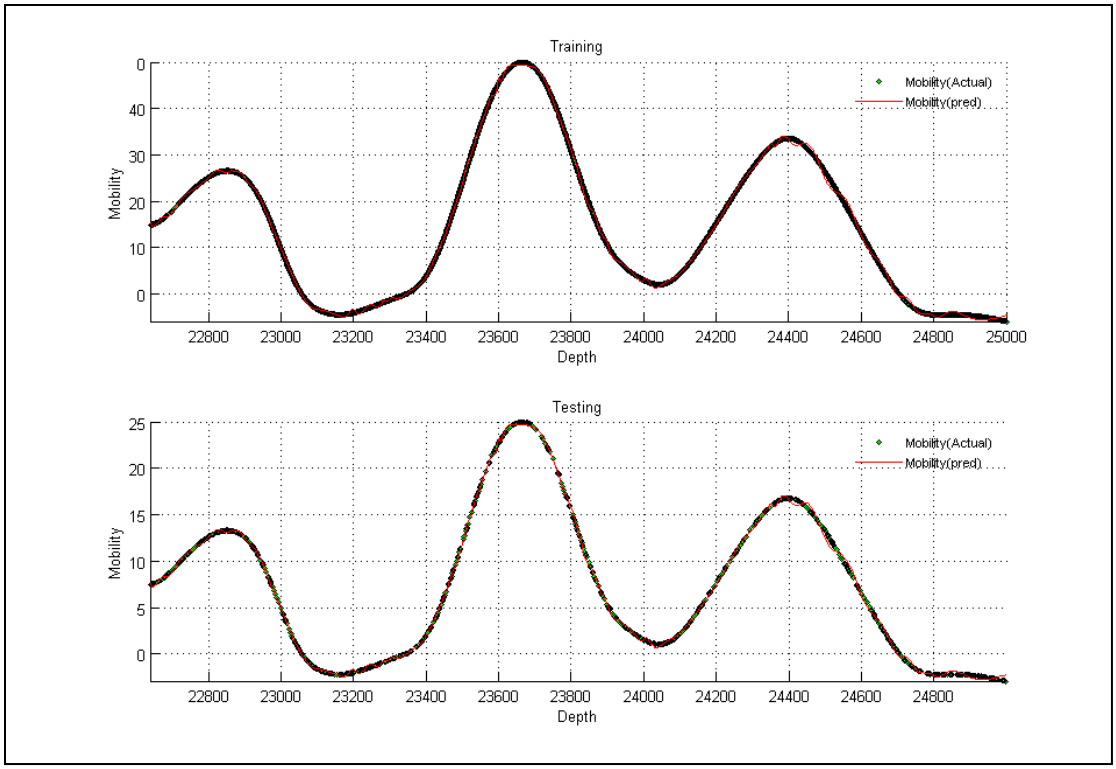

Figure A- 73: Well-4, Case -7

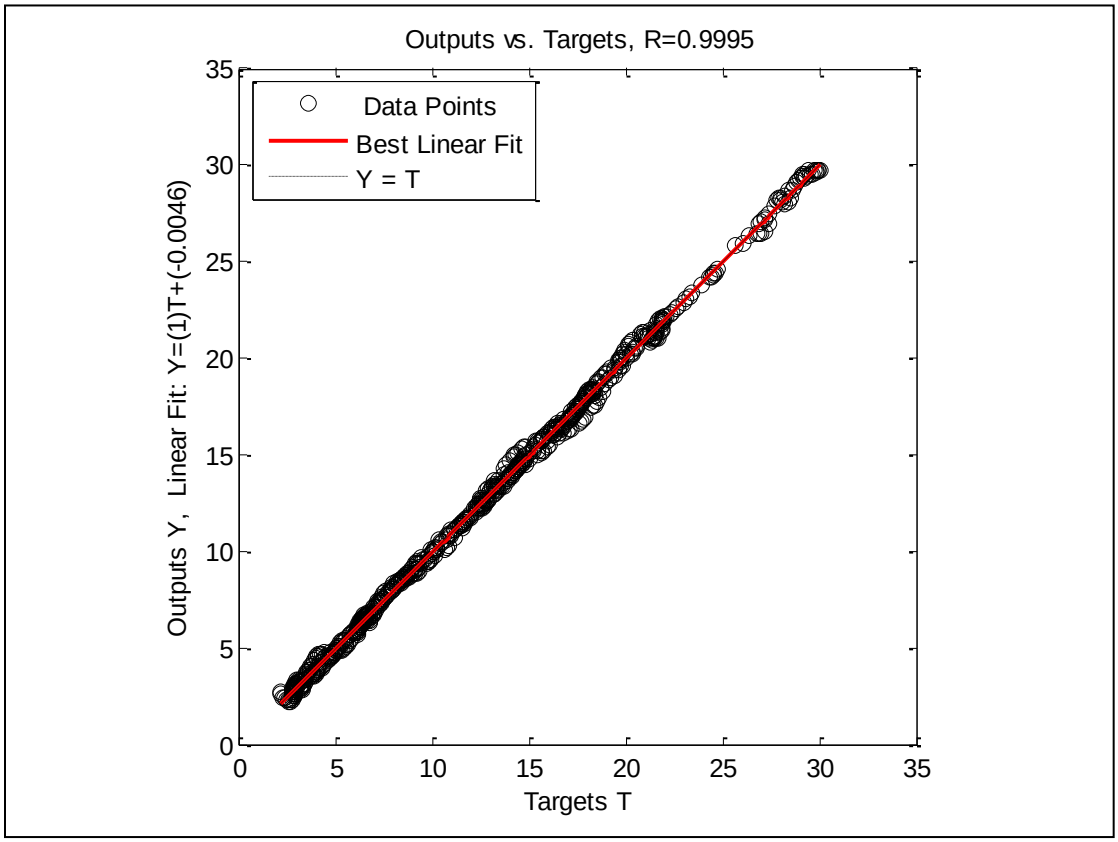

Figure A- 74: Well-4, Case -7, Crossplot

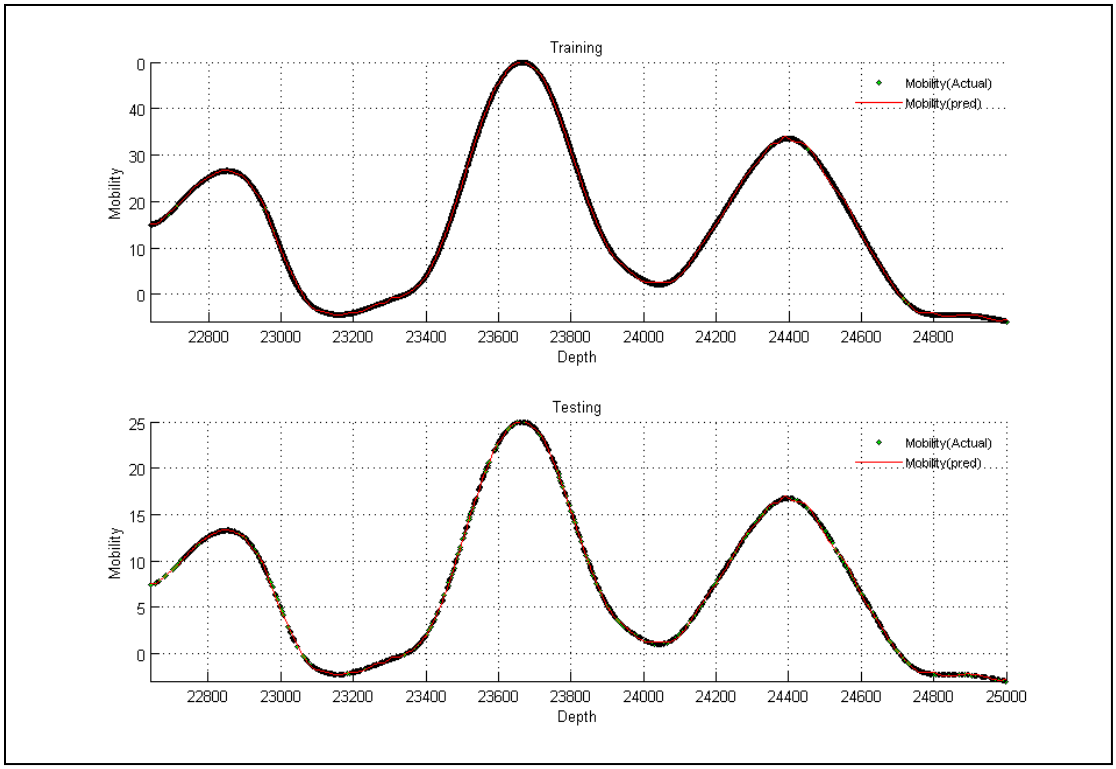

Figure A- 75: Well-4, Case -8

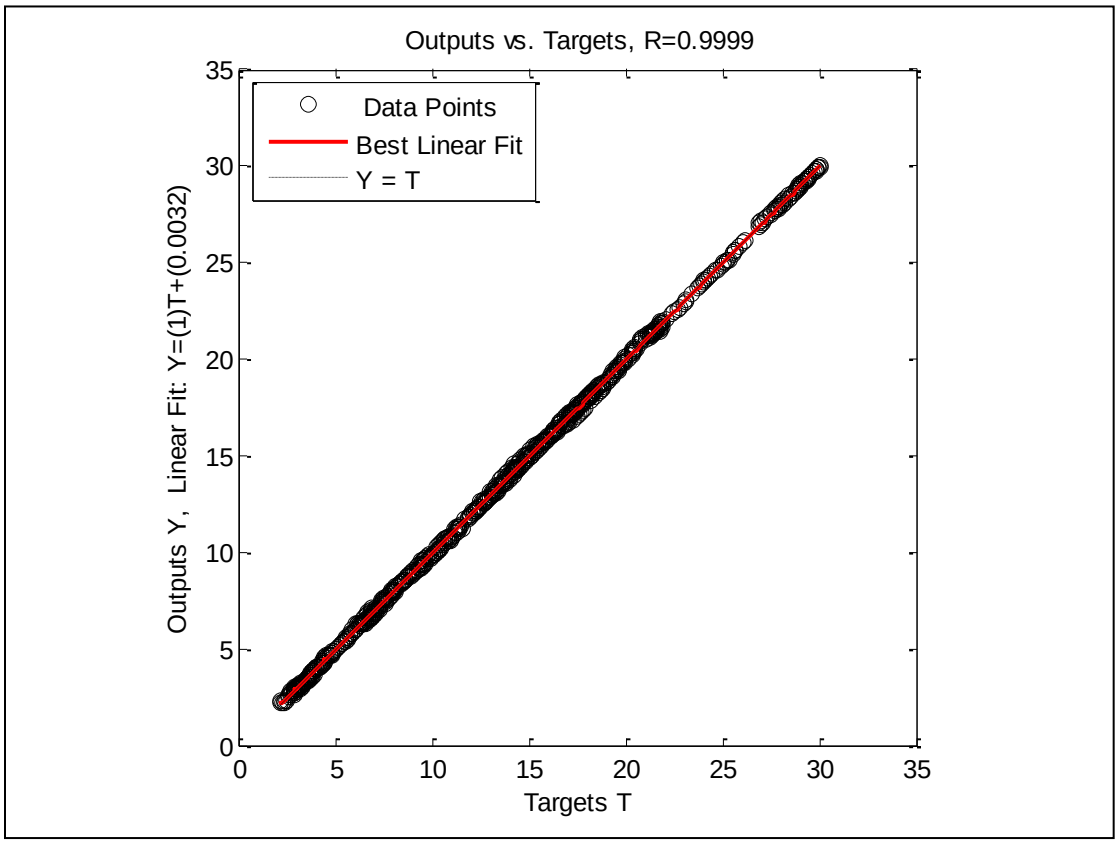

Figure A- 76: Well-4, Case -8, Crossplot

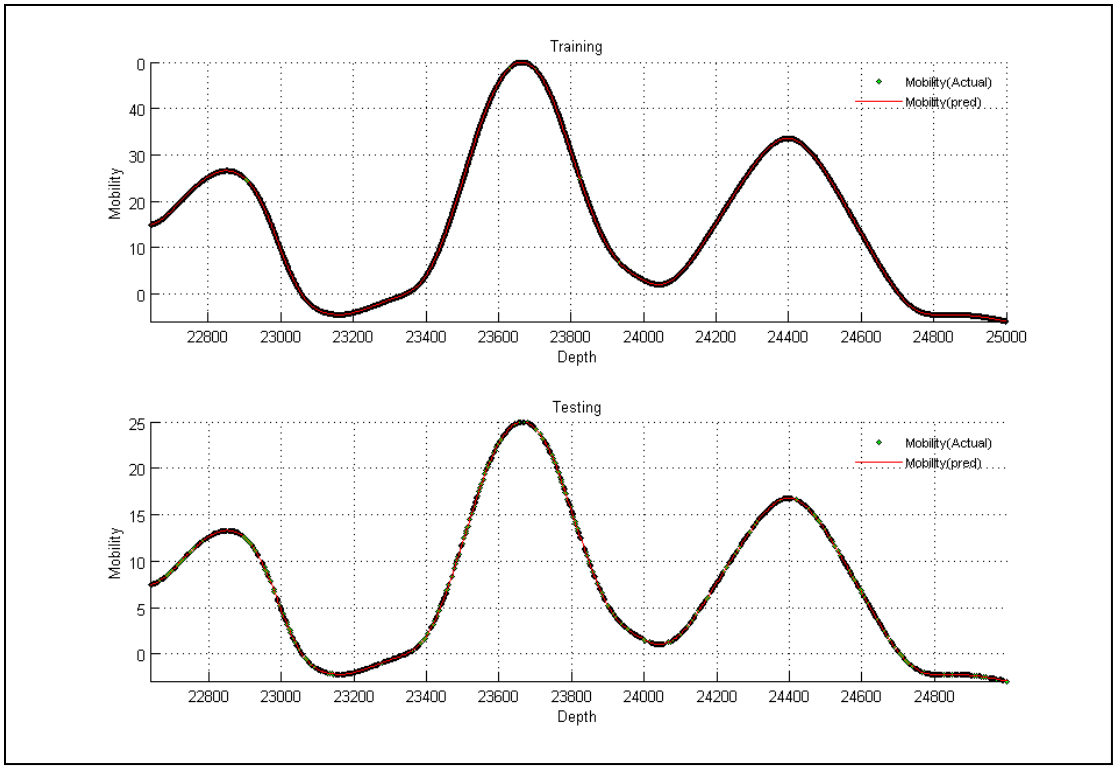

Figure A- 77: Well-4, Case -9

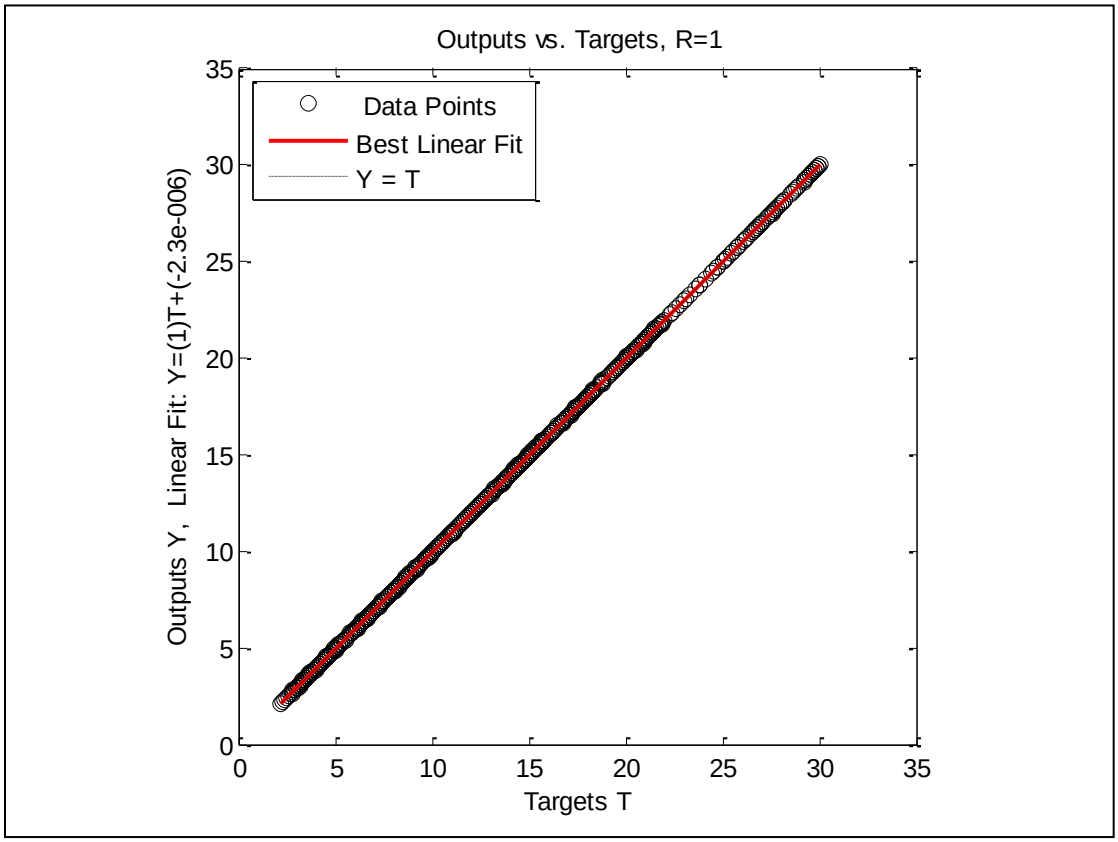

Figure A- 78: Well-4, Case -9, Crossplot

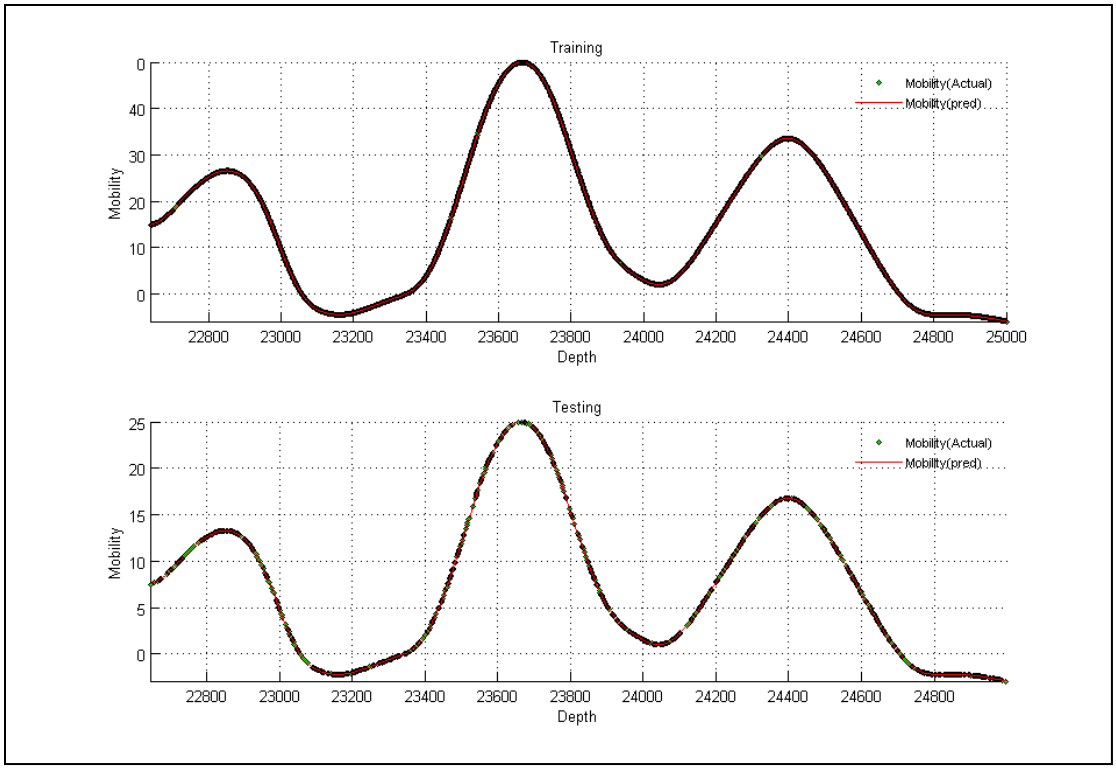

Figure A- 79: Well-4, Case -10

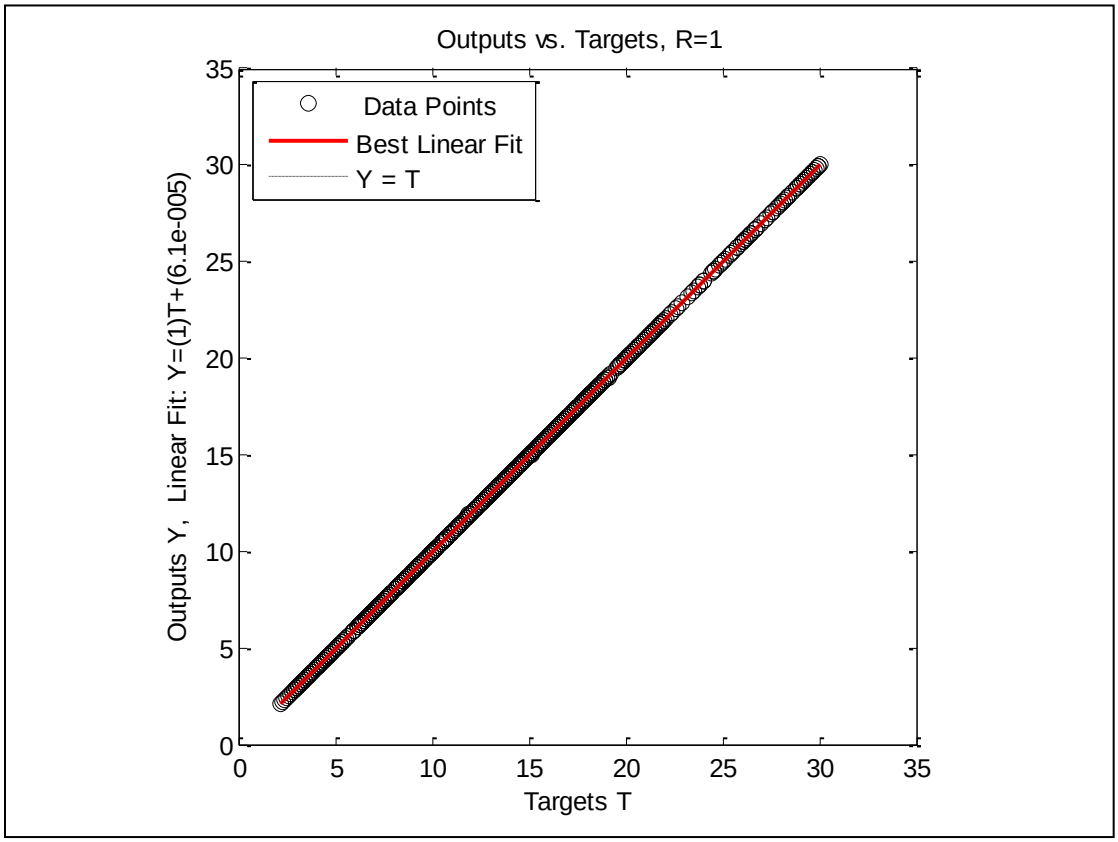

Figure A- 80: Well-4, Case -10, Crossplot

Well No. 5

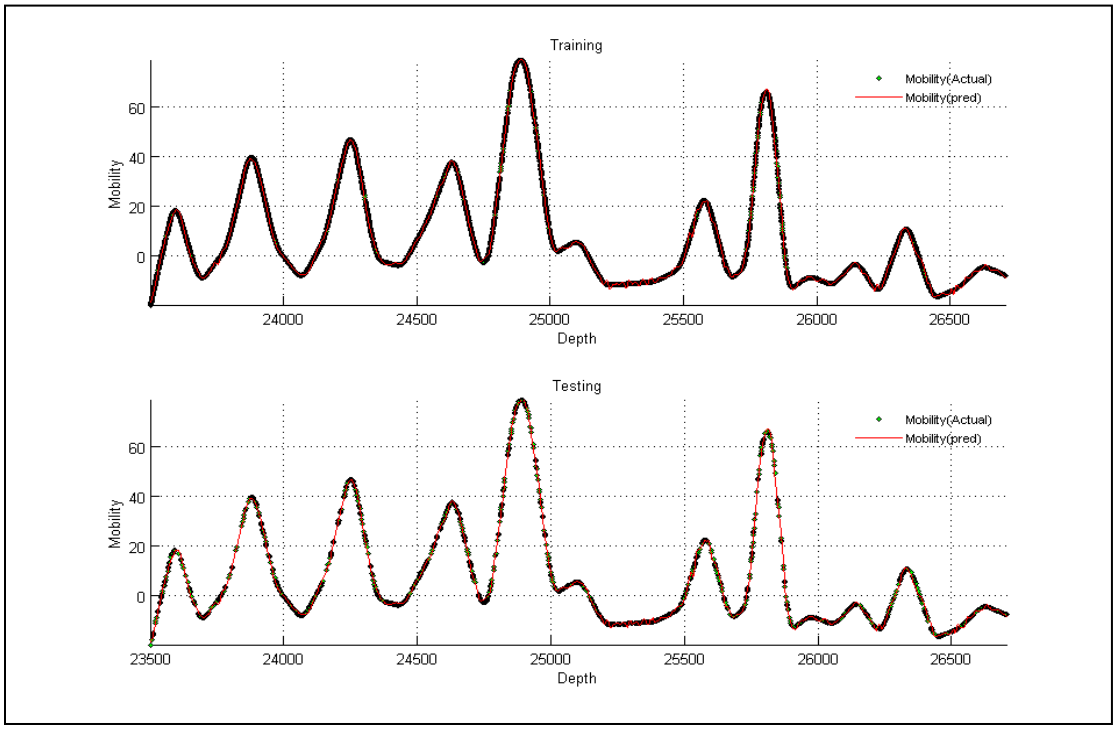

Figure A- 81: Well-5, Case -1

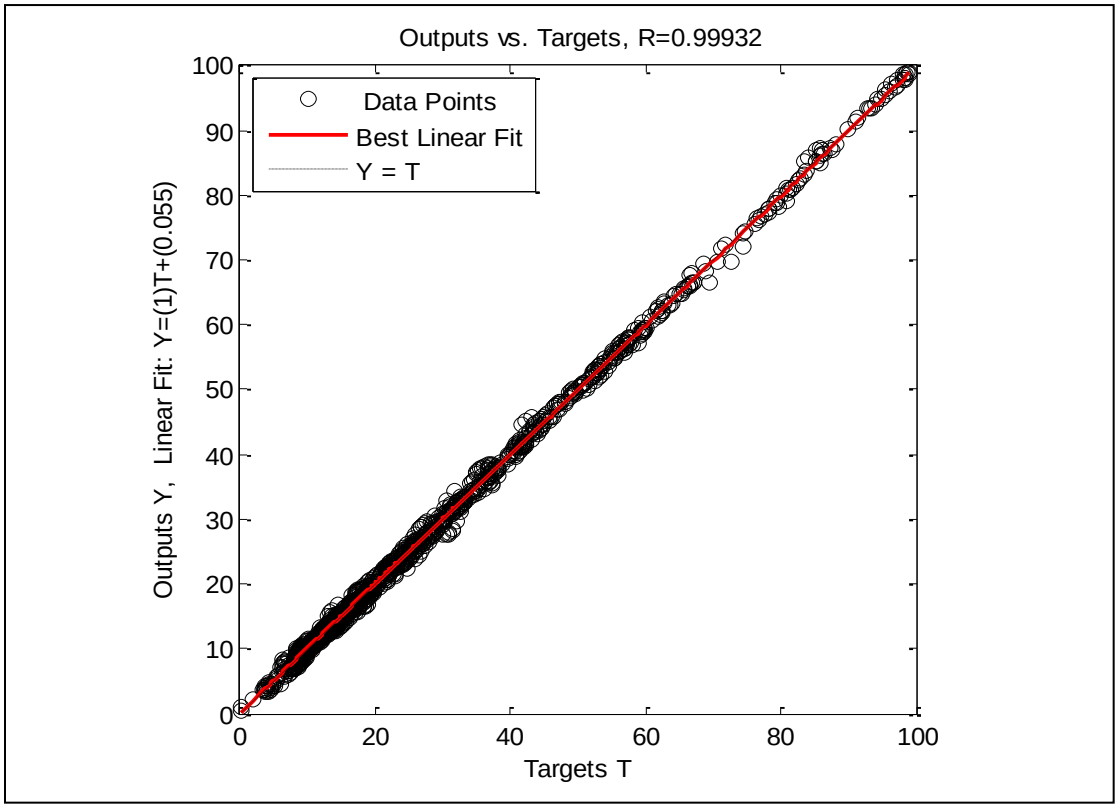

Figure A- 82: Well-5, Case -1, Crossplot

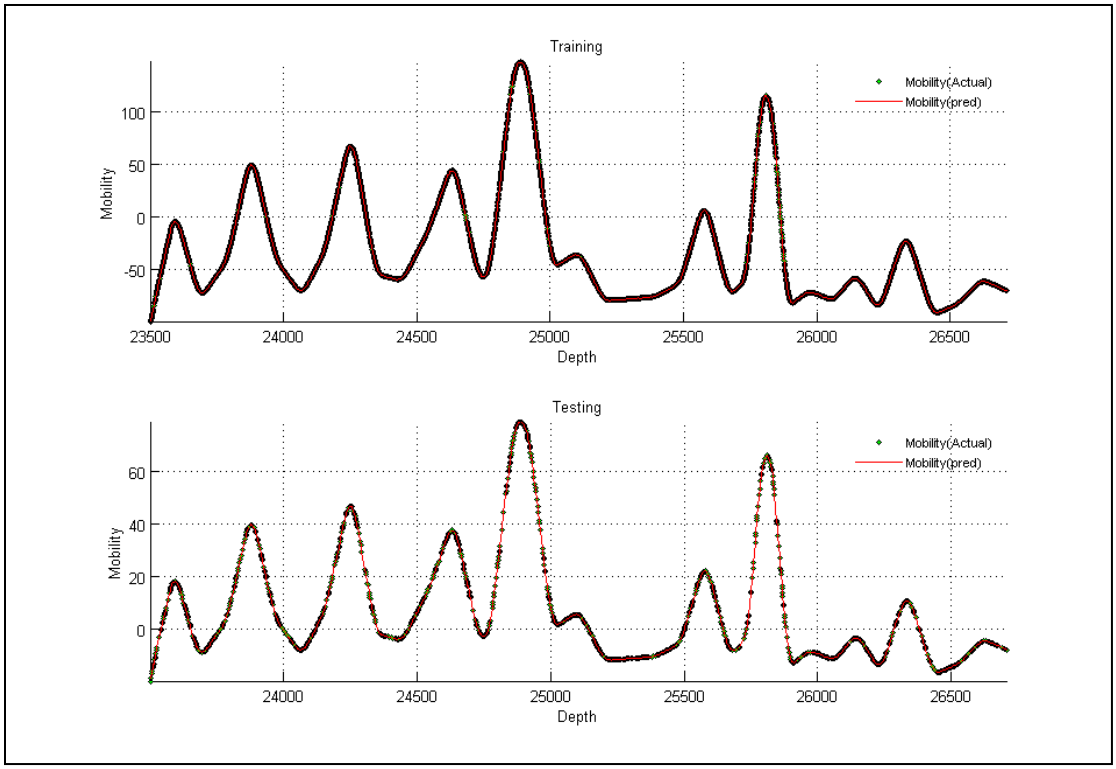

Figure A- 83: Well-5, Case -2

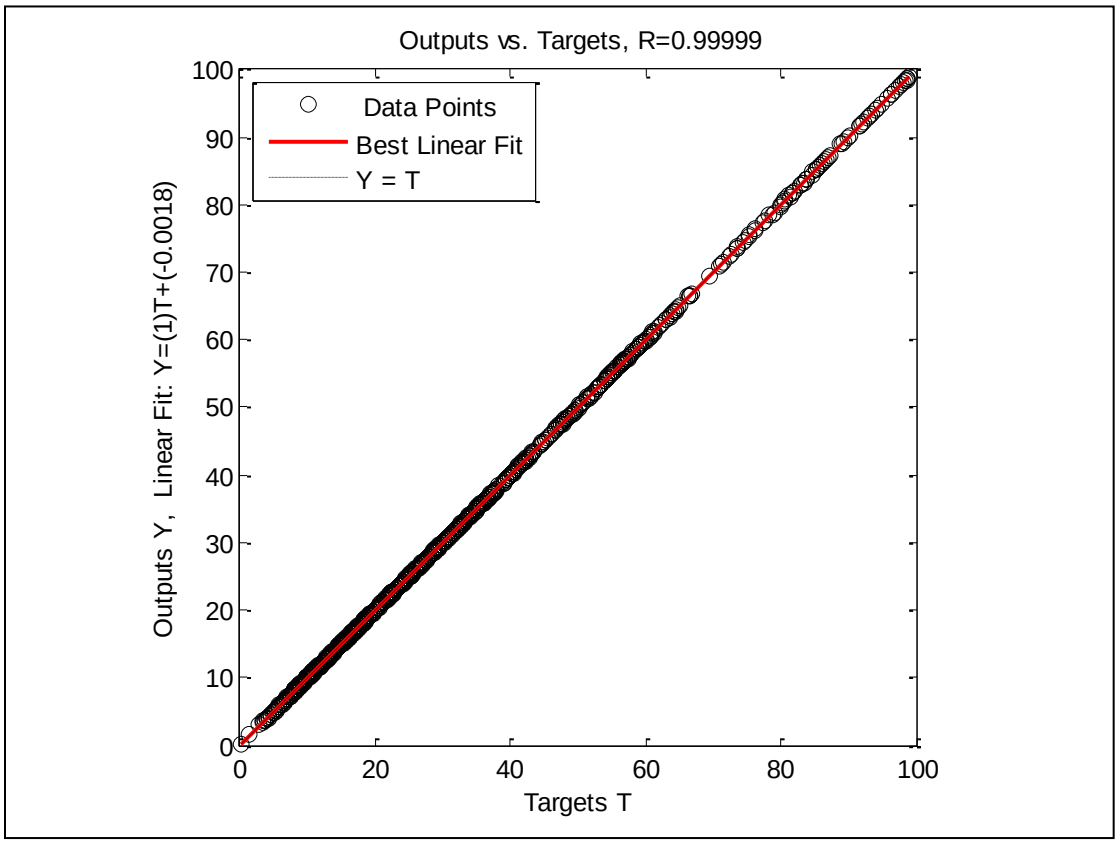

Figure A- 84: Well-5, Case -2, Crossplot

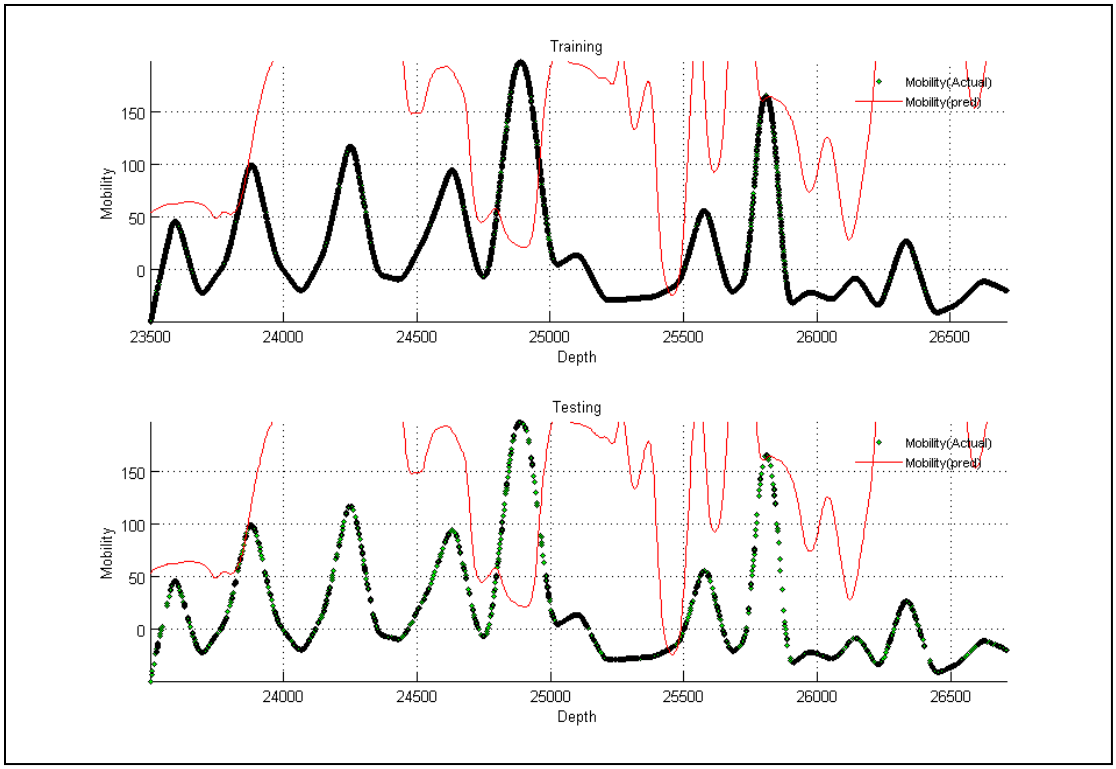

Figure A- 85: Well-5, Case -3

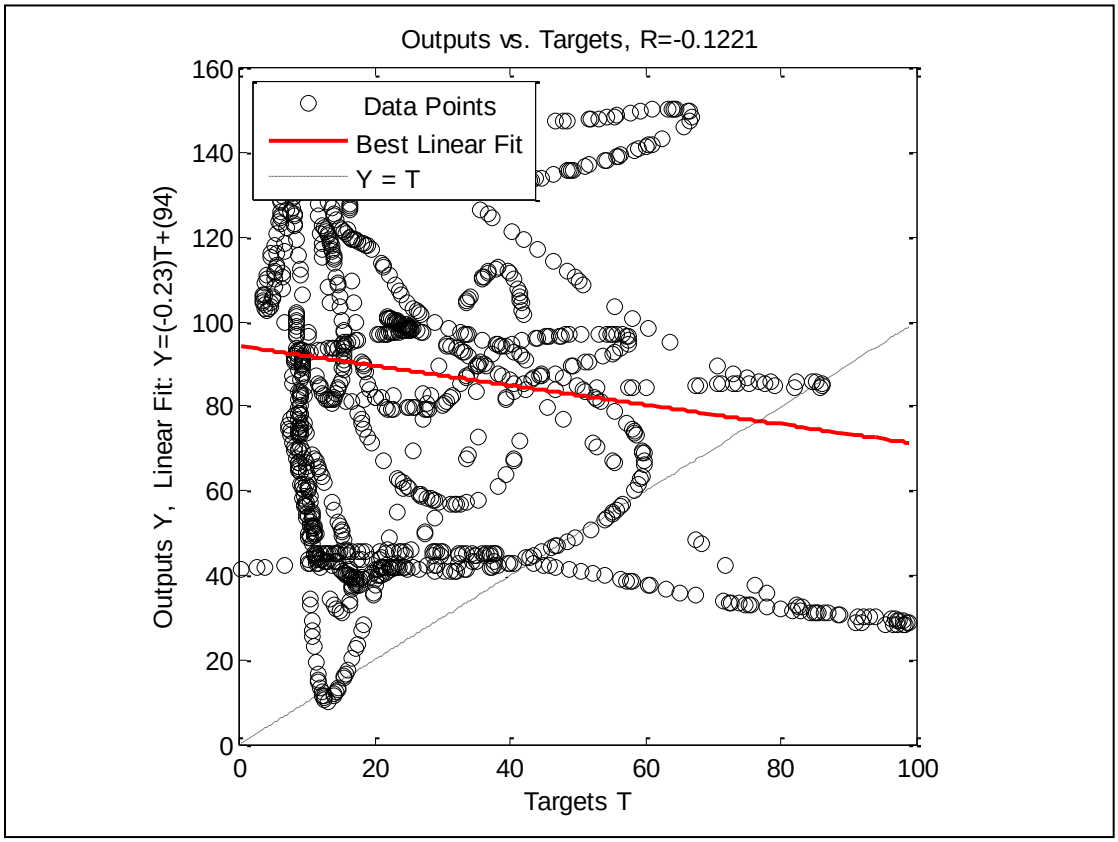

Figure A- 86: Well-5, Case -3, Crossplot

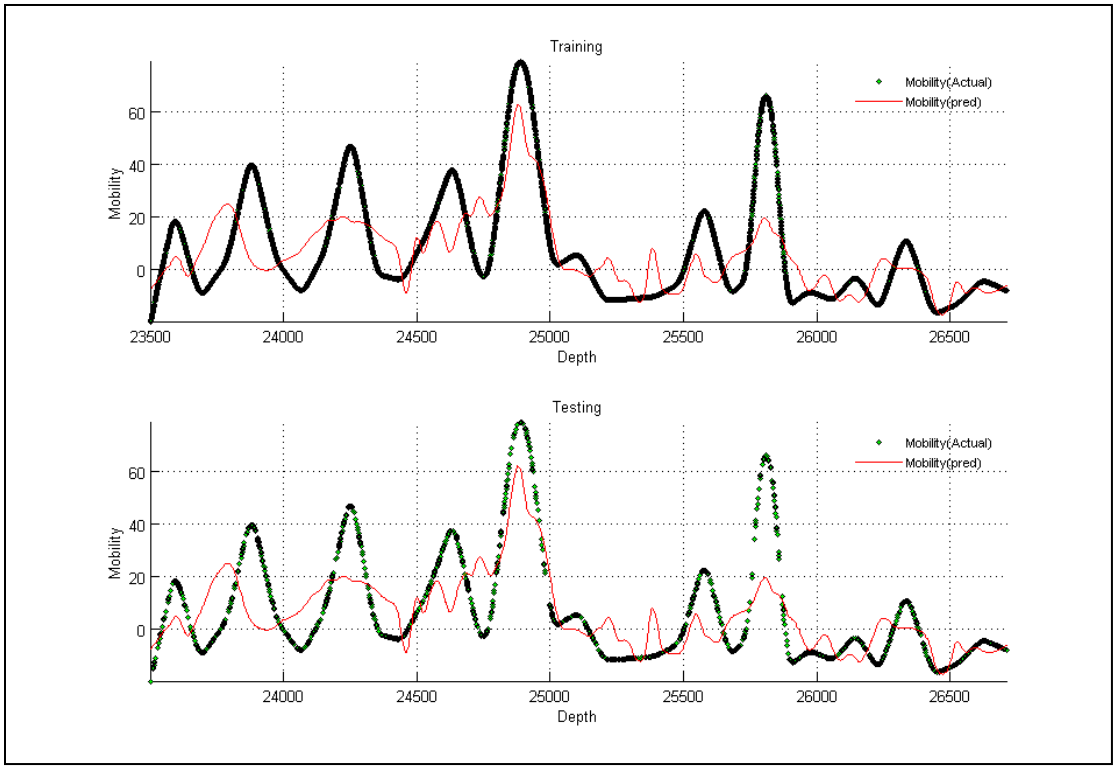

Figure A- 87: Well-5, Case -4

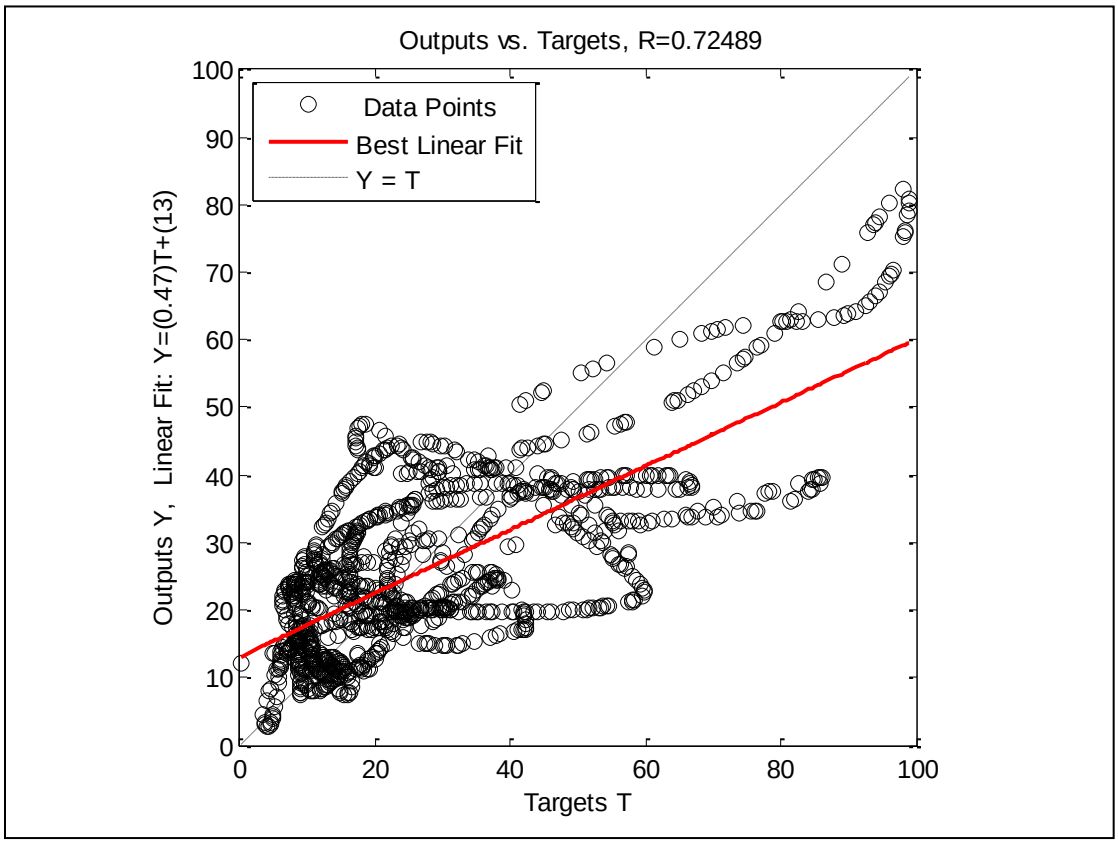

Figure A- 88: Well-5, Case -4, Crossplot

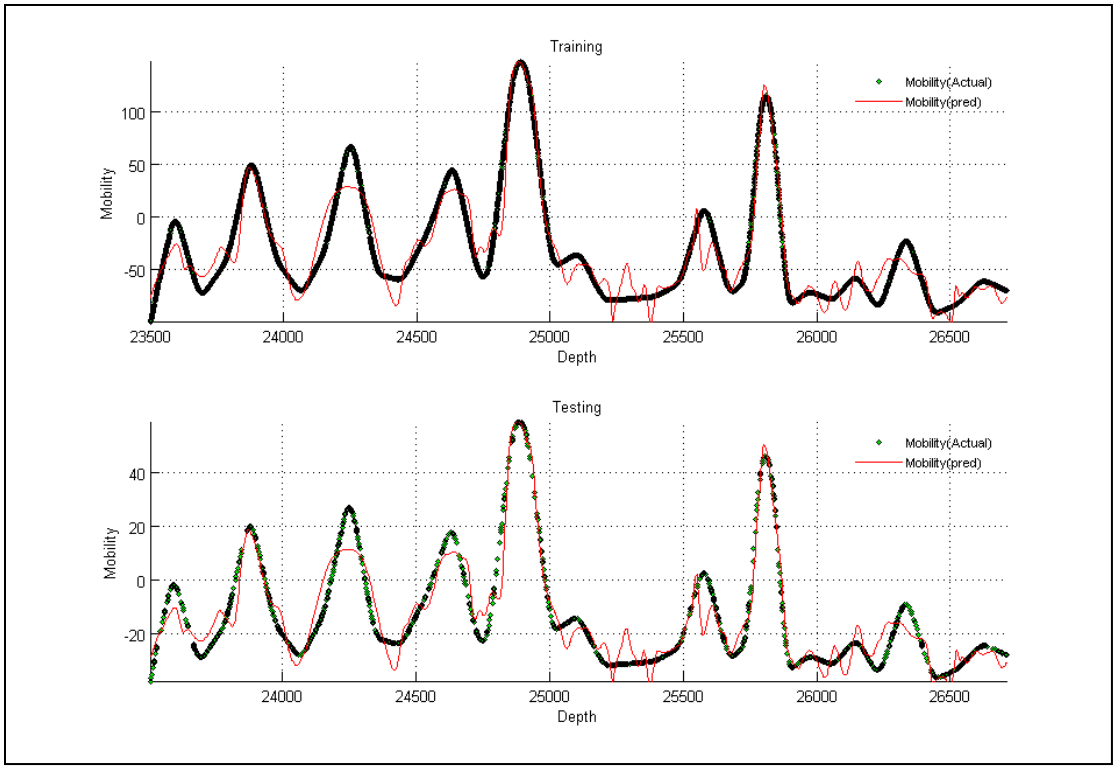

Figure A- 89: Well-5, Case -5

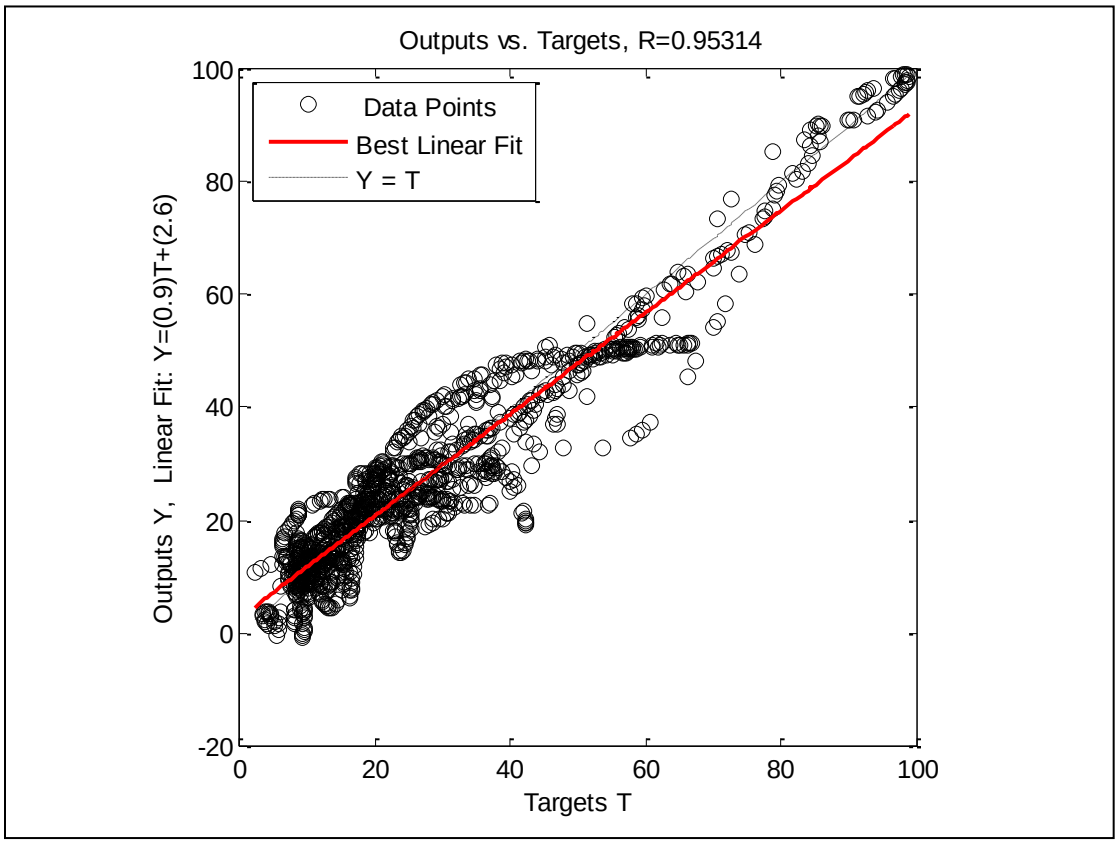

Figure A- 90: Well-5, Case -5, Crossplot

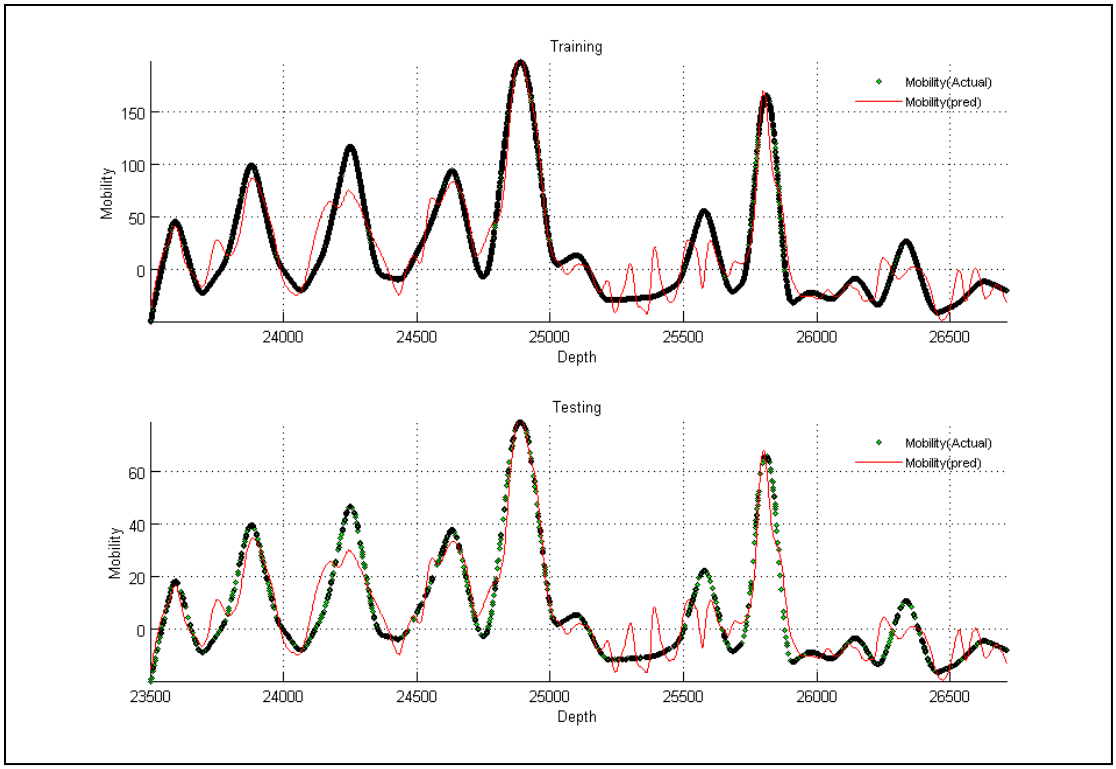

Figure A- 91: Well-5, Case -6

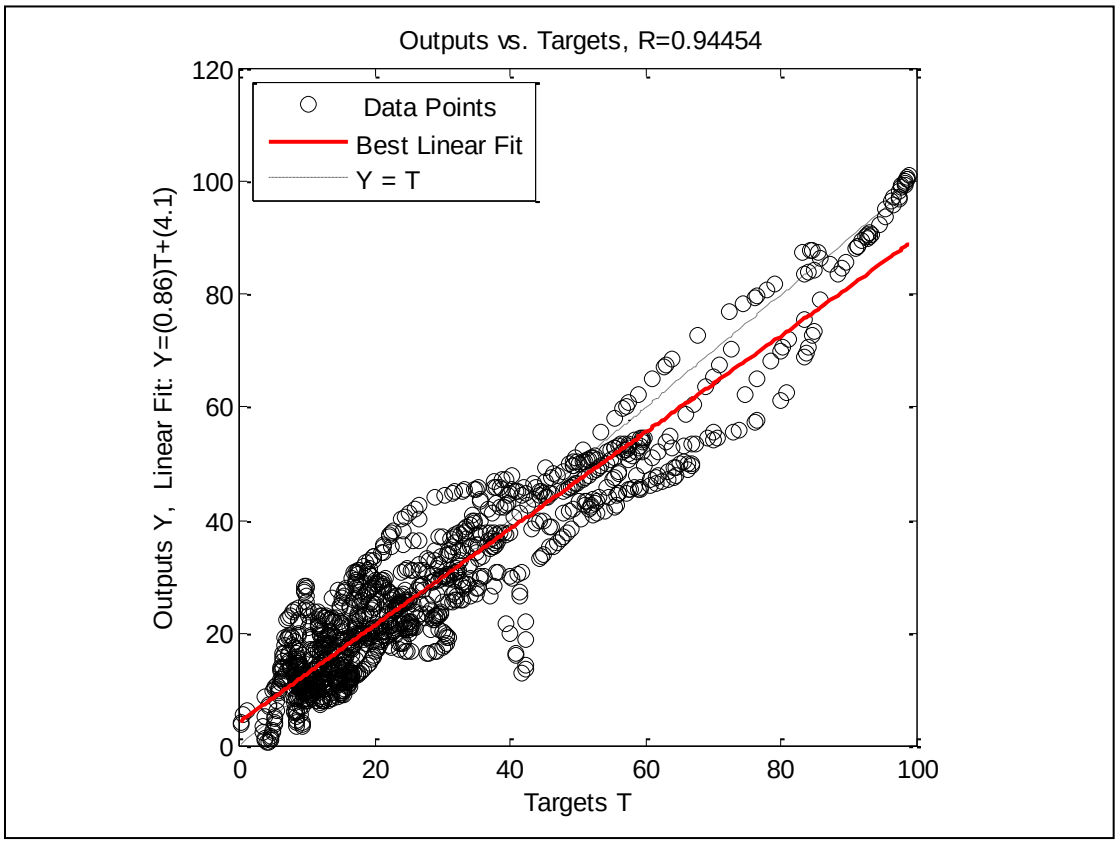

Figure A- 92: Well-5, Case -6, Crossplot

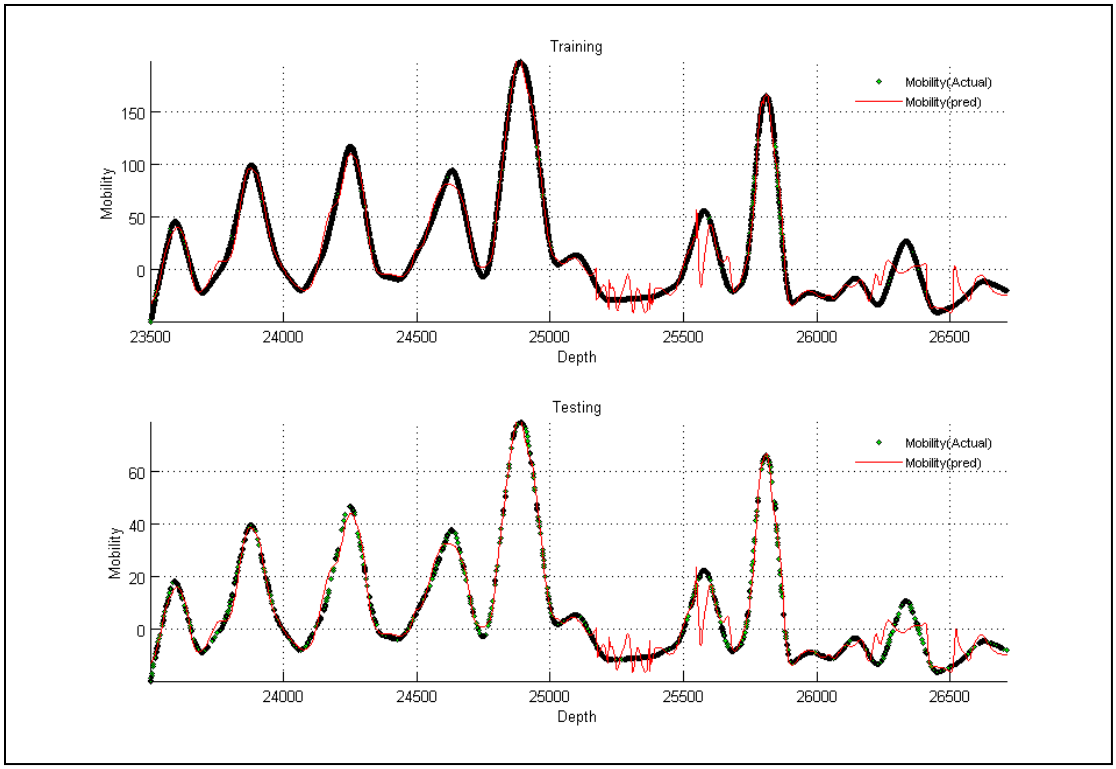

Figure A- 93: Well-5, Case -7

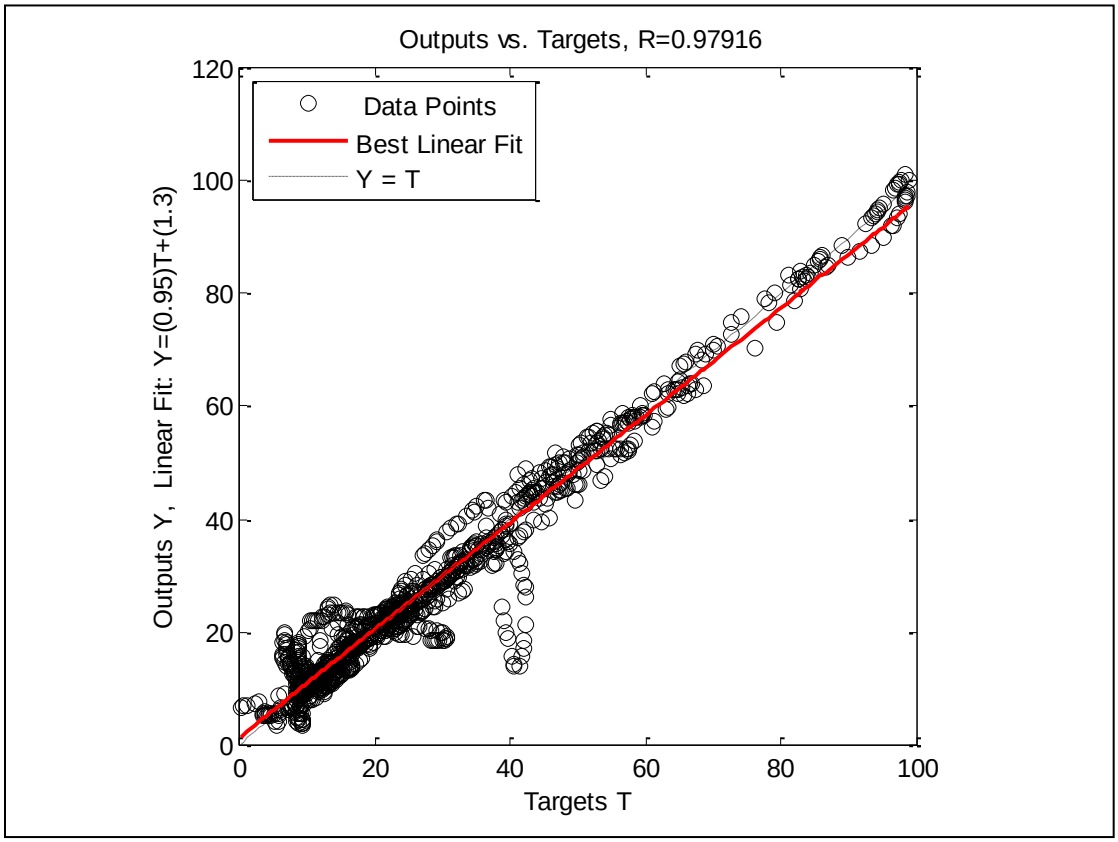

Figure A- 94: Well-5, Case -7, Crossplot

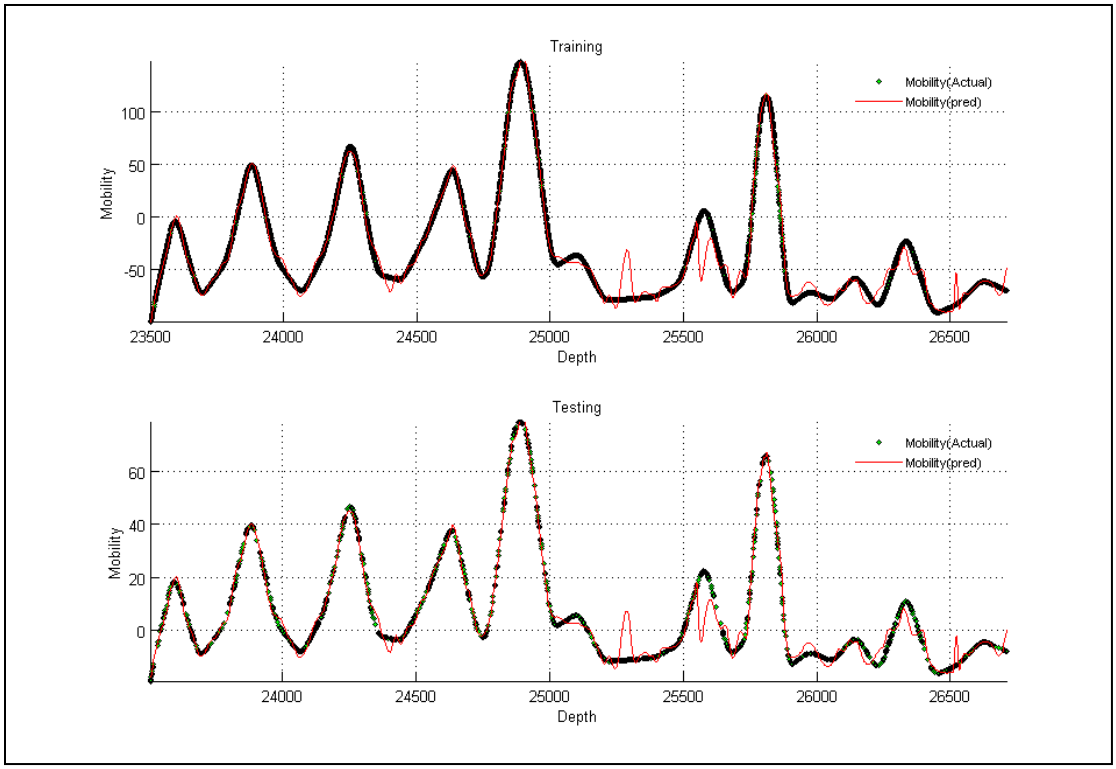

Figure A- 95: Well-5, Case -8

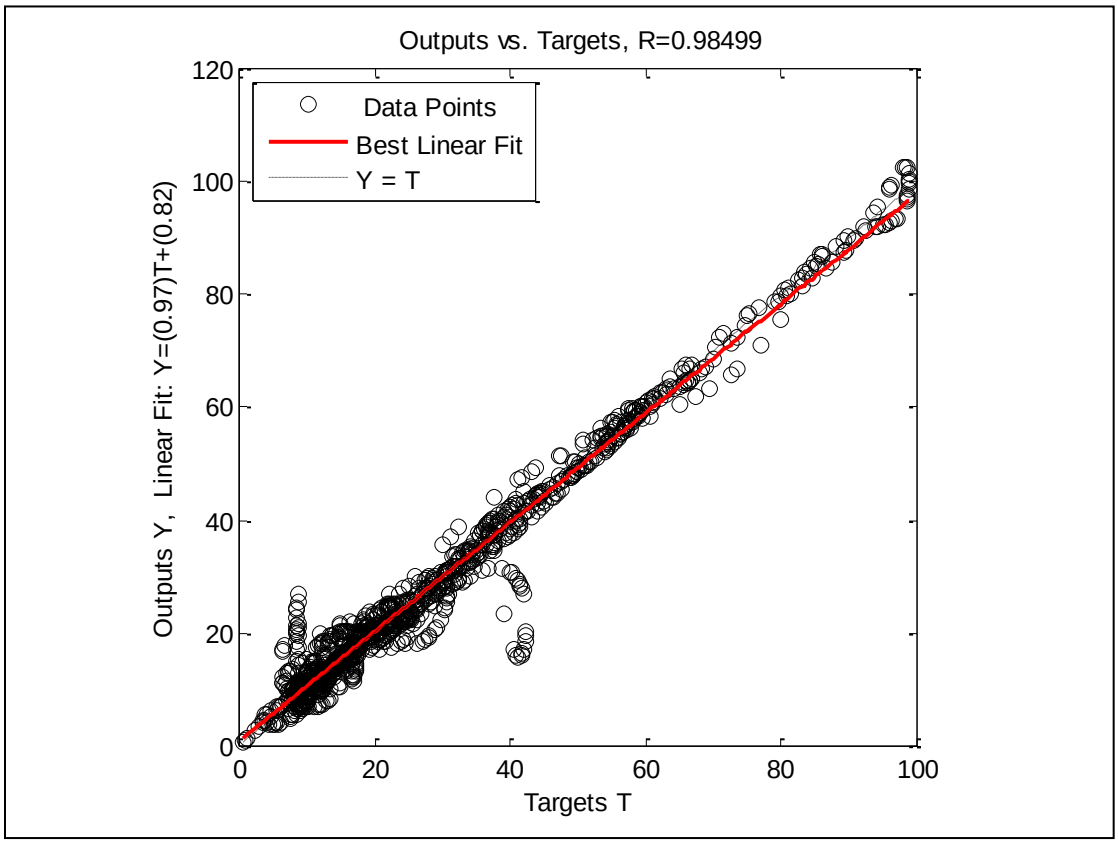

Figure A- 96: Well-5, Case -8, Crossplot

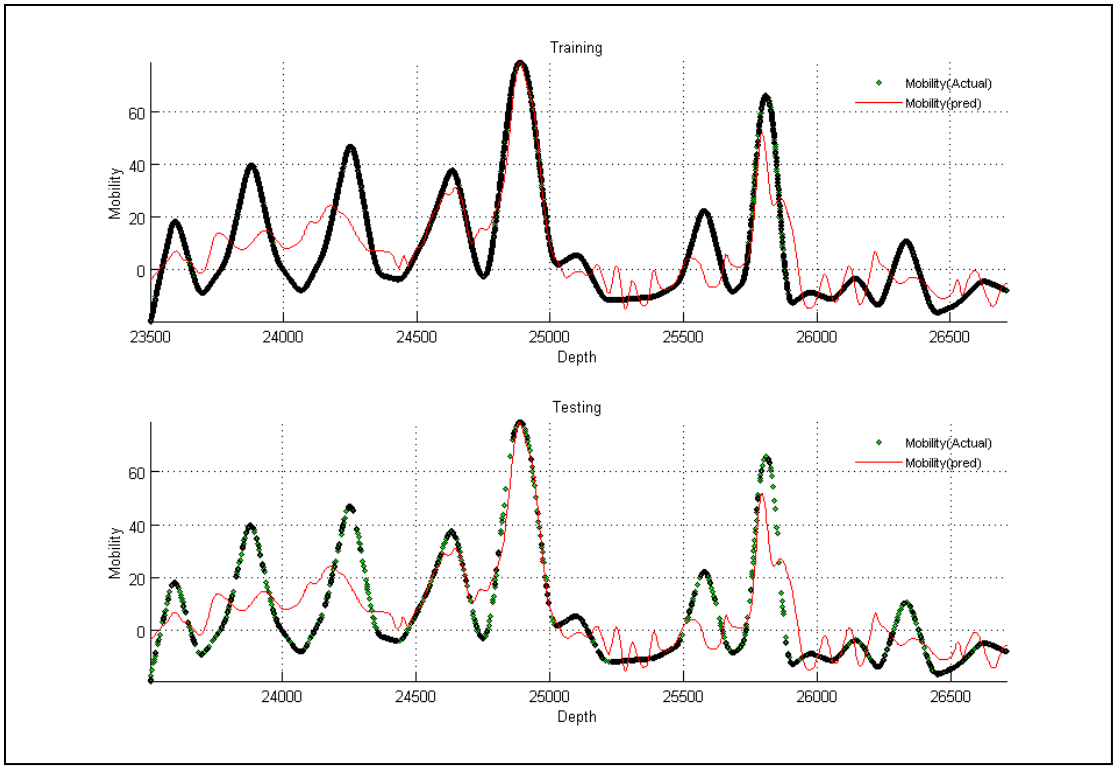

Figure A- 97: Well-5, Case -9

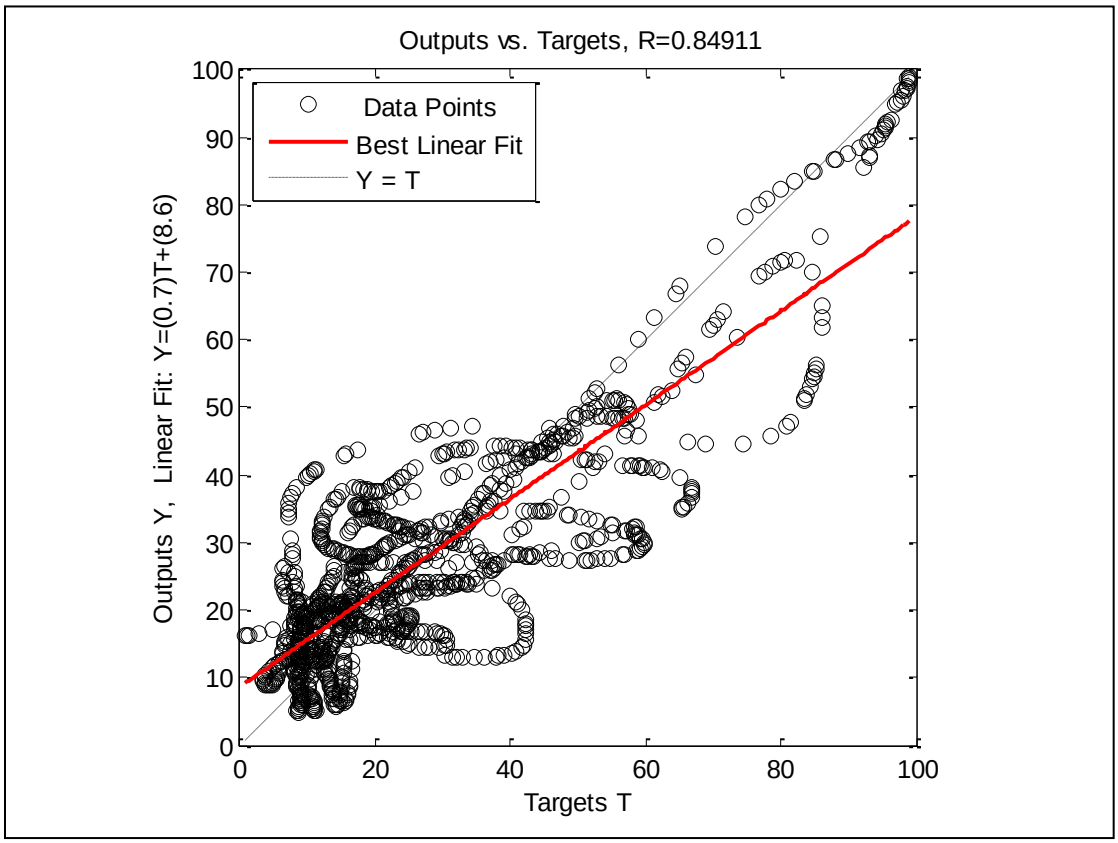

Figure A- 98: Well-5, Case -9, Crossplot

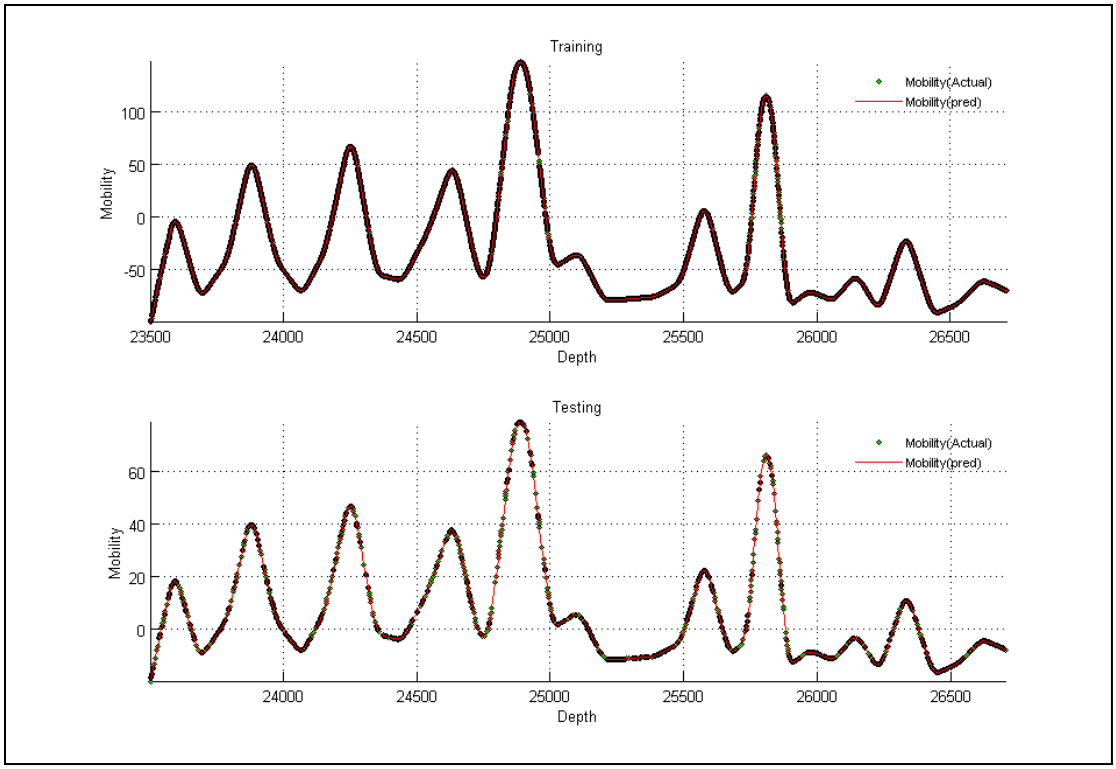

Figure A- 99: Well-5, Case -10

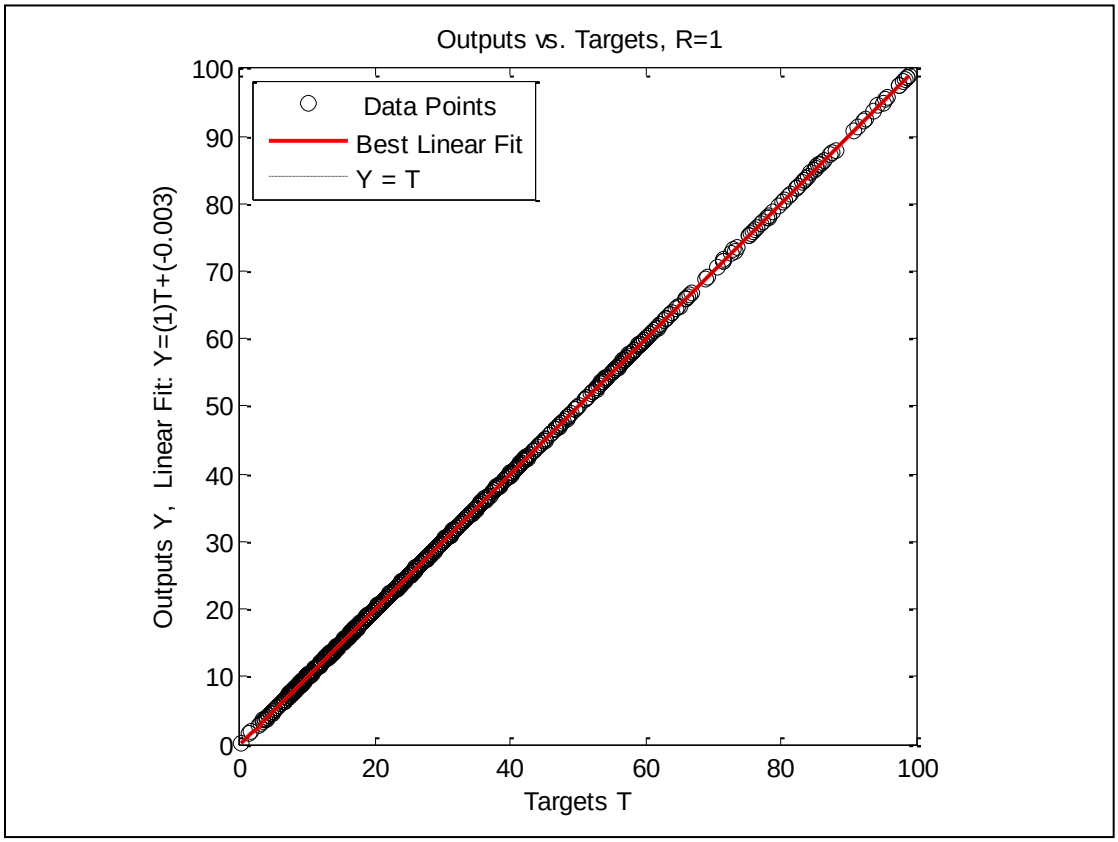

Figure A- 100: Well-5, Case -10, Crossplot

Well No. 6

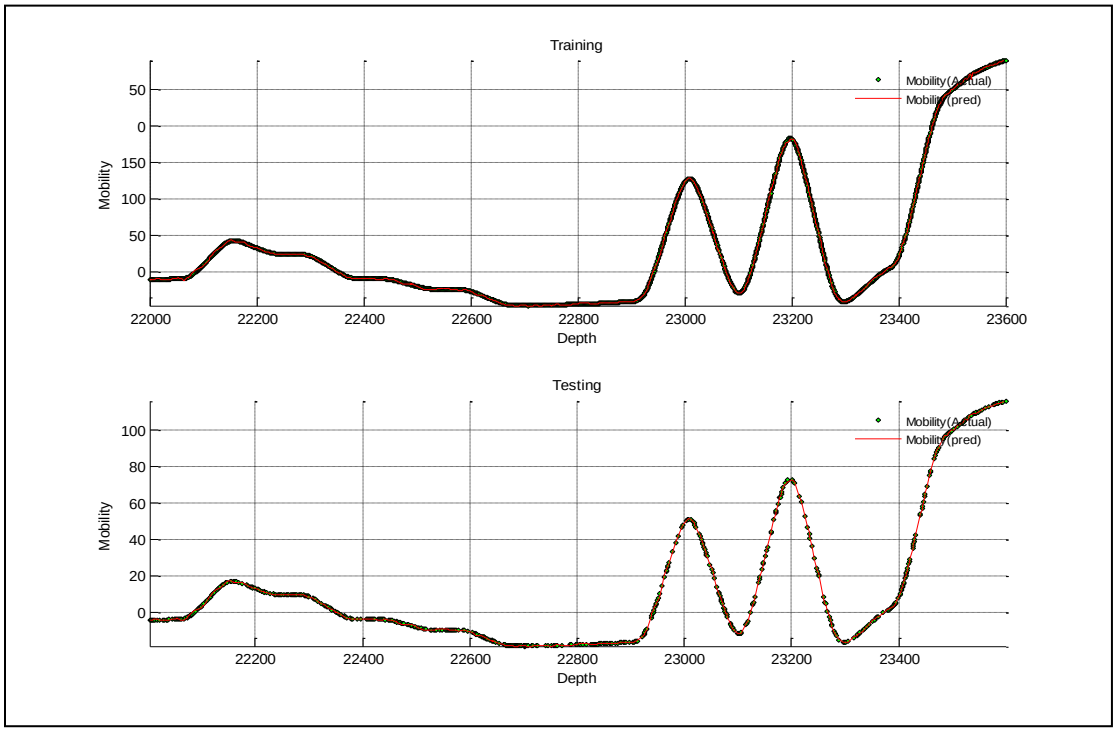

Figure A- 101: Well-6, Case -1

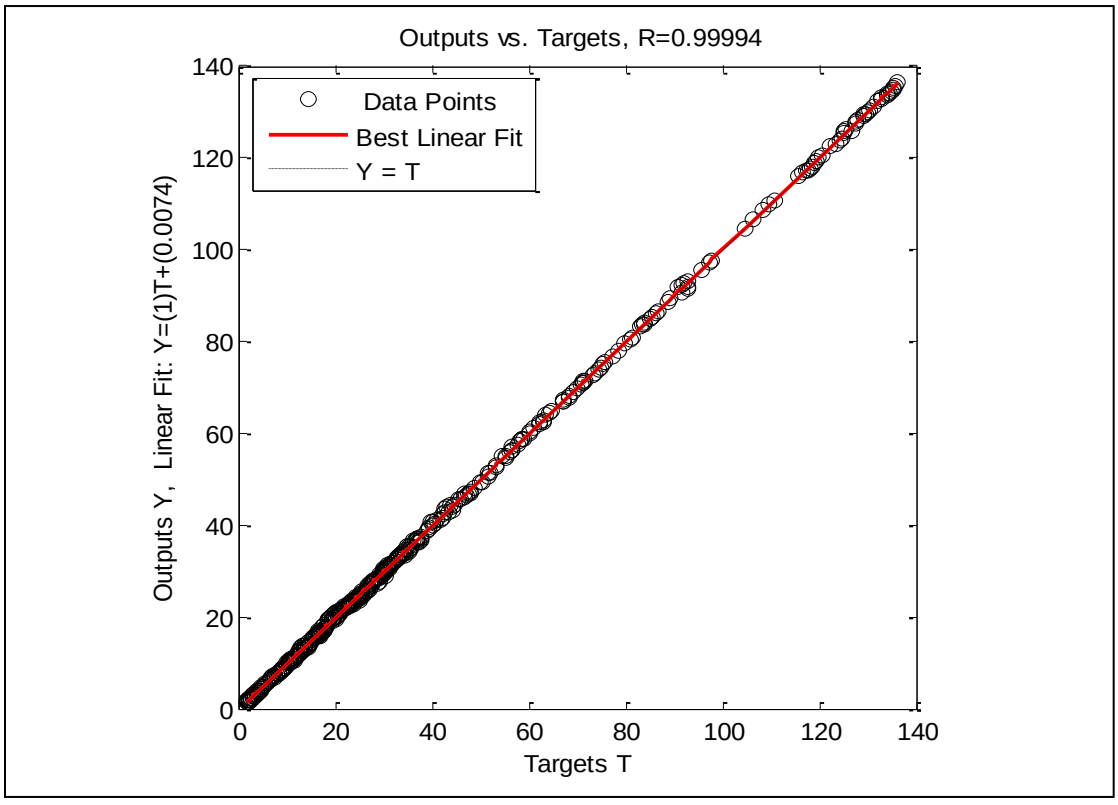

Figure A- 102: Well-6, Case -1, Crossplot

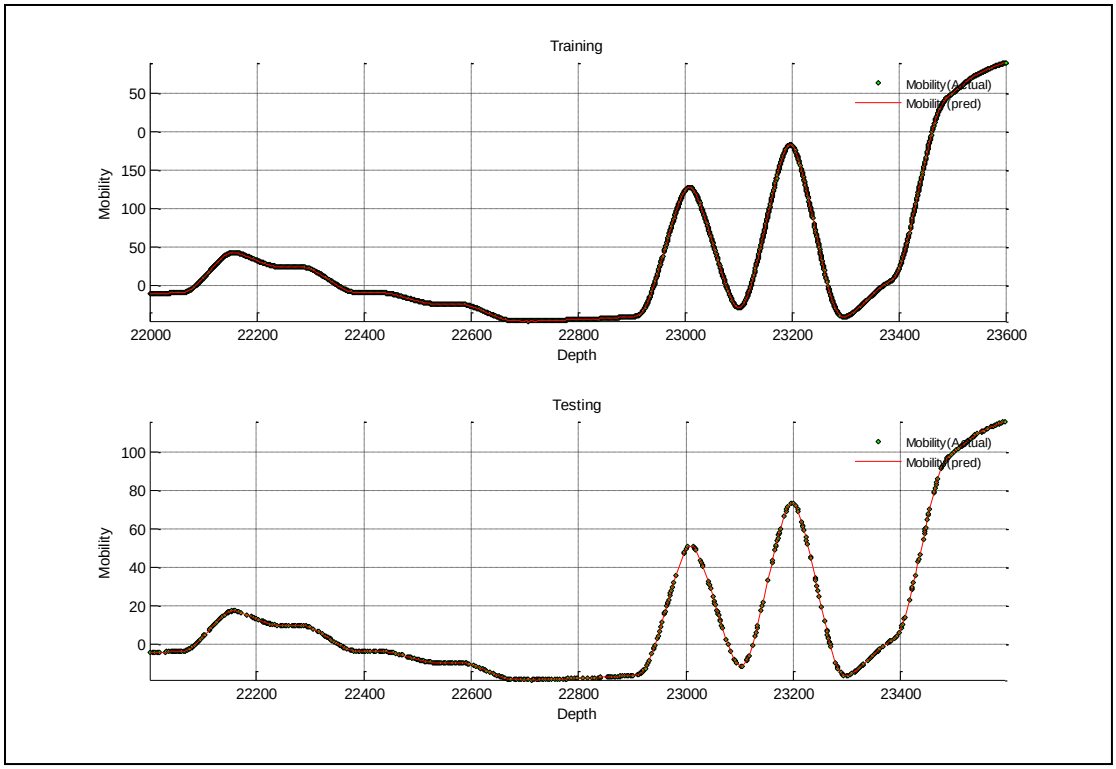

Figure A- 103: Well-6, Case -2

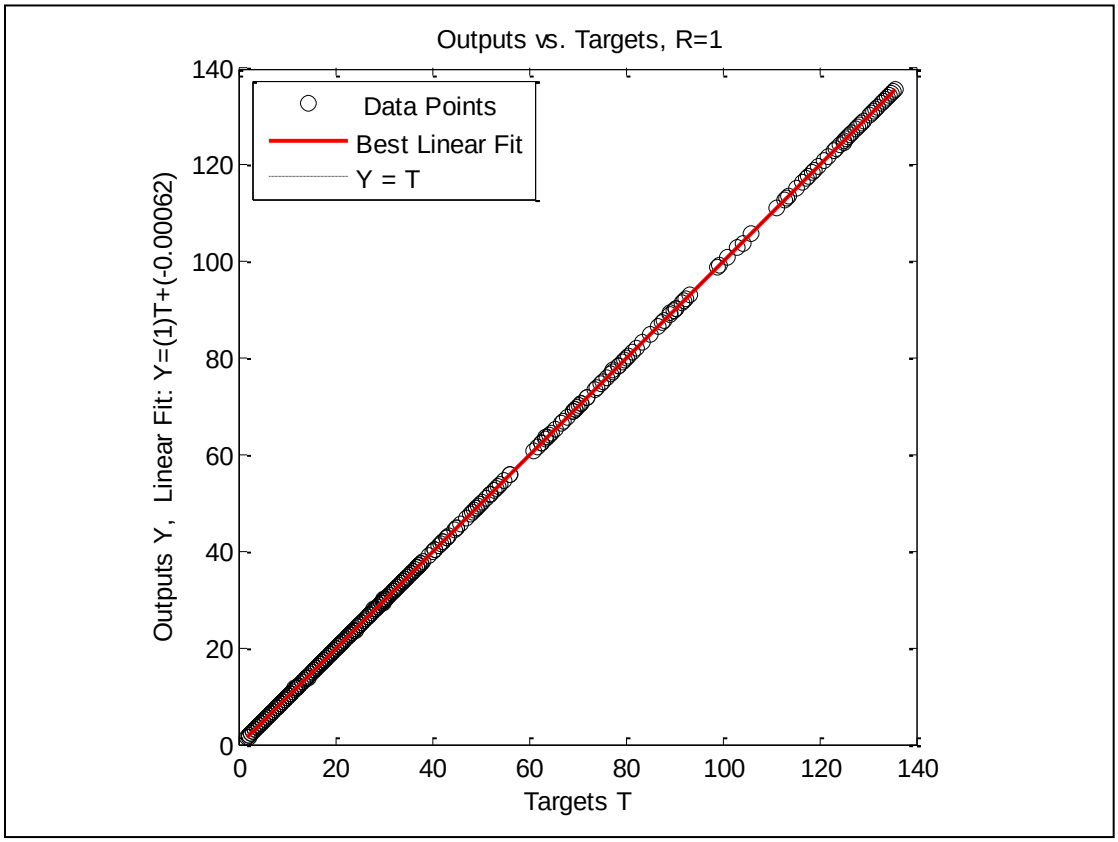

Figure A- 104: Well-6, Case -2, Crossplot

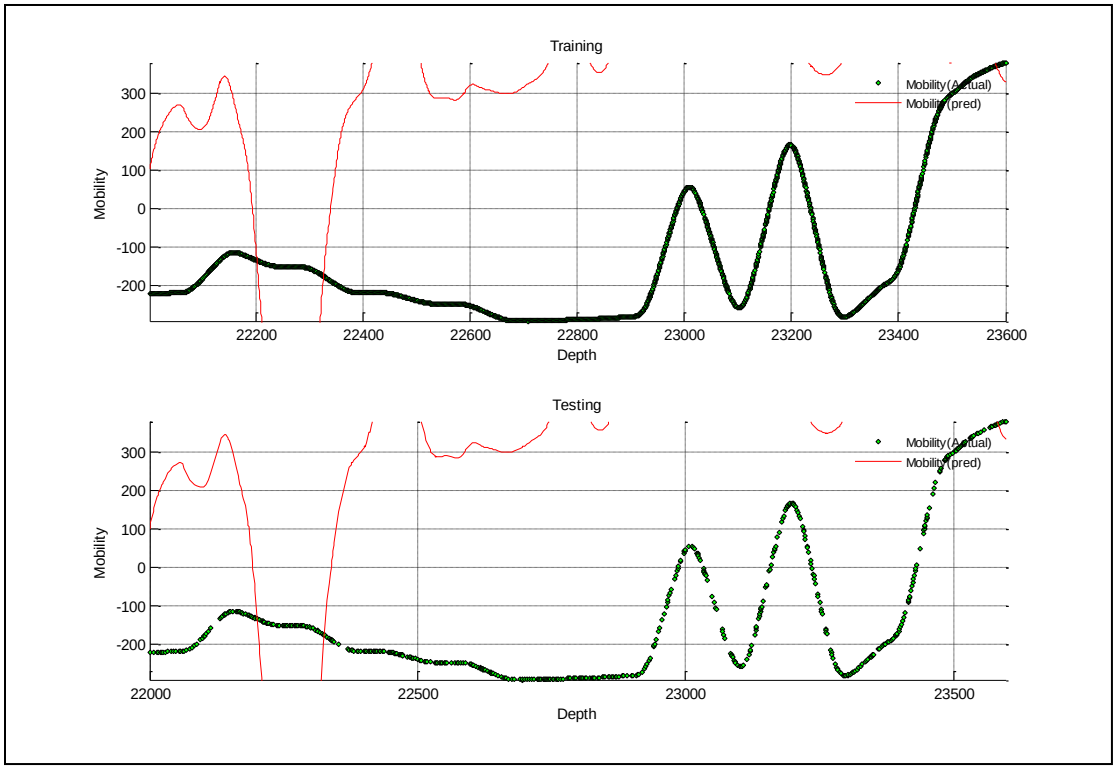

Figure A- 105: Well-6, Case -3

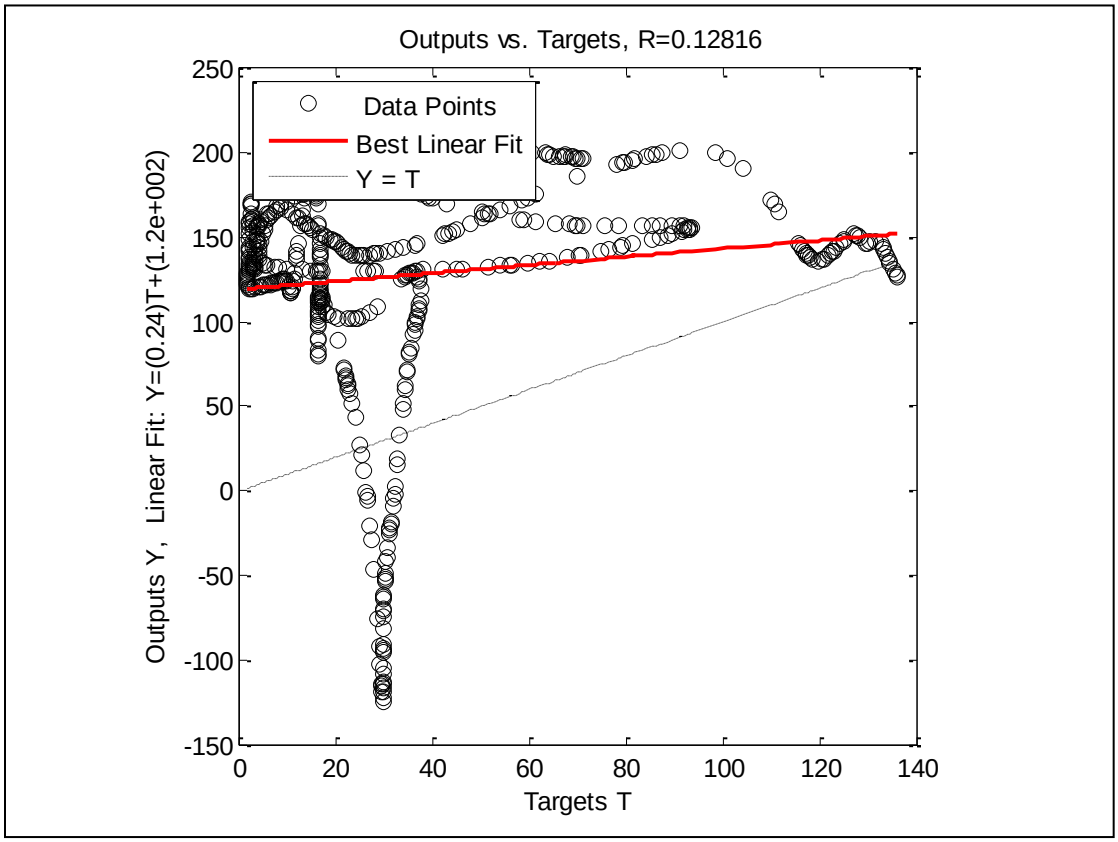

Figure A- 106: Well-6, Case -3, Crossplot

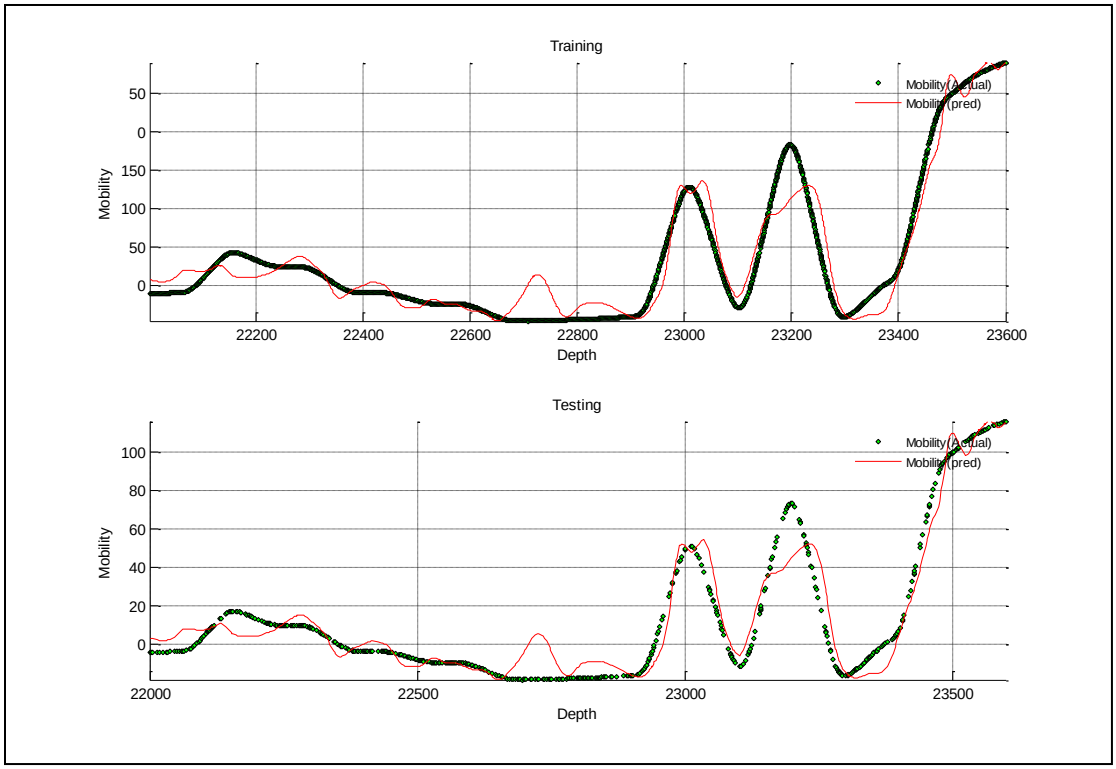

Figure A- 107: Well-6, Case -4

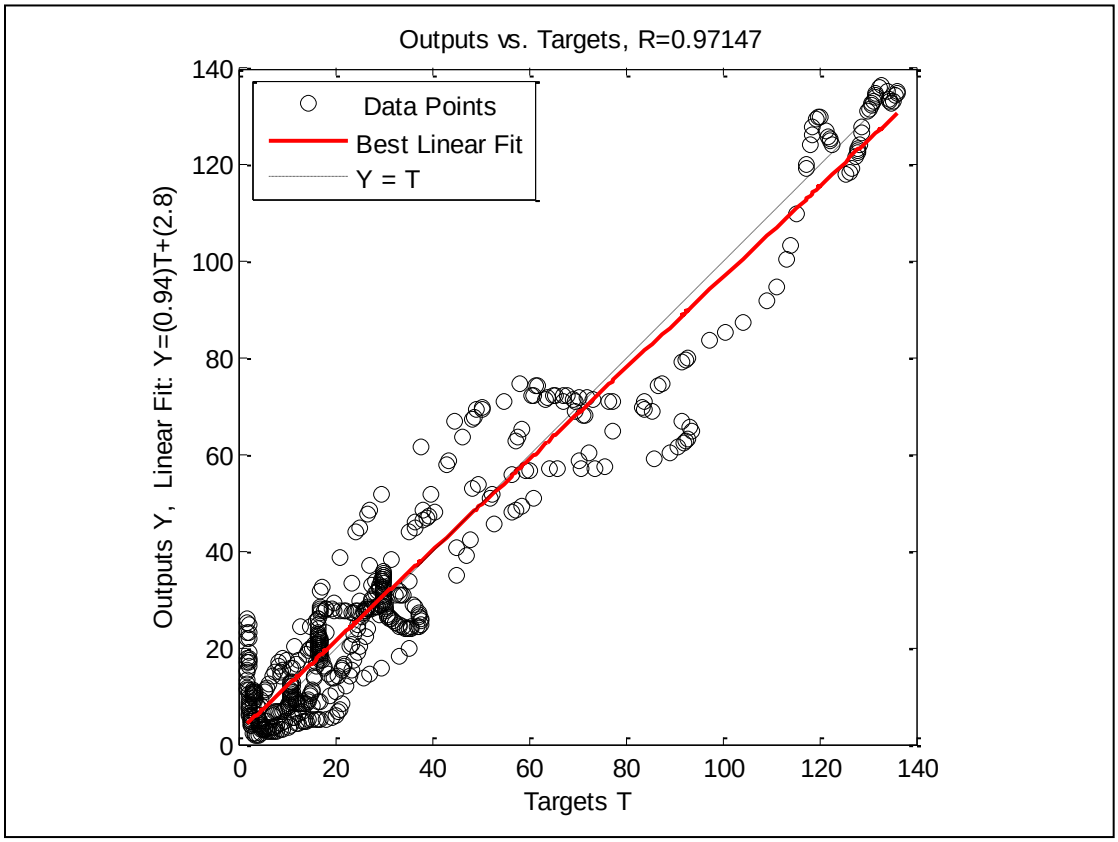

Figure A- 108: Well-6, Case -4, Crossplot

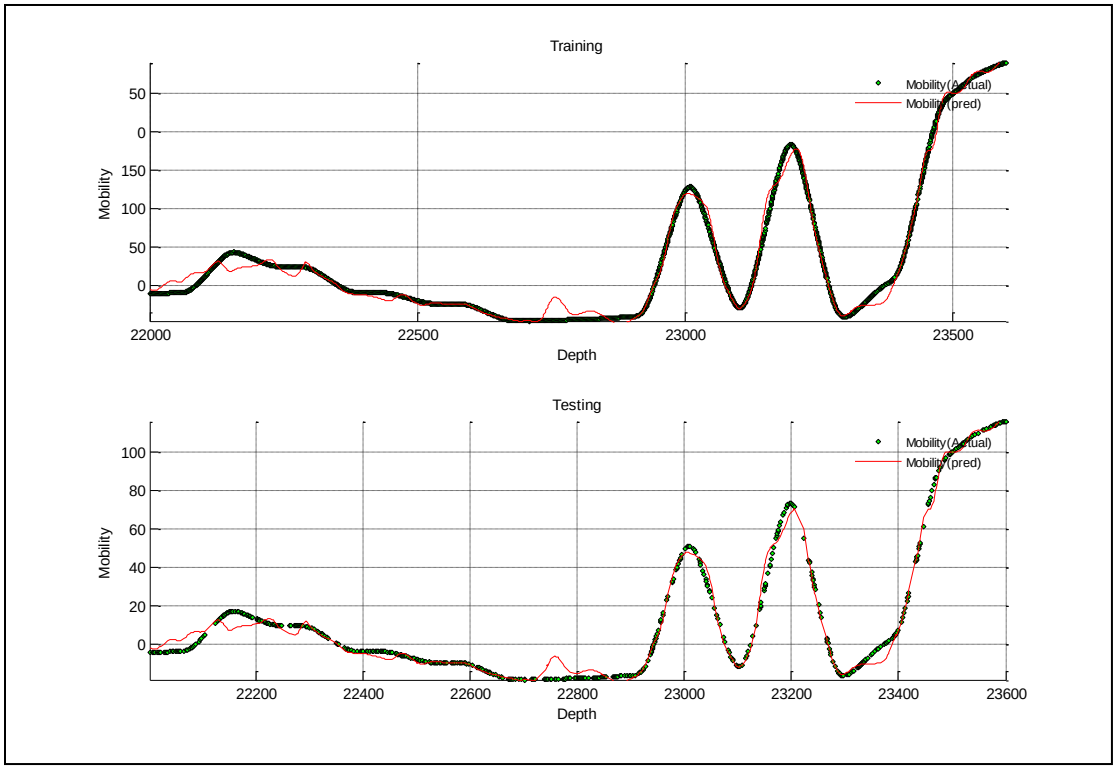

Figure A- 109: Well-6, Case -5

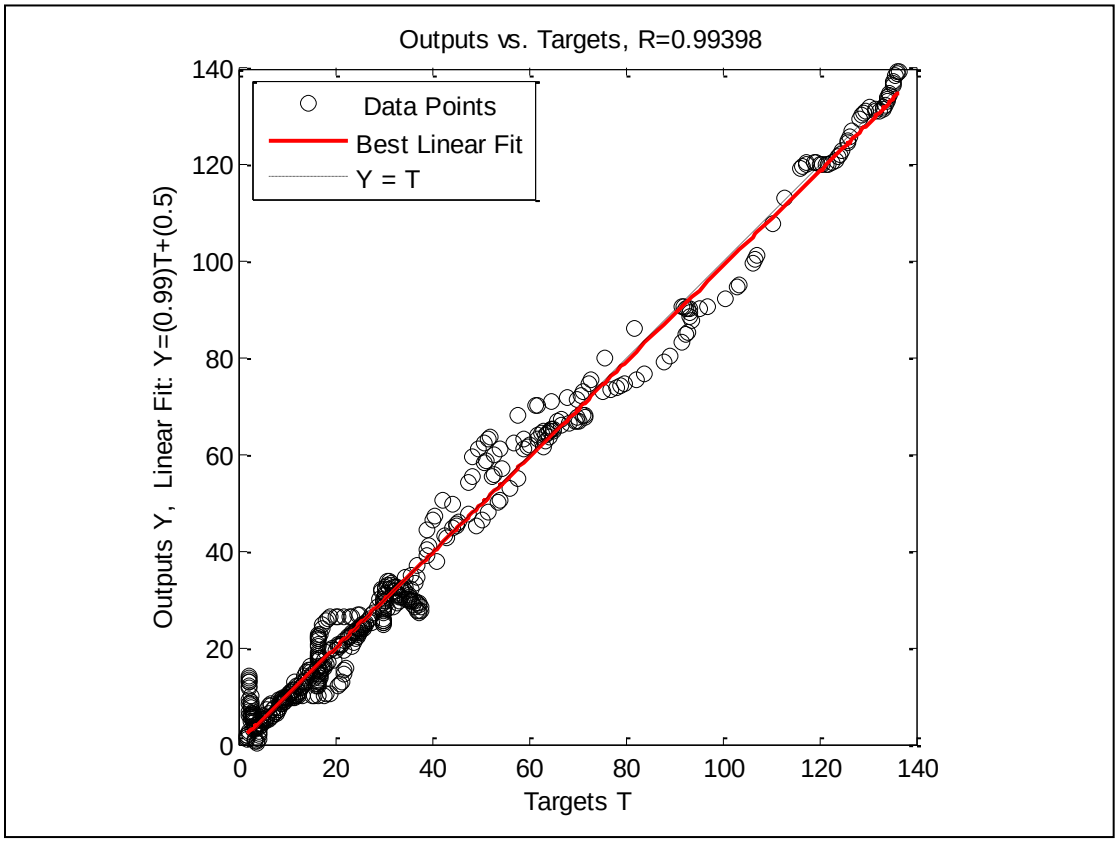

Figure A- 110: Well-6, Case -5, Crossplot

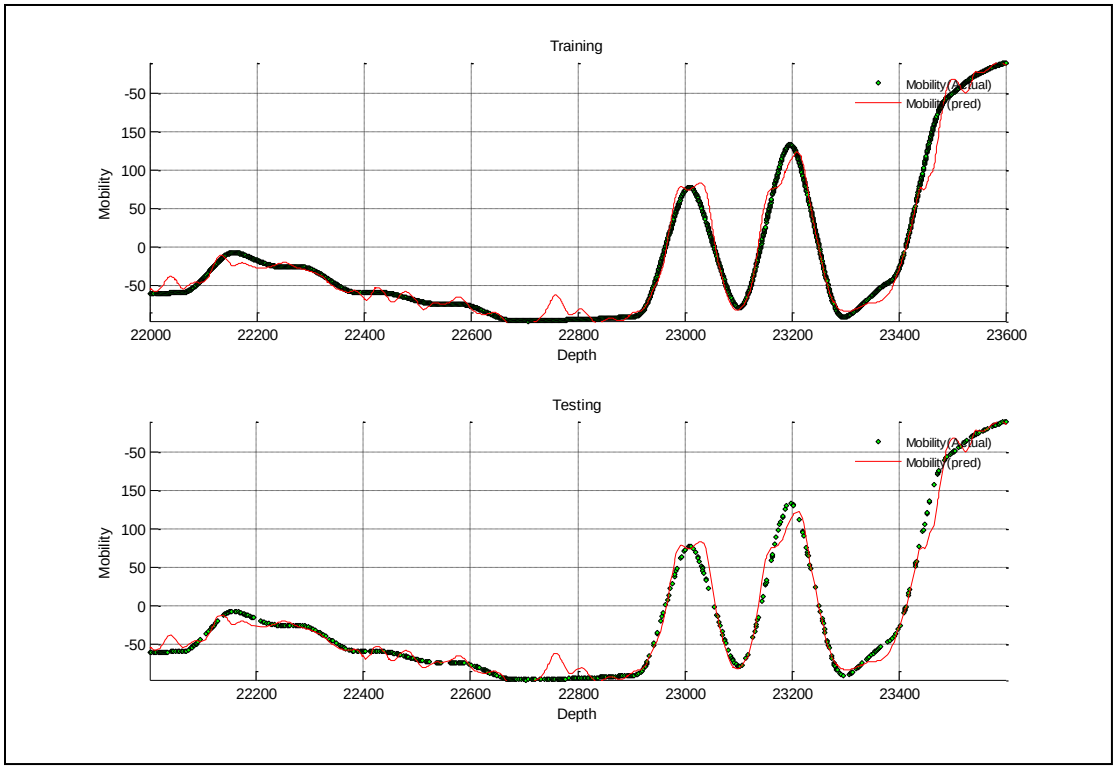

Figure A- 111: Well-6, Case -6

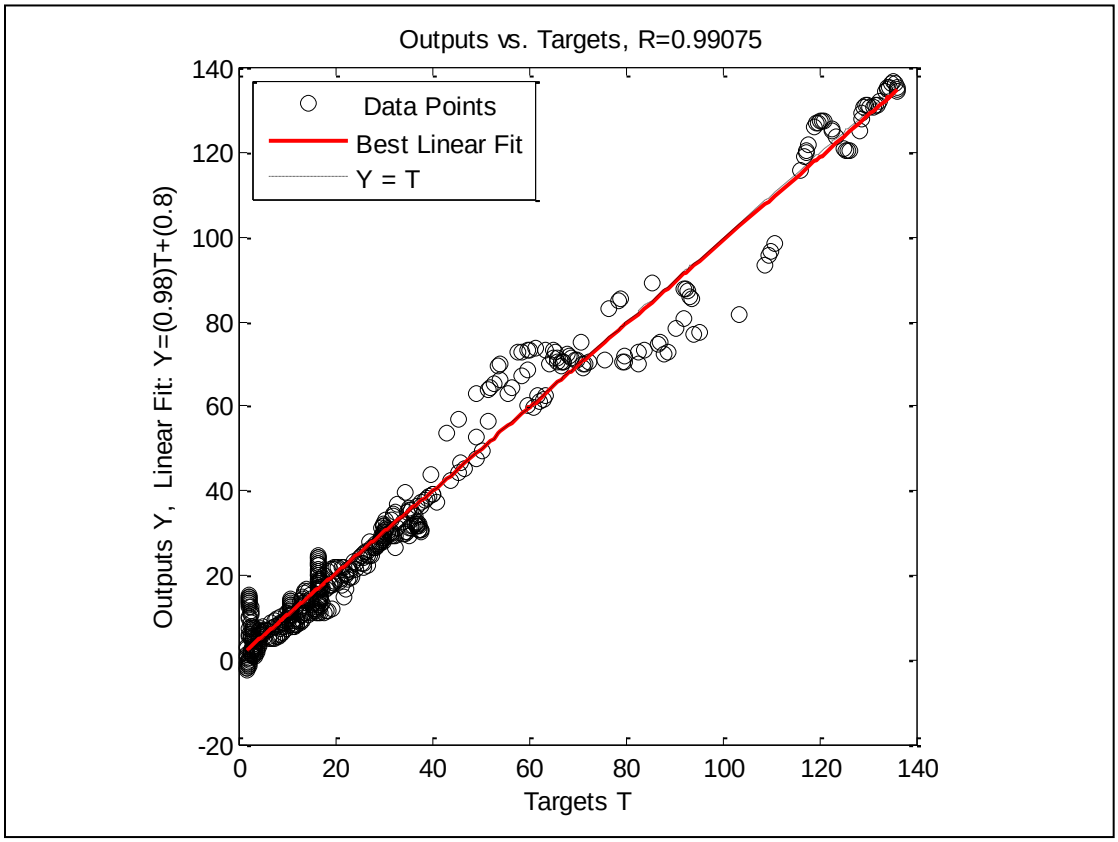

Figure A- 112: Well-6, Case -6, Crossplot

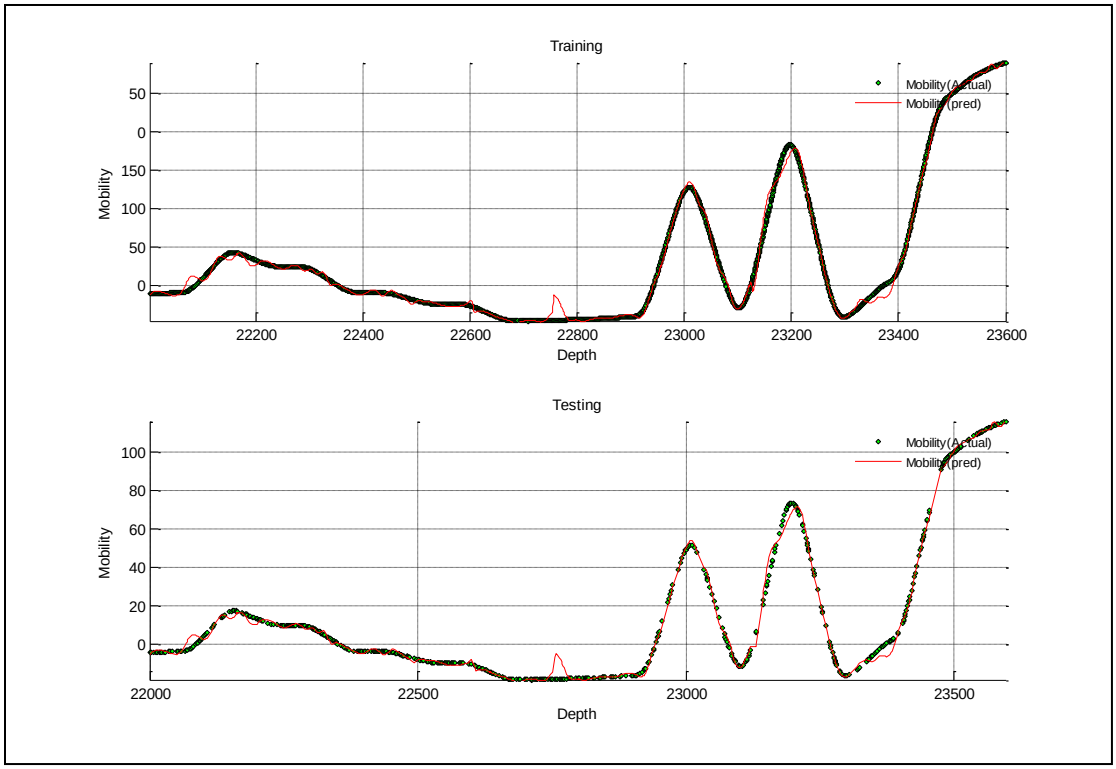

Figure A- 113: Well-6, Case -7

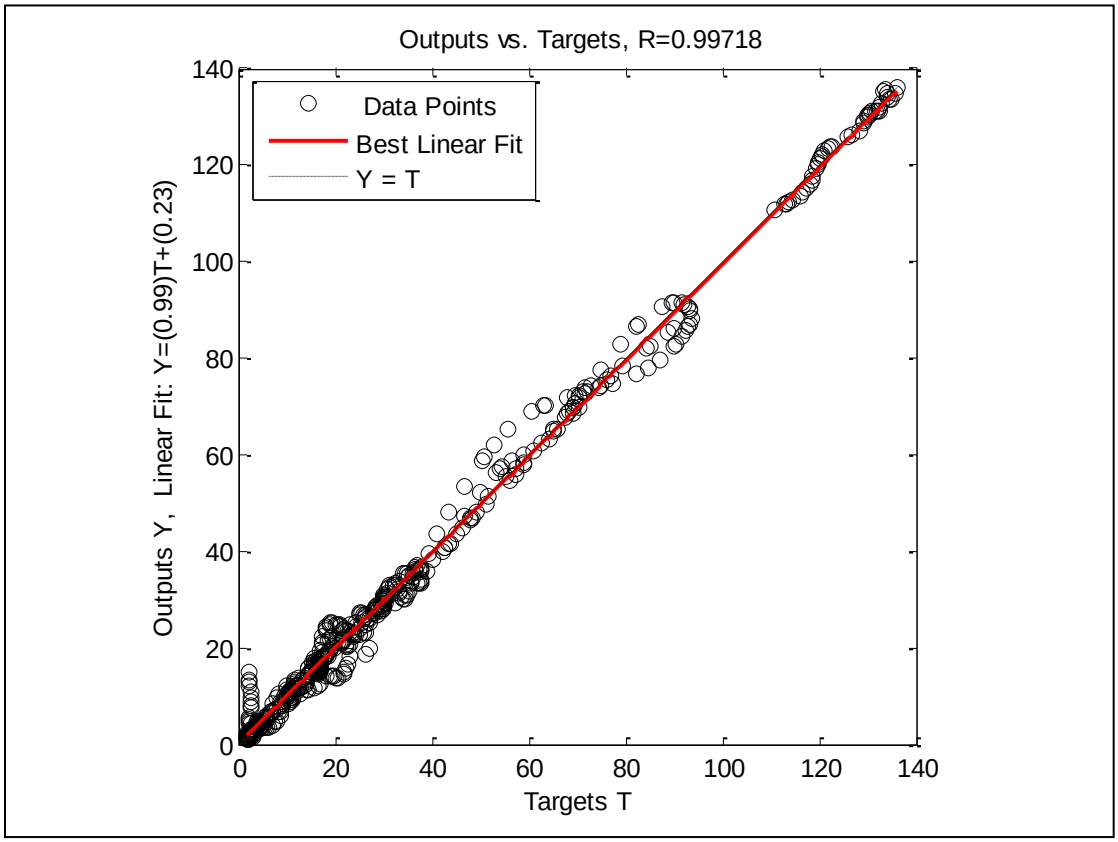

Figure A- 114: Well-6, Case -7, Crossplot

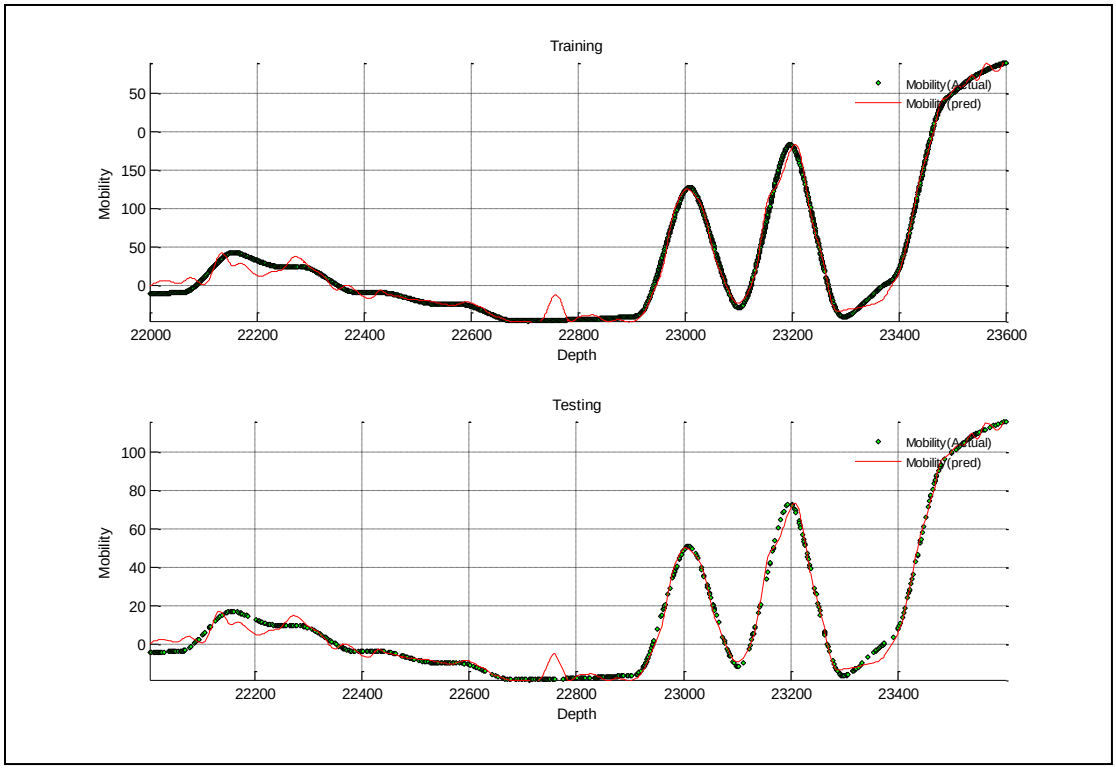

Figure A- 115: Well-6, Case -8

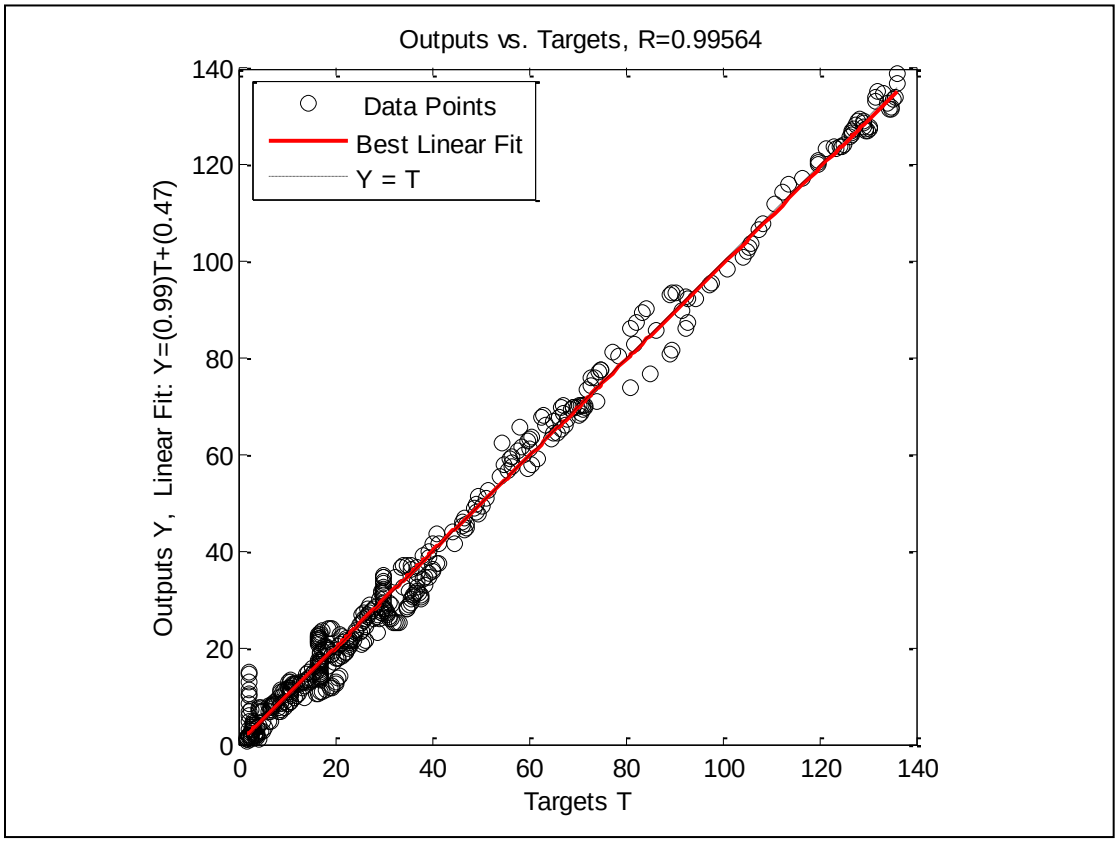

Figure A- 116: Well-6, Case -8, Crossplot

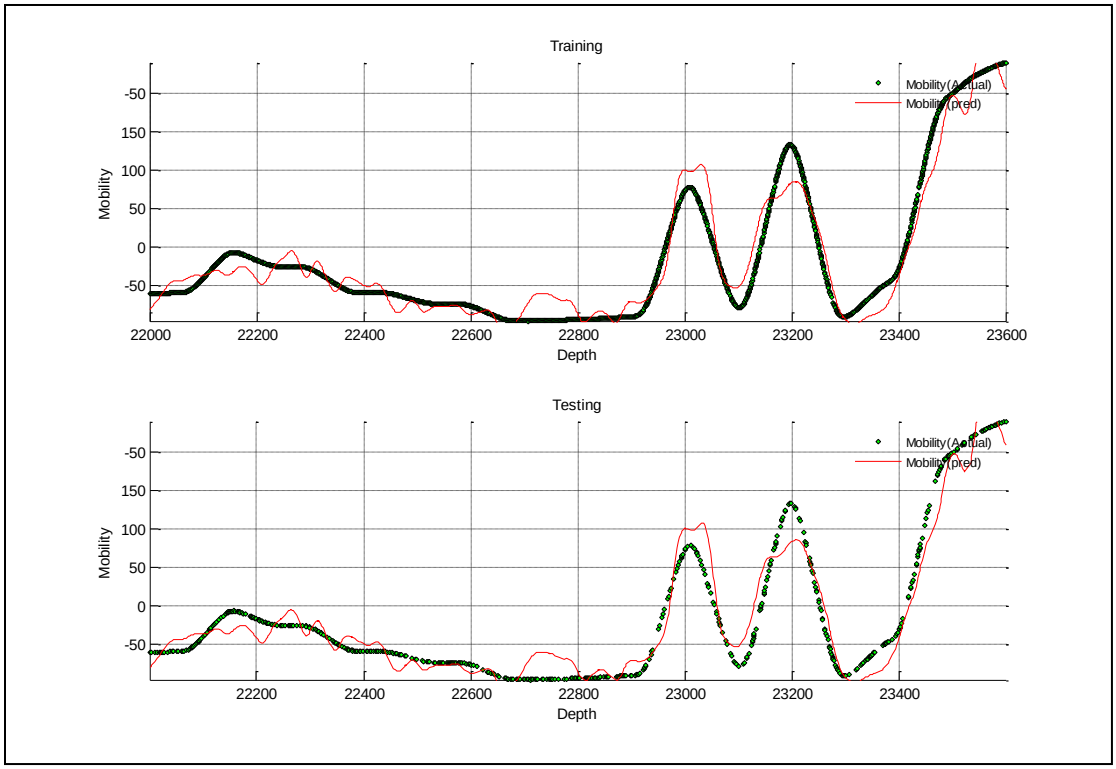

Figure A- 117: Well-6, Case -9

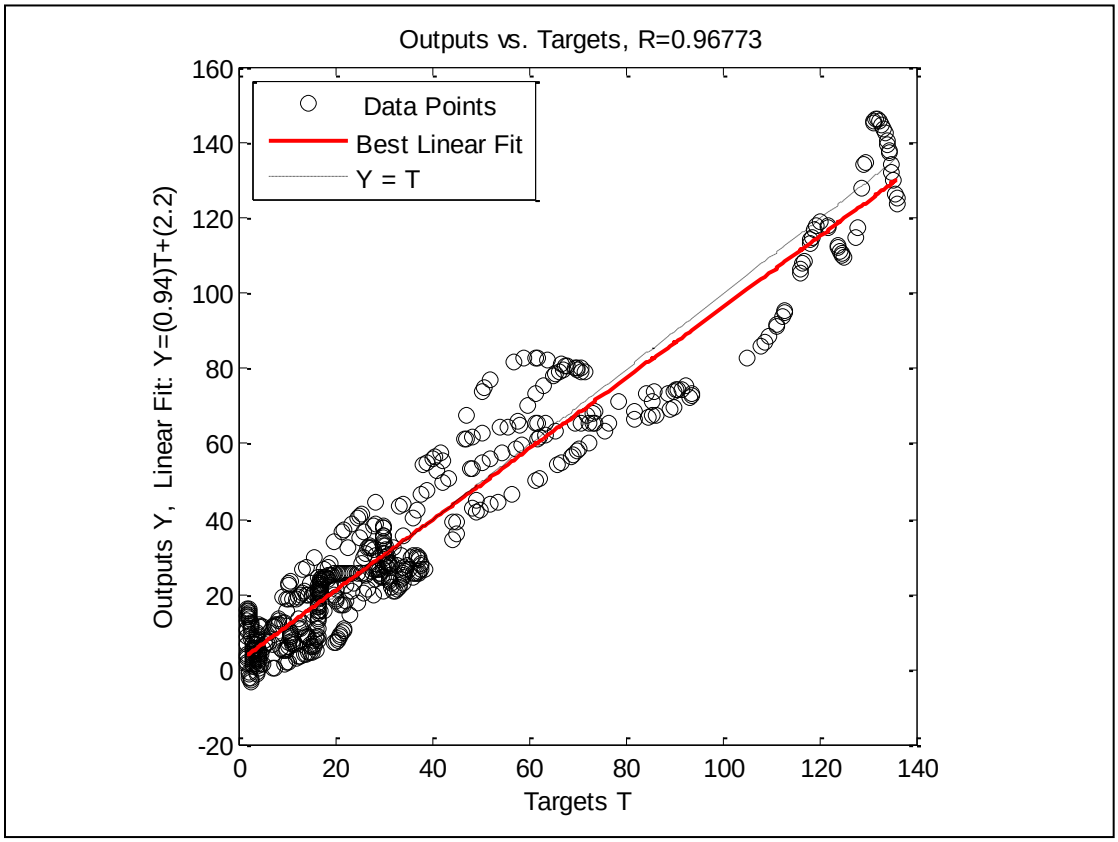

Figure A- 118: Well-6, Case -9, Crossplot

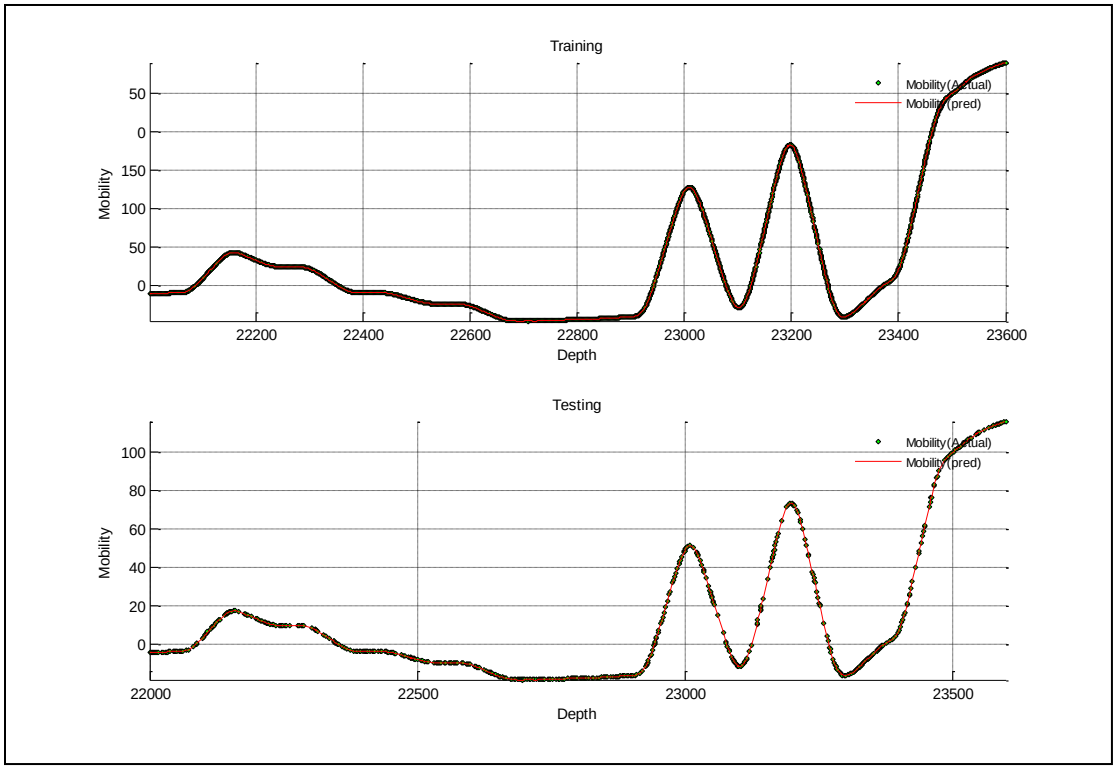

Figure A- 119: Well-6, Case -10

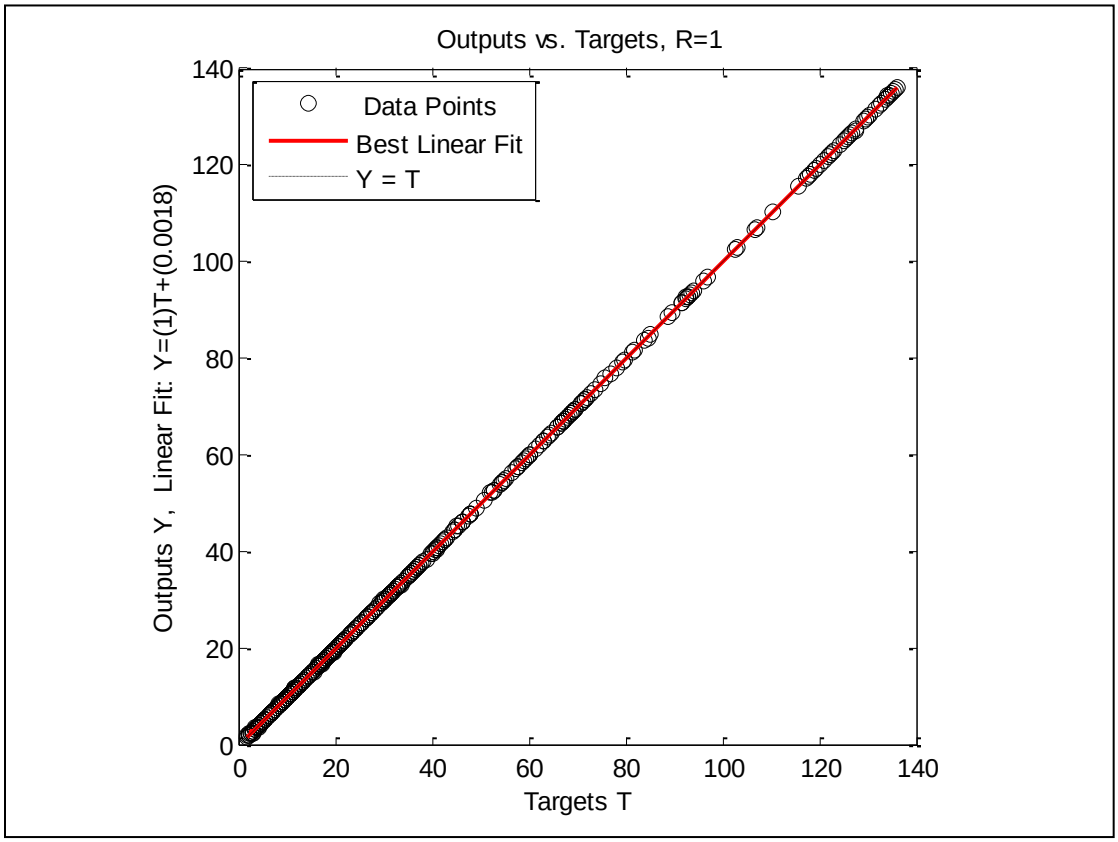

Figure A- 120: Well-6, Case -10, Crossplot

Well No. 7

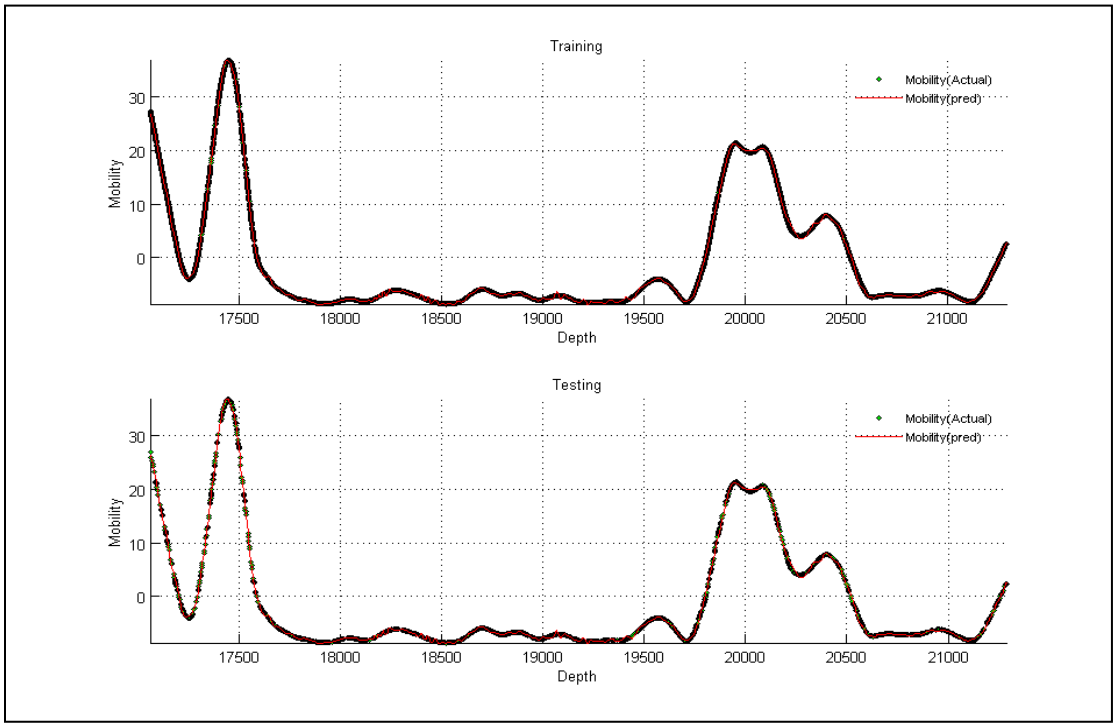

Figure A- 121: Well-7, Case -1

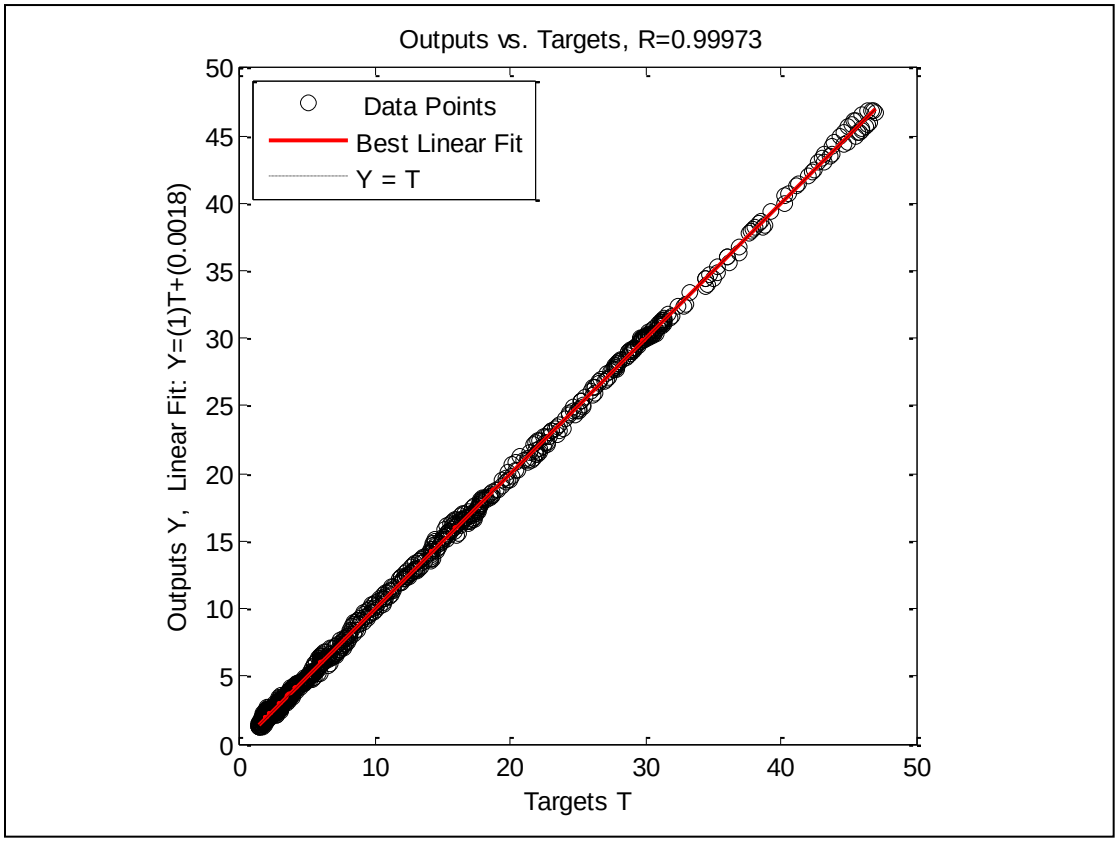

Figure A- 122: Well-7, Case -1, Crossplot

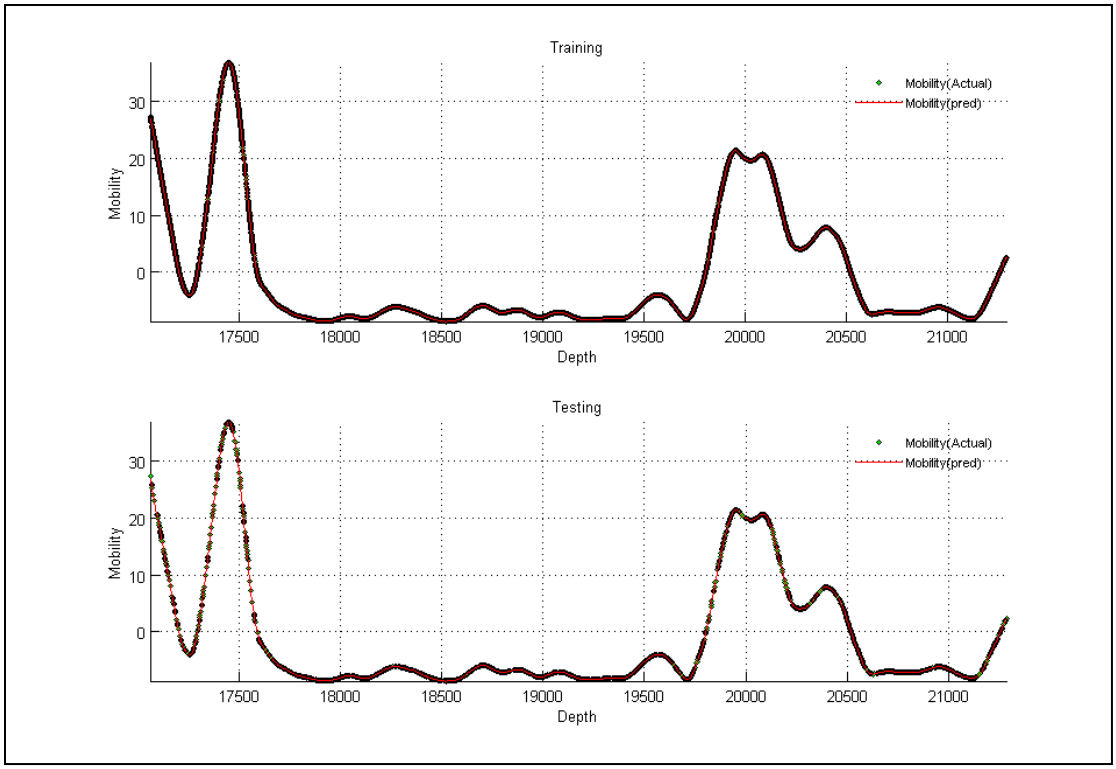

Figure A- 123: Well-7, Case -2

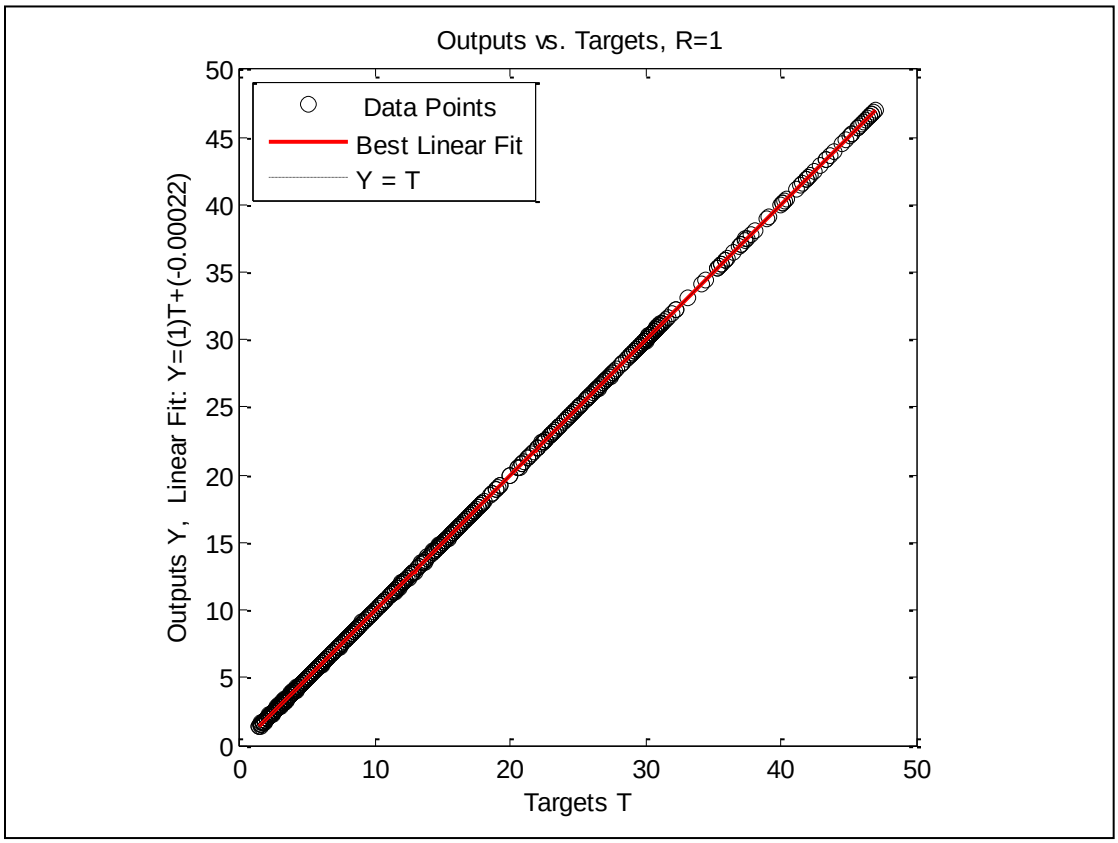

Figure A- 124: Well-7, Case -2, Crossplot

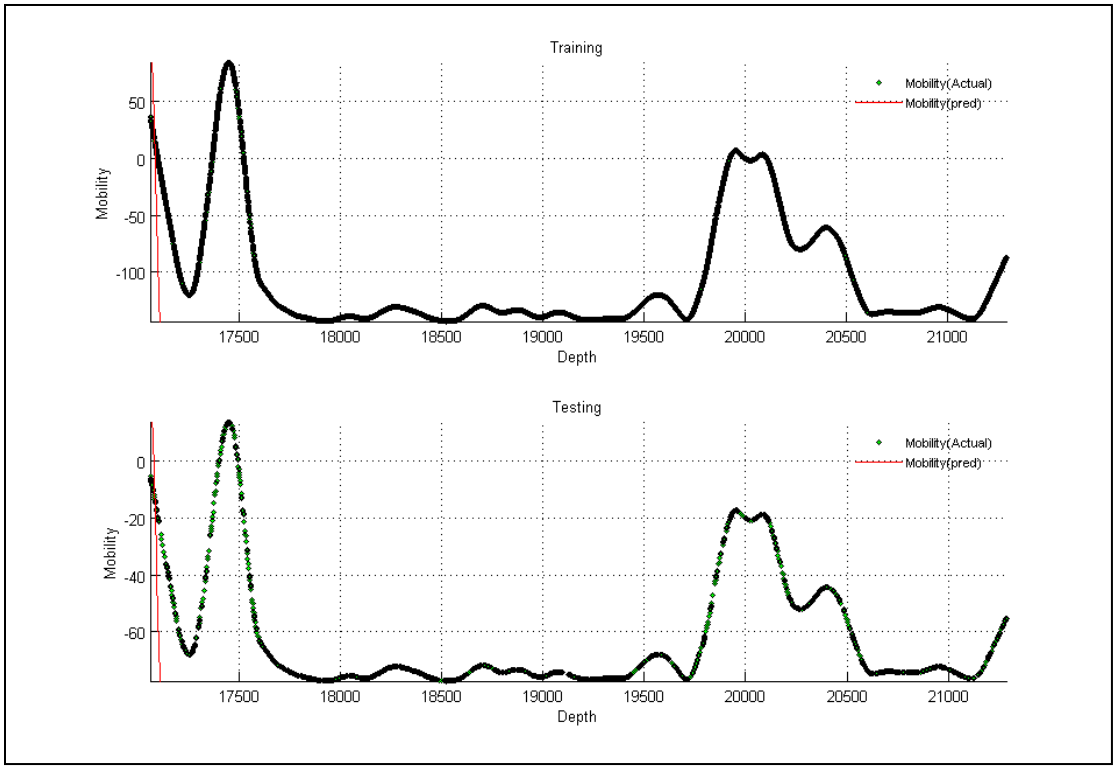

Figure A- 125: Well-7, Case -3

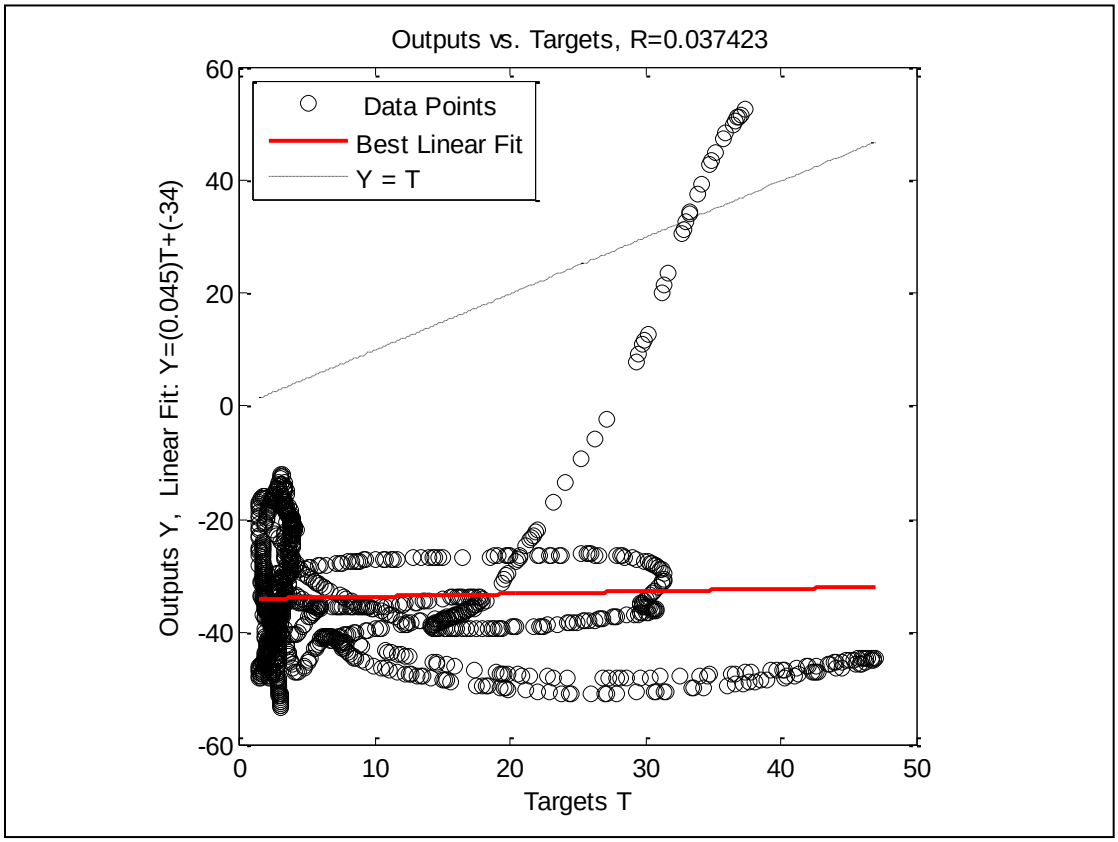

Figure A- 126: Well-7, Case -3, Crossplot

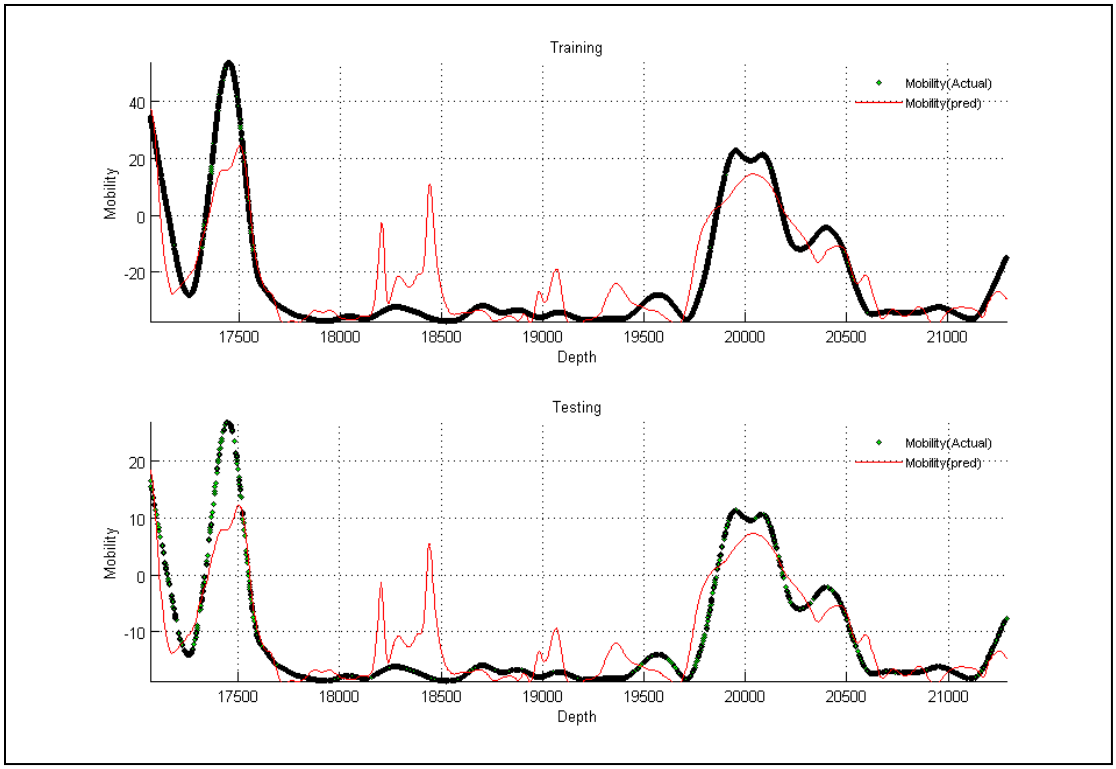

Figure A- 127: Well-7, Case -4

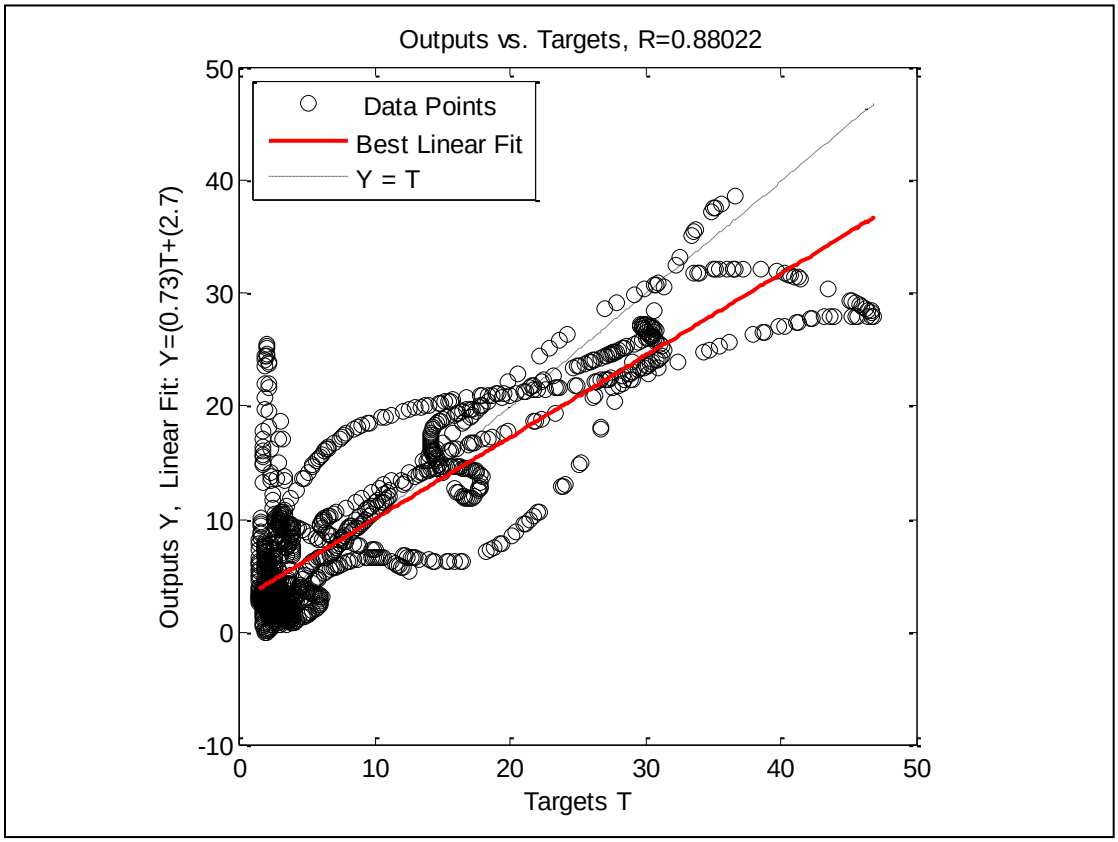

Figure A- 128: Well-7, Case -4, Crossplot

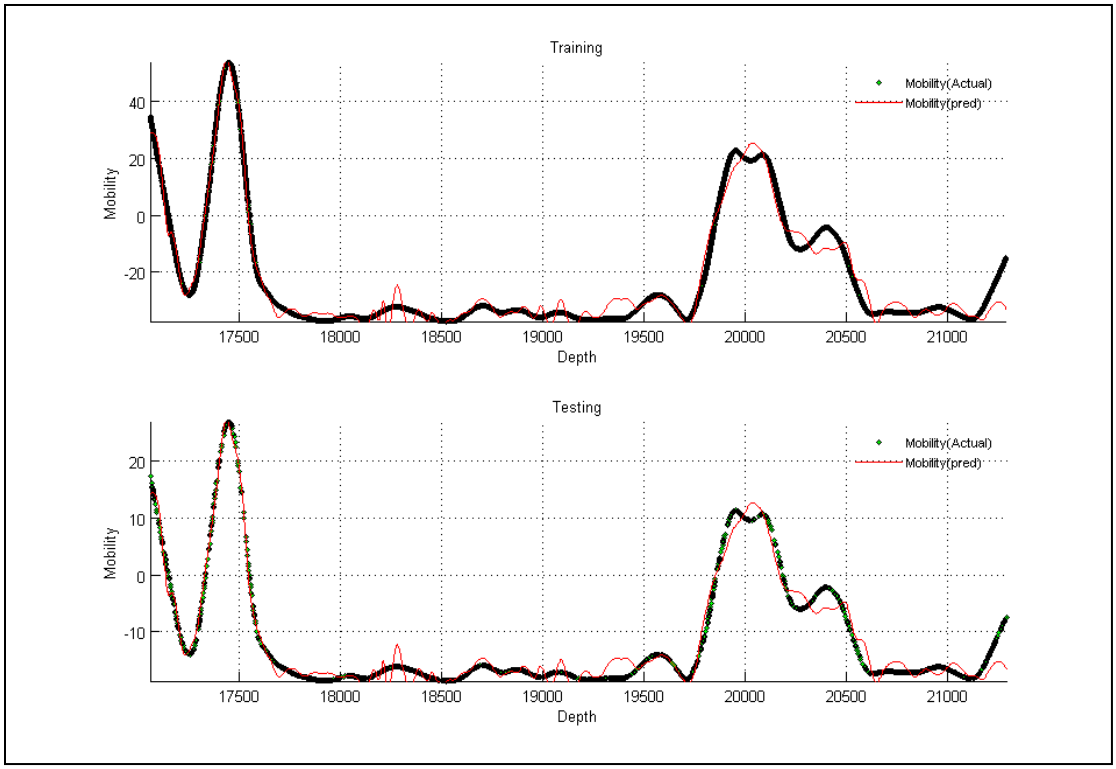

Figure A- 129: Well-7, Case -5

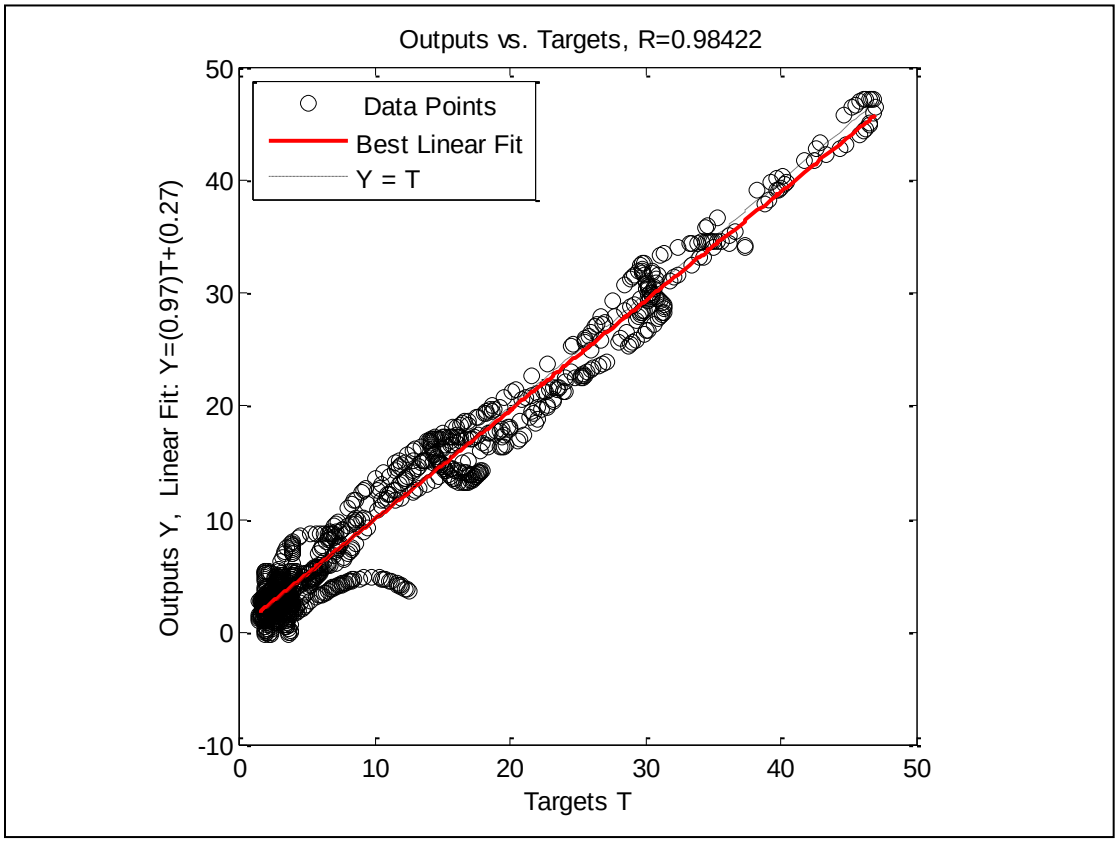

Figure A- 130: Well-7, Case -5, Crossplot

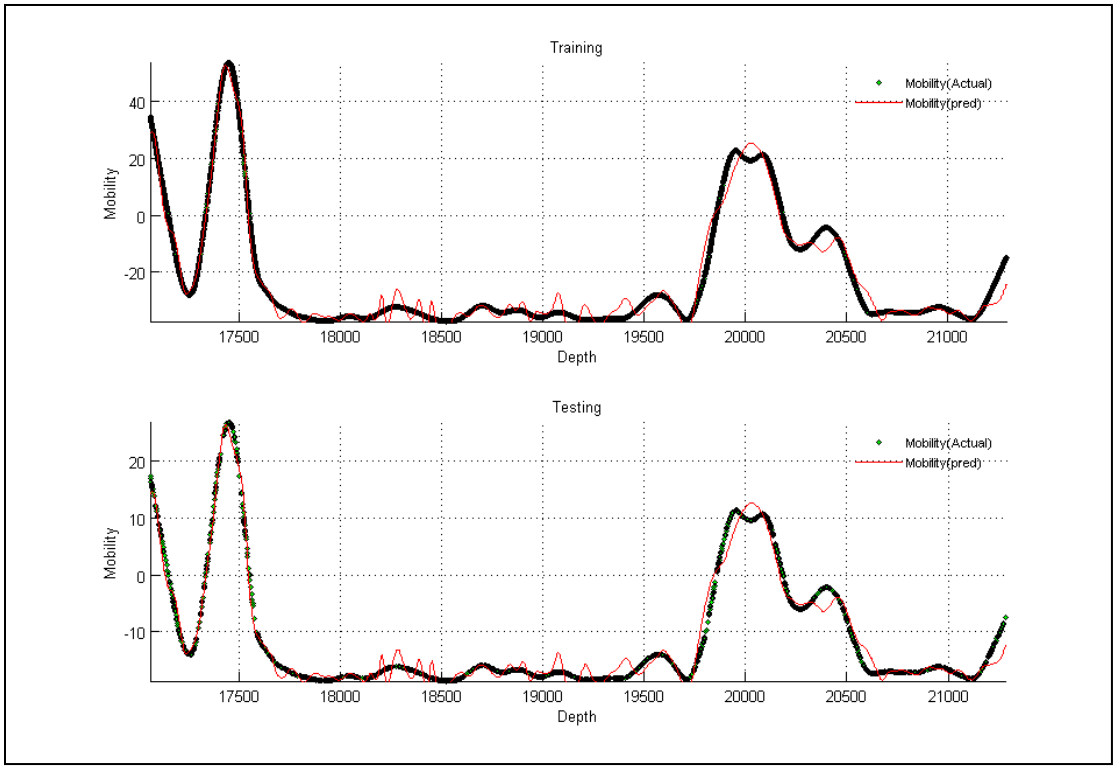

Figure A- 131: Well-7, Case -6

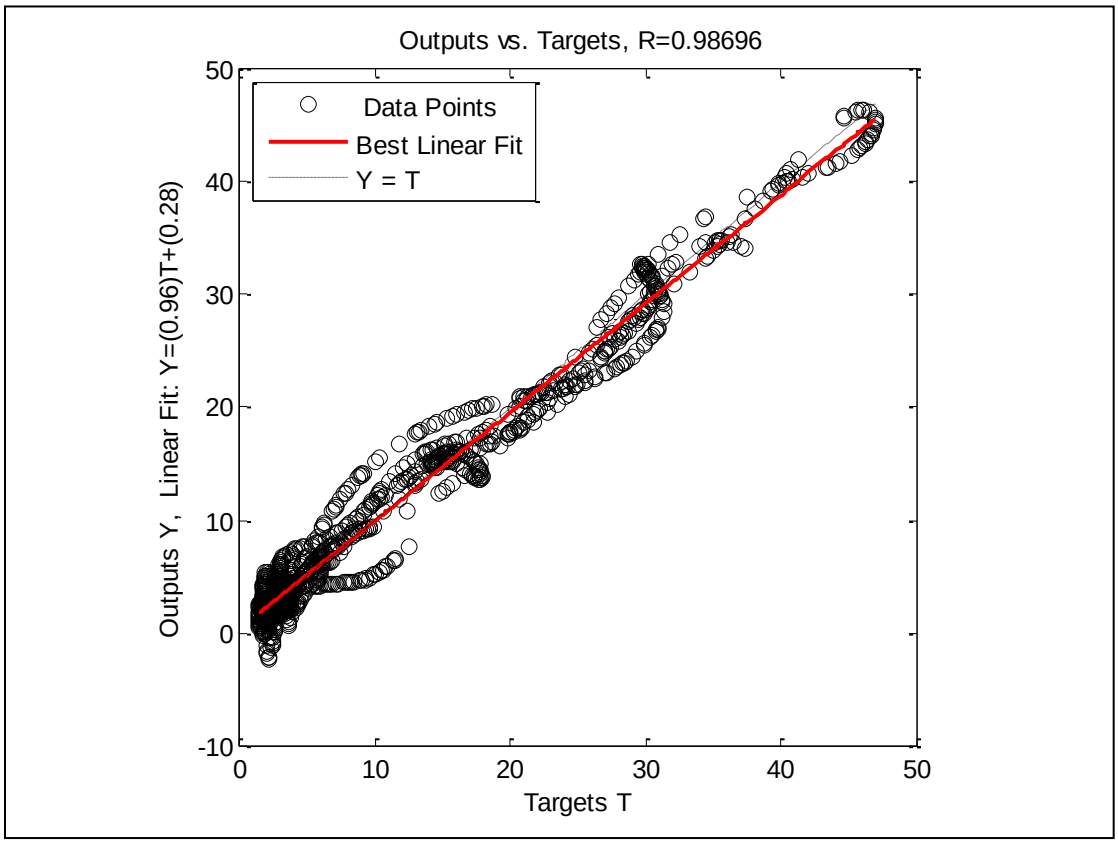

Figure A- 132: Well-7, Case -6, Crossplot

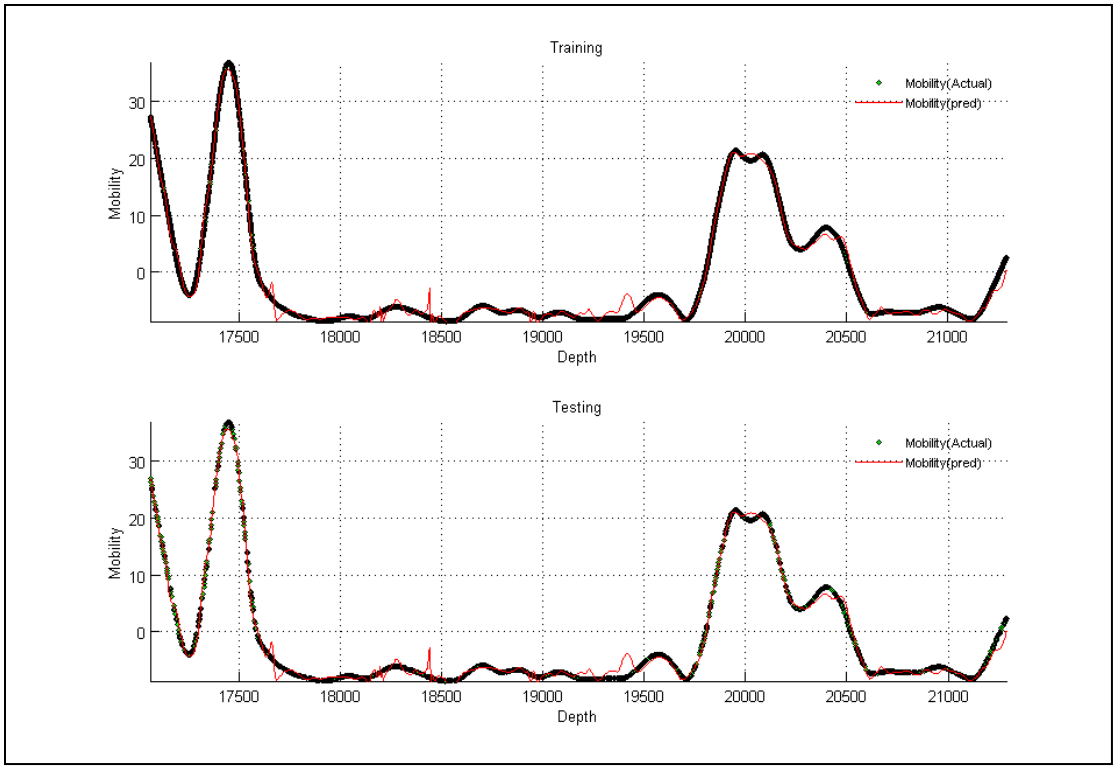

Figure A- 133: Well-7, Case -7

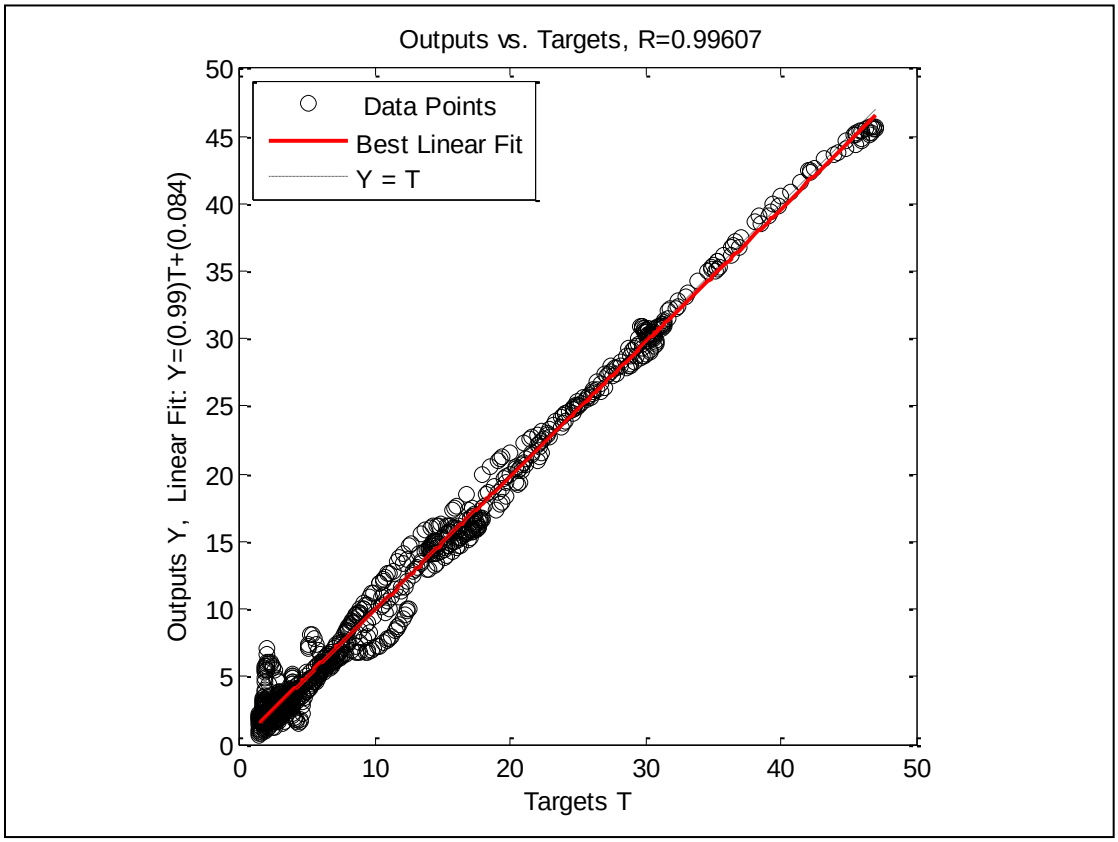

Figure A- 134: Well-7, Case -7, Crossplot

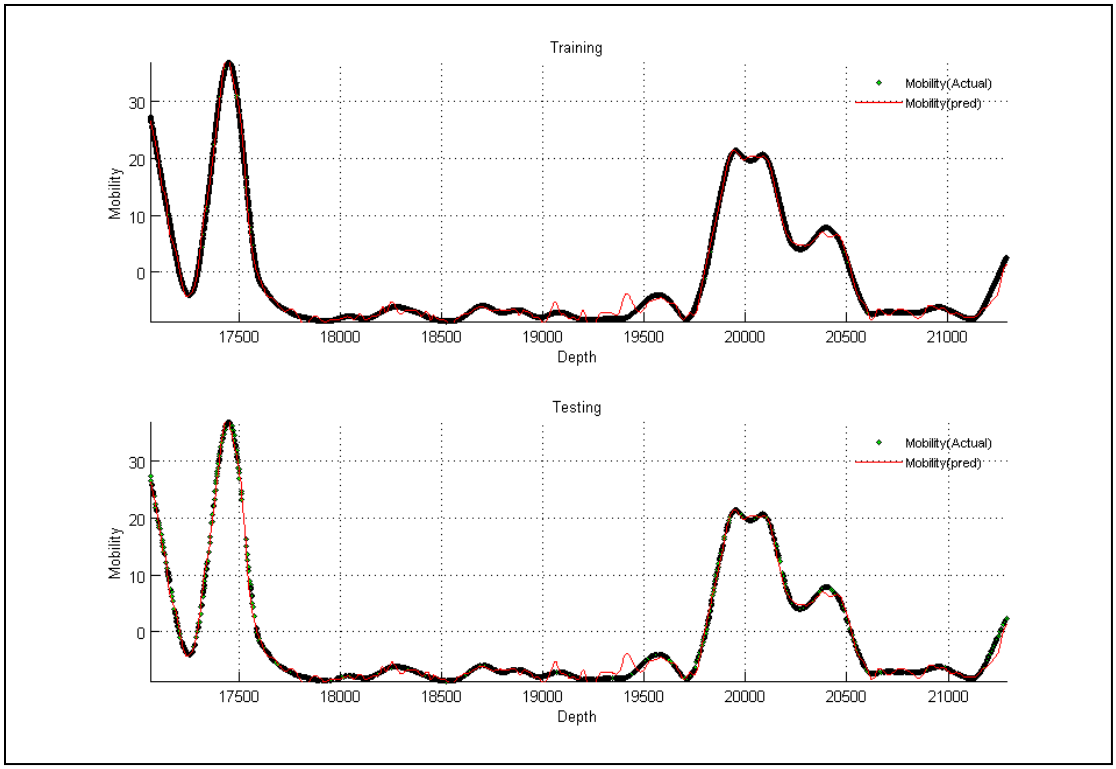

Figure A- 135: Well-7, Case -8

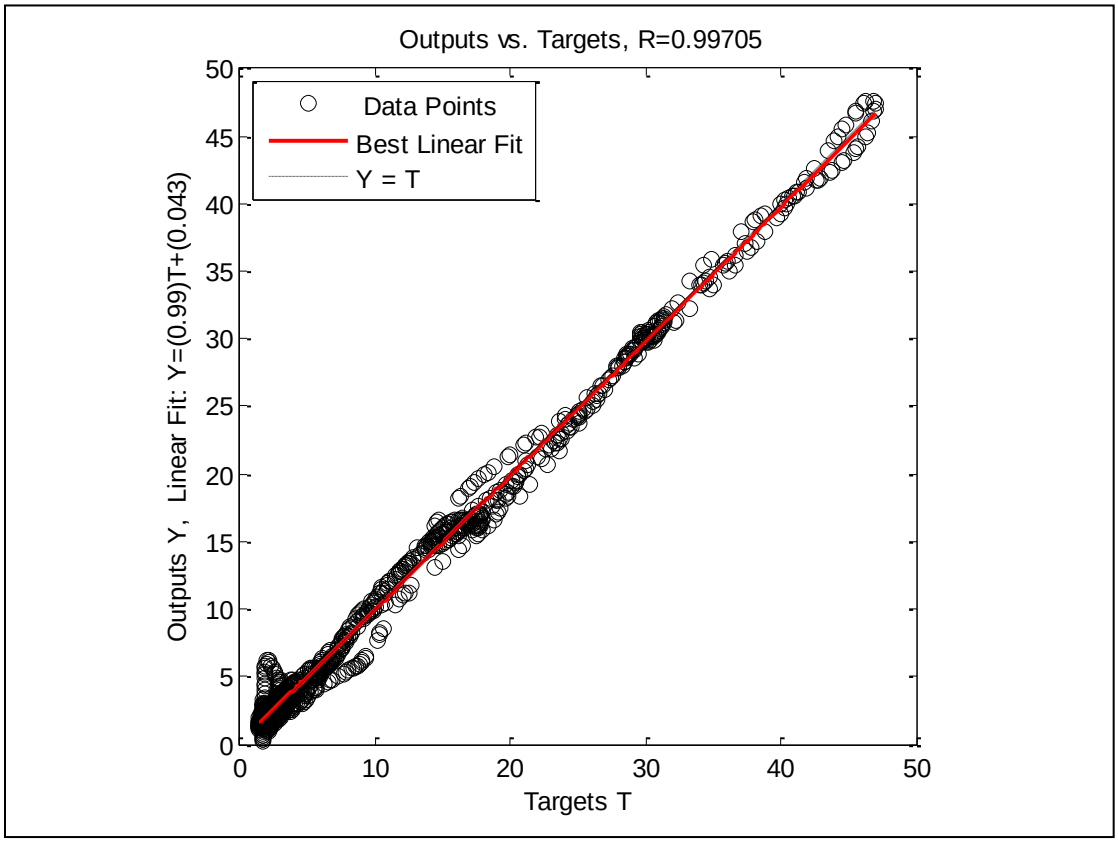

Figure A- 136: Well-7, Case -8

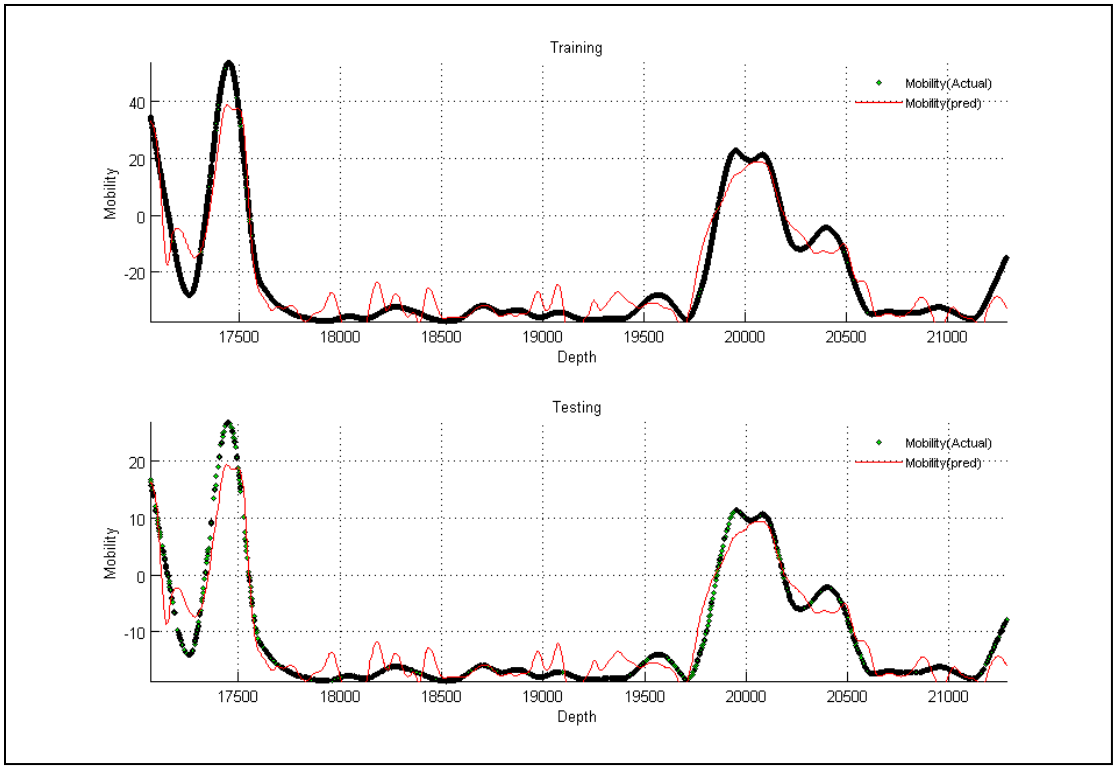

Figure A- 137: Well-7, Case -9

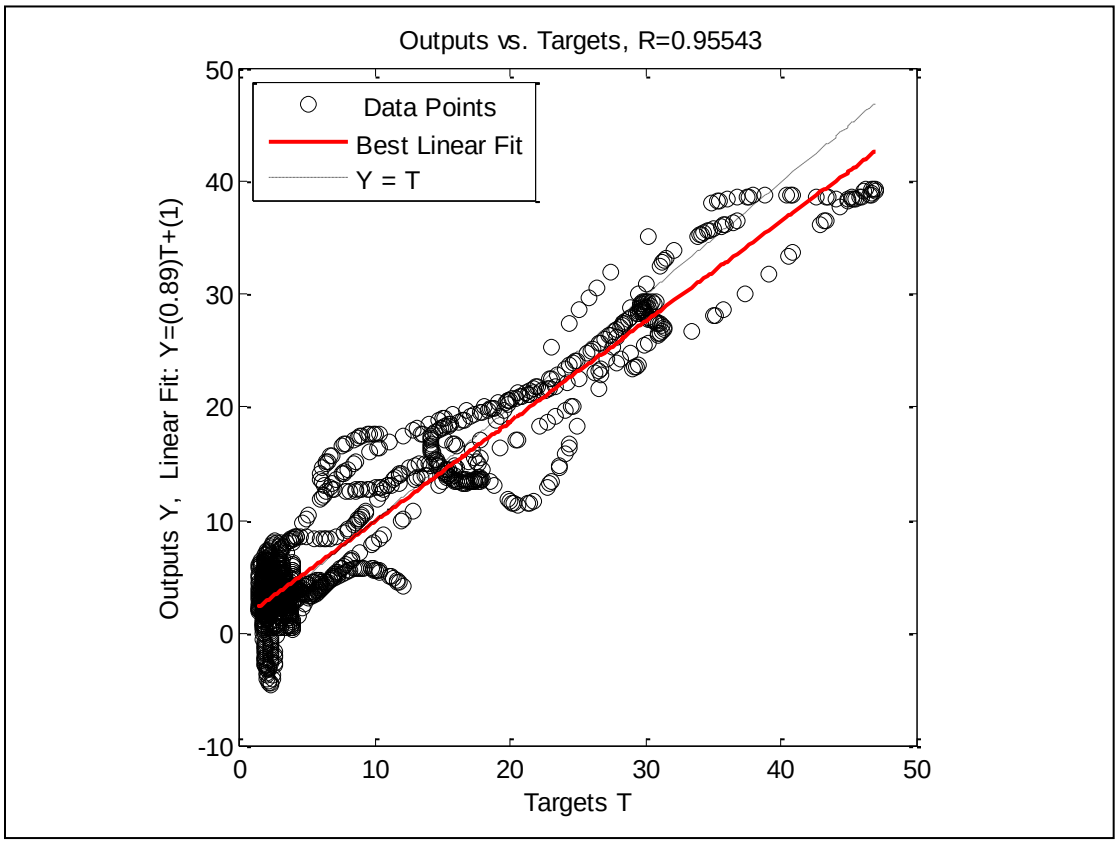

Figure A- 138: Well-7, Case -9, Crossplot

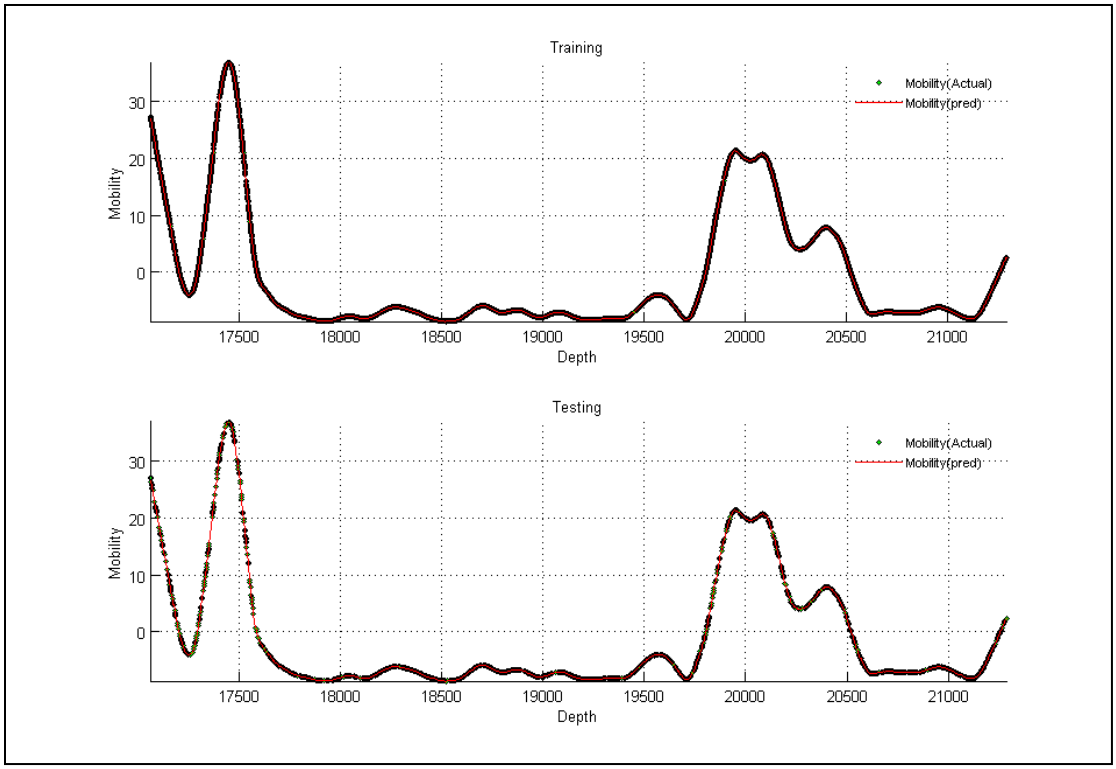

Figure A- 139: Well-7, Case -10

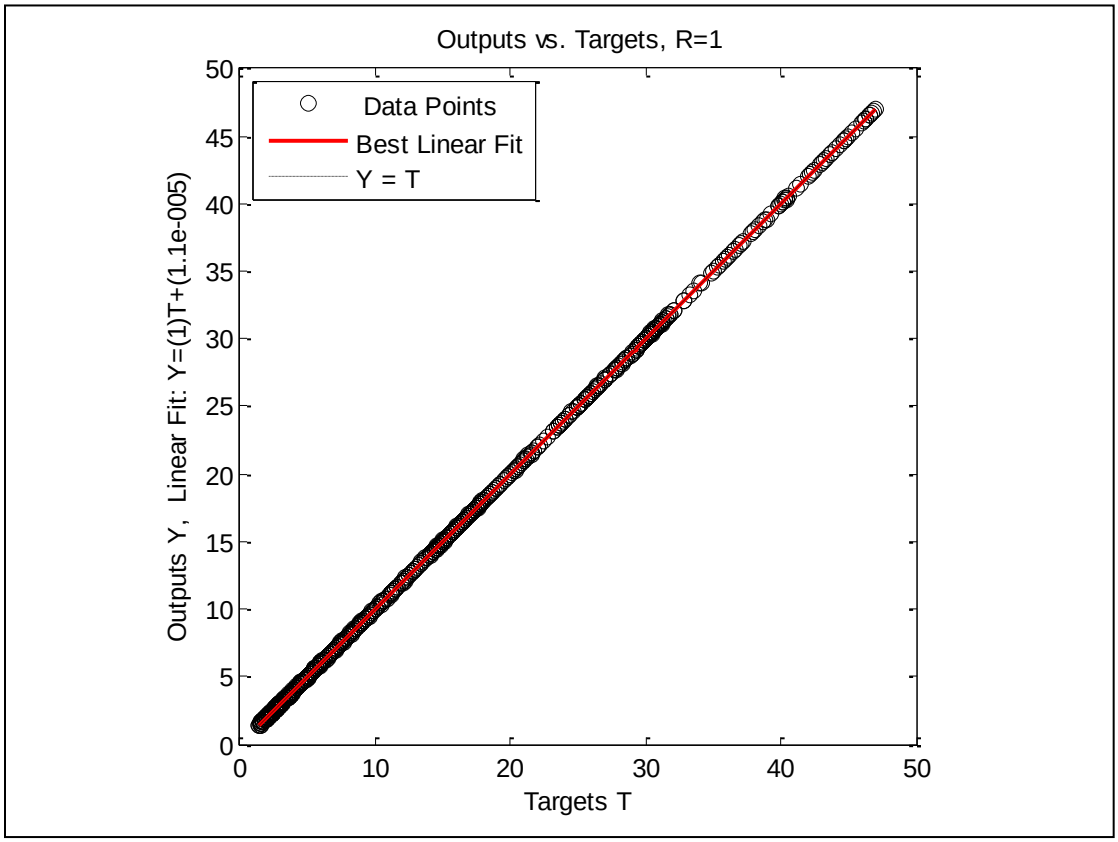

Figure A- 140: Well-7, Case -10, Crossplot

Well No. 8

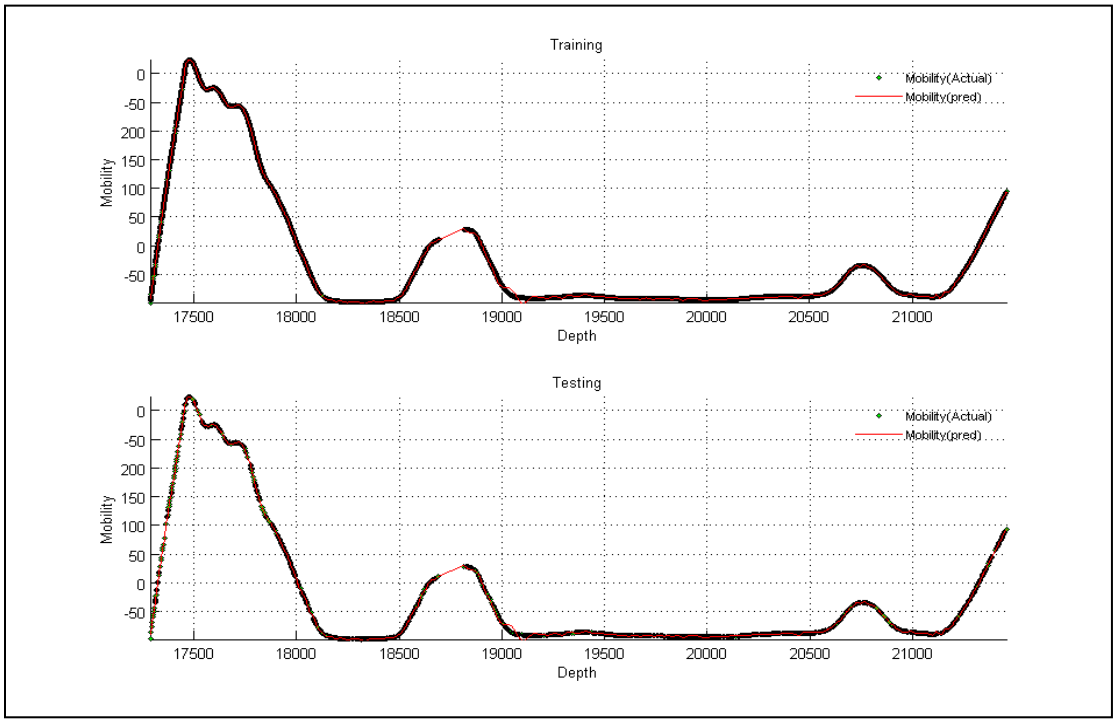

Figure A- 141: Well-8, Case -1

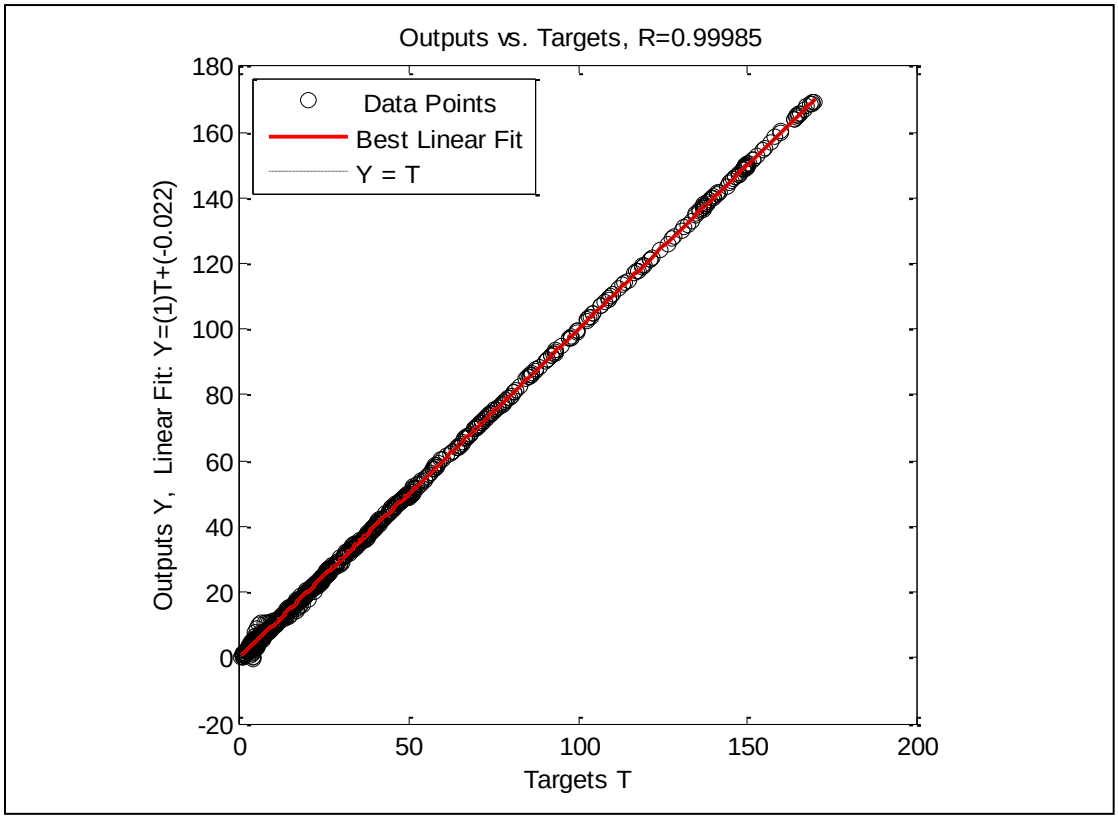

Figure A- 142: Well-8, Case -1, Crossplot

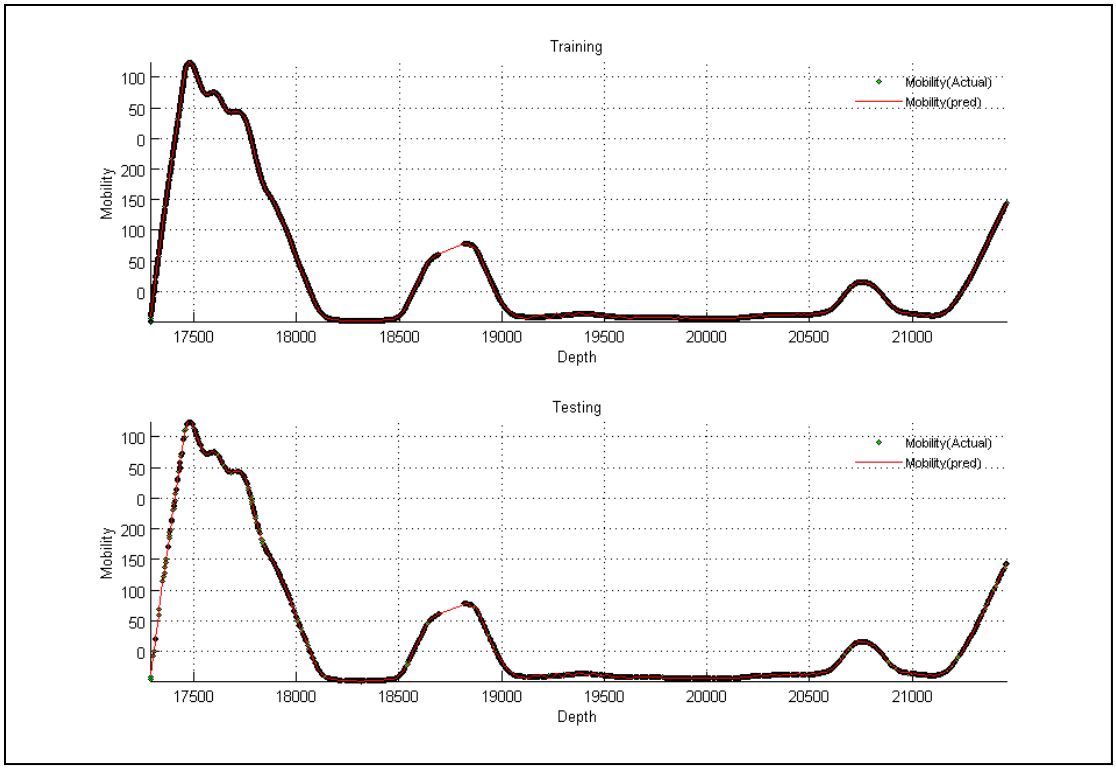

Figure A- 143: Well-8, Case -2

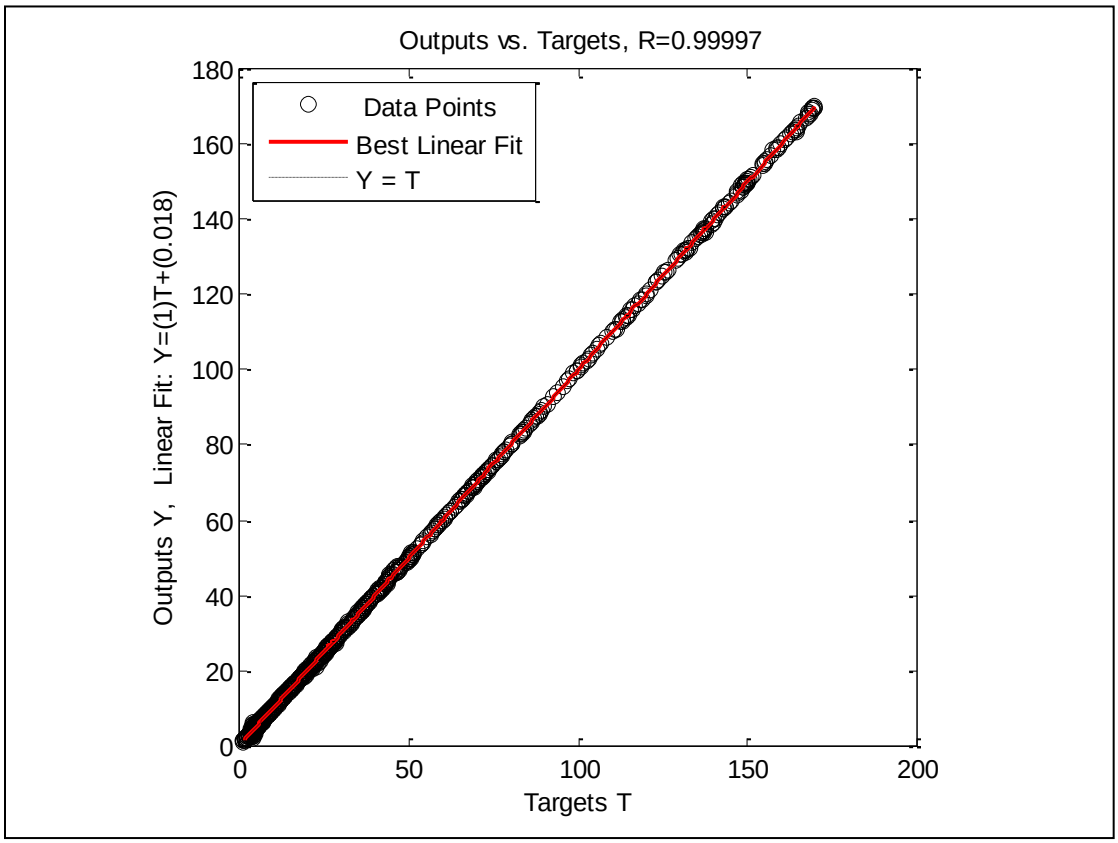

Figure A- 144: Well-8, Case -2, Crossplot

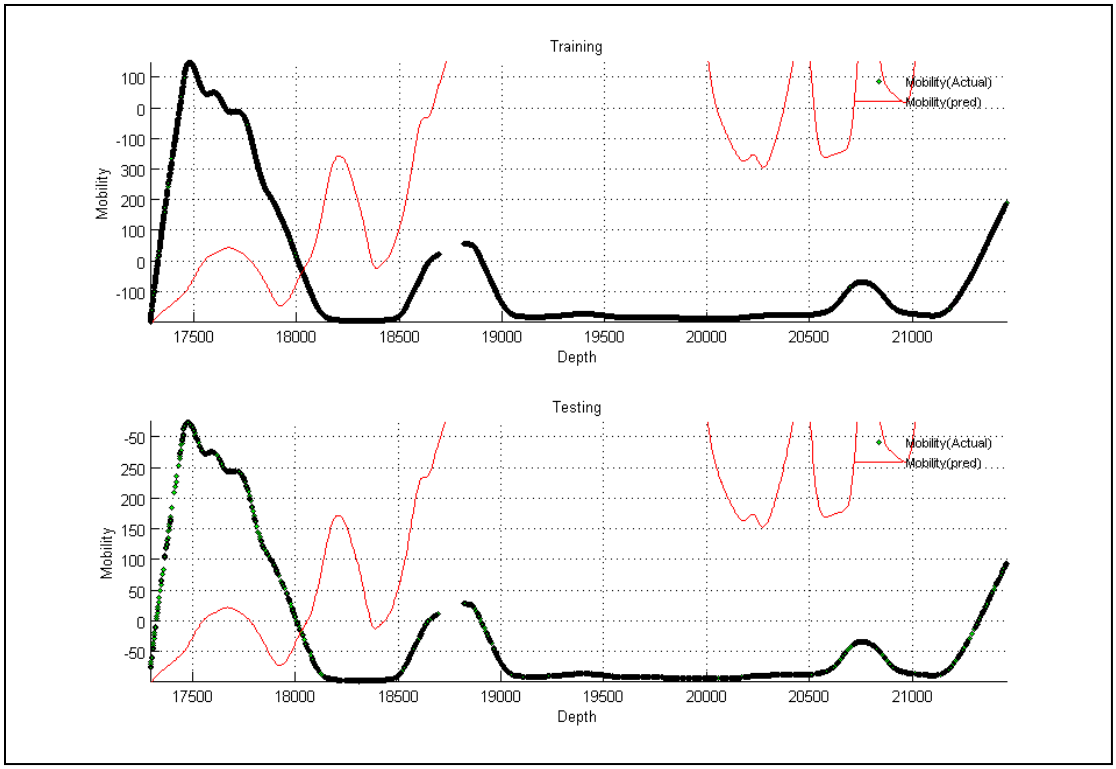

Figure A- 145: Well-8, Case -3

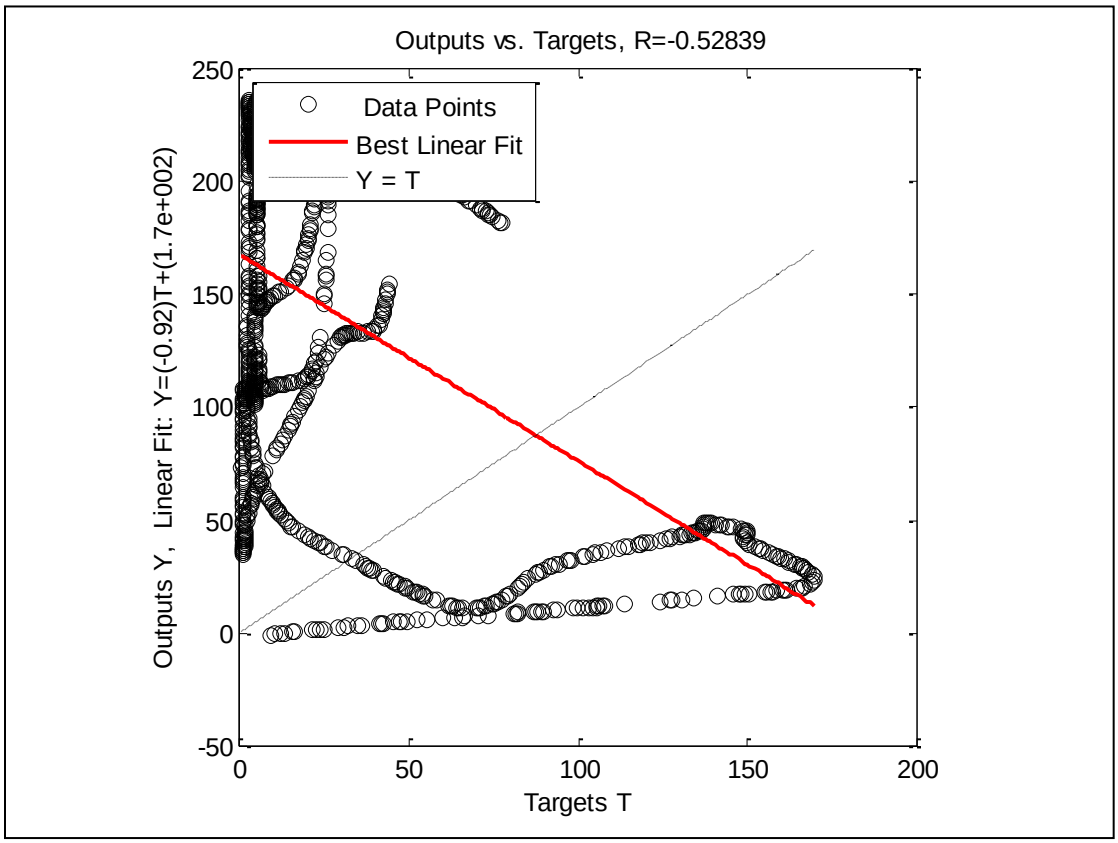

Figure A- 146: Well-8, Case -3, Crossplot

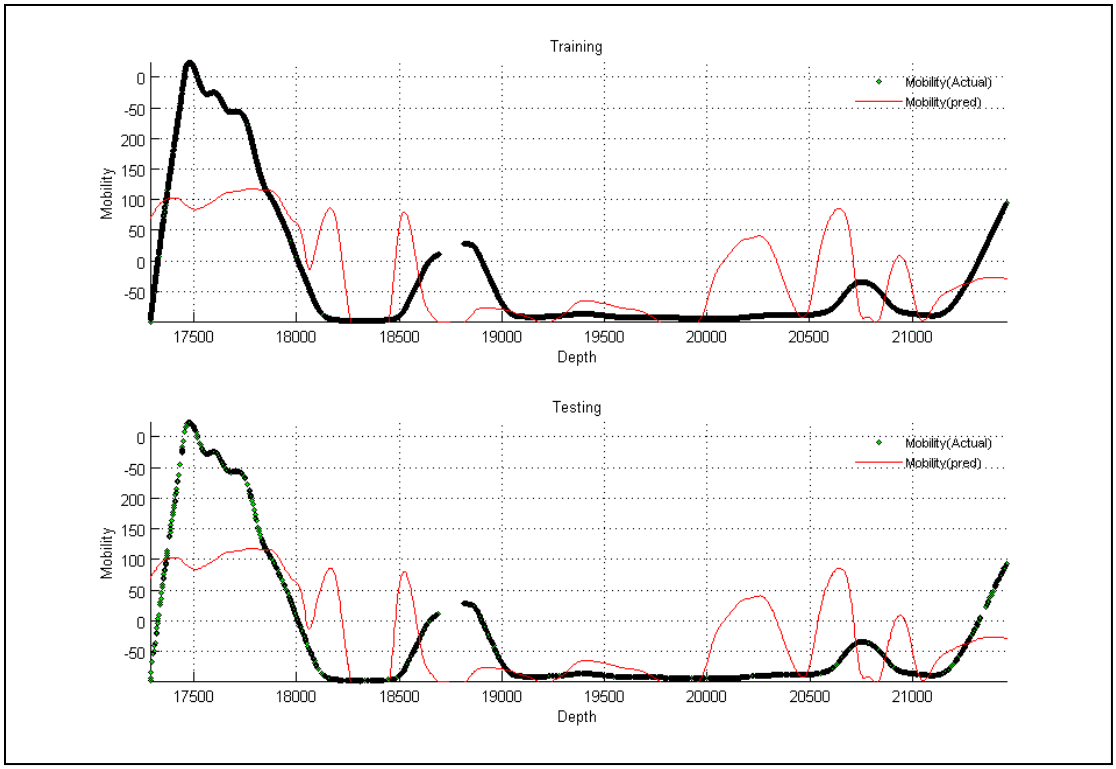

Figure A- 147: Well-8, Case -4

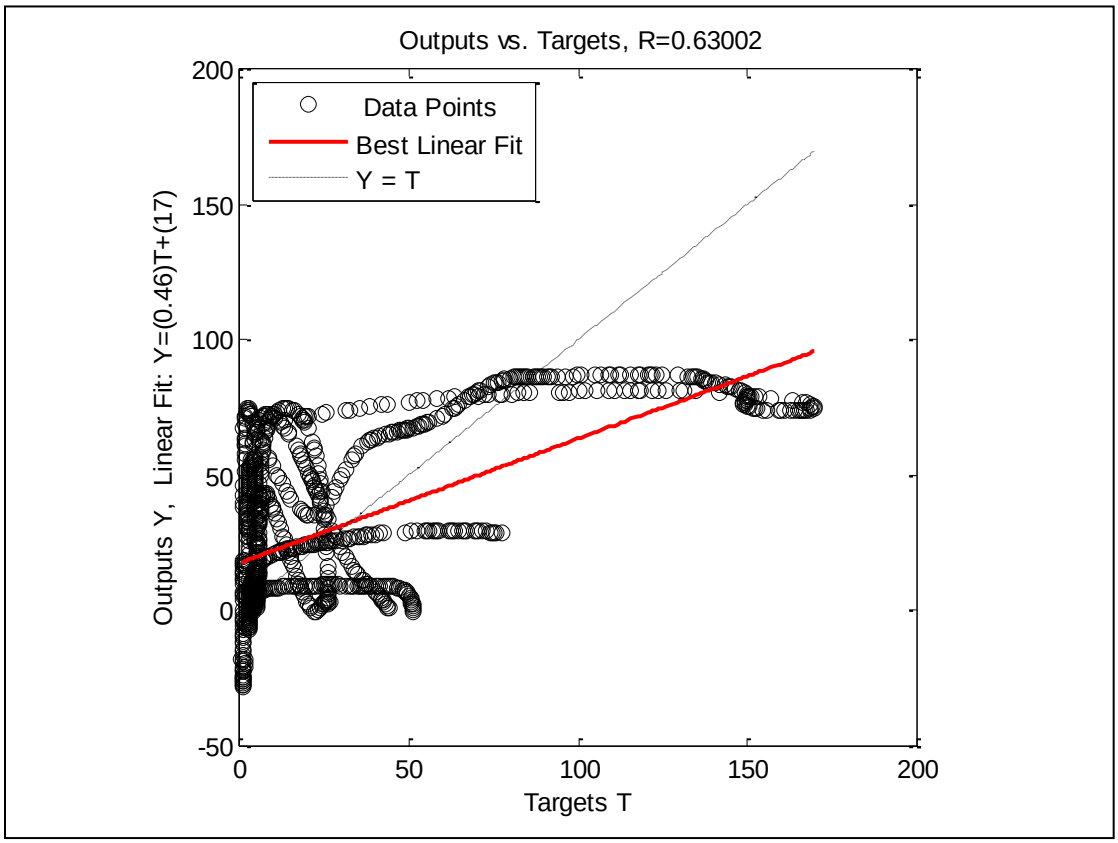

Figure A- 148: Well-8, Case -4, Crossplot

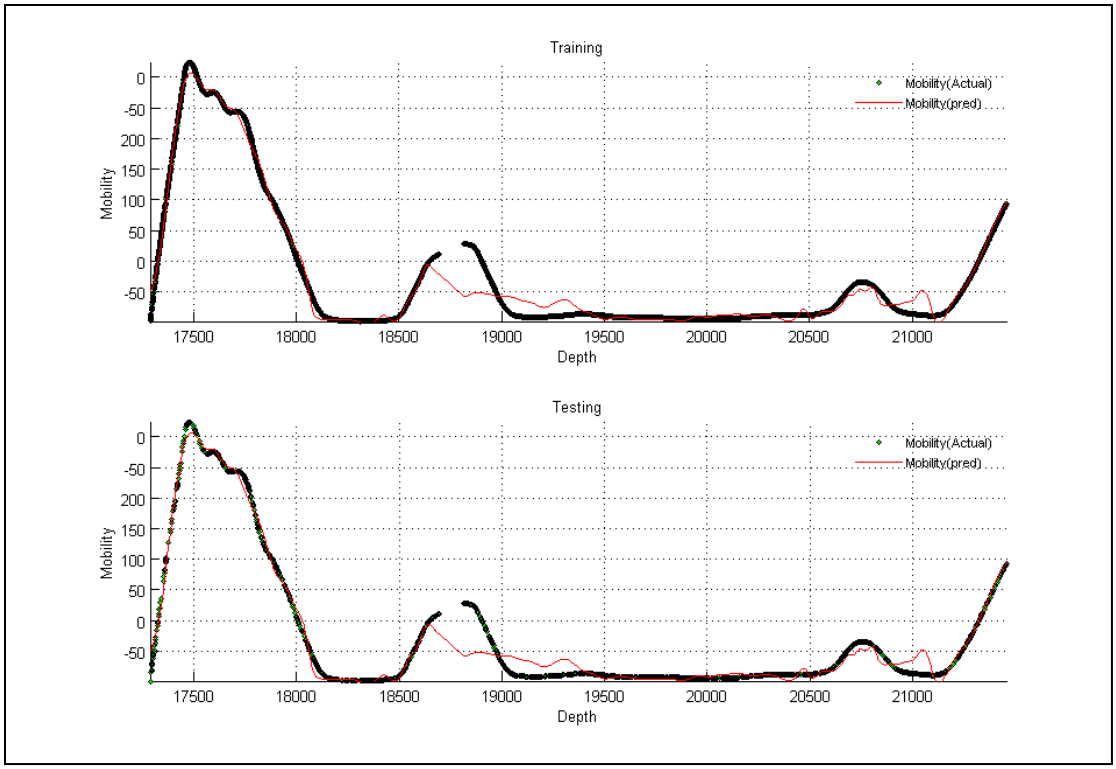

Figure A- 149: Well-8, Case -5

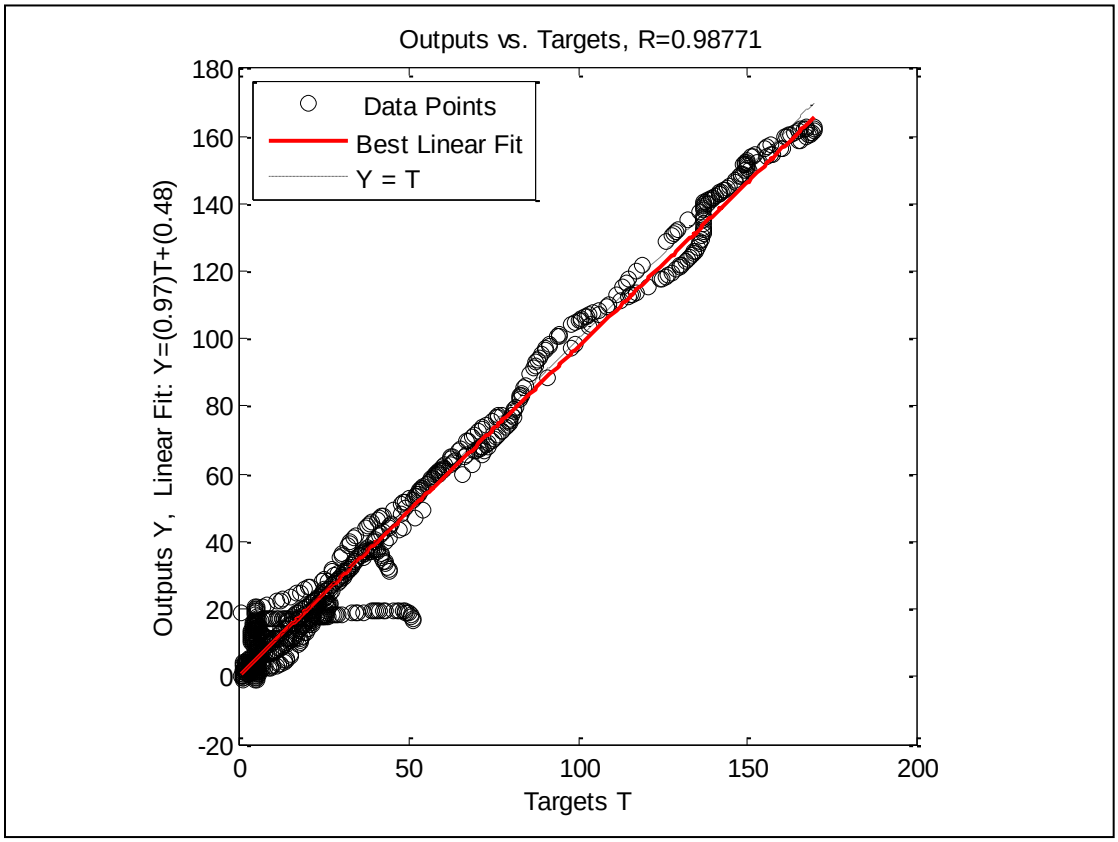

Figure A- 150: Well-8, Case -5, Crossplot

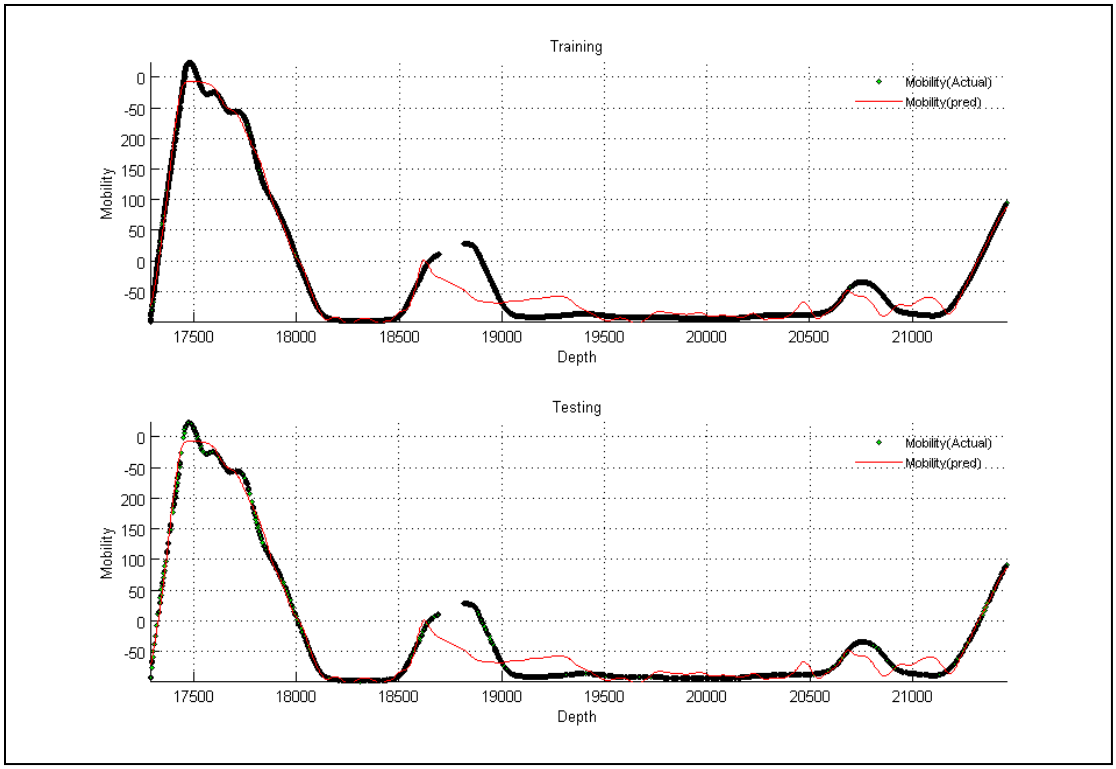

Figure A- 151: Well-8, Case -6

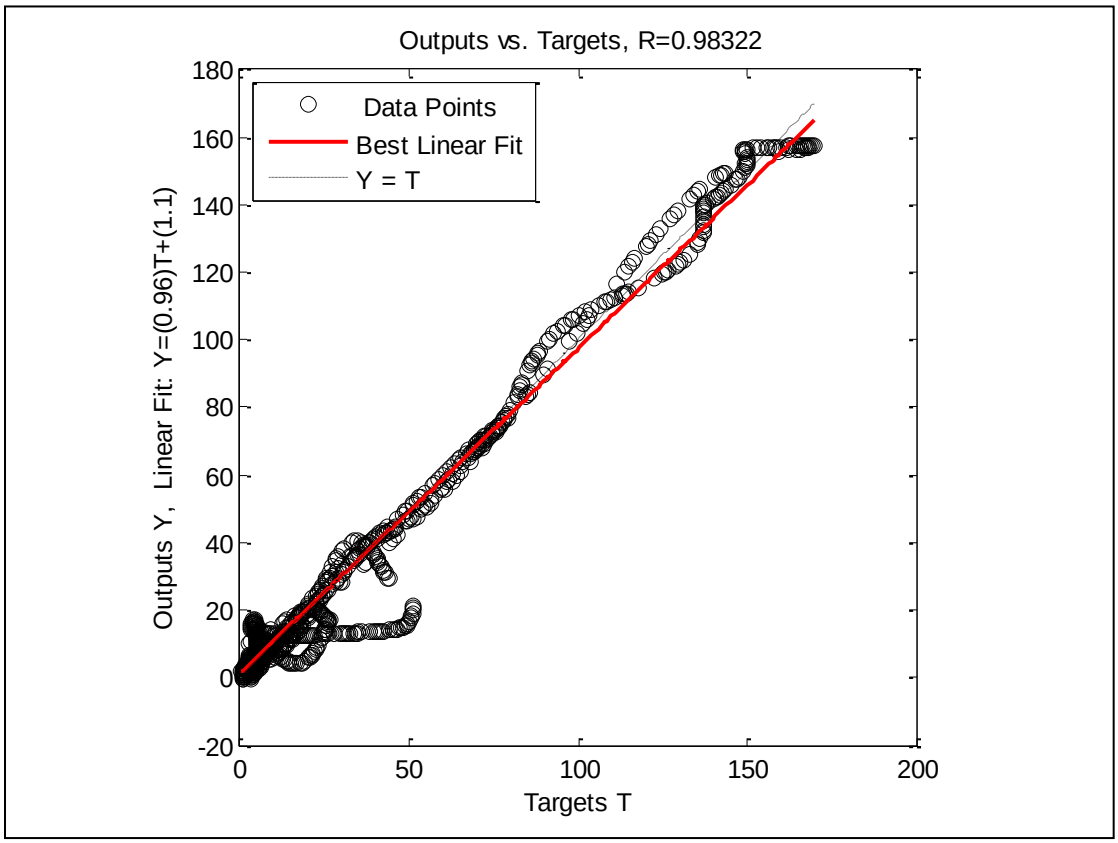

Figure A- 152: Well-8, Case -6, Crossplot

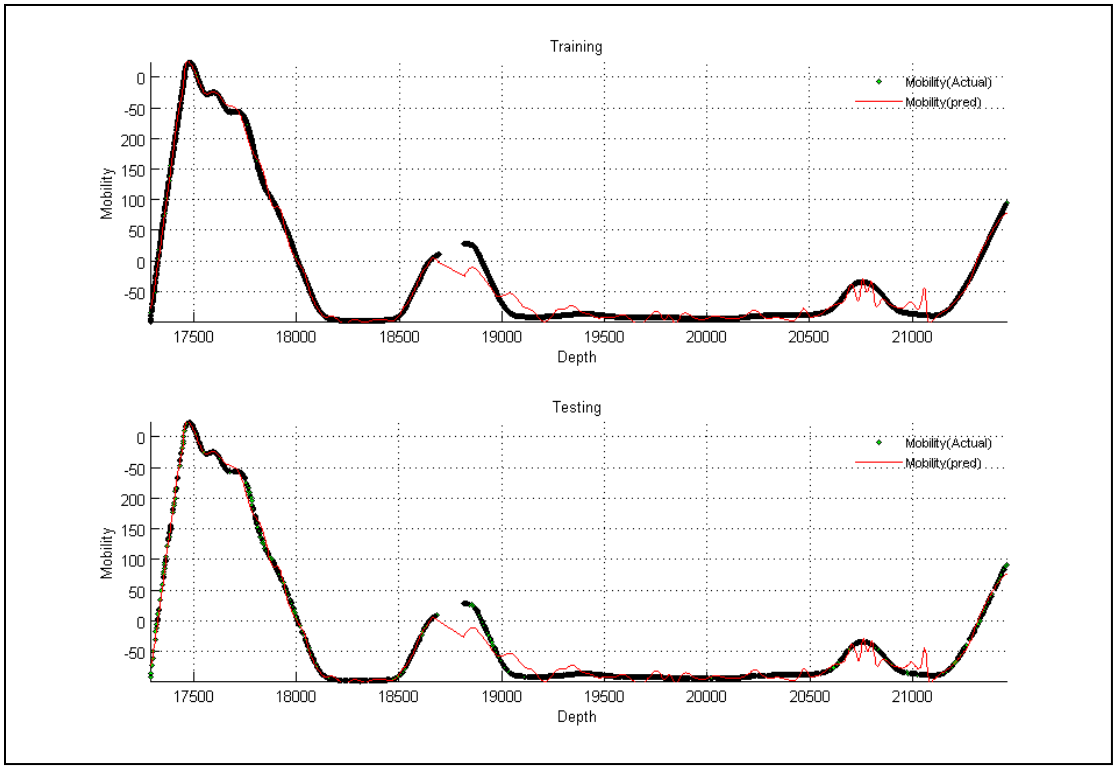

Figure A- 153: Well-8, Case -7

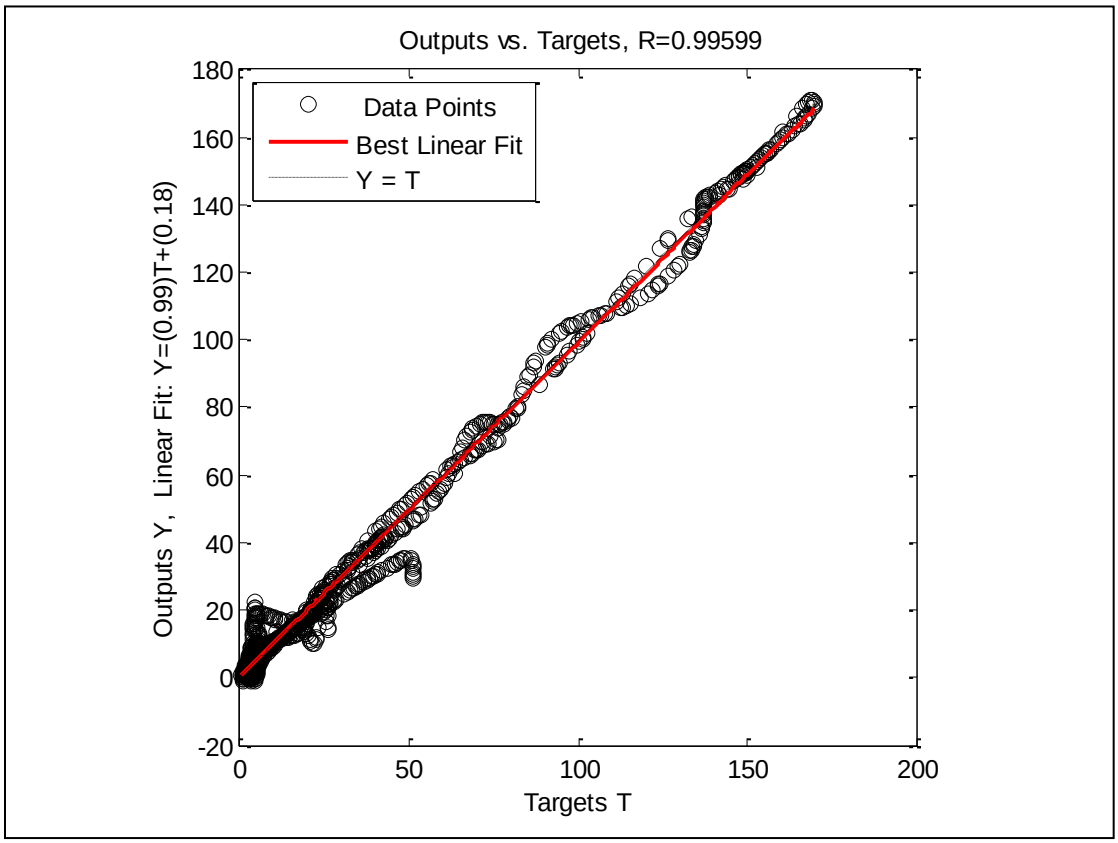

Figure A- 154: Well-8, Case -7, Crossplot

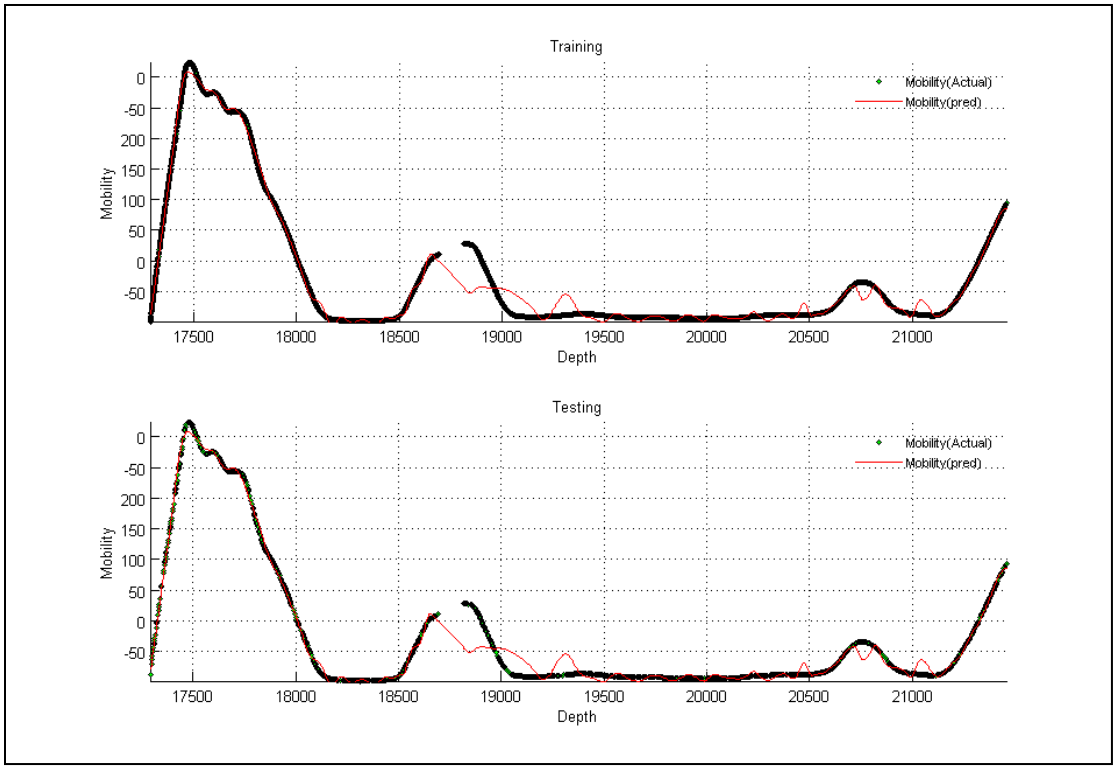

Figure A- 155: Well-8, Case -8

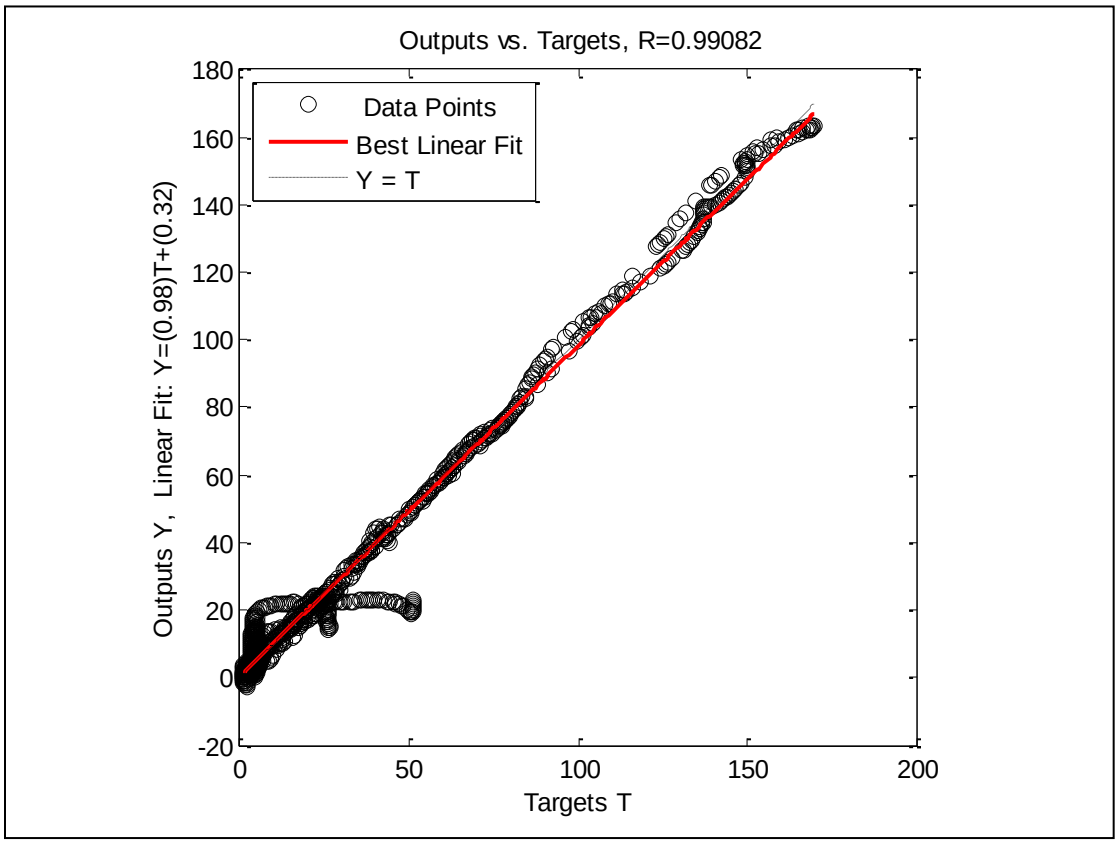

Figure A- 156: Well-8, Case -8, Crossplot

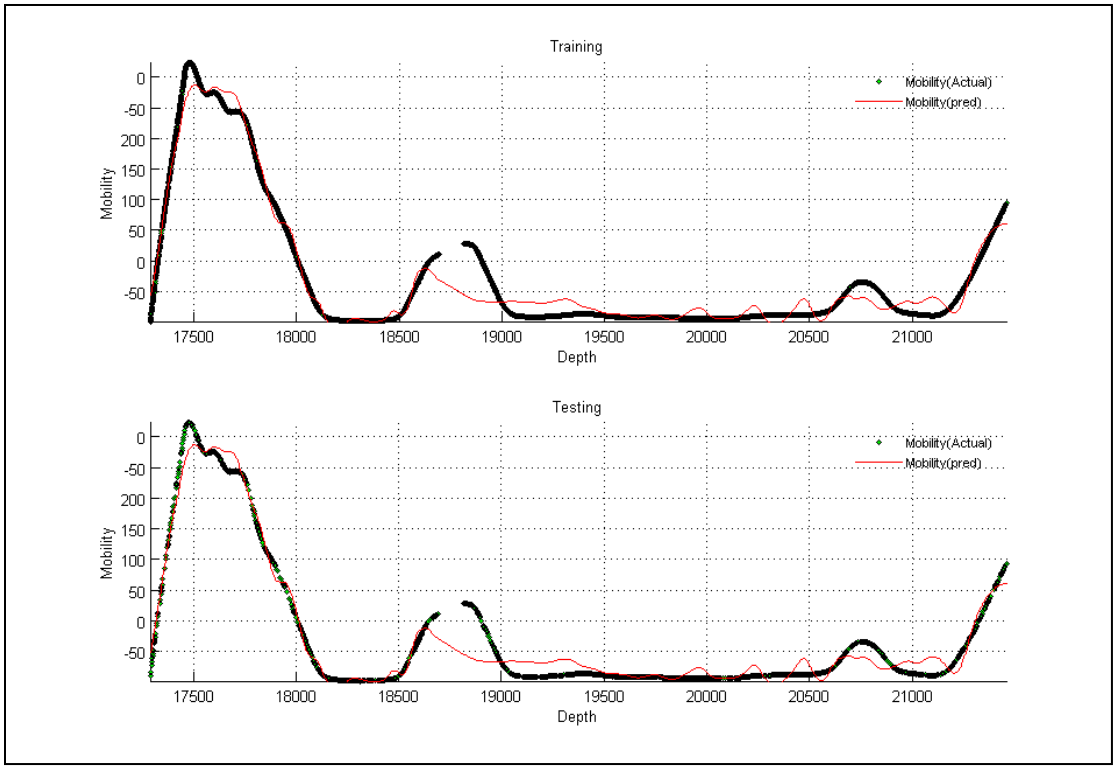

Figure A- 157: Well-8, Case -9

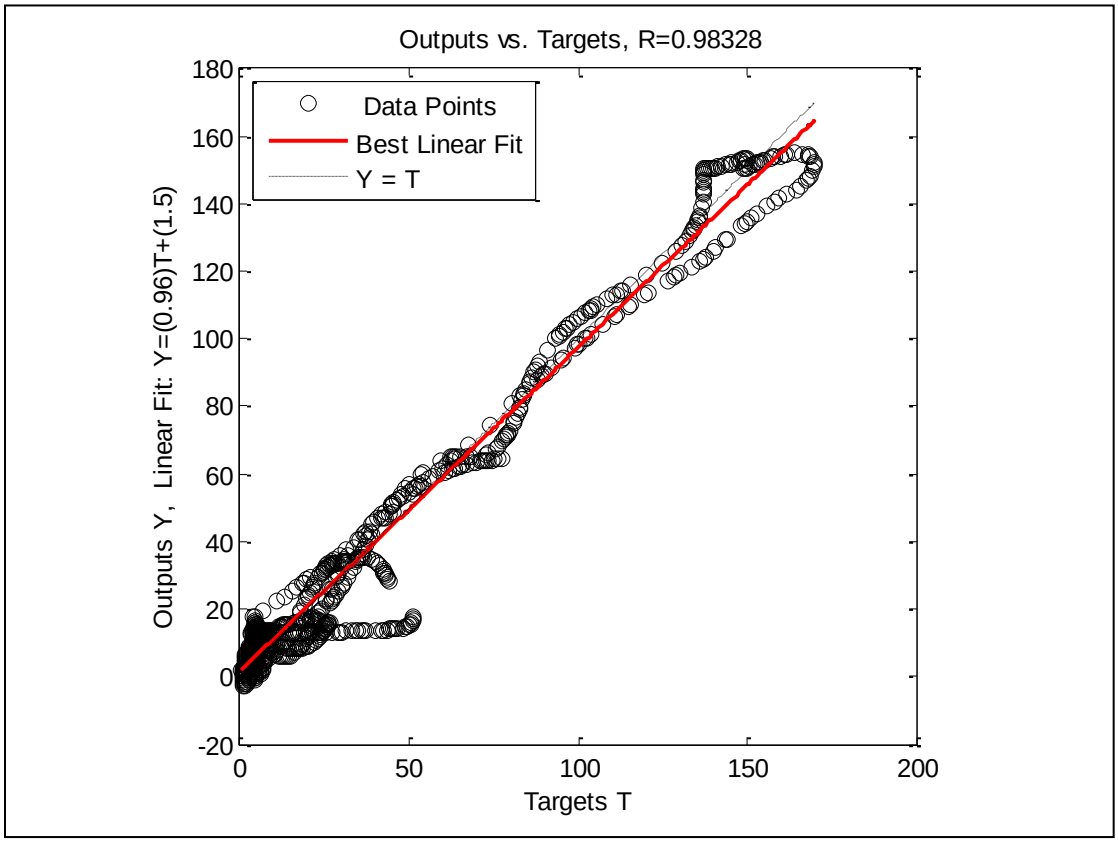

Figure A- 158: Well-8, Case -9, Crossplot

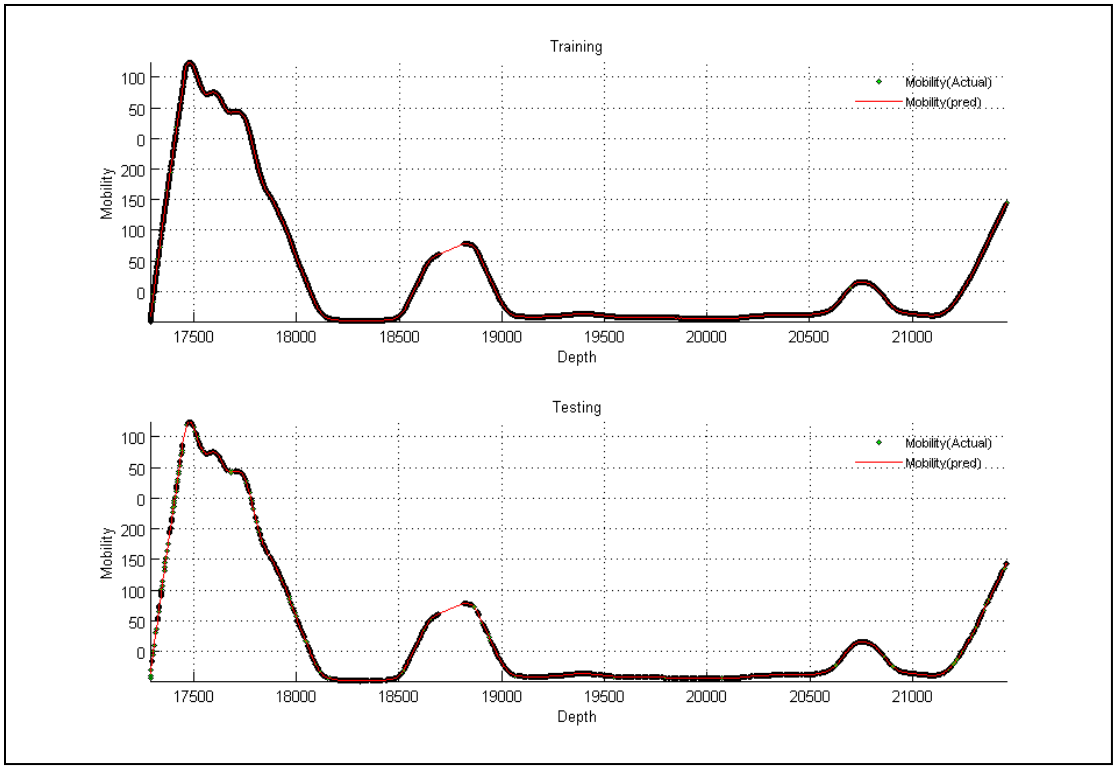

Figure A- 159: Well-8, Case -10

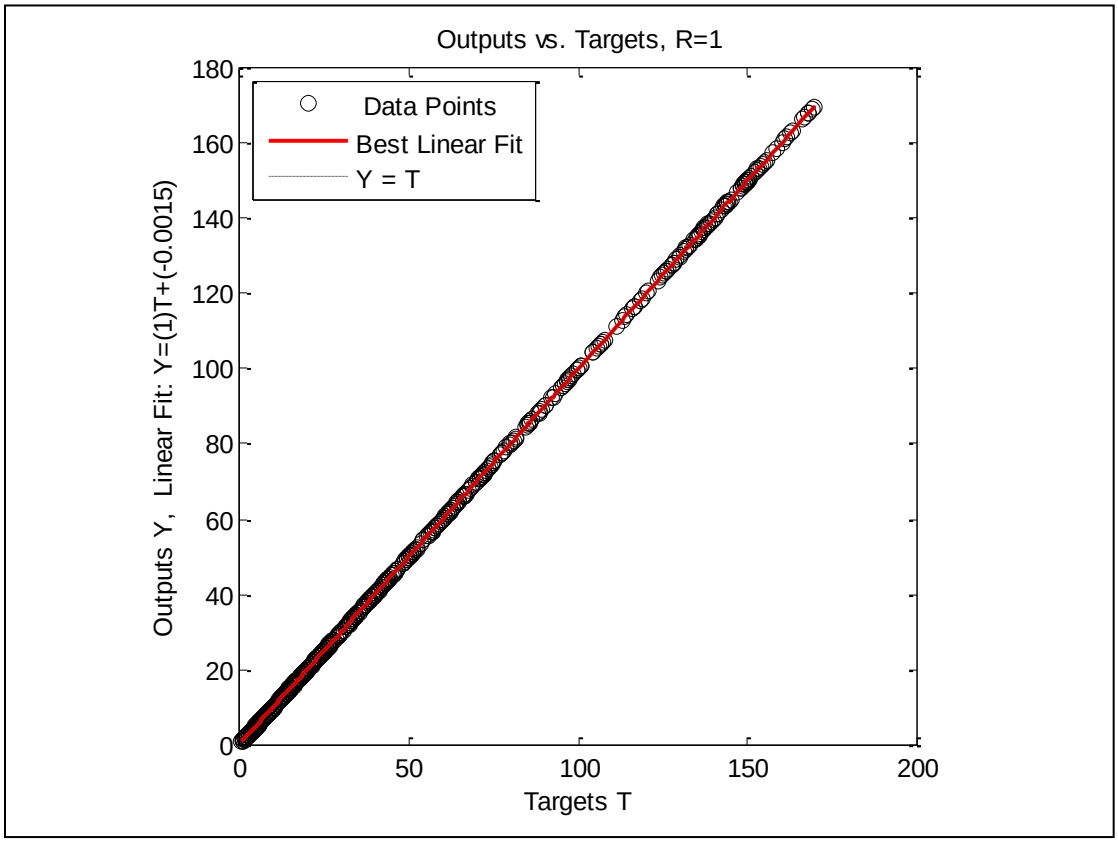

Figure A- 160: Well-8, Case -10, Crossplot

Well No. 9

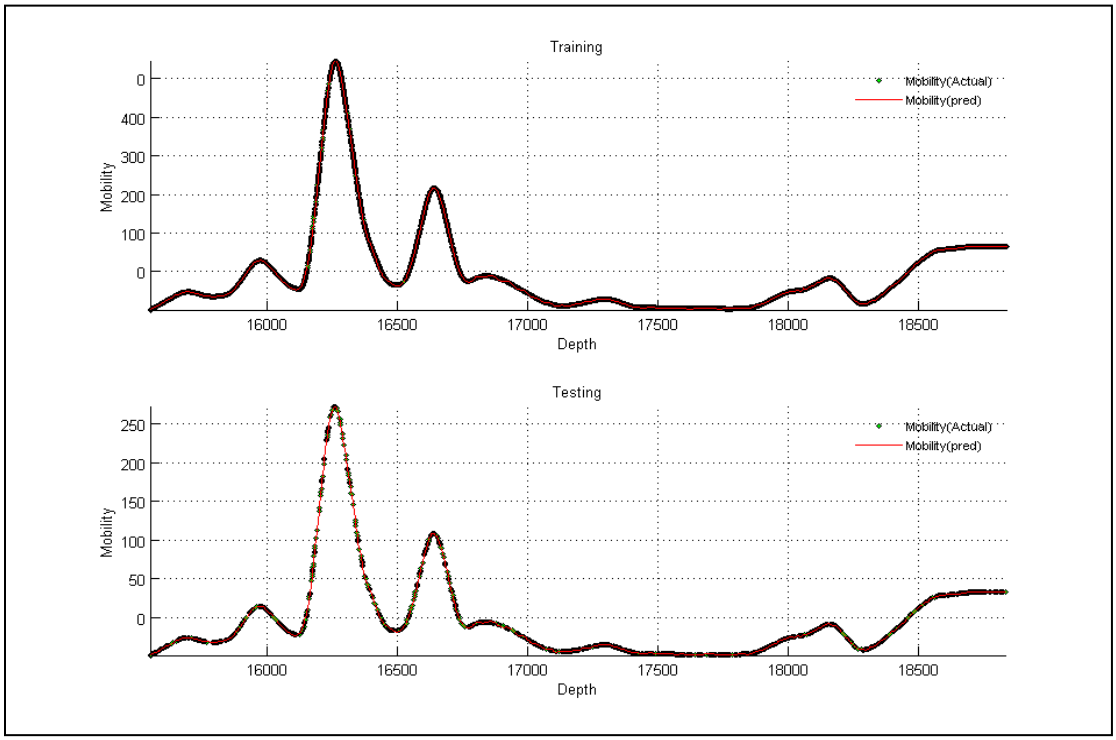

Figure A- 161: Well-9, Case -1

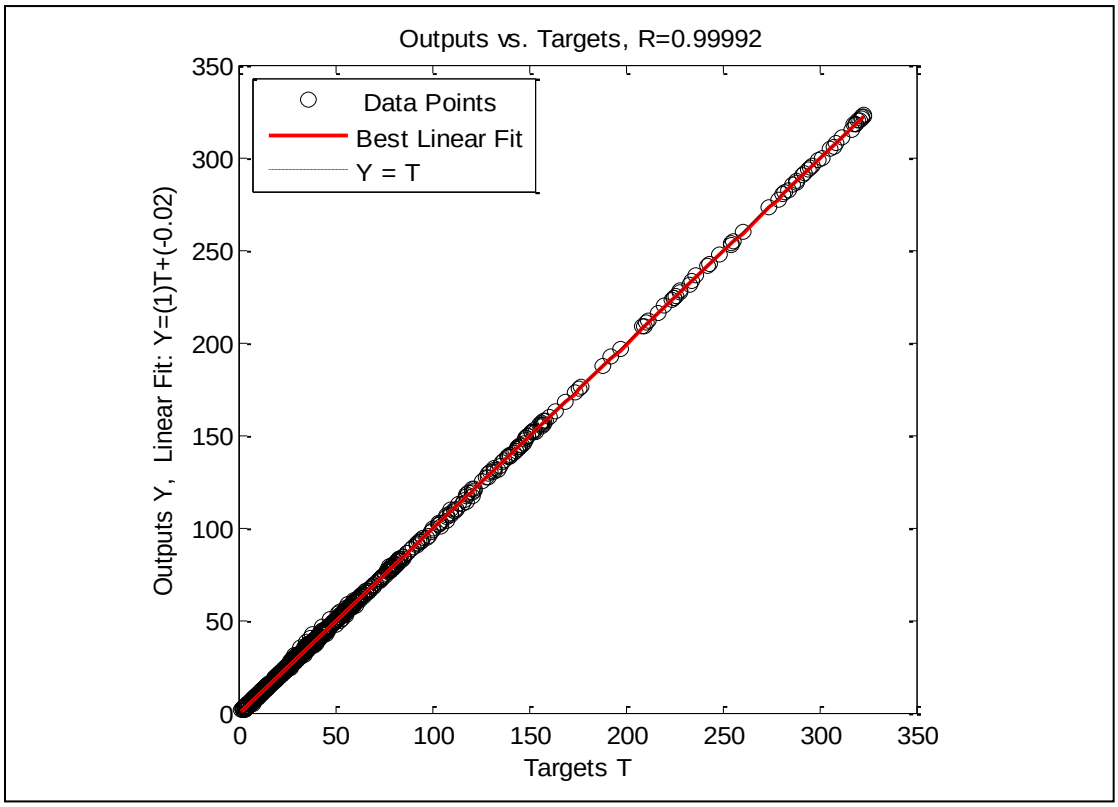

Figure A- 162: Well-9, Case -1, Crossplot

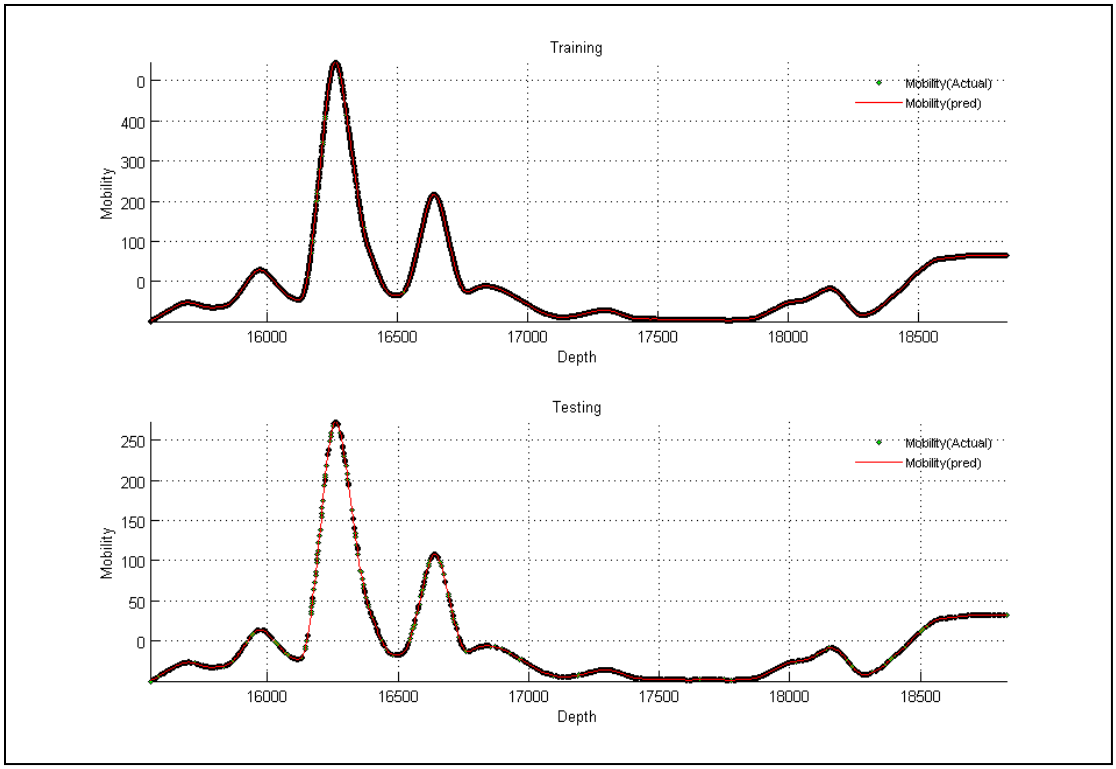

Figure A- 163: Well-9, Case -2

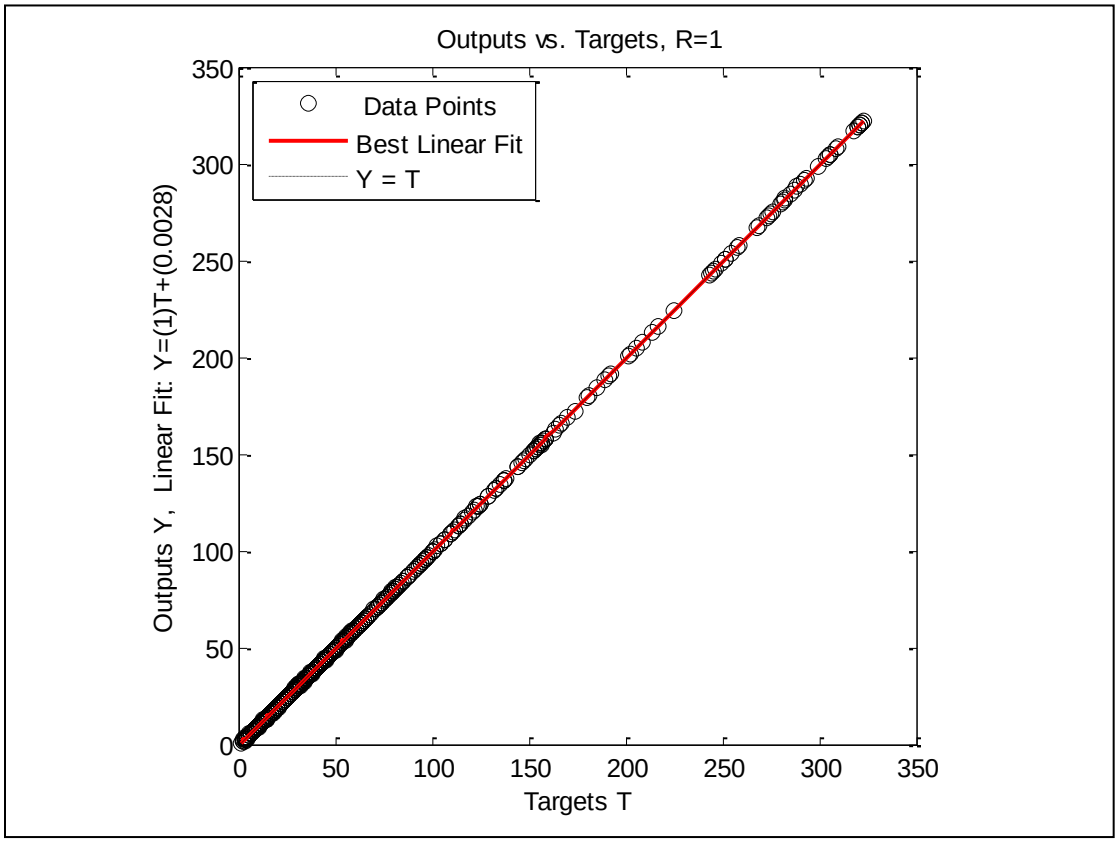

Figure A- 164: Well-9, Case -2, Crossplot

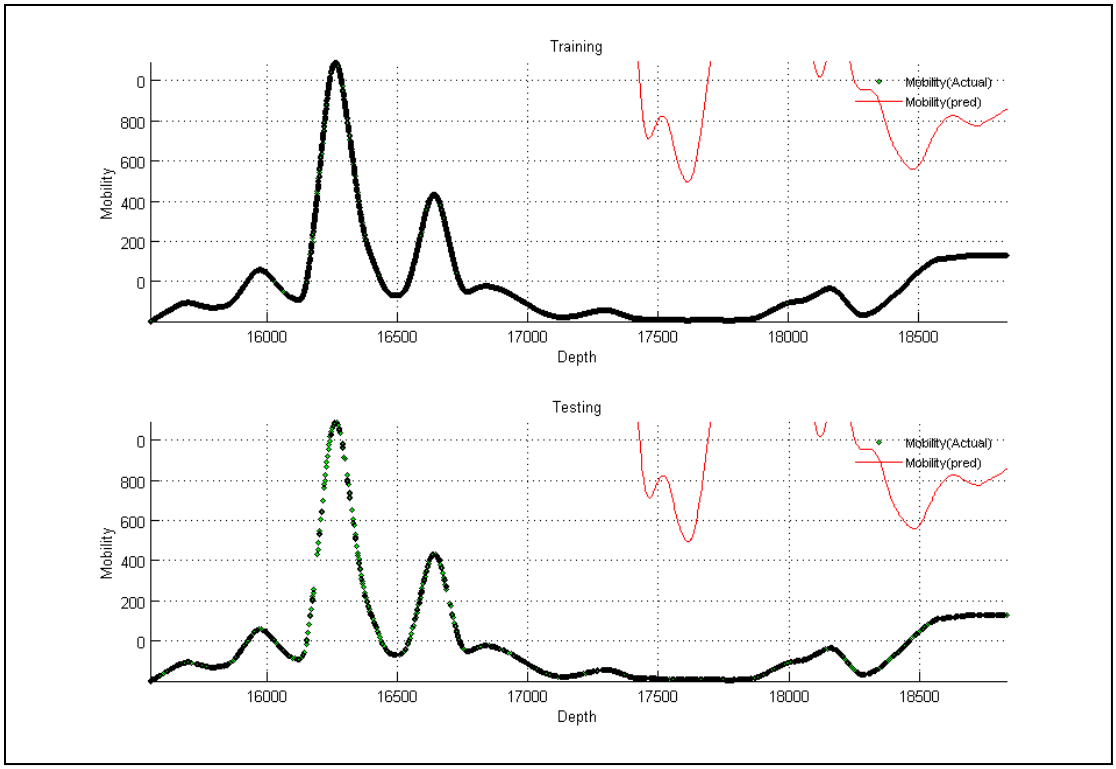

Figure A- 165: Well-9, Case -3

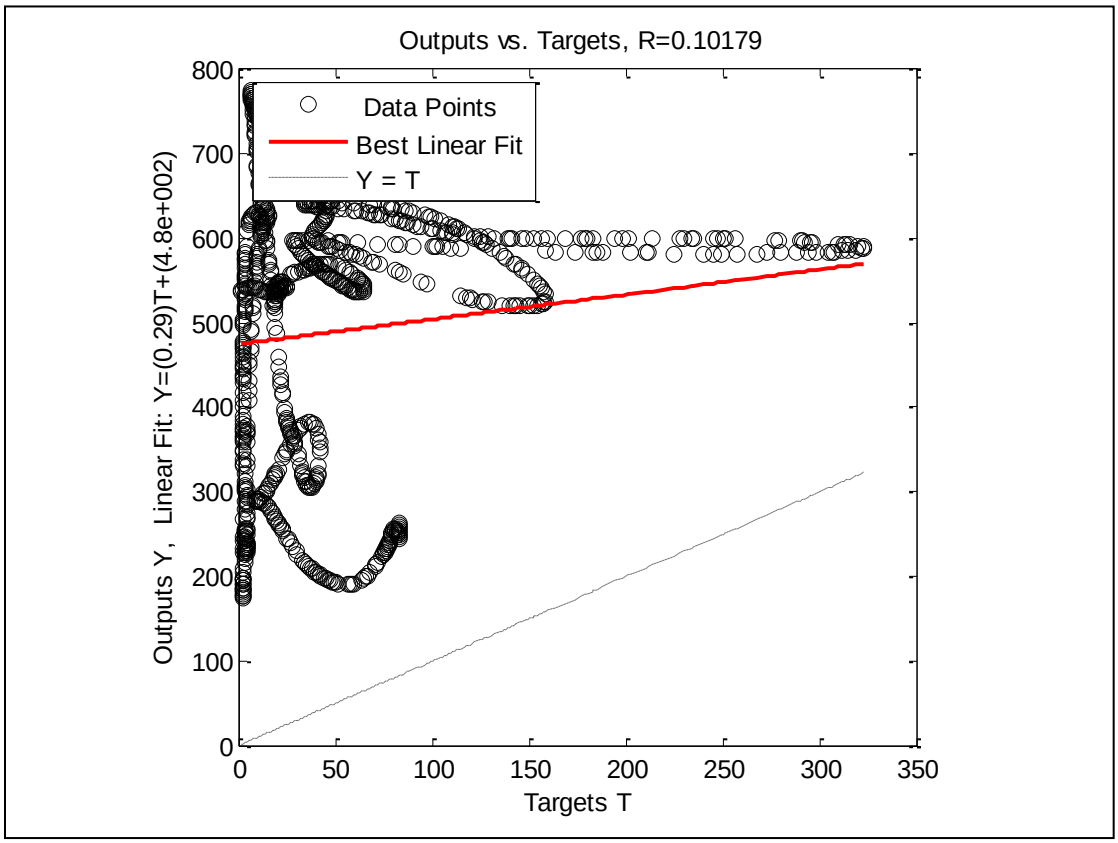

Figure A- 166: Well-9, Case -3, Crossplot

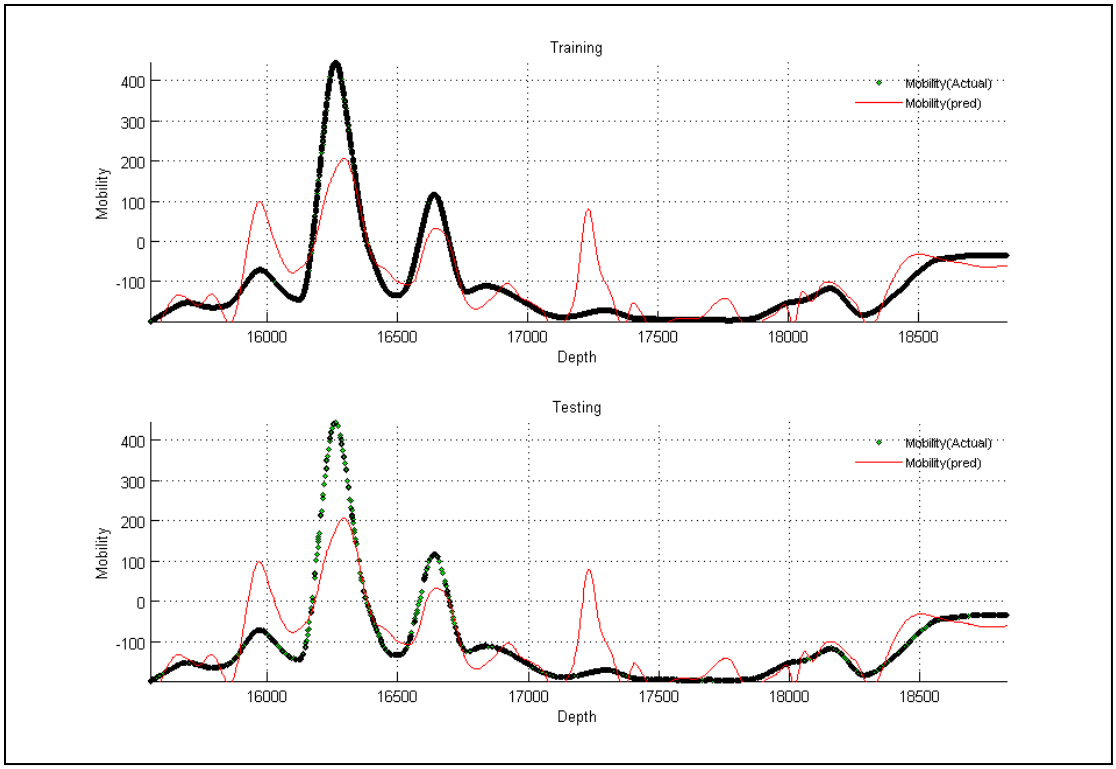

Figure A- 167: Well-9, Case -4

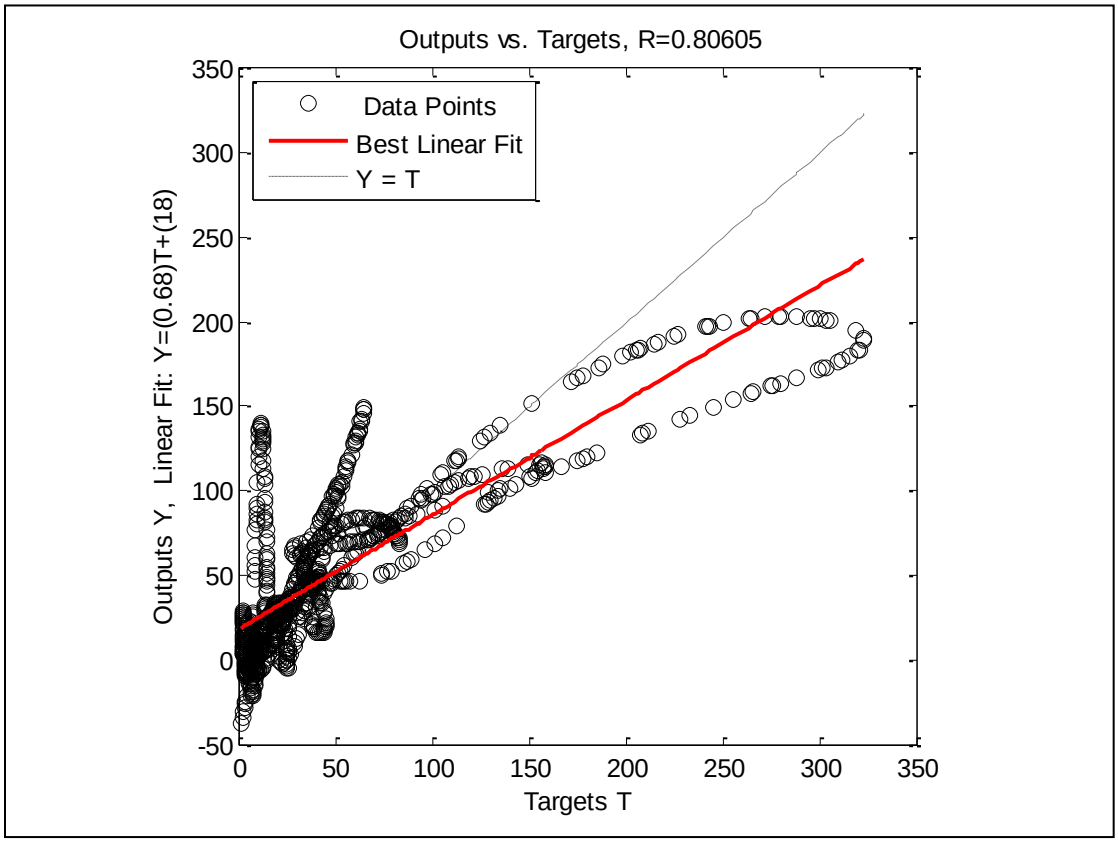

Figure A- 168: Well-9, Case -4, Crossplot

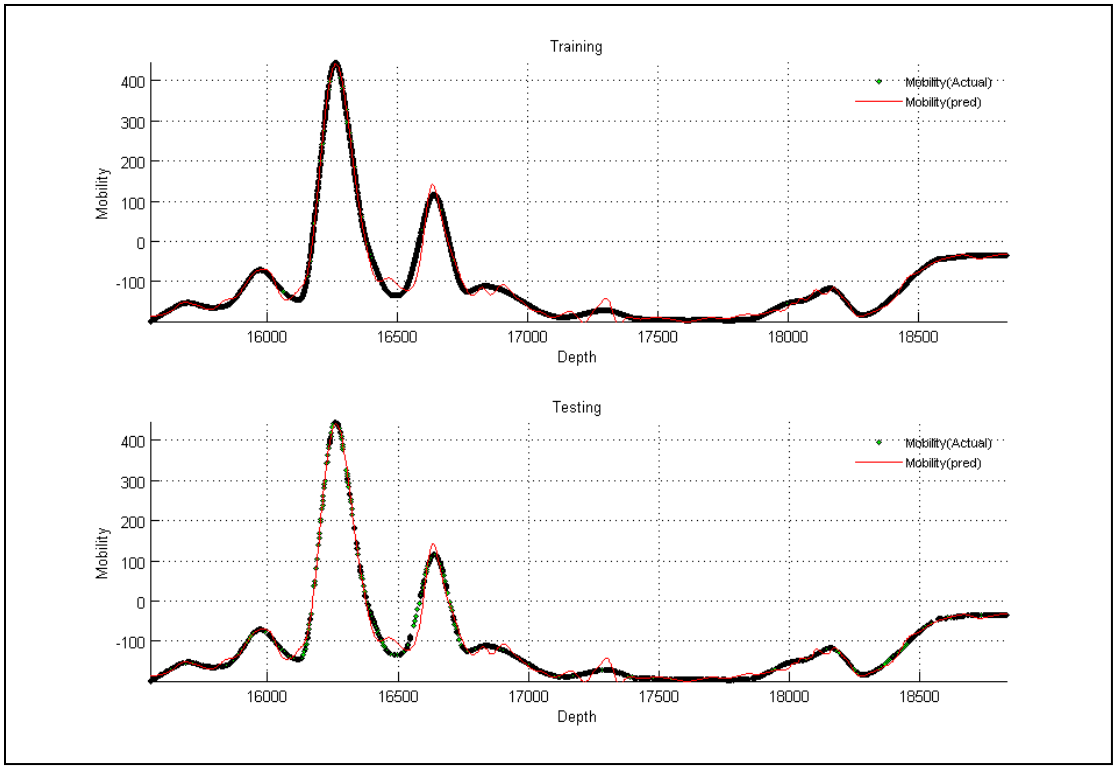

Figure A- 169: Well-9, Case -5

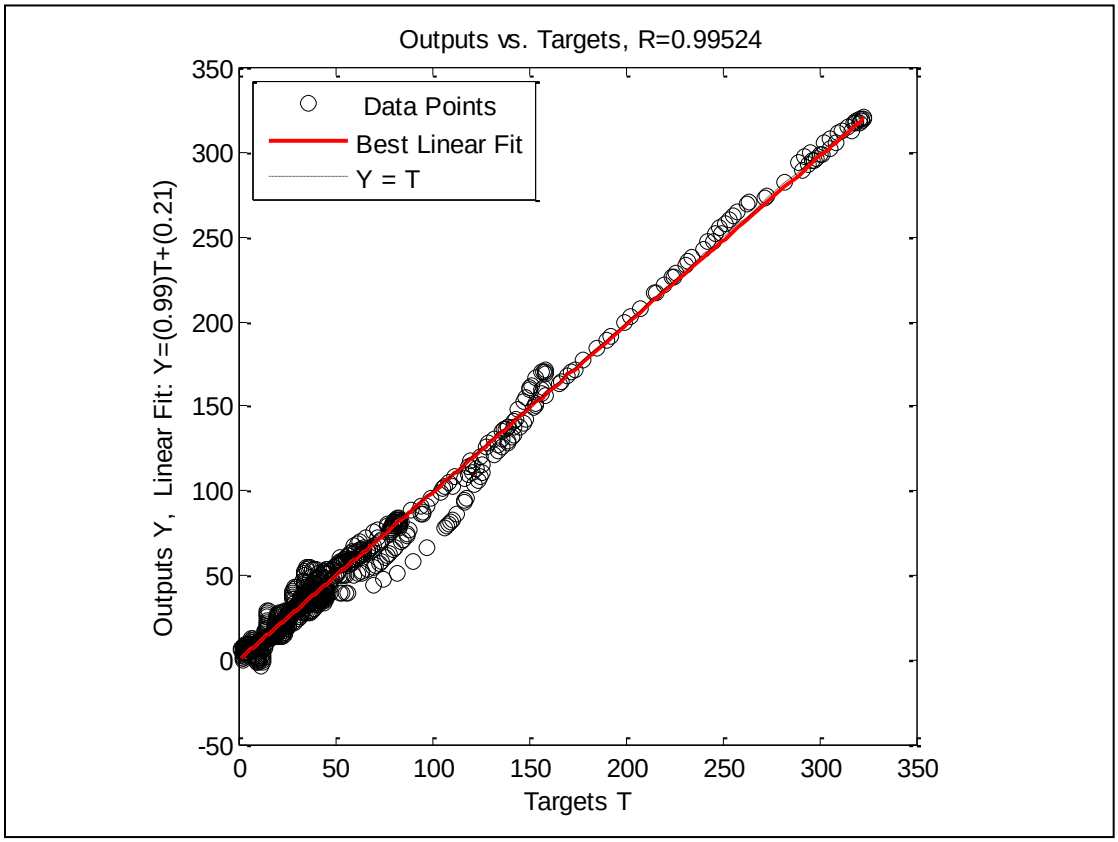

Figure A- 170: Well-9, Case -5, Crossplot

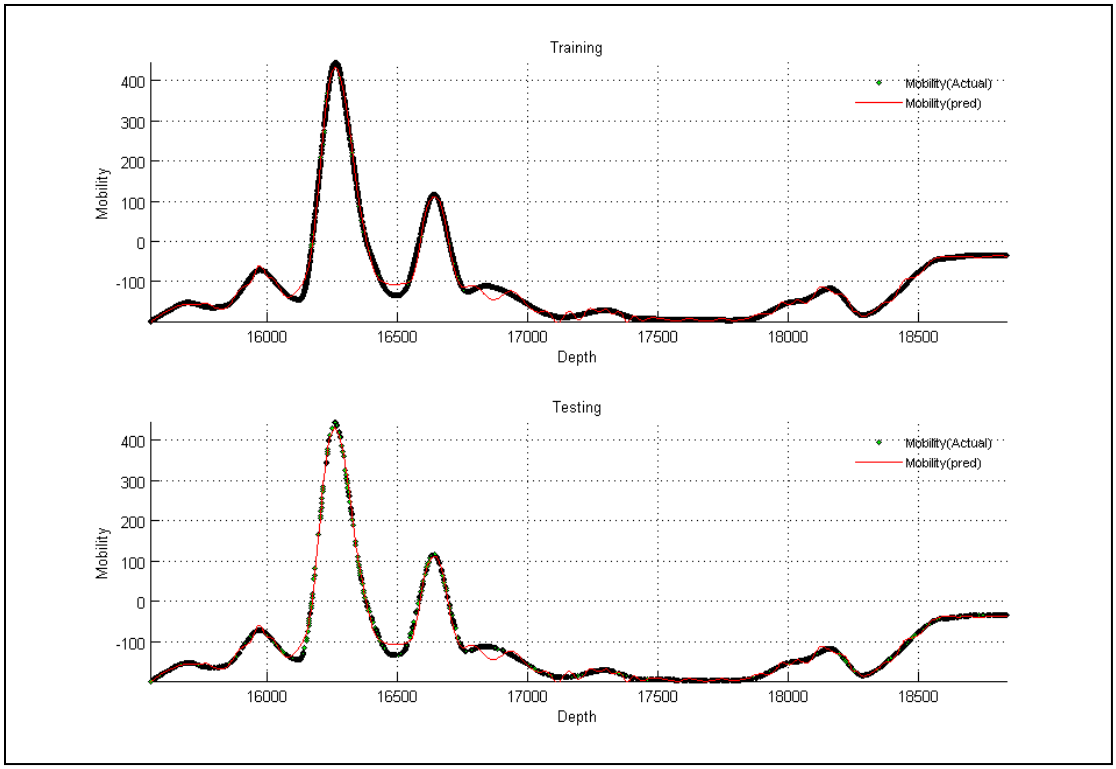

Figure A- 171: Well-9, Case -6

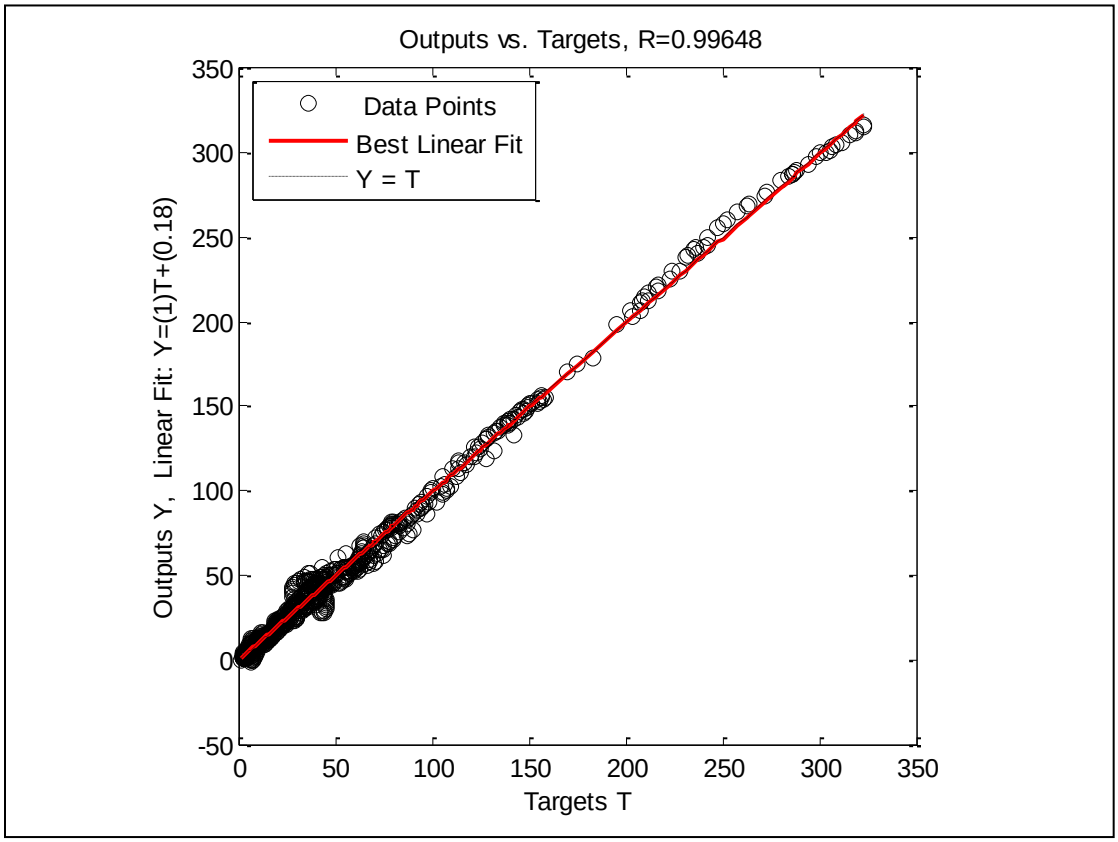

Figure A- 172: Well-9, Case -6, Crossplot

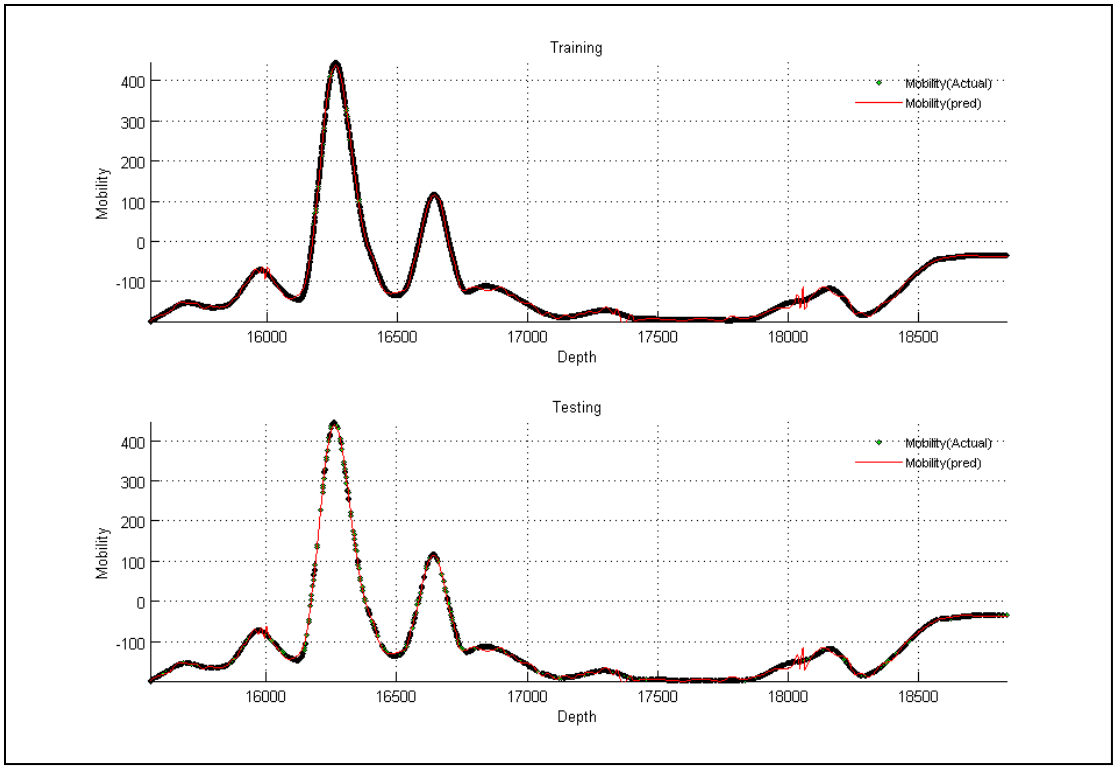

Figure A- 173: Well-9, Case -7

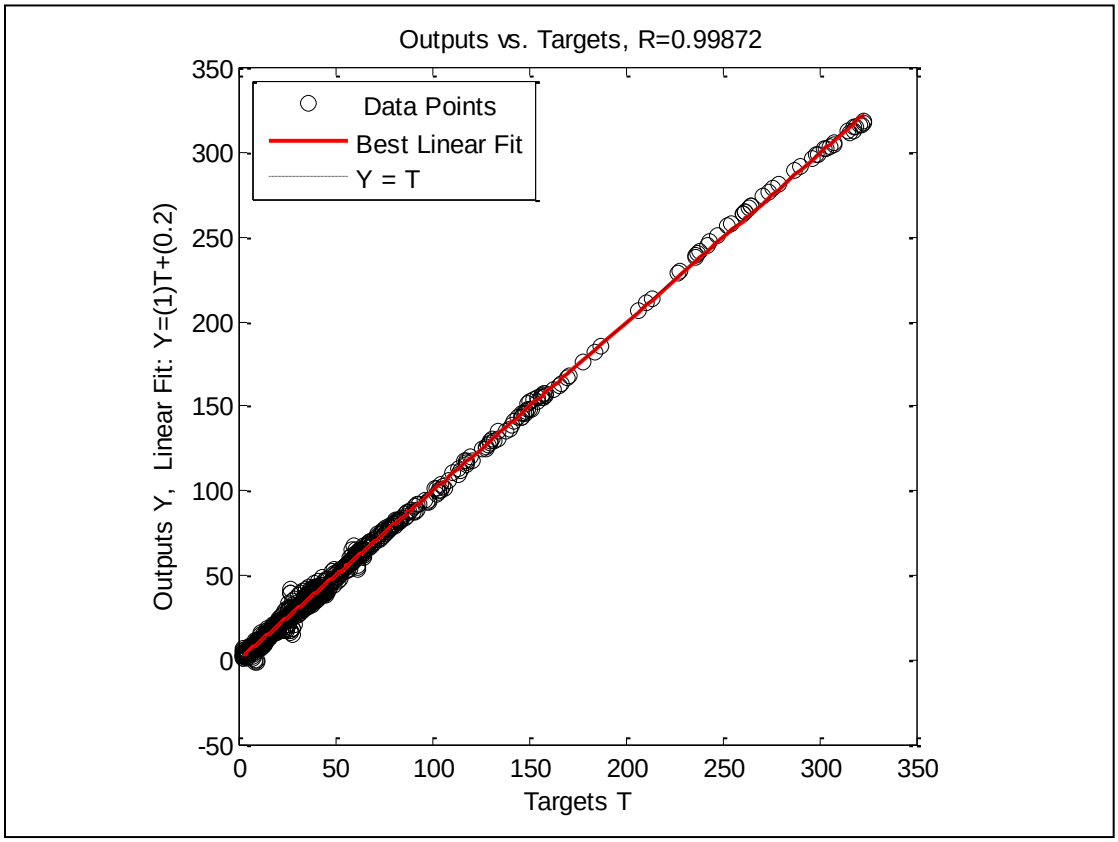

Figure A- 174: Well-9, Case -7, Crossplot

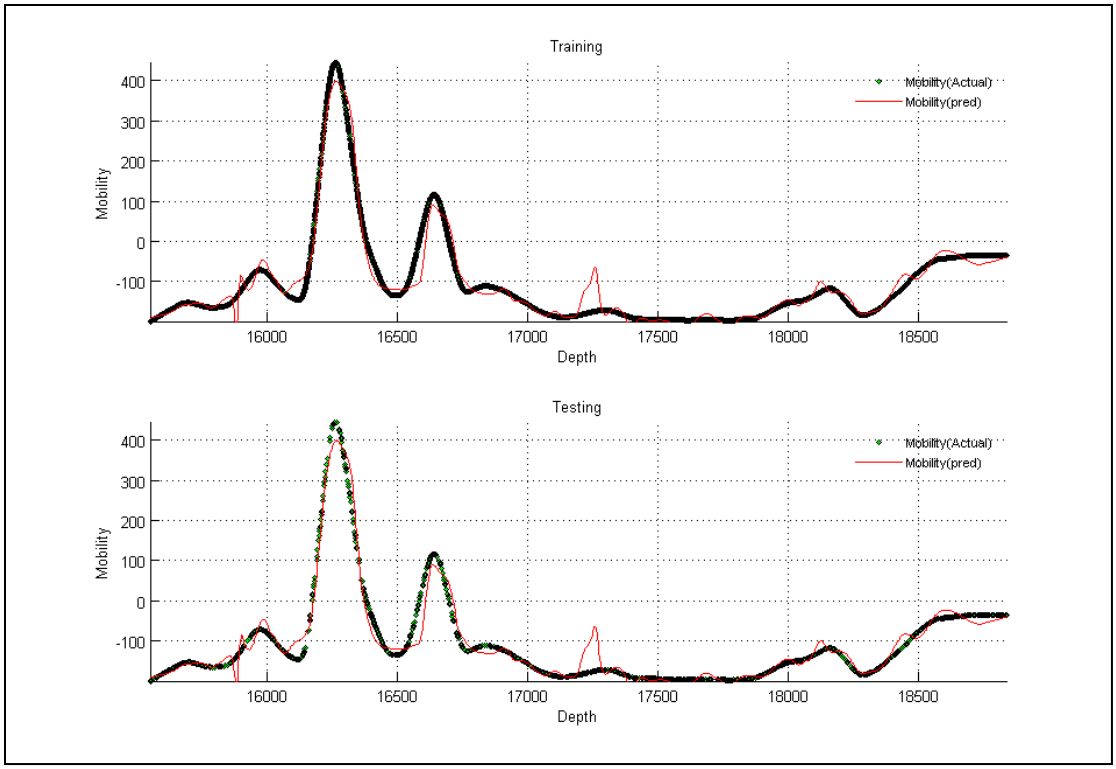

Figure A- 175: Well-9, Case -8

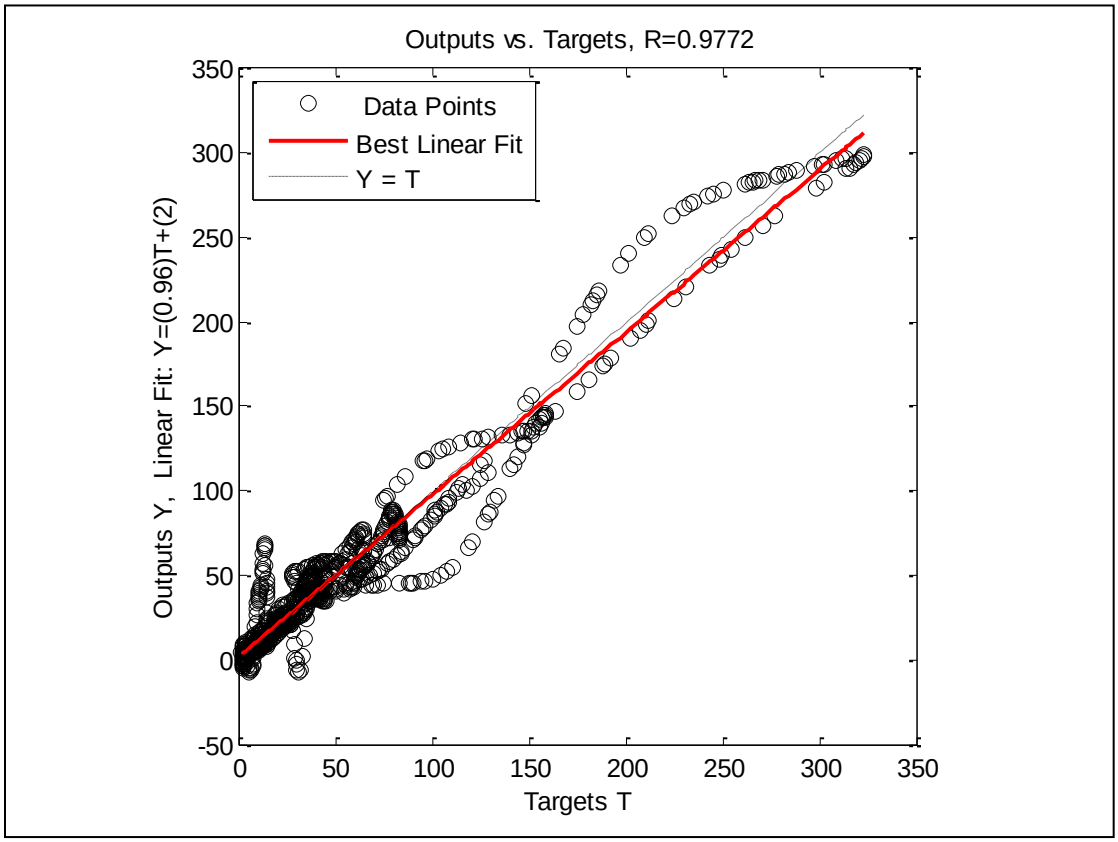

Figure A- 176: Well-9, Case -8, Crossplot

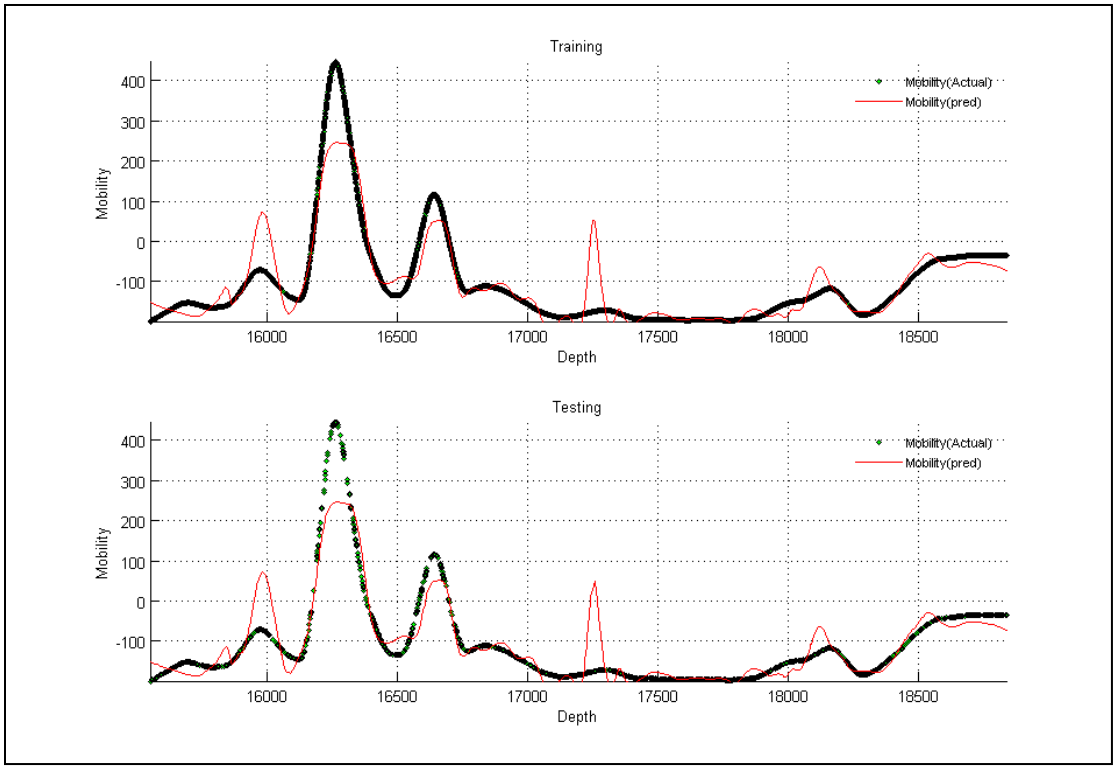

Figure A- 177: Well-9, Case -9

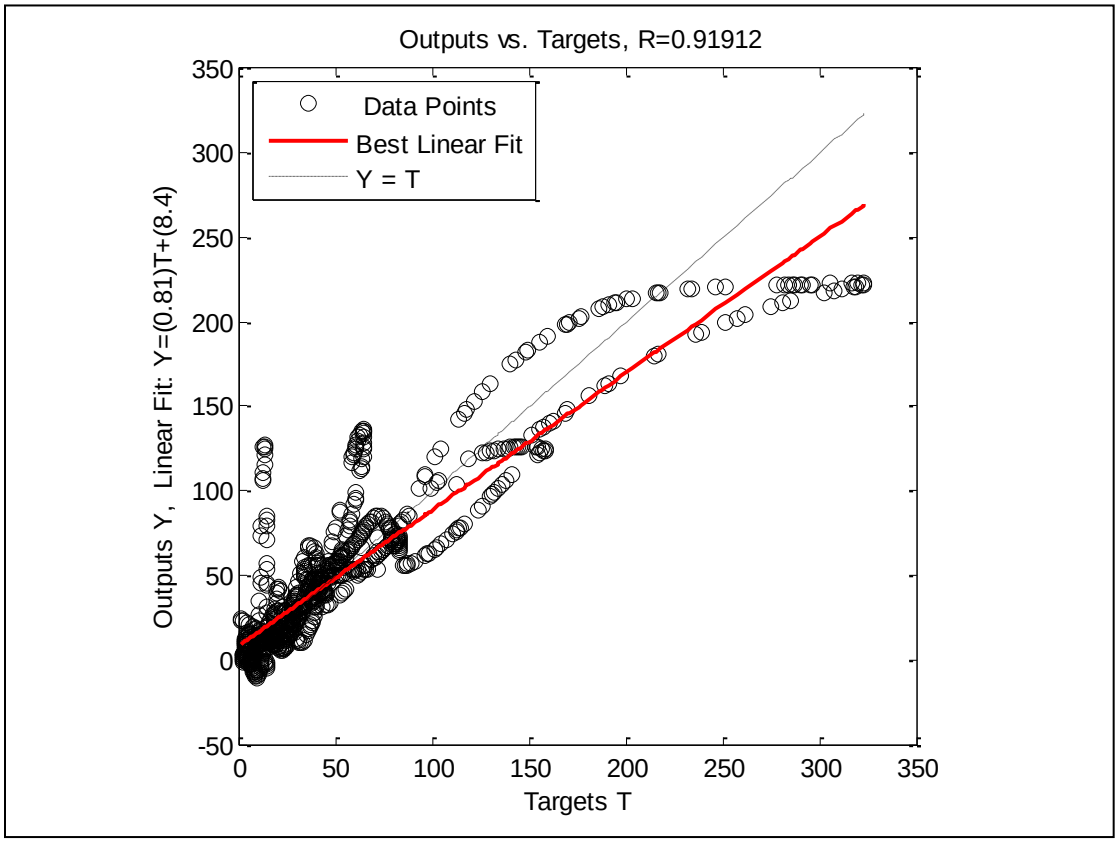

Figure A- 178: Well-9, Case -9, Crossplot

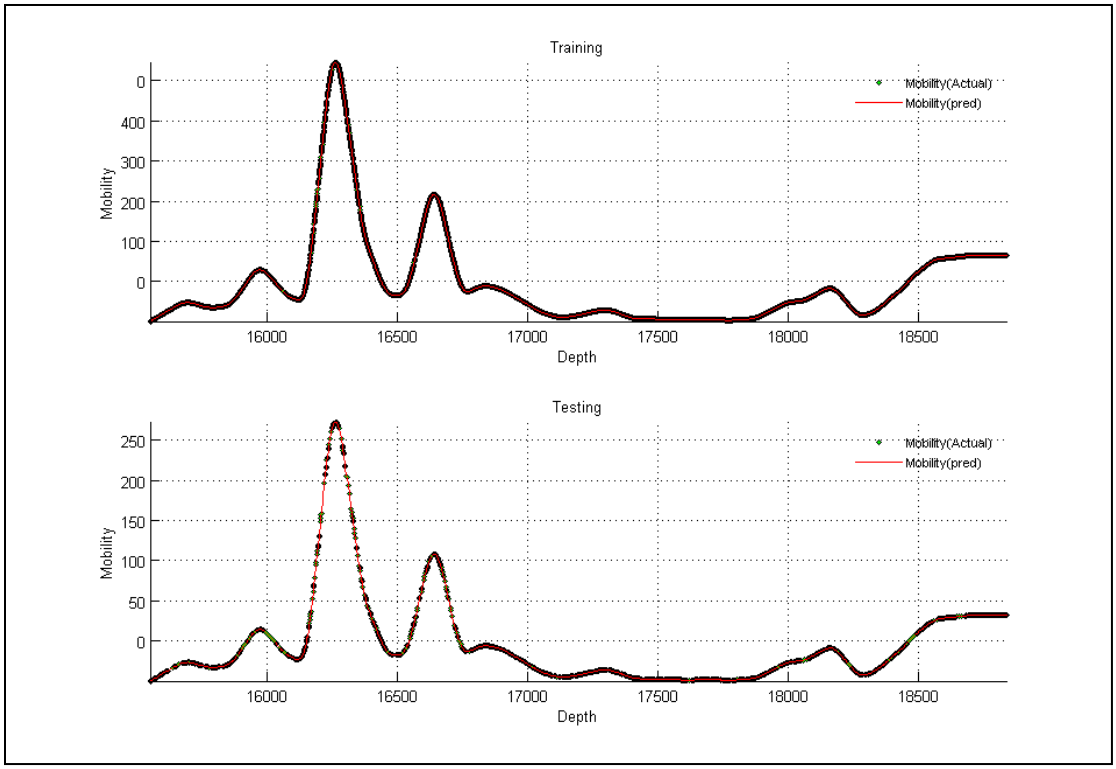

Figure A- 179: Well-9, Case -10

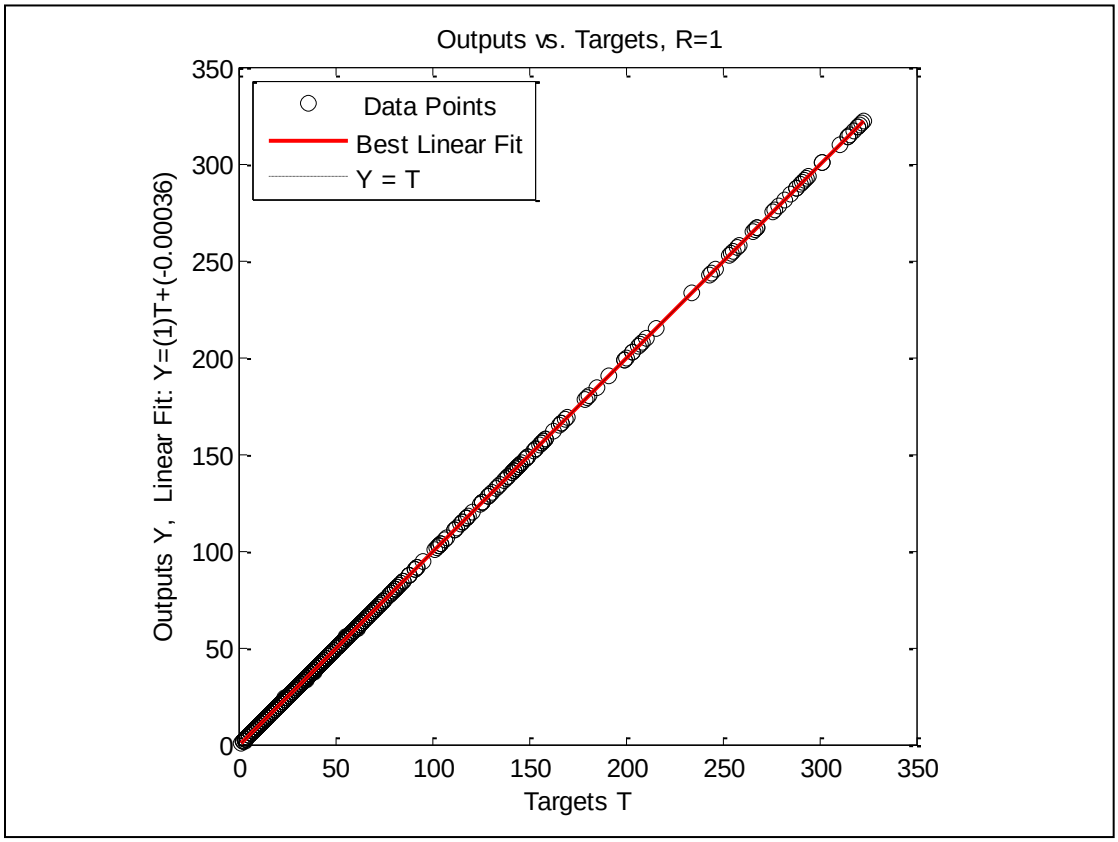

Figure A- 180: Well-9, Case -10, Crossplot

Well No. 10

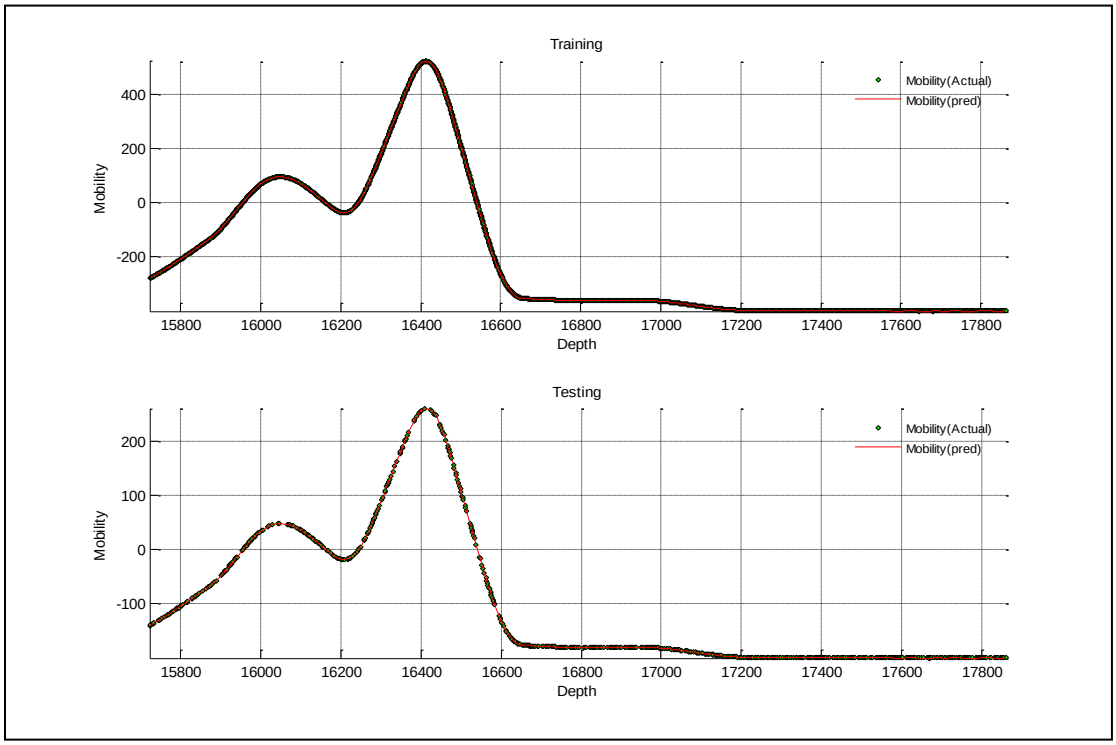

Figure A- 181: Well-10, Case -1

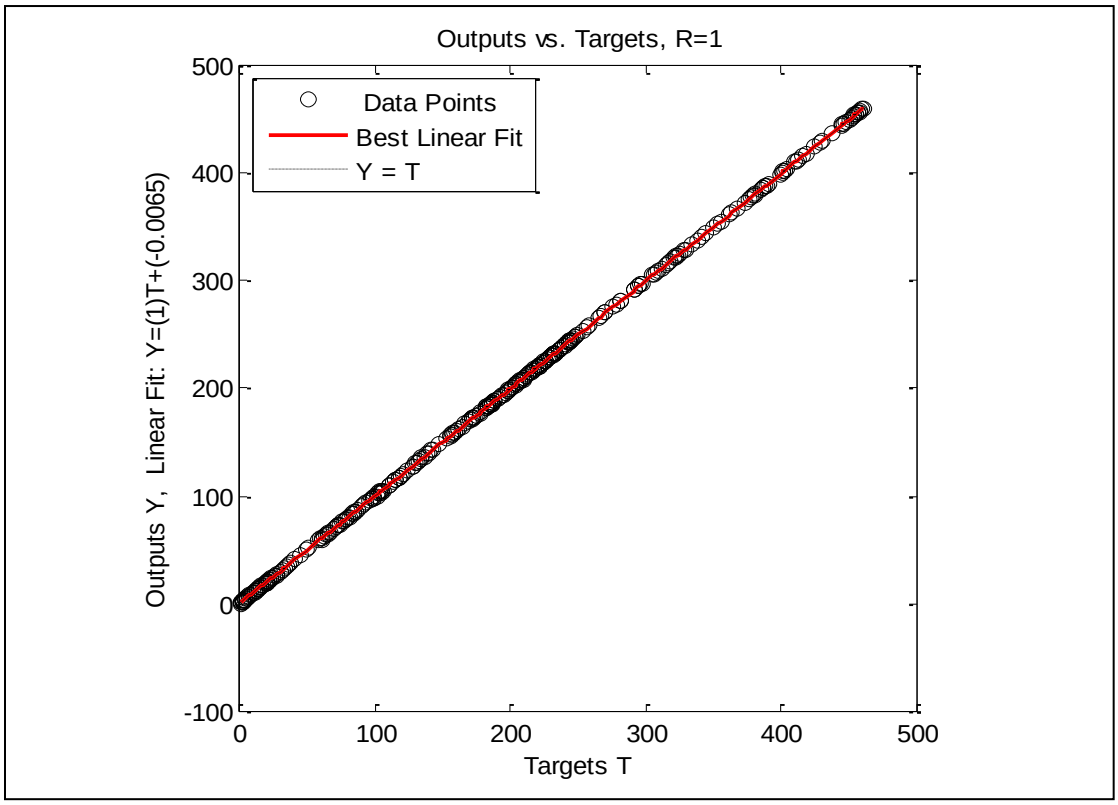

Figure A- 182: Well-10, Case -1, Crossplot

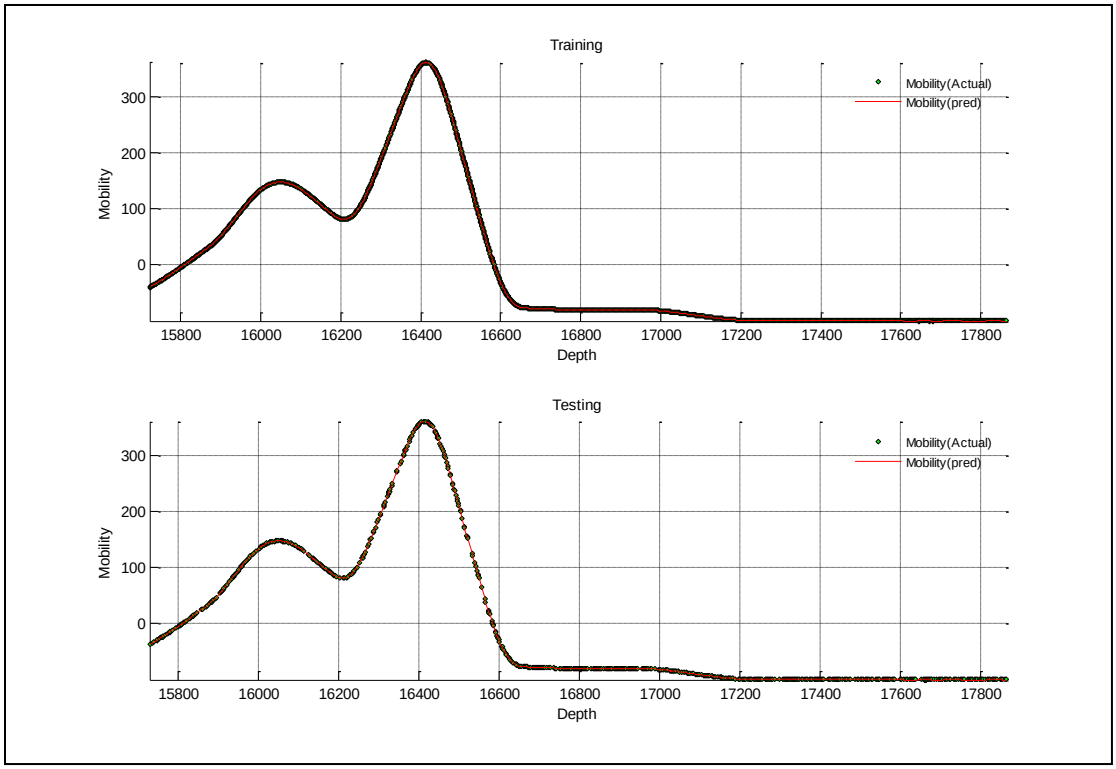

Figure A- 183: Well-10, Case -2

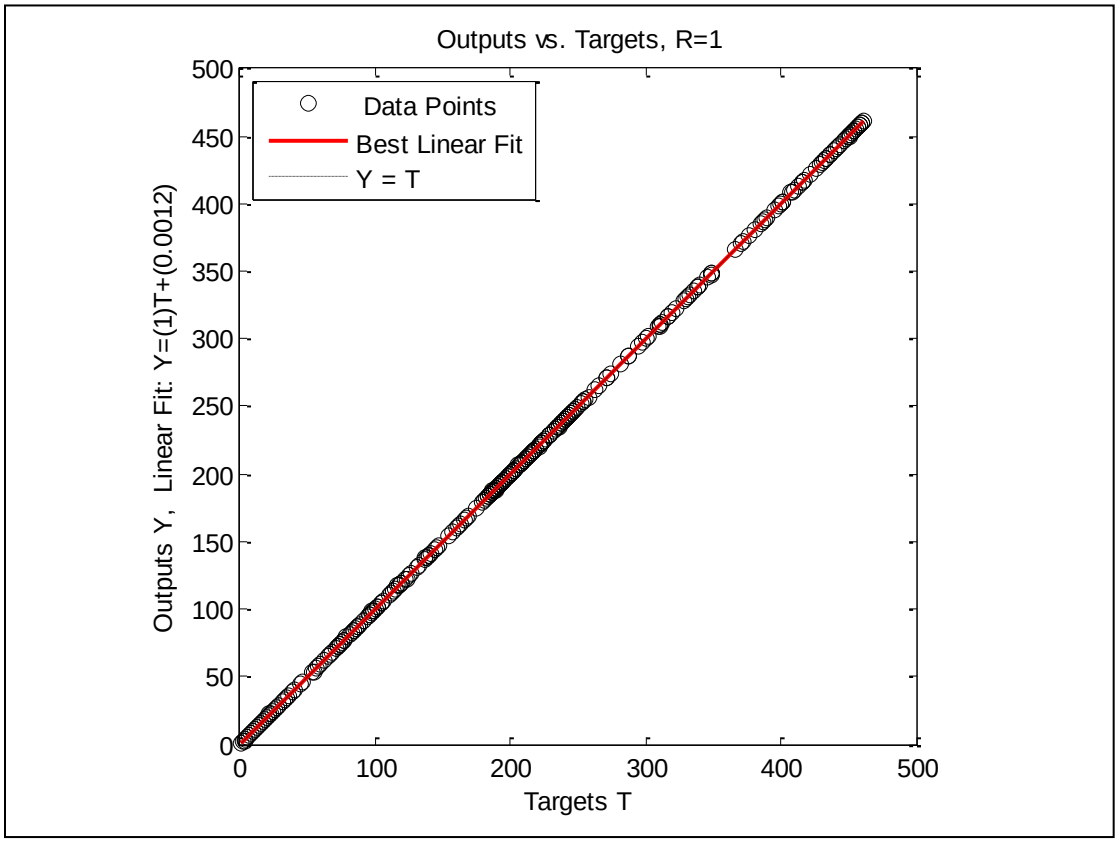

Figure A- 184: Well-10, Case -2, Crossplot

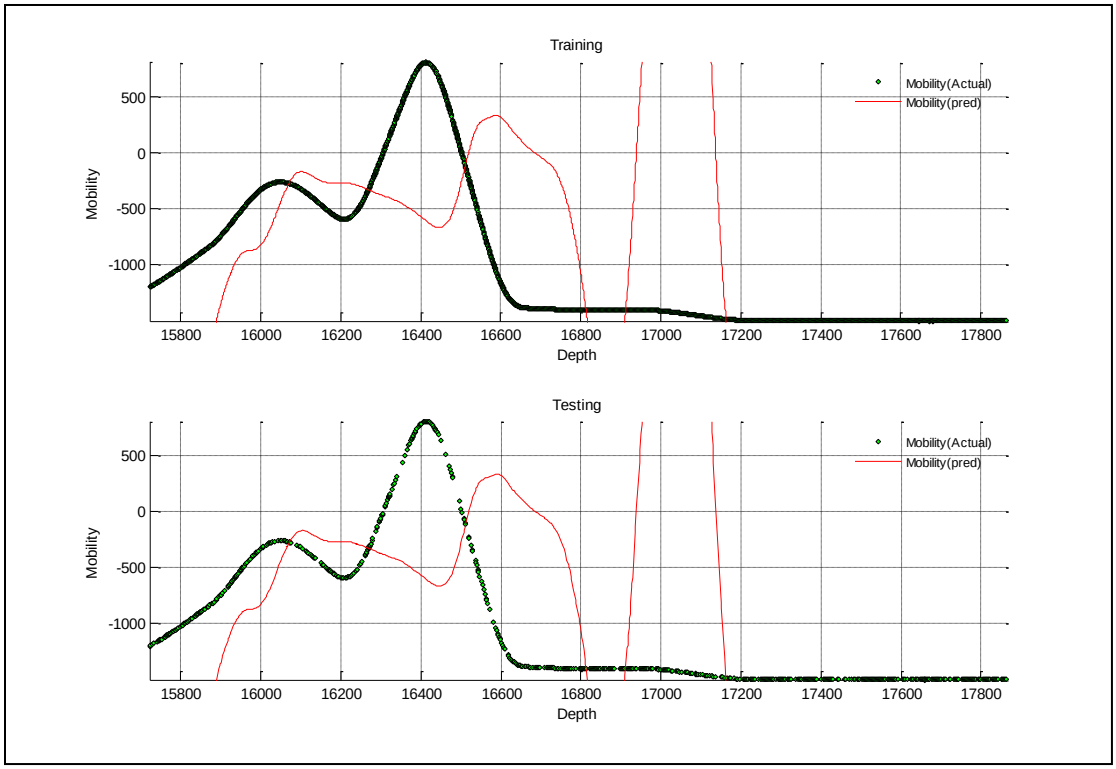

Figure A- 185: Well-10, Case -3

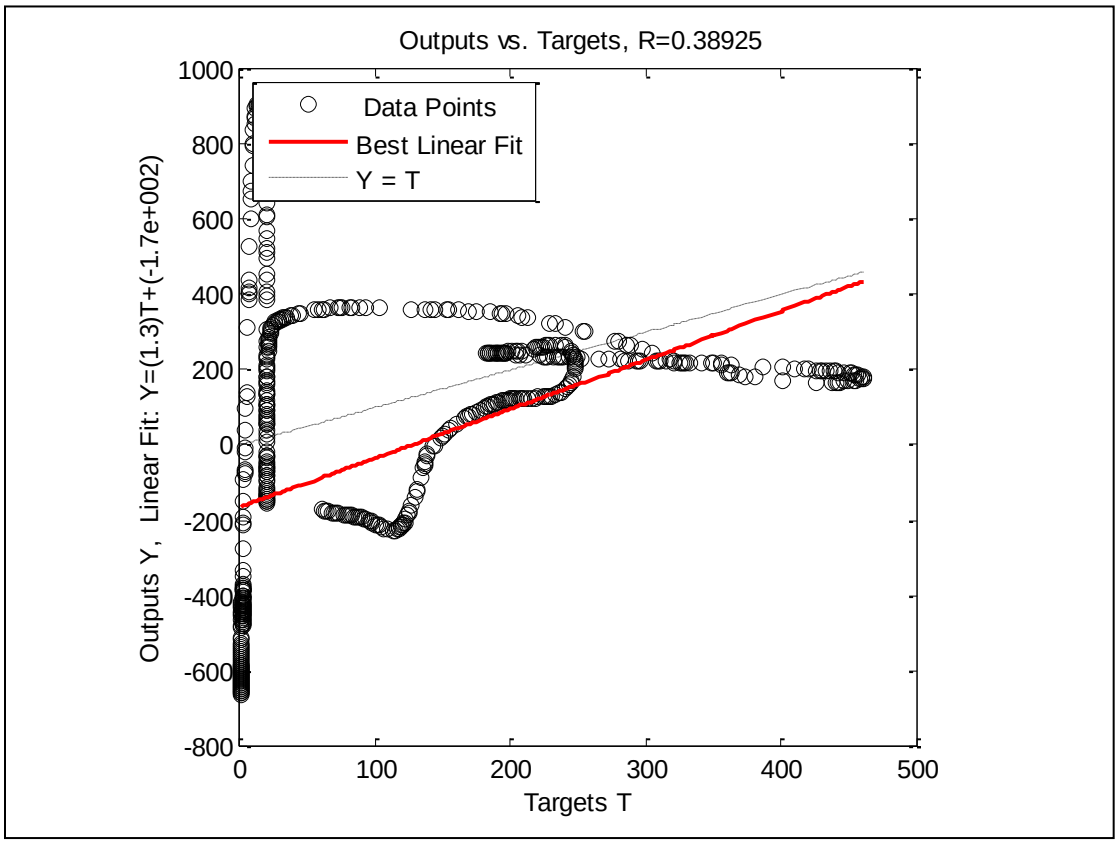

Figure A- 186: Well-10, Case -3, Crossplot

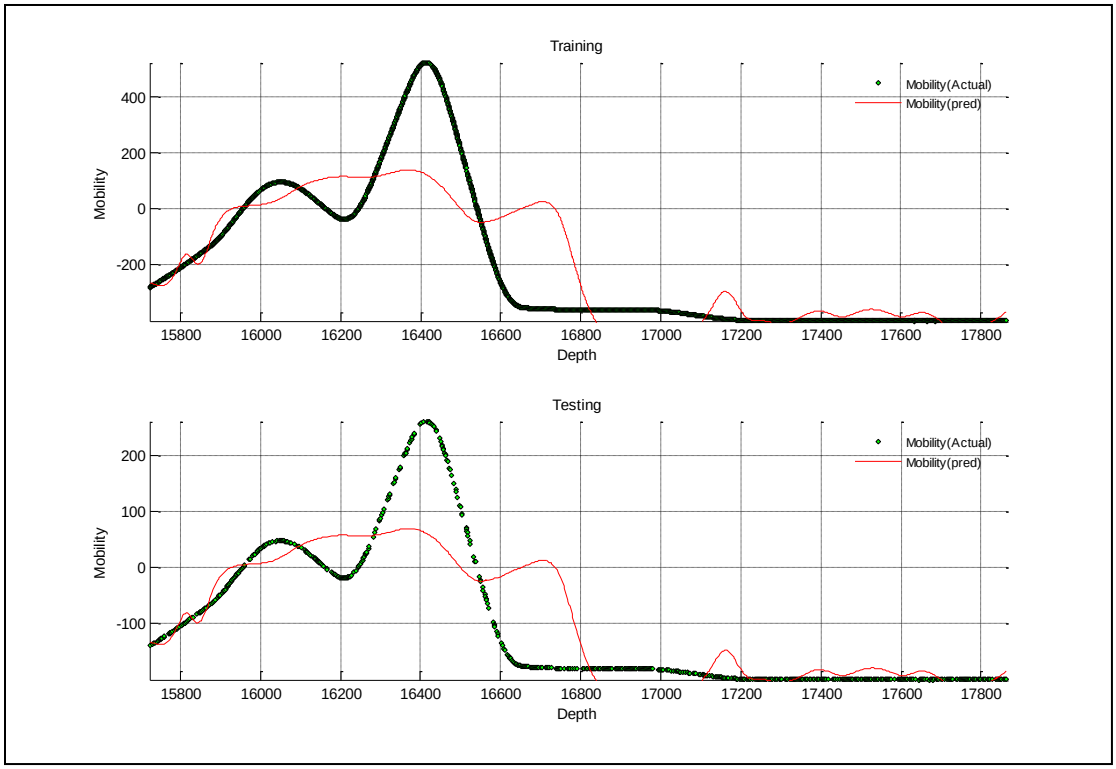

Figure A- 187: Well-10, Case -4

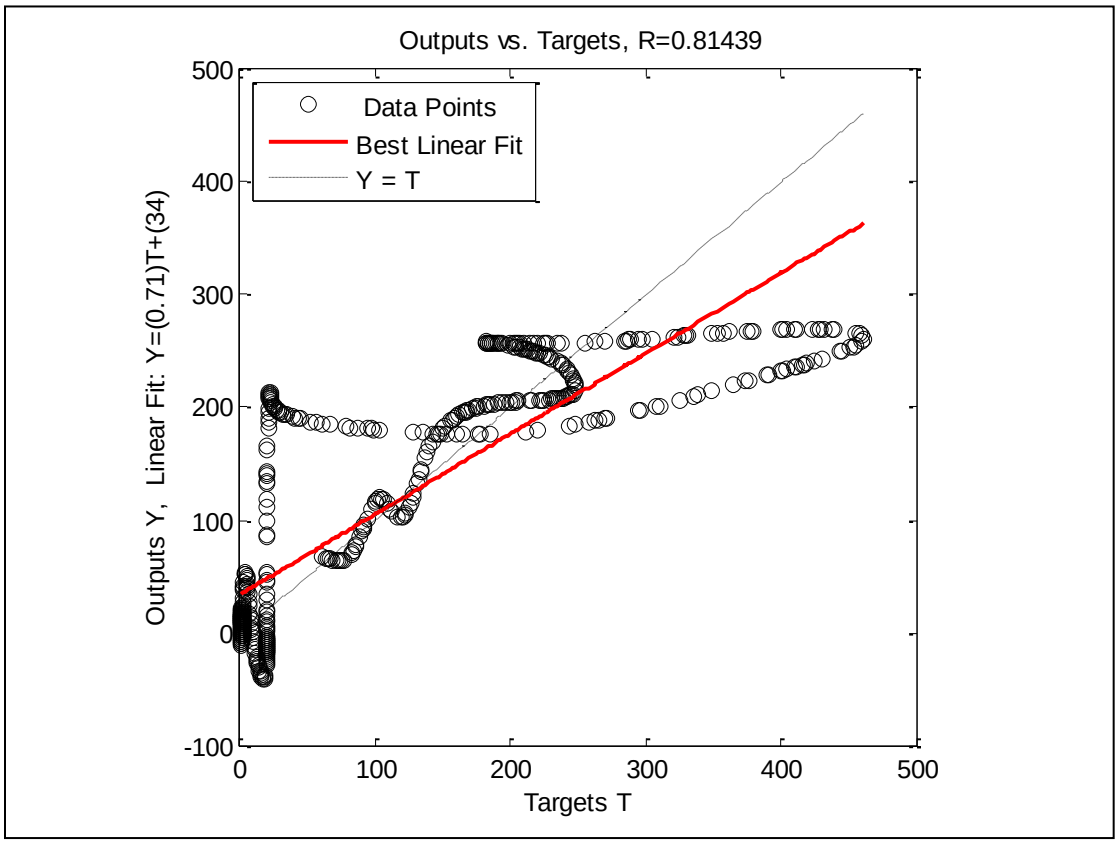

Figure A- 188: Well-10, Case -4, Crossplot

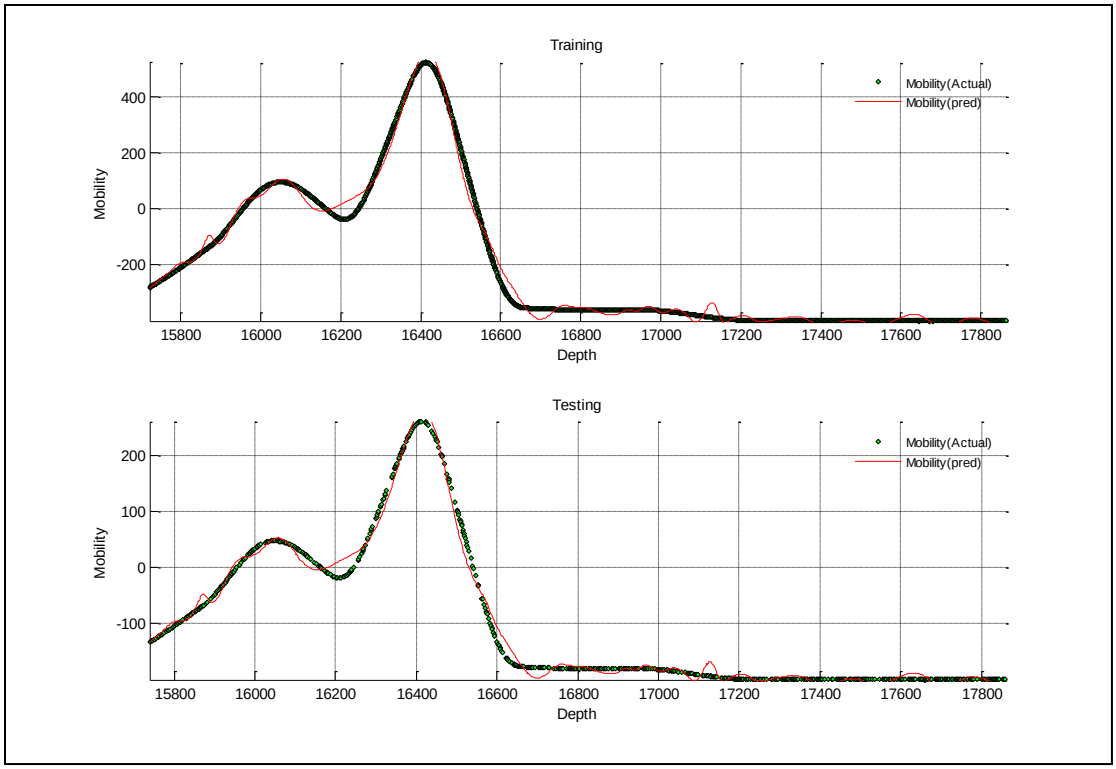

Figure A- 189: Well-10, Case -5

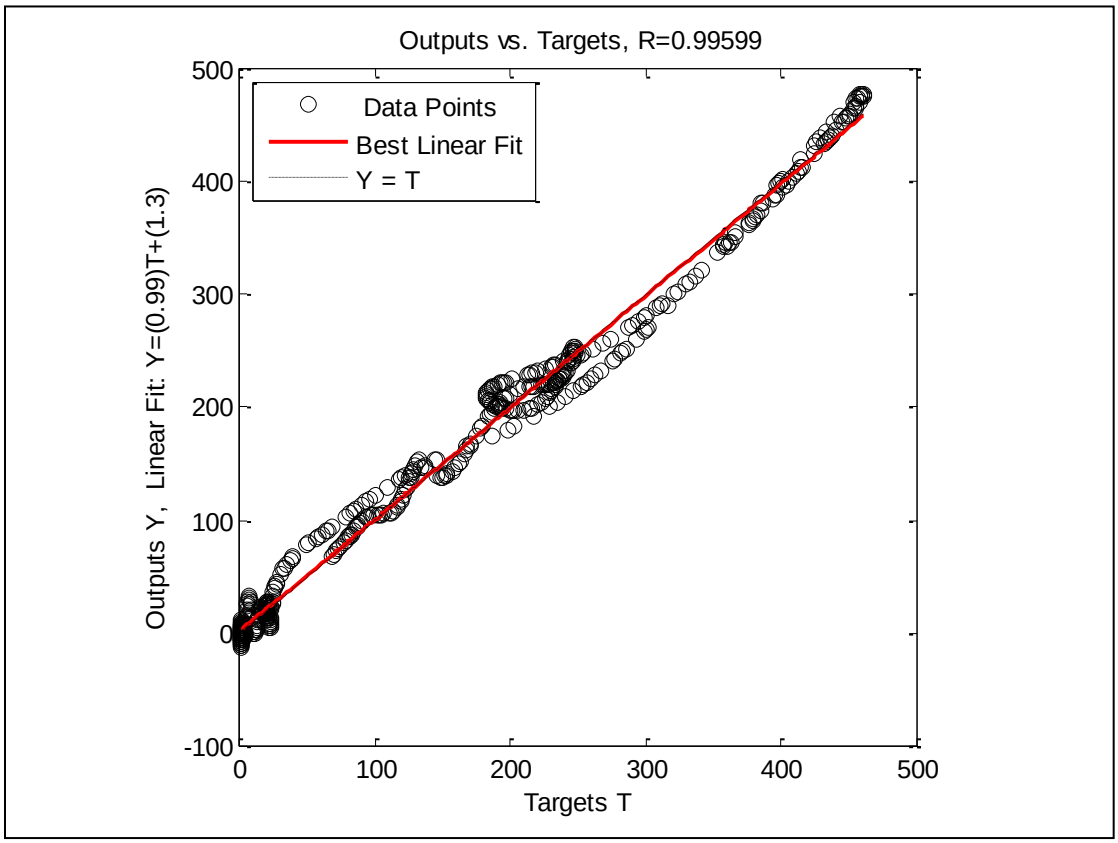

Figure A- 190: Well-10, Case -5, Crossplot

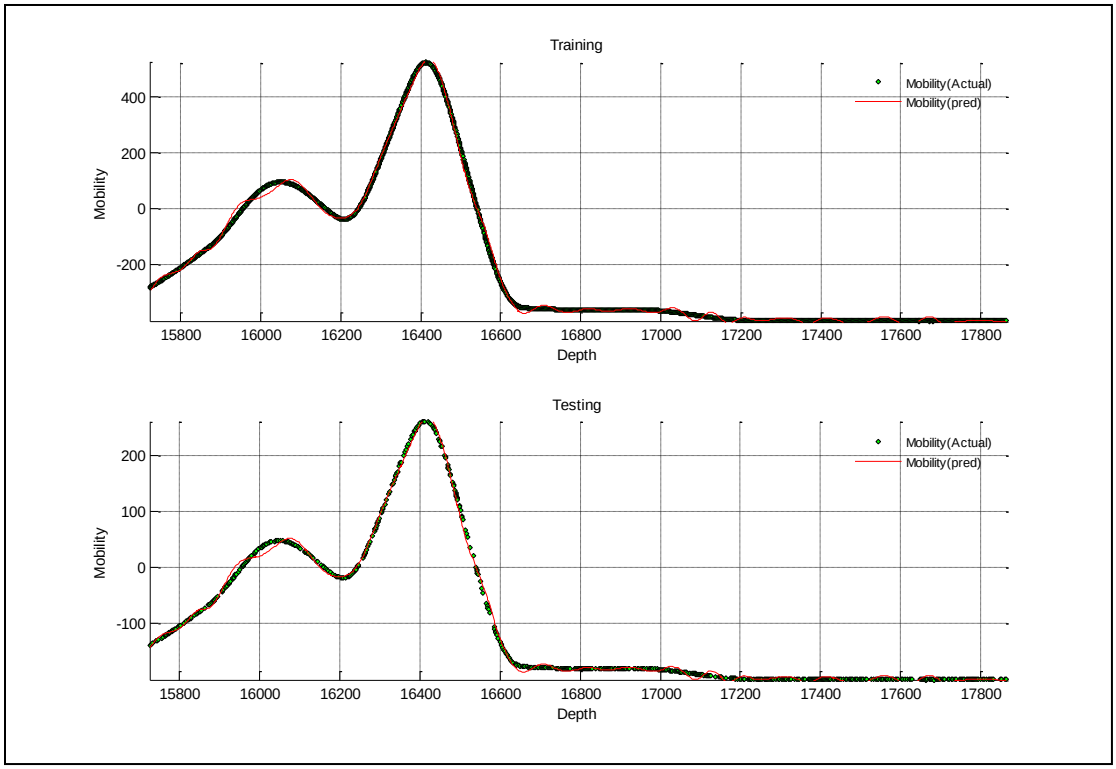

Figure A- 191: Well-10, Case -6

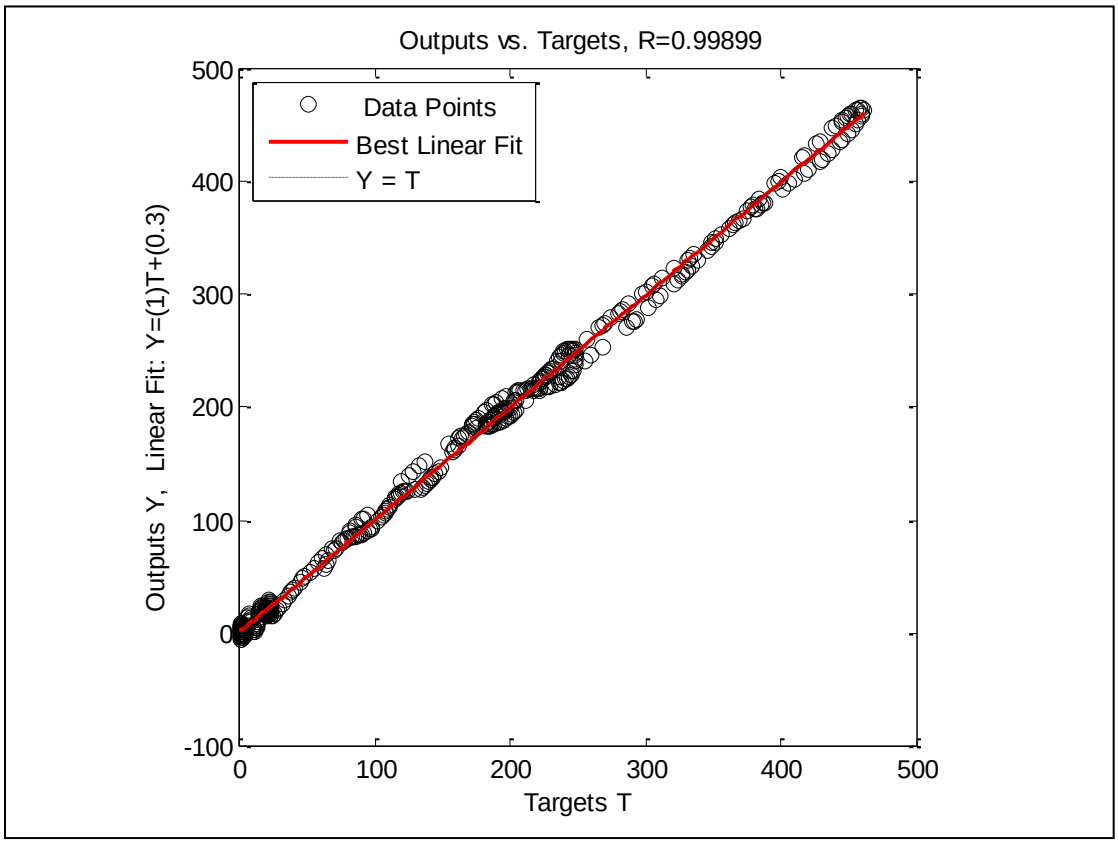

Figure A- 192: Well-10, Case -6, Crossplot

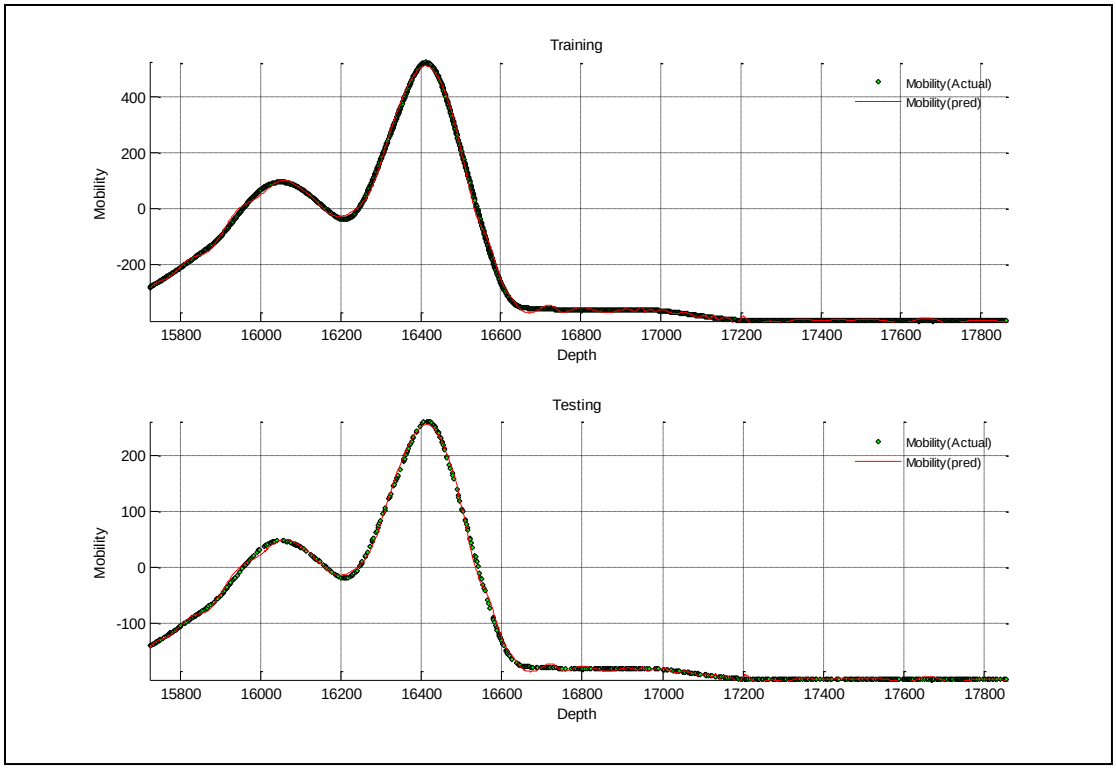

Figure A- 193: Well-10, Case -7

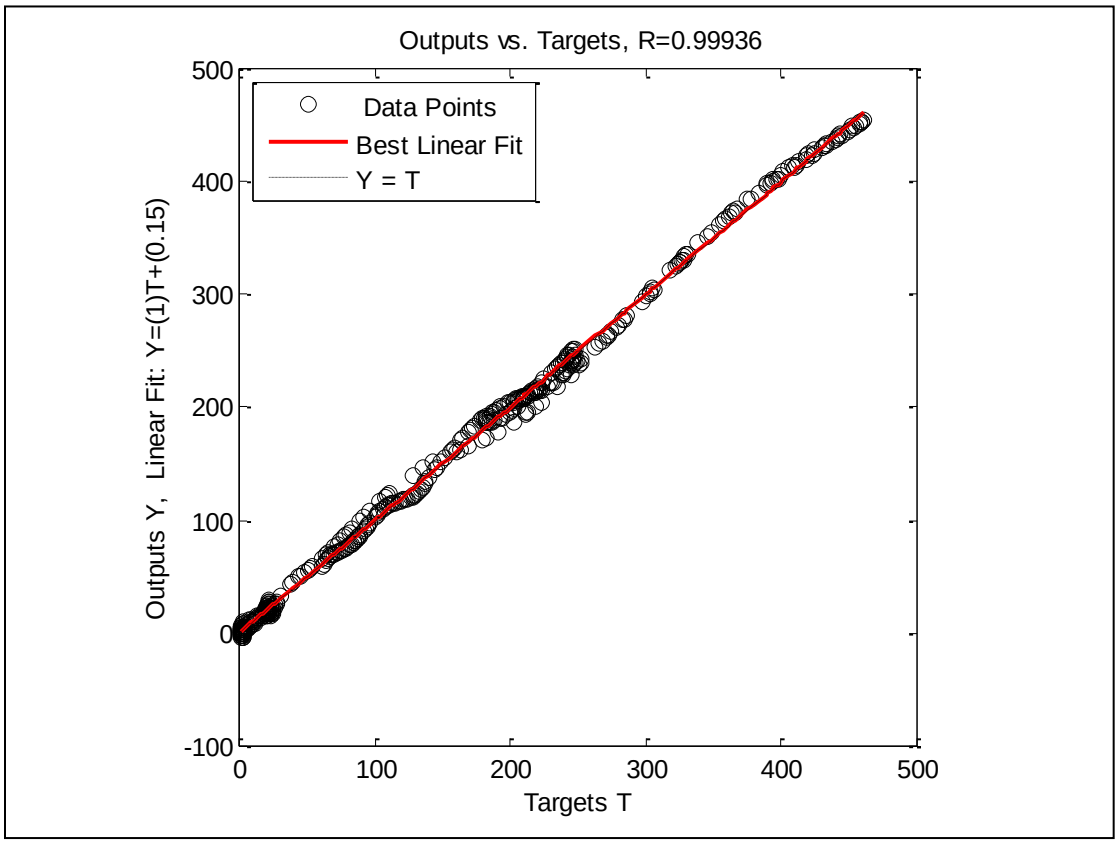

Figure A- 194: Well-10, Case -7, Crossplot

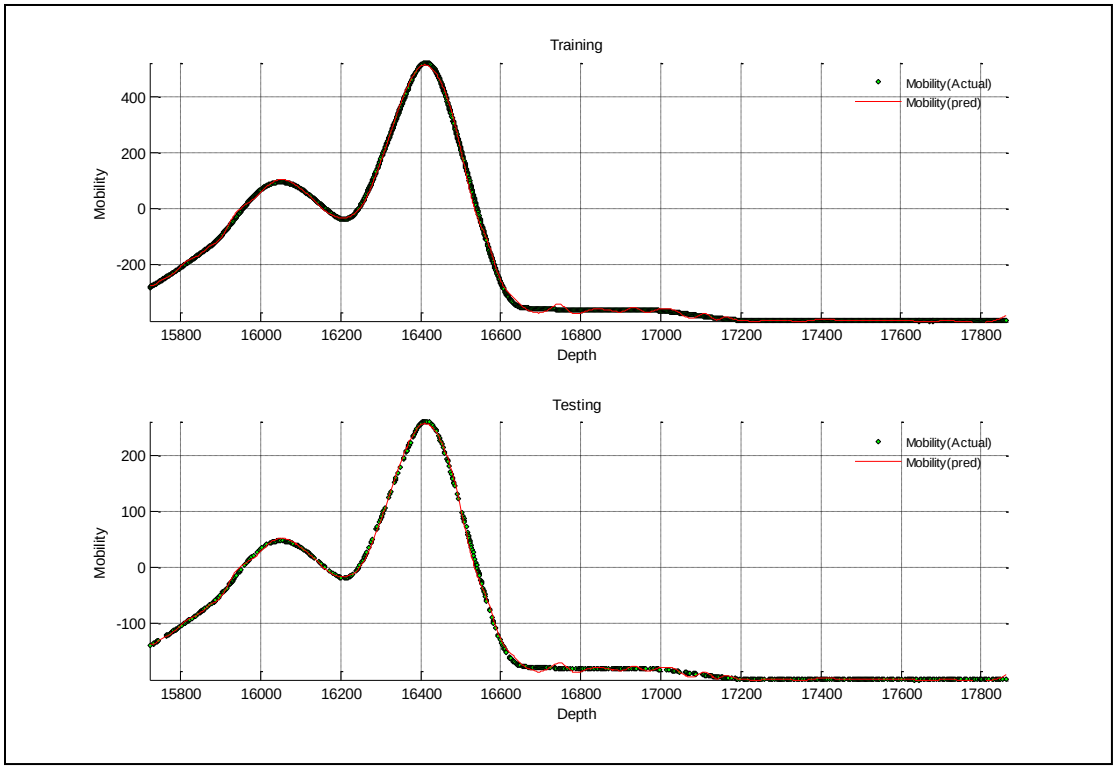

Figure A- 195: Well-10, Case -8

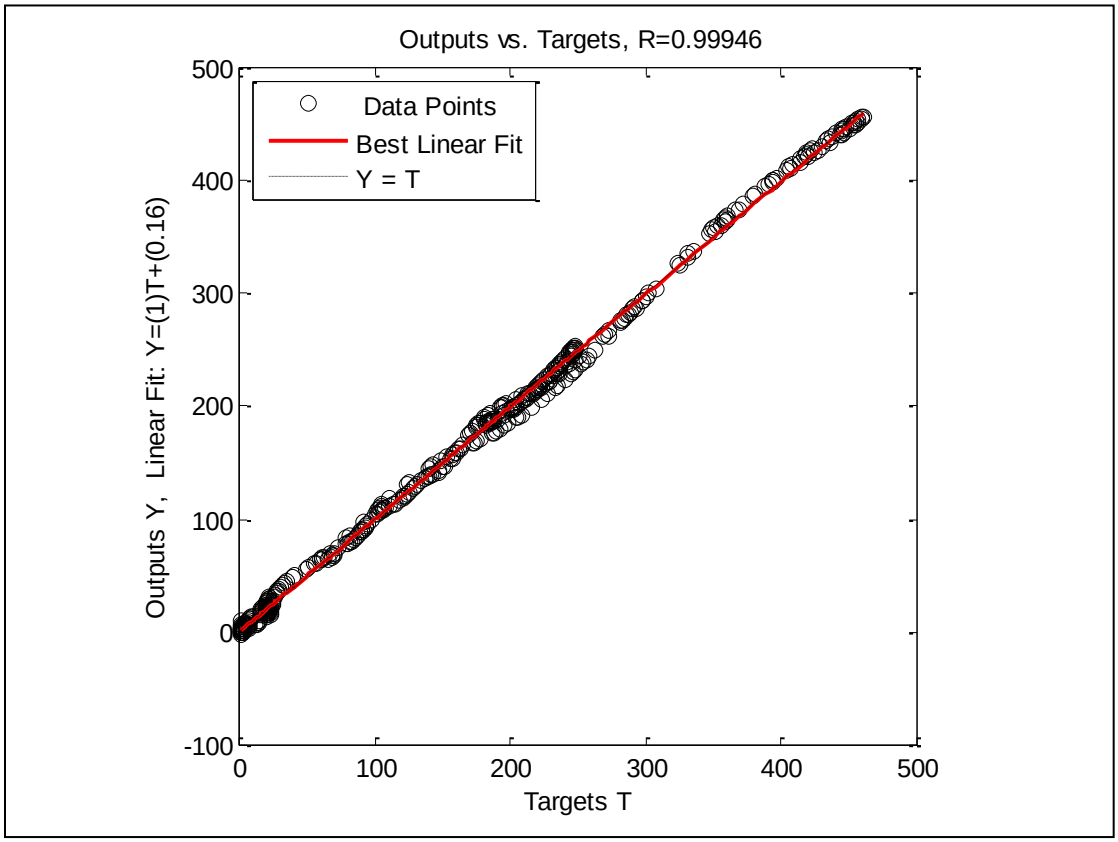

Figure A- 196: Well-10, Case -8, Crossplot

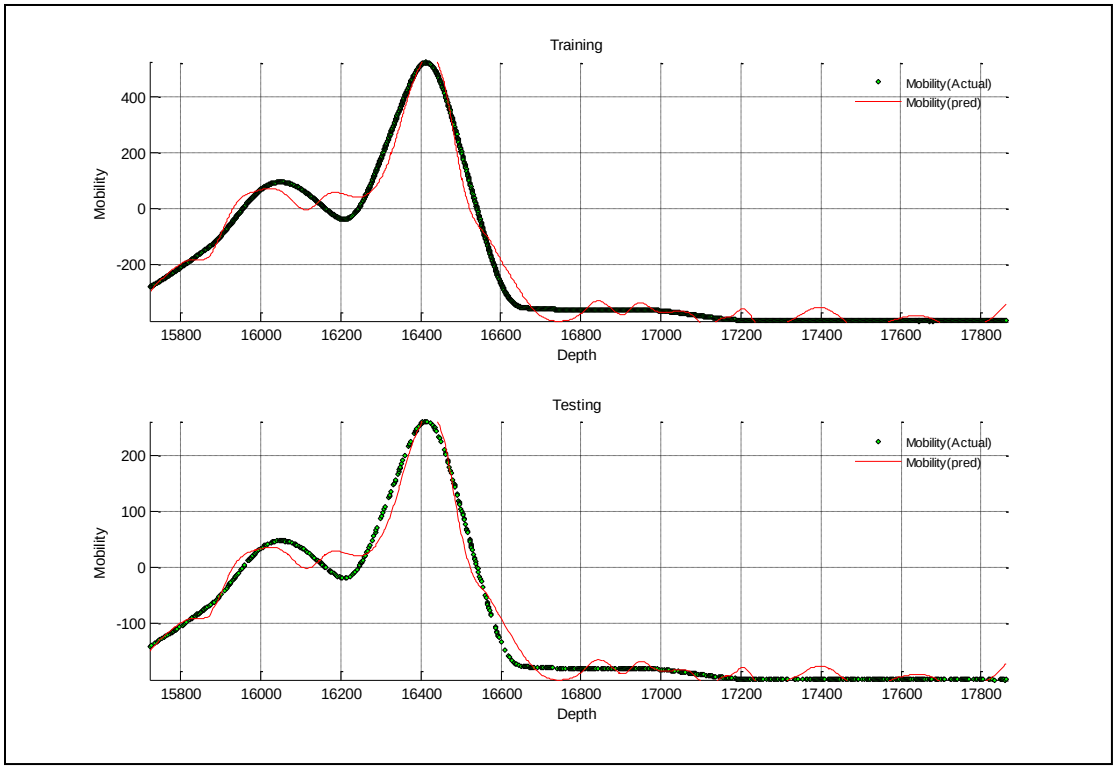

Figure A- 197: Well-10, Case -9

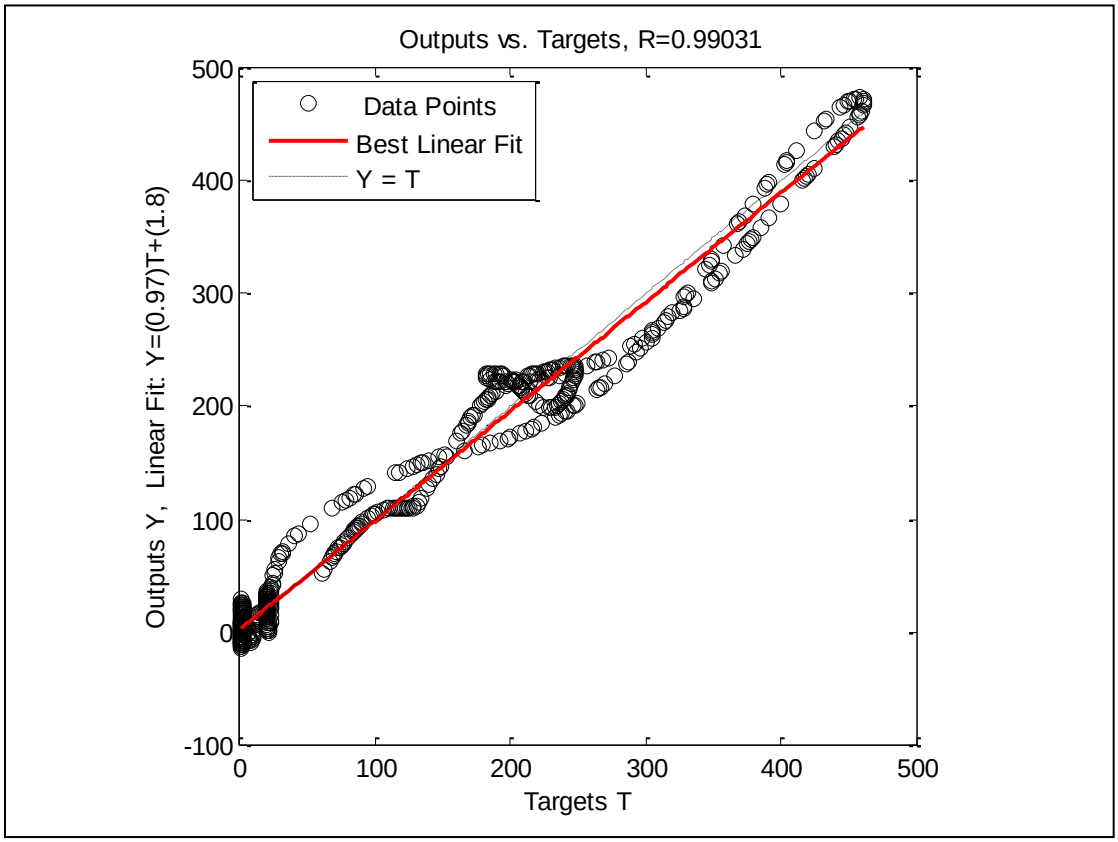

Figure A- 198: Well-10, Case -9, Crossplot

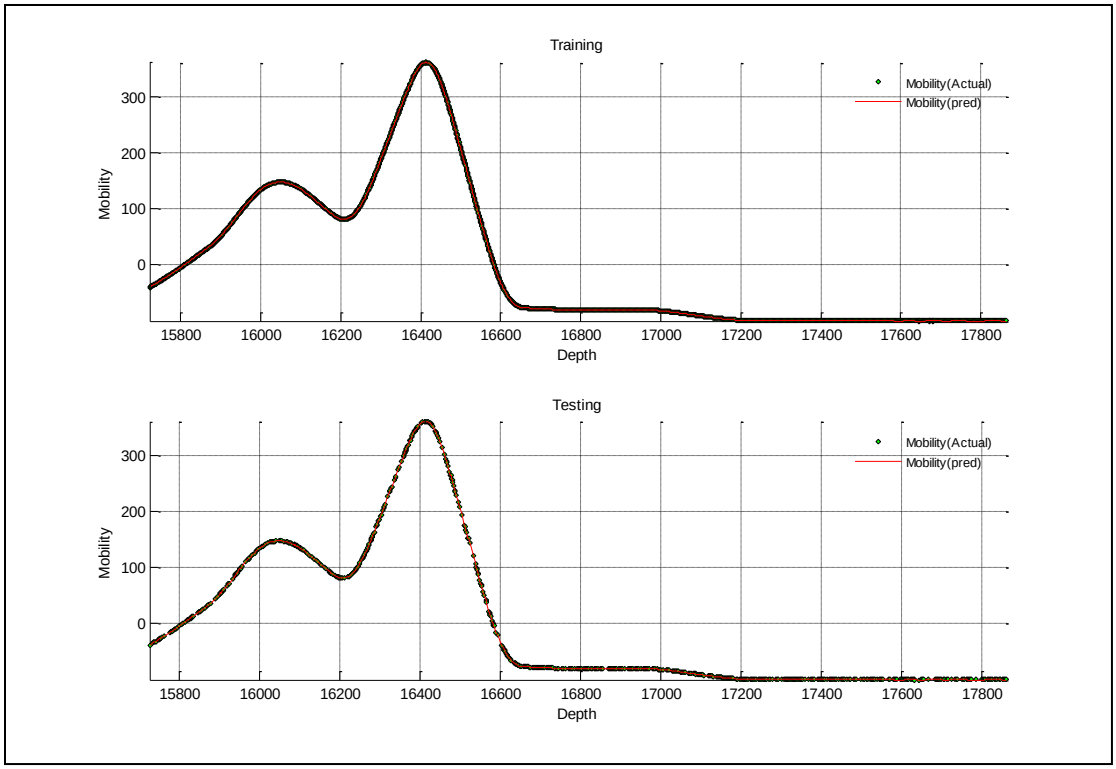

Figure A- 199: Well-10, Case -10

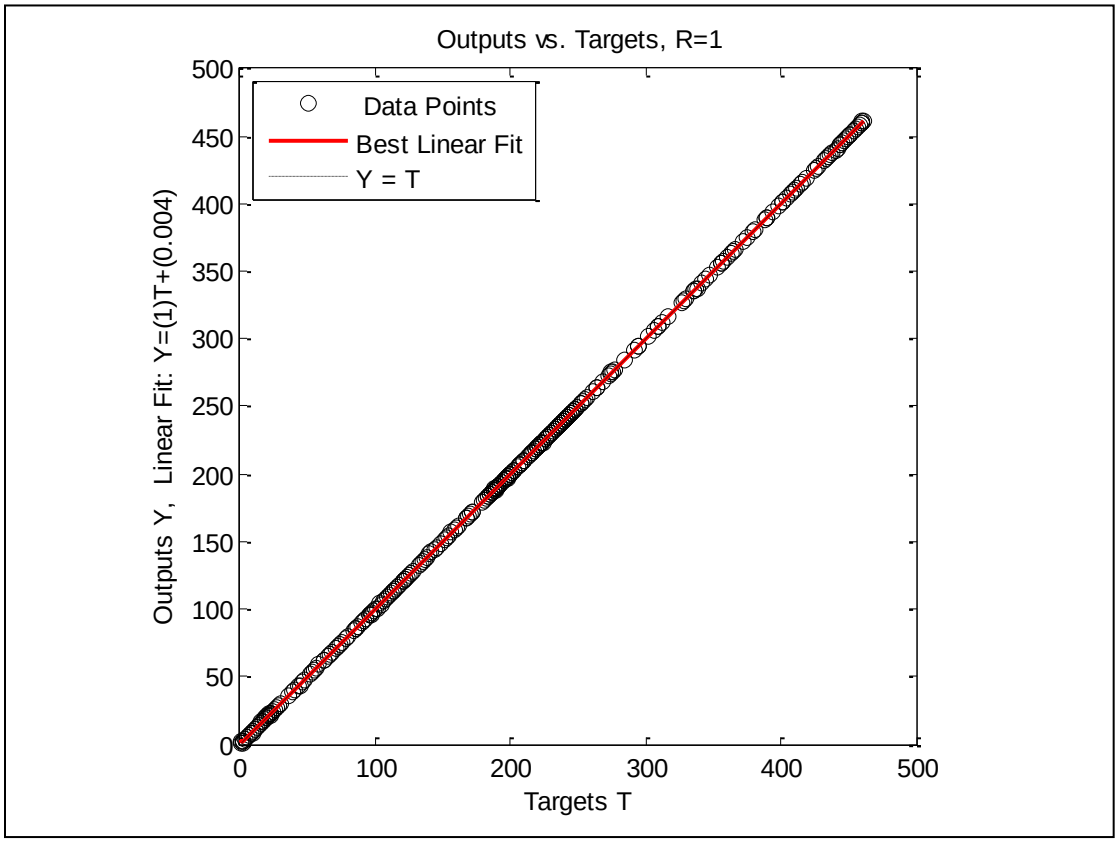

Figure A- 200: Well-10, Case -10, Crossplot

APPENDIX B

FUNCTIONAL NETWORK (FunNet) RESULTS SUMMARY

This appendix is showing all the FunNet results of graphical plots of the actual verses the predicted outputs of all the ten wells under different selection methods.

METHODS USED

Method-1	Functional Network Elimination Selection Method
Method-2	Functional Network Forward Selection Method
Method-3	Functional Network B-ackward Elimination Method
Method-4	Functional Network Forward B-ackward Selection Method
Method-5	Functional Network B-ackward Forward Selection Method

TYPES USED

Type-1	Linear
Type-2	Non-Linear of the 1st order

RESULTS

Well No. 1

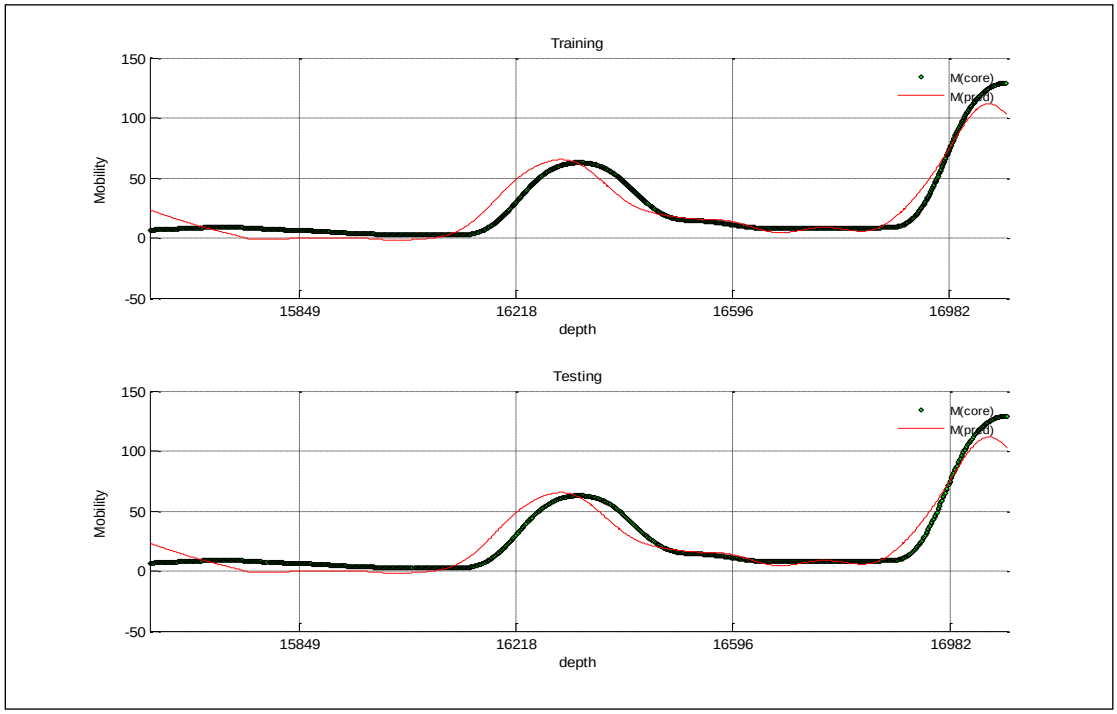

Figure B- 1: Well-1 Method-1, Type-1

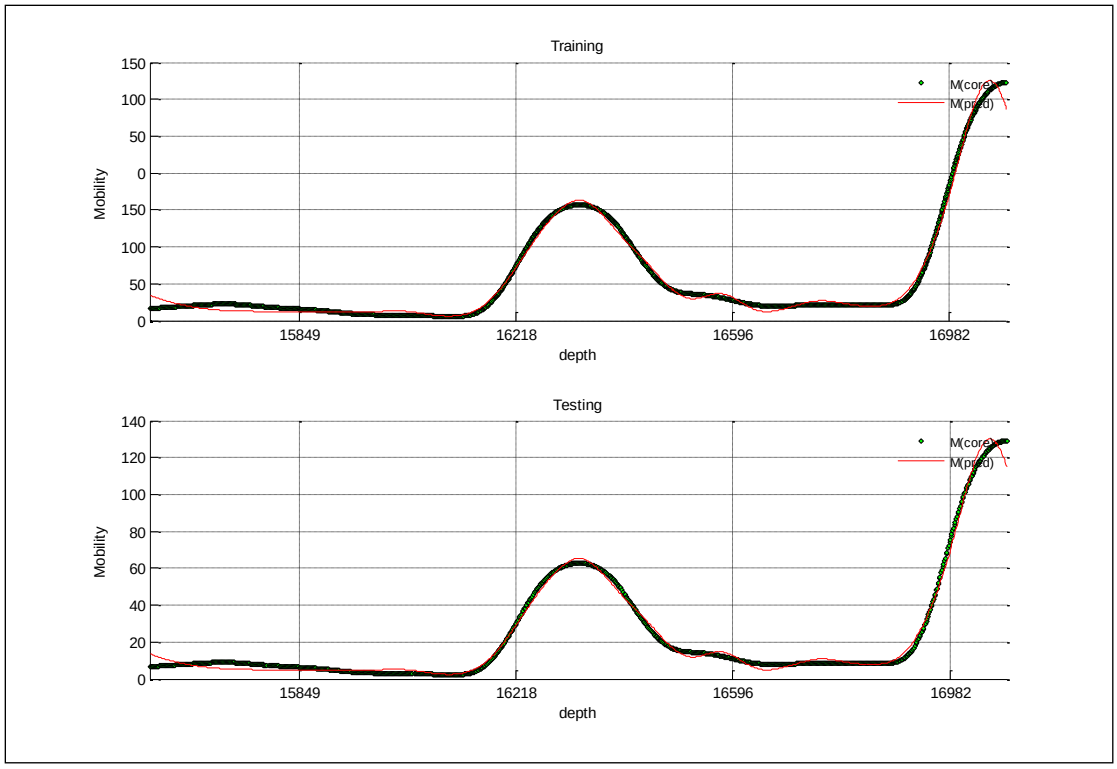

Figure B- 2: Well-1 Method-1, Type-2

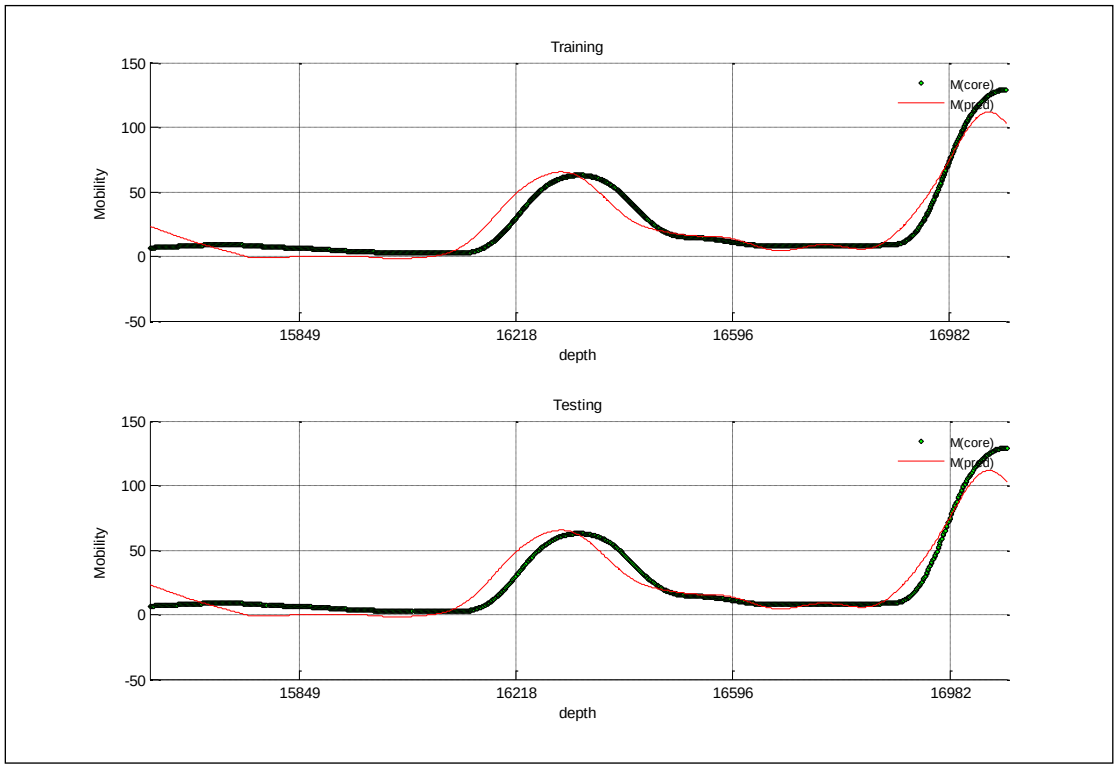

Figure B- 3: Well-1 Method-2, Type-1

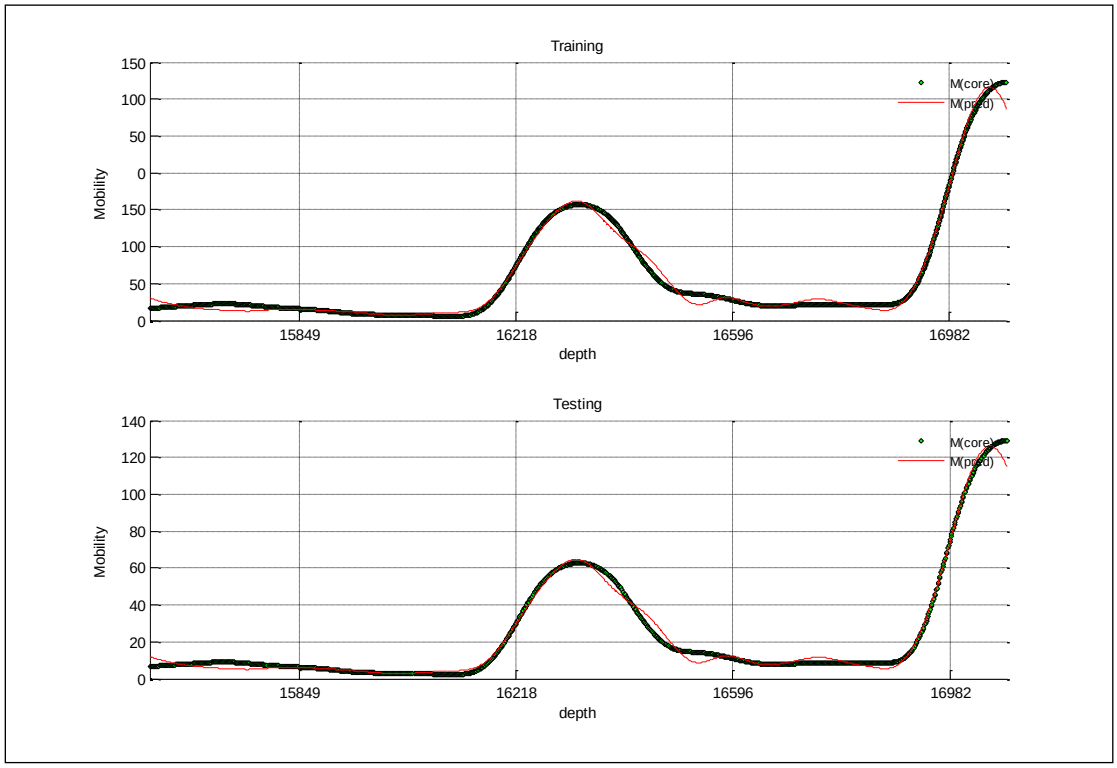

Figure B- 4: Well-1 Method-2, Type-2

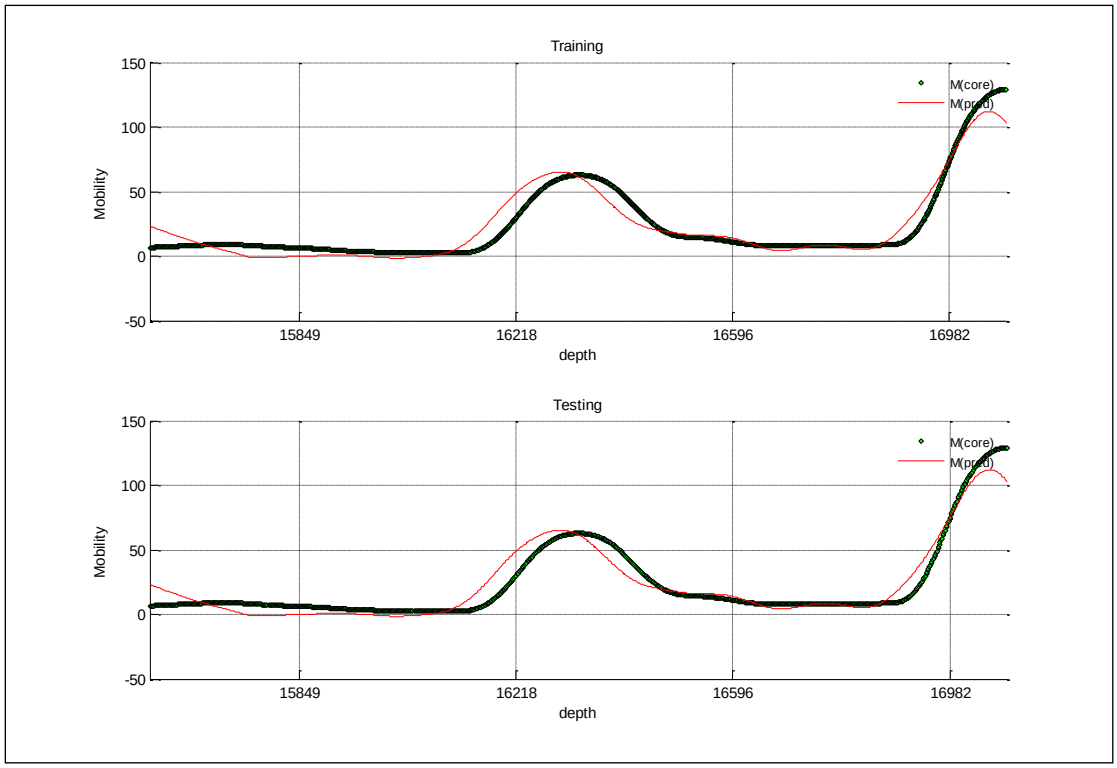

Figure B- 5: Well-1 Method-3, Type-1

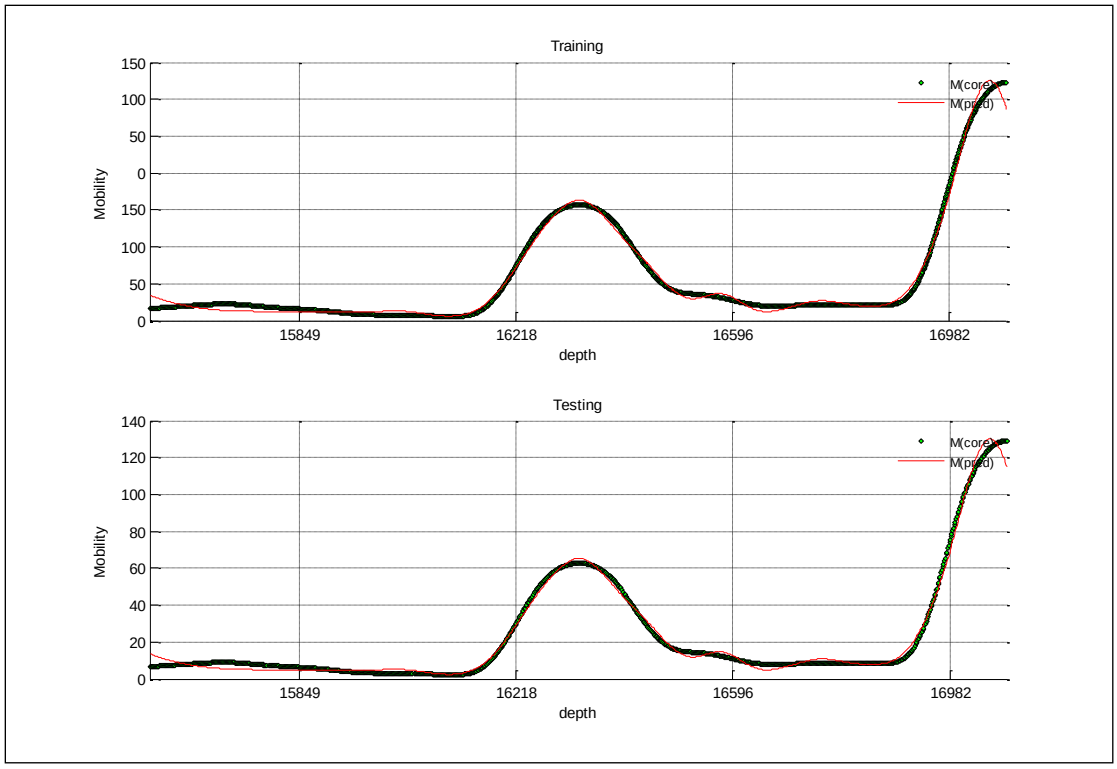

Figure B- 6: Well-1 Method-3, Type-2

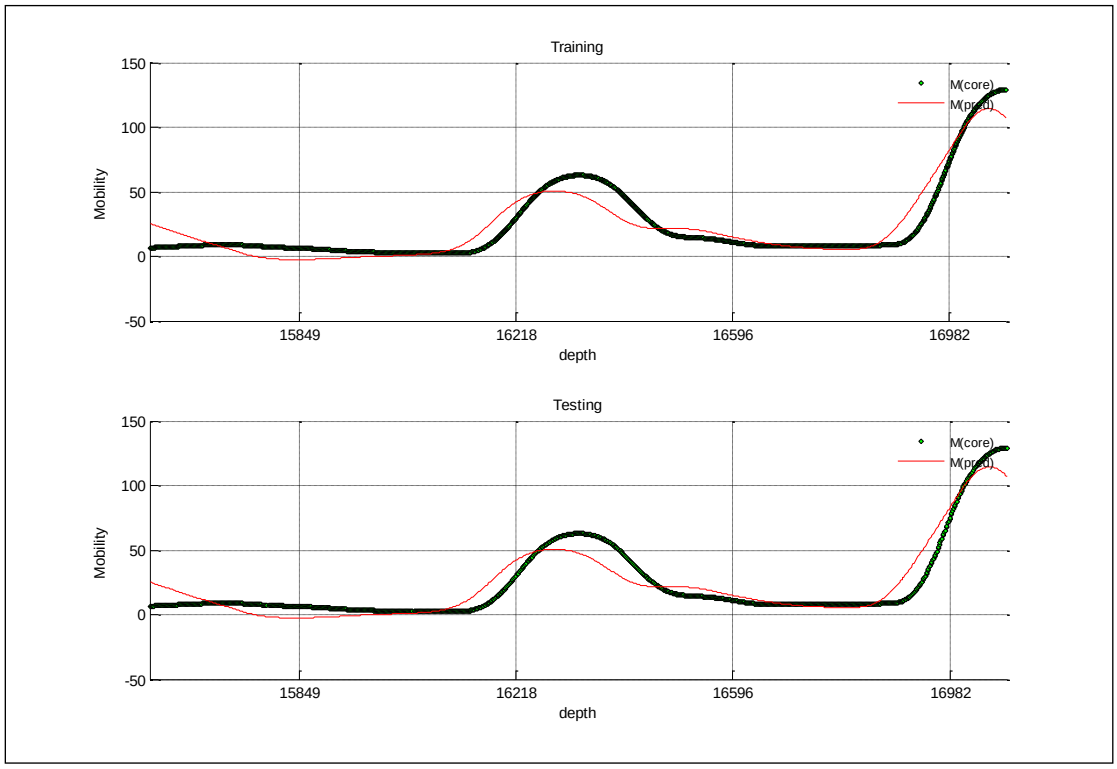

Figure B- 7: Well-1 Method-4, Type-1

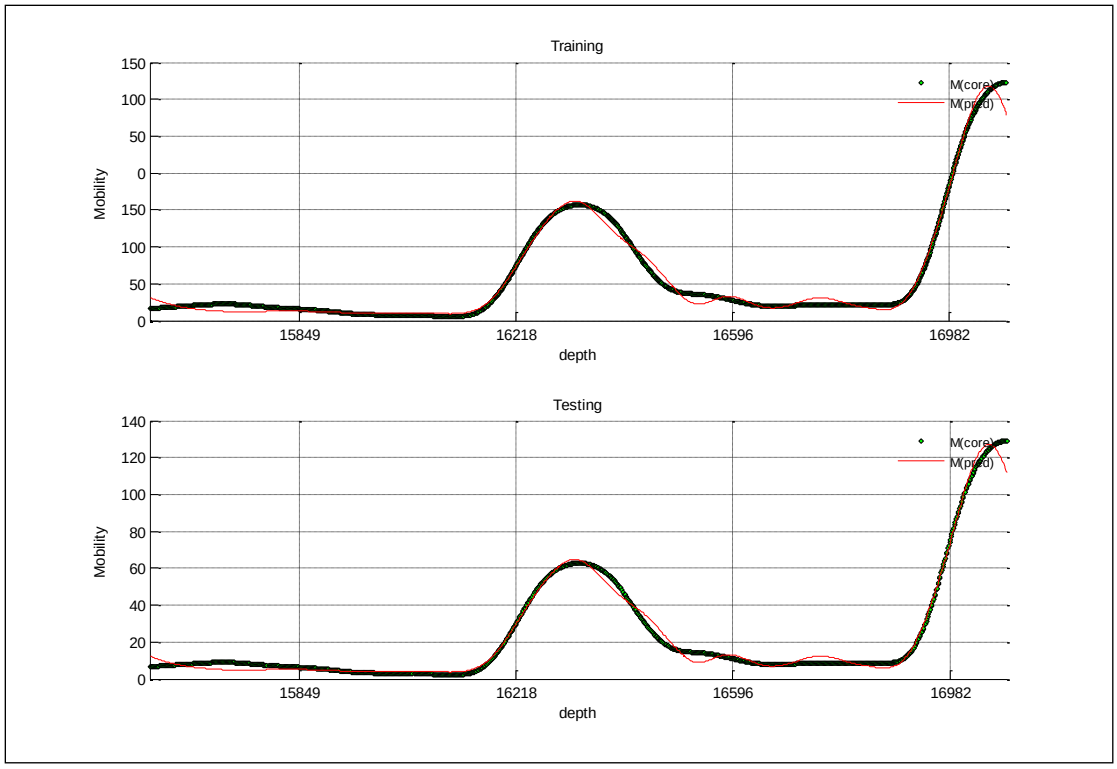

Figure B- 8: Well-1 Method-4, Type-2

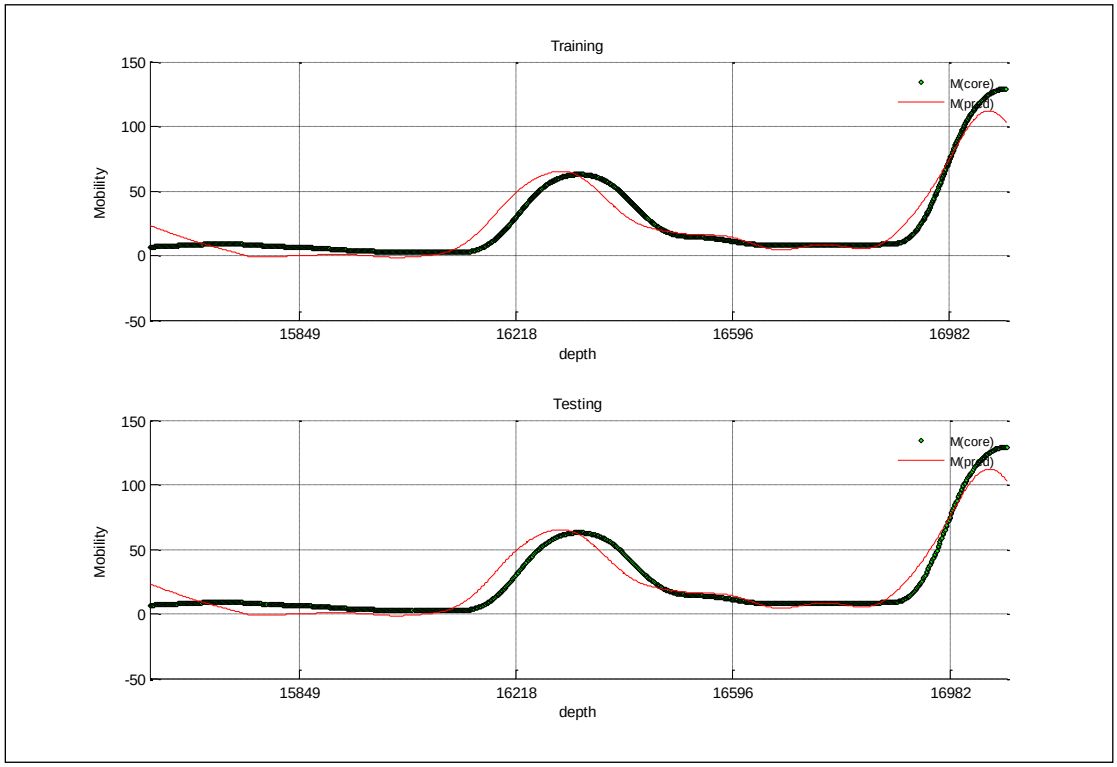

Figure B- 9: Well-1 Method-5, Type-1

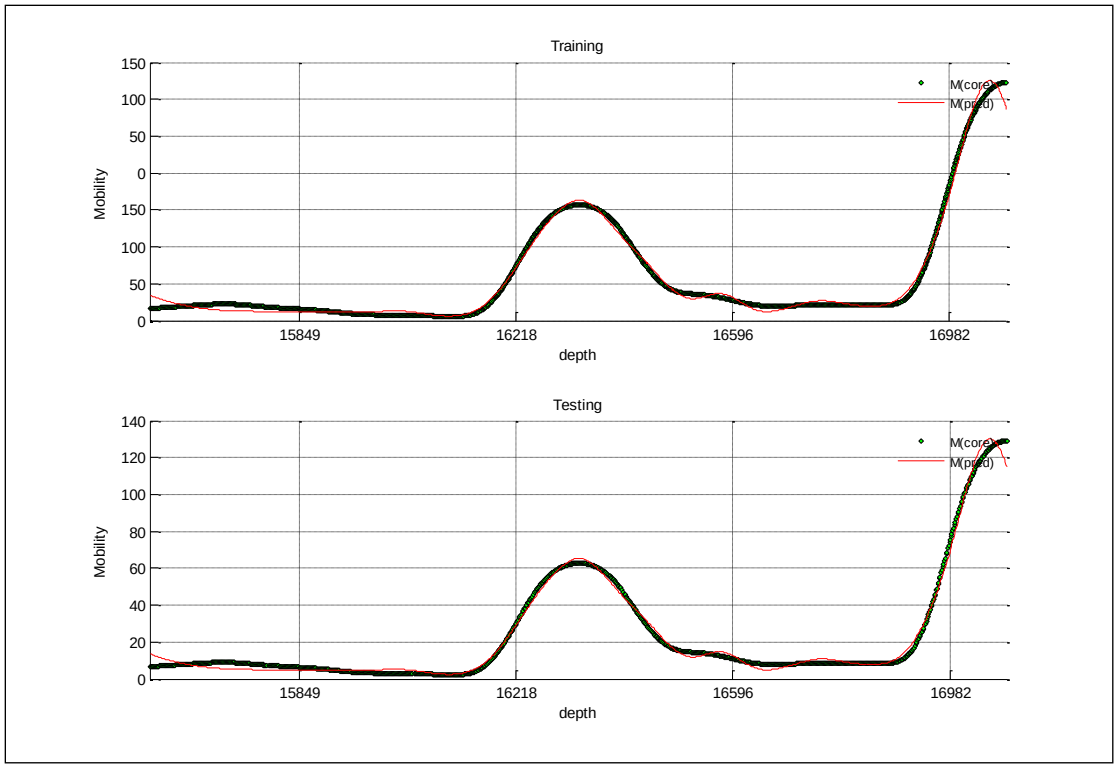

Figure B- 10: Well-1 Method-5, Type-2

Well No. 2

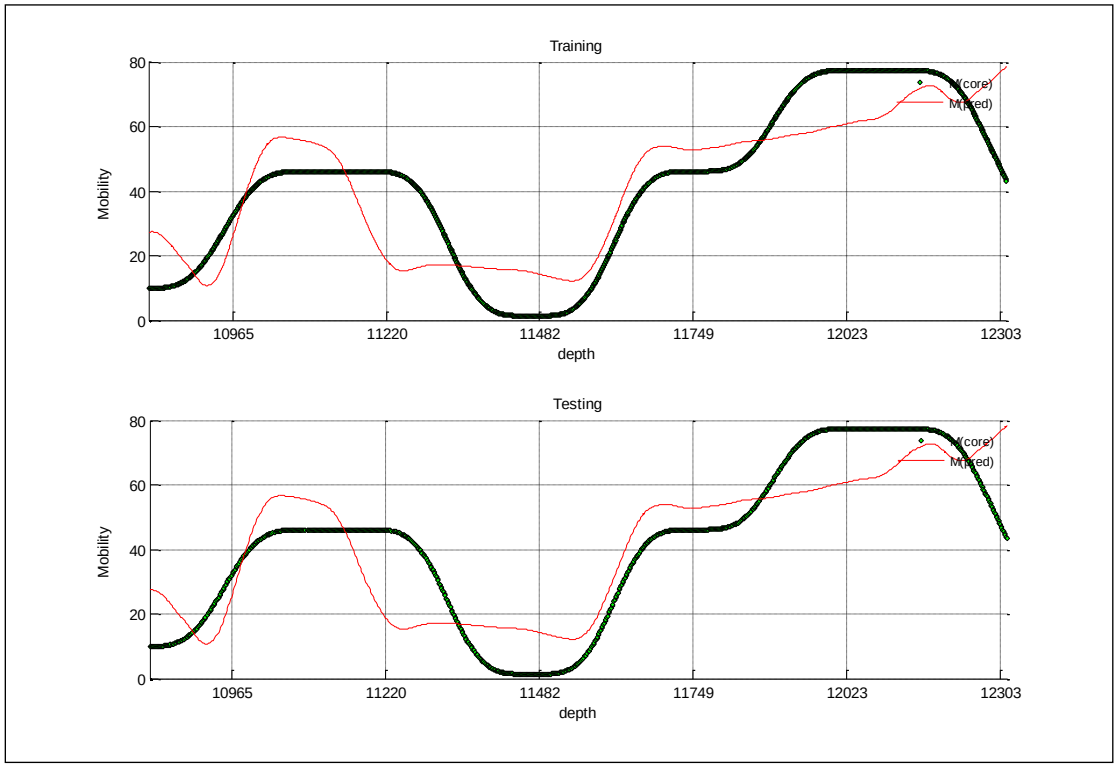

Figure B- 11: Well-2 Method-1, Type-1

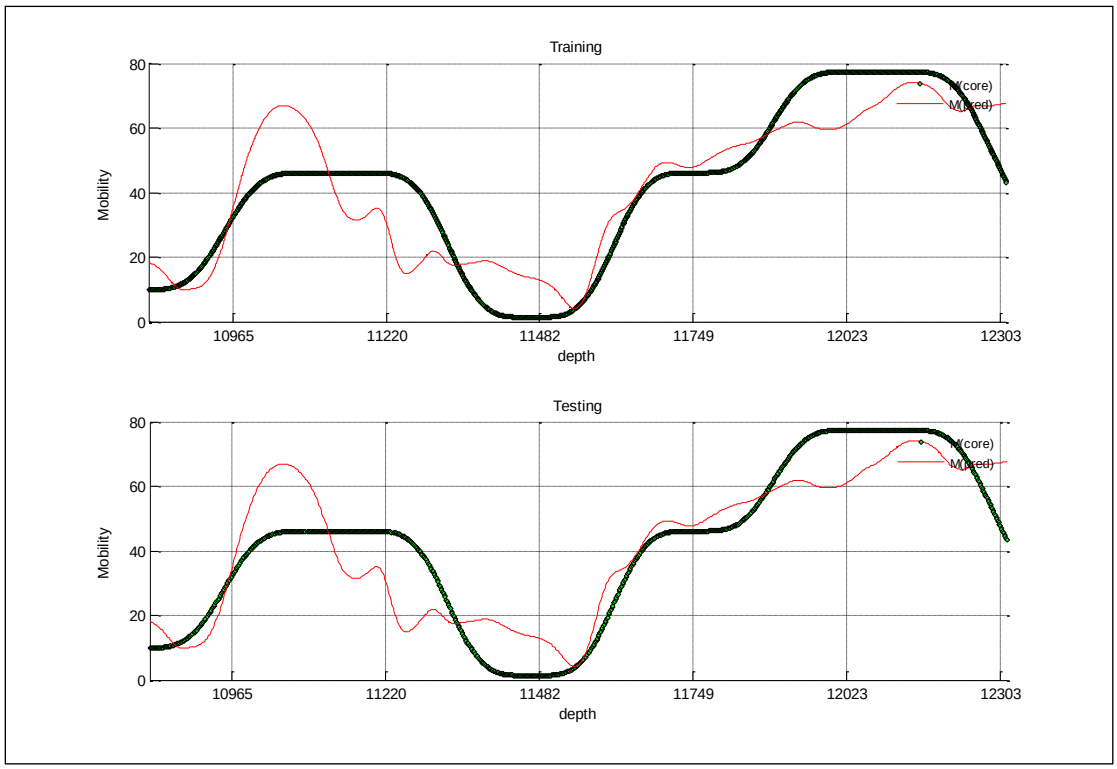

Figure B- 12: Well-2 Method-1, Type-2

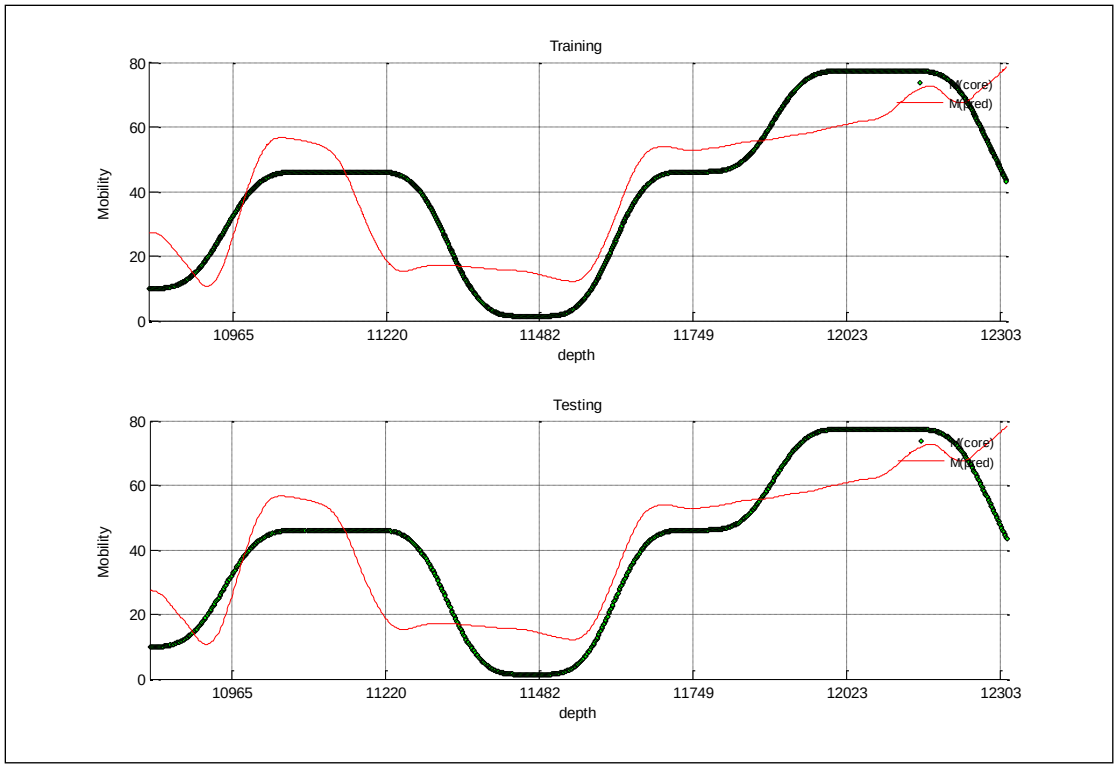

Figure B- 13: Well-2 Method-2, Type-1

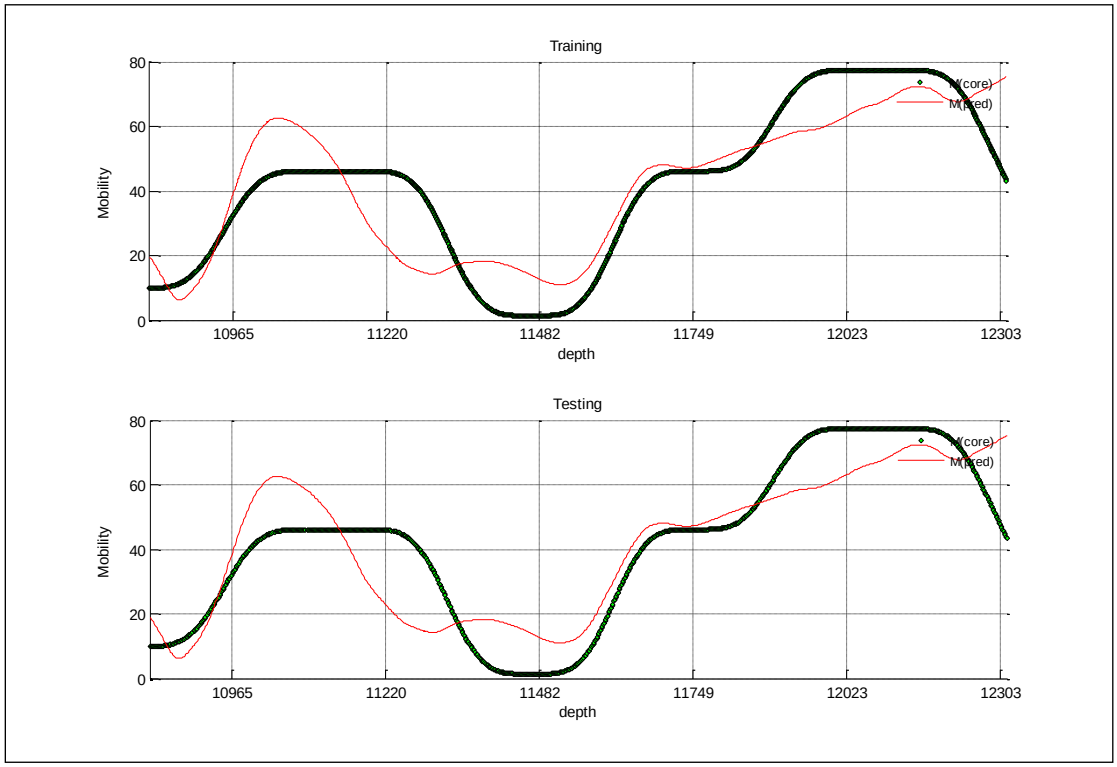

Figure B- 14: Well-2 Method-2, Type-2

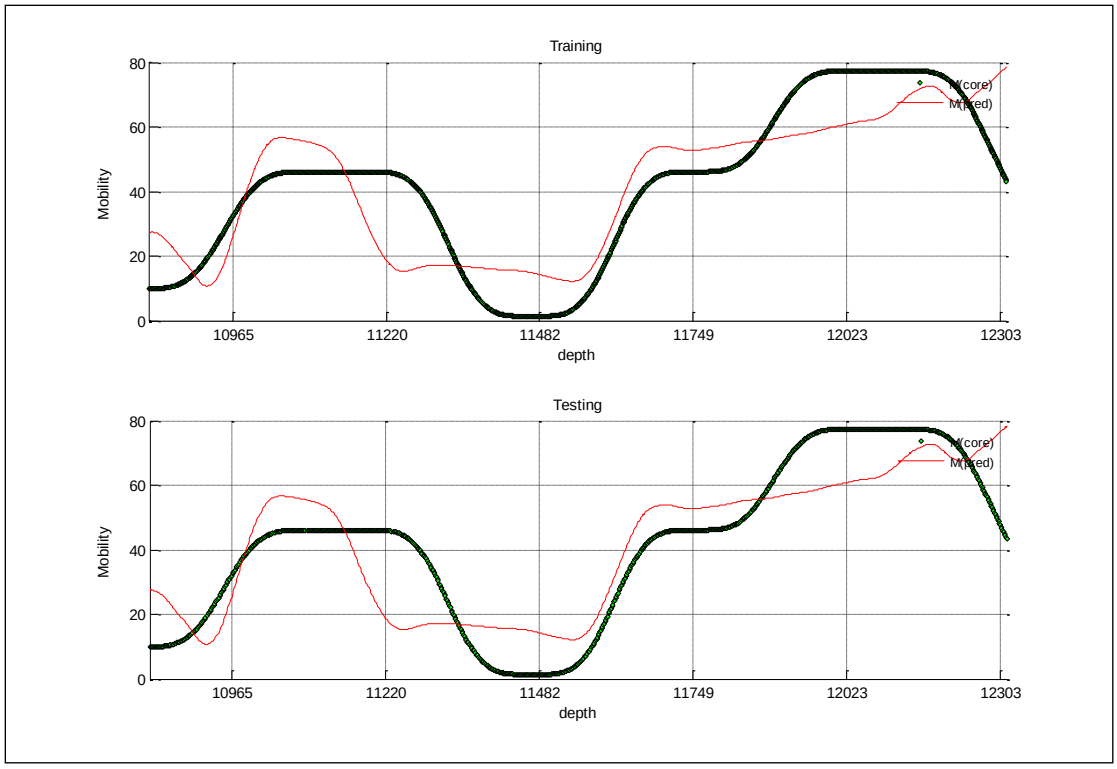

Figure B- 15: Well-2 Method-3, Type-1

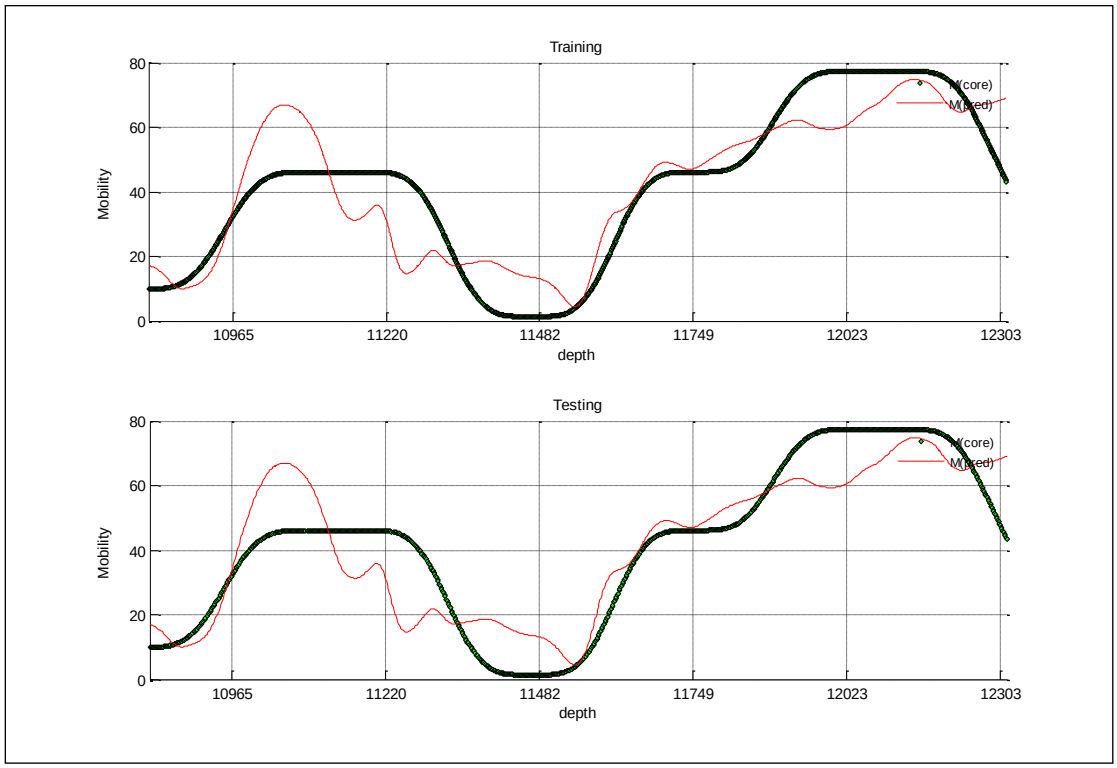

Figure B- 16: Well-2 Method-3, Type-2

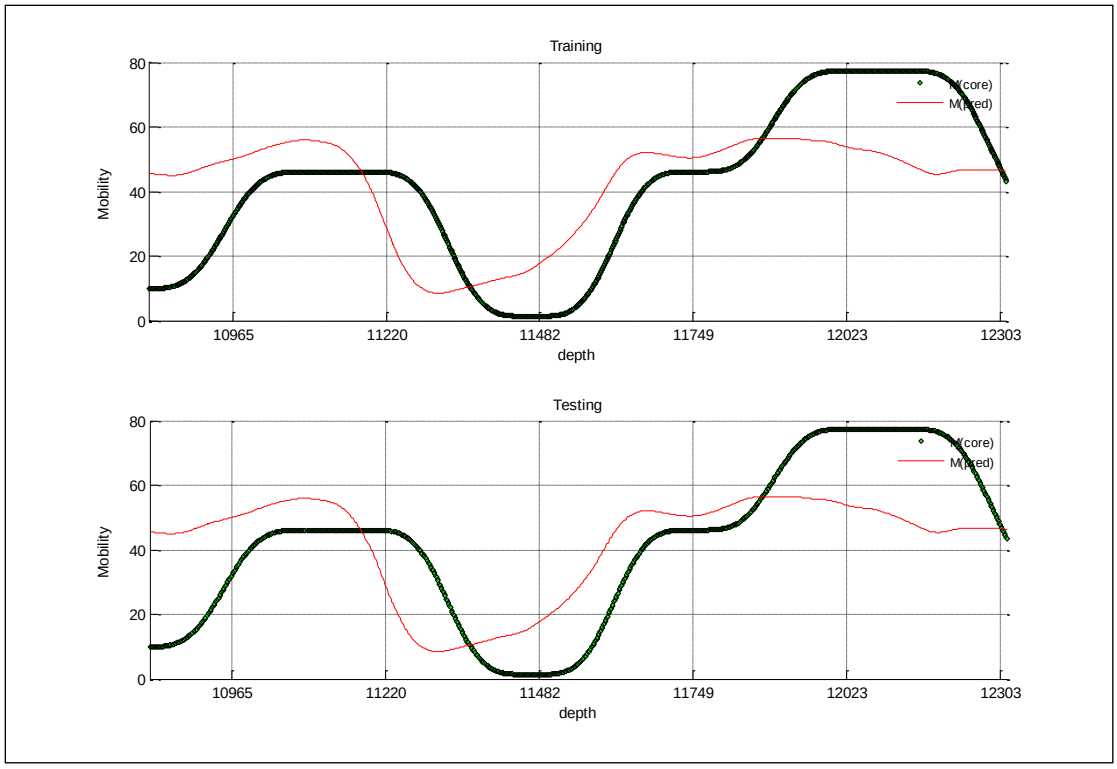

Figure B- 17: Well-2 Method-4, Type-1

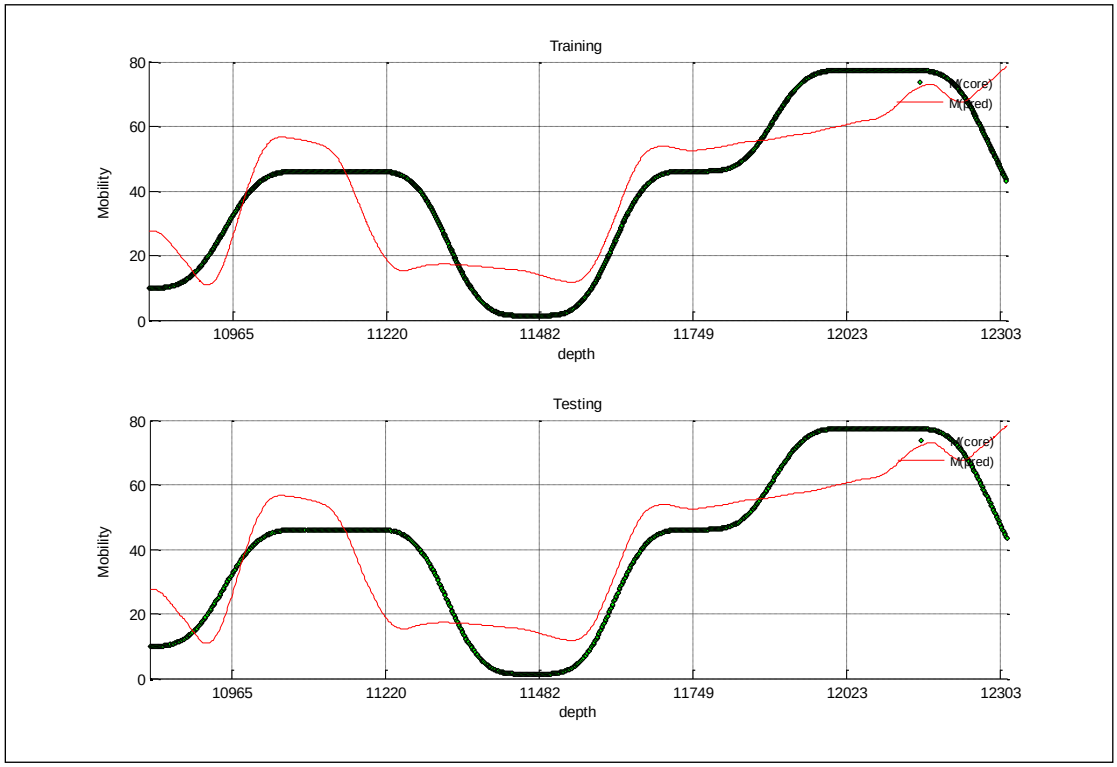

Figure B- 18: Well-2 Method-4, Type-2

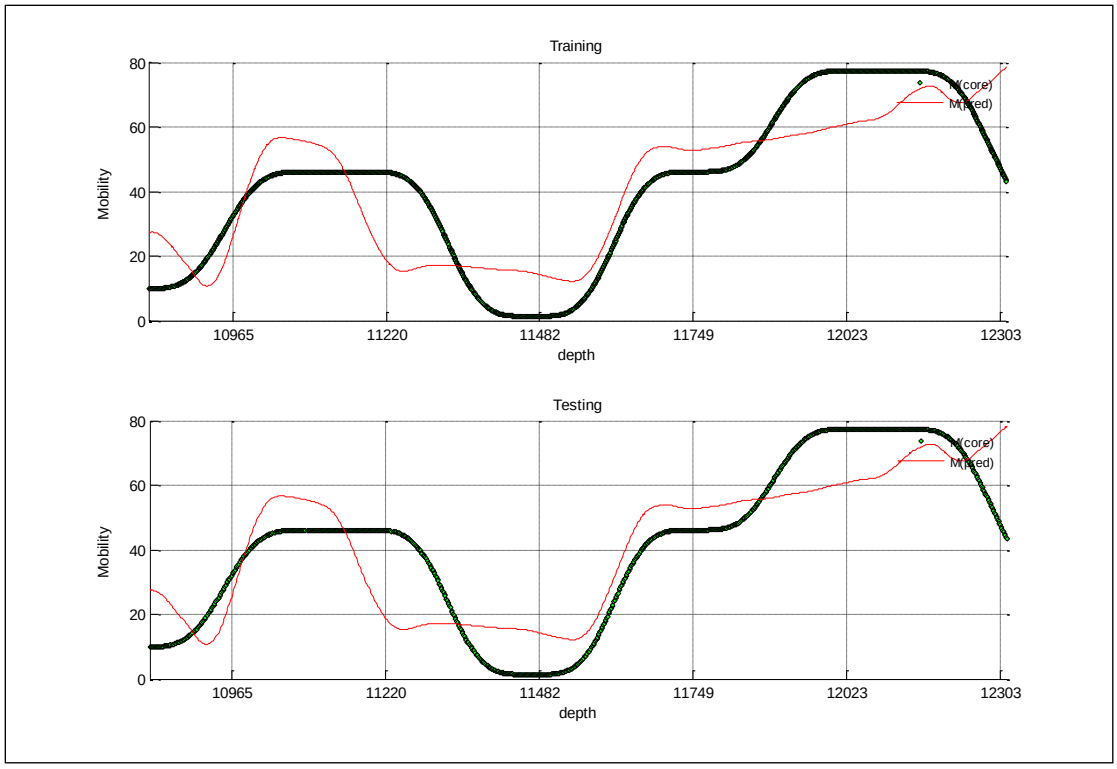

Figure B- 19: Well-2 Method-5, Type-1

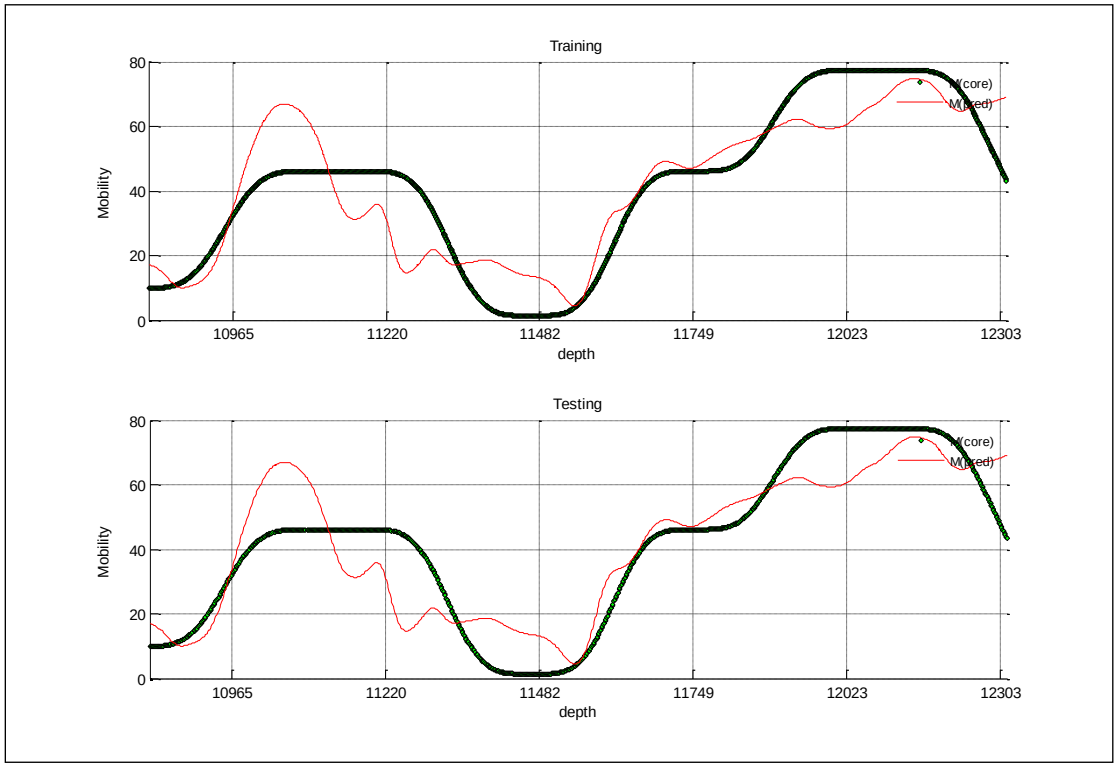

Figure B- 20: Well-2 Method-5, Type-2

Well No. 3

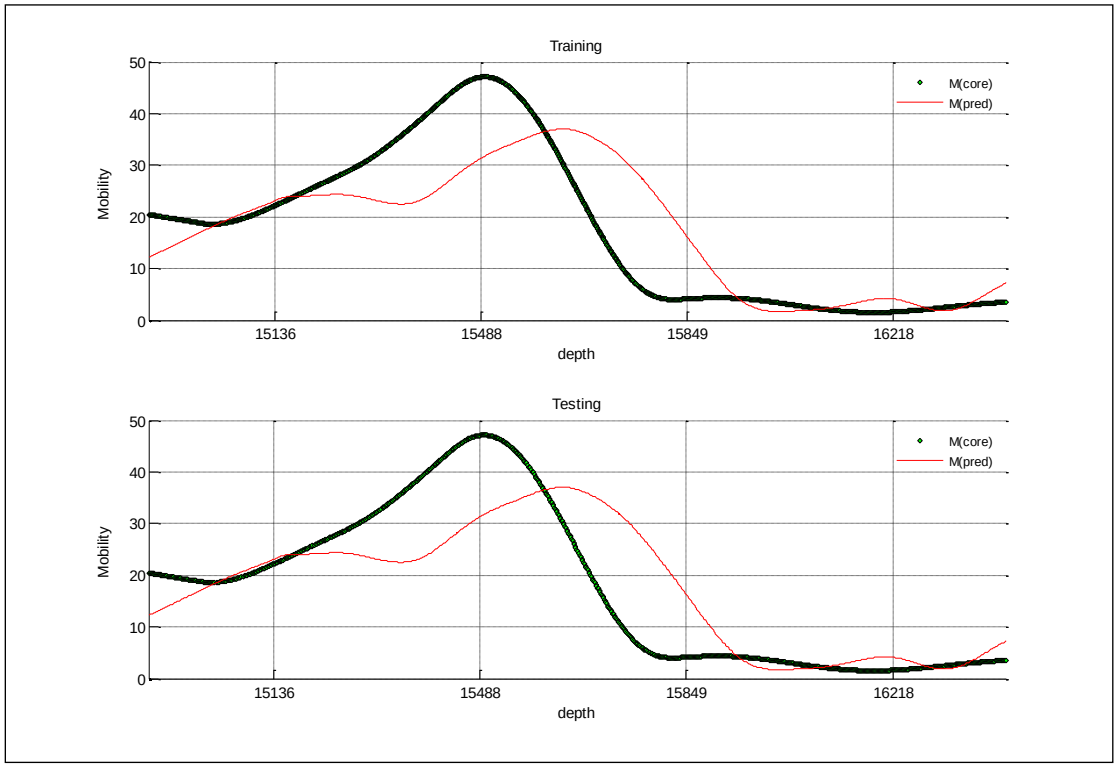

Figure B- 21: Well-3 Method-1, Type-1

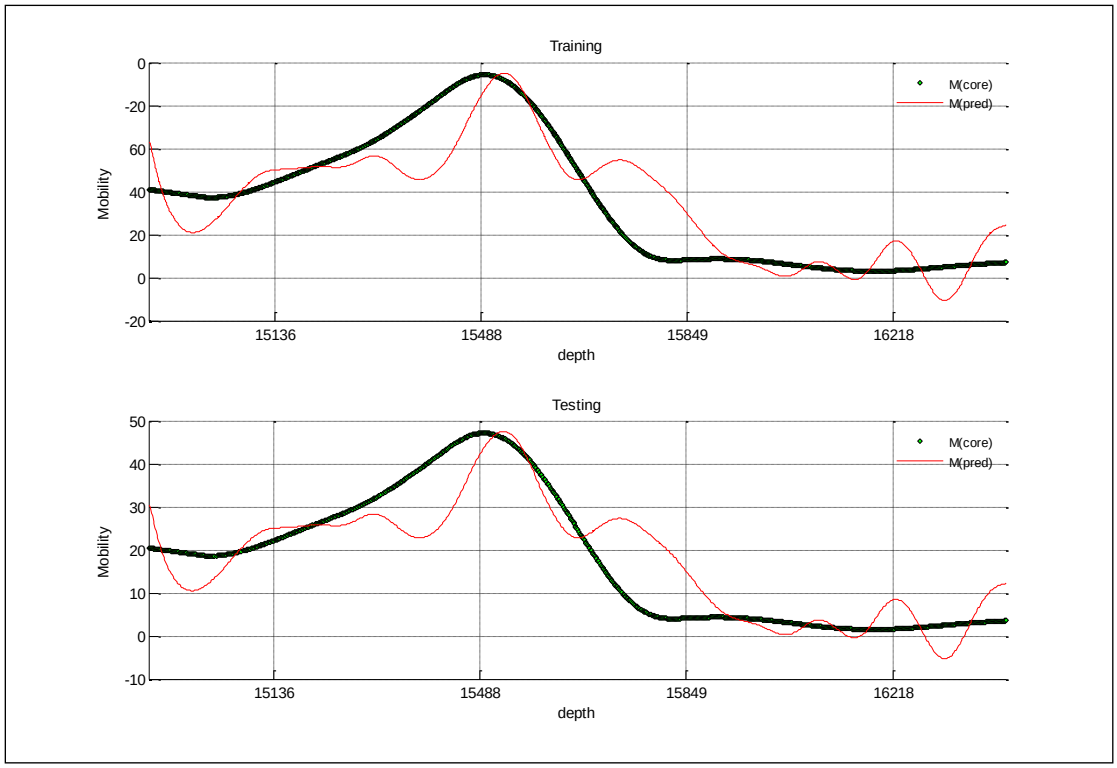

Figure B- 22: Well-3 Method-1, Type-2

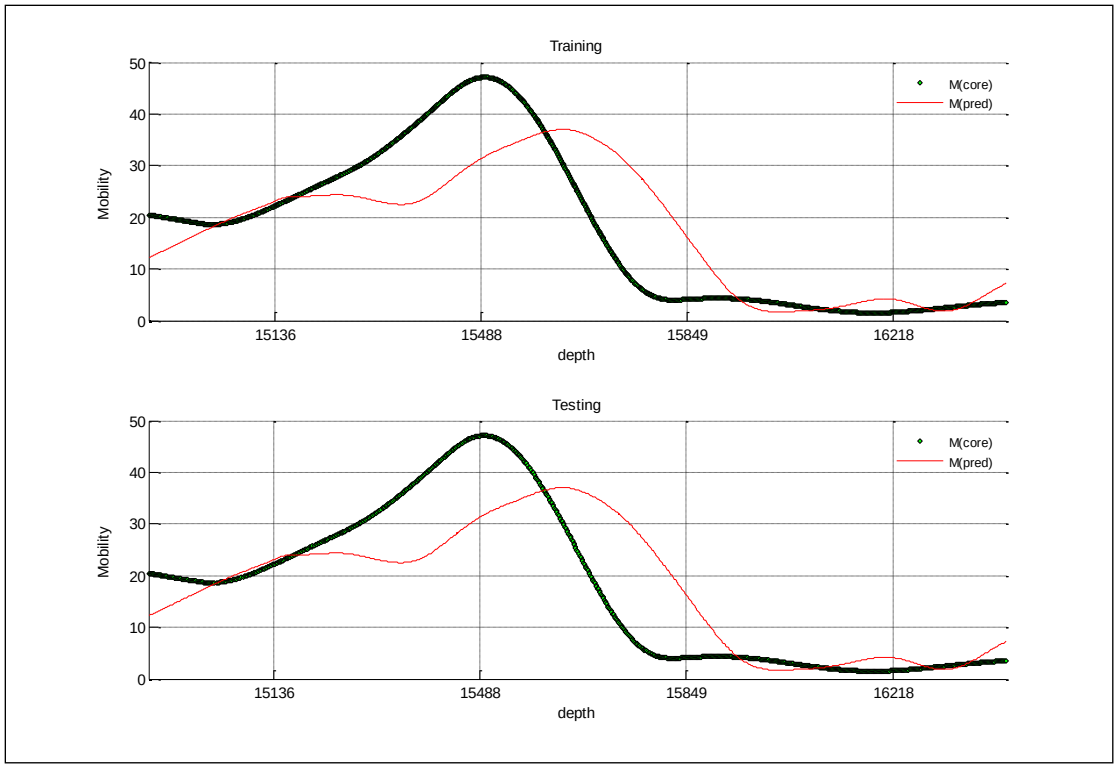

Figure B- 23: Well-3 Method-2, Type-1

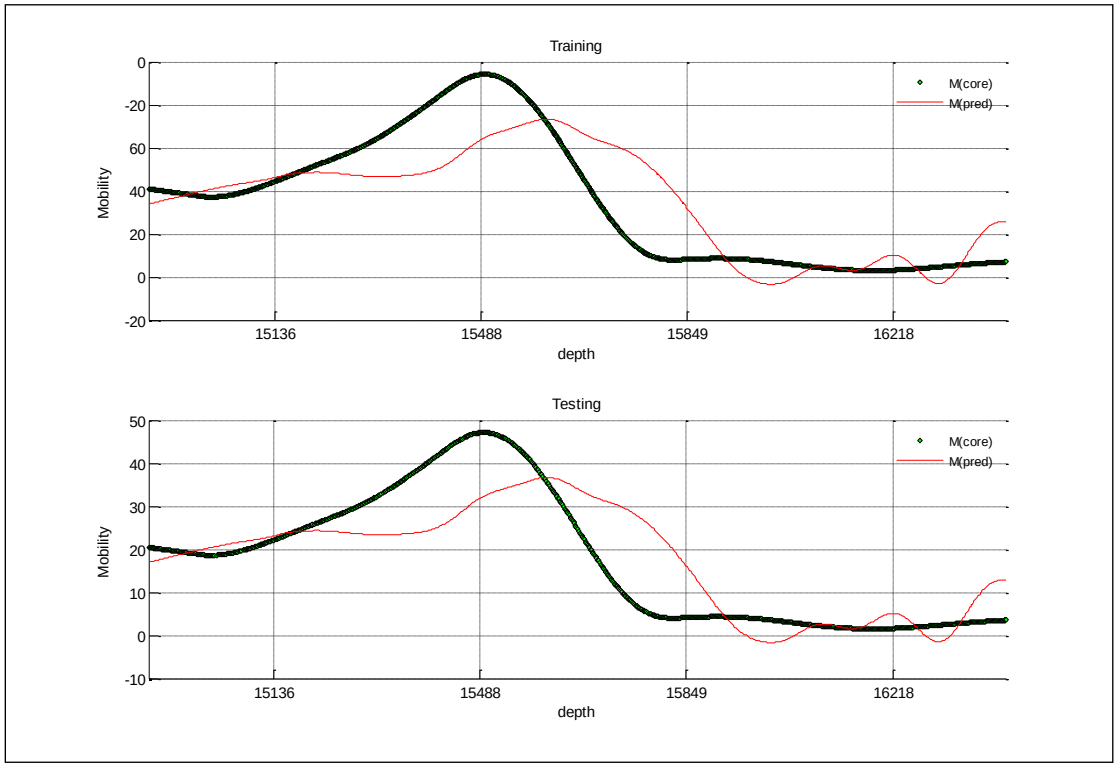

Figure B- 24: Well-3 Method-2, Type-2

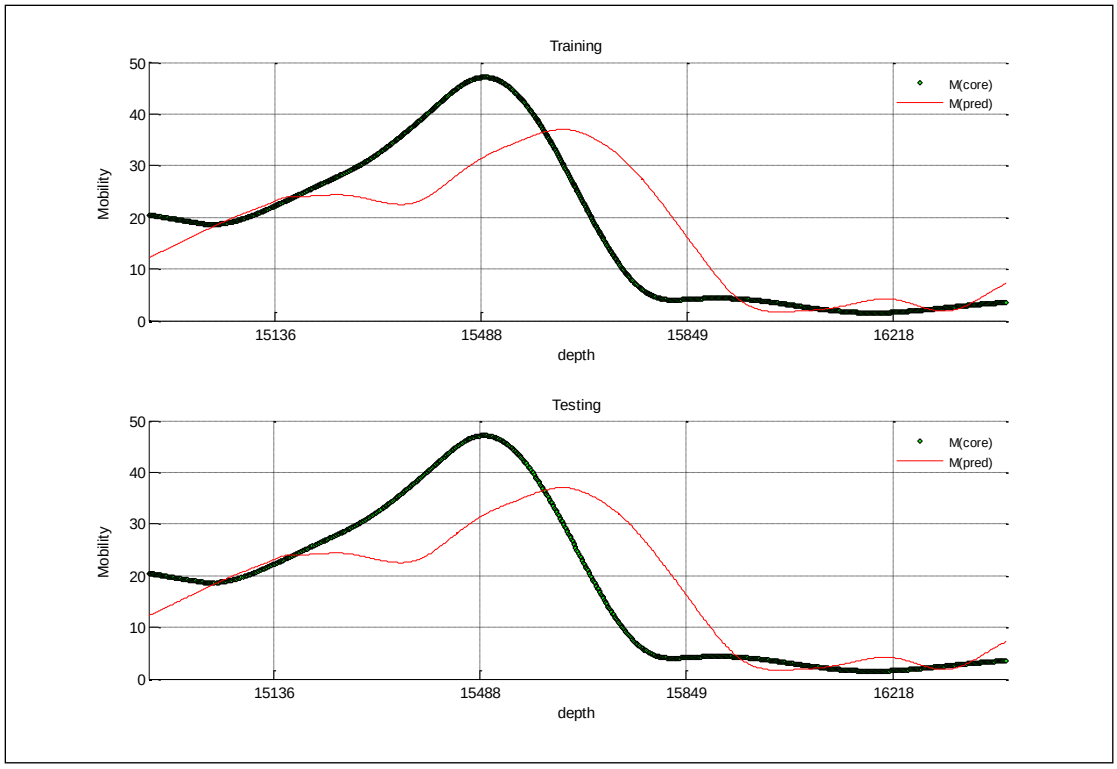

Figure B- 25: Well-3 Method-3, Type-1

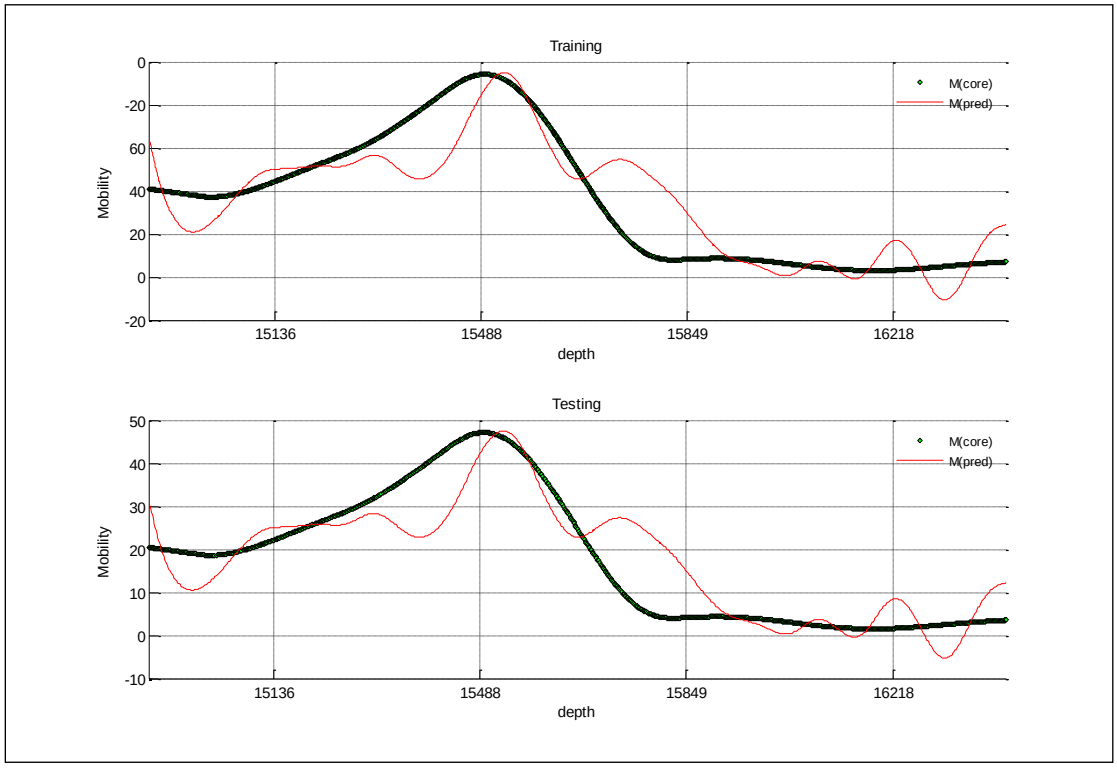

Figure B- 26: Well-3 Method-3, Type-2

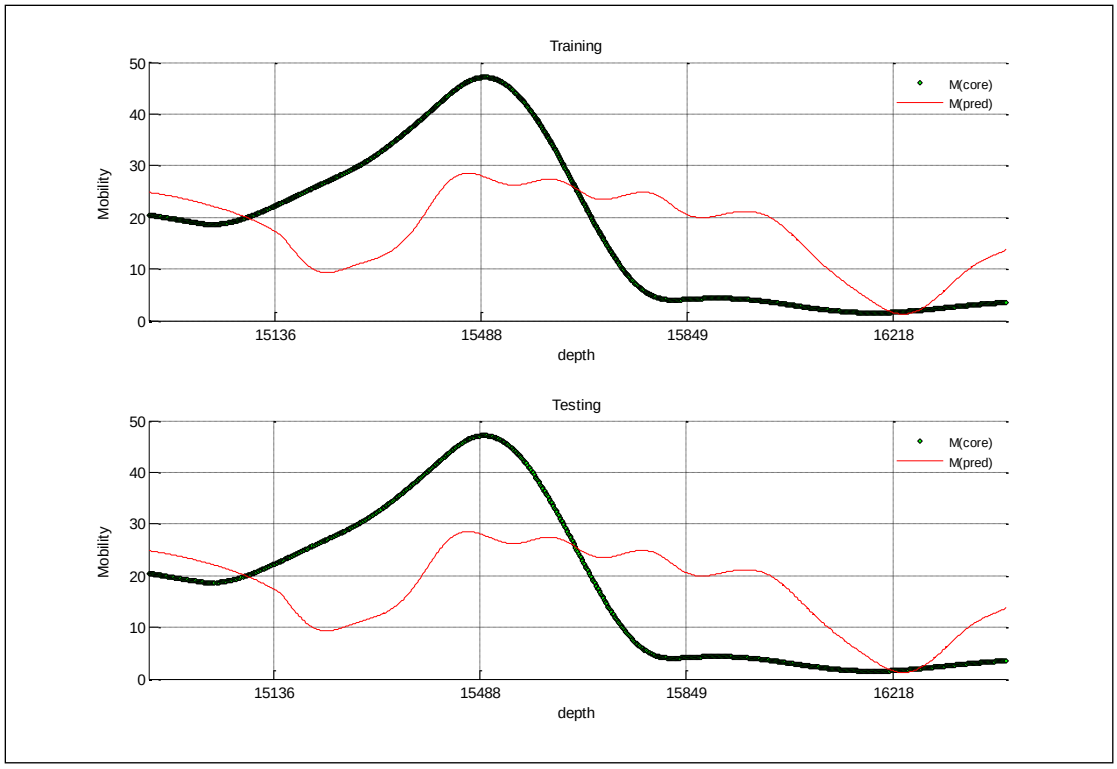

Figure B- 27: Well-3 Method-4, Type-1

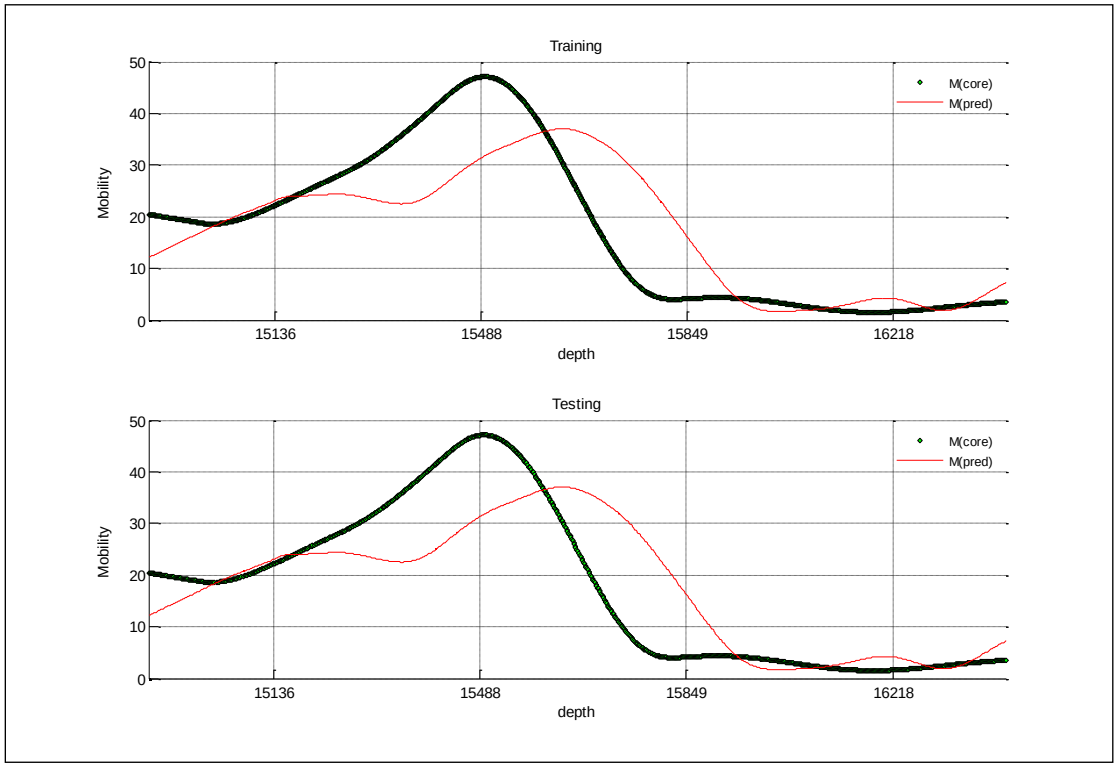

Figure B- 28: Well-3 Method-4, Type-2

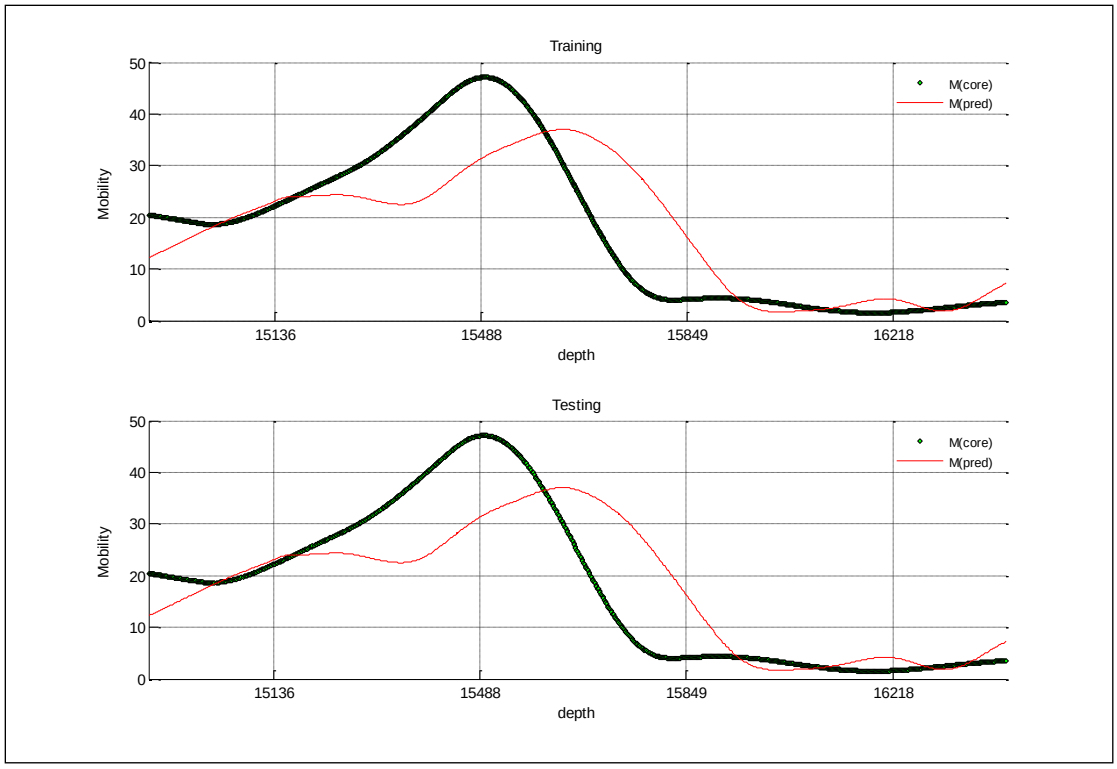

Figure B- 29: Well-3 Method-5, Type-1

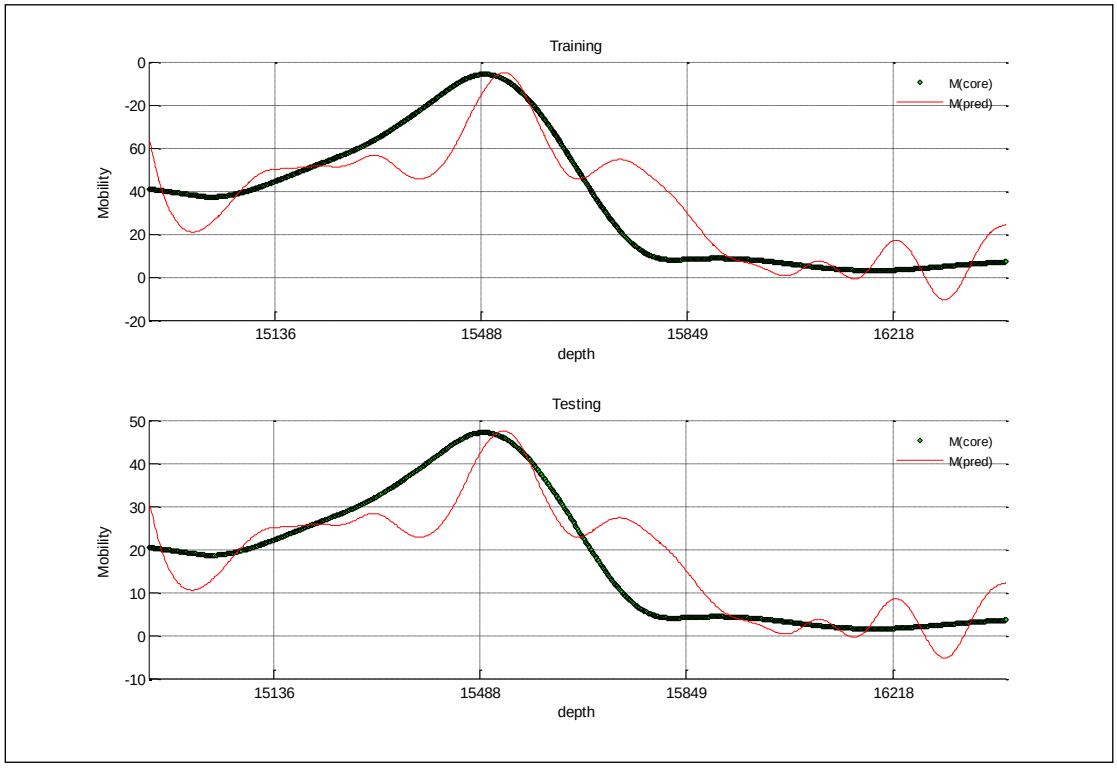

Figure B- 30: Well-3 Method-5, Type-2

Well No. 4

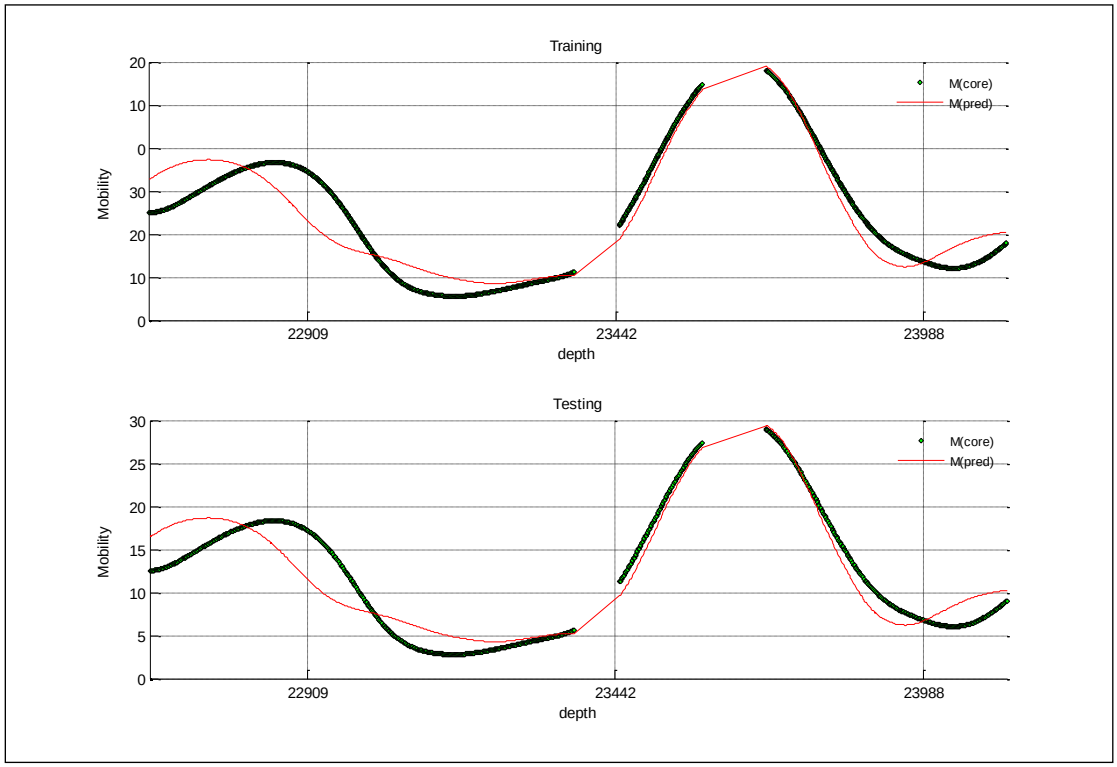

Figure B- 31: Well-4 Method-1, Type-1

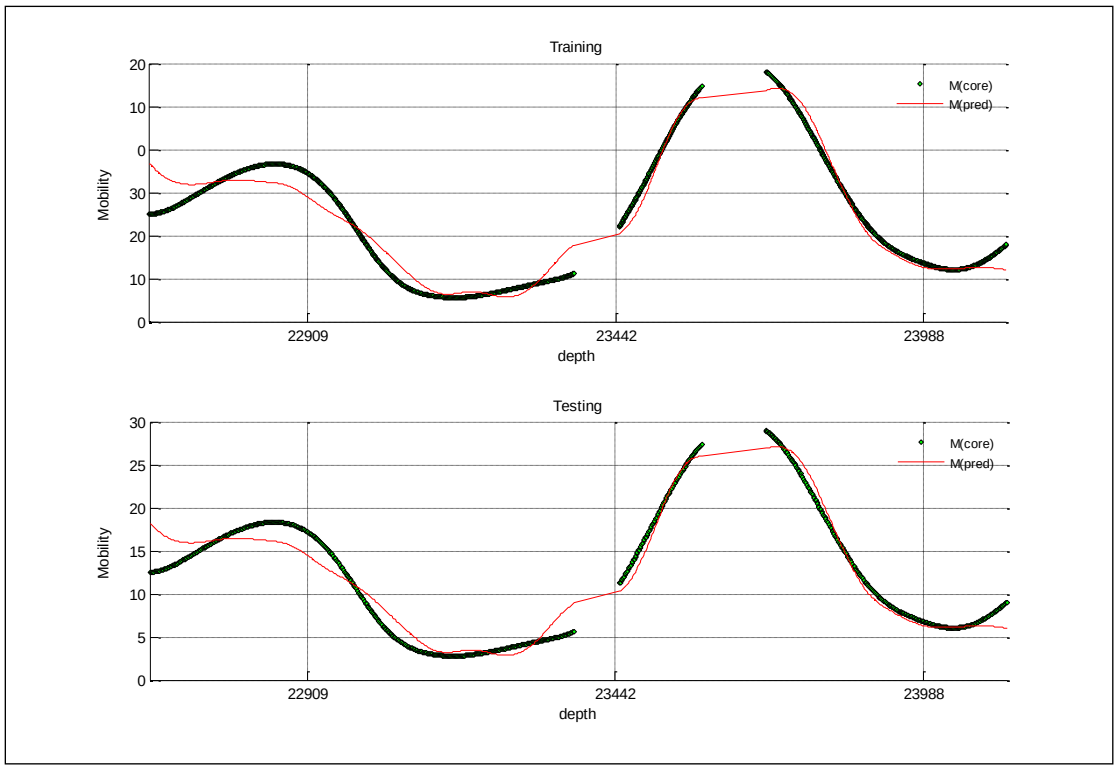

Figure B- 32: Well-4 Method-1, Type-2

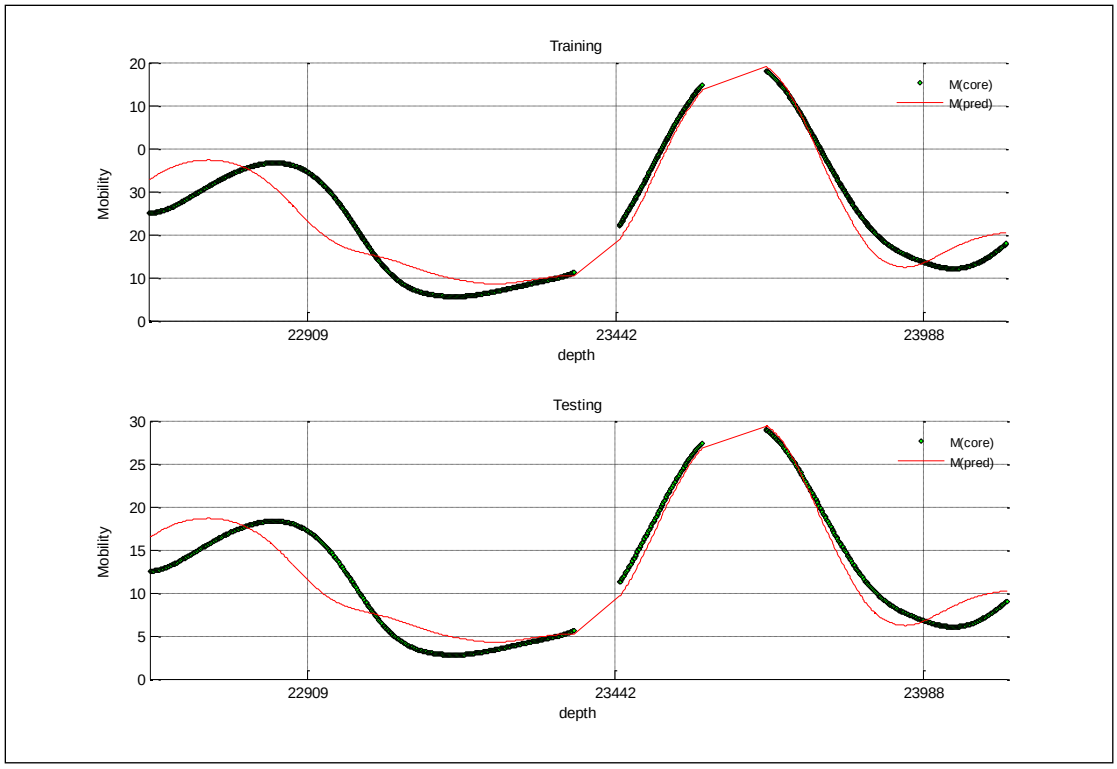

Figure B- 33: Well-4 Method-2, Type-1

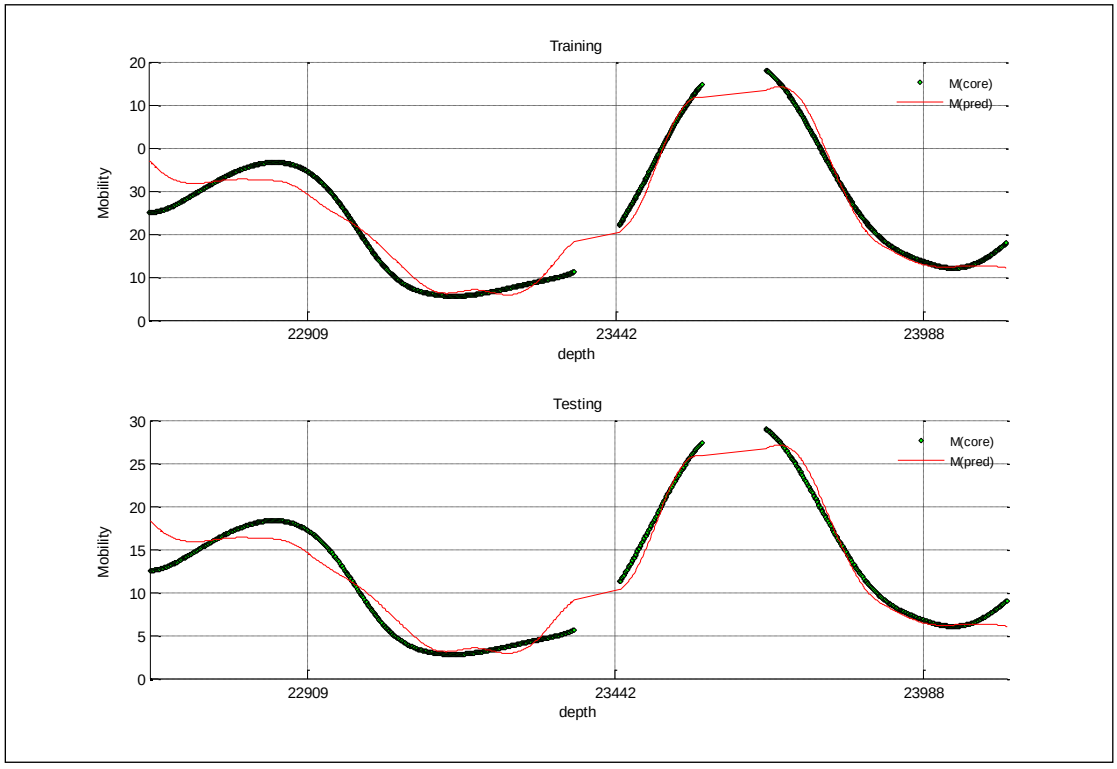

Figure B- 34: Well-4 Method-2, Type-2

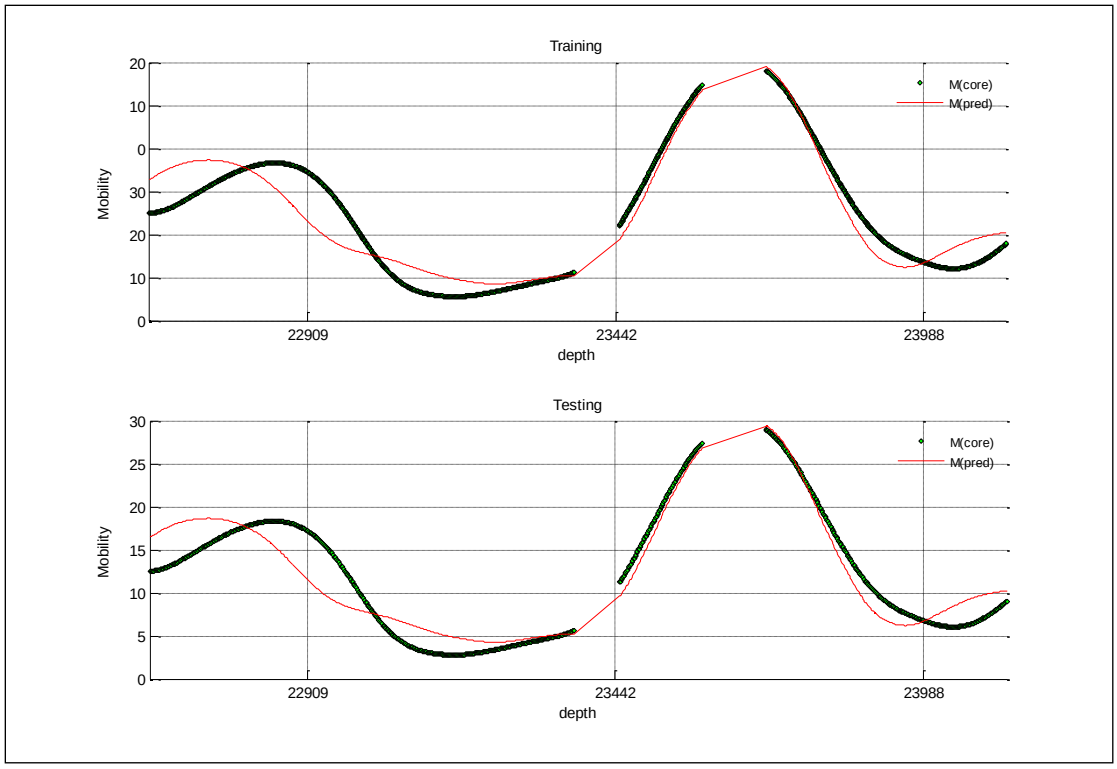

Figure B- 35: Well-4 Method-3, Type-1

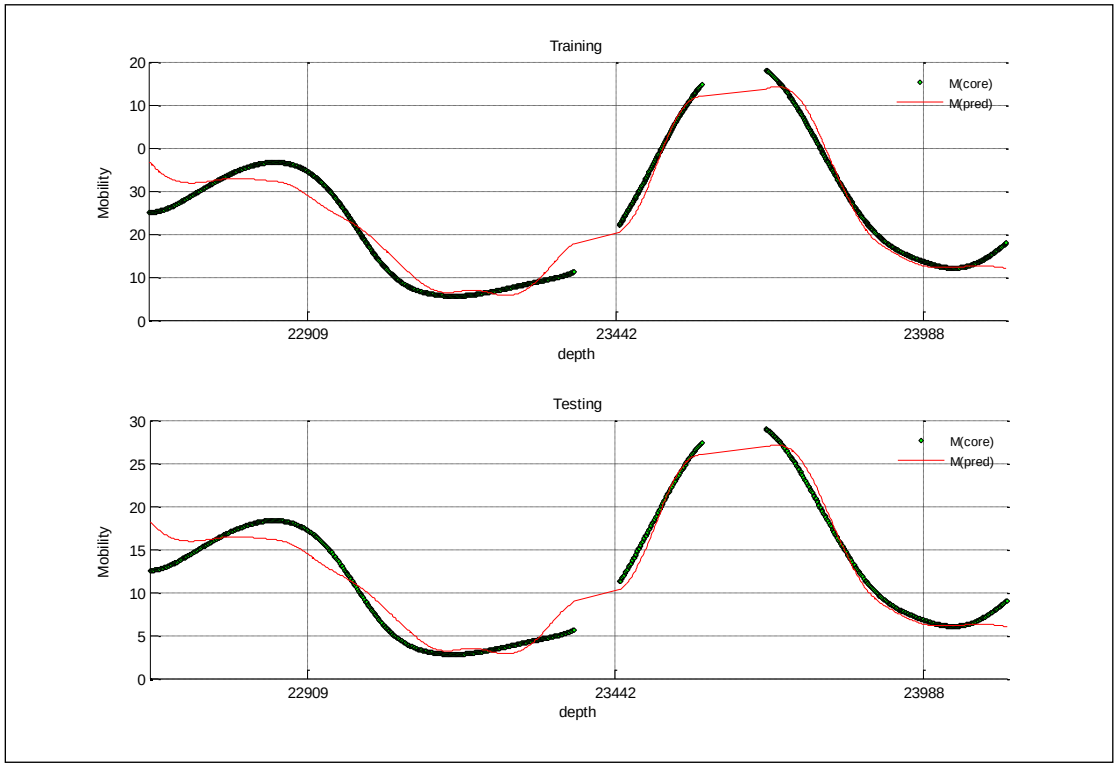

Figure B- 36: Well-4 Method-3, Type-2

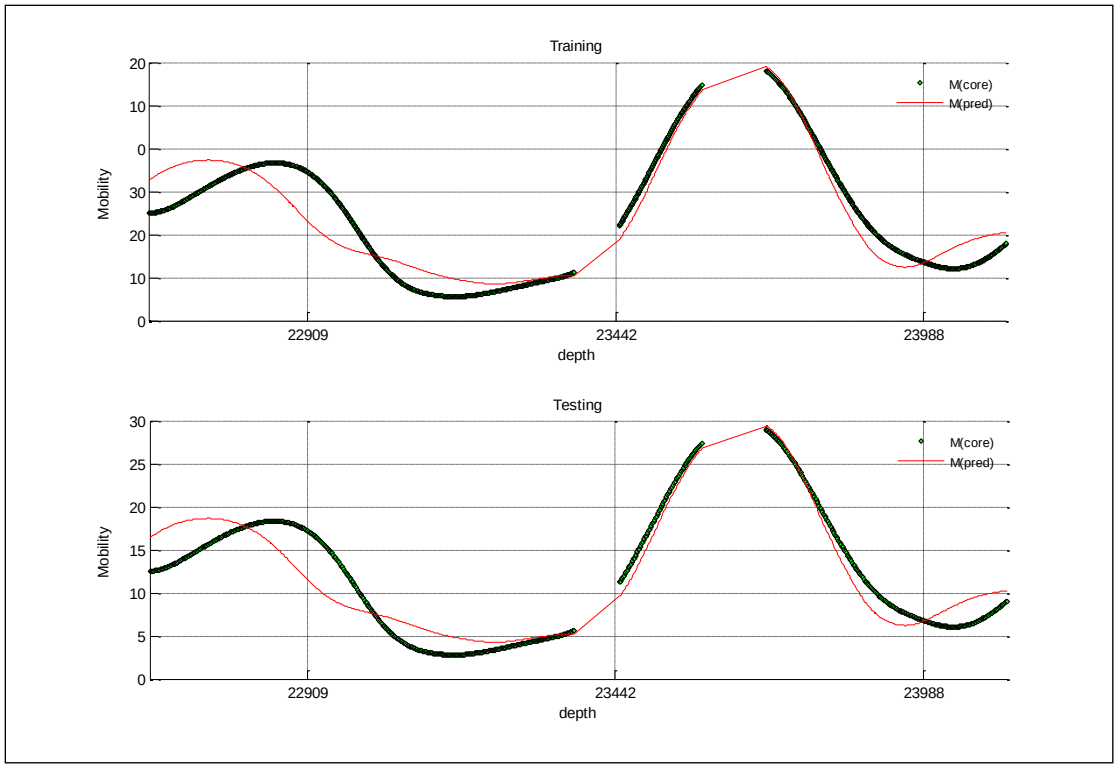

Figure B- 37: Well-4 Method-4, Type-1

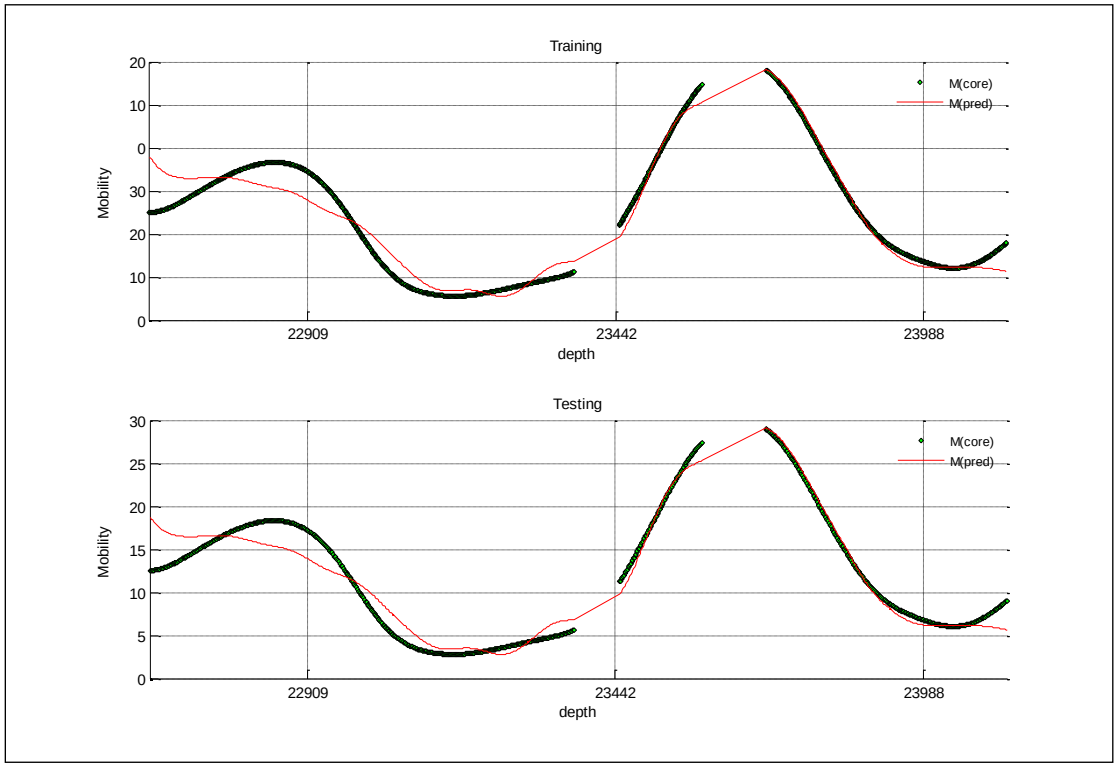

Figure B- 38: Well-4 Method-4, Type-2

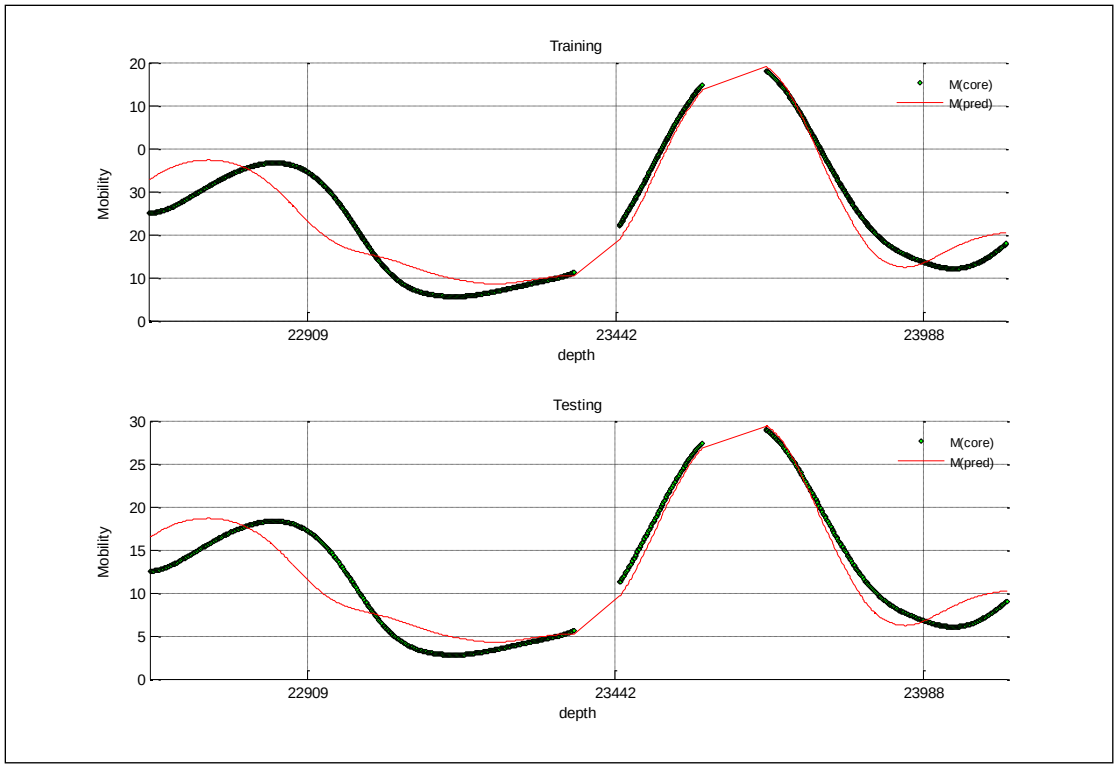

Figure B- 39: Well-4 Method-5, Type-1

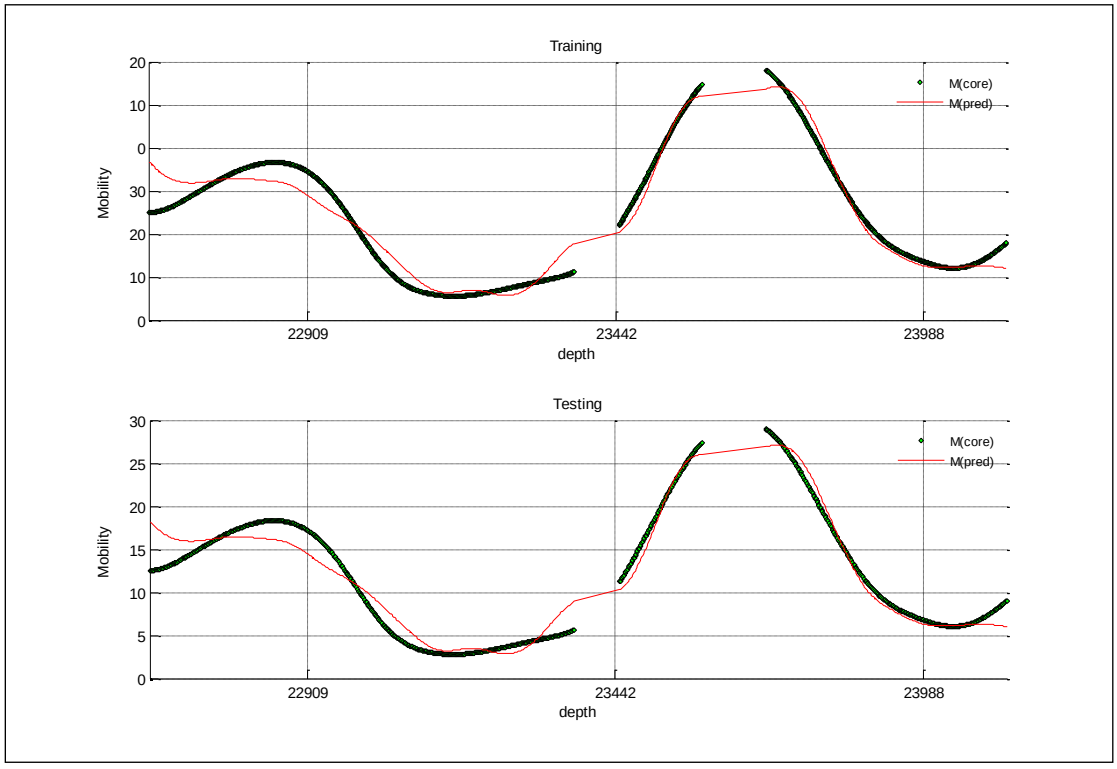

Figure B- 40: Well-4 Method-5, Type-2

Well No. 5

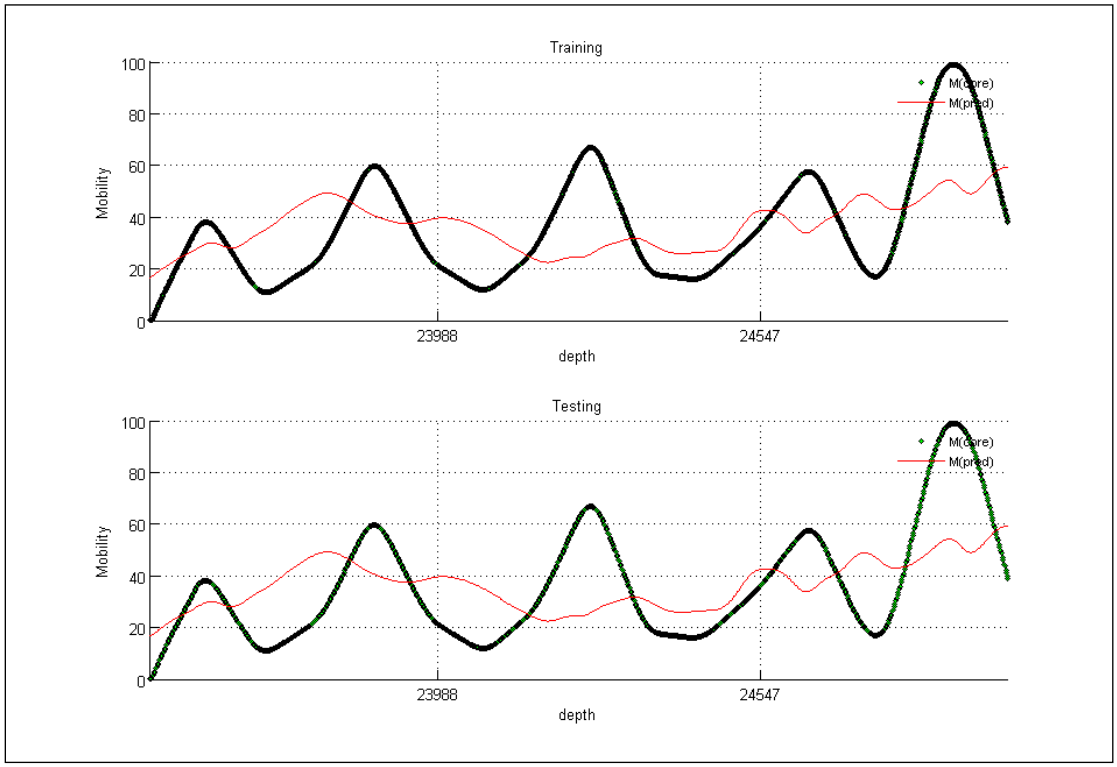

Figure B- 41: Well-5 Method-1, Type-1

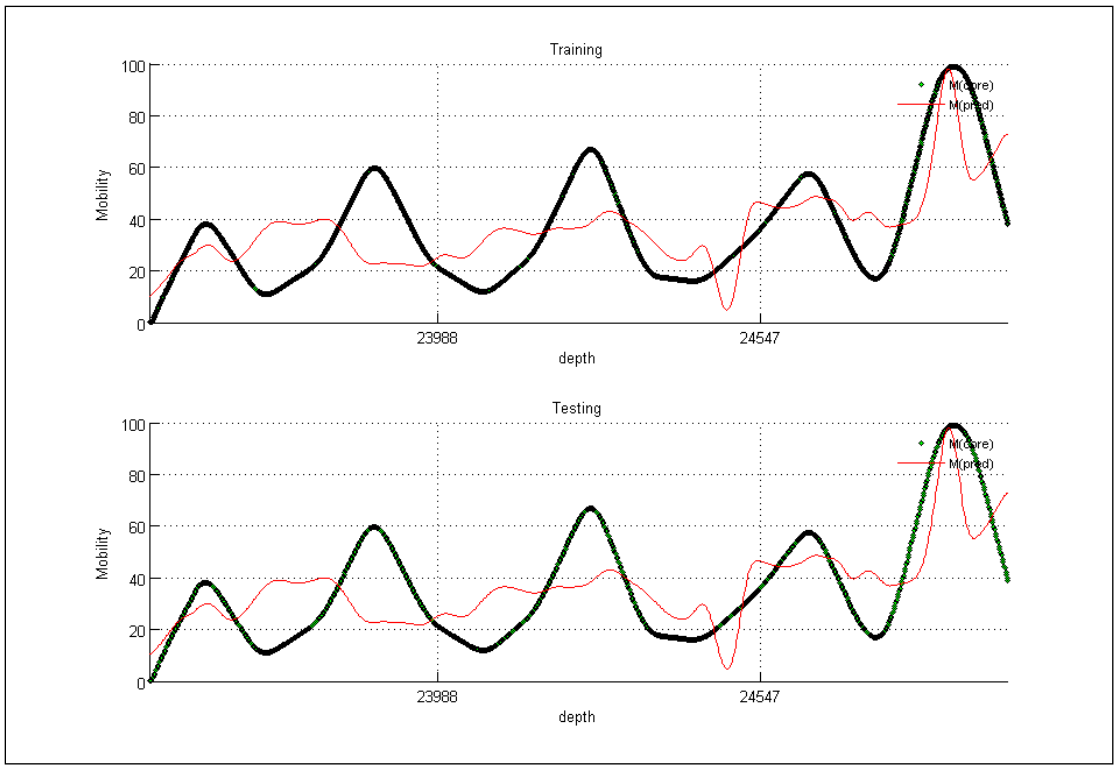

Figure B- 42: Well-5 Method-1, Type-2

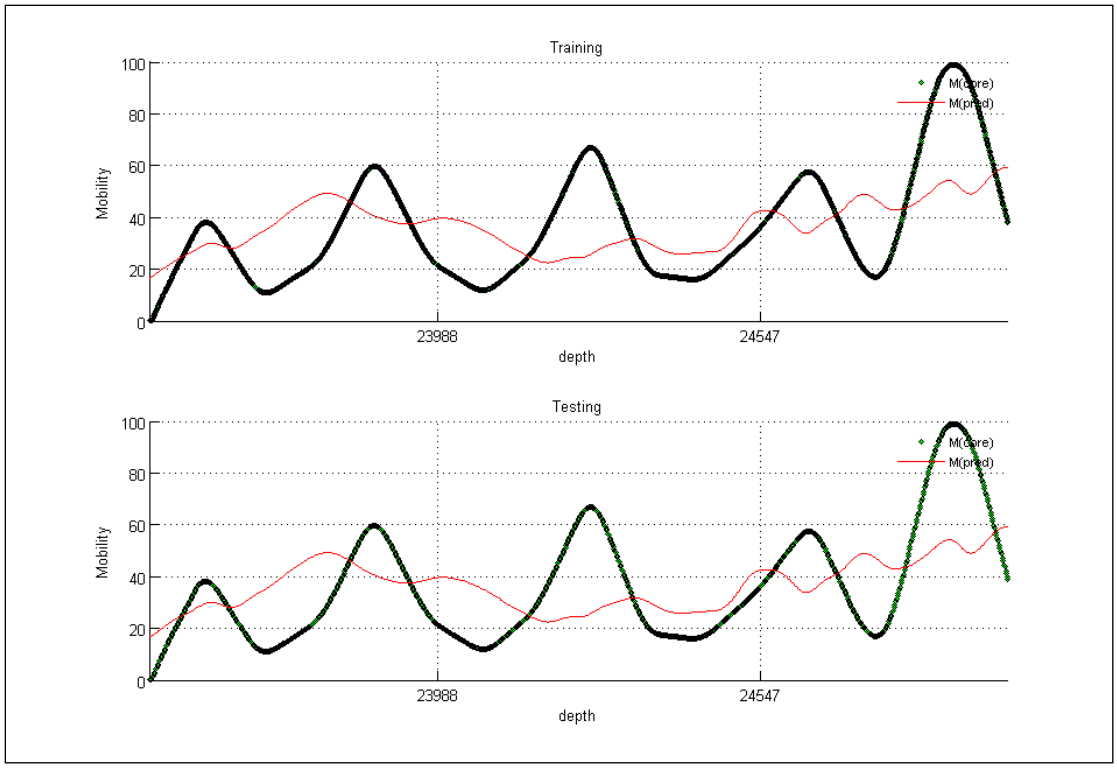

Figure B- 43: Well-5 Method-2, Type-1

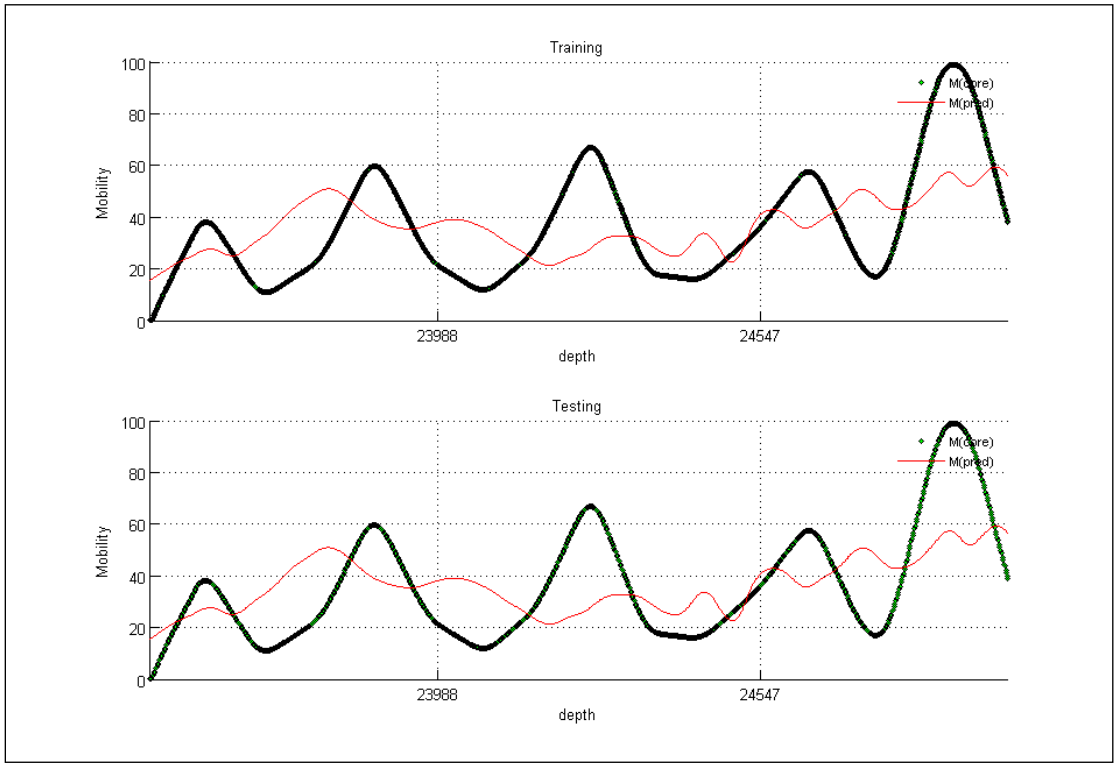

Figure B- 44: Well-5 Method-2, Type-2

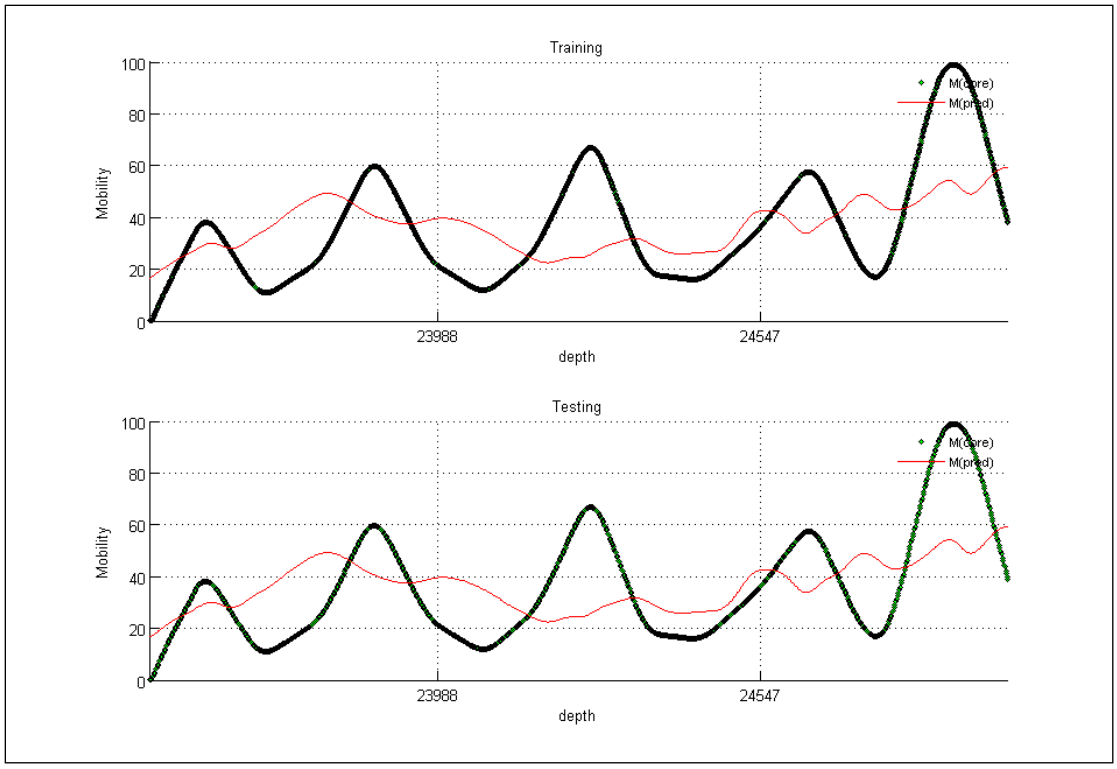

Figure B- 45: Well-5 Method-3, Type-1

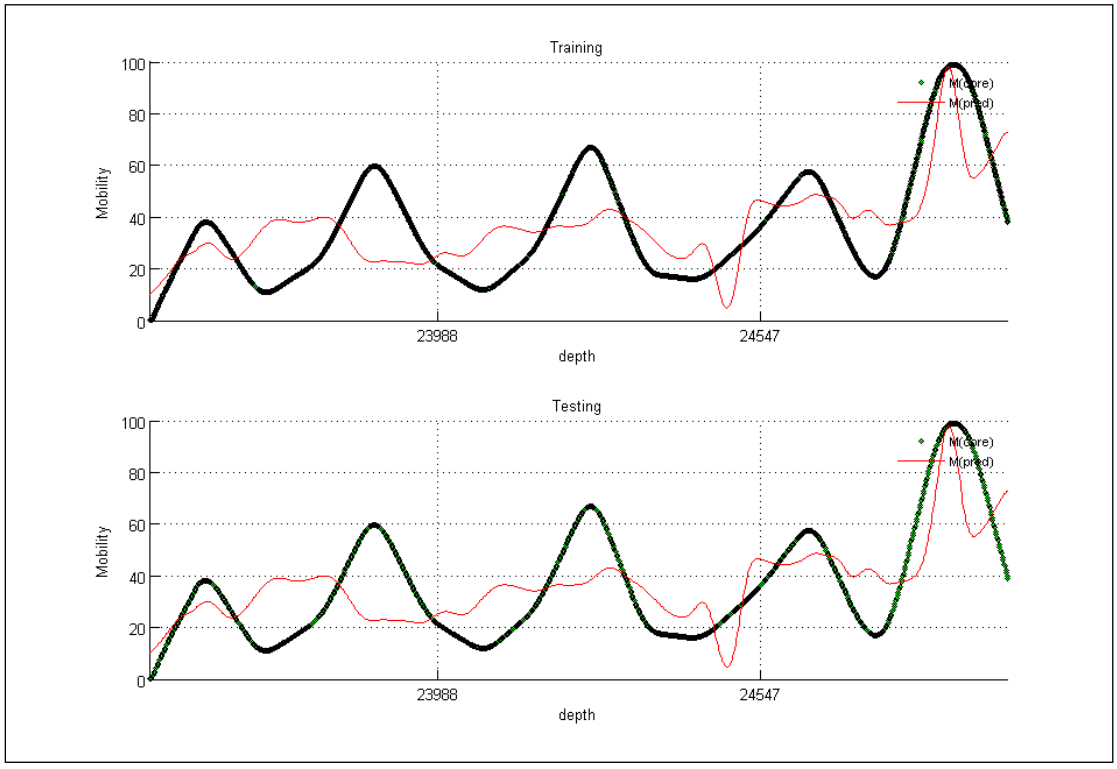

Figure B- 46: Well-5 Method-3, Type-2

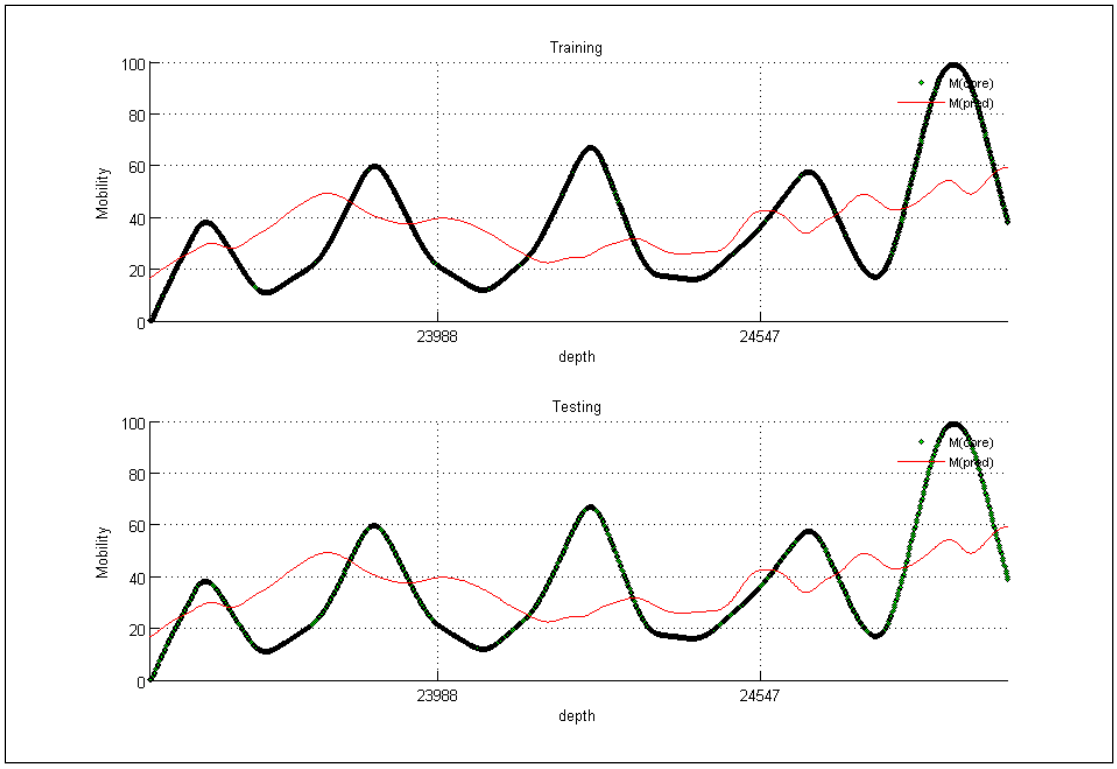

Figure B- 47: Well-5 Method-4, Type-1

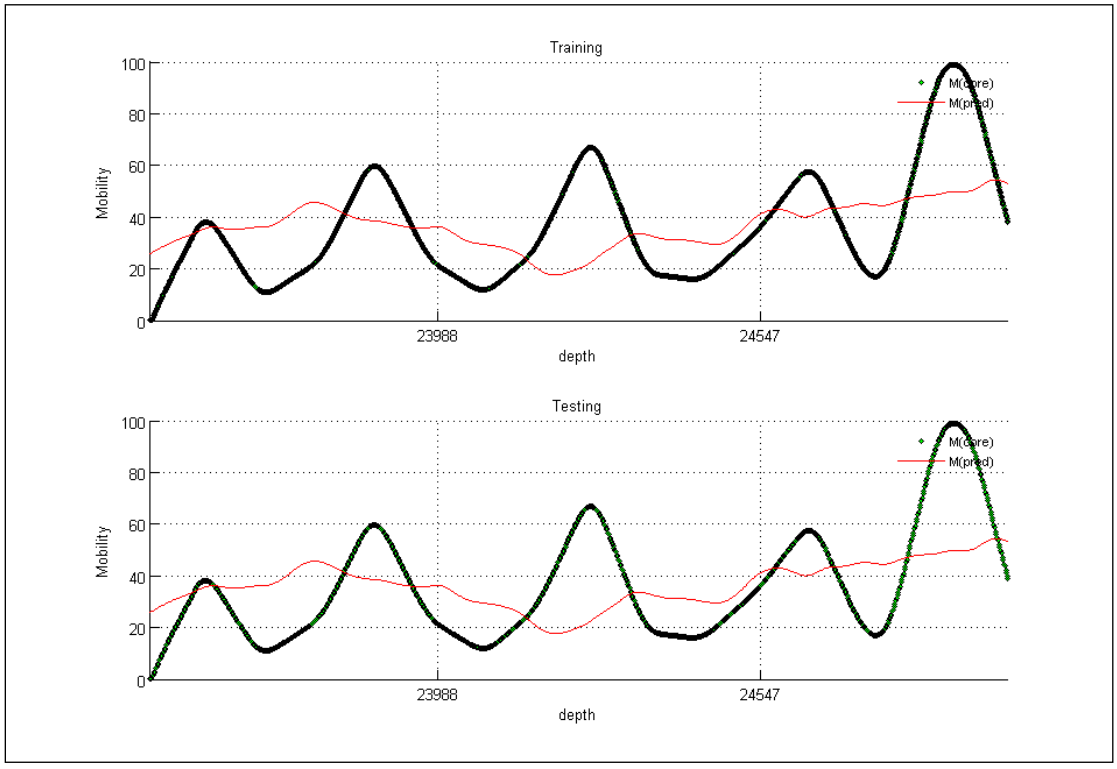

Figure B- 48: Well-5 Method-4, Type-2

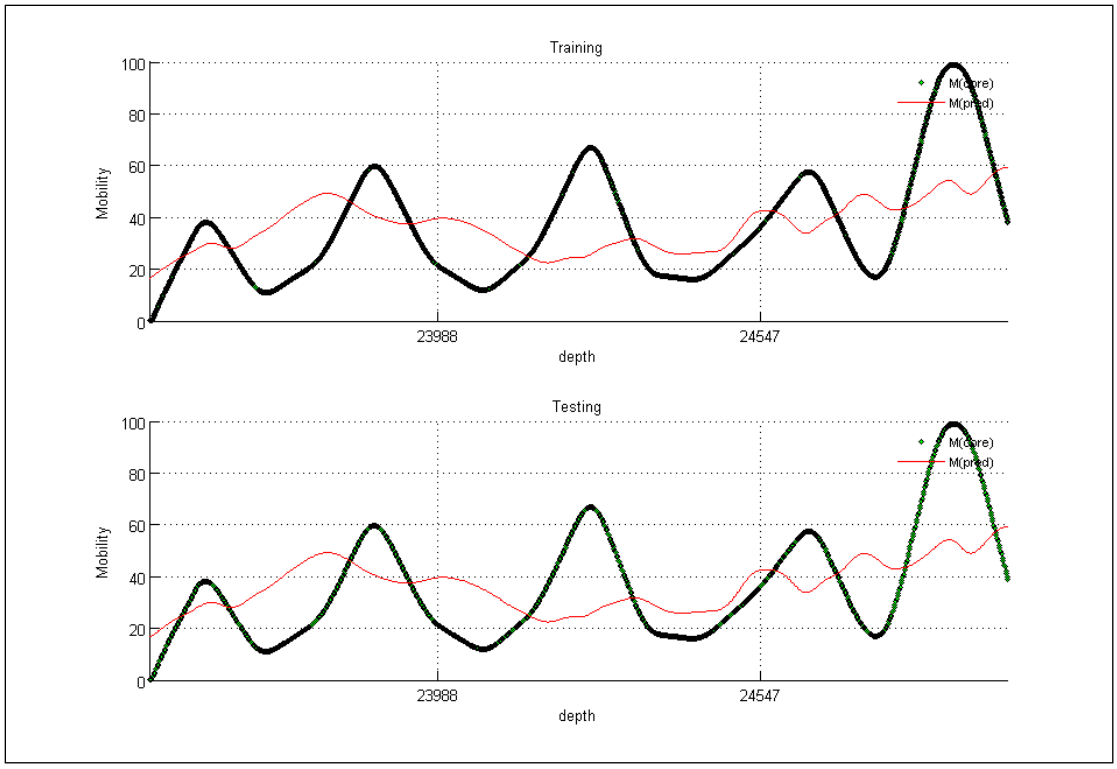

Figure B- 49: Well-5 Method-5, Type-1

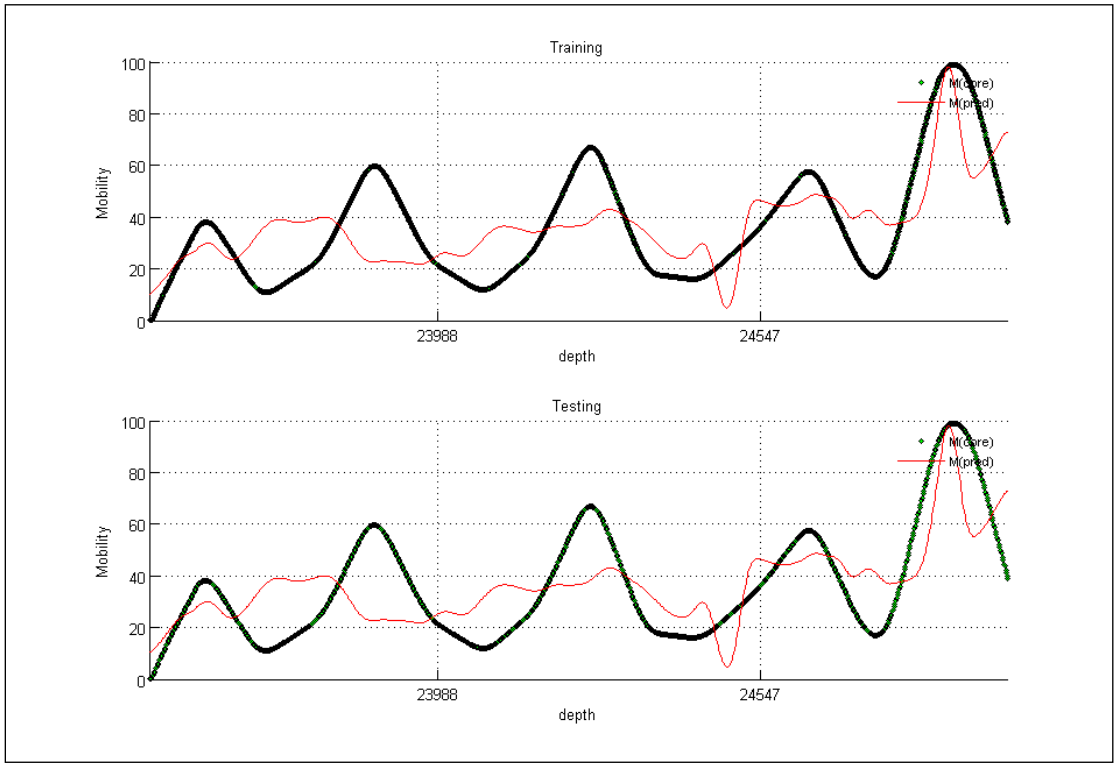

Figure B- 50: Well-5 Method-5, Type-2

Well No. 6

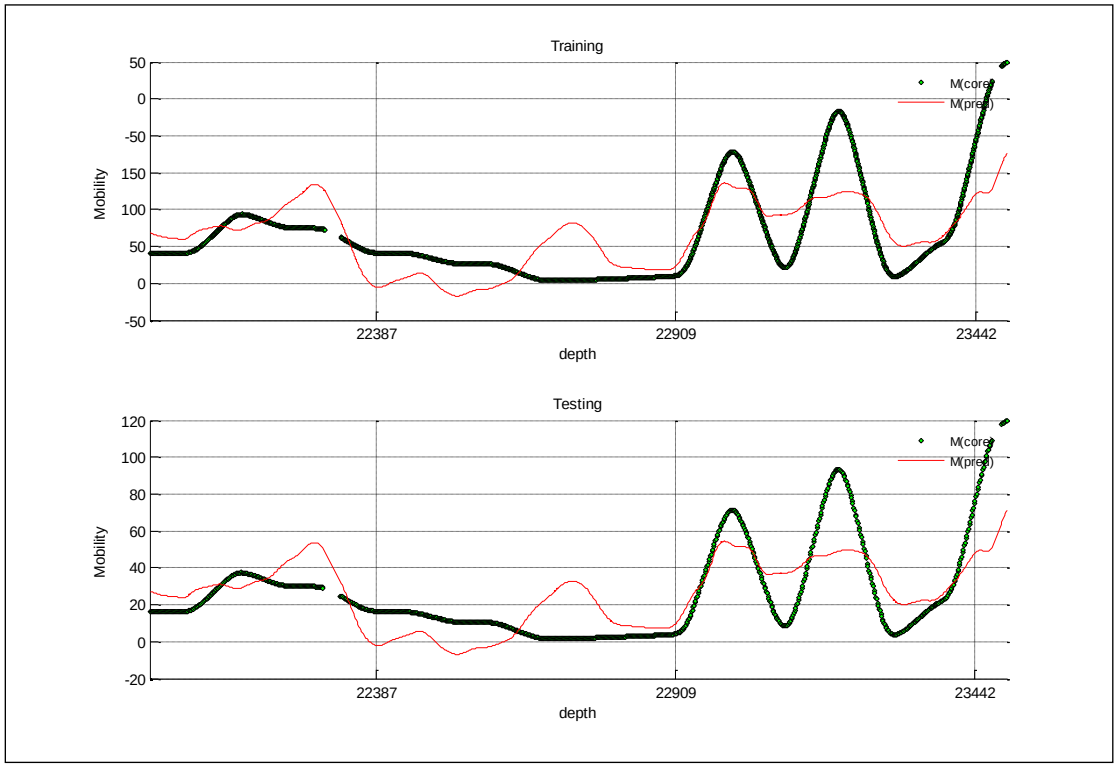

Figure B- 51: Well-6 Method-1, Type-1

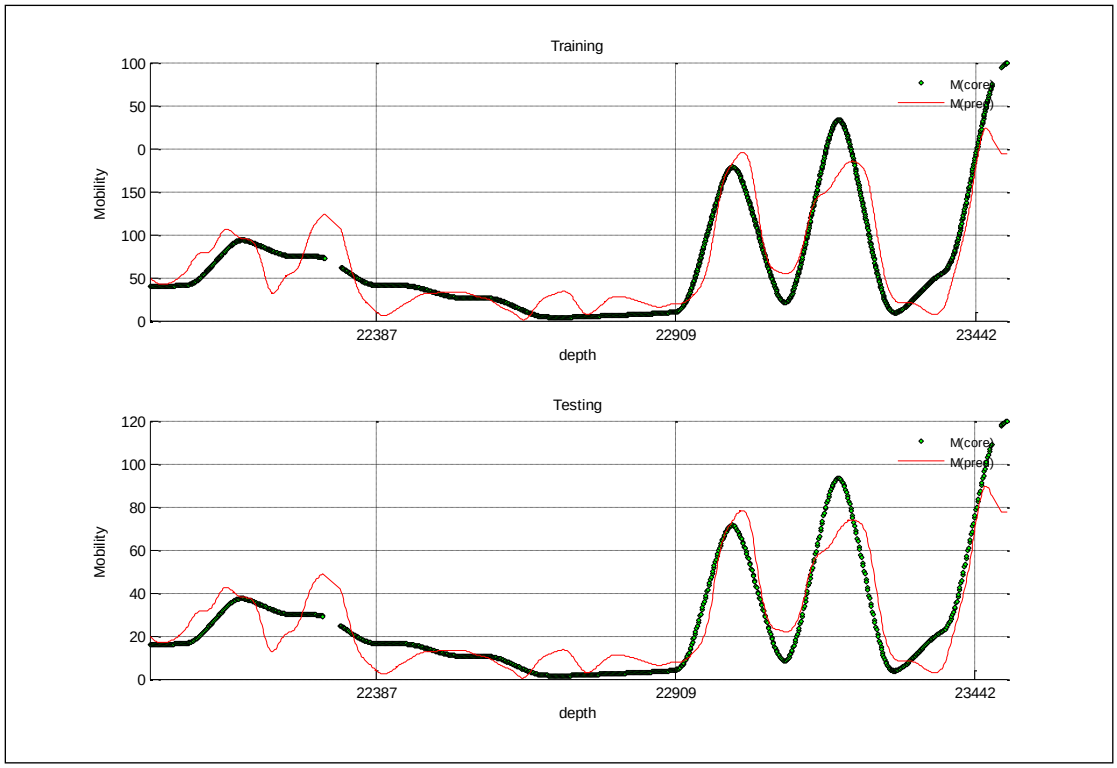

Figure B- 52: Well-6 Method-1, Type-2

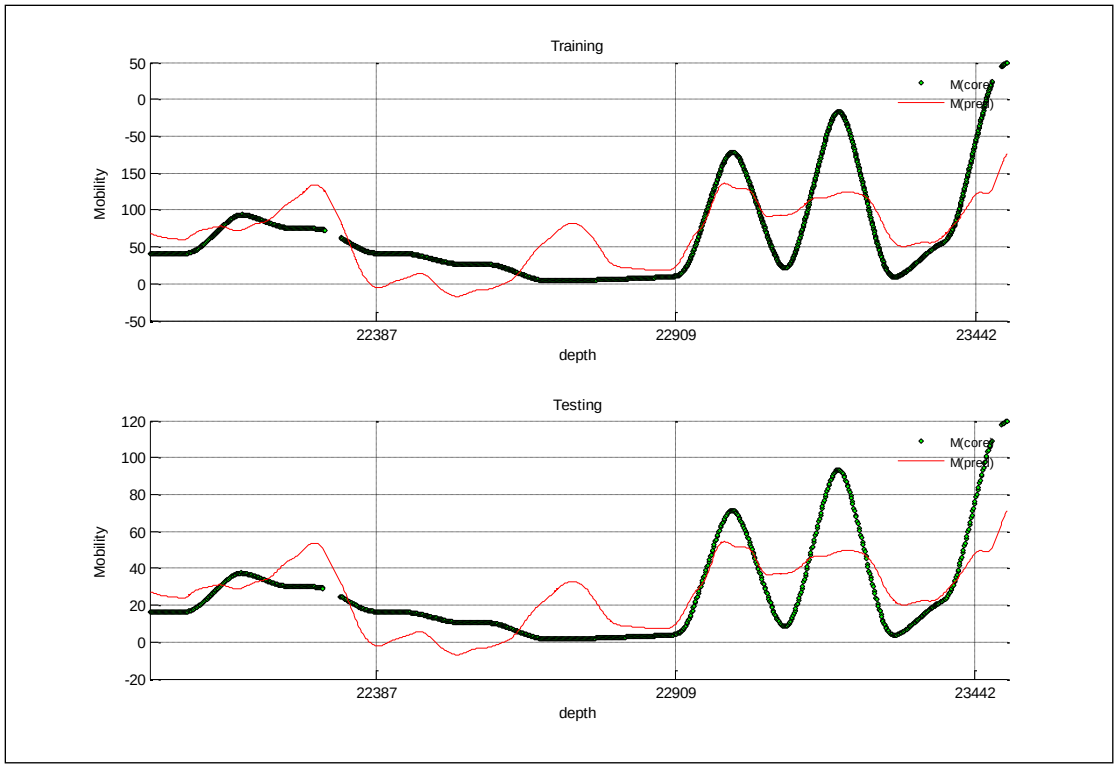

Figure B- 53: Well-6 Method-2, Type-1

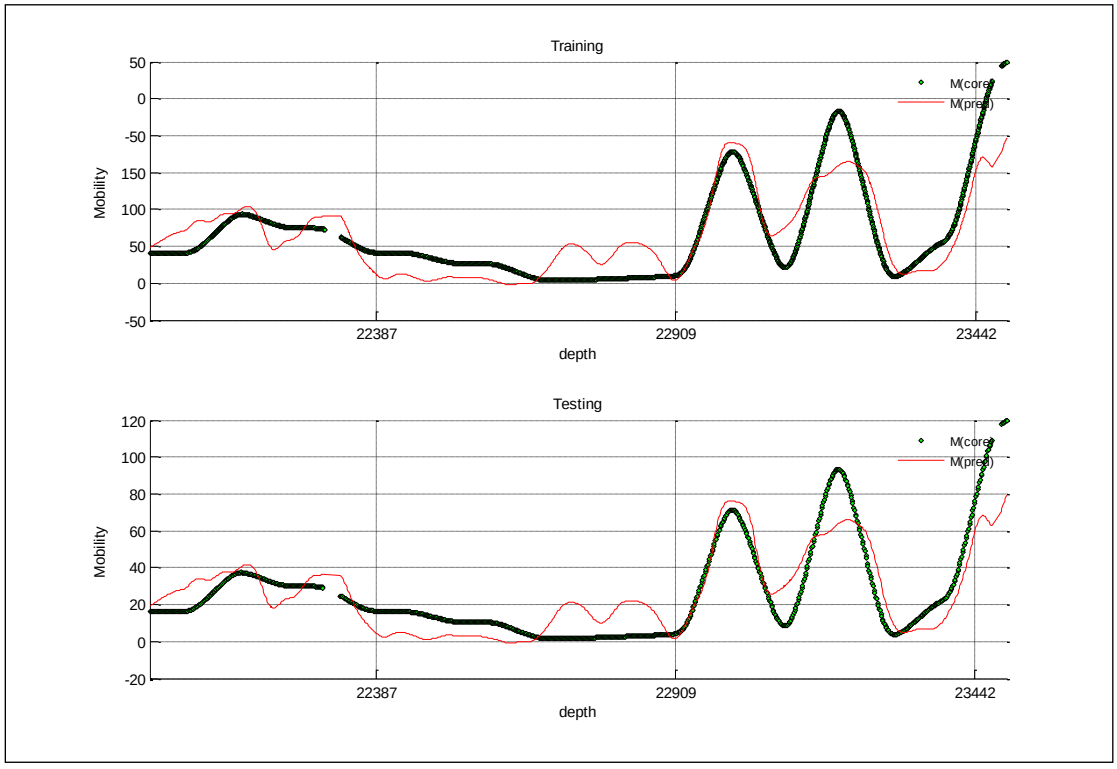

Figure B- 54: Well-6 Method-2, Type-2

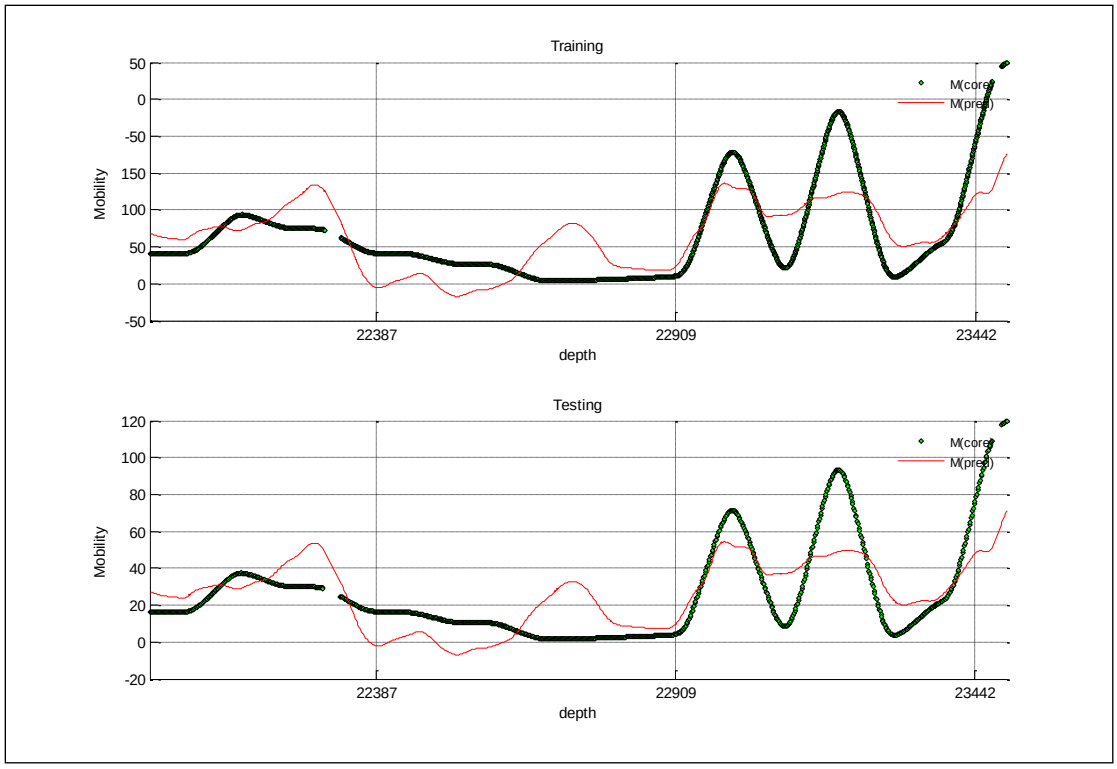

Figure B- 55: Well-6 Method-3, Type-1

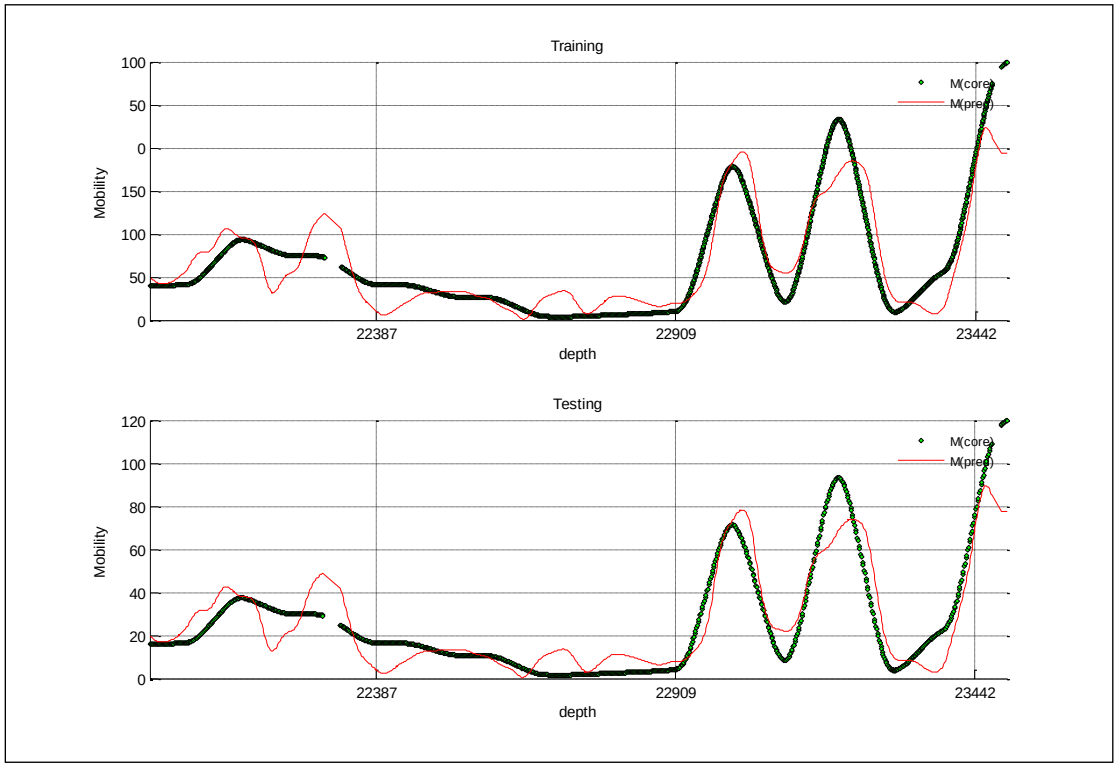

Figure B- 56: Well-6 Method-3, Type-2

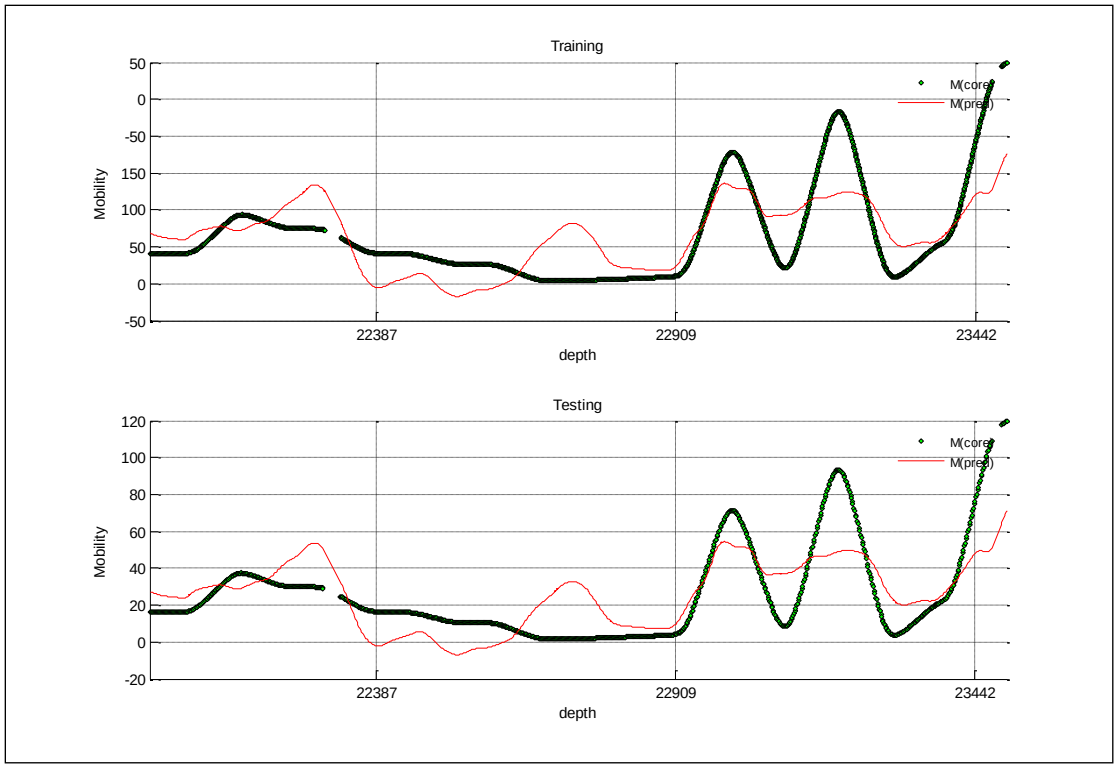

Figure B- 57: Well-6 Method-4, Type-1

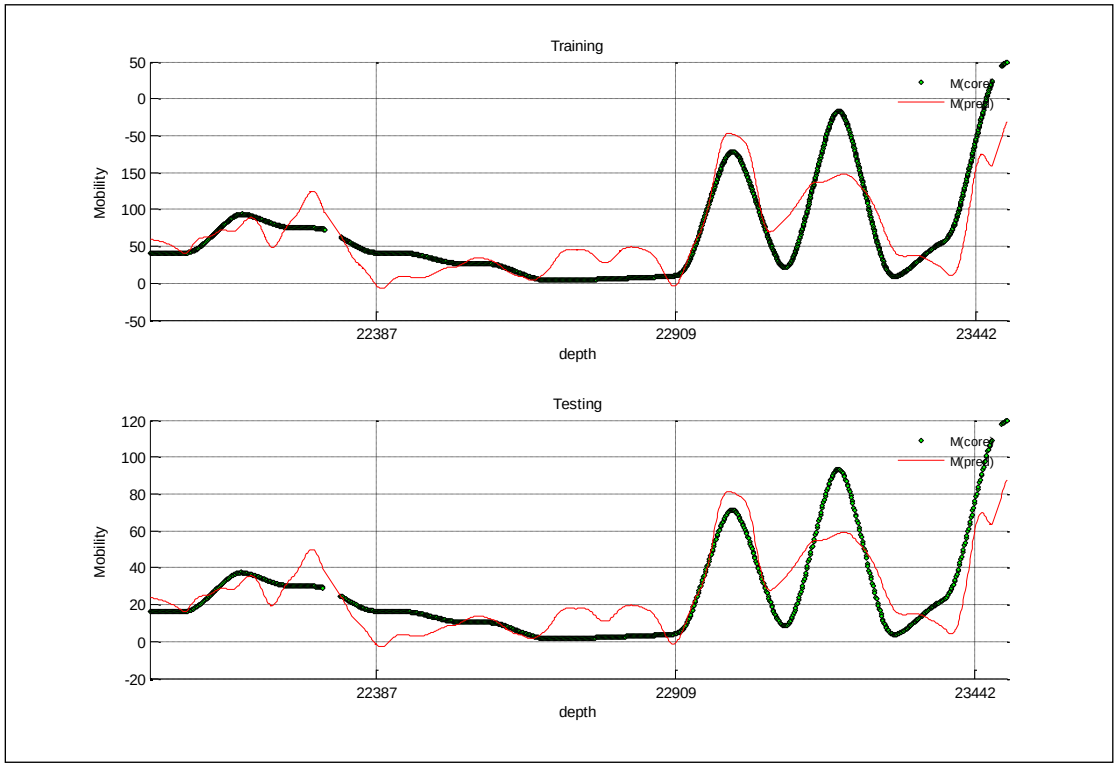

Figure B- 58: Well-6 Method-4, Type-2

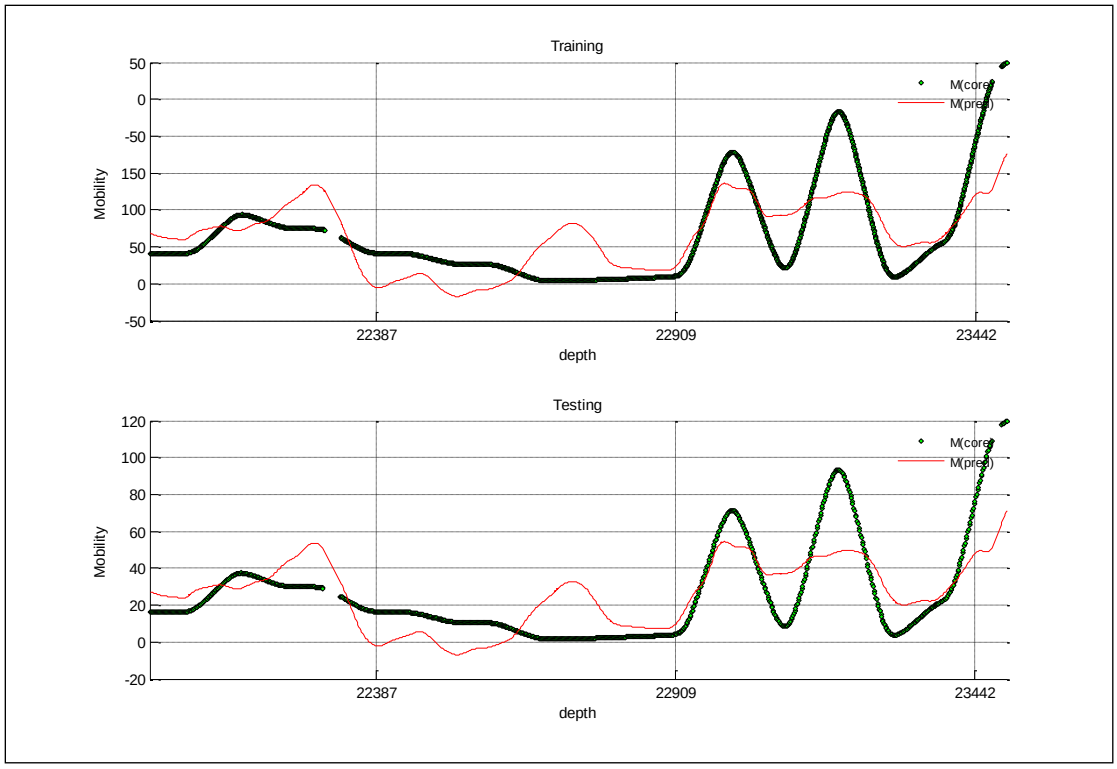

Figure B- 59: Well-6 Method-5, Type-1

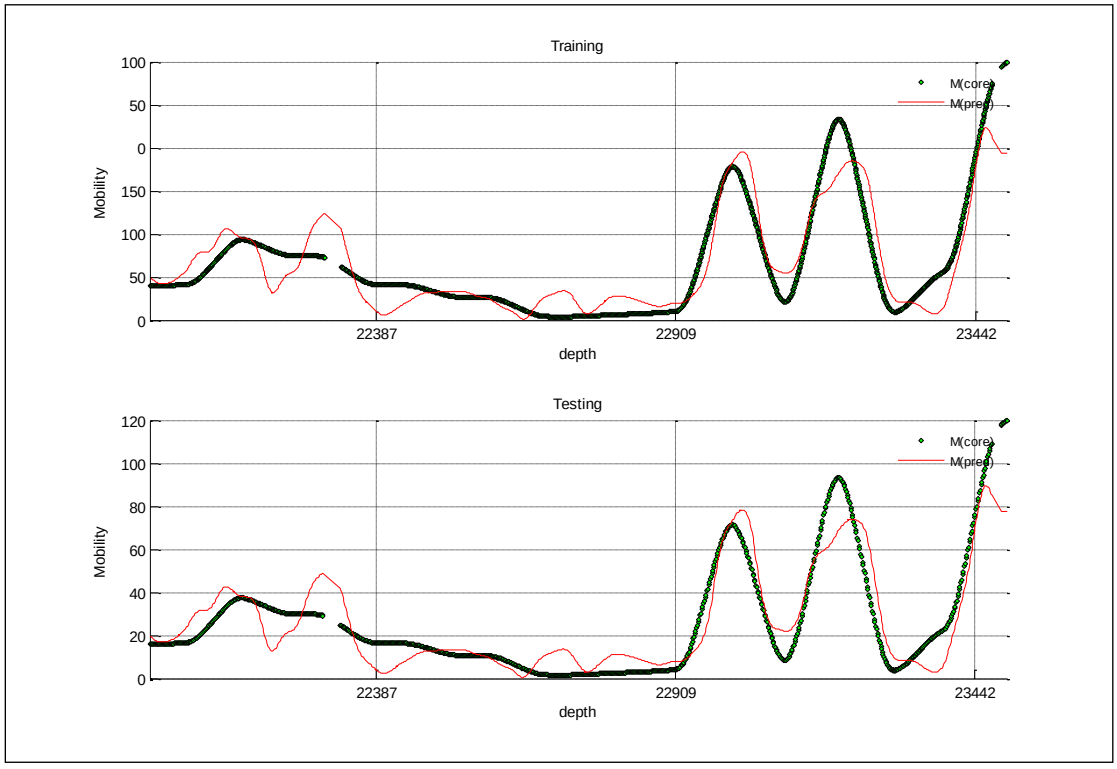

Figure B- 60: Well-6 Method-5, Type-2

Well No. 7

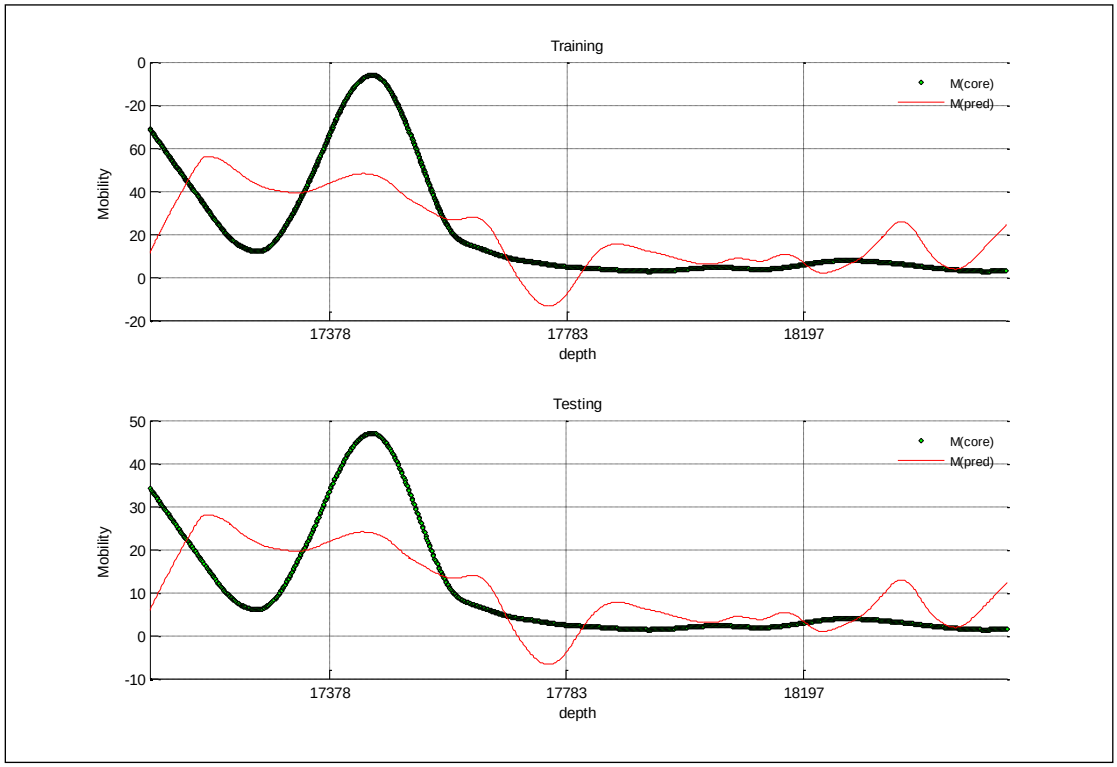

Figure B- 61: Well-7 Method-1, Type-1

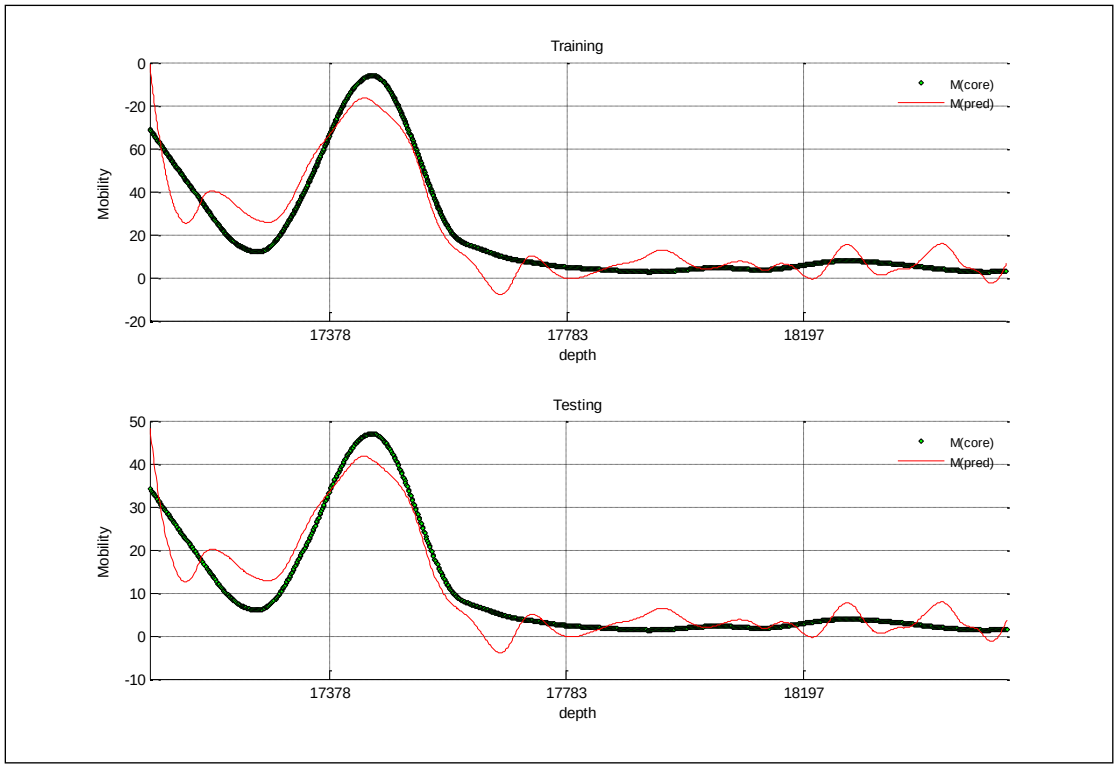

Figure B- 62: Well-7 Method-1, Type-2

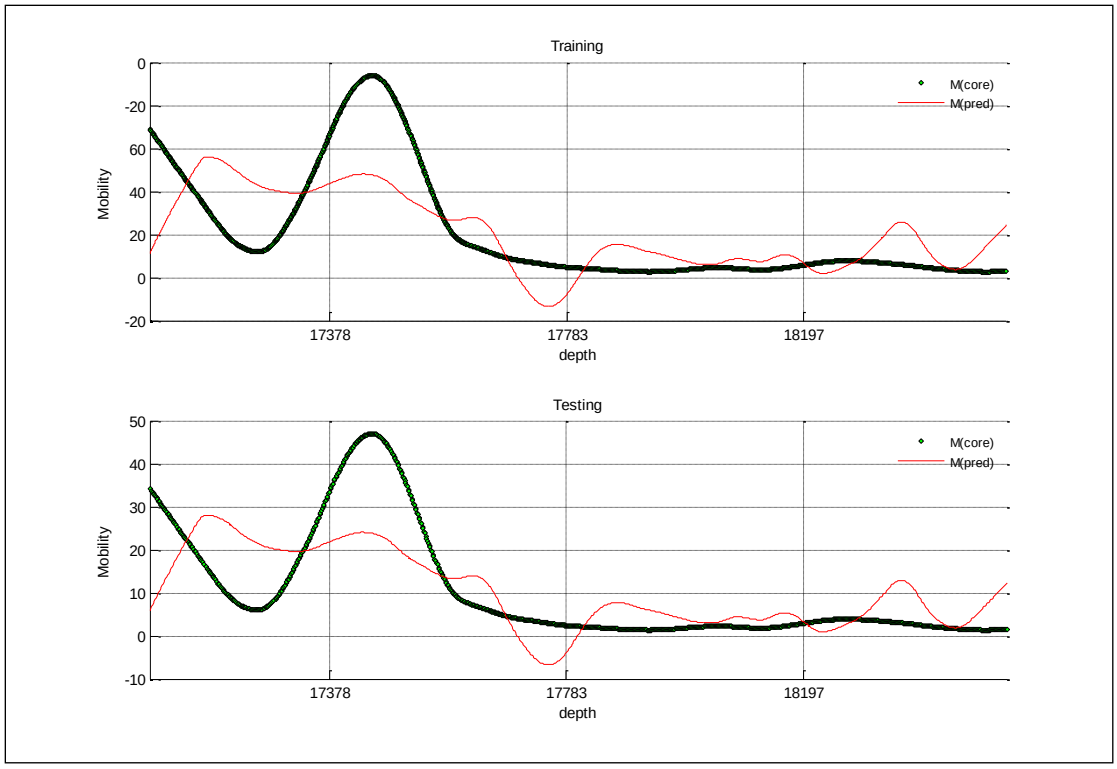

Figure B- 63: Well-7 Method-2, Type-1

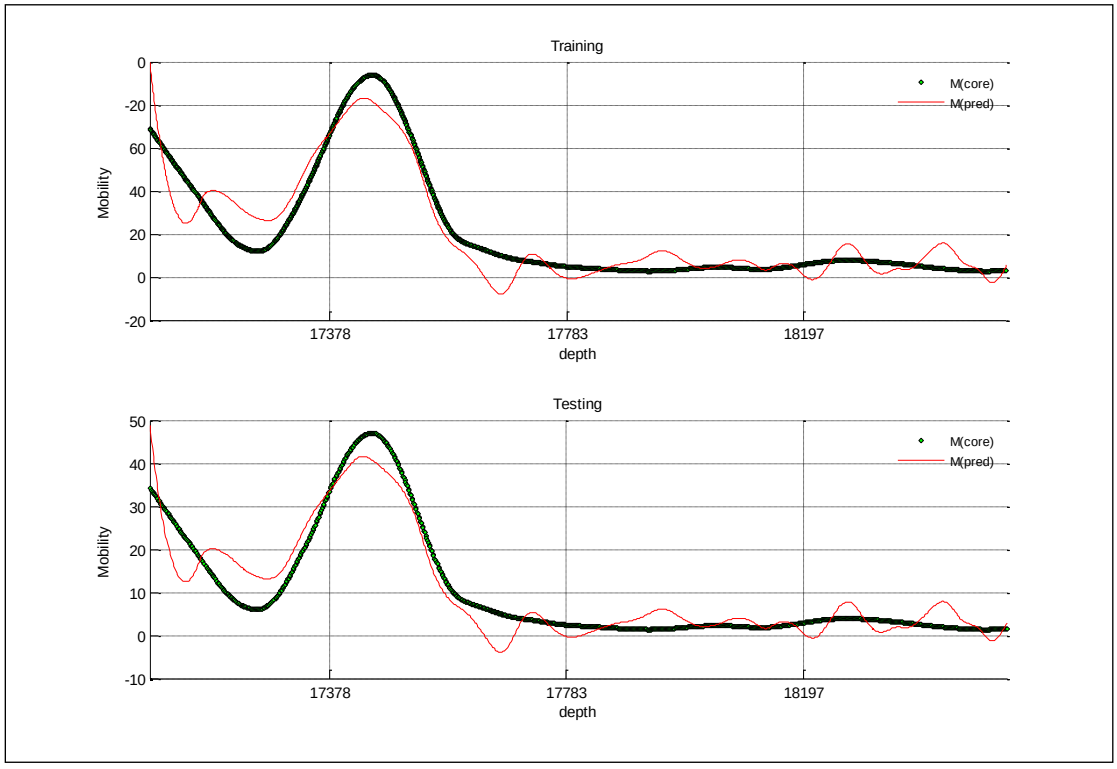

Figure B- 64: Well-7 Method-1, Type-2

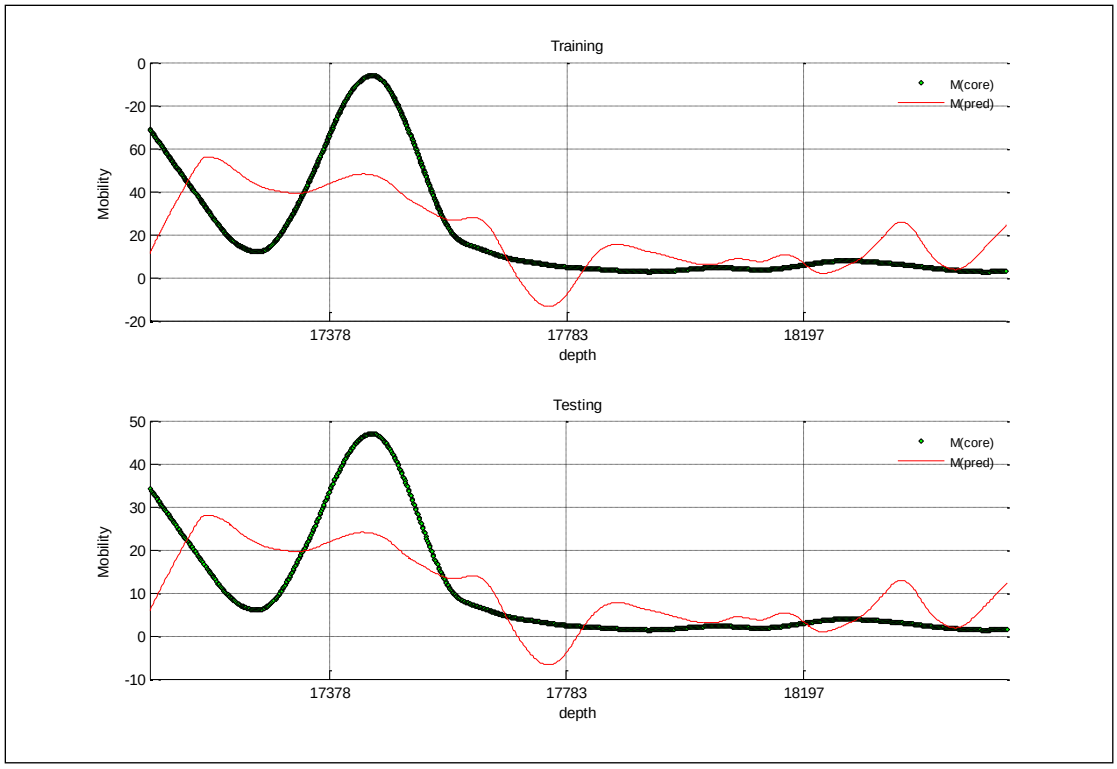

Figure B- 65: Well-7 Method-3, Type-1

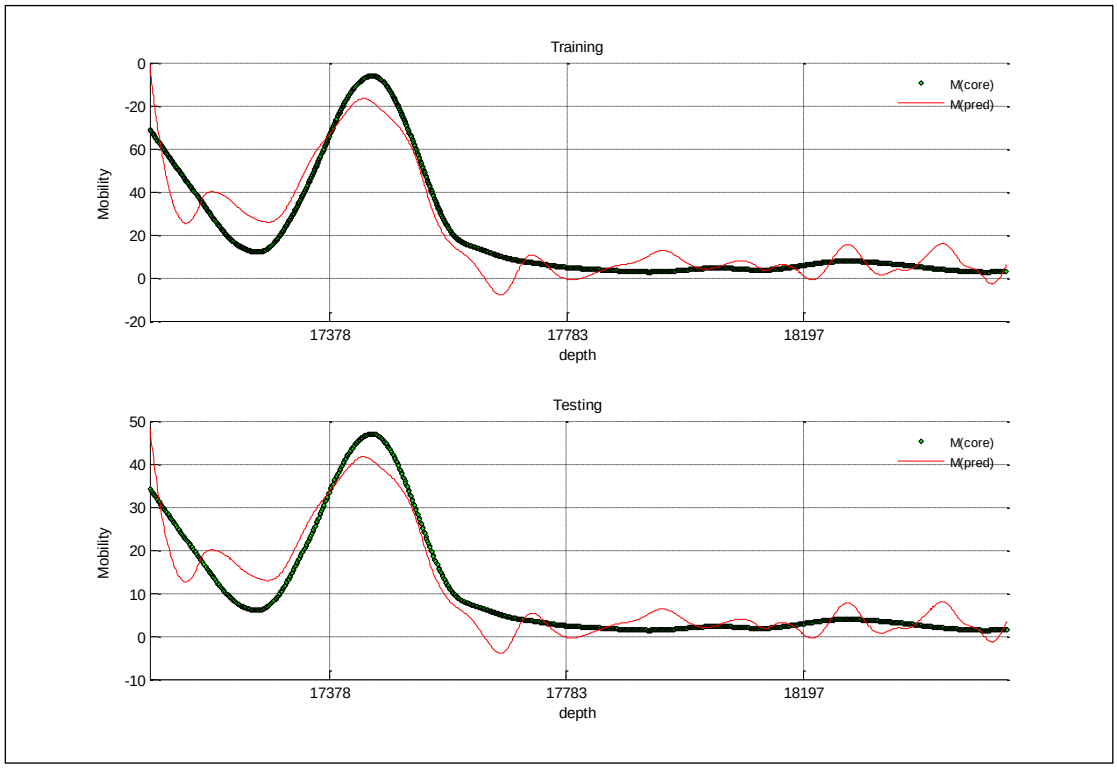

Figure B- 66: Well-7 Method-3, Type-2

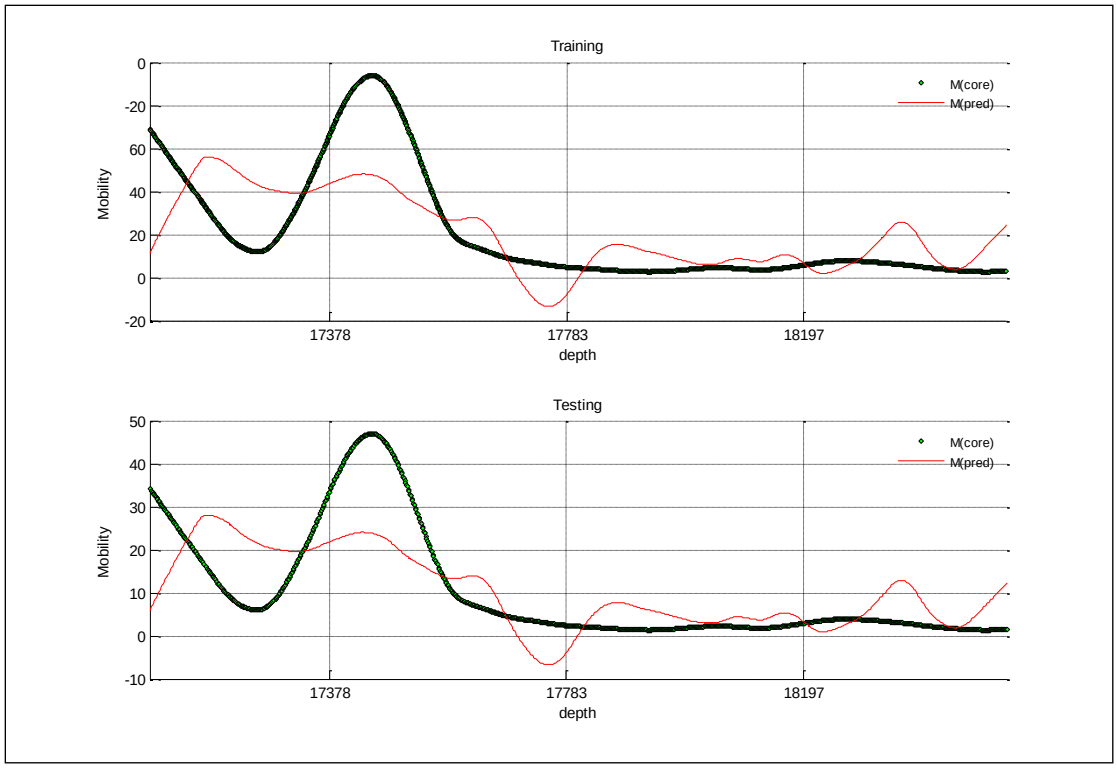

Figure B- 67: Well-7 Method-4, Type-1

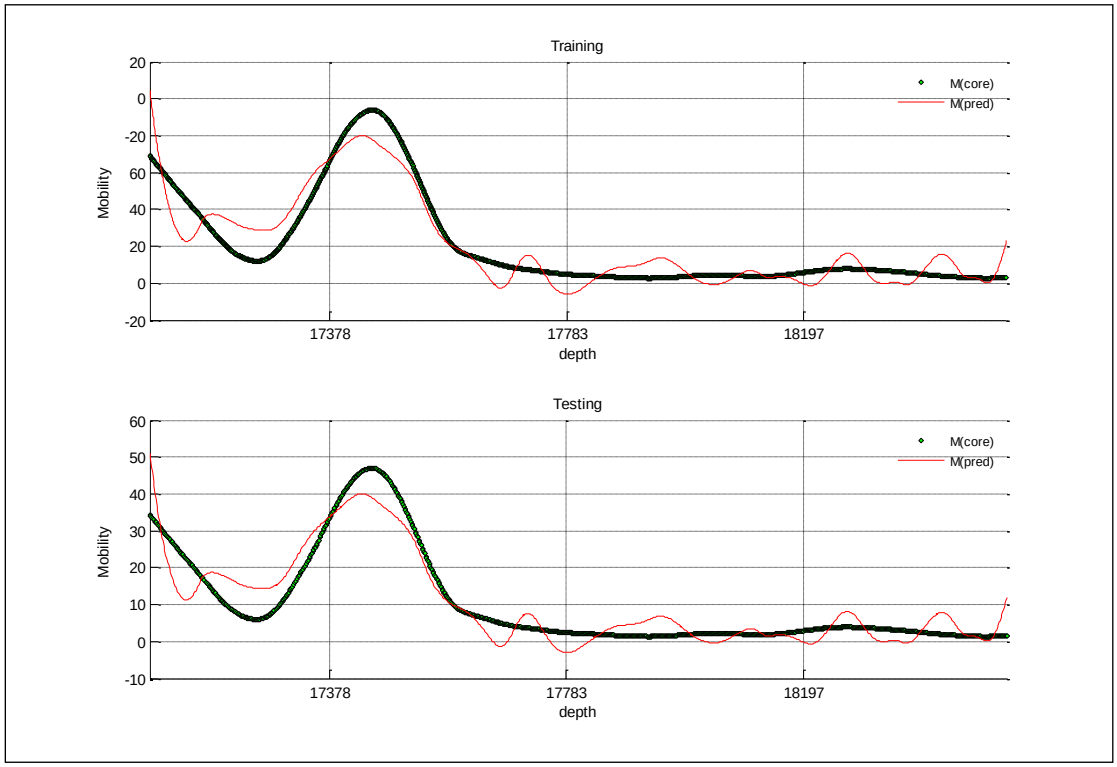

Figure B- 68: Well-7 Method-4, Type-2

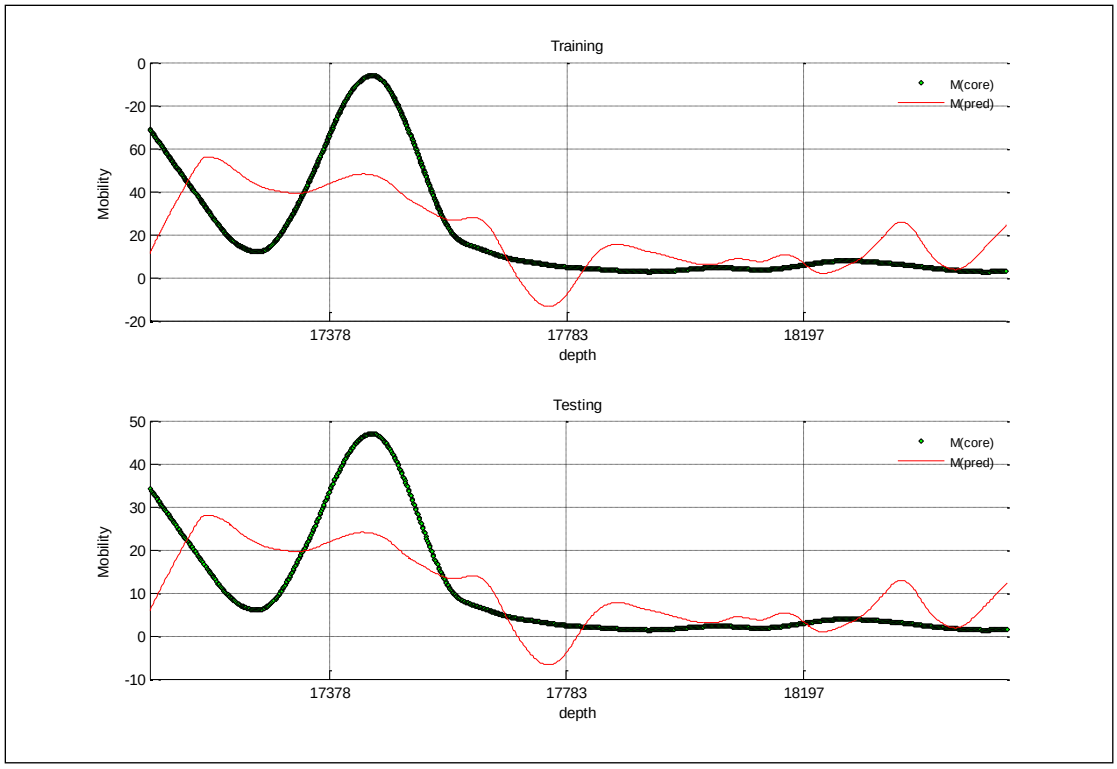

Figure B- 69: Well-7 Method-5, Type-1

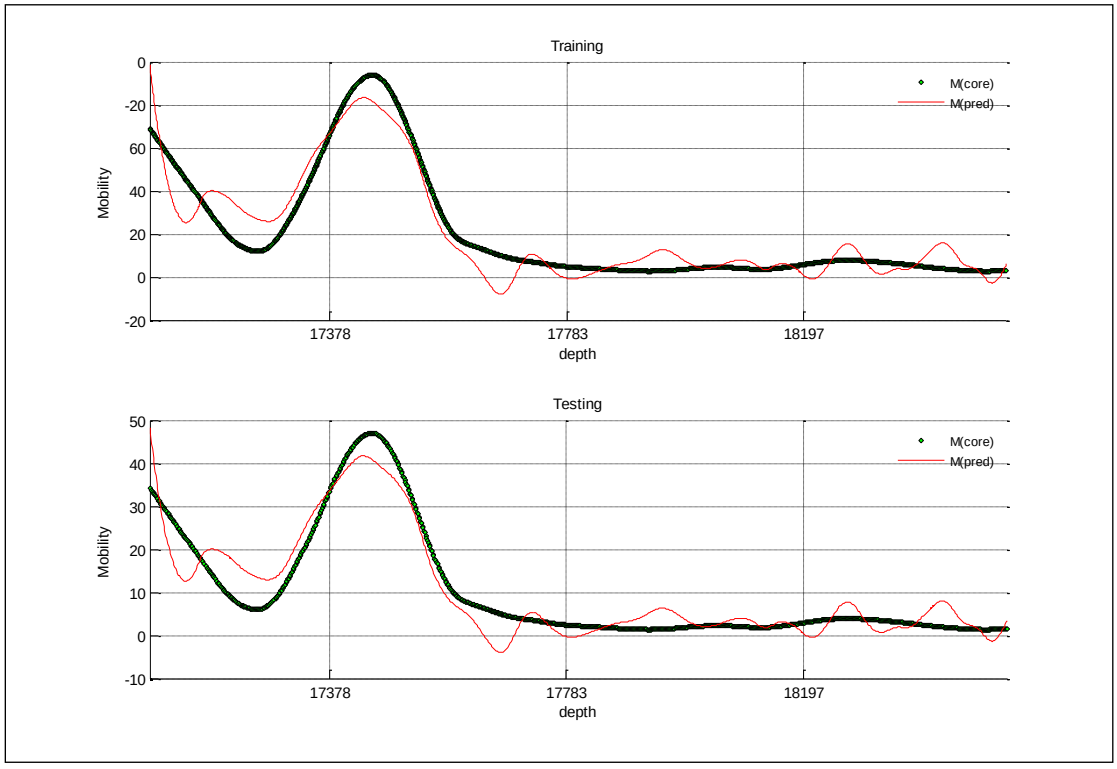

Figure B- 70: Well-7 Method-5, Type-2

Well No. 8

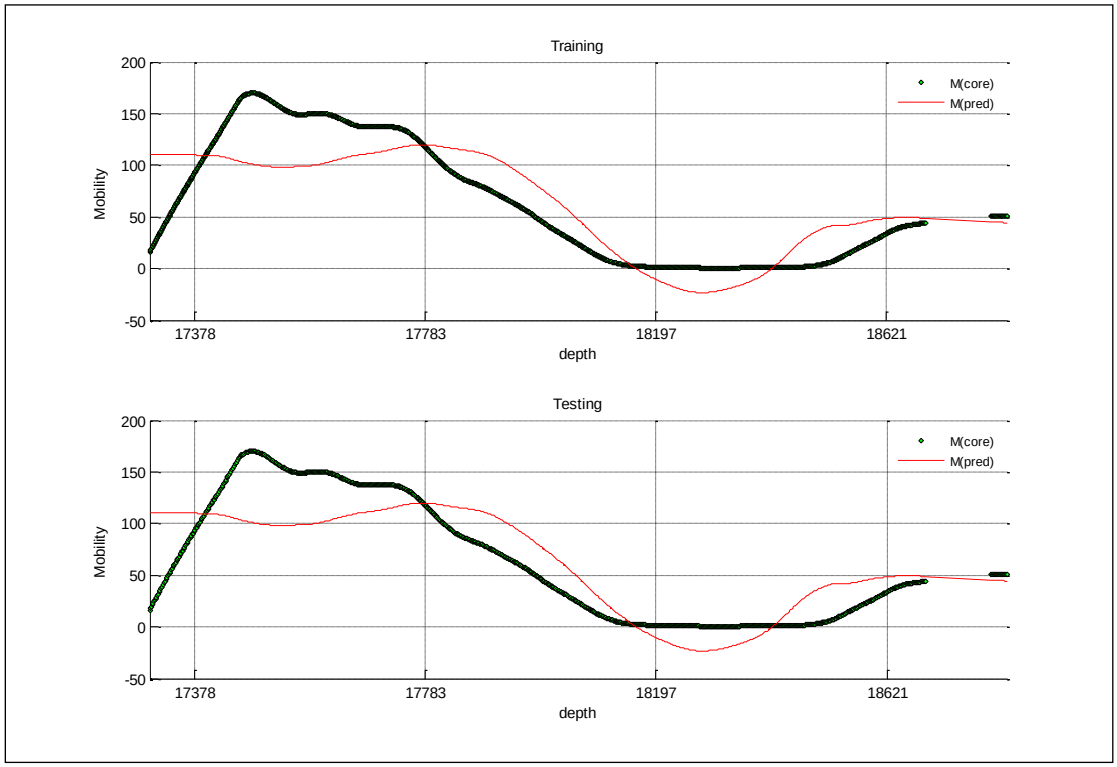

Figure B- 71: Well-8 Method-1, Type-1

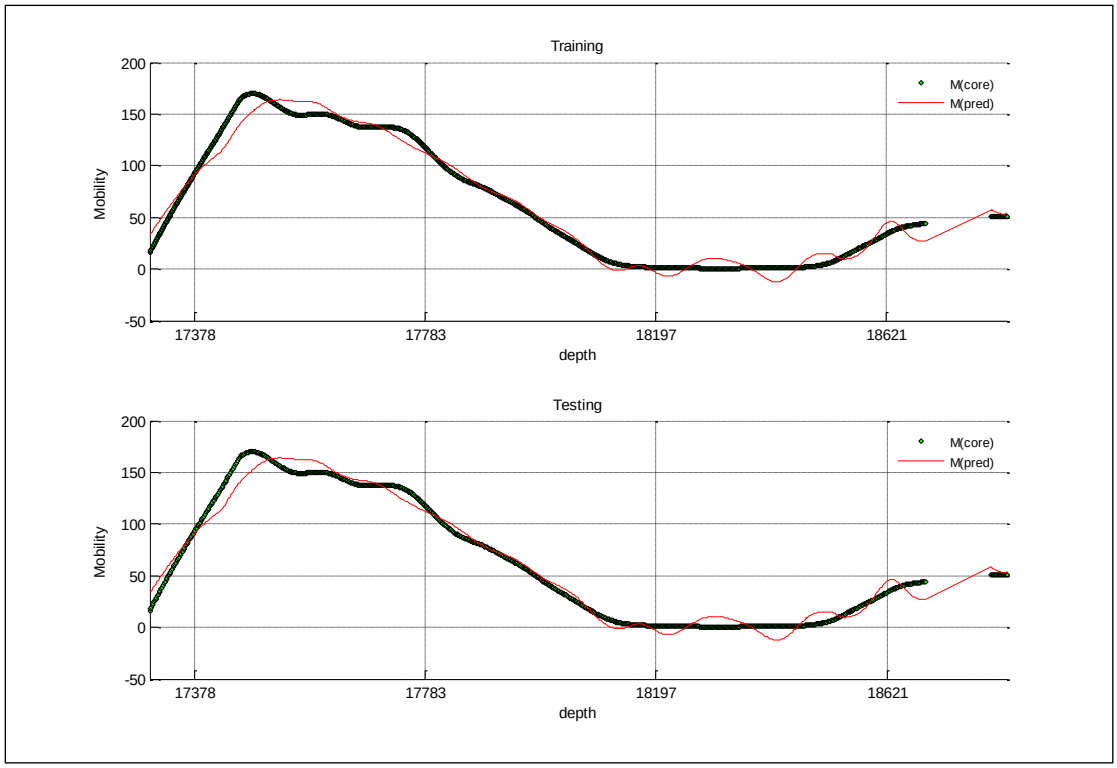

Figure B- 72: Well-8 Method-1, Type-2

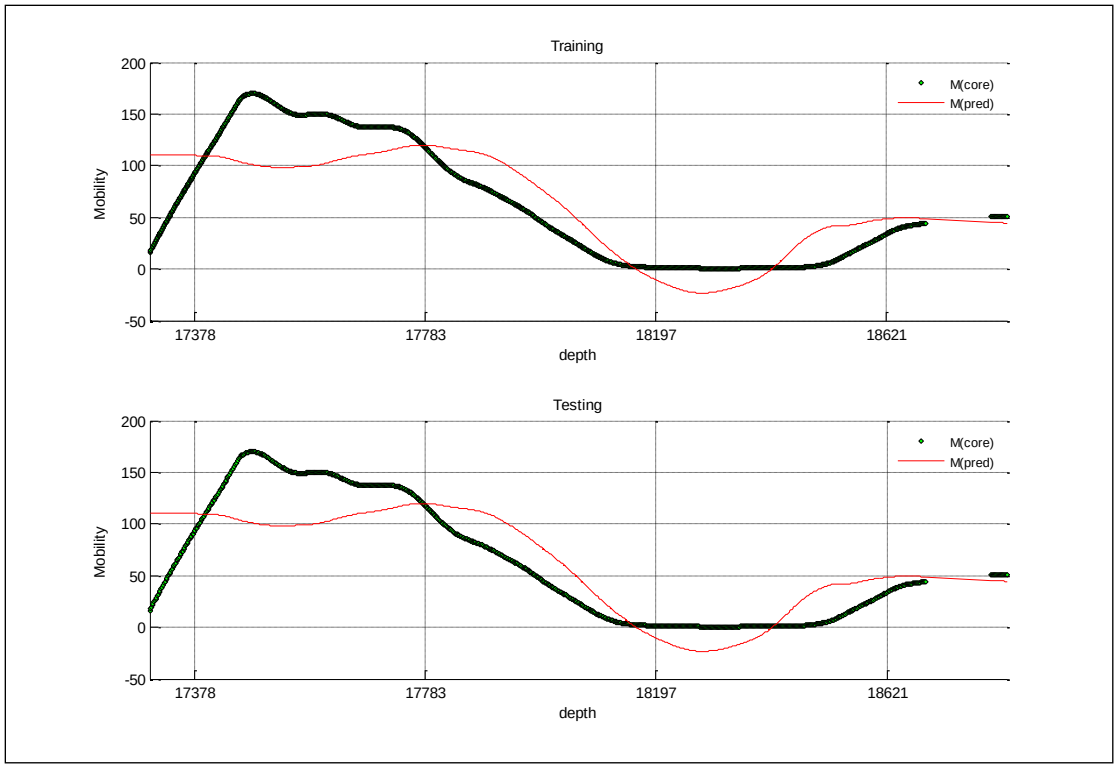

Figure B- 73: Well-8 Method-1, Type-2

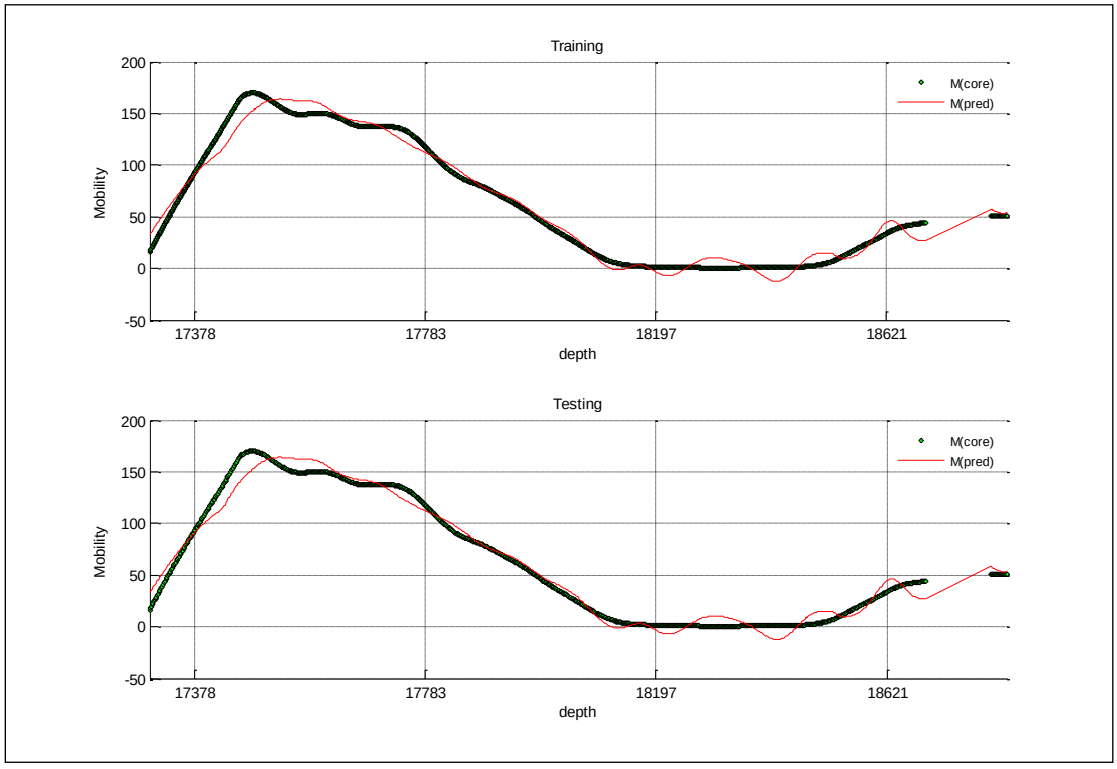

Figure B- 74: Well-8 Method-2, Type-2

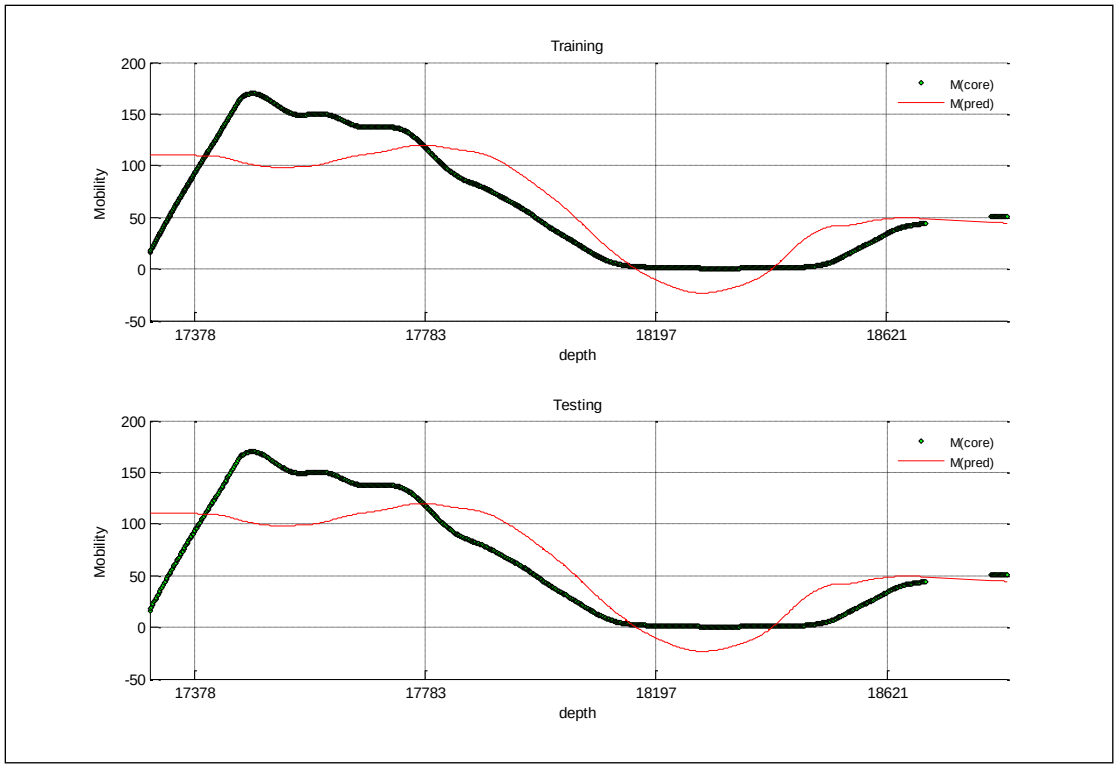

Figure B- 75: Well-8 Method-3, Type-1

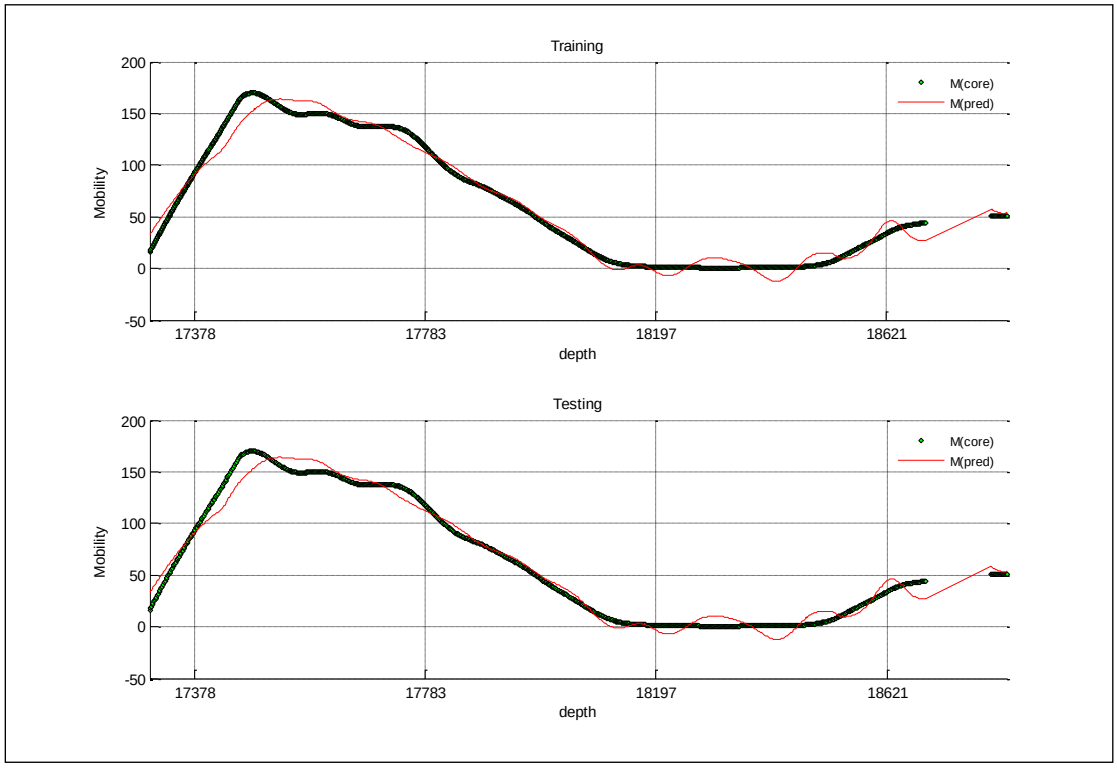

Figure B- 76: Well-8 Method-3, Type-2

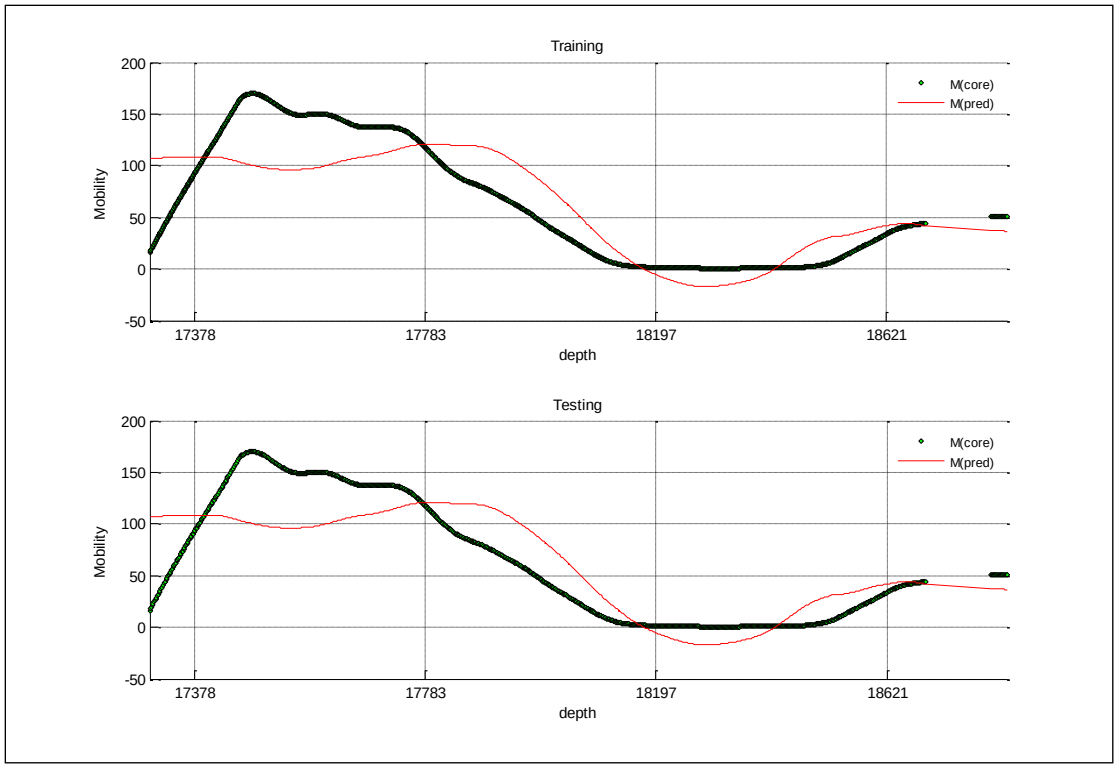

Figure B- 77: Well-8 Method-4, Type-1

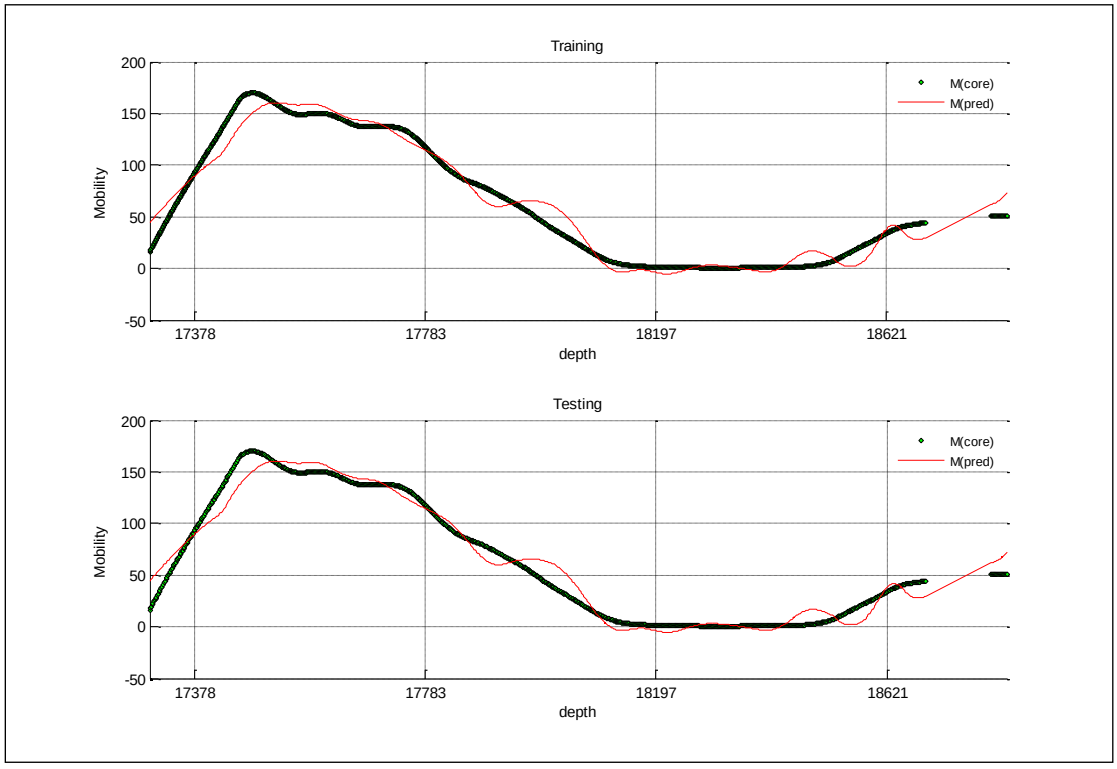

Figure B- 78: Well-8 Method-4, Type-2

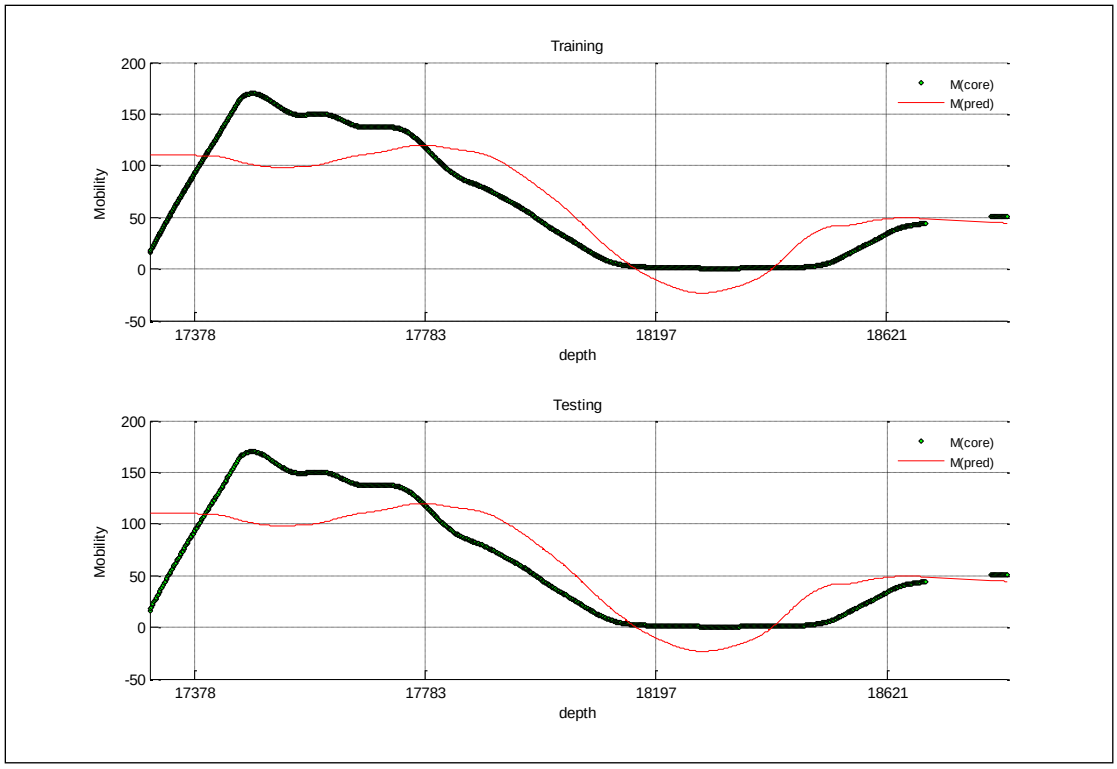

Figure B- 79: Well-8 Method-5, Type-1

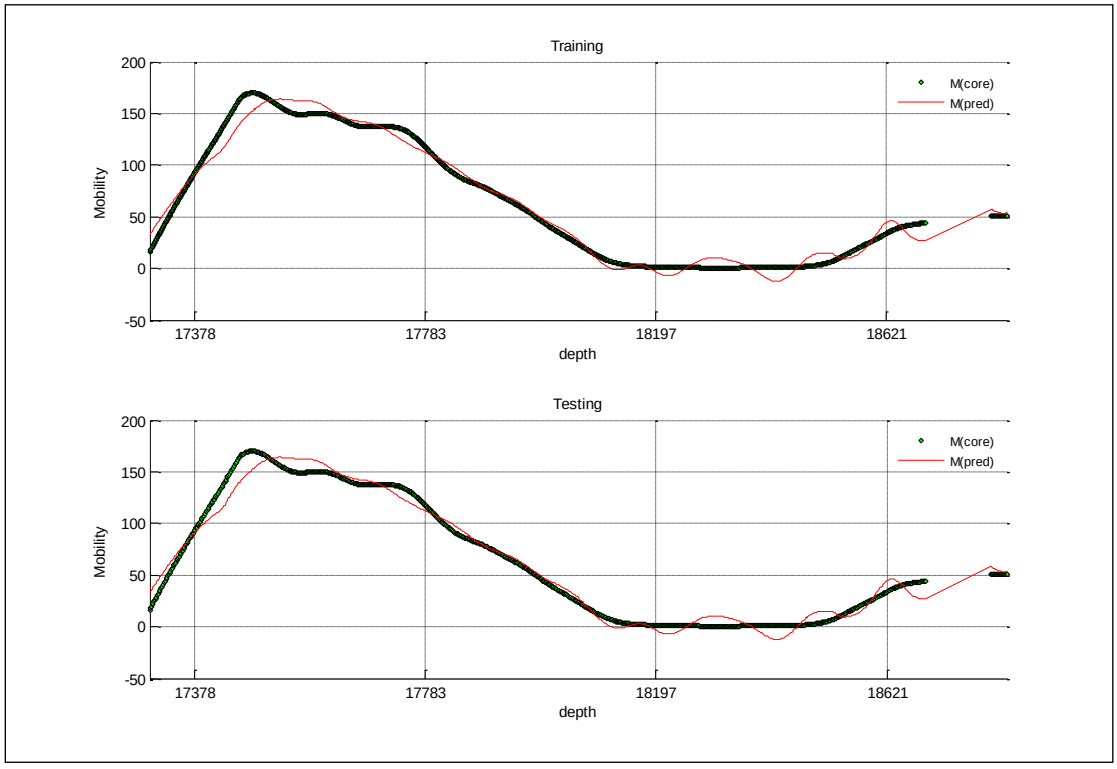

Figure B- 80: Well-8 Method-5, Type-2

Well No. 9

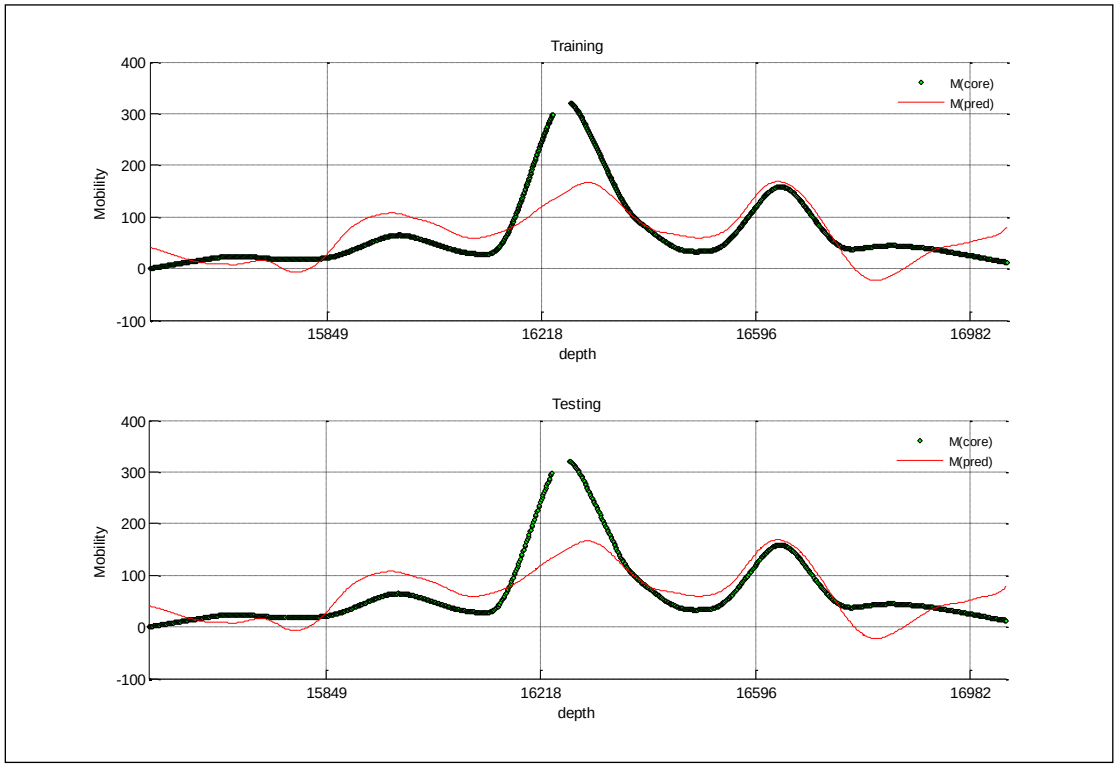

Figure B- 81: Well-9 Method-1, Type-1

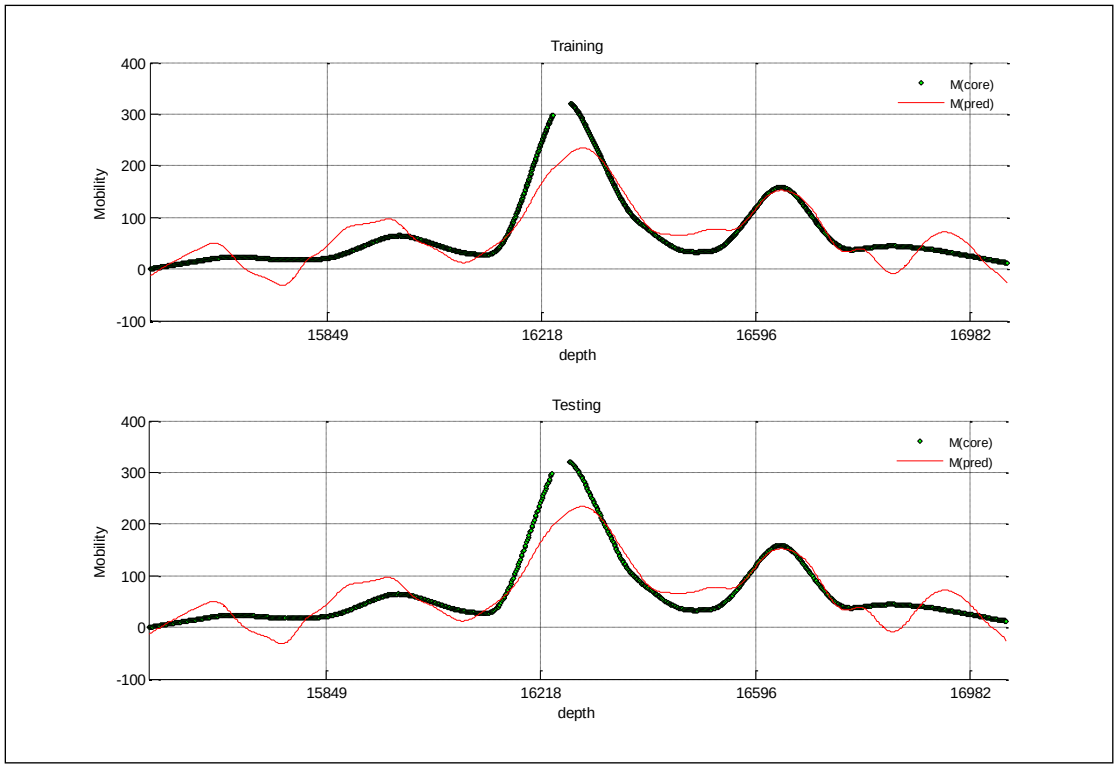

Figure B- 82: Well-9 Method-1, Type-2

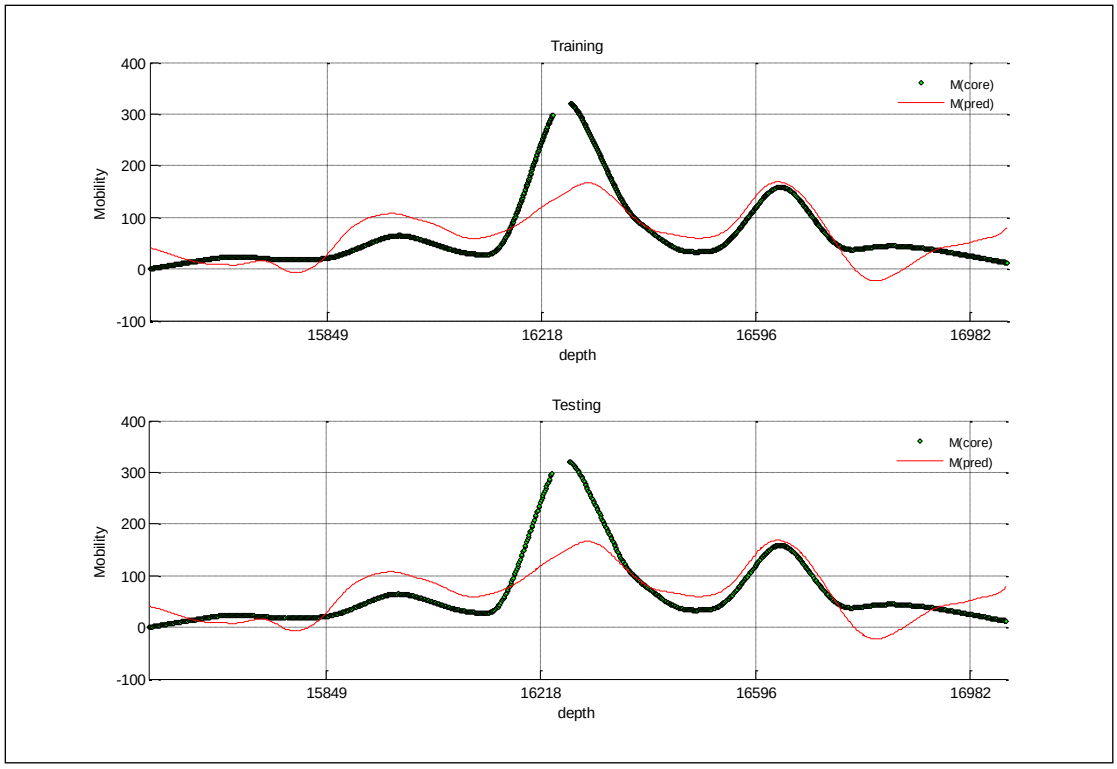

Figure B- 83: Well-9 Method-2, Type-1

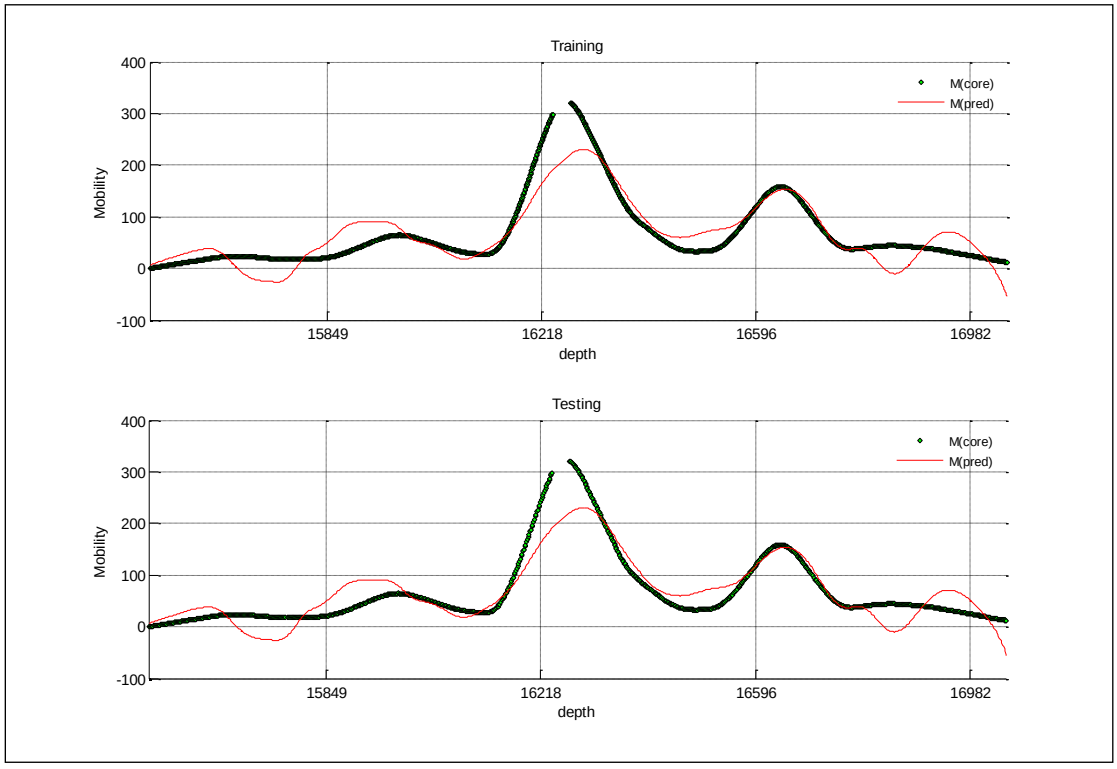

Figure B- 84: Well-9 Method-2, Type-2

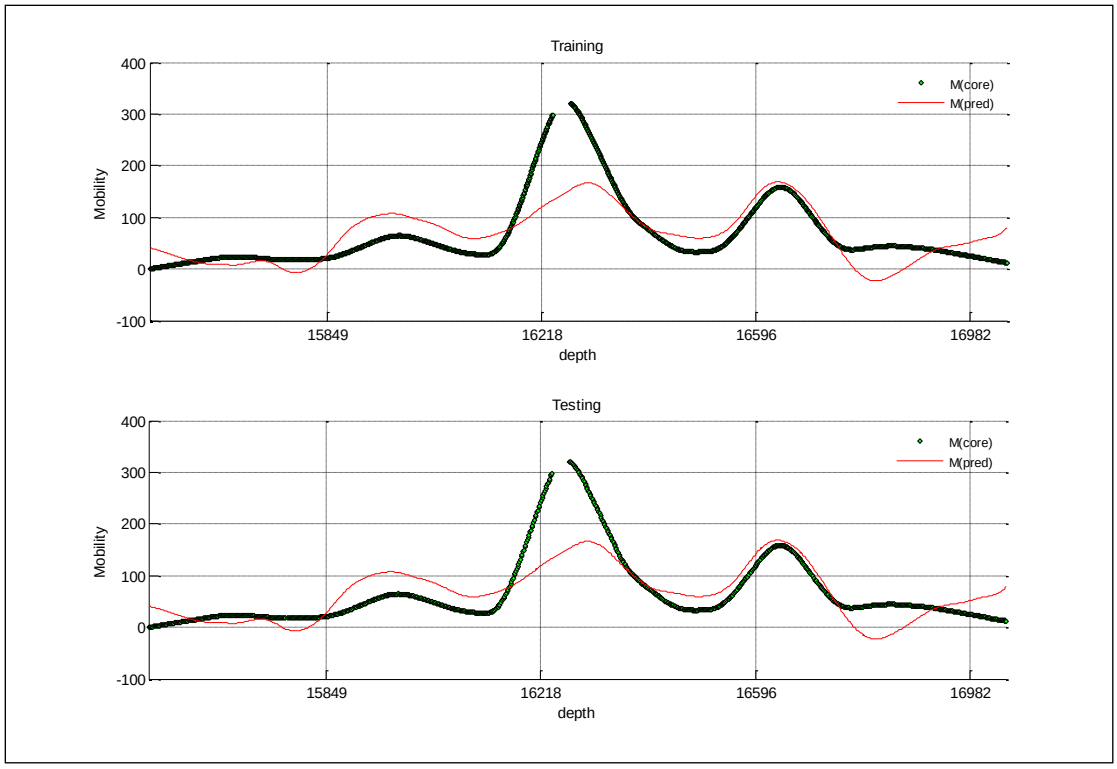

Figure B- 85: Well-9 Method-3, Type-1

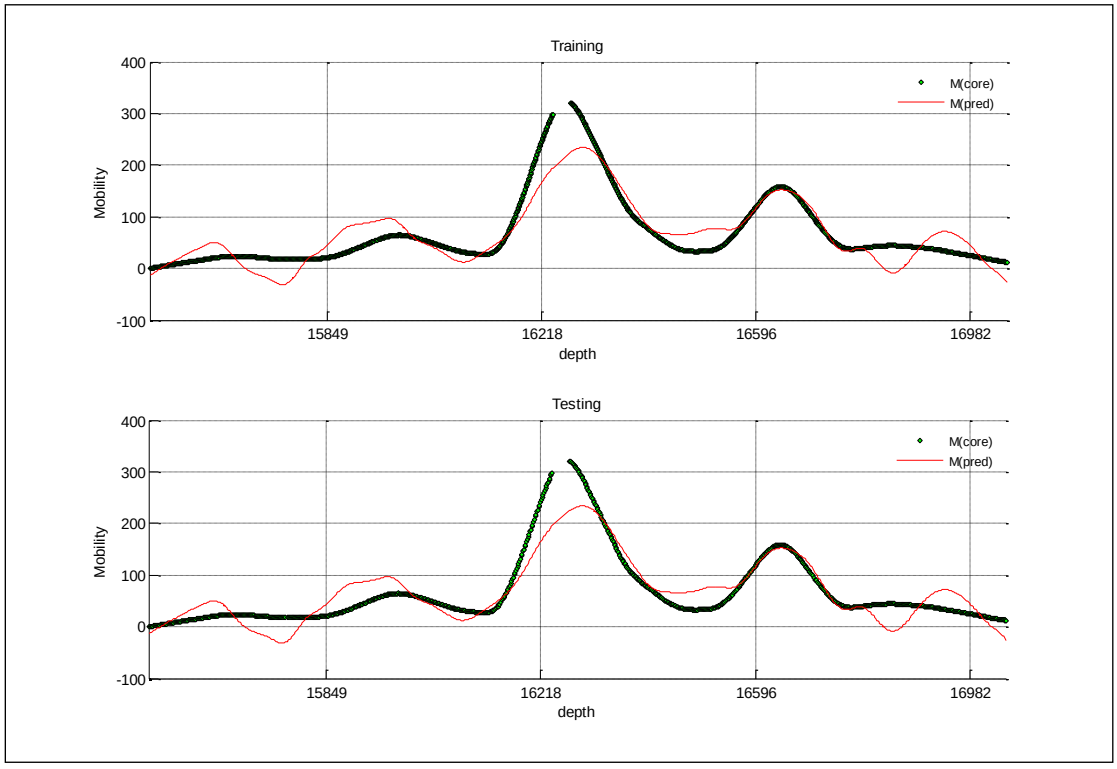

Figure B- 86: Well-9 Method-3, Type-2

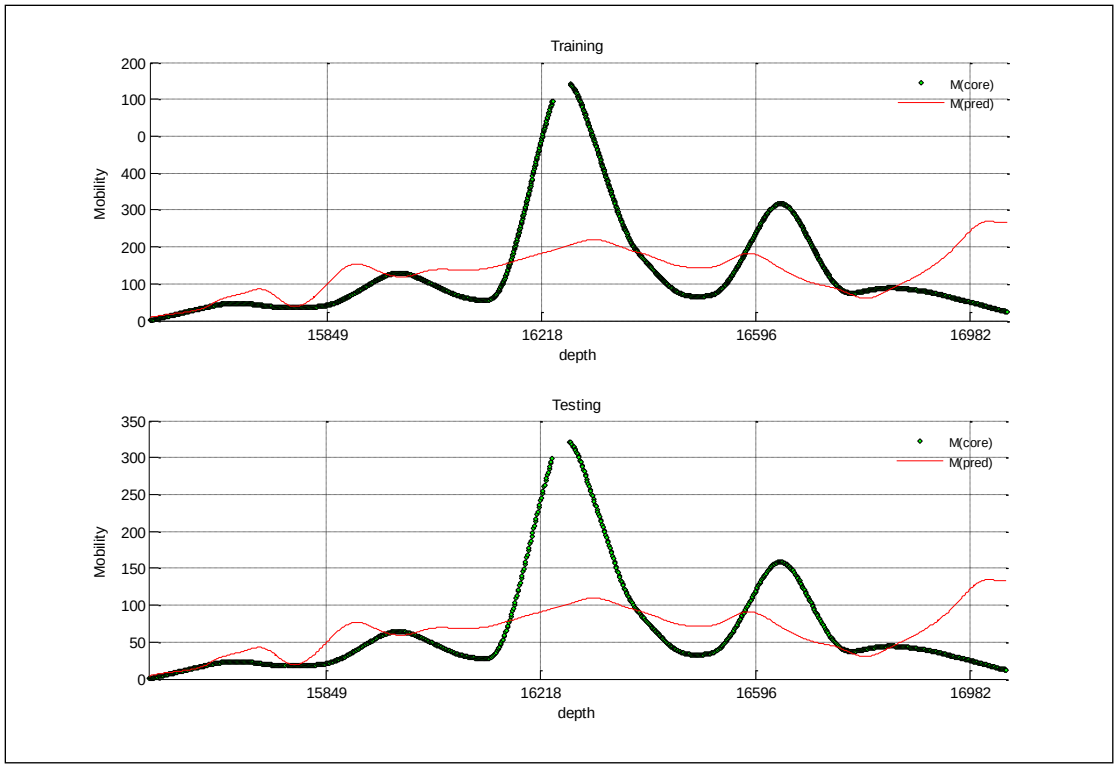

Figure B- 87: Well-9 Method-4, Type-1

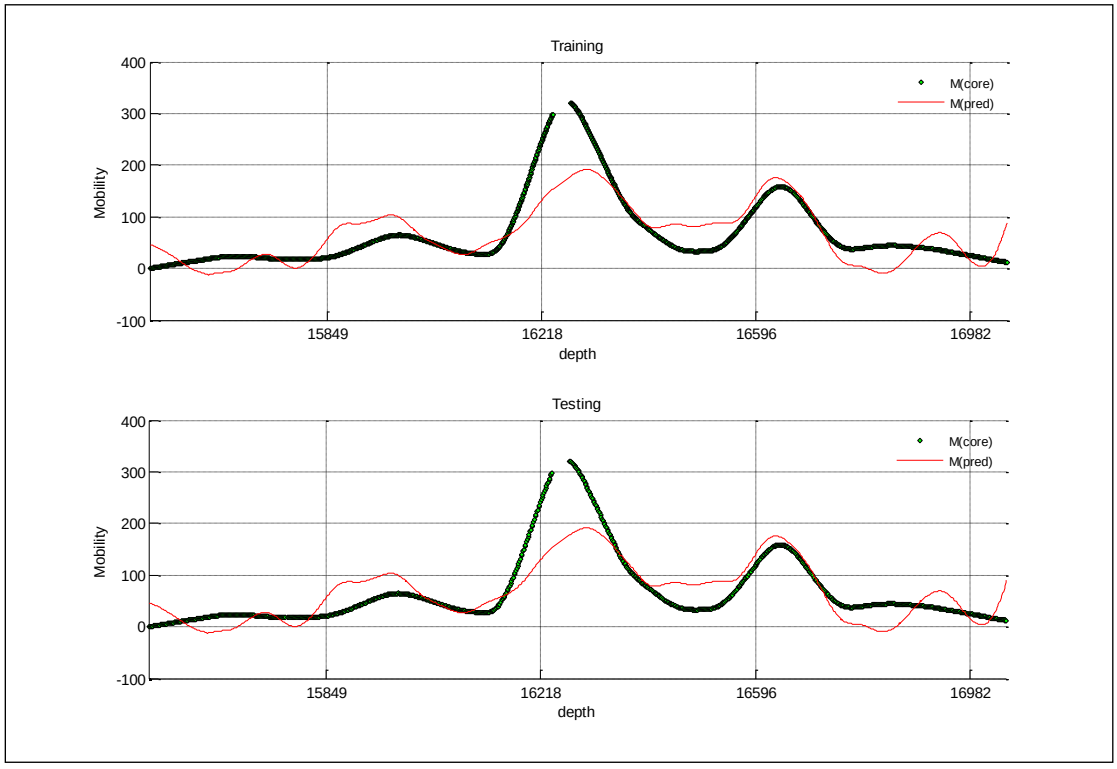

Figure B- 88: Well-9 Method-4, Type-2

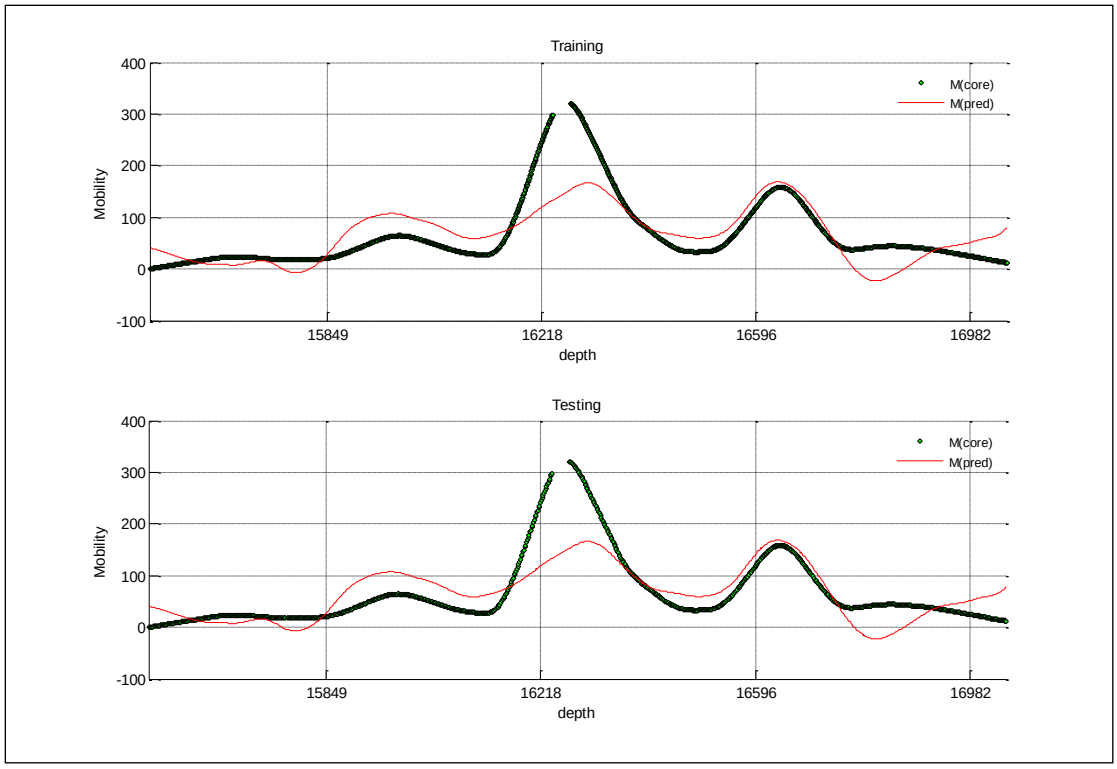

Figure B- 89: Well-9 Method-5, Type-1

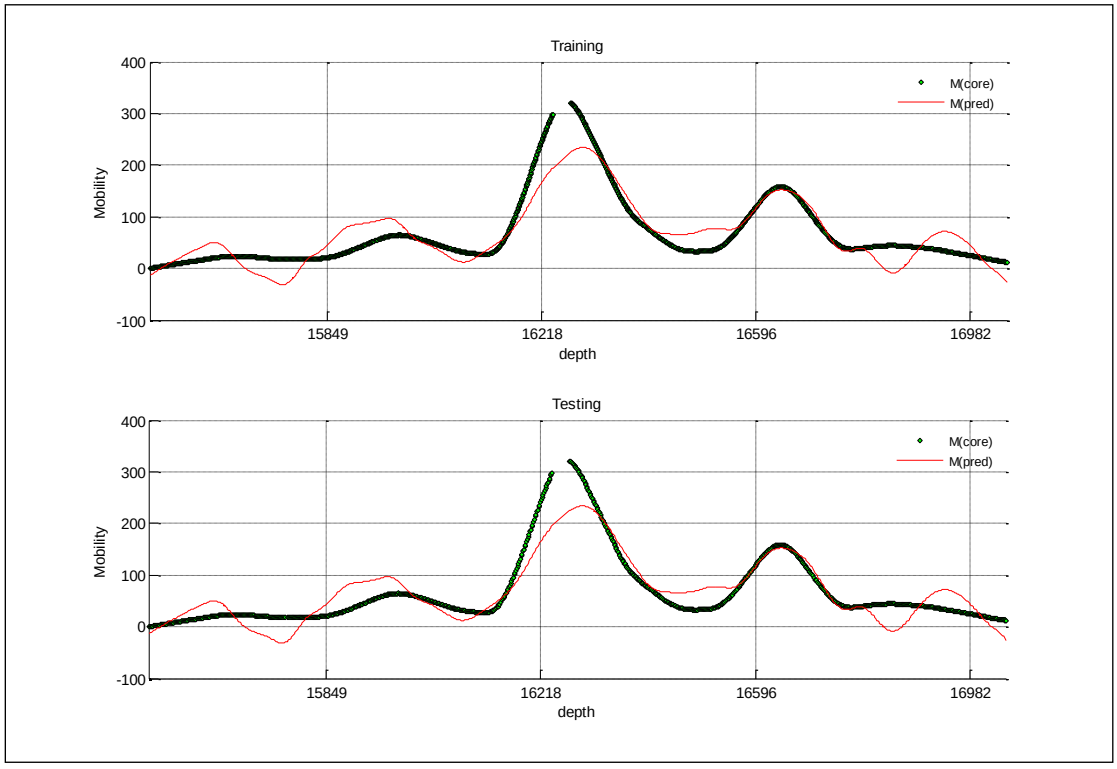

Figure B- 90: Well-9 Method-5, Type-2

Well No. 10

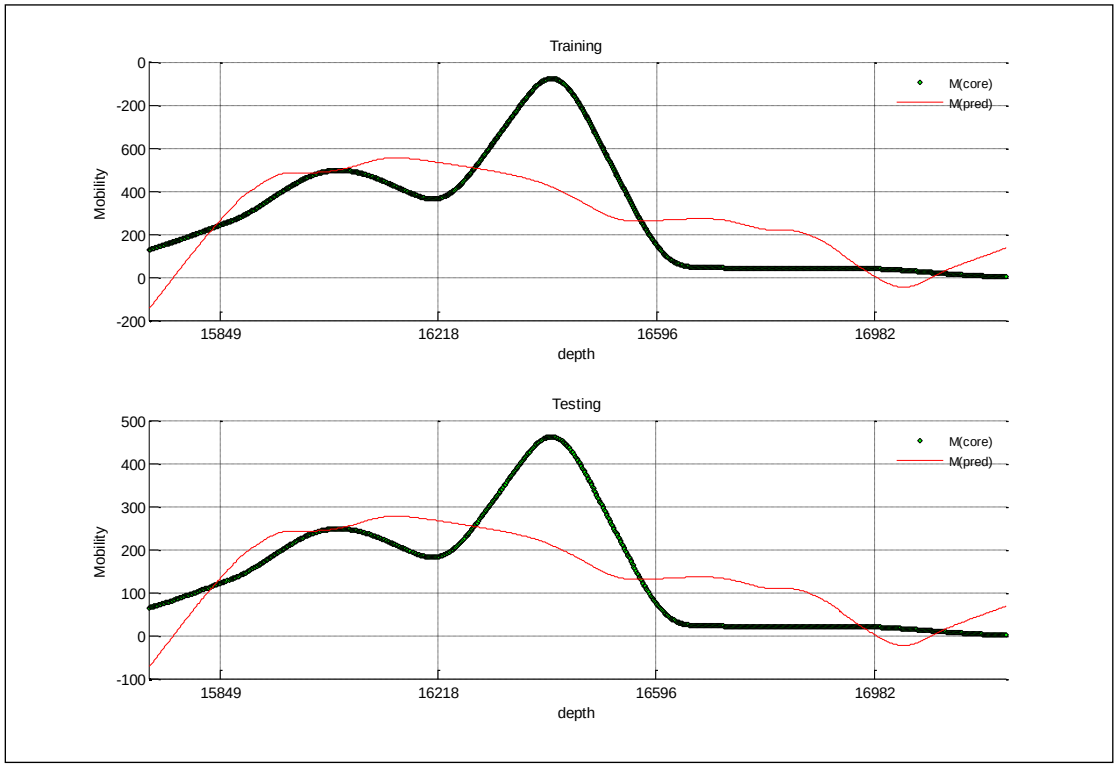

Figure B- 91: Well-10 Method-1, Type-1

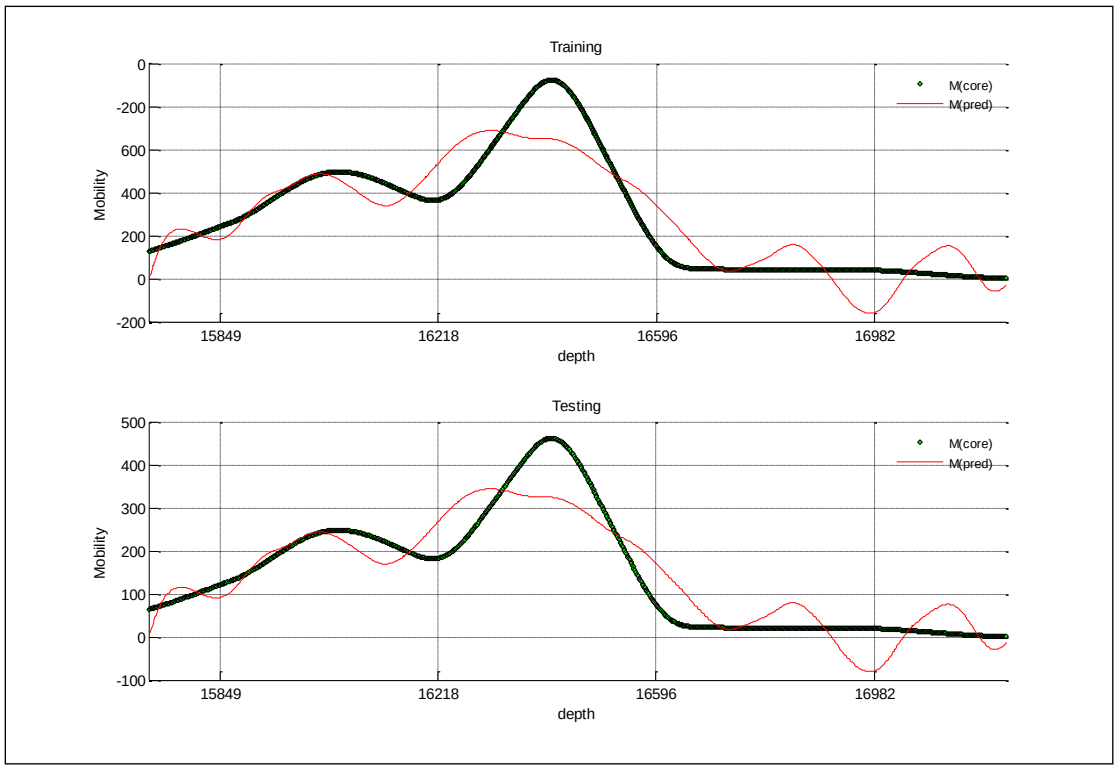

Figure B- 92: Well-10 Method-1, Type-2

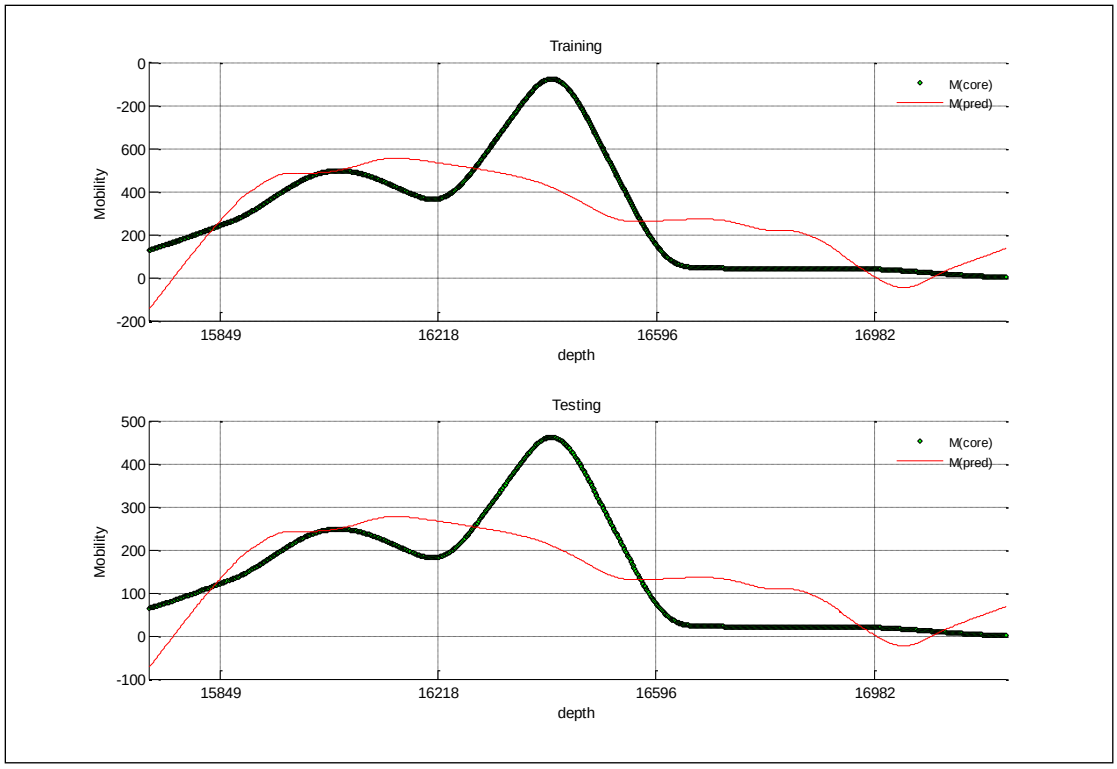

Figure B- 93: Well-10 Method-2, Type-1

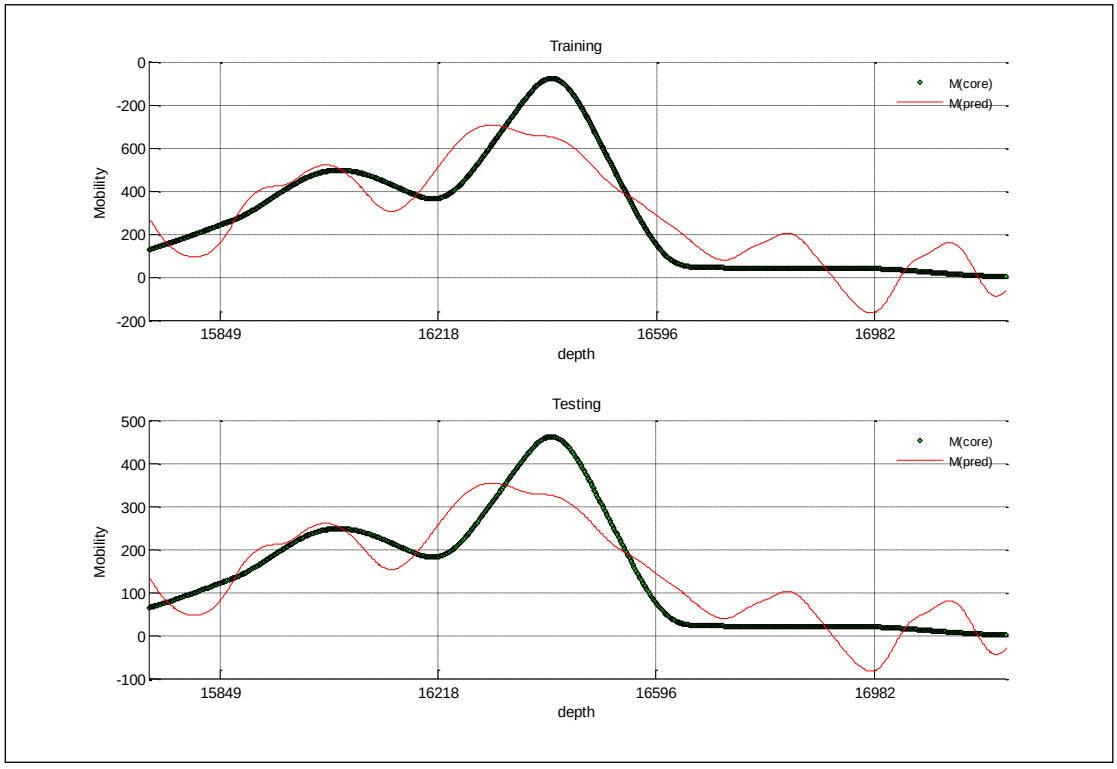

Figure B- 94: Well-10 Method-2, Type-2

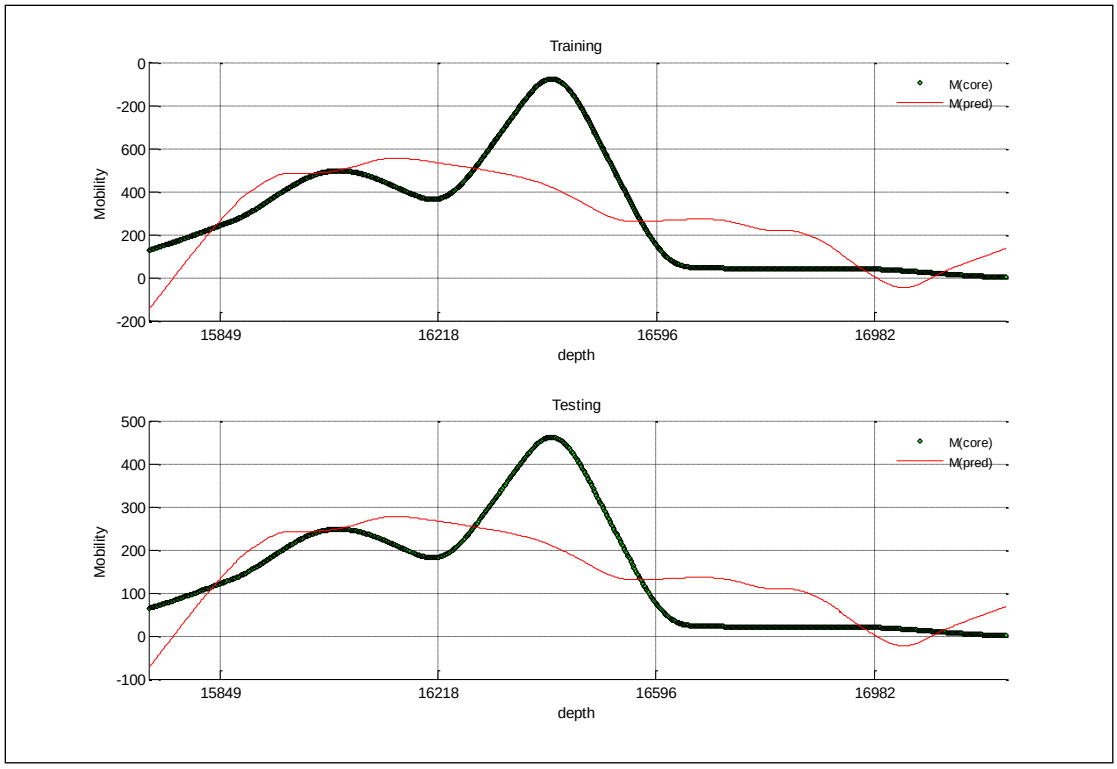

Figure B- 95: Well-10 Method-3, Type-1

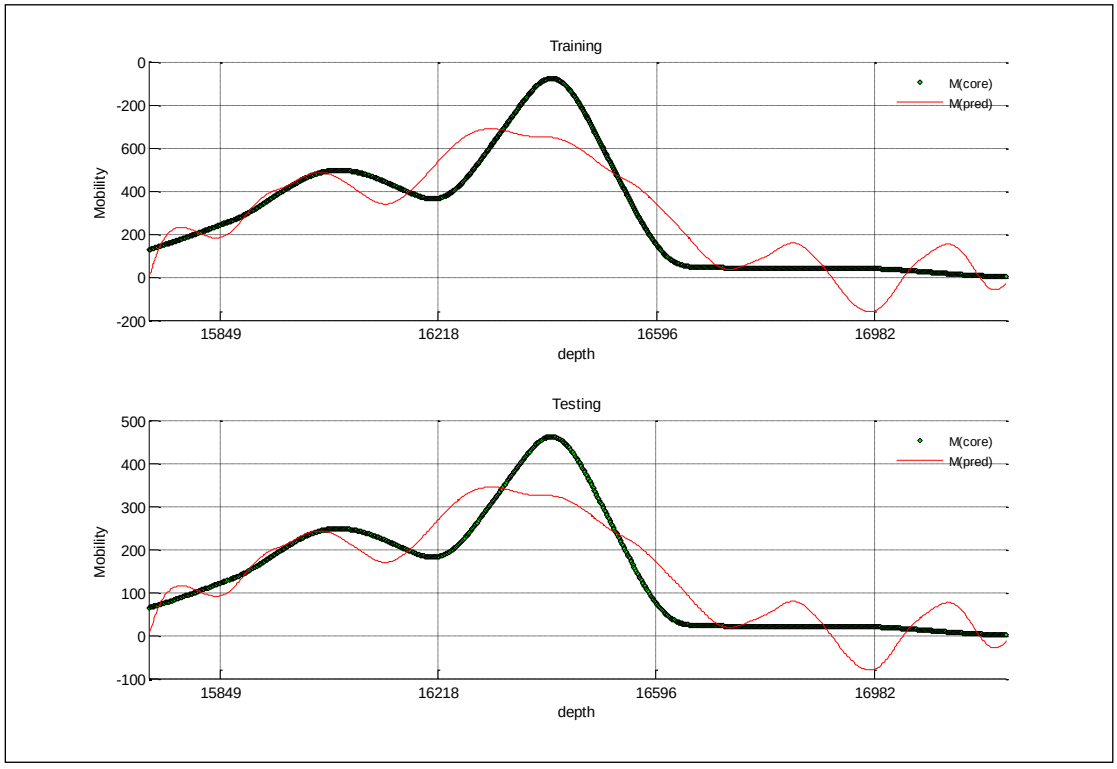

Figure B- 96: Well-10 Method-3, Type-2

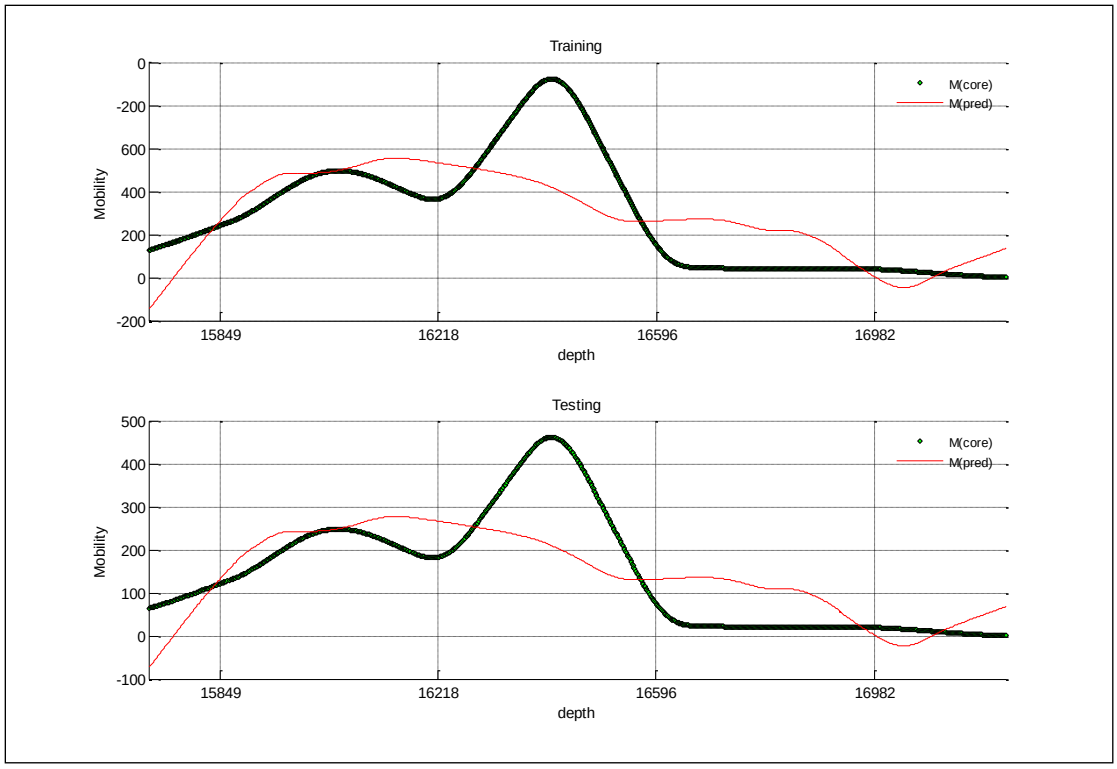

Figure B- 97: Well-10 Method-4, Type-1

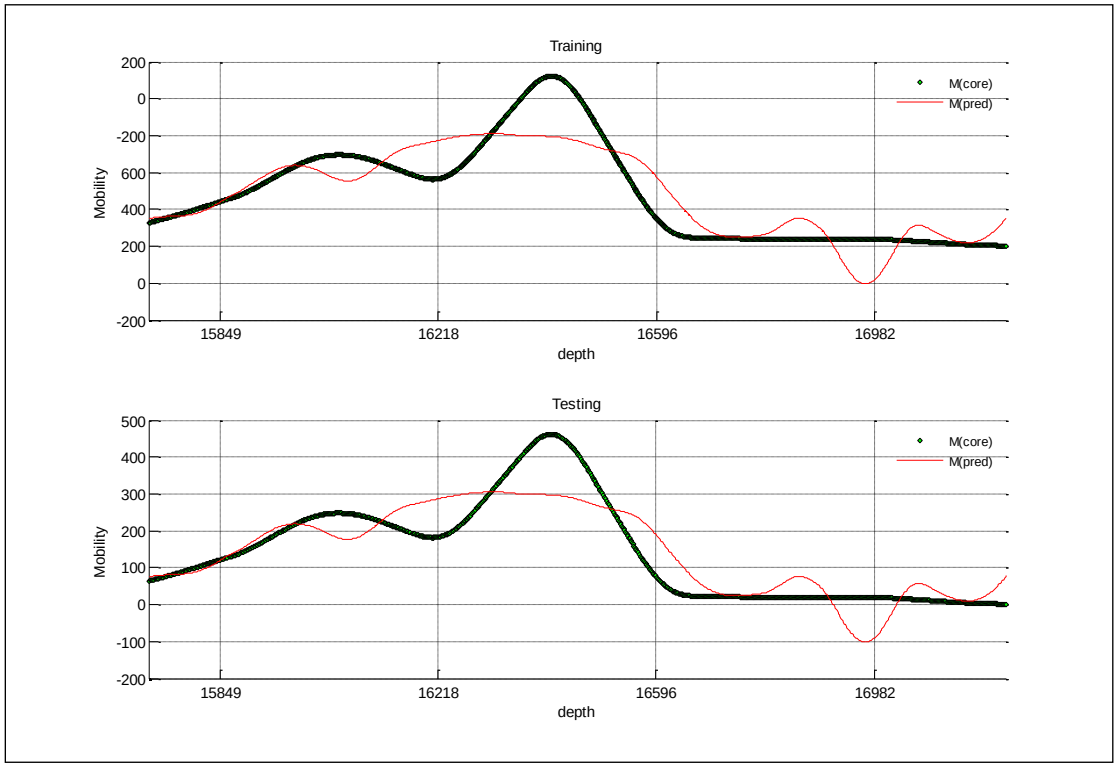

Figure B- 98: Well-10 Method-4, Type-2

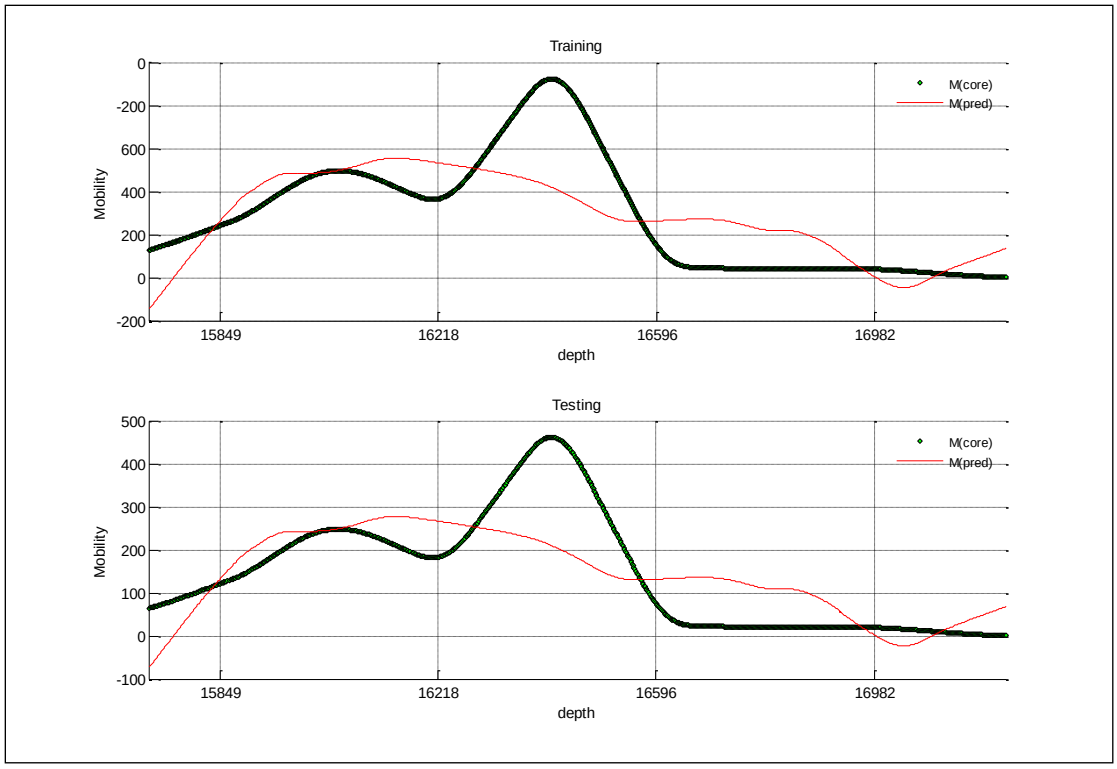

Figure B- 99: Well-10 Method-5, Type-1

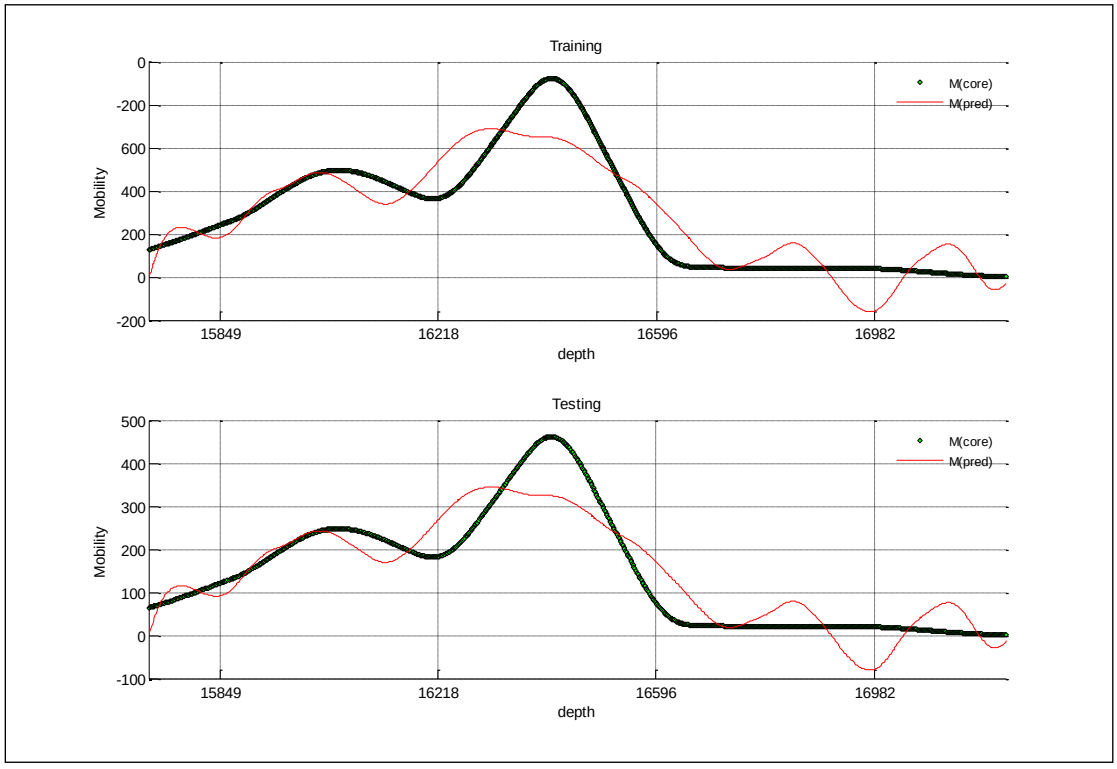

Figure B- 100: Well-10 Method-5, Type-2

APPENDIX C

SUPPORT VECTOR MACHINE (SVM) RESULTS SUMMARY

This appendix is showing all the SVM graphical plots of the actual verses the predicted outputs of all the ten wells under four different kernels.

KERNELS USED

- GAUSSIAN
- POLY
- POLYHOMOG
- JCB

Results

Well No. 1

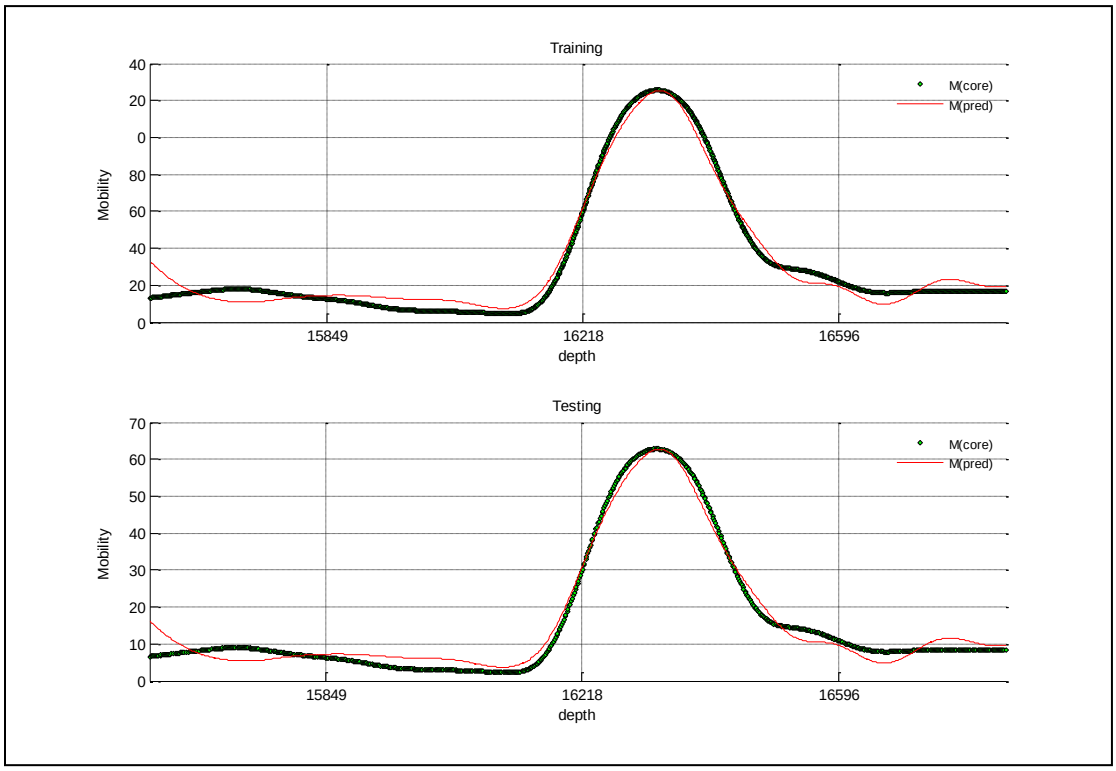

Figure C- 1: Well-1 Gaussian Kernel

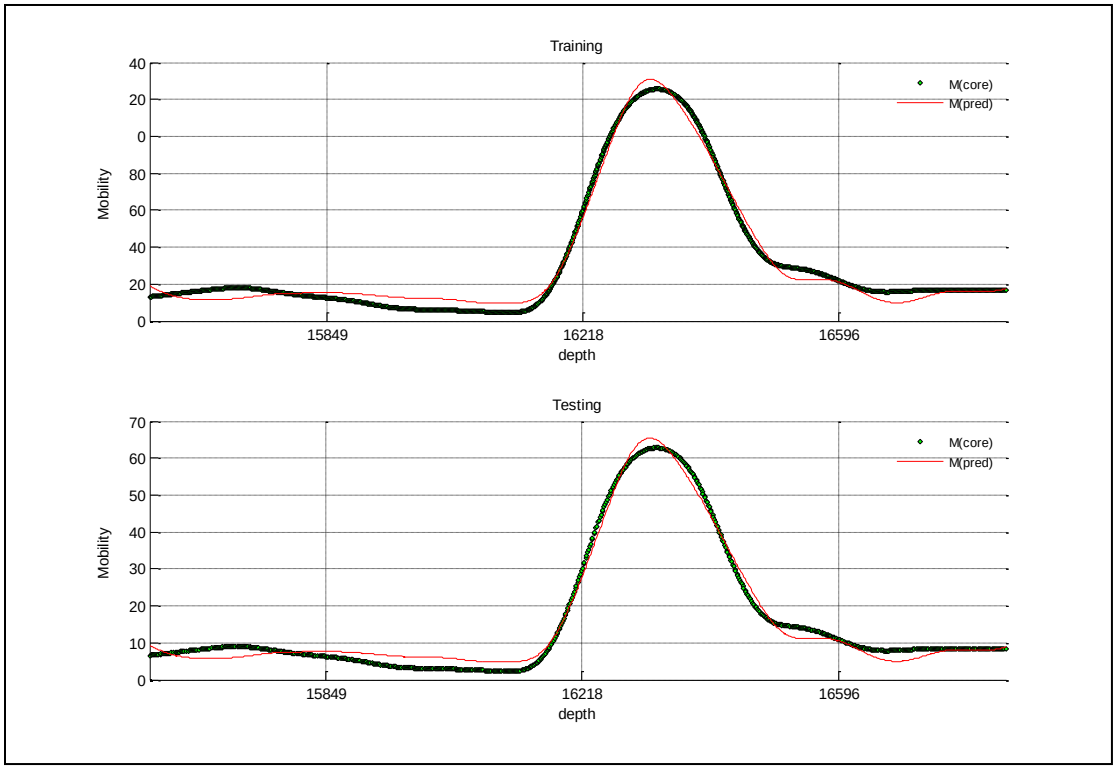

Figure C- 2: Well-1 Poly Kernel

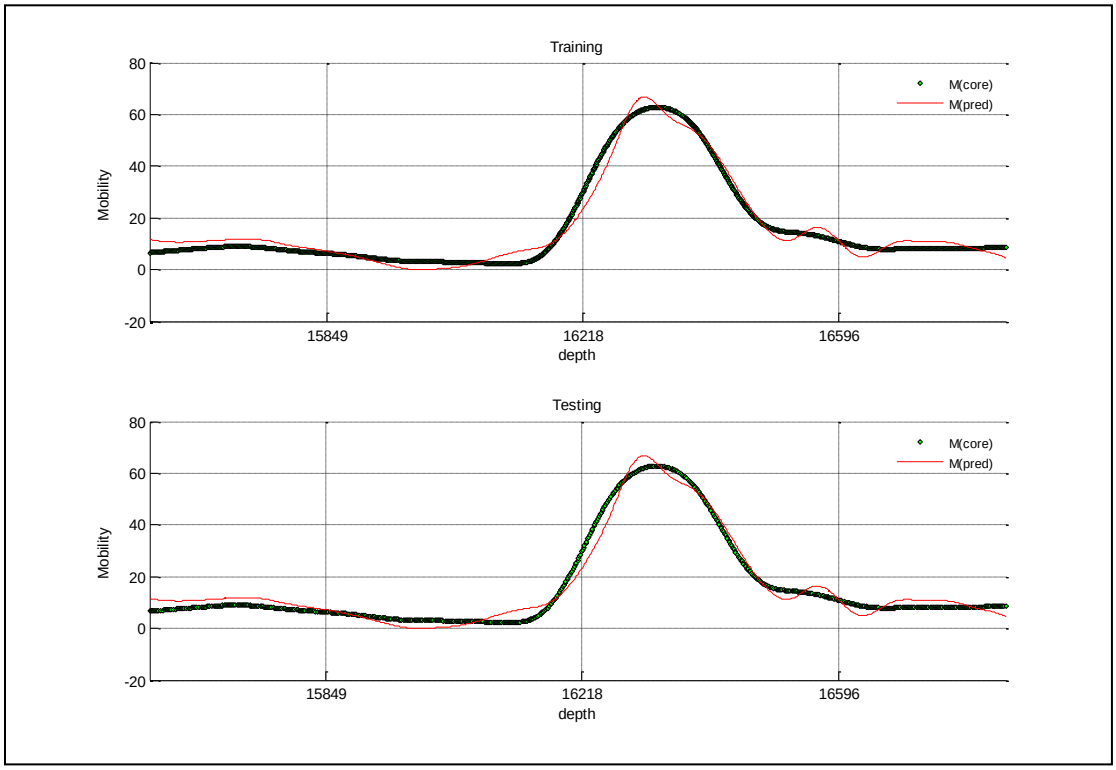

Figure C- 3: Well-1 Polyhomog Kernel

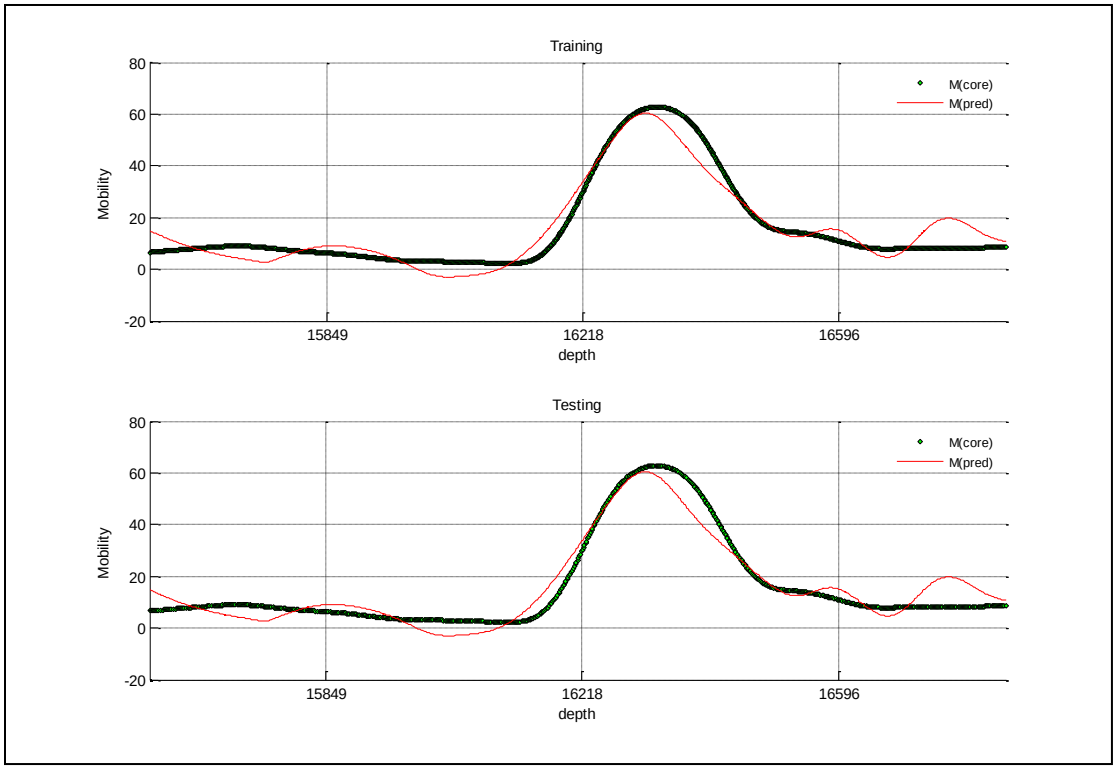

Figure C- 4: Well-1 jcb Kernel

Well No. 2

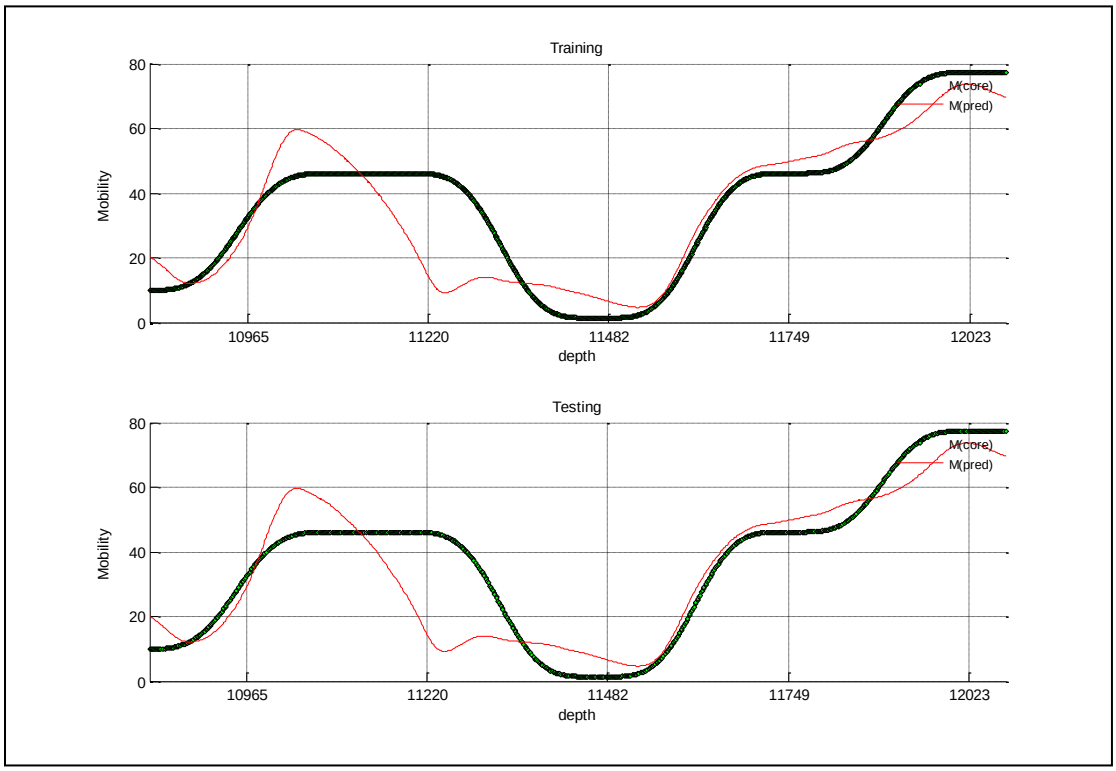

Figure C- 5: Well-2 Gaussian Kernel

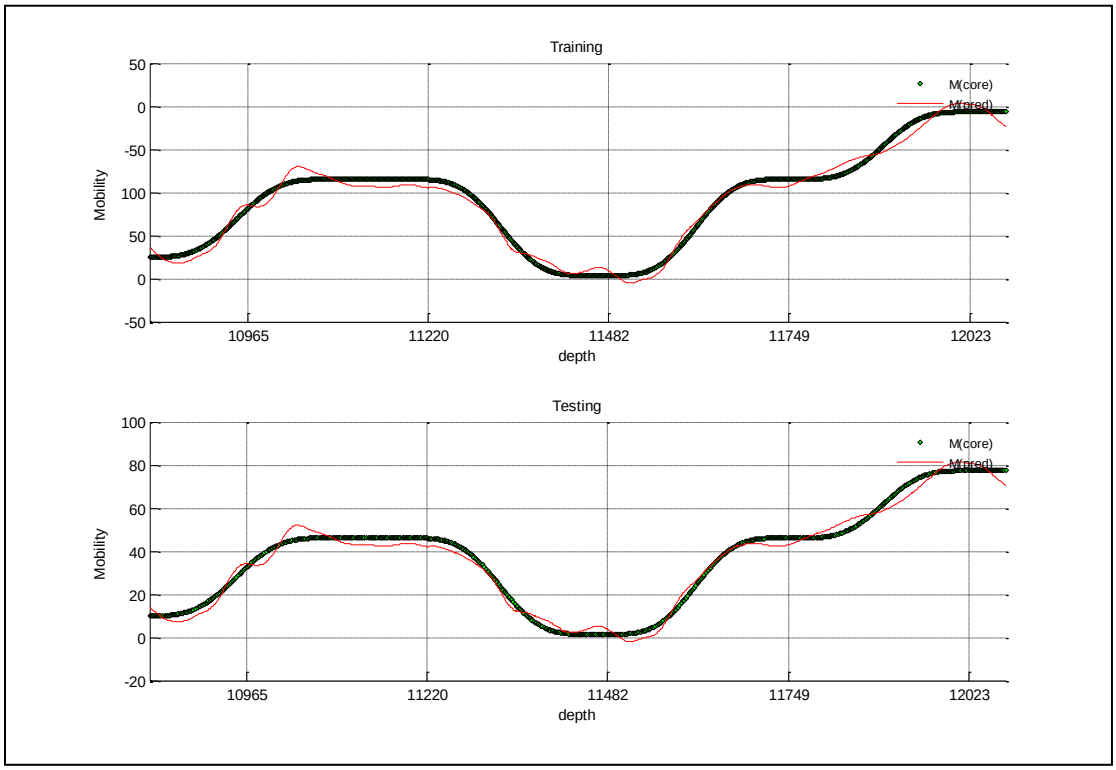

Figure C- 6: Well-2 Poly Kernel

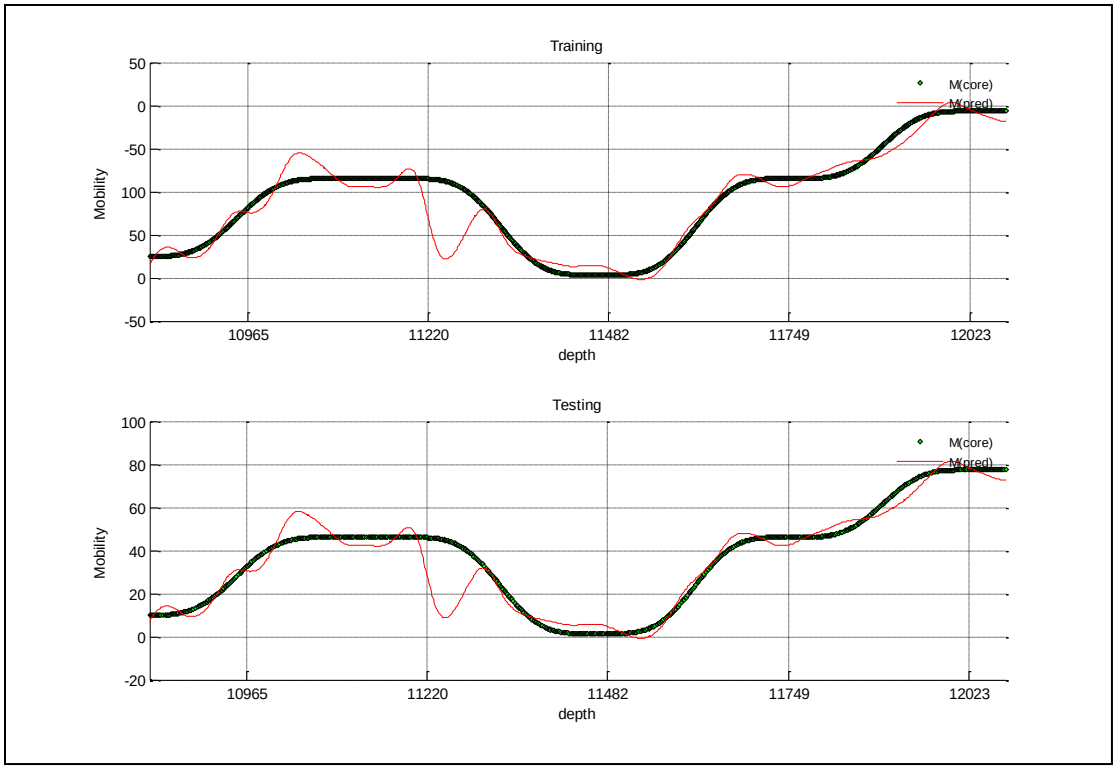

Figure C- 7: Well-2 Polyhomog Kernel

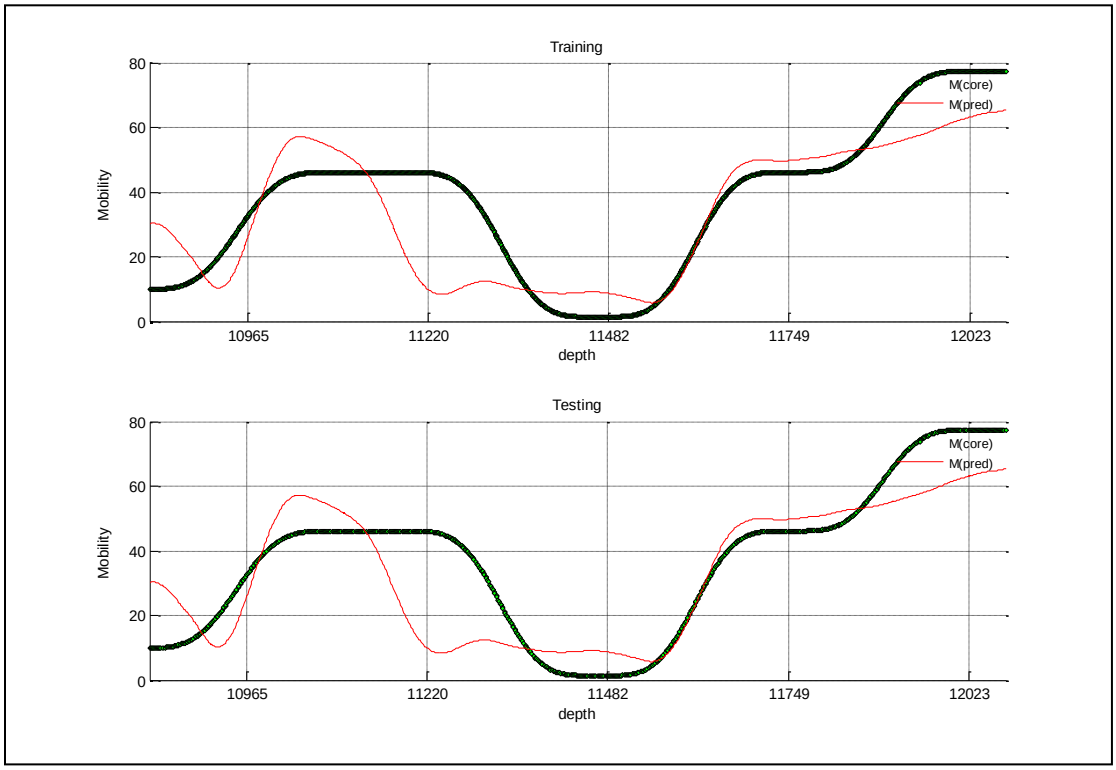

Figure C- 8: Well-2 jcb Kernel

Well No. 3

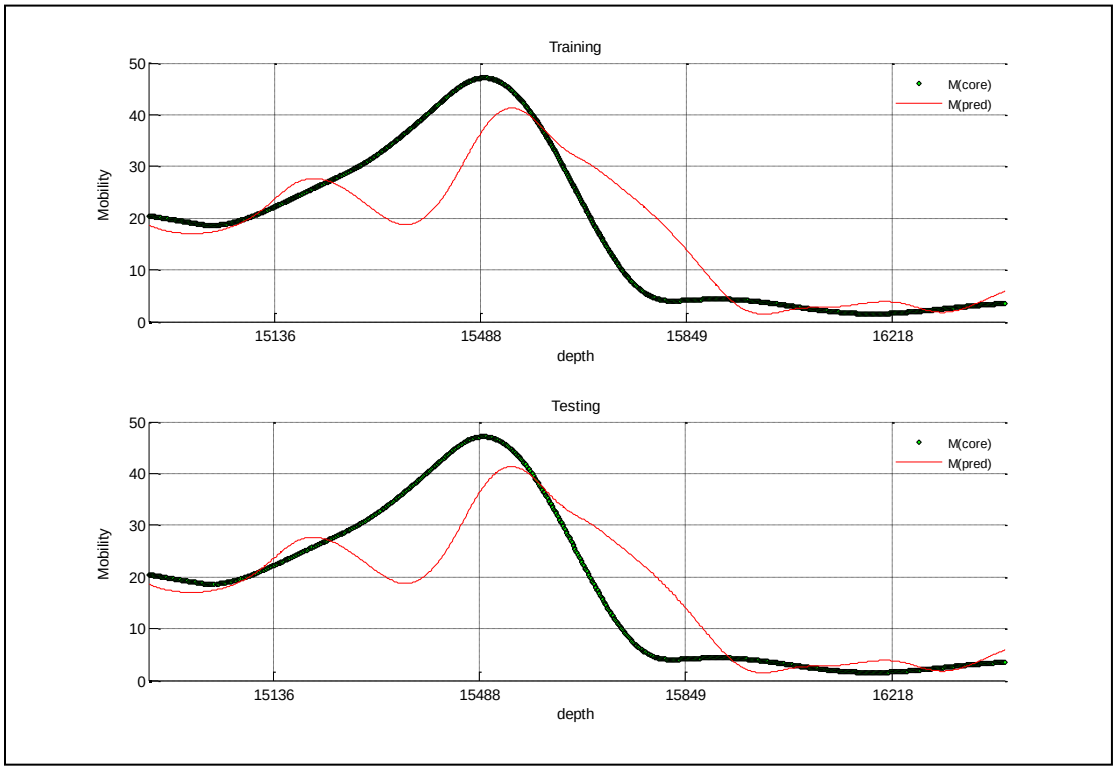

Figure C- 9: Well-3 Gaussian Kernel

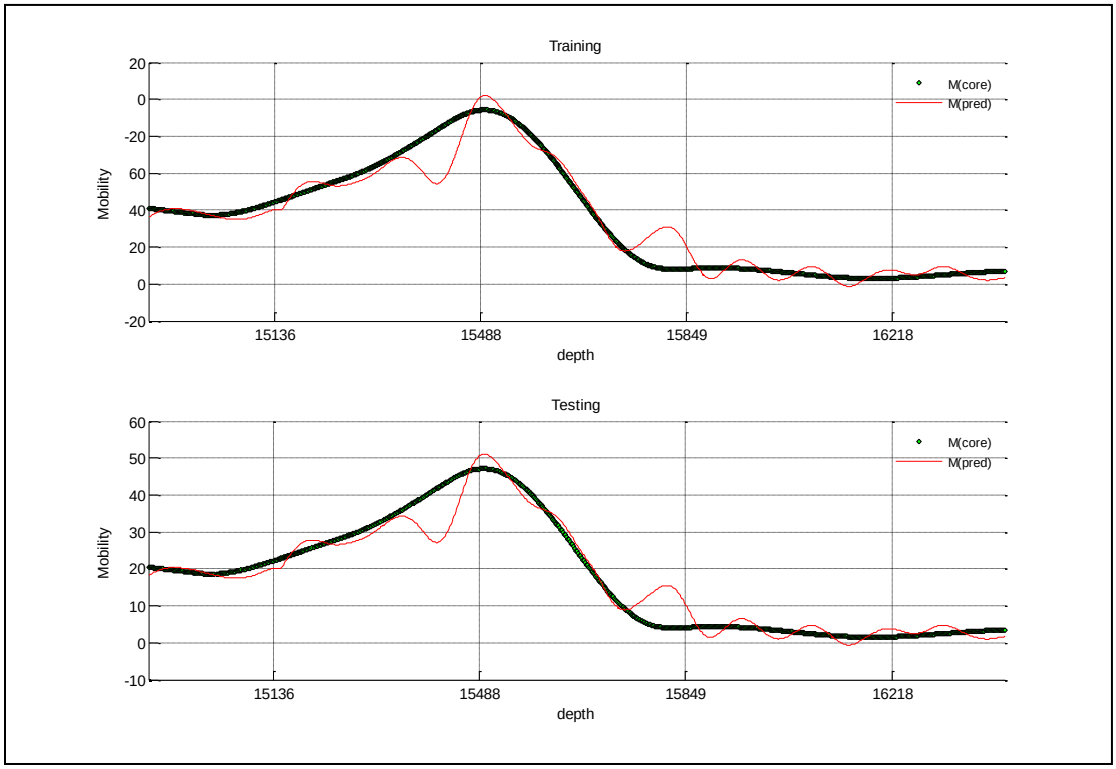

Figure C- 10: Well-3 Poly Kernel

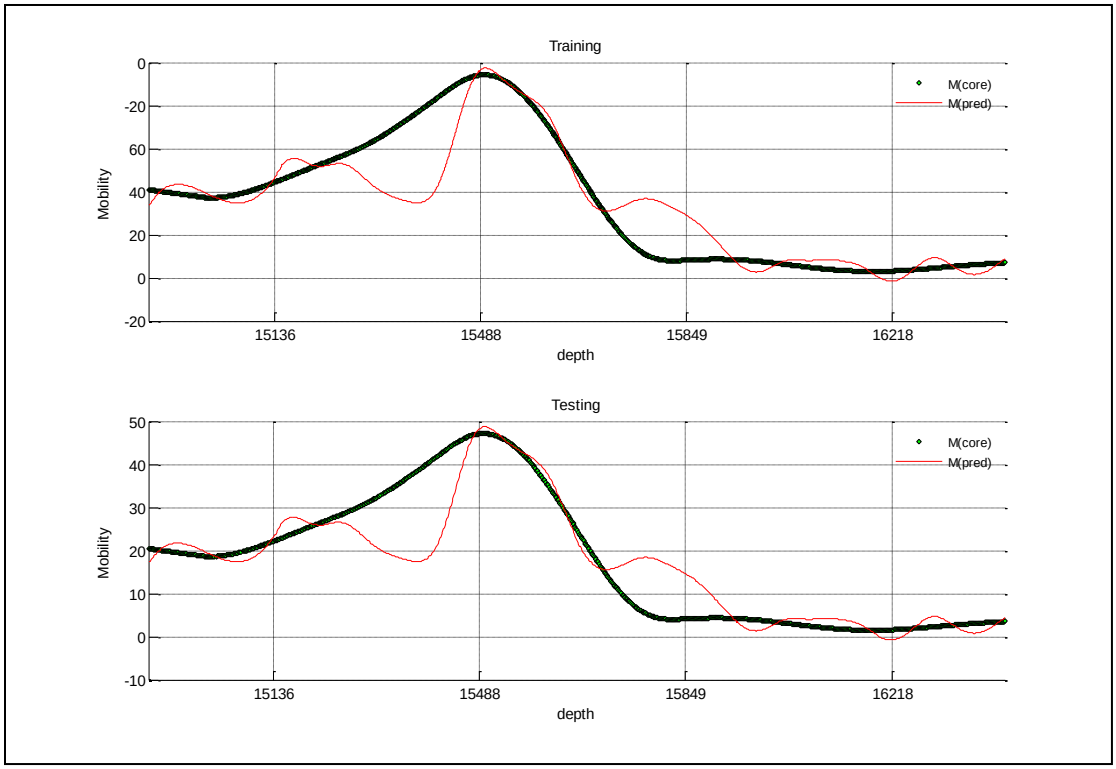

Figure C- 11: Well-3 Polyhomog Kernel

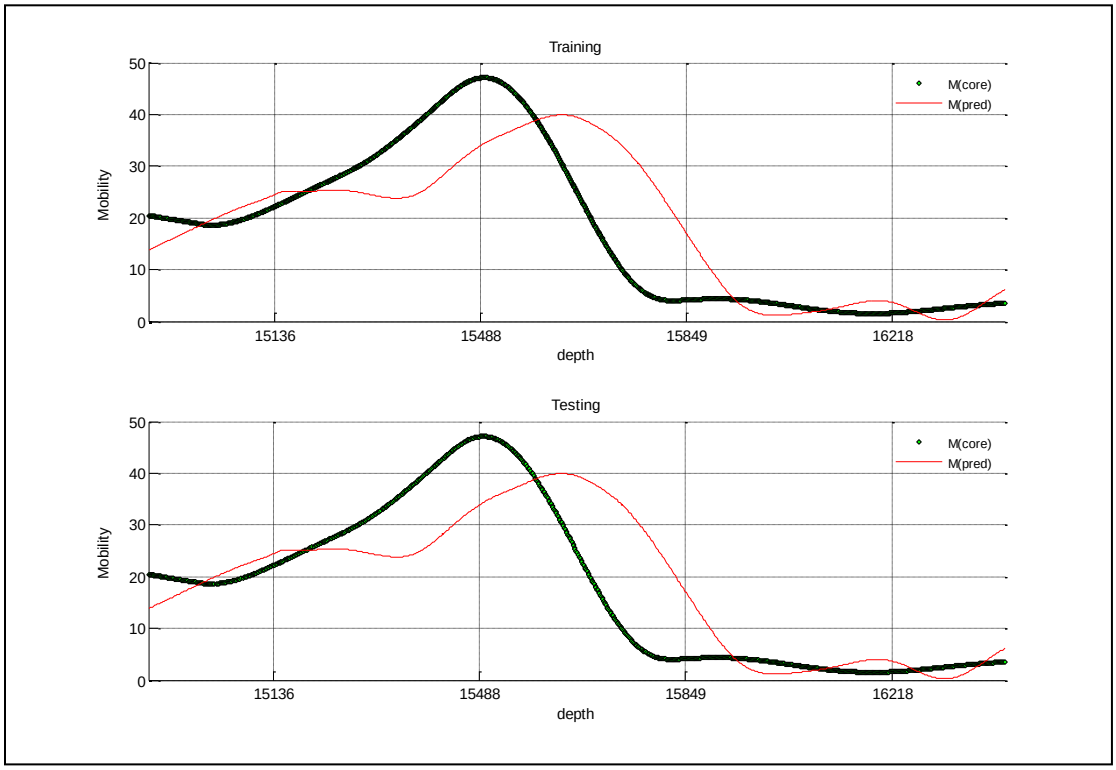

Figure C- 12: Well-3 jcb Kernel

Well No. 4

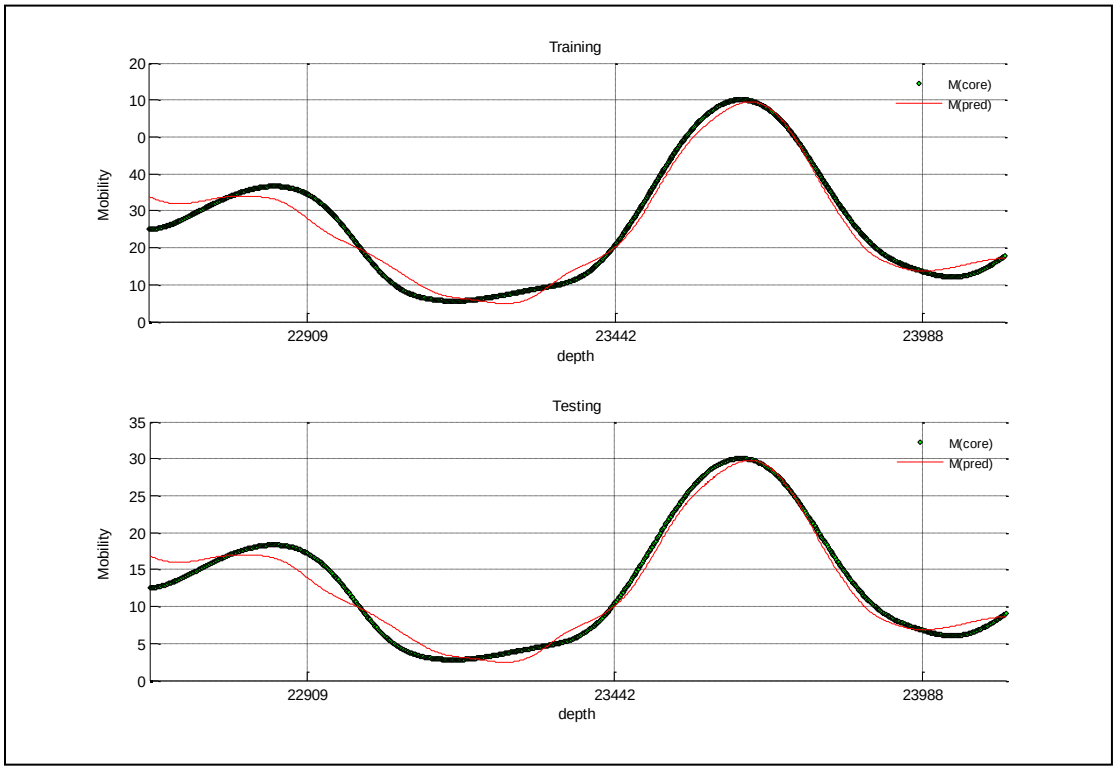

Figure C- 13: Well-4 Gaussian Kernel

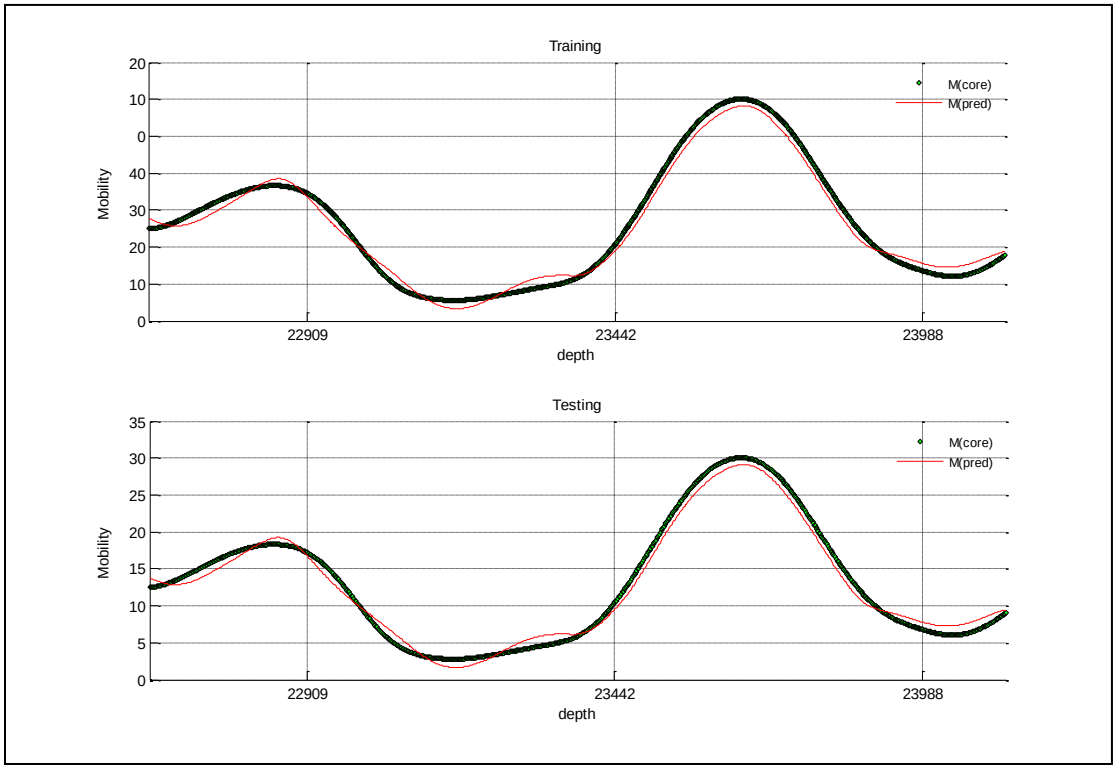

Figure C- 14: Well-4 Poly Kernel

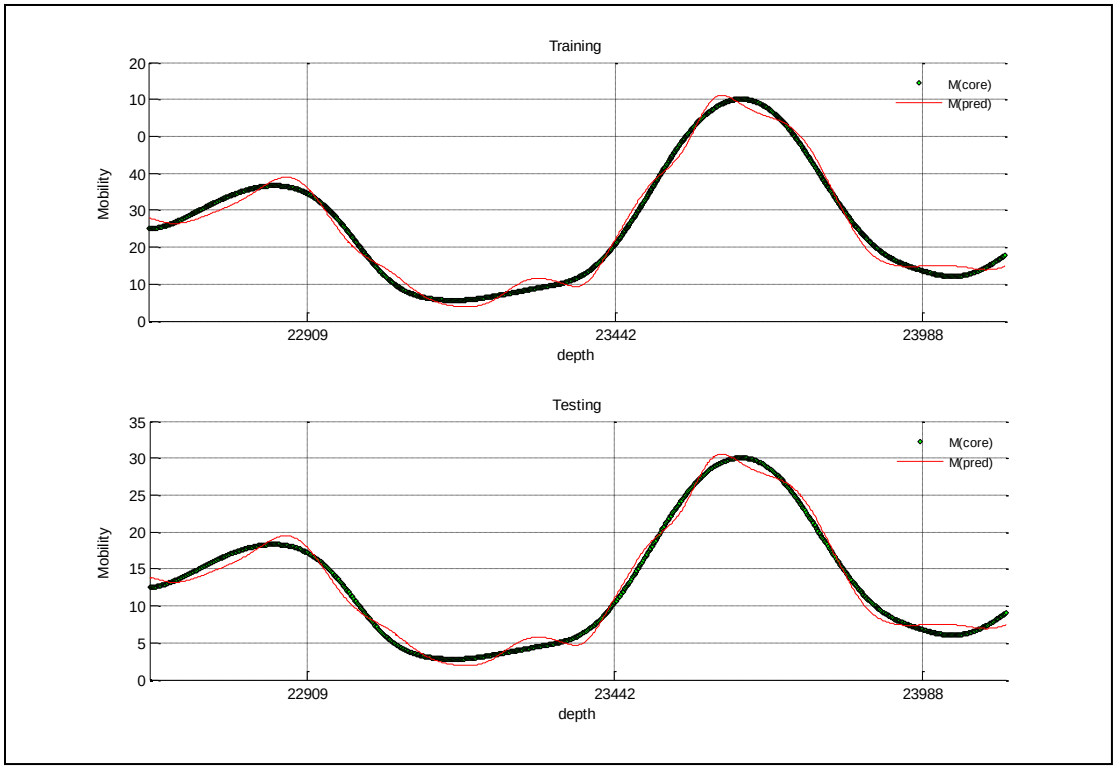

Figure C- 15: Well-4 Polyhomog Kernel

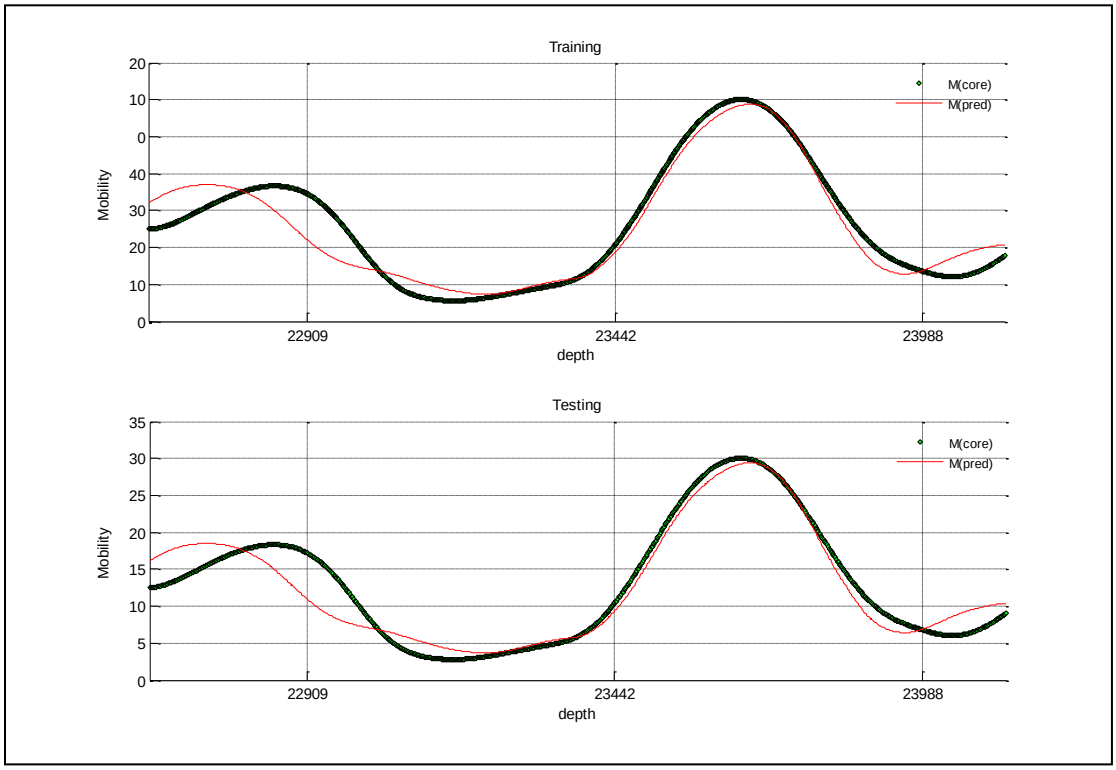

Figure C- 16: Well-4 jcb Kernel

Well No. 5

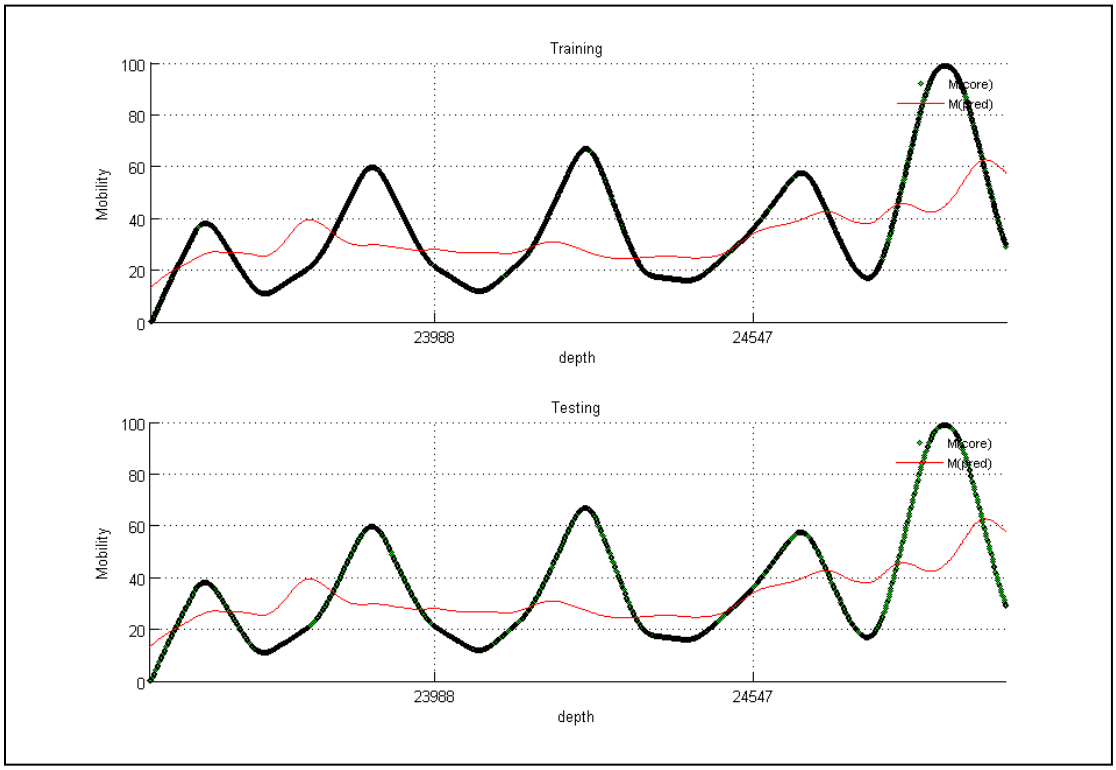

Figure C- 17: Well-5 Gaussian Kernel

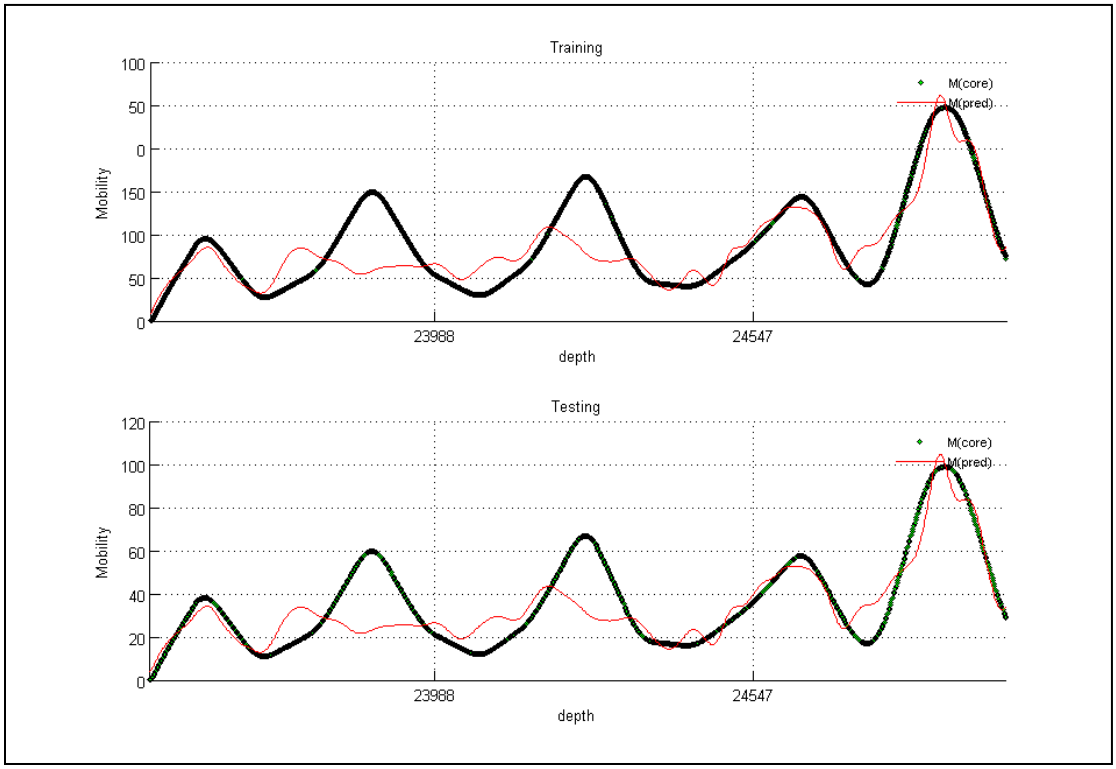

Figure C- 18: Well-5 Poly Kernel

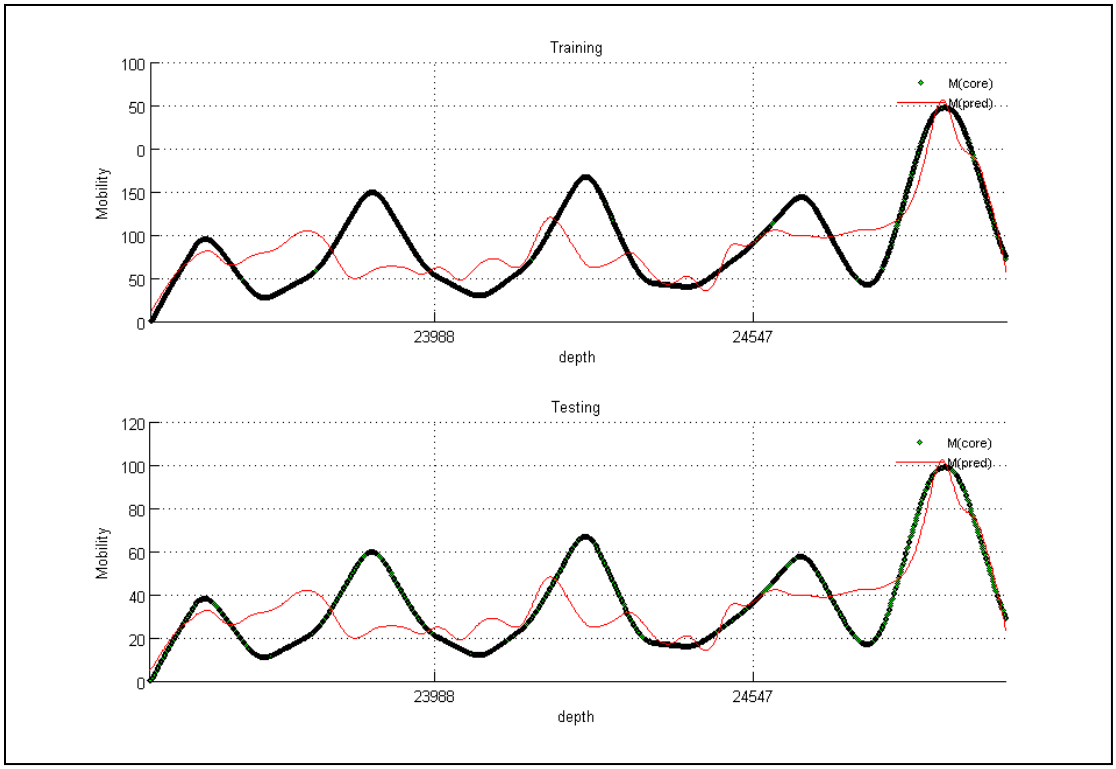

Figure C- 19: Well-5 Polyhomog Kernel

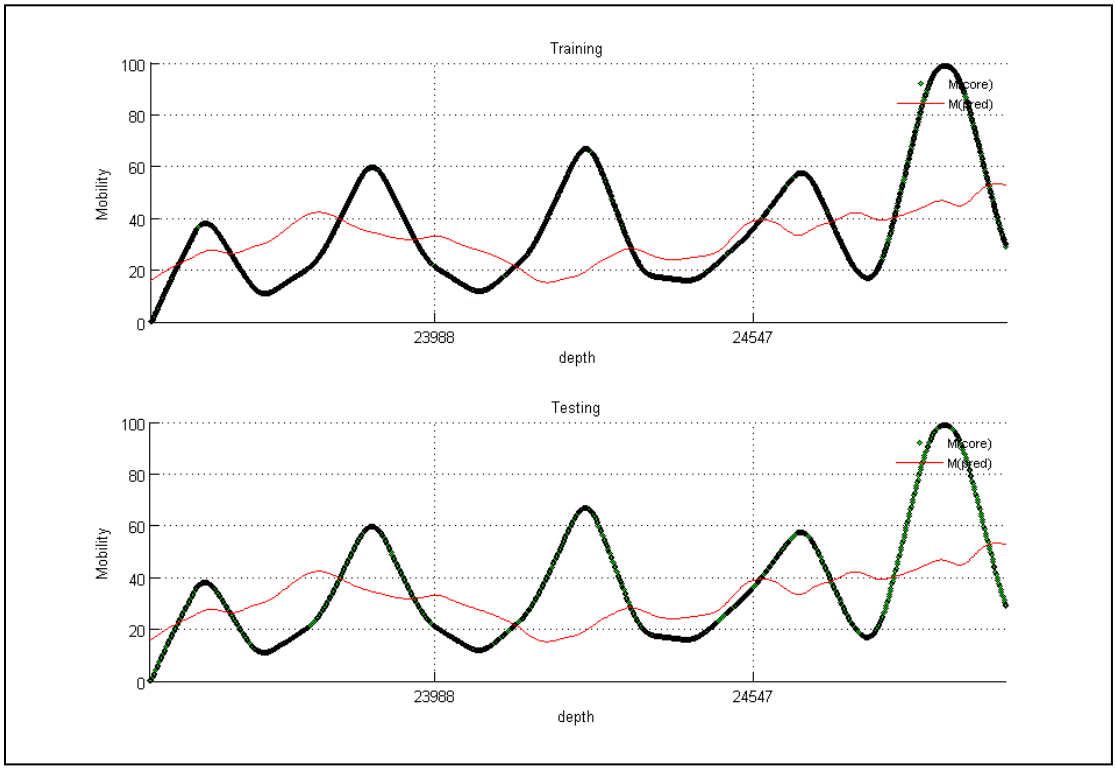

Figure C- 20: Well-5 jcb Kernel

Well No. 6

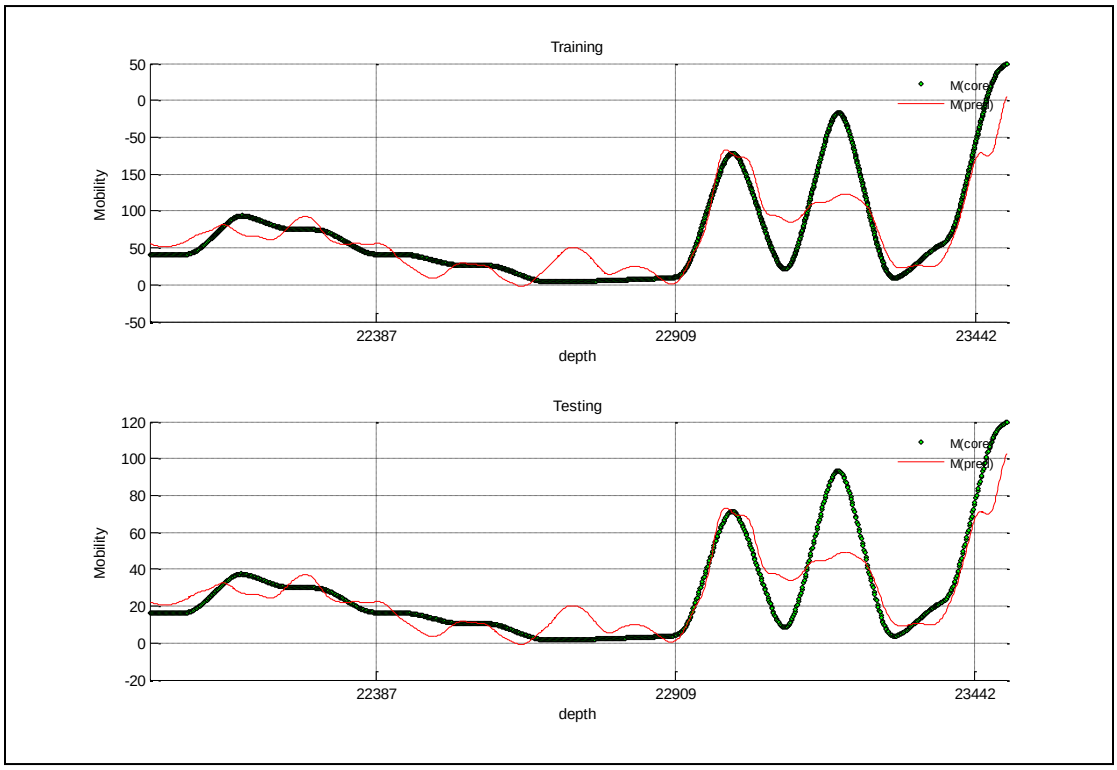

Figure C- 21: Well-6 Gaussian Kernel

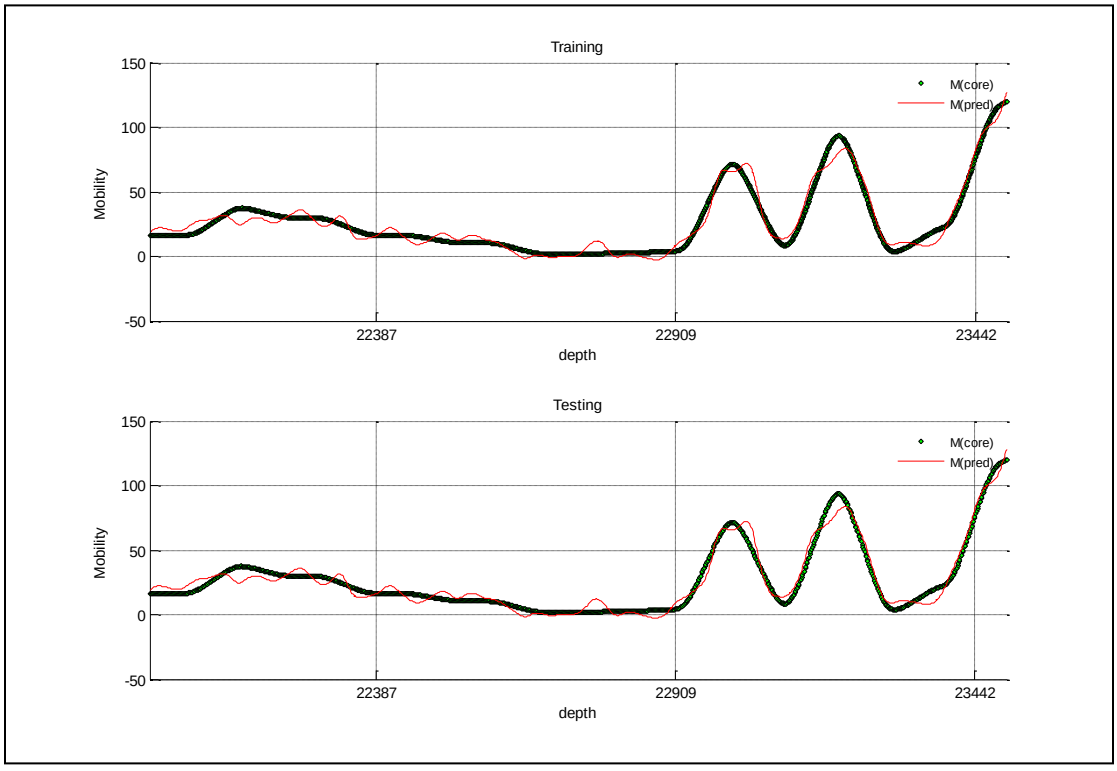

Figure C- 22: Well-6 Poly Kernel

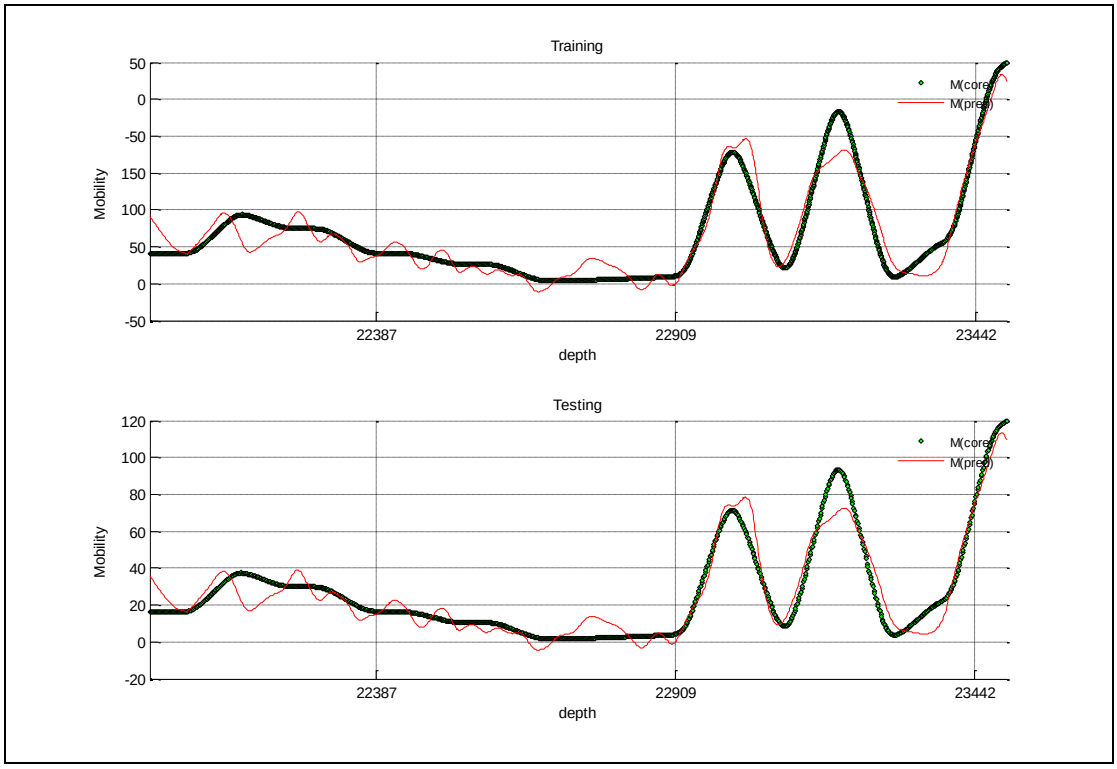

Figure C- 23: Well-6 Polyhomog Kernel

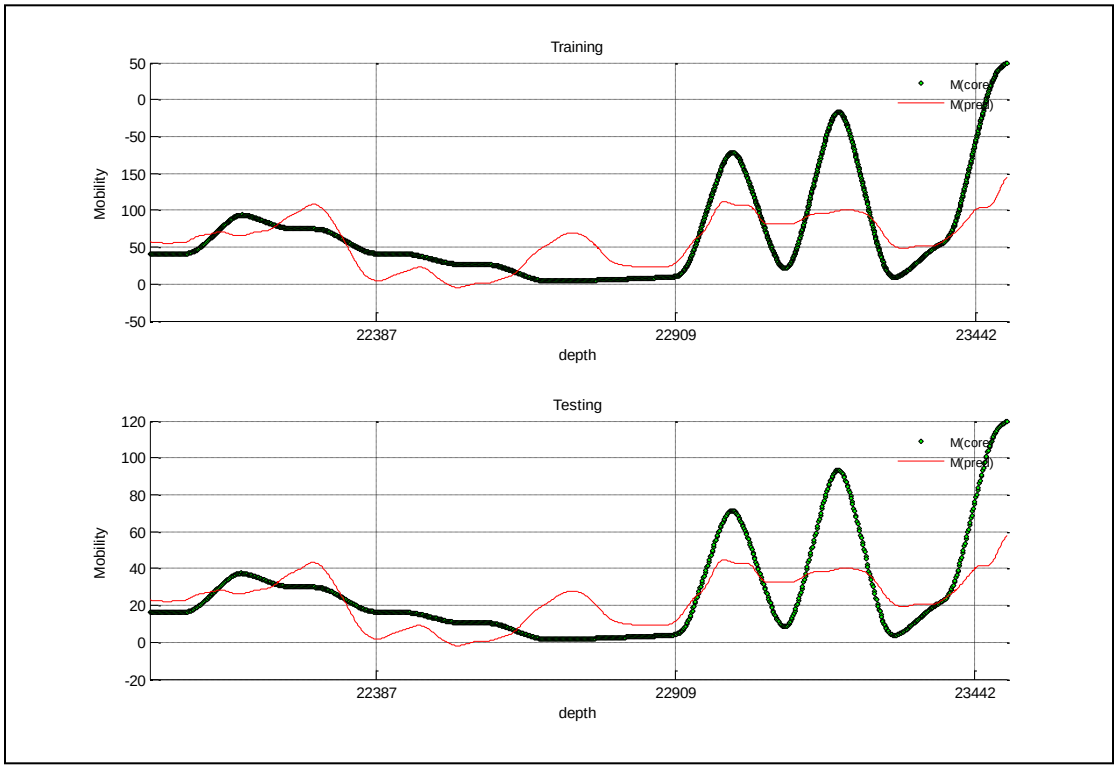

Figure C- 24: Well-6 jcb Kernel

Well No. 7

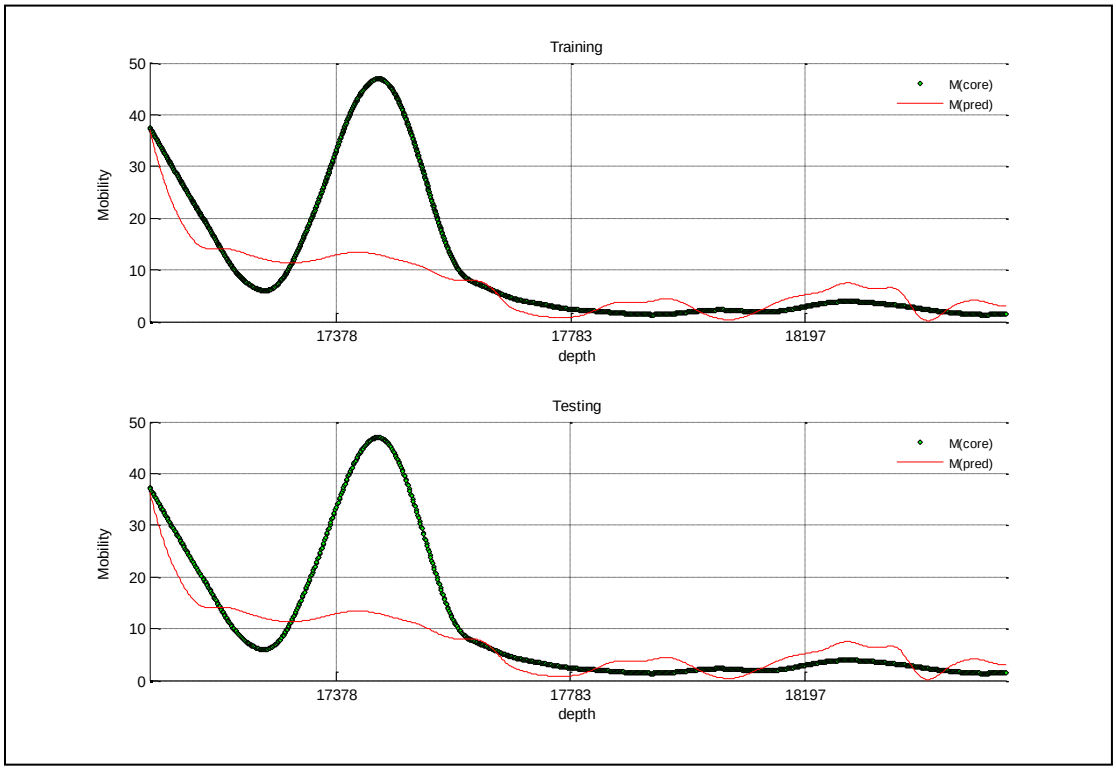

Figure C- 25: Well-7 Gaussian Kernel

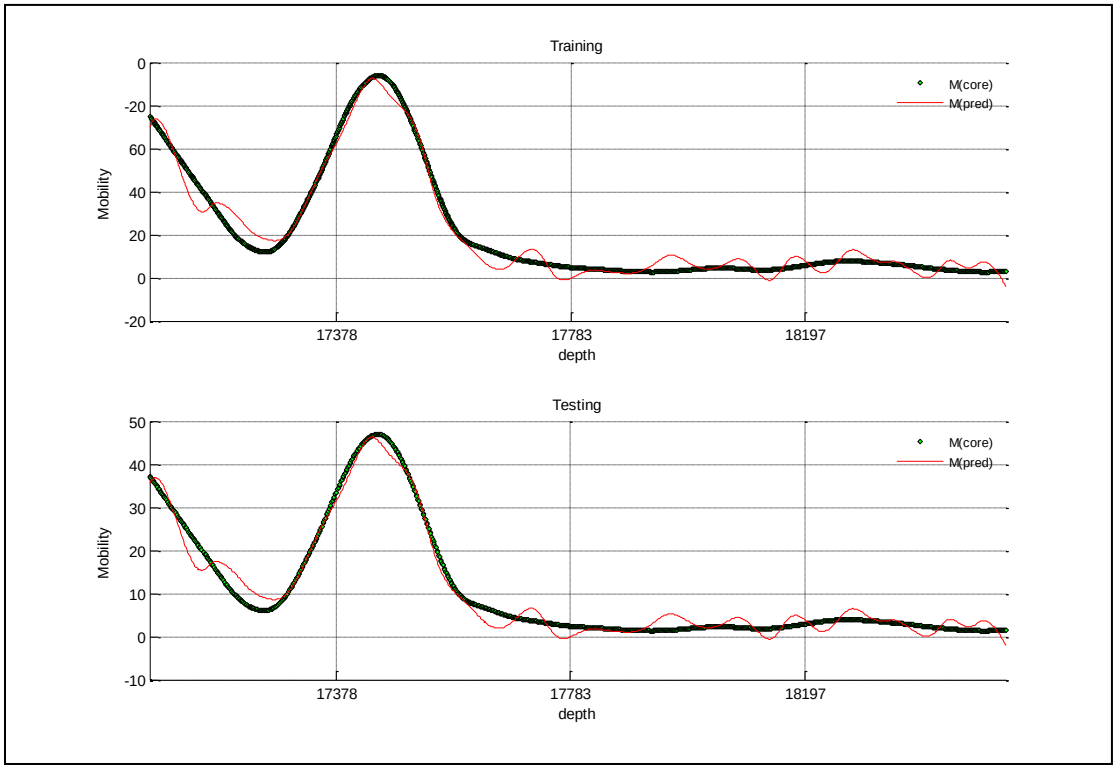

Figure C- 26: Well-7 Poly Kernel

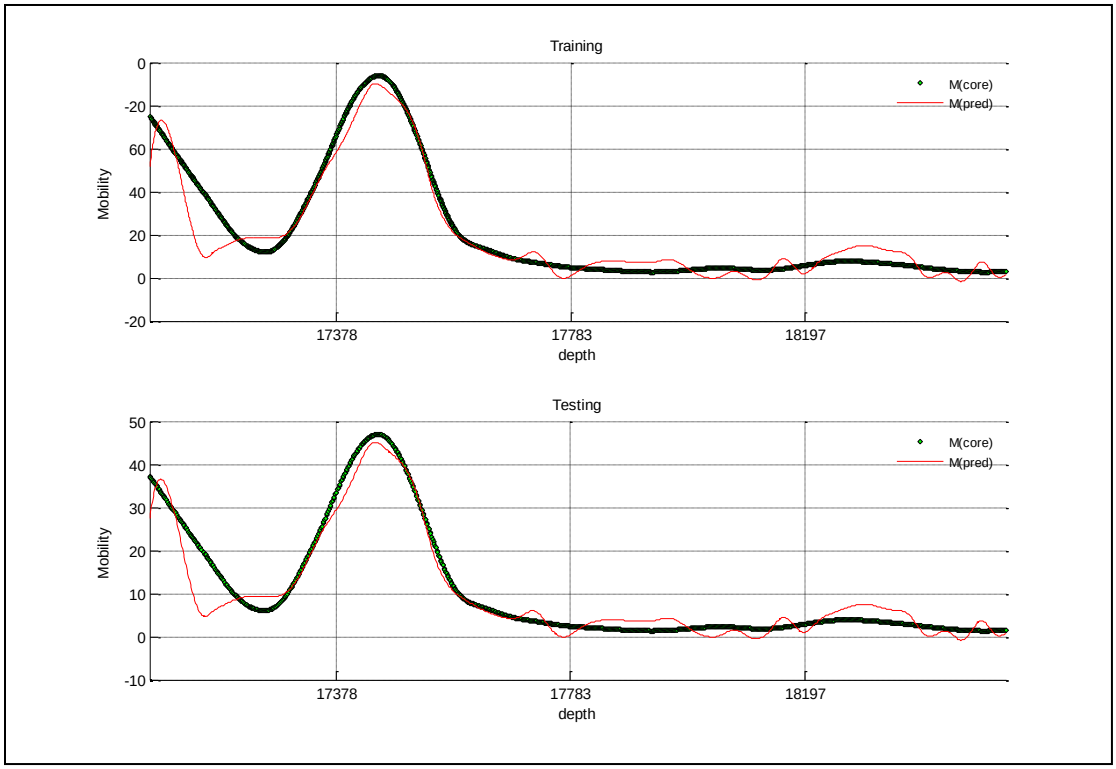

Figure C- 27: Well-7 Polyhomog Kernel

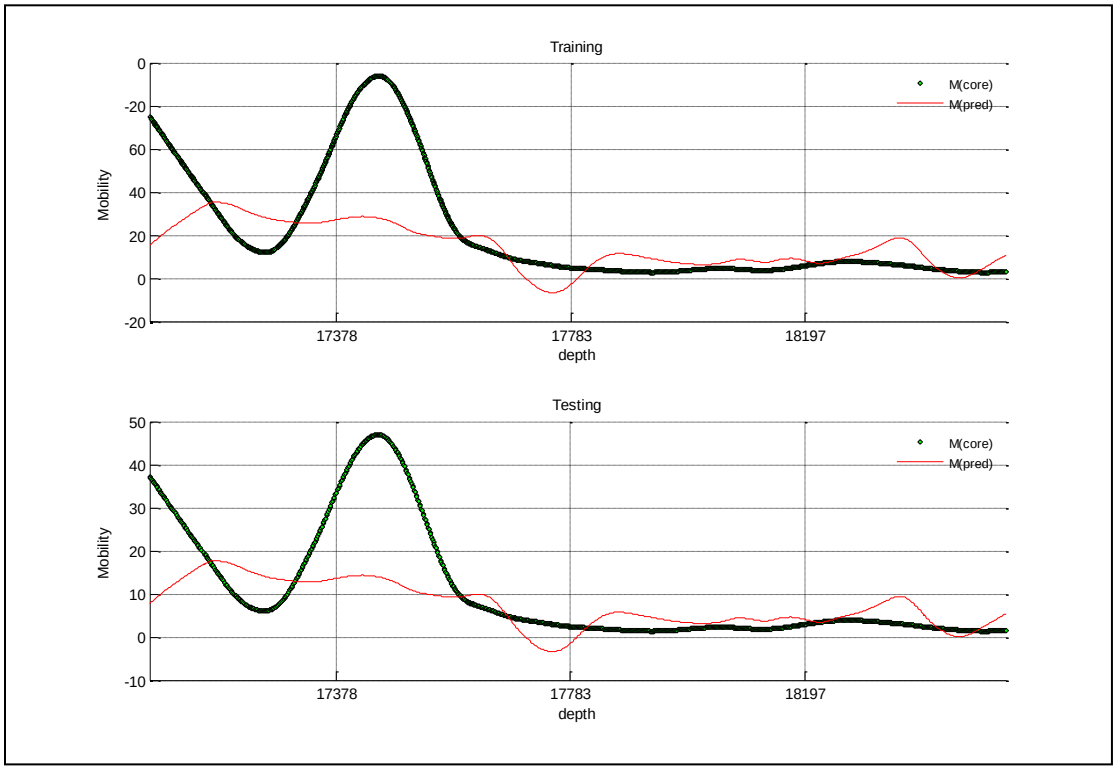

Figure C- 28: Well-7 jcb Kernel

Well No. 8

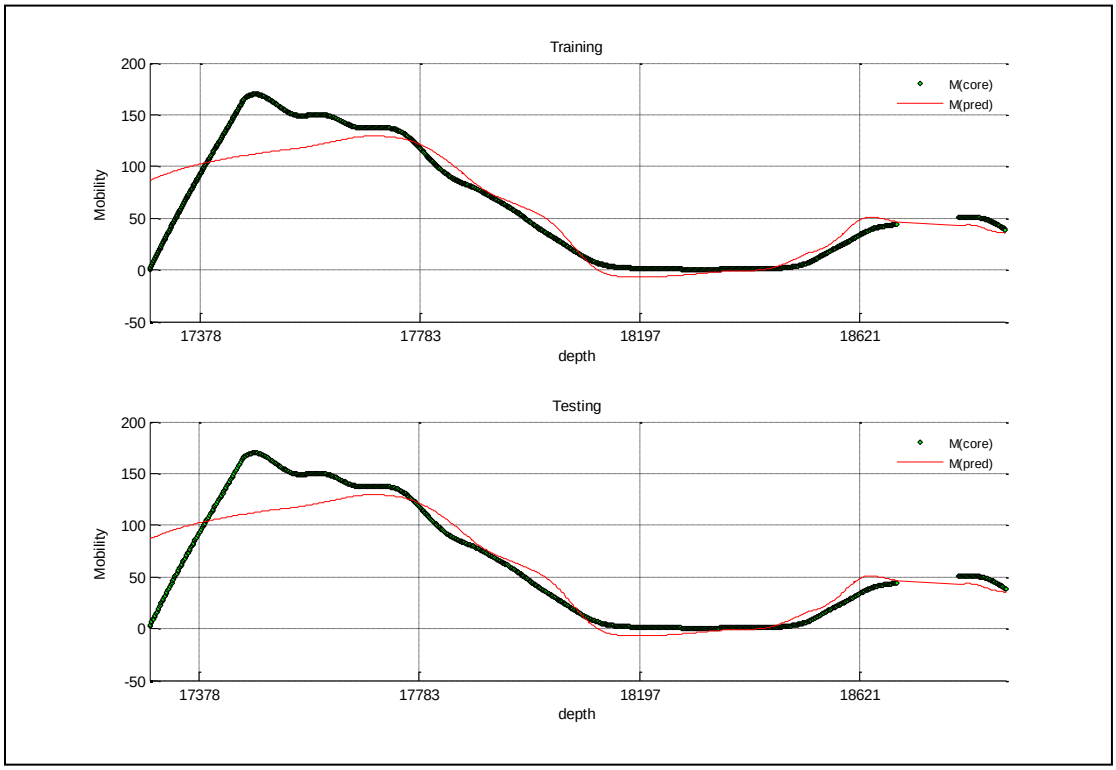

Figure C- 29: Well-8 Gaussian Kernel

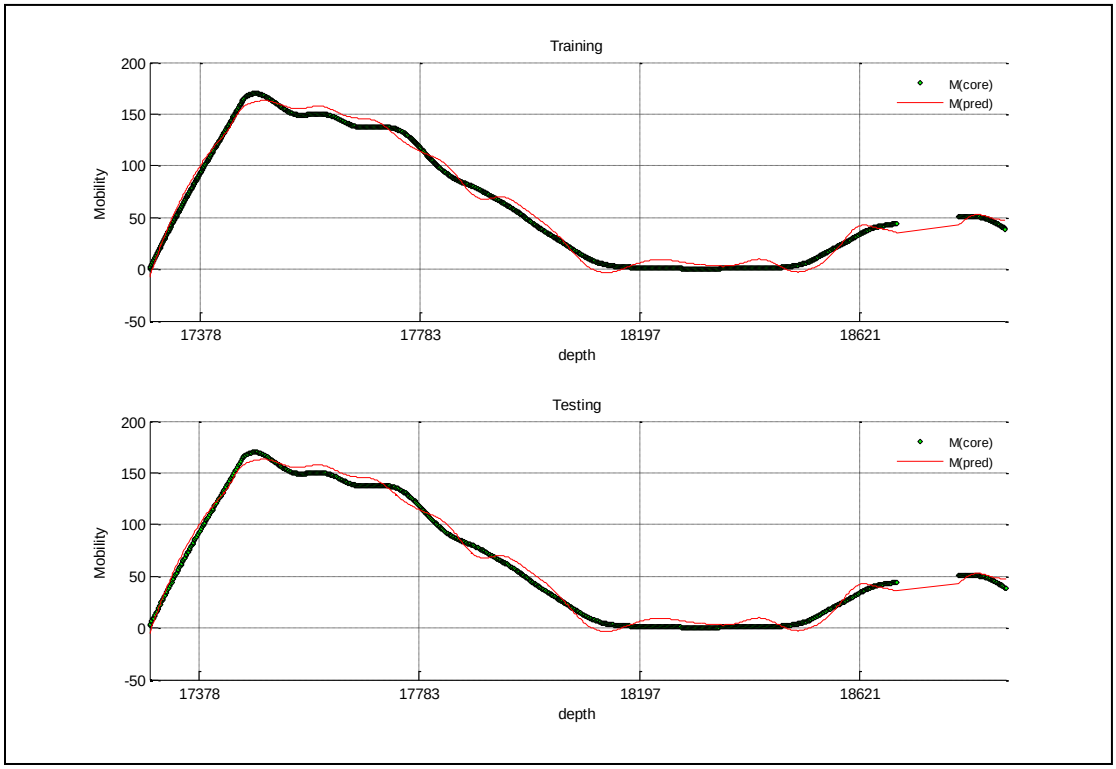

Figure C- 30: Well-8 Poly Kernel

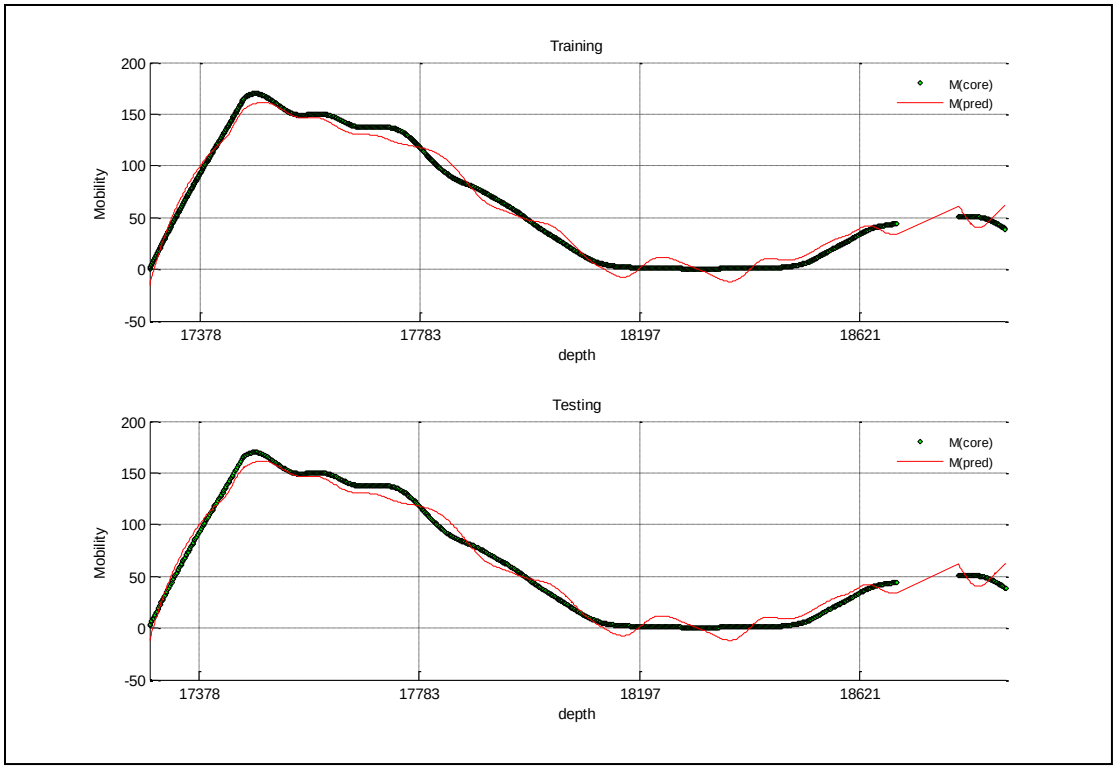

Figure C- 31: Well-8 Polyhomog Kernel

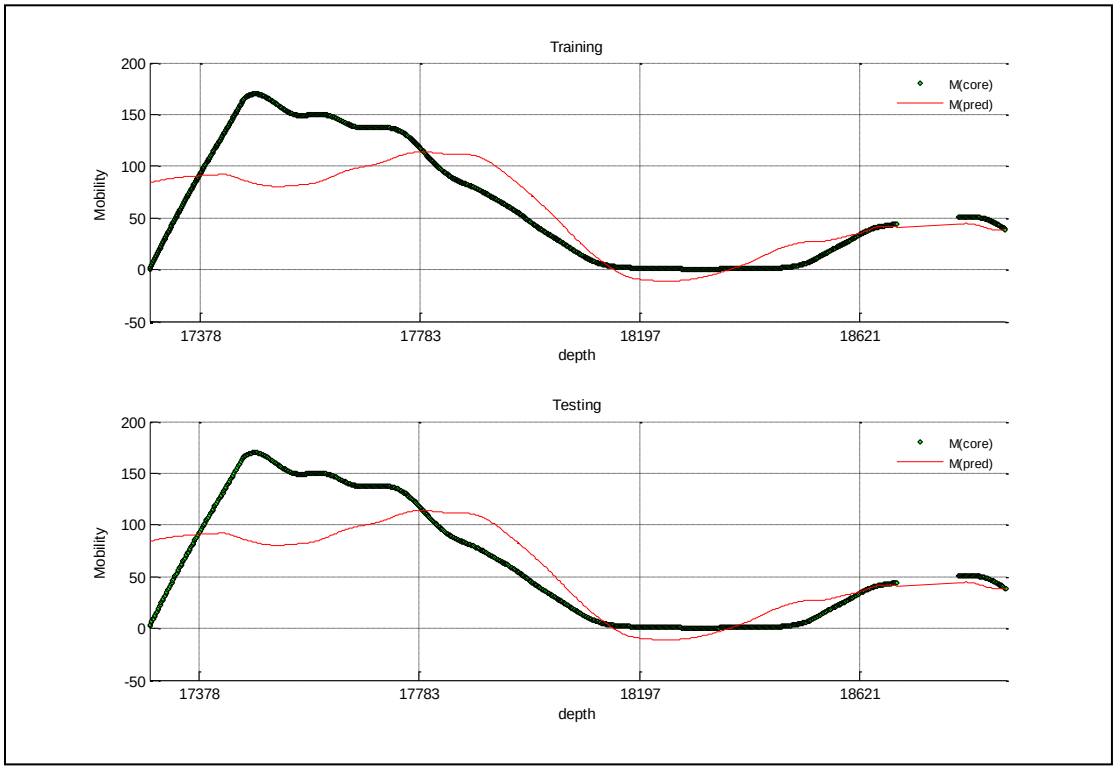

Figure C- 32: Well-8 jcb Kernel

Well No. 9

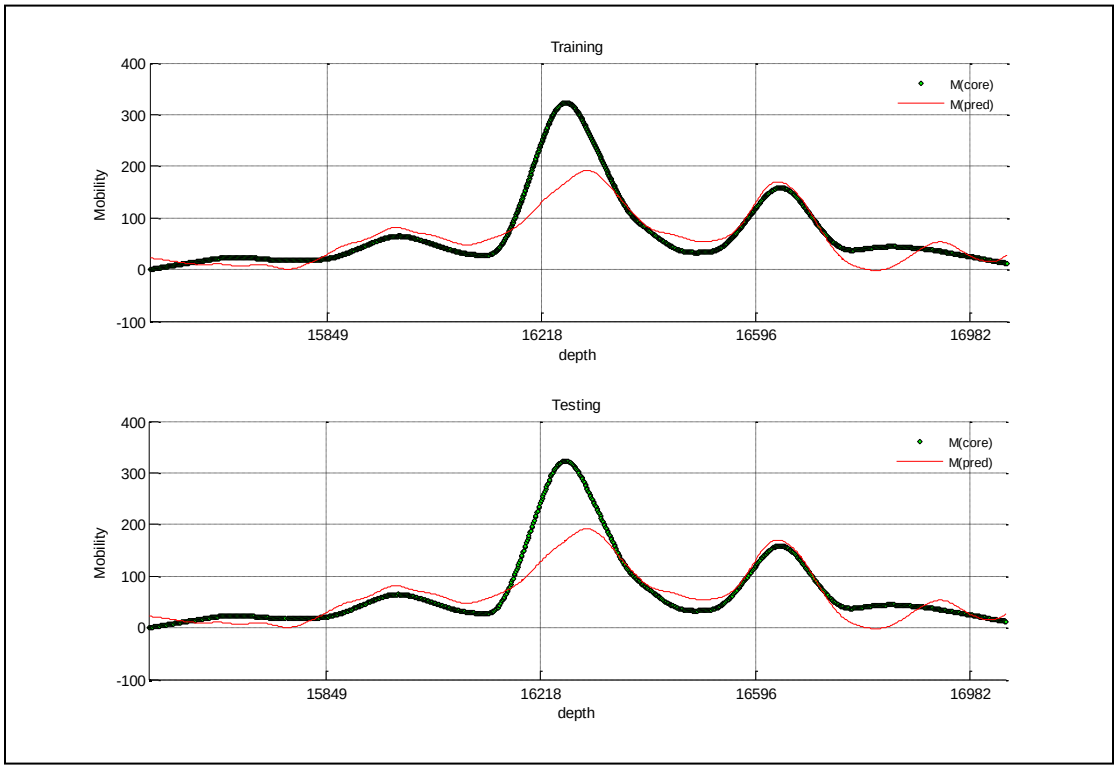

Figure C- 33: Well-9 Gaussian Kernel

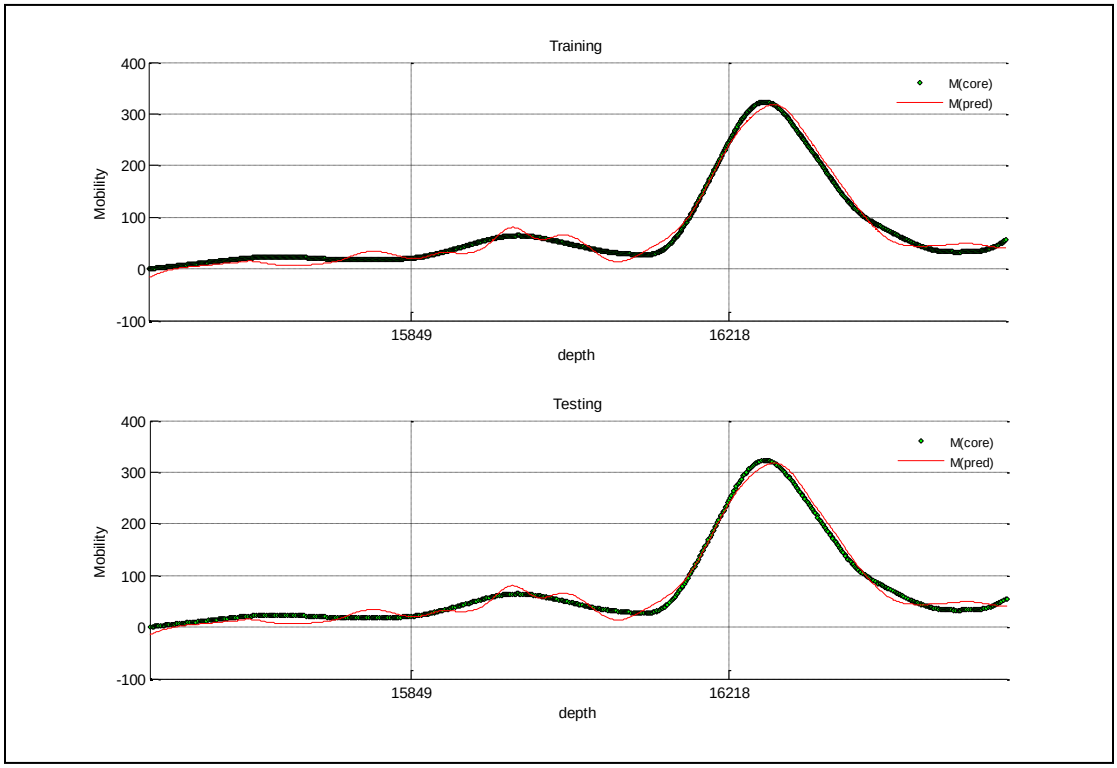

Figure C- 34: Well-9 Poly Kernel

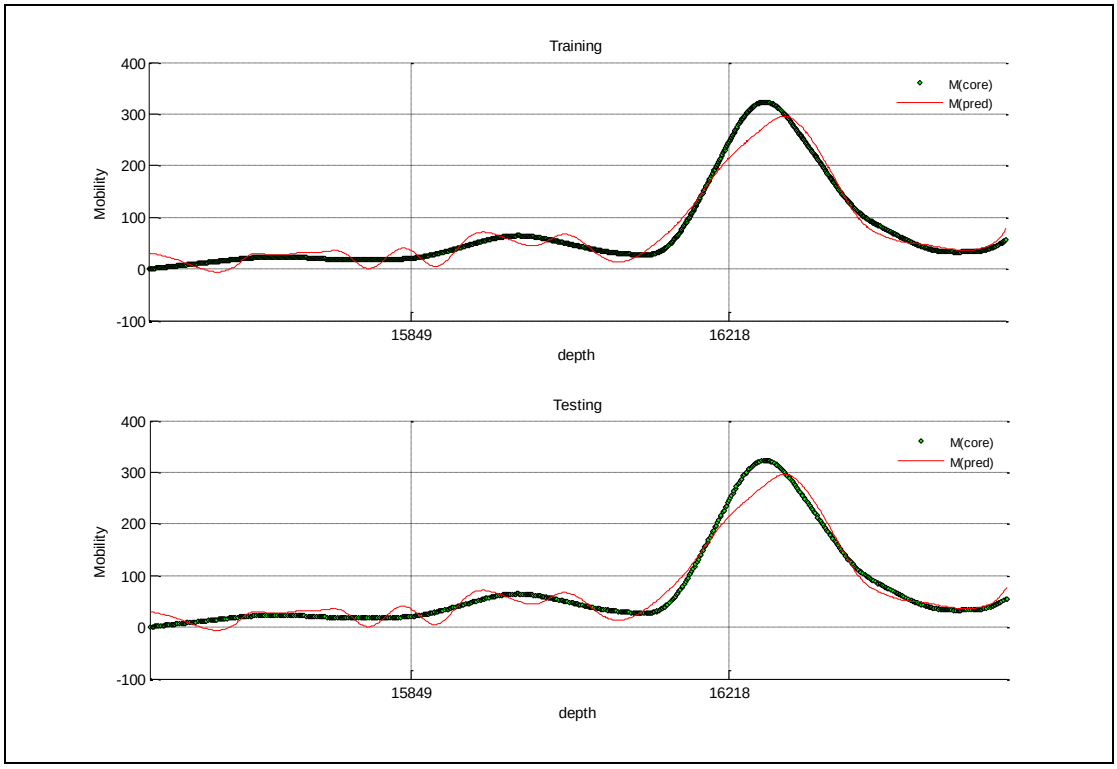

Figure C- 35: Well-9 Polyhomog Kernel

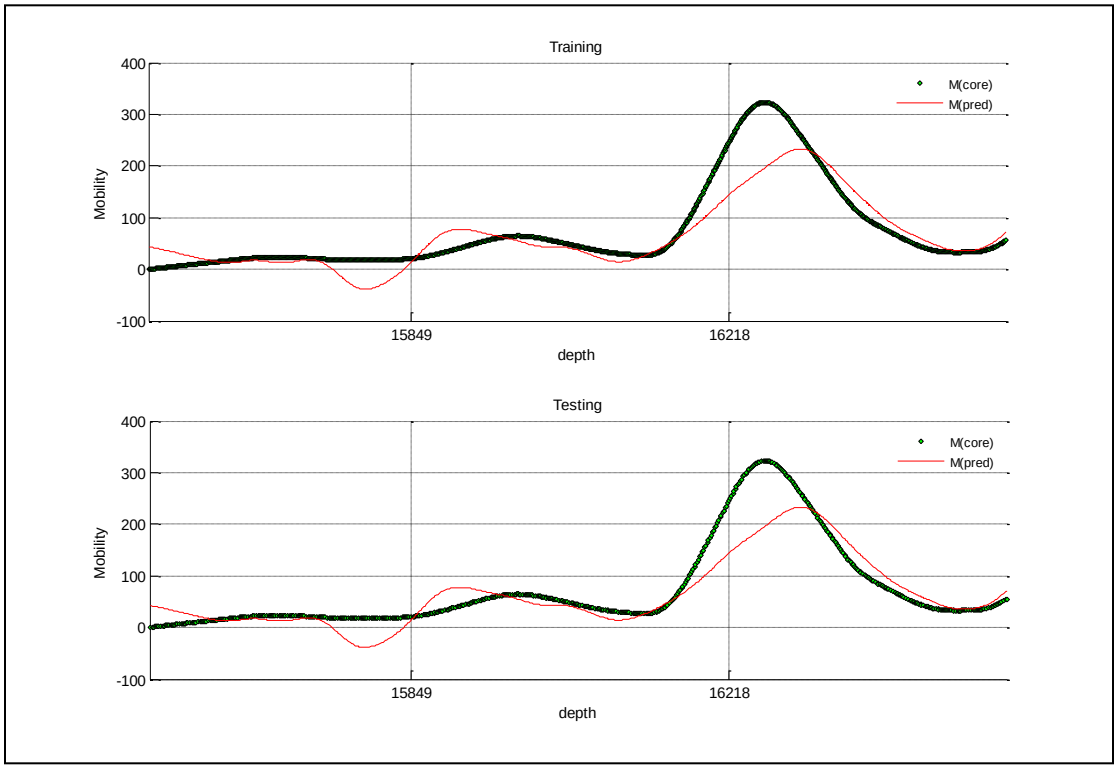

Figure C- 36: Well-9 jcb Kernel

Well No. 10

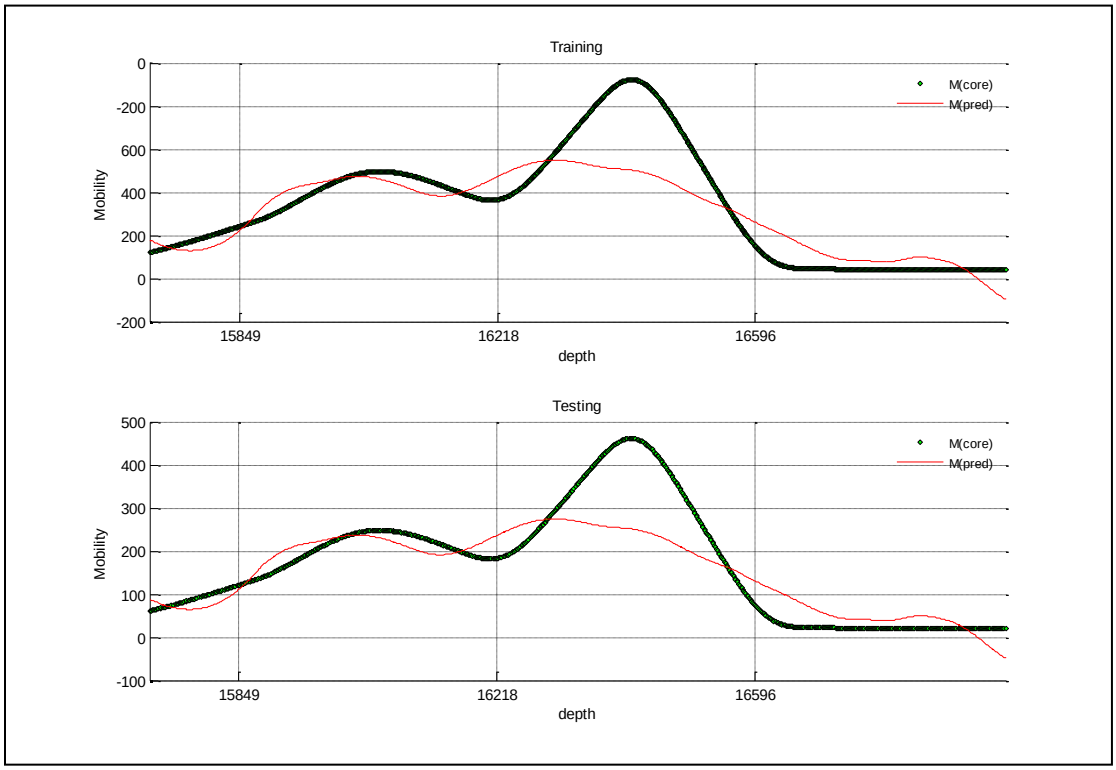

Figure C- 37: Well-10 Gaussian Kernel

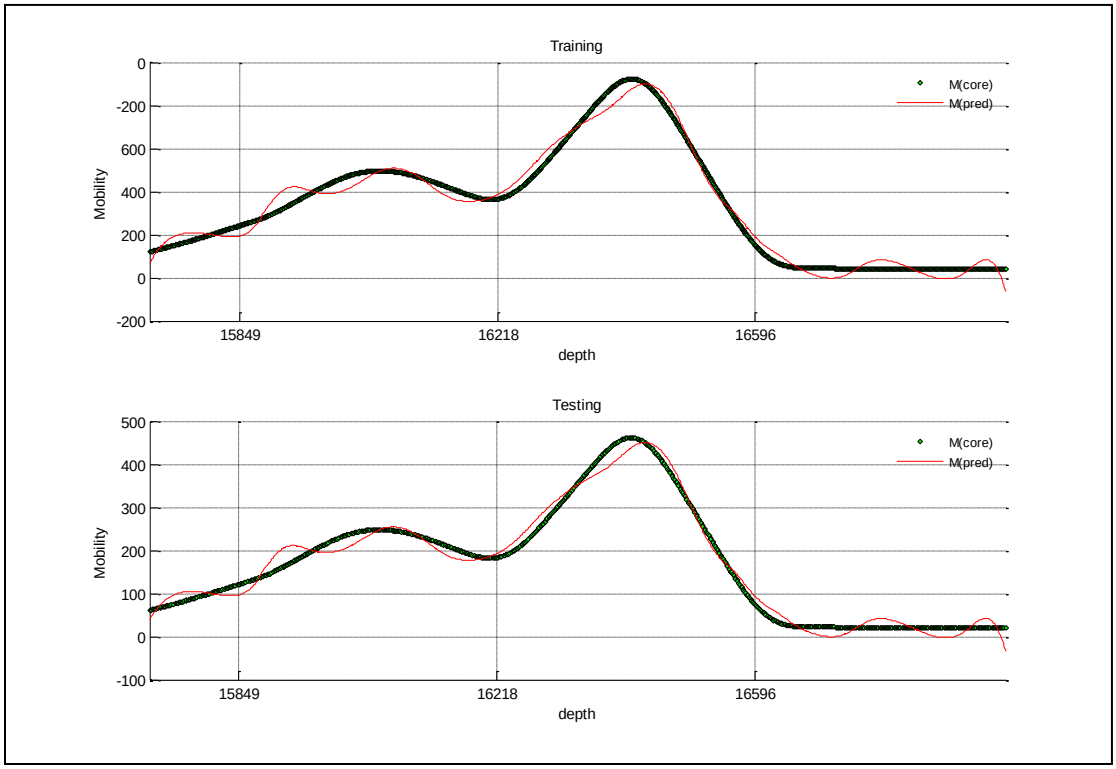

Figure C- 38: Well-10 Poly Kernel

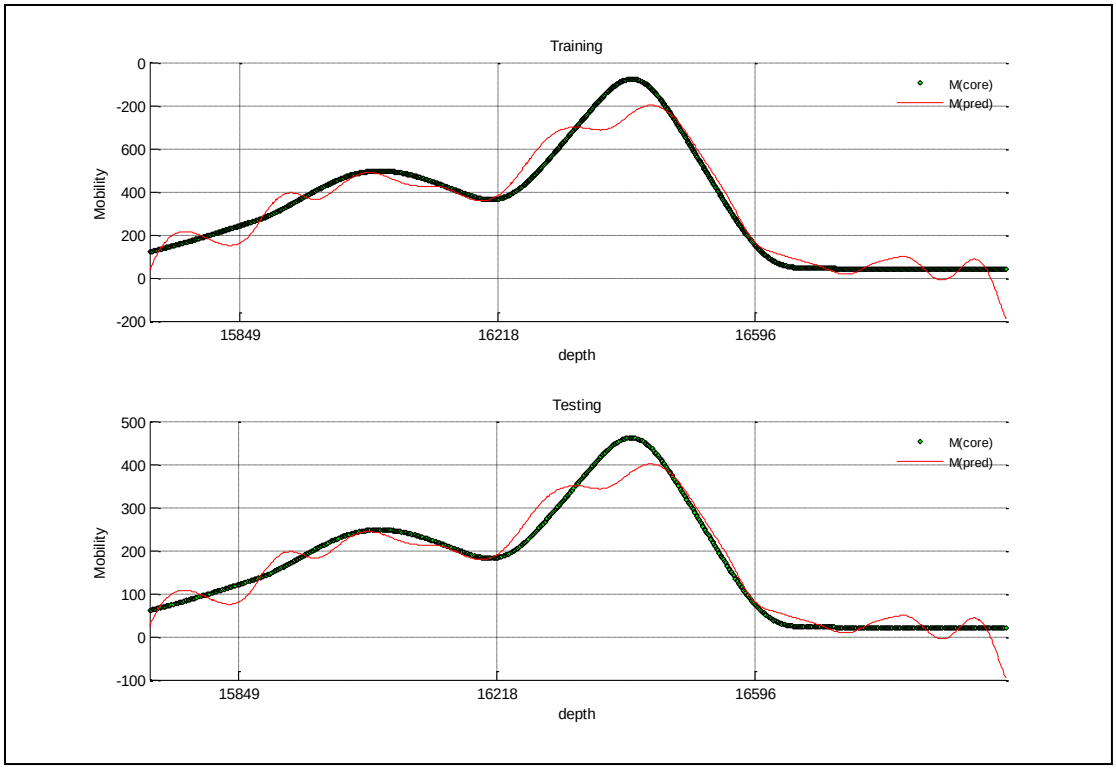

Figure C- 39: Well-10 Polyhomog Kernel

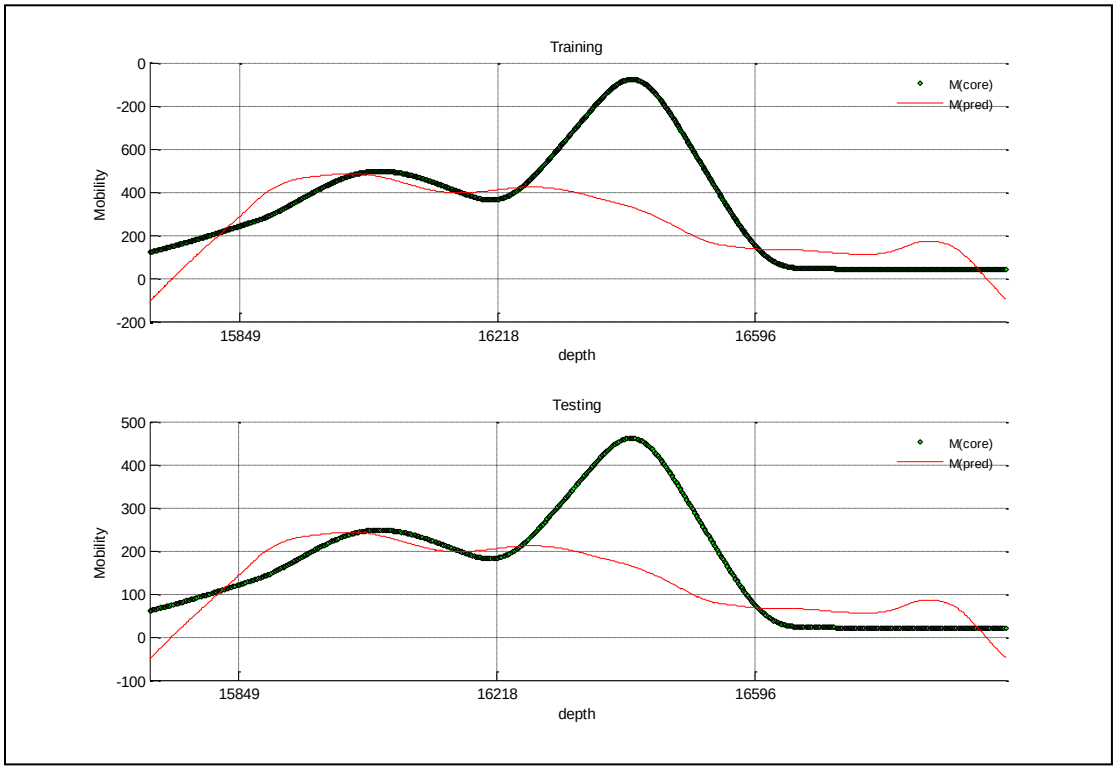

Figure C- 40: Well-10 jcb Kernel

REFERENCES

1. Mohaghegh, S. and Ameri.: “Artificial Neural Network as A Valuable Tool for Petroleum Engineers,” Paper SPE 29220, Prepared as an Unsolicited Paper for Society of Petroleum Engineers (1995).
2. Bilgesu, H. I., Altmis, U., Ameri, Mohaghegh, S., and Aminian, S, K.: “A new Approach to Predict Bit Life Based on Tooth or Bearing Failures,” Paper SPE 51082 Presented at the 1998 SPE East Regional Conference, Pittsburgh, 9-11 November.
3. Dashevskiy, D., Dubinsky, V., and Macpherson D., “Application of Neural Networks for Predictive Control in Drilling Dynamics,” Paper SPE 56442 Presented at the Annual Technical Conference and Exhibition, Houston, 3-6 October.
4. Bilgesu, H. I., Tetrick, T., Altmis, U., Ameri, S. Mohaghegh., and Ameri, S.: “A New Approach for the Prediction of Rate of Penetration (ROP) Values,” Paper SPE 39231 Presented at the 1997 SPE East Regional Conference, Lexington, KY, 22-24 October.
5. Oyeneyin, M. B. and Faga, A. T., "Formation-Grain-Size Prediction Whilst Drilling: A Key Factor in Intelligent Sand Control Completion," Paper SPE 56626 Presented at the 1999 SPE Annual Technical Conference & Exhibition, Huston, Texas, 3-6 October.
6. Holditch, S.A., Xiong, Hongjie, Rueda, Jose, and Rahim, Zillur.: “Using an Expert System To Select the Optimal Fracturing Fluid and Treatment Volume,” Paper SPE 26188 presented at the 1993 SPE Gas Technology Symposium, Calgary, Alberta, Canada, 28-30 June.
7. Mohaghegh, S., Arefi, R., Belgesu, L., Ameri, S, and Rose, D.: “Design and Development of Artificial Neural Network for Estimation of Formation Permeability,” Paper SPE 28237, Presented at the SPE Production Computer Conference, Dallas, 31 July to 3rd August.

8. Hu, Z. and Zhao, B., "A New Method for Discrimination of Automatic Parameters in Horizontal Well Test Analysis," presented at *Natural Gas Industry* (25 March 1997)17, No. 2, 7A, 59-62.
9. Sultan, M. A., and Al-Kaabi, A. U.: "Application of Neural Network to the Determination of Well-Test Interpretation for Horizontal Wells," Paper SPE 77878 presented at the 2002 SPE Asia Pacific Oil and Gas Conference and Exhibition, Melbourne, Australia, 8-10 October.
10. Al-Kaabi, A., and Lee, W. J.: "Using Artificial Neural Nets to Identify the Well Test Interpretation Model," *SPE Formation Evaluation Journal* (September 1993) 233-240. 103
11. Elmo, R. O. and Jabbar Elmatalab.: "A Practical Artificial Neural Network Model for Estimating Tight Gas Sand Permeability," Paper SPE 39703 Presented at the 1998 Asia Pacific Conference, Kuala Lampur, Malaysia, 23-24 March.
12. Osman, E. A., O. A. Abdel-Wahab, and Al-Marhoun, M. A.: "Prediction of Oil PVT Properties Using Neural Networks," Paper SPE 68233, Presented at the12th MEOS (Middle East Oil and Gas Show and Conference), 17-20 March 2001.
13. Varotsis, N., Nighswander, J., Guieze, P., and Gaganis, V.: "A Novel Non-Iterative Method for the Prediction of The PVT Behavior of Reservoir Fluids," Paper SPE 56745 Presented at the 1999 SPE Annual Technical Conference & Exhibition, Houston, Texas, 3-6 October.
14. Boukadi, F., Al-Alawi, S., Al-Bemani, A., and Al-Qassabi, S.: "Establishing PVT Correlations for Omani Oils," *Petroleum Science Technology* (June-July 1999)17, No. 5-6, 637-662.
15. Garrouch, A. and Smaoui, N. H.: "An Artificial Neural Network Model for Estimating Tight Gas Sand Permeability," Paper SPE 39703 Presented at the 1998 Integrated Modeling for Asset Manage Asia Pacific Conference, Kuala Lampur, Malaysia, 23-24 March.

16. Ali, J. K.: "Neural Networks: A New Tool for the Petroleum Industry?" Paper SPE 27561, presented at the 1994 European Petroleum Computer Conference, Aberdeen, K. U., 15-17 March.
17. Ali, J.K.: “Neural Networks: A New Tool for the Petroleum Industry” European Petroleum Computer Conference, 15-17 March 1994, Aberdeen, United Kingdom
18. L. Saputelli, H. Malki, J. Canelon, Universidad del Zulia, M. Nikolaou.: “A Critical Overview of Artificial Neural Network Applications in the Context of Continuous Oil Field Optimization”, SPE Annual Technical Conference and Exhibition, 29 September-2 October 2002, San Antonio, Texas
19. Shahab Mohaghegh: “ Virtual-Intelligence Applications in Petroleum Engineering: Part 1Â—Artificial Neural Networks” Journal of Petroleum Technology, Vol.52, No.9, 9,2000, Pp:64-73
20. Asha Ramgulam, Turgay Ertekin, and Peter B. Flemings.: “ An Artificial Neural Network Utility for the Optimization of History Matching Process “,Latin American & Caribbean Petroleum Engineering Conference, 15-18 April 2007, Buenos Aires, Argentina
21. C. Alimonti, G. Falcone,:. “Knowledge Discovery in Databases and Multiphase Flow Metering: The Integration of Statistics, Data Mining, Neural Networks, Fuzzy Logic, and Ad Hoc Flow Measurements Towards Well Monitoring and Diagnosis” SPE Annual Technical Conference and Exhibition, 29 September-2 October 2002, San Antonio, Texas
22. Shahab D. Mohaghegh: “Recent Developments in Application of Artificial Intelligence in Petroleum Engineering” Journal of Petroleum Technology, Vol.57, No.4, 4,2005, Pp:86-91

23. Hussam M. Goda, Khaled A. Fattah, Eissa M. El-M Shokir, Mohamed H. Sayyouh,: "Prediction of the PVT Data using Neural Network Computing Theory" Nigeria Annual International Conference and Exhibition, 4-6 August 2003, Abuja, Nigeria
24. T.P. Sampaio, V.J. M. Ferreira Filho, and A. de Sa Neto.: "An Application of Feed Forward Neural Network as Nonlinear Proxies for Use During the History Matching Phase" Latin American and Caribbean Petroleum Engineering Conference, 31 May-3 June 2009, Cartagena de Indias, Colombia
25. E. El-Sebakhy, T. Sheltami, S. Al-Bokhitan, Y. Shaaban, I. Raharja, and Y. Khaeruzzaman: "Support Vector Machines Framework for Predicting the PVT Properties of Crude Oil Systems" SPE Middle East Oil and Gas Show and Conference, 11-14 March 2007, Kingdom of Bahrain
26. Ternyik, IV, J., Bilgesu, H.I., Mohaghegh, S.: "Virtual Measurement in Pipes: Part 2-Liquid Holdup and Flow Pattern Correlations" SPE Eastern Regional Meeting, 18-20 September 1995, Morgantown, West Virginia
27. Saeedi, SPE, K.V. Camarda, and J.T. Liang :" Using Neural Networks for Candidate Selection and Well Performance Prediction in Water-Shutoff Treatments Using Polymer Gels - A Field-Case Study", SPE Production & Operations, Vol.22, No.4, 11,2007, Pp. 417-424
28. El-Sayed A. Osman," Artificial Neural Network Models for Identifying Flow Regimes and Predicting Liquid Holdup in Horizontal Multiphase Flow", SPE Production & Facilities, Vol.19, No.1, 4,2004, Pp. 33-40
29. F. Farshad, J.D. Garber, J.N. Lorde.: " Predicting Temperature Profiles in Producing Oil Wells Using Artificial Neural Networks" Latin American and Caribbean Petroleum Engineering Conference, 21-23 April 1999, Caracas, Venezuela

30. E.A. Osman, O.A. Abdel-Wahhab, M.A. Al-Marhoun :"Prediction of Oil PVT Properties Using Neural Networks" SPE Middle East Oil Show , 17-20 March 2001, Bahrain
31. A.Popa, R. Ramos, A. Cover, C. Popa.: "Integration of Artificial Intelligence and Lean Sigma for Large Field Production Optimization: Application to Kern River Field" SPE Annual Technical Conference and Exhibition, 9-12 October 2005, Dallas, Texas
32. Christian Oberwinkler, Gerhard Ruthammer, Georg Zangl, Michael J. Economides :" New Tools for Fracture Design Optimization" SPE International Symposium and Exhibition on Formation Damage Control, 18-20 February 2004, Lafayette, Louisiana
33. S. Singh, Maharashtra. :" Permeability Prediction Using Artificial Neural Network (ANN): A Case Study of Uinta Basin" SPE Annual Technical Conference and Exhibition, 9-12 October 2005, Dallas, Texas, U.S.A.
34. Saud M. Al-Fattah, "Artificial Intelligence Technology Predicts Relative Permeability of Giant Carbonate Reservoirs" Offshore Europe, 4-7 September 2007, Aberdeen, Scotland, U.K.
35. Ahmed, T., Link, C.A., Porter, K.W., Wideman, C.J., Himmer, P., Braun, J."Application of Neural Network Parameter Prediction in Reservoir Characterization and Simulation - A Case History: The Rabbit Hills Field" Latin American and Caribbean Petroleum Engineering Conference, 30 August-3 September 1997, Rio de Janeiro, Brazil
36. Mohaghegh, Shahab, Arefi, Reza, Ameri, Samuel, Hefner, M.H.," A Methodological Approach for Reservoir Heterogeneity Characterization Using Artificial Neural Networks" SPE Annual Technical Conference and Exhibition, 25-28 September 1994, New Orleans, Louisiana

37. A.Saeedi, K.V. Camarda, J.T. Liang, “Using Neural Networks for Candidate Selection and Well Performance Prediction in Water-Shutoff Treatments Using Polymer Gels - A Field-Case Study” SPE Asia Pacific Oil & Gas Conference and Exhibition, 11-13 September 2006, Adelaide, Australia
38. Burak Yeten, J. Durlofsky, Khalid Aziz,”Optimization of Nonconventional Well Type, Location, and Trajectory”, SPE Journal Vol.8, No.3, 9,2003, Pp.200-210
39. Meisam Karbalaee Akbari, Farhang Jalali Farahani, Yaser Abdy, “ Using Artificial Neural Network's Capability for Estimation of Gas Condensate Reservoir's Dew point Pressure” EUROPEC/EAGE Conference and Exhibition, 11-14 June 2007, London, U.K.
40. Munirudeen A. Oloso, Amar Khoukhi, Abdulazeez Abdulraheem, and Moustafa Elshafei,” Prediction of Crude Oil Viscosity and Gas/Oil Ratio Curves Using Recent Advances to Neural Networks”, SPE/EAGE Reservoir Characterization and Simulation Conference, 19-21 October 2009, Abu Dhabi, UAE
41. El-Sayed A. Osman, “Artificial Neural Networks Models for Identifying Flow Regimes and Predicting Liquid Holdup in Horizontal Multiphase Flow “SPE Middle East Oil Show , 17-20 March 2001, Bahrain
42. Ekwere J. Peters: PetroPhysics, The university of Texas at Austin
43. Akkurt, R., Seifert, 2008, Real-time Detection of Tar in Carbonates Using LWD Triple-Combo, NMR and Formation Tester in Highly-Deviated Wells, presented at the SPWLA 49th Annual Logging Symposium in Edinburgh, Scotland.
44. Burcaw, L, Kleinberg, R., et al, 2008, Improved Methods for Estimating the Viscosity of Heavy Oils from Magnetic Resonance Data, presented at the SPWLA 49th Annual Logging Symposium in Edinburgh, Scotland.

45. “RDD Petrophysics Manual”, Saudi Aramco, 2006

46. “Modular Formation Dynamics Tester booklet” Schlumberger, 2005

47. Christopher J. C. B., (1998), A tutorial on support vector machines for pattern recognition. Data mining and Knowledge Discovery 2, 121-167.

48. Soman K. P., Loganathan R., and Ajay V., (2009), Machine Learning with SVM and other Kernel Methods. PHI Learning, publisher, first edition.

49. John Shawe-Taylor and Nello Cristianini, (2000), Support Vector Machines and other kernel-based learning methods. Cambridge University Press. http://www.support-vector.net/.

50. Thomas Hofmann, Bernhard Sch¨olkopf, and Alexander J. Smola, (2008), KERNEL METHODS IN MACHINE LEARNING. The Annals of Statistics, Vol. 36, No. 3, 1171–1220. DOI: 10.1214/009053607000000677. Institute of Mathematical Statistics.

51. Schölkopf, B., C. J.C. Burges and A. J. Smola: Advances in Kernel Methods - Support Vector Learning. MIT Press, Cambridge, MA (1999)

52. El-Sebakhy E., Raharja I. and Khaeruzzaman Y., “*Machine Learning and Data Mining Tools for the Pattern Recognition: Theory and Applications*”, submitted to Elsevier Science, pp. 1-117, 2006.

53. El-Sebakhy E., Sheltami T., Al-Bokhitan S., Shaaban Y., Raharja I. and Khaeruzzaman Y., "*Support Vector Machines Framework for Predicting the PVT Properties of Crude-Oil Systems*", 15th Society of Petroleum Engineers Middle East Oil & Gas Show and Conference, Bahrain, March 2007.

54. El-Sebakhy E., "*Artificial Neural Networks, Probabilistic Networks, Support Vector Machines, Adaptive-Neuro Fuzzy Systems, and Functional Networks*", submitted to Elsevier Science, 2006.

55. Littman W., "*Introduction to Support Vector Machines*", Lecture notes on CS 536: Machine Learning, Department of Computer Science, Rutgers, The State University of New Jersey, USA.

56. Terrence S.F., Nello C., Nigel D., David W.B., Michel S. and David H., "*Support Vector Machine Classification and Validation of Cancer Tissue Samples using Microarray Expression Data*", Bioinformatics, Vol. 16, 10, 2000, Pp. 906-914.

57. Goda H.M., Maier, H.R. and Behrenbruch, P., "*Use of Artificial Intelligence Techniques for Predicting Irreducible Water Saturation - Australian Hydrocarbons Basins*", Society of Petroleum Engineers Asia Pacific Oil & Gas Conference and Exhibition, Jakarta, Indonesia, 2007.

58. Zhao C.Y., Zhang H.X., Liu M.C., Hua Z.D. and Fan B.T., "*Application of Support Vector Machine (SVM) for Predicting Toxic Activity of Different Data Sets*", Toxicology 217, 2006, Pp. 105–119.

59. Vannerem P., Muller K.R., Scholkopf B., Smola A. and Soldner-Rembold S., "*Classifying LEP Data with Support Vector Algorithms*", Proceedings of AIHENP'99, hep-ex/9905027, Crete, April 1999.

60. Jian H. and Wenfen H., "*Novel Approach to Predict Potentiality of Enhanced Oil Recovery*", Society of Petroleum Engineers Intelligent Energy Conference and Exhibition, Amsterdam, The Netherlands, 2006.

61. Van G.T., Baesens, B., Suykens, J., Espinoza, M., Baestaens, D.E., Vanthienen, J. and De-Moor, B., "*Bankruptcy Prediction with Least Squares Support Vector Machine Classifiers*", Proceedings of IEEE International Conference on Computational Intelligence for Financial Engineering, pp. 1-8, 20-23 March 2003.
62. Stephan K.C., Tobias D. and Detlef S., "*Classification of Ebay Bidding Characteristics*", International Association of Development of the Information Society International Journal on WWW/Internet, Vol. 4, No. 1, pp. 111-125, 2005.
63. Christopher J.C., "*A Tutorial on Support Vector Machines for Pattern Recognition*", Data Mining and Knowledge Discovery 2, 121-167, 1998.
64. Gang W. and Edward Y.C., "*Class-Boundary Alignment for Imbalanced Dataset Learning*", Workshop on Learning from Imbalanced Datasets II, International Conference on Machine Learning (ICML), Washington DC, 2003.
65. Emre C., Ahmet A. and Türkoglu I., "*A Decision Support System Based on Support Vector Machines for Diagnosis of the Heart Valve Diseases*", Computers in Biology and Medicine 37, 2007, Pp. 21 – 27.
66. Kristof C. and Dirk V.P., "*Churn prediction in Subscription Services: An Application of Support Vector Machines while Comparing Two Parameter-Selection Techniques*", Expert Systems with Applications 34, 2008, Pp. 313–327.
67. Kemal P. and Salih G., "*Breast Cancer Diagnosis using Least Square Support Vector Machine*", Digital Signal Processing 17, 2007, Pp. 694–701.
68. Taboada J., Matías J.M., Ordóñez C. and García P.J., "*Creating a Quality Map of a Slate Deposit using Support Vector Machines*", Journal of Computational and Applied Mathematics 204, pp 84 – 94, Elsevier, 2007.

69. Jin-Hyuk H., Jun-Ki M., Ung-Keun C. and Sung-Bae C., "*Fingerprint Classification using One-vs-All Support Vector Machines Dynamically Ordered with Naïve Bayes Classifiers*", Pattern Recognition, Vol. 41, 2008, Pp. 662 – 671.
70. Kemal P., Salih G. and Ahmet A., "*A Cascade Learning System for Classification of Diabetes Disease: Generalized Discriminant Analysis and Least Square Support Vector Machine*", Expert Systems with Applications 34, 2008, Pp. 482–487.
71. Elish, K.O. and Elish, M.O., "*Predicting Defect-Prone Software Modules Using Support Vector Machines*", The Journal of Systems and Software (2007), doi: 10.1016/j.jss.2007.07.040
72. Cheng-Lung H., Hung-Chang L. and Mu-Chen C., "*Prediction Model Building and Feature Selection with Support Vector Machines in Breast Cancer Diagnosis*", Expert Systems with Applications 34, 2008, Pp. 578–587.
73. Li, X., Luan, F., Si, H., Hu, Z. and Liu, M., "*Prediction of Retention Times for a Large Set of Pesticides or Toxicants Based on Support Vector Machine and the Heuristic Method*", Toxicology Letters (2007), doi:10.1016/j.toxlet.2007.10.005
74. Jie W., Hongying D., Huanxiang L., Xiaojun Y., Zhide H. and Botao F., "*Prediction of Surface Tension for Common Compounds Based on Novel Methods using Heuristic Method and Support Vector Machine*", Talanta 73, 2007, 147–156.
75. Ciwei G., Ettore B., Roberto N. and Haozhong C., "*Price Forecast in the Competitive Electricity Market by Support Vector Machine*", Physica A 382, 2007, 98–113.
76. El-Sebakhy A. E., Functional Networks Training Algorithm for Statistical Pattern Recognition; IEEE Symposium on Computers and Communications, ISCC 2004. Ninth International Symposium on Volume, vol. 1, pp. 92 –97, 28 June–1 July, 2004.

77. El-Sebakhy A. E., Hadi S. A., and Faisal A. K., Iterative Least Squares Functional Networks Classifier; IEEE Transactions Neural Networks, vol. 18, no. 2, pp. 91 –100, May 2007.
78. El-Sebakhy E., Faisal K., El-Bassuny T., Azzedin F., and Al-Suhaim A., (2006), "Evaluation of Breast Cancer Tumor Classification with Unconstrained Functional Networks Classifier**";** the 4th ACS/IEEE International Conf. on Computer Systems and Applications. 281-287.
79. El-Sebakhy A. E., "Relative Solvent Accessibility of Residues in Proteins Using Unconstrained Functional Networks", International Journal of Bioinformatics (2007).
80. El-Sebakhy A. E., "Forecasting PVT Properties of Crude Oil Systems based on Support Vector Machines Modeling Scheme". International journal of petroleum science and engineering (2007).
81. Li C, Liao X, Wu Z, Yu J. Complex functional networks. Math Comput Simul 2001;57:355–65.
82. Castillo E., Functional networks. *Neural Process. Lett.,* 7(3):151–159, 1998.
83. Castillo E, Cobo A, Gutierrez JM, Pruneda E., Functional networks with applications-a neural-based paradigm. Boston/Dordrecht/London: Kluwer Academic Publishers; New York, 1998.
84. Castillo E, Cobo A, Gutierrez JM, and Hadi A. S., A general framework for functional networks. Networks, 35:70–82, 1999.
85. Castillo E. and Gutierrez JM,, A comparison of functional networks and neural networks. In Proceedings of the IASTED International Conference on Artificial Intelligence and Soft Computing, pages 439–442, IASTED ACTA press 1998.

86. Castillo E, Cobo A, Gutierrez J. M, Nonlinear time series modeling and prediction using functional networks. Extracting information masked by chaos. Phy. Letters A 244 (1998) 71-84.

87. Castillo, E., Hadi, A., and Lacruz, B. (2001), "Optimal Transformations in Multiple Linear Regression Using Functional Networks," Proceedings of the International Work-Conference on Artificial and natural Neural Networks. IWANN 2001, in *Lecture Notes in Computer Science* 2084, Part I, 316–324.

88. Castillo, E., Gutiérrez, J. M., Hadi, A. S., and Lacruz, B. (2001), "Some Applications of Functional Networks in Statistics and Engineering," *Technometrics*, 43, 10–24.

89. Pruneda, B. Lacruz, and C. Solares, A First Approach to Solve Classification Problems Based on Functional Networks. ICANN 2005, LNCS 3697, pp. 313–318. Springer-Verlag Berlin Heidelberg 2005.

90. Solares C., Vieira E. W., and Minguez R., Functional Networks and the Lagrange Polynomial Interpolation. E. Corchado et al. (Eds.): IDEAL 2006, LNCS 4224, pp. 394–401, 2006. Springer-Verlag Berlin Heidelberg 2006.

91. Rajasekaran S., Mohan V. S., and Khamis O., The optimization of space structures using evolution strategies with functional networks. *Engineering with Computers* (2004) 20: 75-87

92. Bruen M. and Yang J., Functional networks in real-time flood forecasting- a novel application. Advances in Water Resources 28 (2005) 899–909.

93. Alan J. Cann " Maths from Scratch for Biologists", university of Leicester, UK, 2003

VITAE

Name	:	Mubarak Aoudah Al-Dhufairi
Birth Date	:	November 24, 1977
Birth Place	:	Al-Qaissomah, Saudi Arabia
Status	:	Married
Nationality	:	Saudi Arabia
Address	:	Saudi Aramco, P. O. Box 5380
	:	Dhahran 31311, Saudi Arabia
Email	:	mubarak.dhufairi@aramco.com
Education	:	**MS (Petroleum Engineering), September 2010**
		King Fahd University of Petroleum and Minerals
		Dhahran, Saudi Arabia
		BS (Petroleum Engineering), May-2000
		King Fahd University of Petroleum and Minerals
		Dhahran, Saudi Arabia
Area of Interest	:	Green fields developments
		Production Engineering and well maintenance